



Advances in Printing and Media Technology

Vol. XXXIX

Edited by Nils Enlund and Mladen Lovreček

Darmstadt
MMXII

Advances in Printing and Media Technology

Proceedings of the 39th International Research Conference of iarigai

Ljubljana, Slovenia, September 2012

Published by the International Association
of Research Organizations for the Information,
Media and Graphic Arts Industries

Darmstadt, Germany 2012

Co-edited by

Nils Enlund, Helsinki, Finland
Mladen Lovreček, Zagreb, Croatia

Scientific Committee

Anne Blayo (Grenoble)
Timothy C. Claypole (Swansea)
Edgar Dörsam (Darmstadt)
Wolfgang Faigle (Stuttgart)
Patrick Gane (Espoo)
Ulrike Herzau-Gerhardt (Leipzig)
Gorazd Golob (Ljubljana)
Jon Yngve Hardeberg (Gjøvik)
Gunter Hübner (Stuttgart)
Marie Kaplanova Pardubice)
John Kettle (Espoo)
Helmut Kipphan (Schwetzingen)
Marianne Klaman (Stockholm)
Yuri Kuznetsov (St. Petersburg)
Magnus Lestelius (Karlstad)
Ulf Lindqvist (Espoo)
Patrice Mangin (Trois Rivières)
Erzsébet Novotny (Budapest)
Anastasios Politis (Athens)
Anu Seisto (Espoo)
Johan Stenberg (Stockholm)
Renke Wilken (Munich)
Scott Williams (Rochester)

The facts published in this book are obtained from sources believed to be reliable. However, publishers can accept no legal liability for the contents of papers, nor for any information contained therein, nor for conclusions drawn by any party from it.

No part of this publication may be reproduced, stored in a retrieval system or transmitted in any form or by any means of electronic, mechanical, photocopying, recording or otherwise without the prior written permission of the publisher.

Printed edition

ISBN 978-3-9812704-5-7
ISSN 2225-6067

Online edition

ISBN 978-3-9870704-3-3
ISSN 2409-4021

Contents

Introduction

Preface	3
<i>Nils Enlund</i>	
Recognition of pigments in organic matrices	5
<i>Miran Mozetič</i>	
Materials science meets graphic communication for a joint venture beyond the conventional	11
<i>Marta Klanjšek Gunde</i>	
Photoacoustic measurements of screen-printed conductive layers	17
<i>Nikola Peřinka</i>	
Next media - a unique cooperation between industry and research	23
<i>Helene Juhola</i>	
Next media, personal media day	27
<i>Kristiina Markkula</i>	

1. Printed electronics and special printing

Disturbance factors in a one impression gravure printing process for the production of PEM fuel cell electrodes	33
<i>Frank Siegel, Albert Kohl, Eugen Enns, Andreas Willert, Wolfgang Deger, Holger Dziallas, Reinhard Baumann</i>	
Advantage of customized battery integration as self-sustaining and embedded device within print products	43
<i>Michael Espig, Sebastian Heinz, André Stark, Frank Siegel, Andreas Willert, Reinhard R. Baumann</i>	
Investigation in the homogeneity of gravure printed polymer films for printed electronics	47
<i>Simon Stahl, Hans-Martin Sauer, Edgar Dörsam</i>	
Graphene inks for printed electronics	53
<i>Veronika Husovska, Alexandra Pekarovicova, Paul D. Fleming III, Mike Knox, Hiroyuki Fukushima, Kathy Roberts</i>	
Thermochromic composition on the base of cyanine dyes as smart packaging element	61
<i>Irina Nagornova, Evgeny Bablyuk</i>	
Hot stamping technology for functional printing	69
<i>Alexandra Lyashenko, Larisa Salun, Edgar Dörsam</i>	
Photoacoustic characterization of a printed electroluminescent panel	75
<i>Markéta Držková, Tomáš Syrový, Nikola Peřinka, Martin Roch</i>	
Printed UHF RFID antenna on coated cardboard	83
<i>Tadeja Muck, Matej Pivar, Miloje Đokić, Diana Gregor Svetec, Urška Bogotaj, Marijan Maček, Leon Pavlovič, Boštjan Batagelj</i>	

Introducing a new anaglyph method: compromise anaglyph <i>Jure Ahtik</i>	91
Printing Braille with inkjet <i>Manfred Schär, Urs von Arx, Fritz Bircher, Reinhold Krause, Pascal Bernet, Karl-Heinz Selbmann</i>	97
Understanding graphic protection methods in print production <i>Branka Morić Kolarić, Ivan Budimir, Jana Žiljak Vujić</i>	107
Accelerated light aging of digital prints <i>Ákos Borbély, Csaba Horváth, Rozália Szentgyörgyvölgyi</i>	117
Reproduction of art paintings with their status in the near infrared spectrum <i>Jana Žiljak Vujić, Ivana Žiljak Stanimirović, Ana Hoić</i>	123
2. Determinators of quality in printed products	
Towards a fully digital computer-to-screen workflow for an improved product quality and quality assurance in screen printing <i>Janko Jesenko, Bojan Petek</i>	131
Leaner and better. How can the setup time and waste at the sheet-fed presses be reduced? <i>Csaba Horváth</i>	139
Digitisation of old printed typeface <i>Klementina Možina, Tanja Urbanc</i>	145
Surface patterning of flexo plates for improved ink transfer <i>Anja Hamblyn, Davide Deganello, Tim C. Claypole</i>	153
Effects of solvents on flexographic printing plates <i>Alexandra Theopold, Jann Neumann, Daniel Massfelder, Edgar Dörsam</i>	159
Permanent flexographic plate changes through nip contacts <i>David Beynon, Tim C. Claypole</i>	169
Ink splitting: The influence of structured surfaces on the contact angle in flexo printing <i>Stefan Griesheimer, Edgar Dörsam</i>	175
The influence of engagement on the flexographic printing of fine lines <i>Tim C. Claypole, Glyn R. Davies, Simon M. Hamblyn, David Galton, Richard Hall</i>	181
Effect of flexographic press parameters on the reproduction of colour images <i>Tim C. Claypole, Eifion H. Jewell, David C. Bould</i>	187
Developing a laboratory simulation of tail edge pick <i>Eveliina Jutila, Cathy J. Ridgeway, Patrick A. C. Gane</i>	195
Control of the breakup of ink filaments in offset printing <i>James Claypole, Phylip R. Williams, Davide Deganello</i>	207
Hardness and electric conductivity of copper in gravure form production <i>Armin Weichmann, Matthias Galus, Tim Wolber</i>	213
Characterization of gravure cells using confocal microscopy <i>Nils Bornemann, Tim Guck, Thorsten Bitsch, Edgar Dörsam</i>	221

Adhesive strength of surface coatings on digital printed products <i>Dragan Milosavljević, Johannes Backhaus</i>	227
Printing ink modified with hyperbranched polymer rheological behaviour and print quality <i>Zuzanna Żolek Tryznowska, Joanna Izdebska, Maciej Szymanowski</i>	233
Printing quality characteristics of rich mineral paper for offset commercial printing <i>Yung-Cheng Hsieh, Kuo-Kun Lee, Ssu-Yi Cheng, Chih-Cheng Kao</i>	241
Influence of surface free energy of biodegradable films on optical density of ink coated fields of prints <i>Joanna Izdebska, Halina Podsiadlo, Liliya Harri</i>	245
Measuring forces appearing while cutting a stack of sheets with the aim to improve post press processes <i>Jann Neumann, Michael Desch, Dieter Spiehl, Edgar Dörsam</i>	253
Wear of packaging during transport simulation <i>Peter Rättö, Thomas Trost, Erik Blohm</i>	261
3. Media and the consumer	
Augmented Reality as a technology bringing interactivity to print products <i>Anu Seisto, Maiju Aikala, Ravi Vatrapsu, Timo Kuula</i>	271
A graphic designer's view on the interaction design for mobile application development <i>Klemen Vadnjak, Ana Praprotnik, Bojan Petek</i>	281
Legibility on Apple iPhone 4S <i>Blaž Rat, Klementina Možina</i>	287
Visualizing a content scenario for mobile devices towards inexperienced user <i>Chrysoula Gatsou, Anastasios Politis, Dimitrios Zevgolis</i>	293
Linking physical print and digital media: opportunities and challenges of quick response codes in the face of mobile visual search technology <i>Natalia Lumby</i>	303
Legibility of offset prints after exposure to light <i>Blaž Rat, Sabina Bračko, Klementina Možina</i>	313
Brand experience as a tool for brand communication in multiple channels <i>Aino Mensonen, Janne Laine, Anu Seisto</i>	321
On the definition of a multi-criteria model for the evaluation and adoption of packaging <i>Marios Tsigonias, Nikolas Kakizis, George Romanos, Antonios Tsigonias, Diana Tsimis, Anastasios Politis, Dimitrios Zevgolis</i>	329
The emotional impact of packaging design. An eye tracking analysis <i>Ulrich Nikolaus, Denise Lipfert</i>	337
Index of authors	347





Introduction

Preface

Nils Enlund

Co-editor, Chairman of the **iarigai** Program and Publishing Committee

E-mail: nilse@kth.se

What, how and when to print - and when not to

Printing has been defined as the art of rapidly and accurately placing "stuff on stuff". By habit and centuries old tradition, we are used to thinking of printing as a technology for putting ink on paper in order to reproduce text and images. But, nowadays, the technologies and methods for efficiently and on an industrial scale placing other substances on other substrates are increasingly capturing the attention of researchers and industry alike.

At the 39th International Research Conference of **iarigai**, the International Association of Research Organizations for the Information, Media and Graphic Arts Industries, held in Ljubljana, Slovenia, on September 9 -12, 2012, printed electronics and functional printing were strongly in focus. Two keynote presentations, one invited lecture, and eight of the papers selected by a committee of international experts through a double-blind review process were addressing the challenges of printing electronics on different surfaces.

A second emerging focus area at the annual conference was the impact and use of non-printed digital media and the attitudes and expectations of consumers to the changing media landscape. In this emerging multidisciplinary scientific field, the conference offered two keynote lectures and eleven peer-reviewed presentations.

Is the venerable **iarigai** conference, so rich on traditions, moving away from print research, then? Certainly not. The main body of the conference is still centered on the problems and challenges of achieving quality and productivity in the printing process. The main body of papers in these proceedings is concerned with investigating the factors that determine quality in printed products of different kinds. This is a wide and stimulating research field.

But printing technology and science are now being applied in new and exciting areas. At the same time, traditional printed products are encountering competition and potential extensions in the digital realm. These developments open up new intriguing and important fields of research that certainly will be further explored at future **iarigai** conferences.

This proceedings volume contains the research contributions presented at the 39th **iarigai** International Research Conference. It also includes the non-reviewed manuscripts of the keynote and invited lectures. The editors and publisher hope that you will find the contents of these proceedings informative and interesting.

Last, but not the least: from this volume on, the Advances in Printing and Media Technology are formally recognized not only as a book, but as well as an international serial publication.



Recognition of pigments in organic matrices*

Miran Mozetič

Jozef Štefan Institute
Jamova cesta 39, SI-1000 Ljubljana, Slovenia
E-mail: miran.mozetic@ijs.si

Abstract

The quality of paints and inks depends not only on the type, size and shape of fillers but often also on distribution and sometimes even orientation of pigments and other particles in organic matrices. The structure of such materials is rather difficult to determine due to a lack of appropriate experimental techniques. An advanced technique is presented in this contribution. The technique applies treatment of materials by highly non-equilibrium gases, usually oxygen plasma, and subsequent surface morphology characterization by scanning electron microscopy. Reactive oxygen species which abound in highly non-equilibrium gases even at room temperature readily interact with the organic matrices causing slow removal in a highly controlled manner. Since the processing takes place at room temperature the fillers in the matrices remain essentially intact. Appropriate treatment conditions therefore allow for removal of the surface layer of organic matrix thus revealing the original distribution of fillers. Several examples are presented and the reaction mechanisms discussed to some details.

Keywords: advanced inks, polymer composite, gaseous plasma, selective etching, functional printing inks

1. Introduction

Enormous progress in printing technology in the past decade is also a consequence of development of advanced functional printing inks. A modern paint is a composite material with a variety of different particles embedded in a polymer matrix. The quality of inks depends not only on the type of polymer used as the matrix and the type, size and shape of functional particles but also on distribution and sometimes even orientation of pigments and other particles in organic matrices. The structure of such complex materials is rather difficult to determine due to a lack of appropriate experimental techniques. A commonly applied technique is scanning electron microscopy (SEM). Since the escape depth of back-scattered as well as secondary electrons is often below a micrometer, this technique cannot reveal the morphological properties of bulk materials such as prints. In order to overcome this limitation many researchers cut investigated films using different mechanical techniques. Such a procedure followed by polishing the sample is usually suitable for characterization of hard solid materials but often fails in the case of composites with unevenly distributed particles of different hardness. Polishing of such composite materials is usually far from being uniform so the original structure of the composite is lost.

An ideal method for sample preparation prior to SEM characterization would be removal of the polymer matrix without touching the embedded particles. Such a procedure cannot be realized by mechanical treatment since the particles found in advanced inks are often sub-microscopic and dense in polymer matrix. Wet chemical methods could be applied in specific cases where the applied chemical interacts only with the polymer matrix but the embedded particles are left intact. This is rarely the case of advanced inks and there is always a threat of destruction of the original distribution and orientation of the particles so this method has limited applicability.

An advanced technique for selective removal of polymer matrix from the surface of modern composite materials is based on low-temperature oxidation. Under thermodynamically equilibrium environment polymer materials are oxidized at reasonably high rates only at elevated temperature. Thermal shocks often cause destruction of the original distribution of particles in the composite materials so oxidation is preferably performed at room temperature. This requirement dictates application of non-equilibrium environments which allow for rapid oxidation even at room temperature. Recent results show that such oxidation could be performed in a highly controllable manner, atom by atom¹. The technology is based on application of extremely non-equilibrium oxygen plasma². Such plasma is created using either radiofrequency³ or microwave⁴ discharges at the pressure of about 100 Pa where the density of neutral oxygen atoms is often at its maximum. The technique was found suitable for revealing the morphological characteristics of ink-jet paper⁵ as well as for studying the distribution of particles in various paint coatings⁶⁻¹¹. It is also a suitable technique for modification of graphite - polymer composites prior to metallization^{11,12}.

2. Materials and methods

Commercially available thermochromic inks were printed on paper substrates and dried according to the recommended procedures. The printed samples were mounted into a plasma reactor. The reactor was made of borosilicate glass, a material with a low probability for heterogeneous surface recombination of neutral oxygen atoms in the ground state. The reactor was pumped with a two stage rotary vacuum pump with the nominal pumping speed of $2.2 \times 10^{-3} \text{ m}^3\text{s}^{-1}$ in a broad range from the atmospheric pressure down to the pressure of 1 Pa. After evacuation of the reactor below the detection limit of the pressure gauge (below 1 Pa) oxygen of commercial purity was leaked continuously into the plasma reactor. Since it was also pumping by the vacuum pump steady conditions were met where the pressure equilibrated at 75 Pa. The reactor was powered with a radiofrequency (RF) generator of nominal power up to 700 W. The reactor was coupled to a copper coil mounted onto the reactor. Due to rather poor matching the power dissipated at the coil was estimated to about 200 W only. As soon as the RF generator was turned on, luminous plasma appeared in the reactor. The plasma treatment time was selected according to the previous experiences⁶⁻¹¹. After plasma treatment the samples were imaged by scanning electron microscopy. The samples were coated with a thin gold film using a commercial sputter device and investigated by SEM.

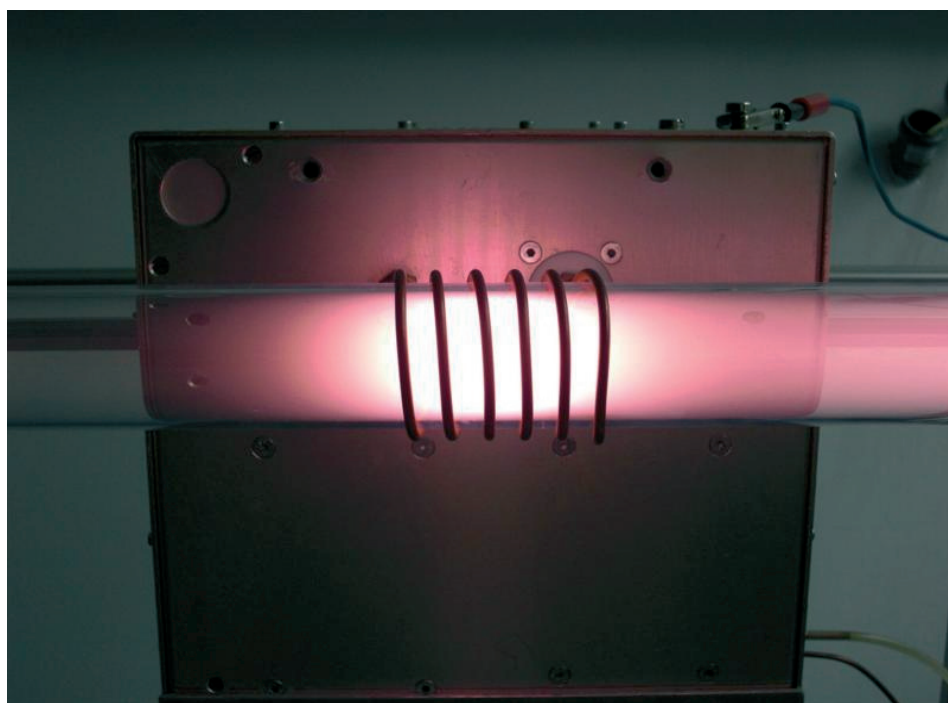


Figure 1: A photo of plasma created by electrode-less radiofrequency discharge

3. Results and discussion

A typical SEM image of untreated sample is shown in Figure 2. As expected, the particles embedded in the polymer matrix are hardly visible since they are covered with the polymer material. The polymer is rather smooth on micrometer scale and fills the available space between functional particles as well as forms a thin coating on top of the particular particle appearing on the layer's surface. A different picture is shown in Figure 3 which represents a typical SEM image of a sample treated with oxygen plasma for half a minute. Now the topmost particles are clearly visible. They are not coated with polymer any more. The removal of polymer is obviously the result of interaction between oxygen plasma and the sample. Reactive particles created in plasma at room temperature interact chemically with the surface atoms on the uppermost layer of the solid material. The interaction is extremely selective: while a layer of polymer is removed the spherical particles appear intact. This is the major feature of the applied technology. The feature is based on the proper selection of reactive gaseous species. In general, plasma is known as partially ionized gas so it contains positively charged oxygen molecules. They are accelerated in the sheath next to the sample but they cannot gain much kinetic energy since the samples are kept at floating potential during plasma treatment (the samples are not biased). The density of charged particles in plasma described above is low - typically below 10^{16} m^{-3} .

This is very important because much larger densities would cause excessive heating of the material and thus a loss of etching selectivity. Namely, a positively charged molecule touching the surface brings excessive kinetic and potential energies. The kinetic energy comes from acceleration across the sheath between unperturbed plasma and the sample and is at our experimental conditions about 10 eV. The positively charged ion meets an electron on the surface of the sample and neutralizes with a very high probability. The neutralization is also an exothermic process and the energy dissipated is equal to the ionization energy of the oxygen molecule (about 12 eV). An ion therefore brings more than 20 eV of energy and the flux should be kept low in order to prevent thermal degradation.

The particles which play a major role in removal of polymer from the sample surface are neutral oxygen atoms in the ground state. They abound in plasma created in glass plasma reactors. They are produced by dissociation of parent molecules. Since the dissociation energy is rather low at 5.2 eV the probability for dissociation upon a collision with energetic electrons is reasonably high. Furthermore, the oxygen molecules are known to have 2 metastable states with long life-times². An electron of medium energy excites a molecule to an excited state and another electron finishes the job by dissociation of the molecule.

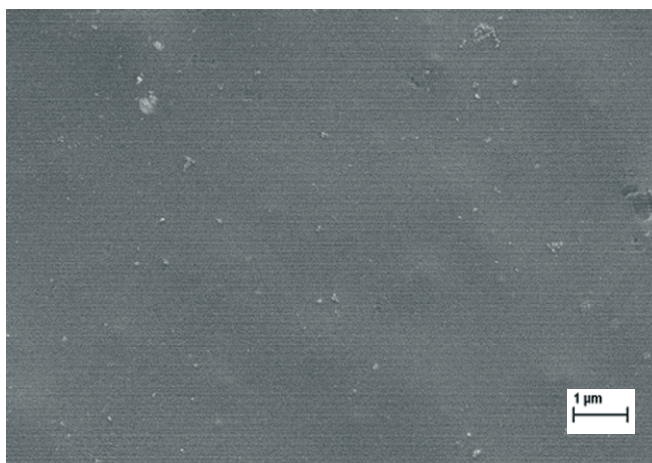


Figure 2: A SEM image of an untreated sample

The required kinetic energy of the electron is solely the difference between the excitation and the dissociation energies - about 3 eV for the case of the molecule found in the second excited state². The density of atoms is large also due to minimized loss in the gas phase as well as on the surfaces. The loss in the gas phase by three body collision is negligible below the pressure of several 100 Pa as explained in² and that's why the rather low pressure was used during plasma treatment of the samples. The loss of atoms by heterogeneous surface recombination on the reactor walls is minimized by proper selection of the plasma facing material. As mentioned earlier the probability for recombination on borosilicate glass is very low so the atom density is really high - the order of magnitude is close to 10^{22} m^{-3} . Such a high density is needed since the interaction probability leading to etching is low, too. Recent results showed the probability of the order of 10^{-4} as revealed in¹.

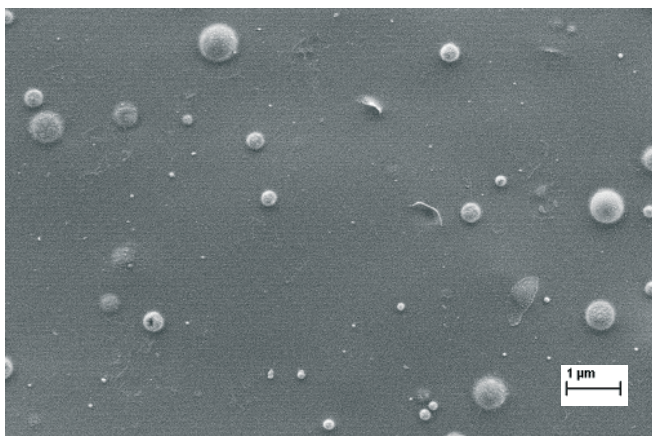


Figure 3: A SEM image of an sample treated with oxygen plasma for 30 s

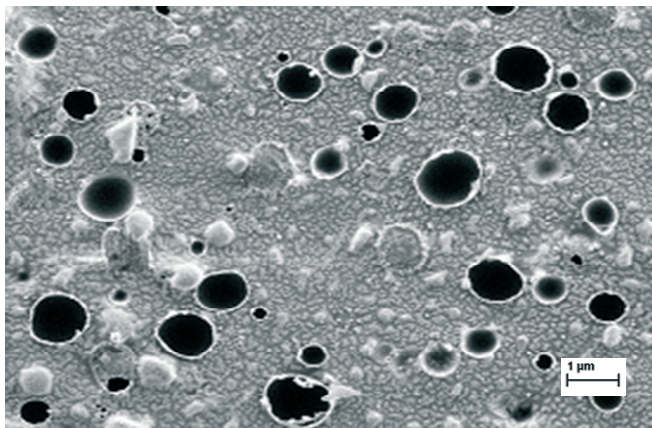


Figure 4: SEM image of an sample treated with oxygen plasma for 60 s

Neutral oxygen atoms are therefore suitable for selective removal of polymer from the surface of our samples so the particles are clearly visible after 30 s of plasma treatment as shown in Figure 3. Also worth discussing is the image presented in Figure 4. This sample was exposed to oxygen plasma for one minute. Now the spherical particles observed on the surface of plasma treated sample are denser. Polymer is, of course, etched more intensively so more spheres are revealed. Most particles are nicely shaped but some of them are empty. This effect could be explained by the fact that the spheres are also etched upon exposure to oxygen plasma. Since such empty spheres are not observed in Figure 3 one should consider another etching mechanism. A suitable one is thermal effect. As mentioned earlier, oxygen plasma created by RF or MW discharges is basically cold - the kinetic energy of molecules, atoms and positively charged particles is essentially the same as for gas at room temperature under thermal equilibrium. There are, however, numerous surface reactions that do cause heating of the material. First there is interaction with ions which has been already discussed. Next, there is heterogeneous surface recombination of atoms which means that each atom will bring the potential energy equal to half the dissociation energy of an oxygen molecule multiplied with the recombination coefficient. Furthermore, the oxidation of polymer or any other carbon containing material is an exothermic process and several eV of energy is dissipated at chemical interaction. The fact that some spheres are empty in Figure 4 can be therefore explained by thermal effects. Such a hypothesis is confirmed taking into account the image presented in Figure 5. In this figure, no sphere is observed. Instead, numerous spherical holes are visible. The effect looks contradictory to what was explained above. Namely, it was claimed that polymer was etched at higher rate than the fillings. Such explanation obviously holds only for rather short treatment times - perhaps up to between 30 and 60 s. For longer treatment times the thermal effects prevail and that's why only holes are observed in Figure 5.

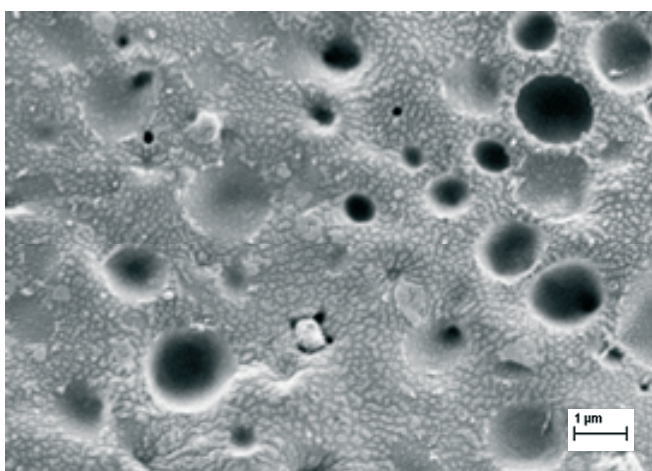


Figure 5: A SEM image of an sample treated with oxygen plasma for 90 s

An experimentalist therefore has to be careful when selecting treatment parameters. Not all particles that form in oxygen plasma are suitable for treatment of prints. As mentioned earlier, ions are very reactive but on the other hand they cause too much heating of the materials so should be avoided. The appropriate flux of

ions onto the sample surface depends on the properties of polymers. Those which are etched easily should not be exposed to large ion fluxes. The density of ions could be selected by choosing the right type of electrical discharge. Electrode-less discharges are recommended since the charged particle density as well as kinetic energy is rather low.

As revealed from Figure 1, the plasma is rather uniform within the coil but its luminosity decreases rapidly away from the coil. Delicate polymer matrix composites should therefore not be placed directly into the coil but a certain distance away where the density of charged particles is much lower than within the coil. In any case it is advisable to use plasma with a large density of neutral oxygen atoms in the ground state. Such plasma is difficult if not impossible to create in metallic chambers where extensive surface recombination prevents high density of atoms at reasonable discharge power.

Also, sputtering effects could be annoying in plasma created by classical discharges such as a DC glow discharge and a capacitively coupled radio-frequency discharge. In these discharges a sheath is formed next to the cathode or powered electrode. The corresponding potential fall across the sheath is several 100 V. Gaseous ions accelerate in this potential fall and bombard the electrode with the kinetic energy of several 100 eV. Although the sputtering coefficient is small at such kinetic energy the effect cannot be neglected in practical cases¹⁵. Even an extremely thin metal film which deposits onto a sample due to sputtering of the powered electrode causes a huge increase of the heat dissipated on the sample surface and thus loss of etching selectivity. This effect is due to very high coefficient for heterogeneous surface recombination of neutral oxygen atoms on metallic surfaces¹⁶.

Finally it is worth mentioning that the optimal etching selectivity is not obtained in plasma but rather in a flowing afterglow. If gas is forced passing a discharge by pumping on one side and continuous leakage on the other side of reactor gaseous molecules will be ionized, dissociated and excited. As explained earlier the best reactants are neutral atoms in the ground state so other particles (ions and metastable atoms) should be avoided when treating extremely delicate materials¹⁷.

The particles are best avoided by placing a sample far away from the plasma region, sometimes half a meter or more in the direction of gas flow. At that position the density of any reactive particles but atoms in the ground state is negligible so extremely high etching selectivity is observed¹⁷. Such a treatment is recommended in cases where the affinity of the polymer matrix to oxidation is very large.

4. Conclusions

The SEM images supported by discussion above enlighten the advantages as well as drawbacks of the technology presented in this paper. First is it clear that treatment of entirely organic composites such as thermochromic inks by oxygen plasma enables studying of the distribution of particles in the polymer matrix. On the other hand, one should be careful when selecting treatment conditions. In this paper it is shown that too long treatment results in destruction of fillings and the optimal treatment time should be selected. Not explained, but worth mentioning, is also the proper choice of plasma parameters. This is the crucial point and the parameters have to be optimized for each particular application¹³. As a general rule, one should choose plasma with a low concentration of charged particles (since they cause unwanted heating of solid materials) and a high density of neutral reactive species such as neutral oxygen atoms in the ground state. Such atoms abound in plasma created at moderately low pressure (about 100 Pa) providing plasma is sustained in a glass reactor. Reactors made for metals (especially stainless steel, nickel, cobalt, copper and alike, should be avoided since these metals act as catalyst for heterogeneous surface recombination and thus prevent a high concentration of atoms needed for appropriate treatment of the composite samples.

Acknowledgments

The financial support from the state budget by the Slovenian Research Agency (program No. P2-0082) is acknowledged.

References

1. A. Doliška, A. Vesel, M. Kolar, K. Stana - Kleinschek and M. Mozetič: "Interaction between model poly(ethylene terephthalate) thin films and weakly ionised oxygen plasma", *Surf. interface anal.* 44 (2012) 56-61.

2. M. Mozetič: "Extremely non-equilibrium oxygen plasma for direct synthesis of metal oxide nanowires on metallic substrates", J. Phys. D, Appl. phys. 44 (2011) 174028-1-174028-9.
3. R. Zaplotnik, A. Vesel and M. Mozetič: "Transition from E to H mode in inductively coupled oxygen plasma : hysteresis and the behaviour of oxygen atom density" Europhys. Lett. 95 (2011) 55001-1-55001-5.
4. A. Vesel, M. Mozetič and M. Balat - Pichelin: "Oxygen atom density in microwave oxygen plasma", Vacuum 81 (2007) 1088-1093.
5. A. Vesel, M. Mozetič, A. Hladnik, J. Dolenc, J. Zule, S. Milošević, N. Krstulović, M. Klanjšek - Gunde and N. Hauptman: "Modification of ink-jet paper by oxygen-plasma treatment", J. Phys., D, Appl. Phys. 40 (2007) 3689-2696.
6. M. Mozetič, A. Zalar, P. Panjan, M. Bele, S. Pejovnik and R. Grmek: "A method of studying carbon particle distribution in paint films", Thin solid films 376 (2000) 5-8.
7. M. Klanjšek - Gunde, M. Kunaver, M. Mozetič, P. Pelicon, J. Simčič, M. Budnar and M. Bele, "Microstructure analysis of metal-effect coatings", Surf. Coat. Int. B: Coat. Trans. 85 (2002) 115-121.
8. M. Kunaver, M. Klanjšek - Gunde, M. Mozetič and A. Hrovat: "The degree of dispersion of pigments in powder coatings and the origin of some surface defects", Surf. Coat. Int., B: Coat. Trans. 86 (2003) 175-179.
9. M. Kunaver, M. Klanjšek - Gunde, M. Mozetič and A. Hrovat: "The degree of dispersion of pigments in powder coatings", Dyes Pigment. 57 (2003) 235-243.
10. M. Kunaver, M. Mozetič and M. Klanjšek - Gunde: "Selective plasma etching of powder coatings. Thin solid films 459 (2004) 115-117.
11. M. Klanjšek - Gunde, M. Kunaver, M. Mozetič and A. Hrovat: "Method for the evaluation of the degree of pigment dispersion in powder coatings. Powder technol. 148 (2004) 64-66.
12. U. Cvelbar, S. Pejovnik, M. Mozetič and A. Zalar: "Increased surface roughness by oxygen plasma treatment of graphite/polymer composite", Appl. Surf. Sci. 210 (2003) 255-261.
13. M. Mozetič and A. Zalar: "Improved affinity to metallization of graphite/polymer composites by oxygen plasma treatment", Mater. Sci. Forum 437 (2003) 81-84.
14. R. Kulčar, M. Friškovec, N. Hauptman, A. Vesel, M. Klanjšek Gunde: "Colorimetric properties of reversible thermochromic printing inks", Dyes and Pigments 86 (2010) 271-277.
15. A. Vesel, M. Mozetič: "On the functionalization of polypropylene with CF₄ plasma created in capacitively coupled RF discharge", Inform. MIDEM 40 (2010) 67-73.
16. M. Mozetič, U. Cvelbar: "Determination of the neutral oxygen atom density in a plasma reactor loaded with metal samples". Plasma sources sci. technol. 18 (2009) 034002-1-034002-5.
17. U. Cvelbar, M. Mozetič, N. Hauptman, : "Degradation of Staphylococcus aureus bacteria by neutral oxygen atoms". J. appl. phys. 106 (2009) 103303-1-103303-5.

Materials science meets graphic communication for a joint venture beyond the conventional*

Marta Klanjšek Gunde

National Institute of Chemistry
Hajdrihova 19, SI-1000 Ljubljana, Slovenia
E-mail: marta.k.gunde@ki.si

Abstract

The applications beyond conventional are complex and diverse. Enormous combinations of different materials used in these applications are not necessarily compatible and may not work properly in a particular functionality. To be efficient enough and to retain the position of print and paper industry among most sustainable and green technologies, it is necessary to be aware of all benefits and drawbacks of new printing materials that may be applied in printed functionalities. Few examples are shown here. They may illustrate the complexity of problems and the scientific approach to understand them. Such knowledge may help to establish a fruitful joint venture between graphic communication and materials science and prepare applications well beyond conventional, benefit to the customer and producers. The area of printed functionality is, however, still far from being mature enough for high profits and adequate sustainability. The market must recognise the need for new products and the industry has to make novel applications. Environmental and safety issues must also be fully addressed.

Keywords: printed functionality, paper electronics, functional printing inks, electrically functional inks, special effects

1. Introduction

Enormous progress of electronic media in the last decade may support an opinion that diversity of e-based applications will be used instead of paper-based or printed media. This is often interpreted as a need for saving forest and energy for pulp, paper and printing. Digital media are not necessarily more environmentally friendly than print^{1,2,3}. However, the internet is crucial for a low carbon world by minimising transport which is the most energy demanding action.

Printing is the only media having only one-time carbon footprint; all other media require energy every time they are looked at. The figures could be improved further by reducing drying energy by minimising design and ink coverage, improving de-inkability of printed products, reduce the average weight of packaging, enlarge point-of-sale or end-user printing and similar.

Print provides practically endless combinations of colours, special effects, surface finishes, shapes, substrates, touches and even smells. Therefore it is the only media which is able to address all human senses. However, vast majority of products provides visual information only, thus address only seeing. Many alternative possibilities are nowadays rapidly entering the area. It is not only human sensation that is progressively addressed, but also electronic reading and communicating. The most complex domain for such integrated applications is packaging, which must be safe for transport and storage and must provide more and more information for all persons taking part in the entire chain from producer to a customer.

New applications are complex and diverse; they address the issues beyond the conventional graphic communication. On the simplest side are printed indicators which show a short-term information or short-range data in a most simple way, whereas on the other appears to be printed electronics with more complex materials and much different printed structures when compared with conventional printing. The new application may predict a very bright future for the entire graphic community. Many products are on the market already and a great many in the research labs or industrial pipelines.

However, the entire area beyond conventional is still far from being mature enough to give high profits and sustainable future. Lot of efforts are still required to reach stable working technologies and optimised functional materials. The market area must recognise the need for such products. Environmental and safety issues have to be addressed seriously.

New functionalities that enable graphic communication products beyond conventional are inevitably connected to the broad knowledge from the area of material science. End applications frequently address imaginary needs (better to say some yet undefined requirements) outside of the traditional field of electronic applications and also of the conventional graphic communication. The number of end products is still small not only due to technological limitations but also due to very tight demands of properties which printing industry was not aware yet. The required combinations of different materials are not necessarily compatible - they seem to be printable in an acceptable quality for conventional prints, but the product do not necessarily serve properly in a particular functionality.

We are entering a new area of graphic communication sector. To be efficient enough and to retain the position among most sustainable and green technologies, it is necessary to be aware of all benefits and drawbacks of new printing materials that will be applied for different functionalities. A few examples will be considered here to illustrate the complexity of problems. To be aware of them and to know possible solutions may help in establishing a fruitful joint venture between graphic communication and materials science. It is reasonable to expect that this way applications well beyond conventional will be feasible to produce, benefit to the customer and producers and with the smallest possible carbon footprint.

2. Methods

There are several possibilities for new printed products, the so-called smart graphic products. They are a synthesis of functional materials, special printing design and suitable substrates.

Printing of functionalities on paper was encouraged by the applications named "paper electronics", especially those where rough and porous paper surface is even beneficial over the smooth and impermeable surfaces⁴⁻⁶. Special coatings were developed to improve the properties of paper substrates for better functioning in electronic applications. However, such improvements are beneficial for the first (bottom) printed layer only. Modification of conventional printing substrate cannot approach perfect properties of semiconductor substrates used in conventional microelectronics.

We refer to printing inks serving other issues than conventional printing for visual purposes as "functional printing inks". Most important classes are conductive, semiconductive and insulator (dielectric), but special effects such as electroluminescence, electrochromism, thermochromism or even shape memory⁷ are also becoming more and more important⁷⁻¹¹. All of them base on polymeric material which enables printing at reasonable conditions.

Printed electronics is based on materials with tightly controlled electrical properties. Simplified structures have to be printed using minimal number of different printing inks, so that the lowest possible price is assured. The target value was estimated to be below 0.2 € per piece¹². Conductive and semiconducting polymers are one of the most important candidates for electrically functional printing inks. They were invented in 1976 as a fourth generation of polymeric materials¹³. It opened fundamental research on chemistry and physics of π -bonded macromolecules which remains of large interest to quantum-effect research and condensed matter physics for decades. Conjugated polymers are typically semiconductors. The HOMO-LUMO difference depends on the molecular structure which offers a big challenge for synthetic chemists to control the energy gap (E_g) by molecular level design. Together with doping, the electrochemical potential (i.e. the Fermi level) moves, and when it becomes into a region of highest density of electronic states, the polymer becomes metallic-like¹⁴. Doped conjugated polymers are relatively good (semi)conductors, but they cannot approach their inorganic representatives. The most important fundamental reason is a certain degree of disorder, which is inevitable intrinsic property of any polymer. It limits the mobility of charges but enables suitable properties of the material at printing conditions. Another possibility for preparation of conductive polymer-based materials is application of metal particles. Materials with high conductivity are applied for this purpose such as silver, gold, copper, nickel, platinum or carbon¹⁵⁻¹⁷. Such conductive inks have various resistivity; the lower was obtained with silver particles. Such electrically functional printing inks are available for screen printing, offset and pad-printing technologies, some of them also for ink-jet. In most cases producers provide sheet resistivity for a layer with specified thickness prepared by a recommended printing and drying conditions. However, the resistivity of a shape, printed by a particle-based conductive ink, depends on the internal microstructure of printed lines which is influenced by printing parameters and may affect the functional properties of the final application¹⁸⁻²¹. This is an intrinsic structural effect that could be understood by the help of percolation theory^{22,17}.

Undoped conjugated polymers are insulators (dielectrics) with dielectric constant $\varepsilon = 3$, similar to all other polymers. However, this is rather low, especially for applications in capacitors where dielectric constant is linearly connected to their capacitance. The dielectric constant of polymers is enlarged by application of particles with high dielectric constant such as magnesium silicate and barium titanate²³.

Electrically functional printing inks are commercially available for extremely broad resistivity region, from $10^{14} \Omega\text{cm}$ for undoped polymers to $10^{-1} \Omega\text{cm}$ for polyaniline and carbon-based conductors and up to $10^{-5} \Omega\text{cm}$ for composites with other conductive particles²⁴. The basic data for dielectrics (ε , breakdown voltage) and semiconductors (E_g , charge mobility, Fermi level) are given rarely, which confirm their great dependence on processing properties.

Printed electronics is capable of producing significantly bigger sensors than conventional microelectronics technology. They could be divided to resistance- and capacitance-based sensors, respect to which changes they are measuring during absorption of analyte, the change of resistance, or the change of capacitance in sensor layer of a capacitor. Printed sensors detect the external factors such as moisture, volatile organic compound, pressure and opening/closing of the electric charge circle by some change in electrical property. Some applications could be transferred directly from microelectronic applications but its intrinsic material properties are of crucial importance and have to be regarded together with structure design²⁵.

3.Results and discussion

The available literature data for specific resistivity of electrically functional printing inks were collected. They show very broad resistivity/conductivity region, compared to other classes of materials (Figure 1). The electrically functional printing inks cover a very wide range and may therefore replace several other non-printable materials.

The inks with pure polymers and their blends have resistivity above $10^4 \Omega\text{cm}$. Much lower values are typical for conductive polymers and carbon-based polymer composites, within 10^2 and $10^{-2} \Omega\text{cm}$. Much smaller resistivity is characteristic composites with highly conductive particles and high loadings. Such inks are frequently called "pastes". Most frequently applied conductive fillers are copper, nickel and silver. The resistivity of such materials range from $10^{-2} \Omega\text{cm}$ up to $10^{-4} \Omega\text{cm}$; the smallest resistivity (the largest conductivity) was obtained for silver paste ($10^{-5} \Omega\text{cm}$). The overview of specific resistivities of functional printing inks is shown in Figure 2.

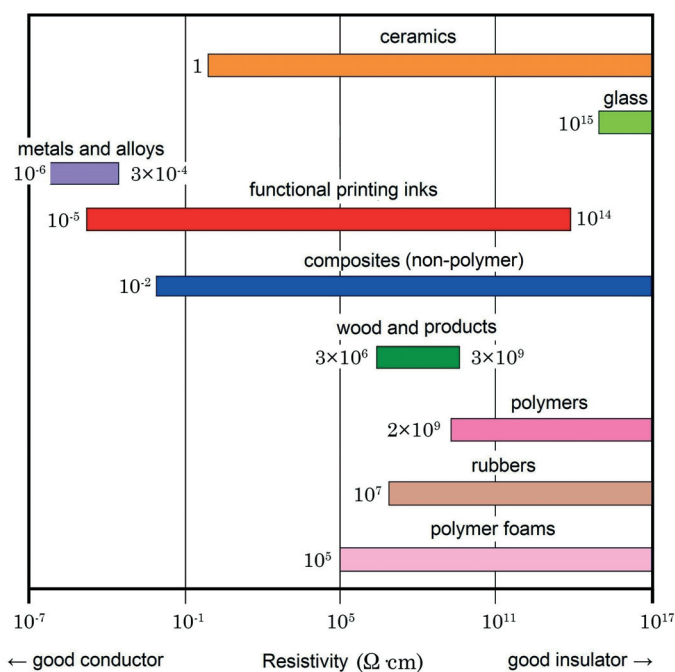


Figure 1: Specific resistivity of materials

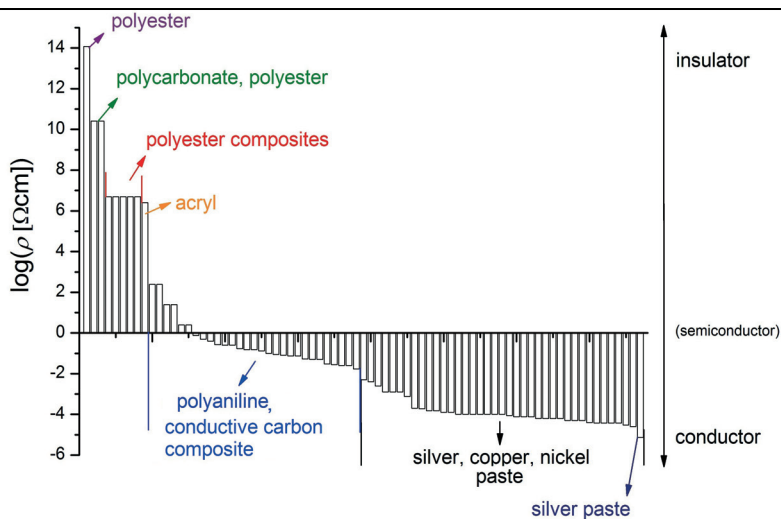


Figure 2: Specific resistivity of electrically functional printing inks²⁴

For printing applications are particularly interesting polymer composites acting as conductors or isolators. The conductivity of particle-based polymer functional printing inks (frequently named "pastes" to point out heavy particle loadings) depends on volume concentration of particles, their distribution within polymer matrix and on internal structure. Such a material is a disordered system; the conditions in which it becomes opened to a sort of flow (fluid, heat, electric current, moving objects, ...) is described by percolation theory. At small concentration of conductive particles, the average distance between them are too large for the electric current to flow while the insulating polymer limits it. At a sufficient concentration, particles form conductive paths throughout, which gives rise to several orders of magnitude diminish of specific resistivity. The corresponding concentration is the so-called percolation threshold. It divides composites into conductive and non-conductive²⁶. The percolation threshold of simple nearly round-shaped particles is higher than of branched particles with higher structure. In the former case the almost close-packed network of spheres is 'connected' by nearest-neighbour tunnelling while in the later the structure of particles may provide larger areas of close contact, therefore more conductive pathways. This is the reason why highly structured carbon black gives, in general, composites with higher conductivity²⁷. However, the conductive network is not the only factor influencing specific resistivity of the material. The interface between particle and polymer matrix is also important. Conductive particles need some wetting and dispersing additive to be dispersed in a polymer matrix. A layer of additive can screen the charges on particle surfaces. It was shown that this effect is the smallest when the monolayer of additive was chemically bond on particle surfaces²⁸. Nevertheless, the role of polymer matrix is not negligible; it may support the electric current or not. The effect depends on the polymer structure, especially on crosslinking properties. In photoresist polymer up to five order of magnitude drop in specific resistivity was confirmed after UV exposure compared to unexposed dry material²⁹. Such a polymer matrix enables electron transport over larger distances than tunnelling.

Good insulators are poor conductors which have large dielectric strength, i.e. direct current voltage at which dielectric breakdown occurs when such a material is applied between both terminals of a capacitor. Most polymers have breakdown voltage 100-300 kV/cm. When such material is applied as an insulator in capacitors, it must have large dielectric constant ϵ to support the capacitance of the device and the electric field between the conductive plates. Polar polymers have ϵ above 3, but non-polar below this value. The properties of insulator ink are frequently changed by incorporating particles with larger ϵ . Such systems are described by effective medium theories. The basic assumption is that the properties of the composite can be described by effective parameters, taking into account the corresponding properties of all constituent materials in bulk. For inks with high dielectric constant different particles are applied, such as silicates, alumina or titanates.

The most important representatives of functional printing inks for special effects are electroluminescent inks. They luminesce when in an electric field. Such conditions are met in flat-plate capacitors. However, at least one conductive plate must be transparent for the light comes out. Electroluminescent ink is a dielectric; however, additional dielectric layer is advised to print to ensure the operating of the device³⁰.

Other interesting functional printing inks are thermochromics. The functional material is in most cases entirely organic material which is protected in polymer capsules, and these "pigments" are embedded in a sui-

table polymer matrix. Such inks, in general, show color hysteresis. Commercial inks with the same activation temperature may have very different loops, wide or narrow, symmetric or unsymmetric⁸. Hysteresis loop of a mixture of such inks reveals its binary nature only if the individual pure inks have well-separated hysteresis⁹. The thermochromic inks are not very stable. When exposed to UV light, color hysteresis gets smaller, wider and become lower slopes. A 24 hour exposure in Suntest could destroy the complete effect. However, the printed samples are stable enough against 10 h heating in laboratory dryer at 150 °C. Stability therefore appear as a combined effect of the binder, the polymeric shell and the active core inside the pigment capsules. Poor stability against light and high temperatures has different origins; exposure to light influences mostly the active core inside capsules, while heating affects pigment capsules. Exposure to light broadens the corresponding hysteresis loop, while heating makes it narrower¹⁰. The core material in pigment capsules contains leucodye, developer and solvent. Leucodye define the colour shade whereas melting point of the solvent gives activation temperature where the colour change occurs. Concentration ratio of the three components defines the dynamic colour properties¹¹.

4. Conclusions

The conventional printing addresses basically only human visual sense which limits the required materials and the features of final product. The demands of the so-called printed functionality or smart printed matter remove these boundaries, but introduce many very tight conditions which must be met. The possibly useful materials were developed more or less for some target applications using the highest impact of advance material science. The research is devoted to complex materials which have to provide full advantage of the uniqueness and peculiarities of novel materials. The tight cooperation between materials science and graphic communication is likely to form a prosperous joint venture that offers yet unimaginable applications well beyond conventional.

One of the serious issues of all printed functionalities is recyclability. Electrical conductivity of polymer-based materials inevitably needs application of heavy metals to enhance conductivity; however, they should be avoided by the environmental and health reasons. Printed functionalities require much thicker structures than conventional printings. Multilayered applications may quickly reach 2.5 g/m², which is regarded to impair recycling. The deinkability issues of these applications were not addressed yet. These problems have to be considered for the paper and printing industry remain among most sustainable sectors also after wide implementation of printed functionalities.

A joint venture between materials science and graphic communication offers yet unimaginable applications well beyond conventional. This will be beneficial also in solving sustainability issues.

Acknowledgements

The financial support from the state budget by the Slovenian Research Agency (project No. J2-9455 and program No. P1-0030) is acknowledged.

References

1. "The facts of our value chain", European mail industry platform, 2011.
2. Zerocarbon footprint http://www.zerocarbonfootprint.co.uk/green_computing.htm (accessed on 11th July 2012).
3. Newspaper performs well in environmental comparison, <http://www.forest.fi/smyforest/foresteng.nsf/95f358fafb7d84d8c2256f4b003725e1/5c5a49462ac05185c22574ba001ba997>, (accessed on 11th July 2012).
4. D. Tobjörk, R. Österbacka, "Paper electronics", *Advanced Materials* 23 (2011) 1935-1961.
5. C. Mercier, M. Peralba, M. Dube, J.F. Bloch, J.P. Mangin, "Effects of drops interactions on ink-jet print quality", *Advances in Printing Science and Technology* 34 (2007) 221-230.
6. R. Ballström, A. Määttänen, D. Tobörk, P. Ihlainen, N. Kaihtovirta, J. Österbacka, M. Toivakka, "A multilayer fiber-based substrate for printed functionality", *Organic Electronics* 10 (2009) 1020-1'23.j
7. A. Seeboth, D. Löttsch, "Thermochromic phenomena in polymers". Shawbury: Smithers Rapra technology Limited; 2008.
8. R. Kulčar, M. Friškovec, N. Hauptman, A. Vesel, M. Klanjšek Gunde, "Colorimetric properties of reversible thermochromic printing inks", *Dyes and Pigments* 86 (2010). 271-277.

9. R. Kulčar, M. Friškovec, M. Klanjšek Gunde, N. Knešaurek, "Dynamic colorimetric properties of mixed thermochromic printing inks", *Coloration technology* 127 (2011) 411-417.
10. M. Friškovec, R. Kulčar, M. Klanjšek Gunde, "Light fastness and high temperature stability of reversible thermochromic printing inks", *Coloration technology*, accepted (2012).
11. O. Panak, N. Hauptman, M. Klanjšek Gunde, M. Kaplanova, "Colorimetric characterization of thermochromic composites with different molar ratios of compounds", *JPMTR* 1 (2012), in press.
12. M. Berggren, D. Nilsson, N.D. Robinson, "Organic materials for printed electronics", *nature Materials* 2 (2007) 3-5.
13. A.J. Heeger, "Semiconducting and metallic polymers: the fourth generation of polymeric materials", *Synthetic Metals* 125 (2002) 23-42.
14. Kwanghee Lee, Shinuk Cho, Sung Heum Park, A. J. Heeger, Chan-Woo Lee, Suck-Hyun lee, "Metallic transport in polyaniline", *Nature* 441 (2006) 65-68.
15. R. Strümpfer, J. Glatz-Reichenbach, "Conducting polymer composites", *Journal of Electroceramics* 3 (1999) 329-346.
16. B.K. Park, S. Jeong, J. Moon, J. S. Kim, "Direct writing of copper conductive patterns by ink-jet writing", *Thin Solid Films* 515 (2007) 7706-7711.
17. N. Hauptman, M. Žveglič, M. Maček, M. Klanjšek Gunde, "Carbon based conductive photoresist", *Journal of Materials Science* 44 (2009) 4625-4632.
18. M. Pudas, N. Halonen, P. Granat, J. Vähäkangas, "Gravure printing of conductive polymer inks on flexible substrates", *Progress in Organic Coatings* 54 (2005) 310-316.
19. J. Perelaer, B. J de Gans, U.S. Schubert, "Ink-jet printing and Microwave Sintering of Conductive Silver Tracs", *Advanced Materials* 18 (2007) 2101-2104.
20. M. Žveglič, N. Hauptman, M. Maček, M. Klanjšek Gunde, "Screen-printed electrically conductive functionalities on paper substrates", *Materials and Technology* 45 (2011) 627-632.
21. K. Reuter, H. Kempa, N. Brandt, M. Bartzsch, A. C. Heuber, "Influence of process parameters on the electrical properties of offset printed conductive polymer layers", *Progress in Organic Coatings* 58 (2007) 312-315.
22. F. Lux, "Models proposed to explain the electrical conductivity of mixtures made of conductive and insulating materials", *Journal of Materials Science* 28 (1993) 285-301.
23. T. Leghnet, P. Herbeck-Engel, J. Adam, G. Klein, T. Kolouoma, M. Veith, "Dielectric properties of a printed sol-gel matrix composite", *Advanced Engineering Materials* 12 (2010) 379-384.
24. M. Žveglič, M. Klanjšek Gunde, "Printing materials for printed electronics", *Vakuumist* 31 (2011) 3-7.
25. M. Klanjšek Gunde, N. Hauptman, M. Maček, M. Kunaver, "The influence of hard-baking temperature applied for SU8 sensor layer on the sensitivity of capacitive chemical sensor", *Applied Physics A* 95 (2009) 673-680.
26. R. Strümpfer and J. Glatz-Reichenbach, "Conducting Polymer Composites", *Journal of Electroceramics* 3 (1999) 329-346
27. I. Balberg, "A comprehensive picture of the electrical phenomena in carbon black-polymer composites", *Carbon* 40 (2002) 139-143.
28. N. Hauptman, M. Klanjšek Gunde, M. Kunaver, M. Bešter-Rogač, "Influence of dispersing additives on the conductivity of carbon black pigment dispersion", *Journal of Coatings Technology and Research* 8 (2011) 553-561.
29. N. Hauptman, M. Žveglič, M. Maček, M. Klanjšek Gunde, "Carbon based conductive photoresist", *Journal of Materials Science* 44 (2009) 4625-4632.
30. K. Weigelt, E. H. Jewell, C. O. Phillips, T. C. Claypole, A. C. Hübler, "Bidirectional flexible mouldable electroluminescent lamps fabricated by screen printing", *JPMTR* 1 (2012) 97-102.

Photoacoustic measurement of screen-printed conductive layers*

Nikola Peřinka, Lucie Syrová, Markéta Držková, Tomáš Syrový, Marie Kaplanová

University of Pardubice

Faculty of Chemical Technology

Department of Graphic Arts and Photophysics

Studentská 95, Pardubice CZ-53210, Czech Republic

E-mails: nikola.perinka@student.upce.cz; lucie.syrova@student.upce.cz; marketa.drzkova@upce.cz;

tomas.syrovy@upce.cz; marie.kaplanova@upce.cz

Abstract

The main parameters, which may influence the resulting quality of the printed functional layers, are the thickness and the layer homogeneity. For evaluation of these parameters, currently, different methods can be used. However some of these methods may have various drawbacks and therefore new methods are still being searched and developed. The layer thickness can be determined by mechanical (or optical) profilometers. Another approach is represented by using the spectroscopic methods, e.g. UV-VIS or the photoacoustics. After some promising results have been received during the first photoacoustic measurements of spiral coated functional layers, further measurements have been carried out to prove the capability of this method for the evaluation of layer thickness with the screen printed transparent PEDOT:PSS based conductive polymer layers and also silver based conductive composite inks. As the substrate material, flexible polymer foil was used. This paper discusses the progress in photoacoustic measurements of different functional materials, represented by two commercially available conductive screen-printable dispersions of PEDOT:PSS (Clevios S V3 and Orgacon EL-P 3040) and conductive silver ink CI-1001. The two different PEDOT:PSS based conductive dispersions are compared as well.

Keywords: conducting polymers, screen-printing, photoacoustics, PEDOT:PSS

1. Introduction

The area of application of new functional materials by means of the printing is already established since several years under the term "Printed electronics" (Perelaer, 2010). The printing processes enable the low cost large area roll-to-roll (R2R) production (Bae, 2010). The main advantages are also the possibility of patterning and application on flexible substrates (Mannerbro 2008; Denneulin 2011). The layers of various functional materials can be printed on each other and layer-to-layer aligned (Street, 2006). The thickness of the printed layers ranges from the several tens of nanometers to micrometers (Clemens, 2004). Currently, one of the widely used printing technologies in the printed electronics is the screen printing technique (Faddoul, 2012; Krebs, 2009; Parashkov, 2005). The screen printing technology is applied for manufacturing of functional layers for various electronic applications, such as electro-optic devices (Winther-Jensen, 2006), radio frequency identification (RFID) (Subramanian, 2005), sensor arrays and biosensors (Piano, 2010), printed organic circuits (Hübler, 2011), batteries (Hilder 2009; Braam 2012), diodes (Lilja, 2009), printed wiring boards (PWB) (Lian, 2009), micro-electro-mechanical systems (MEMS) structures (Cheneler, 2011), etc. During the fabrication process, the quality and the properties of the functional layers and final electronic devices need to be evaluated. For these reasons various methods are investigated to be applied in this field.

The photoacoustics represents a new approach to the assessment of the properties of printed conductive materials (Peřinka, 2009; Peřinka, 2011). Since the layer thickness and the thickness homogeneity of conductive layers are of great importance for the final functionality of printed electronic devices, the current processes for the thickness determination are still being improved and the new methods are still being searched. In some cases, the utilization of the mechanical and laser profilers may not be suitable. The reasons are for instance low accuracy of these methods or the dependence on other factors (e.g. unevenness of the substrate). Moreover, these methods usually require the mechanical contact and hence the studied matter can be often damaged after the measurement (Mendeleyev, 1997; Mattia, 2003). For instance, for the full printed areas, it is necessary to scratch the printed area to receive "the valley" in the printed layer to detect the distance between the substrate surface and the printed layer surface. The other limitations of the mechanical techniques are the facts that they cannot be realized in inline processes and the measurement and evaluation of the data usually may take a long time. By the mechanical methods, only the layer surface can be examined. Since the functionality of the layers in printed electronics is often influenced by the structure of the printed

material, the properties within layer volume should be also evaluated. The spectroscopic assessment is therefore of advantage, so that the parameters inside of the examined layer can be obtained as well. The currently available optical techniques, such as the interferometry or spectroscopic ellipsometry suffer from the fact that the accuracy of these methods depends on the radiation source wavelength (Juárez, 1999) or the examined layers must be at least partially transparent (Woollam, 2003). Since the photoacoustics does not deal with the detection of the photons but rather the energy relaxed by the studied matter, the transparency of the examined layer does not stand for the limitation, in this case (Rosencwaig, 1980). The photoacoustics was chosen as contactless and mostly non-destructive method. The main aim of this work was to prove the capability of photoacoustics as the method for the detection of the layer properties, such as the thickness or layer homogeneity of various functional materials (e.g. conducting polymers or conductive composites). Under the term photoacoustics should be understood the measurement of the heat, which is produced after the periodical irradiation of the examined sample by the frequency modulated laser light. The heat created in the sample is produced through the non-radiative de-excitation processes. The heat changes, which arise after the interaction of light with the sample, are usually registered indirectly by means of the corresponding pressure changes in a form of acoustic waves, detected by a microphone. The theoretical background of this phenomenon was explained by Rosencwaig and Gersho in 1970's (Rosencwaig, 1980).

2. Materials and methods

The studied samples comprised single functional layer deposited on flexible transparent PET foil. Three conductive inks were utilized for the study: two dispersions (Clevios™ S V3 and Orgacon™ EL-P 3040) based on PEDOT:PSS [poly(3,4-ethylenedioxythiophene) poly(styrenesulfonate)] from different producers and conductive composite ink based on Silver (CI-1001). The printed layers of PEDOT:PSS were prepared on the transparent flexible PET substrate Melinex® ST504.

During the experiment, various samples prepared via screen-printing semiautomatic machines were examined. To obtain a scale of various thicknesses, a set of five screens frames with different mesh densities was prepared. Each mesh density refers to particular thickness of resulting layer. For the Clevios™ S V3 all five mesh densities were applied. In the case of the Orgacon™ EL-P 3040 only two meshes with different mesh densities and in the case of the CI-1001 meshes with four different densities were available. The highest mesh densities correspond to the lowest values of the thickness. All examined layers were conductive. The measured surface resistance (measured by simple contact 2-point probe for samples printed using the mesh with the density of 62 cm^{-1}) of the samples of Clevios™ S V3 was approximately $10 \text{ k}\Omega/\text{Sq}$; for Orgacon™ EL-P 3040 the surface resistance was higher up to several tens of $\text{k}\Omega/\text{Sq}$. In the case of the Silver based sample, the measured resistance was amounted to $0.020 \Omega/(\text{Sq Mil})$.

The photoacoustic measurement was carried on the laboratory built device, consisting of four main parts - the closed photoacoustic cell connected to the pre-amplified $\frac{1}{2}$ " microphone (4137 from Brüel & Kjaer), DSP lock-in amplifier (SR830 from Stanford Research Systems) and the computer to control the measurement and process the measured signal and data. The samples placed in the photoacoustic chamber were impinged by the light emitted by diode pumped solid-state laser with the wavelength of 532 nm, which was intensity modulated in the frequency range from 10 to 995 Hz by means of the lock-in amplifier. The measured photoacoustic signal was normalized after the measurement using the reference sample comprising a Gold layer deposited on the polypropylene foil via high vacuum evaporation. Each sample was examined once it was placed into the photoacoustic chamber four times by two consecutive scans in measured range of modulation frequencies.

The profilometric measurements were also proceeded to obtain the absolute values of the thickness and to compare them with the photoacoustic parameters. The profiles were scanned on the printed lines of the nominal width of approximately 0.8 mm using the profilometer Dektak 8 from Veeco (PEDOT:PSS based layers) and SSC01 from R.M.I. (Silver based layers).

3. Results and discussion

According to the measured profiles of the printed layers based on PEDOT:PSS, the thickness was in the range from approximately 200 nm to almost $1 \mu\text{m}$. In contrast to PEDOT:PSS based layers, the thicknesses of the Silver based layers were in the range from approximately 3.5 to $7 \mu\text{m}$. All the calculated thicknesses estimated by means of the profilometer are clearly surveyed in Table 1.

Table 1: Thickness of the examined layers

Mesh density [cm ⁻¹]	Thickness <i>d</i> of Orgacon™ EL-P 3040 (standard deviation) [nm]	Thickness <i>d</i> of Clevios™ SV3 (standard deviation) [nm]	Thickness <i>d</i> of CI-1001 (standard deviation) [μm]
62	-	956 (46)	7.1 (1.3)
77	-	439 (20)	4.8 (0.8)
110	-	382 (13)	3.9 (0.8)
140	337 (19)	205 (8)	3.6 (0.9)
165	284 (33)	195 (14)	-

As it becomes obvious from the Table 1, the thickness of the PEDOT:PSS based layers prepared from the Orgacon™ EL-P 3040 was higher than the thickness of Clevios™ S V3 layers prepared using the same mesh densities. Also the roughness, given by the evaluation of the standard deviation of the mean thickness was higher in the case of Orgacon™ EL-P 3040. These facts are also illustrated in Figure 1 and Figure 2, where the cross-sectional line profiles for the both different dispersions can be compared. The high peaks in the profile in Figure 2 are caused by the higher roughness of the layer, which induces instabilities in the movement of the measuring instrument. During the evaluation process it is then rather more complicated to extract the information about the "real" surface of the examined layer, which leads to some inaccuracies in the final assessment of the measured data. Comparing the PEDOT:PSS based layers with the Silver based layers shows that, although the same mesh densities were used, the thickness of the CI-1001 was much higher. This was caused by the higher solid content of the Silver based ink. Also it should be noted that for the CI-1001 layers, the roughness relative to the absolute value of the thickness is much higher than in the case of PEDOT:PSS based layers.

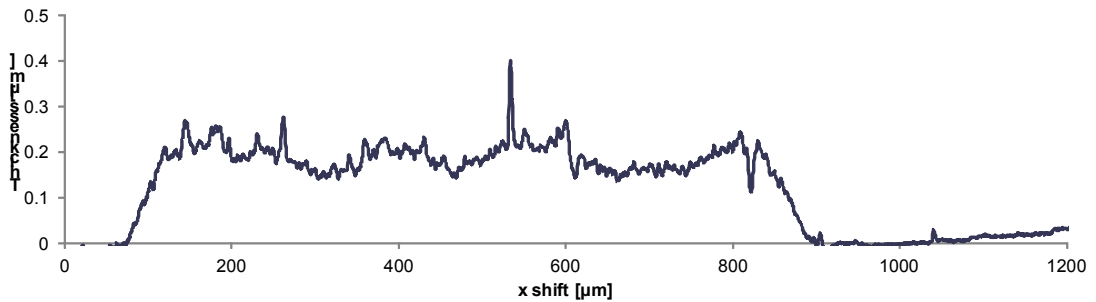


Figure 1: Measured cross-sectional printed line profile of PEDOT:PSS based layers of Clevios™ S V3 on the substrate Melinex® ST 504 (Mesh density 165 cm⁻¹)

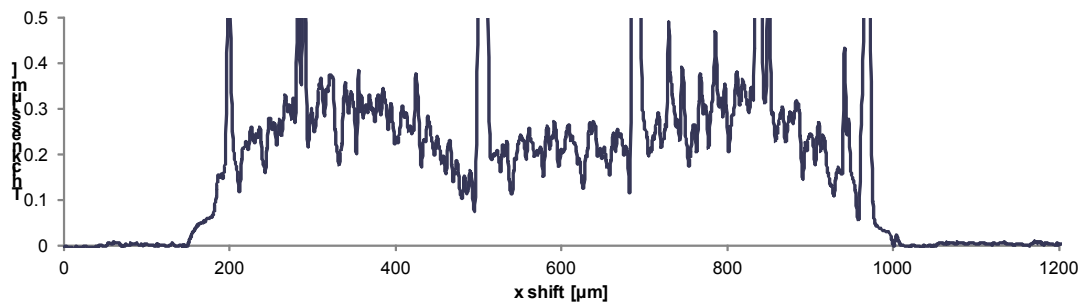


Figure 2: Measured cross-sectional printed line profile of PEDOT:PSS based layers of Orgacon™ EL-P 3040 on the substrate Melinex® ST 504 (Mesh density 165 cm⁻¹)

After the evaluation of the photoacoustic signal measured for the Orgacon™ EL-P 3040 it was found out that the two examined layers with different thickness can be distinguished both in the amplitude and the phase shift of the signal. In the case of the amplitude, the precision was higher and uniform in the whole range of modulation frequencies. The resolution in the amplitude, estimated through the statistical assessment based on the confidence band of 95 % probability evaluated from four measurements of each sample, reached 35 nm (average distance between the upper and lower confidence band). This is in contrast to the phase shift of the measured signal, where the precision was lower and considerably varied for individual modulation frequen-

cies, with the best resolution of 59 nm. It should be noted that the value of the resolution cannot be compared with the value from the profilometer, where just the standard deviation calculated from three measured cross-sectional line profiles is indicated.

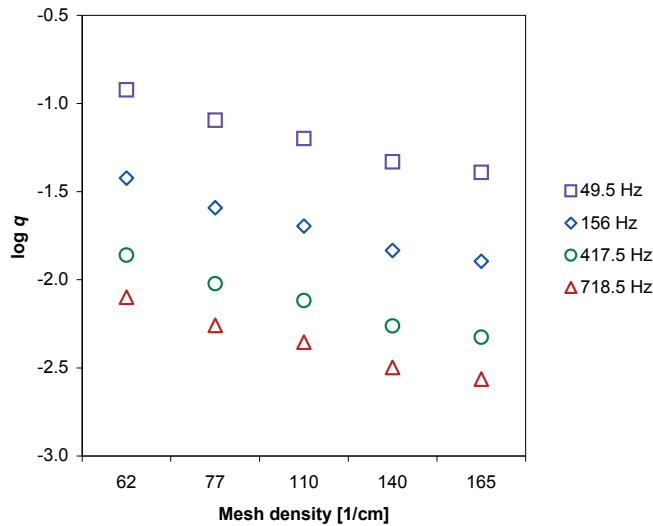


Figure 3: Interdependence between the logarithm of the amplitude of the photoacoustic signal and the mesh density (corresponding to the thickness of the examined layers) for the printed PEDOT:PSS based layers of Clevios™ S V3 at various frequencies of the laser light modulation

For the Clevios™ S V3, all the five different thicknesses can be clearly distinguished in the amplitude of the photoacoustic signal at whole range of modulation frequencies, which is illustrated in the Fig. 3. Comparing to the results for Orgacon™ EL-P 3040, the precision and its uniformity were lower. The resolution estimated using the same statistical approach reached 66 nm. In the case of the phase shift of the photoacoustic signal, the course of the modulation frequency dependence is more complicated and only the higher frequencies were found as possibly suitable for thickness evaluation without elaborate theoretical interpretation. However, due to significantly lower precision obtained in the phase shift (in the order of hundreds of nanometers), the amplitude would be favoured. For the Clevios™ S V3, the correlation between the photoacoustic amplitude for one chosen modulation frequency (222.5 Hz) and the thickness determined with the profilometer (and also the mesh density) was studied as well. In the both cases the high correlation exceeding 90 % was found. Since the correlation between the amplitude of the photoacoustic signal and the mesh density was higher, it rather shows on the questionable assessment of the thickness using the profilometer.

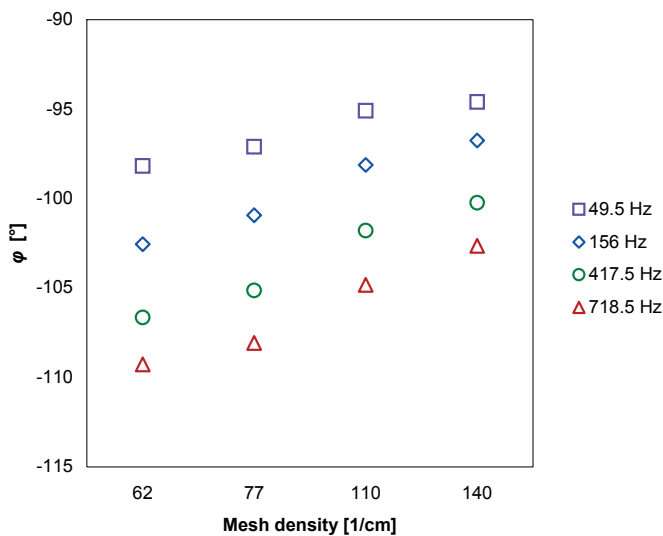


Figure 4: Interdependence between the phase shift of the photoacoustic signal and the mesh density (corresponding to the thickness of the examined layers) for the printed Silver based layers of CI-1001 at various frequencies of the laser light modulation

In the case of the Silver based ink, the different thicknesses could be relatively well resolved in the phase shift of the photoacoustic signal (Fig. 4). The estimated resolution in the phase shift ranged in the order of several hundreds of nanometers, with the best resolution of 0.2 μm for the middle modulation frequencies. In the amplitude of the signal, only slight differences increasing with the modulation frequency were observed between the individual thicknesses. Accordingly, the precision increases with the modulation frequency and for the highest frequencies used, the estimated resolution reached 0.8 μm . Since the Silver based ink beside the conductive particles also contains a higher amount of the binder, it represents more complex system comparing to PEDOT:PSS based ink, contributing to higher variability of layer thickness and roughness, which together with differing material properties leads to lower resolution of the photoacoustic method.

4. Conclusion

In this work it was shown that the thickness and morphology of the printed functional layers of different conductive materials can be examined by the photoacoustics. In the case of the PEDOT:PSS based layers, a high repeatability and sensitivity of this method was confirmed. Also the differences in the quality of the layers prepared from the PEDOT:PSS based dispersions from different manufacturers can be observed using the photoacoustics. Based on the presented statistical evaluations and comparing with the data, received from the profilometer, the resolution of the photoacoustic method for the detection of the thickness differences is high; especially in the case of the studied system of the conducting polymer. This fact was also supported by the high correlation with the data obtained from the profilometer. However, the resolution of this method is always determined by the material properties of the examined conductive material. This is also the reason why the detection of the thickness of the conductive composites is rather sensitive in the phase shift of the photoacoustic signal. The actual results are a good motivation for the further measurements of other functional material and multi-layer system. Also the characterization of the full device structures are studied in the moment and new ones are planned.

Acknowledgments

The main thanks belong to the Institute of Print and Media Technology at the TU-Chemnitz for the cooperation during this work. The financial support of the Czech Ministry of Education (grant no. MSMT 0021627501) and of the FR-TI1/144 from the Ministry of Industry and Trade of the Czech Republic is gratefully acknowledged.

References

- Bae S., Kim H., Lee Y., Xu X., Park J., Zheng Y., Balakrishnan J., Lei T., Kim H. R., Song Y. I., Kim Y., Kim K., Özyilmaz B., Ahn J., Hong B. H., Iijima S., (2010), Roll-to-roll production of 30-inch graphene films for transparent electrode, vol. 5, pp. 574-578.
- Braam K. T., Volkman S. K., Subramanian V., (2012), Characterization and optimization of a printed, primary silver-zinc battery, *Journal of Power Sources*, vol. 199, pp. 367-372.
- Cheneler D., Teng J., Adams M., Anthony C. J., Carter E. L., Ward M., (2011), Printed circuit board as a MEMS platform for focused ion beam technology, *Microelectronic Engineering*, vol. 88, no. 1, pp. 121-126.
- Clemens W., Fixa W., Fickera J., Knoblocha A., Ullmann A., (2004), From polymer transistors toward printed electronics, *Journal of Materials Research*, vol. 19, pp. 1963-1973.
- Denneulin A., Bras J., Blayo A., Neuman Ch., (2011), Substrate pre-treatment of flexible material for printed electronics with carbon nanotube based ink, *Applied Surface Science*, vol. 257, no. 8, pp. 3645-3651.
- Faddoul R., Reverdy-Bruas N., Blayo A., (2012), Formulation and screen printing of water based conductive flake silver pastes onto green ceramic tapes for electronic applications, *Materials Science and Engineering: B*, vol. 177, no. 13, pp. 1053-1066.
- Hilder M., Winther-Jensen B., Clark N. B., (2009), Paper-based, printed zinc-air battery, *Journal of Power Sources*, vol. 194, no. 2, pp. 1135-1141.
- Hübler A. C., Schmidt G. C., Kempa H., Reuter K., Hamsch M., Bellmann M., (2011), Three-dimensional integrated circuit using printed electronics, *Organic Electronics*, vol. 12, no. 3, pp. 419-423.
- Juárez A., Hernández M., Hernández R., (1999), Interferometric thickness determination of thin metallic films, *Superficies y Vacío*, vol. 9, pp. 283-285.
- Krebs F. C., Jørgensen M., Norman K., Hagemann O., Alstrup J., Nielsen T. D., Fyenbo J., Larsen K., Kristensen J., (2009), A complete process for production of flexible large area polymer solar cells entirely using screen printing - First public demonstration, *Solar Energy Materials and Solar Cells*, vol. 93, no. 4, pp. 422-441.

- Lian K., O'Rourke S., Sadler D., Eliacin M., Gamboa C., Terbrueggen R., Chason M., (2009), Integrated microfluidic components on a printed wiring board platform, *Sensors and Actuators B: Chemical*, vol.138, no. 1, pp. 21-27.
- Lilja K. E., Bäcklund T. G., Lupo D., Hassinen T., Joutsenoja T., (2009), Gravure printed organic rectifying diodes operating at high frequencies, *Organic Electronics*, vol. 10, no. 5, pp. 1011-1014.
- Mannerbro R., Ranlöf M., Robinson N., Forchheimer R., (2008), Inkjet printed electrochemical organic electronics, *Synthetic Metals*, vol. 158, no. 13, pp. 556-560.
- Mattia F., Davidson M. W. J., Le Toan T., D'Haese C. M. F., Verhoest N. E. C., Gatti A. M., Borgeaud, M., (2003), A comparison between soil roughness statistics used in surface scattering models derived from mechanical and laser profilers, vol.41, no. 7, pp. 1659-1671.
- Mendeleyev V. Y., (1997), Dependence of measuring errors of rms roughness on stylus tip size for mechanical profilers, *Appl. Opt.*, vol. 36, no. 34, pp. 9005-9009.
- Parashkov R., Becker E., Riedl T., Johannes H.-H., Kowalsky W., (2005), Large Area Electronics Using Printing Methods, *Proceedings of the IEEE*, vol. 93, no. 7, pp. 1321-1329.
- Perelaer J., Patrick J., Smith P. J., Mager D., Soltman D., Volkman S. K., Subramanian V., Korvink J. G., Schubert U. S., (2010), Printed electronics: the challenges involved in printing devices, interconnects, and contacts based on inorganic materials, *J. Mater. Chem.*, vol. 20, pp. 8446-8453.
- Peřinka N., Drřková M., Klřma J., (2009), The possible Applications of Optical Spectroscopy and Photoacoustics for Evaluation of Printed Conductive Thin Layers, *Proceedings of Printing Future Days 2009*, p. 369.
- Peřinka N., Kaplanov M., Drřková M., Tylřov L., Syrov T., (2011), The Photoacoustic Assessment of Printed Conductive Thin Layers, *Proceedings of International Symposium on Organic Electronics 2011*, p. 74.
- Piano M., Serban S., Biddle N., Pittson R., Drago G. A., Hart J.P., (2010), A flow injection system, comprising a biosensor based on a screen-printed carbon electrode containing Meldola's Blue-Reinecke salt coated with glucose dehydrogenase, for the measurement of glucose, *Analytical Biochemistry*, vol. 396, no. 2, pp. 269-274.
- Rosenclwaig A., (1980), *Photoacoustics and Photoacoustic Spectroscopy*, *Chem. Analysis V57*, John Wiley & Sons, New York, 309 p. ISBN 0-471-04495-4.
- Street R. A., Wong W. S., Ready, S. E., Chabynyc M. L., Arias A. C., Limb S., Salleo A., Lujan R., (2006), Jet printing flexible displays, *Materials Today*, vol. 9, no. 4, pp. 32-37.
- Subramanian V., Frechet J. M. J., Chang P. C., Huang D. C., Lee J. B., Molesa S. E., Murphy A. R., Redinger D. R., Volkman S. K., (2005), Progress Toward Development of All-Printed RFID Tags: Materials, Processes, and Devices, *Proceedings of the IEEE*, vol. 93, no. 7, pp. 1330-1338.
- Winther-Jensen B., Krebs F.C., (2006), High-conductivity large-area semi-transparent electrodes for polymer photovoltaics by silk screen printing and vapour-phase deposition, *Solar Energy Materials and Solar Cells*, vol. 90, No. 2, pp. 123-132.
- Woollam J. A., Bungay C., Hilfiker J., Tiwald T., (2003), VUV and IR spectroellipsometric studies of polymer surfaces, *Nuclear Instruments and Methods in Physics Research B: Beam Interactions with Materials and Atoms*, vol. 208, pp. 35-39.

* Paper given as the invited presentation for the awarded contribution of the fourth International student conference *Printing Future Days*, Chemnitz, Germany, November 2011

Next Media - unique cooperation between industry and research*

Helene Juhola

Finnmedia, Lönnrotinkatu 11A,
FI- 00120 Helsinki, Finland
E-mail: helene.juhola@vkl.fi

Abstract

Production and consumption of media is undergoing radical transformation. Digitalisation and exploring usage of broadband and mobile Internet allow rich media content to be distributed to a variety of terminals. Media consumption is becoming more co-creative, participatory and multi-channel, while time and place become increasingly irrelevant. The Finnish Next Media research programme (2010 - 2013) is aimed at tackling these challenges. It is aiming at innovations for new business models, media concepts and technologies providing completely new types of media experience. The development of organisational structures is addressed also. Next Media forms an extensive collaboration structure, an industry-led R&D&I ecosystem for including 8 research participants, 6 different scientific disciplines, 56 companies of which 24 are media companies. The research themes are media business, media eXperience, media usage and media technology and the business oriented work packages eReading, Personal Media Day and Hyperlocal. Next Media is one of TIVIT (Strategic Centre for Science, Technology and Innovation on ICT in Finland) Research Programmes /3/and has been evaluated to be unique in an international comparison. The aim is to continue the work on international level within Horizon 2020.

Keywords: Next Media, TIVIT, media research programme, collaboration, industry and research, media business, media experience, media technology, Horizon 2020

1. Motivation

Production and consumption of media is undergoing radical transformation. The digitalisation of media production, distribution and consumption and the growing penetration of broadband access and mobile Internet allow increasingly rich media content to be distributed to a variety of terminals. Media consumption is becoming more co-creative, participatory and multi-channel, while time and place become increasingly irrelevant. The diversity of terminals and devices in the everyday lives of consumers is increasing and the significance of mobility is emphasised. Media is very much present in the daily life; the average Finn for instance uses media for about eight hours a day.

The Next Media research programme (2010 - 2013) is aimed at tackling these challenges and at producing innovations for new business models, concepts and technologies to help people in their everyday lives, to generate and support interaction, and to provide completely new types of media experience and last but not least to develop organisational structures [1].

2. Background

Next Media is supported by the entire media industry. Businesses joined forces in 2008 and 2009 to create a branch oriented strategy for the media sector. Process resulting to the strategy outlining called "Media sector as a winner" was coordinated by Finnmedia [2]. Simultaneously with this business oriented strategy process businesses and research organisations in the media sector started to draft a strategic research agenda - the Media SRA - and prepare a research programme. This took place within TIVIT which is one of Finland's Strategic Centres for Science, Technology and Innovation (SHOKs) [3]. SHOKs are non-profit private companies owned by industry and research. TIVIT is focusing on ICT and especially ICT-based digital services. The core activity is to run industry driven innovation programmes. TIVIT's role is not only to bring together and systematize research and development, but also to ensure that the results of research are understood, applied and adopted as part of companies' business practice faster than ever before.

3. Objectives

Next Media aims at transforming the media experience on digital platforms to profitable business. This main objective can be divided into four parts:

1. To reform the media business environment by breaking down the conceptual boundaries of media content and changing the way content is created, adapted, distributed, shared and consumed;
2. To significantly improve and promote the productivity and co-creation of content and the effectiveness of the sector;
3. To solve the research problems related to future business operations, and to accumulate knowledge capital and expertise across organisational boundaries;
4. To establish a new kind of ecosystem formed by different operators to produce research results and exploit them for successful business ventures.

4. Resources and organisation

Next Media forms an extensive collaboration structure, an R&D&I ecosystem for the media industry. In an international comparison, Next Media has been evaluated to be unique thanks to its diverse consortium and organisation of the programme. The consortium includes representatives from all media formats, and the programme has been structured with an industry-led approach. There are currently no other media-related research programmes that involve as wide a range of industries and participants.

The altogether 8 research participants include all major Finnish media research organisations representing 6 different scientific disciplines from journalism via graphic design to ICT technologies. All the major publishers are represented and the programme is coordinated by Sanoma, the biggest media house in Finland. All the divisions of Sanoma are involved. The total number of participating companies is 56 of which 24 are media companies. Advertisers, media agencies, ICT providers, bookstores, libraries and other players of the value chain are represented, too. Half of the participating companies are SMEs. The total budget in 2012 is 10 million Euros. All partners are investing their workforce in the programme.

SCRUM methodology is used in the implementation of the common programme plans [4]. All workpackages organise from 4 to 5 result seminars annually, where both the research partners and the companies present their achievements, plans and corrective actions for the next 3 months period. In addition from two to three programme level seminars will be organised. This assures continuous information and knowledge exchange.

Publishers need new tools and enabling technologies in their service development in order to fulfill versatile needs of users and customers. This gives ICT providers and other partners an opportunity to create new technological solution for international market.

5. Programme structure

Next Media consists of three work packages which all have several companies participating with a common business goal with a time span of 3-5 years. The tasks in the work packages have been divided into three groups, each reflecting the content of one of the three research themes.

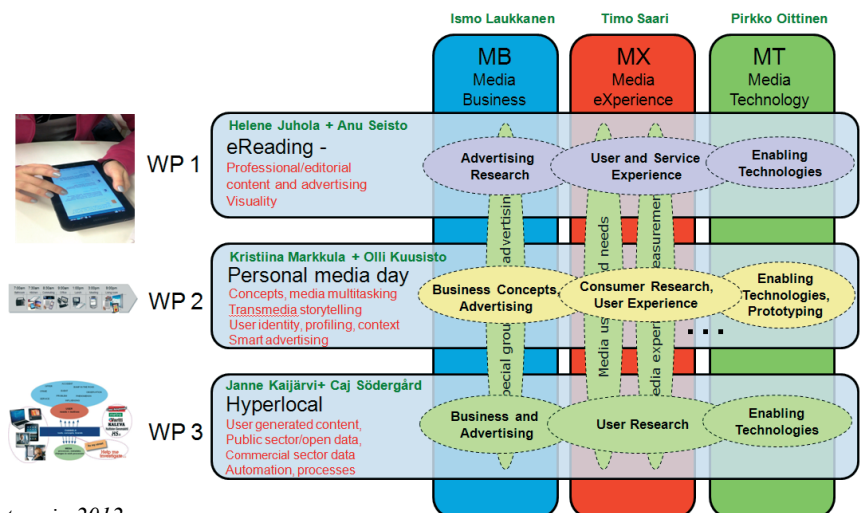


Figure 1: Next Media programme structure in 2012

The three work packages are:

- WP1: eReading
- WP2: Personal Media Day
- WP3: Hyperlocal

The three research themes are:

- Media Business
- Media eXperience
- Media Technology

6. Focuses of the workpackages

6.1 eReading

Business oriented research:

Key question is how to make chargeable editorial content a profitable business in new platforms. The objective is to create a content- and consumer-oriented ways for distributing charged newspaper, magazine and book content on new platforms. New advertising and value creation models, users' media and service experience, knowledge and solutions for brand-aware cross-platform publishing and the development of content management and automation in editorial workflows from the planning to the presentation of layouts. The goal is also to influence the standardization in the industry and to ensure migration to global standards.

Generic research:

Media experience (MX) measurement methods integration and predicting media consumption

Integration of the different MX research methods is a vitally important task to get a comprehensive view of user's media experience. This activity has started in 2011 aiming to integrate self-reporting, psychophysiology, eye-tracking, and media ethnography. MX research identifies the key variables of media experience, defines their optimal measurement methodologies and studies how momentary MX variables predict long-term media consumption and media behaviour.

6.2 Personal Media Day

Business oriented research:

What motivates consumers to use media? What kind of different consumer groups can be identified now and in the near future? Who are the lead users? Consumers use different devices and different content at the same time. Where do users concentrate and what does this mean for content providers? How to make more engaging and relevant content for consumers?

Better information of how consumers use media during the day and week is needed in order to build better media services. The central issue is to study the media usage. Companies have studied their consumers but a wider perspective on consumers' media day is needed.

Generic research:

TV tweeting investigates the phenomenon of live tweeting TV shows. How social media is helping old media and could deepen the viewers' relationship with the show.

6.3 Hyperlocal

Business oriented research:

There are lots of possibilities to monetize new kind of local content. A considerable amount of money can also be saved and quality of content can be improved by developing new tools and concepts around hyper-locality.

Open data, machine-made content, mixed reality and incorporation of user generated content are becoming more and more important part of media's future.

Generic research: Affective Facets of Multimedia Content

Understanding and computation of the properties of multimedia content that evoke affective experiences in users is an emerging research area. A long term vision is that the affective intent of the content may become a new affective metadata category with potential to be used as a criterion for instance in browsing, searching, recommendation and sharing systems.

7. Results so far

The most important is that the programme has already been able to reach business results. Several business concept development projects have been started and the participating companies have launched new services. The efficiency and productivity of cooperation between different partners has continuously improved. Completely new partnerships have been created which is very valuable because media sector will not be able to tackle the challenges on its own. What has been emphasized by the companies is that benchmarking and sparring of one's own ideas within the Next Media network has been one of the most valuable assets. In practice it means that Next Media succeeded to bring open innovation thinking to the sector where tradition has based on reactive development from current and yesterday's needs. This was stated also in the report of an international audit that took place in June this year.

Concrete results have been achieved in boosting the eReading business in Finland in all the media genres from almost zero to everyday business that is already profitable for some of the players. The ecosystem and trials utilizing the thinnest eReader in the world for news delivery in Finland and China has been launched and development continues as a business ecosystem project. HTML5 based applications and publishing for multiple platforms has been in the focus almost from the first beginning and is now widely used by almost all the partners. Automation of content workflows and automatic layout of especially magazine content has produced concrete software modules that can be used in the future publishing systems. Automated tools for helping the news editors to find and analyze currently existing very extensive news sources and the automated news generation have been developed and under trialing.

8. Prospects for the future

Next Media programme will be finished at the end of 2013. The next EU Framework Programme called Horizon 2020 will be started at the beginning of 2014 [5]. Our aim is to assure that media sector will be part of the preparation process of Horizon 2020 in order to be able to continue R & D in European scale.

References

- [1] Finnmedia, Making the media sector a winner. Strategies of the Finnish Media Sector. 5.5.2009, Helsinki 32 p. http://www.vkl.fi/files/588/Viestintaalasta_voittaja_-_viestintaalan_toimialastrategia_-_raportti.pdf
- [2] www.nextmedia.fi
- [3] www.tivit.fi
- [4] <http://scrummethodology.com/>
- [5] http://ec.europa.eu/research/horizon2020/index_en.cfm?pg=responses

Next media, personal media day*

Kristiina Markkula

Federation of the Finnish Media Industry
Lönnrotinkatu 11A
FI-00120 Helsinki, Finland
E-mail: kristiina.markkula@vkl.fi

Abstract

The use of traditional media, such as printed newspapers, magazines or TV, depends very much on time and place. The ways people use media are in constant change, and especially now the changes appear to occur at a remarkable speed. New services, devices and possible ways to use different kind of media are born and consumers also expect them.

The results of the research are presented as preliminary only. It is interesting for example how many media titles young lead-users (16-19 years old) and young adults (25-40 years old) mentioned in a qualitative study. The total number of media titles for lead-users was 200 titles average being 66 titles and for young adults the total number was 240 the average being 97 titles. Only one of the most important titles in young adults mind was a traditional media.

According to news media usage study habitual use of news is common mostly among the elderly (news on certain hours) and their news media consumption did not differ depending on the days. Sharing of news is most common face-to-face. Motivation to share news in a group that uses internet and social media much, is to build an online profile as a news consumer and to build one's identity. The practice is especially common on Twitter but is also practiced on Facebook. Multitasking is very common while watching TV. Two thirds use ICT devices while they were watching TV.

Commercial breaks are used for doing something else than watching tv, for example to do something "useful" or just surfing in the net.

Keywords: media usage, consumer research, motivations for media usage, resistance for media usage

1. Introduction

The use of traditional media, such as printed newspapers, magazines or TV, depends very much on time and place. The ways people use media are in constant change, and especially now the changes appear to occur at a remarkable speed. New services, devices and possible ways to use different kind of media are born and consumers also expect them.

With digital media it is possible to engage users during the whole day and week, regardless of where the users are, if the content is relevant. However, it is important to take into account that consumers need different kind of information and services depending of the time of the day, week or year.

In the future consumers will be offered more and more information and services that know the location of the user and that are able to adapt to the needs of the user. Consumers also use different devices and different content simultaneously. It is important to consider which media the user focuses on and what this means from the viewpoint of the content providers. This leads to evaluating how more engaging and relevant content can be created and offered for the consumers.

A good way to find ideas for new and engaging services and content is to study how the consumers spend their day with media. This is, how, where and why media is consumed and which kind of new media concepts and services could fill the "empty spots" or hidden needs of consumers. What motivates consumers to use media? What kind of different consumer groups can be identified now and in the near future? Who are the lead users? These are some of the research questions that have been brought up in the Personal Media Day (PMD) project that is part of the ongoing Next Media research program in Finland. Better information of how consumers use media during the day and week is needed in order to build better media services. Content providers have studied their consumers but a wider perspective on consumers' media day is needed in order to be able to create something for the future. For this reason the consumer research is at the main focus in the PMD project in 2012.

Three research areas have been chosen for PMD as follows:

- Business concepts and advertising
- Consumer research and user experience
- Enabling technologies and prototyping

Business objectives of PMD

The goal in PMD is to find new business opportunities to media companies by extending the time scale to services along the whole day. In the digital world the income that the content providers get at the moment consists mainly of relatively small sums. One way to increase the income from digital services is by engaging the consumer to media services that can offer personalized content for different kind of needs during the entire day.

Research objectives

The most important research objectives of PMD are:

- to achieve a clear picture of consumer's media day both from the viewpoint of consumption but also from the viewpoint of participating,
- to develop new concepts and prototypes for innovative media services and features
- to collect and analyze user feedback of new concepts and prototypes
- to create viable business concepts for new media products, services and features

The project has started in 2012 with consumer research and especially with clarifying how and when the consumers use media and what are the motives behind the media usage. In this presentation, the focus is on giving an overview of the consumer research and presenting the first results.

2. Research and methods

PMD started at the beginning of 2012 and the first results from consumer research were available just before the summer. In addition to the consumer studies, there are also studies in which advertising and user experience is studied. In this presentation, the results of three consumer studies and one advertising study are summarized.

In the PMD consumer and user experience studies, several different research methods have used including (online) media diaries, complementing interviews, observations, surveys, Delphi-panel, Q sorting and sensory ethnography. More detailed descriptions of the methodology will be available with the reports of each individual study.

3. Results

The change in the media consumers' content behaviour

Understanding media consumption is a complex task, including the consideration of the amount of different technologies/platforms the consumer may be using during the day. This consumption is likely to differ depending on the time of the day and week. For example, one is likely to behave differently depending on whether at home or at work, whether travelling or at the office, during the week days or during the weekend.

The general aim of the PMD consumer research is to better understand WHAT media is consumed during different times of the day, during different times of the week, HOW it is consumed and WHY it is consumed (motivation, preferences). Understanding the drivers and inhibitors of media consumption is an ever increasing trend. This requires a more in-depth understanding of media consumption and proactive stance in designing and managing offerings. This viewpoint has been taken in the first study "Daily media usage".

In the following studies, two especially pertinent topics emerge from the field of media consumption, namely understanding the social dimension of media consumption and understanding consumer resistance to adopt new services.

Daily media usage

The key findings of this study are based on a division of the results according to the age and gender of the respondents. The consumers were divided into three groups based on their age: youngsters (<27 years), workers (27-43) and young elderly (>43). Even though most of the people in the young elderly group were also in working age, in this group people are not considered to be "digital natives". The results focus especially on consuming different content on a computer and in print during different week days and different times of day.

Young elderly consume on average the most time on media in different forms. In the workers group there is a peak in media usage in the middle of the week, whereas the youngsters spend on average most time on media in the end of the week. As could be expected, the youngsters spend significantly more time on the computer than the other age groups and the consumption of traditional media (print, radio, TV) increases with age. In the young elderly group, computer use is fairly steady during the day while in the workers group there is a peak in computer consumption during daytime. The youngsters' computer use is distinguished by a linear growth throughout the day. Print media is consumed more during mornings and evenings in the workers and young elderly groups, indicating that print media is especially consumed at home. However, among youngsters print products are especially consumed at daytime. In this group part of the print products may consist of school books or other studying materials.

Overall, age affects largely the consumed, and preferred, media. While older generations prefer traditional media (TV, radio, print), youngsters' prefer digital devices and content. Also, a younger age correlates strongly with preference and importance of social media, the importance of social networks, and the role of media mostly for entertainment and relaxation. These correlations hold true for both genders.

On average, based on this study, men appeared to consume more media than women. Women's over all media consumption peaks in the end of the week and men's in the middle of the week. However, in the case of computer media, it is consumed the most in the middle of the week by both genders. In addition, a clear peak on computer use can be picked out during daytime among men. Women consume on average more print during evenings compared to men and men tend to have higher print consumption during mornings.

Key findings from this survey concerning current and future expenditure show that print expenditure grows linearly with age, young elderly spend significantly more money on Apps than the other groups and that young elderly expect their print expenditure to decrease in the future while a slight increase is expected by the other age groups. Expenditure on internet media services and on different media Apps are estimated to increase in the future by all three age groups. Men spend somewhat more money on internet services and significantly more on Apps than women, and both genders expect that spending on these services will increase in the future. Men are also more willing to lower their spending on print compared to women. Furthermore, according to the survey men are more tech savvy, i.e. own more smartphones and iPads. Smartphone penetration is very similar in all age groups, as well as the share of iPad owners (14.5% for all age groups).

Understanding the social dimension of media consumption

The current research on the social dimensions of media consumption has focused on exploring the social practices related to news consumption. It has yielded findings regarding the motivation to follow news, their role as a part of the daily regimen, and the social function of news. Consumers are motivated to follow news by a number of different drivers. First, news is followed to feel being up-to-date as well as to feel as a responsive citizen. On the other hand, following news is also used to fill time and as a way of entertaining and stimulating oneself. Reading news is seen very much as a part of the daily regimen. For example, reading the morning newspaper is associated with breakfast. In addition to this, consumers skim online news during the working day and in the public transportation to stay up-to-date on what's happening. Thus, news constitutes different roles at different times of the day.

Sharing news with others constitutes a substantial reason for following news. It can also be used as a way to build or maintain social relationships. Therefore, following and discussing news can be perceived to function as a platform for social interaction.

Disentangling consumer resistance to media services and formats

The research on consumer resistance has focused on a discursive perspective to resistance. Therefore, the focus has been to problematize the assumptions that resistance draws only from the consumers' inadequate

levels of information or incapacity to understand ones best interest. Three frequently recurring and inter-related themes were identified based on the qualitative data analysis. Whereas media innovations are often-times perceived as helping consumers, the first recurring theme was quite the opposite. Consumers can also perceive new media innovations as a life-complicating burden. These related a lot to the challenges of technology adoption, challenges in actual usage of technology and learning how to use the technology. Additionally, the media innovations were also perceived to carry a risk of enslaving the consumers' life.

Consumers also have a tendency to construct themselves as specific individuals. Resistance also manifests in how consumers construct themselves. This could be seen in the data in the form that consumers constructed themselves as being moral persons that resist adopting media innovations due to being analytical, rational and watchful consumers who are not so easily seduced by the lure of new technologies.

Finally, some consumers talked about themselves as being bad media users as they did not adopt the newest innovations in the media field. This creates an interesting tension between the moral adversary identity and the good media user discourses.

User centric approach to advertising

Internet-TVs, smart phones and tablet devices are becoming more common, which enables new possibilities for TV advertisements. TV ads could be integrated into social media services and the ads could include interactive, targeted and entertaining features with the help of second screen applications. This trend means challenges and opportunities for advertisers, advertising agencies and media companies. Also, consumers' requirements and willingness to use new TV ad concepts should be considered and studied comprehensively.

An on-line survey was carried out in this study, with a total of 2473 respondents (1447 men and 1026 women). The survey was conducted in spring 2012. The respondents were recruited via Sonera customer study unit database, VTT's Owela user study volunteer database and Tampere student news groups.

Nearly three fourth of the respondents watched TV daily. Approximately one fourth of the respondents watched recorded TV shows and Internet video services daily or many times per week. The results showed also that Finnish broadcasting company's YLE Areena video service was as popular as Youtube among the respondents.

Two thirds of the respondents used ICT devices while they watched TV. Over half of the smart phone and tablet device owners utilised their smart mobile devices as they watched TV. Typically they browsed the Internet or used social media services.

Half of the respondents were willing to share their personal information for targeting ads. The main motivation to give information for targeting was avoiding unwanted and irrelevant ads.



1

*Printed electronics
and special printing*

Disturbance factors in an impression gravure printing process for the production of PEM fuel cell electrodes

Frank Siegel¹, Albert Kohl³, Eugen Enns³, Andreas Willert², Wolfgang Deger³, Holger Dziallas³, Reinhard R. Baumann^{1,2}

¹ Chemnitz University of Technology

Straße der Nationen 62, D-09111 Chemnitz, Germany

E-mails: frank.siegel@mb.tu-chemnitz.de; reinhard.baumann@mb.tu-chemnitz.de

² Fraunhofer ENAS, Printed Functionalities

Technologie-Campus 3, D-09126 Chemnitz, Germany

E-mails: andreas.willert@enas.fraunhofer.de; reinhard.baumann@mb.tu-chemnitz.de

³ SolviCore GmbH & Co. KG, Hanau-Wolfgang, Germany

Rodenbacher Chaussee 4, D-63457 Hanau-Wolfgang, Germany

E-mails: albert.kohl@eu.unicore.com; eugen.enns@eu.unicore.com; holger.dziallas@eu.unicore.com; wolfgang.deger@eu.unicore.com

Abstract

Alternative technologies for a fast and sufficient production of carbon based electrodes for polymer electrolyte membrane fuel cells are under research to follow the future demand of fuel cells for different applications. The main drives for this trend are governmental programs for the automotive industry. Printing technology has advantages for the continuous production of active electrodes caused by good patterning possibilities and high efficiency. This publication presents an adapted roll-to-roll gravure printing process. Due to the adaptation of the applied gravure structures disturbance factors are searched to quantify their influence on the production process. The influence of doctor-blade abrasion, nip pressure and ink drying within the gravure cylinder are evaluated with printing tests and following optical analysis according to amount and size of defects (pinholes) and layer thicknesses.

Keywords: gravure printing, layer thickness, layer defects, fuel cell, PEMFC, functional printing, membrane electrode assembly (MEA)

1. Motivation

The increasing energy demand of the triad countries and emerging economies causes a future shortage in fossil energies. Therefore, the search for so called green or alternative solutions to decrease the amount of burned fossil resources is getting momentum. Currently, the automotive industry is running through a tremendous change of the thinking of political institutions and customers. The approach of using electrical power trains for cars demands fast and reliable production processes for electrodes that are used for polymer electrolyte membrane fuel cells (PEMFC) or batteries. For both applications the automotive industry is a driver for process research. To quantify this demand the German Government Program "Elektromobilität" (electric mobility program) should be named exemplary. The aim of this program is to manufacture 1 million cars with electric power trains by 2020 and 6 million cars by 2030 in Germany. This means from 2020 to 2030 there is a need to manufacture 500.000 cars each year driven by batteries and/or fuel cells. Even if only 50 % of the cars have fuel cell power trains the need for a fast and reliable production technology is tremendous. Focusing the challenge of the automotive industry following numbers should be of interest. One single fuel cell driven car will contain between 10 and 20 m² active electrode material (anode and cathode). In this case the fuel cell stack of a car consists of several hundred single cells which are built out of anodes and cathodes. For this reason a fast and reliable production technology is required to satisfy the market demands. In Table 1 a model calculation is shown for a laboratory roll-to-roll gravure printing machine which is considered to run under following ideal conditions:

- 8 hour shift per day
- 365 days/year
- 100 % output - no maculate, no maintenance
- 140 mm web width, 0.093 m² (approximately 3 electrodes) per running meter

Table 1: Gravure printed electrodes - productivity under ideal conditions

Printing speed	6 m/min	18 m/min	36 m/min	60 m/min
R2R lab-printer	0.558 m ² /min	1.674 m ² /min	3.348 m ² /min	5.58 m ² /min
m ² /year electrodes / year	97,761.6 3,153,600	293,284.8 9,460,800	586,569.6 18,921,600	977,616.0 31,536,000
Single cells / year	1,576,800	4,730,400	9,460,800	15,768,000
Cars / year	4,888	14,664	29,328	48,880

This calculation shows, that the throughput of a small roll-to-roll gravure printing machine at a high speed of 60 m/min is able to produce electrodes for around 50.000 cars per year which is one tenth of the claimed amount of cars, which should be equipped with alternative power trains only for Germany. To predict the future development another key number should be presented. In 2010 the German car manufactures have produced more than 12 million cars and utility vehicles worldwide (Unknown, 2011). On this account the fuel cell industry is searching for fast manufacturing procedures for the production and hence electrodes as semi-finished parts. Printing methods - especially gravure printing - are very productive technologies which are able to substitute the state of the art manual labor workflow.

For such a high volume production and expensive material usage the yield of the production line is a key parameter for an application on industrial level. To estimate a yield it is necessary to document and verify critical process parameters which are disturbing a continuous production.

2. Objective of the research

There are different approaches to print the electrodes for fuel cell applications. For a stable and adequate electrochemical reaction sufficient active material is necessary. State of the art catalyst layers contain additional to carbon an average loading between 0.5 and 2 mg / cm² of solid functional material - corresponding in a printed layer thickness of about 5 to 20 μ m. Depending on the solid content of the ink traditional printing processes are able to achieve layer thicknesses of around 1 μ m. For that reason multi-layers should be printed (or deposited with other methods) with around 5 to 10 stacked layers to reach the demanded amount of material and further to achieve a catalyst gradient in the manufactured electrode (Bois et al.; Taylor et al., 2007; Yilmaztürk et al., 2012). Another approach is to utilize modified screens for gravure printing to deposit the needed material within one or only a few impressions. Thus, modified line screens are utilized with highest dip volumes and rough screen structures (Siegel et al., 2011; Siegel et al., 2011). These modifications of the printing form are leading to adjustments and changes of the whole printing process. Specifically, the production process of the electrodes is mainly influenced by process parameters like nip pressure, abrasion of the doctor blades, solvent vaporization during the printing process and the quality of the inking device. Furthermore, the drying of the printed electrodes as a post-treatment step limits the productivity of the printing process caused by long drying times and too less dryer length. All these mentioned disturbance parameters have an impact on the layer quality like amounts and sizes of pinholes and layer characteristics like thickness. The following Figure 1 shows the main influencing factors for the gravure printing process and following drying in general. It is a simplified system view containing input parameters like ink, substrate and gravure cylinder and influencing factors like nip pressure, printing speed, doctoring and web tension.

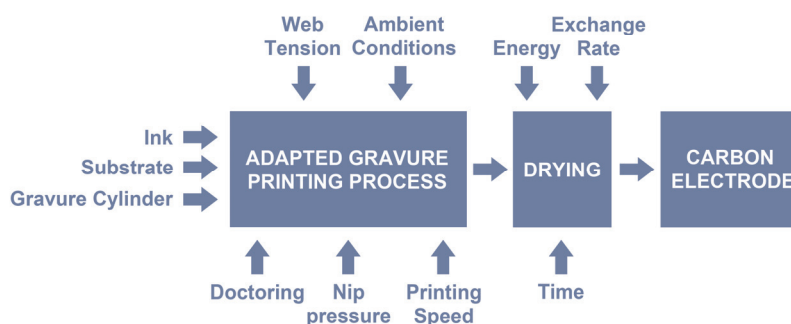


Figure 1: System view on the printing and drying process with influencing/disturbing factors

The present work is mainly focused on obvious parameters which were observed during a lot of previous experiments but not quantified yet. The abrasion of the doctor blade over time and the influence of the nip pressure are varied meanwhile most of the other parameters are fixed like ink, substrate, cylinder, web tension, printing speed and drying procedure. To point out the influence of possible clogging of the printing form the gravure cylinder was inked once and stopped for 2.5 minutes, 5 minutes and 10 minutes in normal ambient conditions before printing. Table 2 is showing the fixed and varied parameter set for the experiments.

Table 2: Overview of fixed and varied parameters for the experiments

Parameter	Status	Value
Ink (Modell-ink)	Fix	Solid Content: 13 wt % Viscosity: shear thinning characteristic, 76.9 mPas (1000 s ⁻¹ , 20 °C)
Substrate	Fix	PET Melinex CW, 100 µm
Web Tension	Fix	Setpoint: 5 kg (49 N)
Web speed	Fix	6 m/min
Dryer Set up	Fix	IR Setpoint: 120 °C Hot air: 100-120 °C
Ambient Conditions	Fix (more or less)	Lab-Temperature: 23 - 26 °C Rel. Humidity: 45 - 50 %
Gravure cylinder	Variable	Open line screen 15 angle 5 L/cm, ca. 160 ml / m ² 7 L/cm, ca. 155 ml / m ²
Doctor blade	Variable	STBR 25x0.2 mm, lamella-tip 0.055 mm/2 (Rolf Mayer GmbH) Lamella abrasion over time
Nip pressure	Variable	Impression roller 80°Shore A Variation of nip pressure

3. Experimental setup

3.1 Ink

All the experiments are done with a carbon black based model-ink with a solid content of 13 wt%, which is made out of the same materials and composition like the fully functional ink but without the added catalyst. Under normal operation conditions, this means at room temperature and relative humidity in the lab, the ink is drying slowly caused by a mixture of the solvents alcohol and water. But it should be noted, that drying processes are occurring exponentially (see Figure 2, right diagram). Experiments have shown that a completely dried film is reached after 60 minutes (for a loading of 0.025 g/cm²) at room temperature of around 20 °C and a relative humidity of 20%. Nevertheless, the mass loss during the first two and half minutes is about 10%.

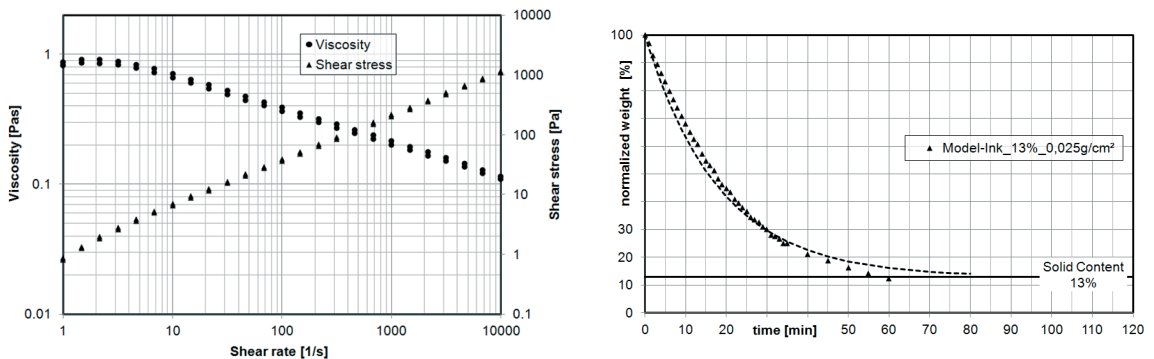


Figure 1: Left: Flowcurve of the applied model-ink; Right: plotted weight loss during drying at room temperature ($T = 20\text{ }^{\circ}\text{C}$, $H_{rel} = 20\%$) for the same model-ink

The rheological characteristics of the ink (Figure 2, left) shows a shear thinning characteristic with a viscosity of 76.9 mPas at 1000 s⁻¹ and a temperature of 20 °C. For fast printing processes this model ink is still to viscous but it has a good printing behavior for slow and mid printing speeds around 6 to 18 m/min.

3.2 Printing machine set up

For printing a roll-to-roll laboratory gravure printing machine from manroland® is applied with a web width of 140 mm and a chamber blade system. The drying section has a length of about 6 m with IR and hot air before turning on the printed side. The machine set up is shown on the left of Figure 3. Two micrographs of the gravure cylinder with a low-resolution line screen of 5 L/cm (top) and 7 L/cm (bottom) is shown on the right of Figure 3.

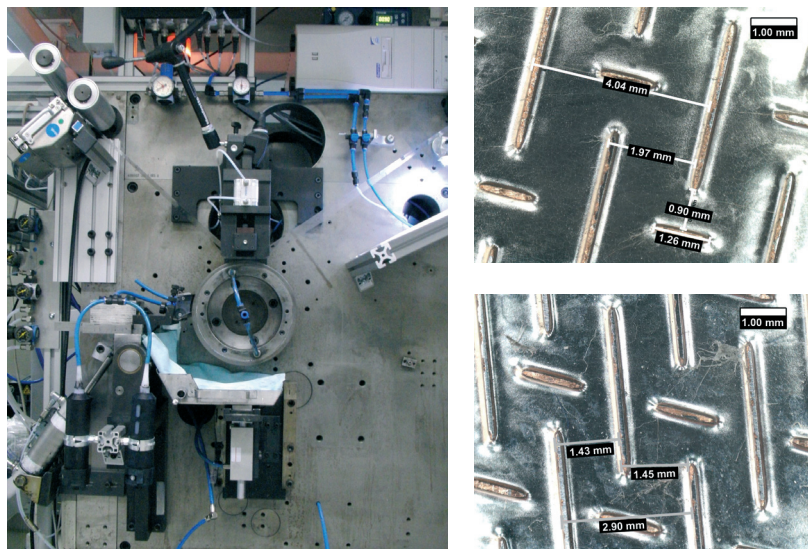


Figure 3: Left: Gravure printing unit with chamber blade system and cartridge system; Right: Top - micrograph of the gravure cylinder with a screen ruling of 5 L/cm and bottom: 7 L/cm

3.3 Analysis set up

The quality of the electrodes is mainly analyzed concerning defects (pinholes) and the layer thicknesses of the electrodes. In Figure 4 the image analysis procedure is shown to count automatically the amount and area of defects within the electrodes. A transmission light web-inspection is applied from Drello V7000 to digitize the electrodes (see image A of Figure 4). Due to the large electrode size of 72x72 mm² and the aim to analyze the whole electrode the resolution is limited to 99 μm / pixel. But to quantify the layer quality in this state of research the resolution is sufficient enough. After digitizing, the electrodes are adjusted with a lens correction procedure and a binarization in Adobe Photoshop® automated batch process (see B). The following analysis is completed with the particle analyze tool in ImageJ, where the amount and area of each defect is detected and documented (see C1 and C2).

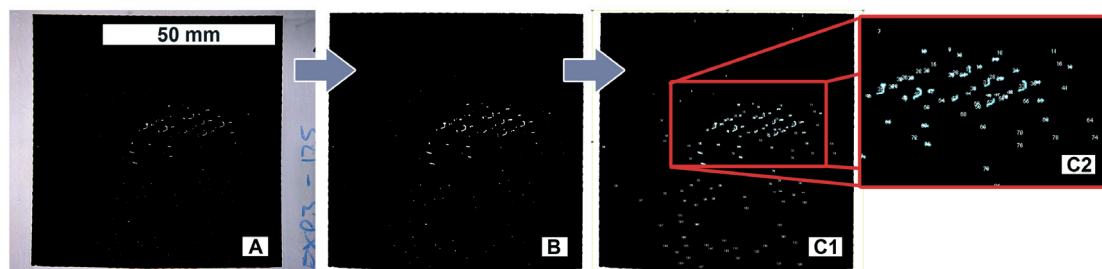


Figure 4: Image analysis procedure: A: Digitalization by Drello V7000 transmission light web-inspection; B: image adjusting with lens correction and threshold in Adobe Photoshop®; C1 and C2: Image analysis applying ImageJ to count the number of defects and their sizes

The layer thickness is measured with a Dektak® 150 stylus profilometer. For each electrode 16 measurements allocated over the whole electrode are done to achieve a homogenous allocation of the measuring points and a mean value.

4. Results

Two major disturbance factors in the printing process were identified. Affected by the rough line screen structures the mechanical load of the doctor blade leads to a significant abrasion result in streaks and splashes on the gravure cylinder and layer defects within the printed electrodes. Furthermore, the nip pressure has a mayor influence, measurable in layer defects. The clogging of the gravure cylinder during a long-term printing test could not be validated, that is why the experiment is changed towards a more considerable experiment with a variation of three waiting times after inking the gravure cylinder and a subsequent printing step.

Taking a closer look to each result, the influence of doctor blade abrasion is the first experiment to mention because of its major influence. Anymore the applied and worn blade was used for the further experiments.

4.1 Doctor blade abrasion

It is well known that new doctor blades should run some impressions to achieve good printing results considering effective wiping. But the lamella-tip should be straight to achieve an even distributed load between blade and gravure cylinder. Caused by the very rough line screen structures which were applied in this printing process the lamella-tip is subjected to high local stress and a constant alternating load.

The results of the abrasion experiments are showing that only a few impressions are necessary to destroy the lamella-tip partly. In Figure 5 the abrasion of the working doctor blade of the chambered inking system is documented. On the left side three scans of the used doctor blade is shown, from top (not used) to bottom (after the second experiment). The red regions are visualizing the distortion of the lamella-tip in the mid region, where the gravure of the electrodes is situated. At right there is a measurement of the size of the lamella on 10 measuring points allocated through the whole doctor blade to illustrate the change of the edge of the lamella-tip. The light grey line shows the original edge of (Lamella - 0) and is set to zero. The mid grey and black line is representing each degree of abrasion after experiment 1 and 2. These measurements are figuring out, that the lamella-tip breaks more than half a millimeter.

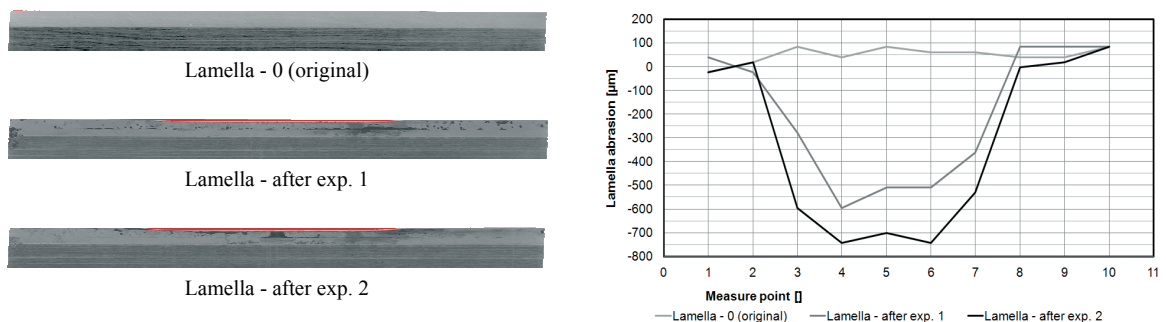


Figure 5: Left: Scans of the damaged lamella-tip before and after experiment 1 and 2; Right: measured lamella-tip abrasion

Due to these results a sufficient doctoring of the printing cylinder is no more guaranteed. In Figure 6 three photographs of the running printing cylinder and the chamber blade system is shown from side (A) and back (B) view as well as a close up of the nip (C2). Some interesting things are observable from these images. Firstly, the lamella is vibrating heavily evoking small droplets of ink spreading on the side wall of the machine and the chamber blade system (see A and B). Secondly, the cylinder is well doctored on the left and right non-printing areas. But in the mid-section of the cylinder where the screens for the electrodes are situated the non-printing areas are covered with streaks of remaining ink (see B).

According to the abrasion of the lamella-tip and the consequently metered ink on the top of the gravure cylinder an ink bulge is occurring at the nip entrance (see the close up of C1 in C2). This ink bulge is leading to a blooming in the non-printing areas but also increasing the layer quality of the printed electrodes. The image analysis of 20 electrodes of 10 impressions for each screen ruling and experiment shows that the amount and size of defects are decreasing significantly with the abrasion of the lamella-tip and an increasing ink bulge at the entrance of the nip. The right diagram of Figure 7 illustrates the amount of defects the left diagram is the according histogram analysis to see the defect size distribution of the printed electrodes. For a fast qualitative recognition of the histogram a bubble diagram was chosen with following rule: the larger the diameter of one of the bubbles, the larger the amount of defects for one defect size.

Considering both diagrams the first experiment with a new doctor blade shows many mid-sized defects (0.04 to 0.5 mm²) and some single large defects with areas above 1 mm². Already the second experiment (compare the image Lamella - after exp. 1 of Figure 5) shows fewer amounts of defects with a similar size distribution, that means a concentration on mid-sized defects. Again, there is an improvement in the layer quality for the third experiment towards less than 40 defects for each analyzed electrodes.

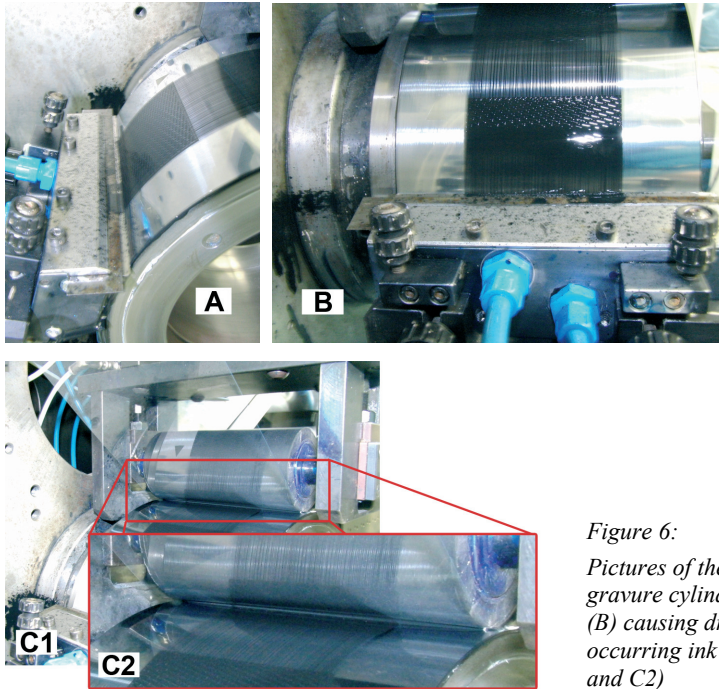


Figure 6: Pictures of the insufficient doctoring of the gravure cylinder from side (A) and back view (B) causing droplets and streaks and an occurring ink bulge at the nip entrance (C1 and C2)

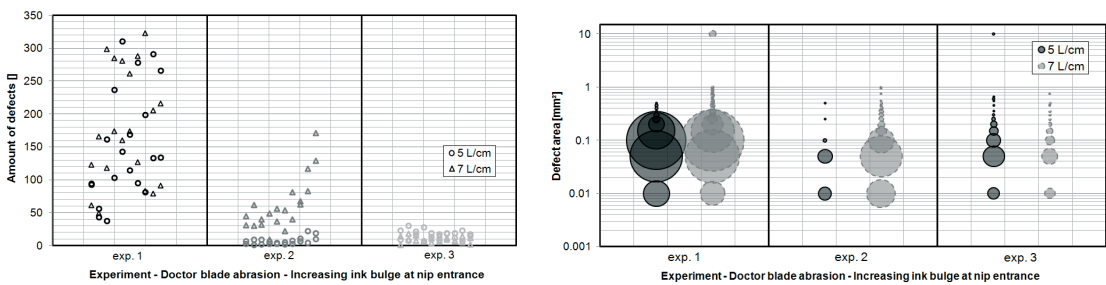


Figure 7: Direct comparison of amount of defects (left diagram) and the histogram of the defect area (right diagram) for the doctor blade abrasion

4.2 Nip pressure

The influence of the nip pressure is remarkably for the amount and size of defects. Figure 8 shows the defect histogram for 5 different nip pressures.

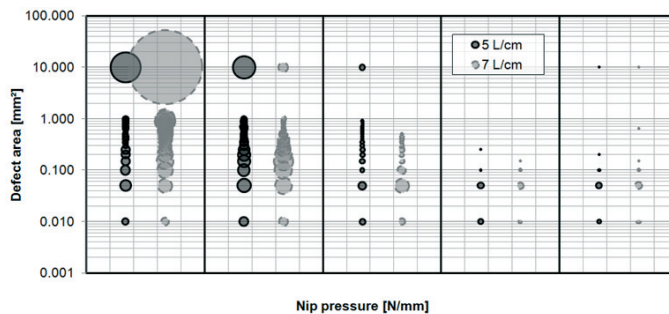


Figure 8: Histogram of the count and area of defects for each nip pressure

From left to right the pressure onto the impression roller is increased and the amount and size of layer defects is decreasing significantly between a calculated nip pressure of 2.47 N/mm and 3.71 N/mm. A stable working area is 4.95 N/mm and 6.19 N/mm with a small amount of defects with sizes below 0.7 mm². The most defects are much smaller with areas around 0.05 mm².

Since the pressure in the nip could have an influence on the geometry of the electrodes, 6 electrodes for each nip pressure are measured in height (printing direction) and width (cross printing direction) on five different positions respectively (Figure 9).

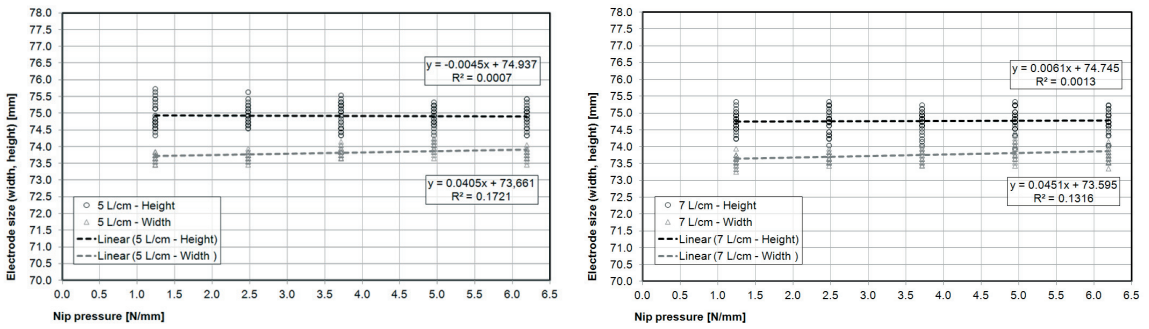


Figure 9: Size of the printed electrodes (in print and cross print direction) depending on the nip pressure

In Figure 9 it is observable that the deviation of the measurements in the height is very high caused by a too slow printing speed and a drain effect.

Due to the high deviation the influence of varying the nip pressure could not be identified surely. The results for the width are achieving a much better deviation and a small increase over the nip pressure but the coefficient of determination R² is very low. It is possible and understandable that the nip pressure has an influence onto the geometry of the printed pattern in microscopic scale. However, for both line screens the size shift very small compared to the electrode size.

The nip pressure has a large influence on the layer quality but only a small effect on the electrode size. Another key value is the electrode thickness which was measured on 16 measuring points of two electrodes for each nip pressure.

Figure 10 compiles the results, beginning with a mean electrode thickness of 4.5 μm for the smallest nip pressure and the highest mean electrode thickness of 5.4 μm for the highest nip pressure. However, a large standard deviation of the single measurements is observable.

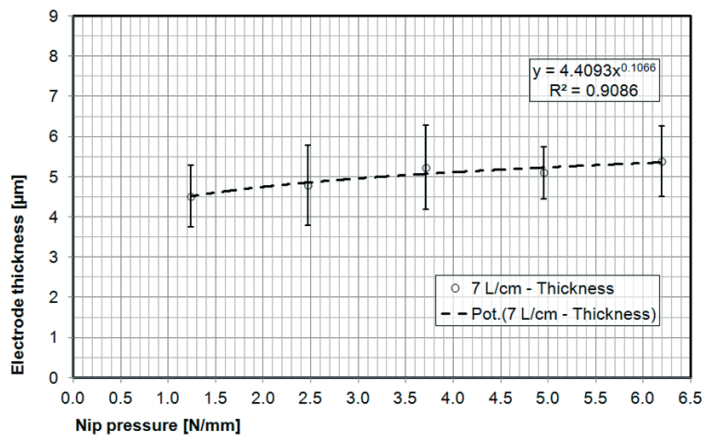


Figure 10: Layer thickness of the printed electrodes - calculated mean and standard deviation with high R²

The high standard deviation of the layer thickness is mainly caused by the leveling characteristics of the applied ink. The topography of the electrodes is showing local thickness differentiations of considerably more than one micron.

4.3 Ink drying within gravure cylinder

Drying processes are occurring also during the printing process itself. The gravure cylinder is inked continuously by a chamber blade system. That is why at a printing speed of 6 m/min a refill and a partly exchange of the ink inside of the gravure cells appears after 7 seconds for each impression. Even if drying processes are progressing exponential significant changes in the model-ink are expectable in a scale of minutes which is mainly influenced by the used solvent. Therefore, the cylinder was inked once and is stopped for 2.5, 5 and 10 minutes. After this waiting time the printing test was done. In Figure 11 the physical appearance of the printing cylinder after each holding time is documented with a photograph.

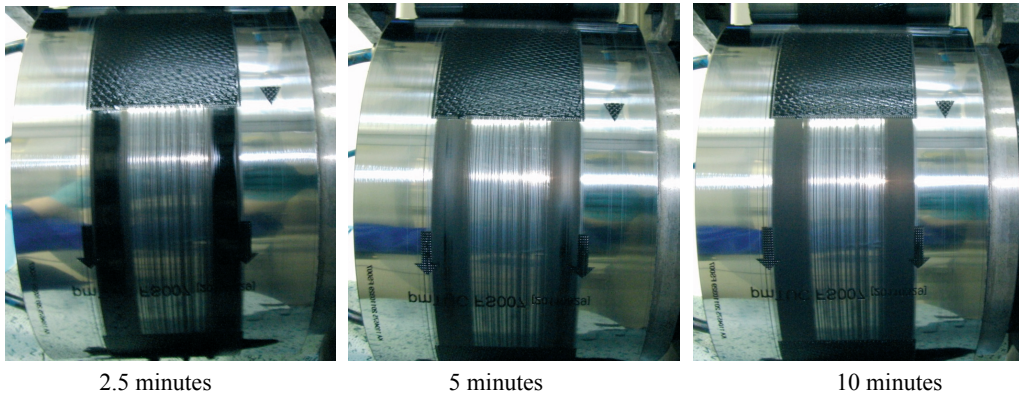


Figure 11: Gravure cylinder after 2.5, 5 and 10 minutes drying

The drying progress is clearly visible especially on the badly doctored parts of the gravure cylinder, where the wet film thickness is low and the open surface is large. To quantify this effect the printed electrodes are analyzed regarding to the amount of defects for 12 following impressions. In Figure 12 the results are plotted.

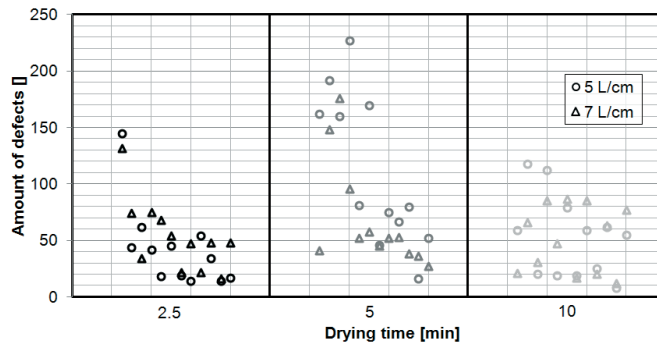


Figure 12: Counted defects for the first 12 impressions after each waiting time (2.5, 5 and 10 minutes)

The amount of defects is decreasing with every new impression of the gravure cylinder. Subsequently, after a certain number of impressions the layer quality is getting better and better caused by new exchange of ink and breaking through dried surfaces. Nevertheless, the achieved layer qualities after 12 impressions are not as good as the best printed electrodes from the nip pressure experiment. Anymore, the influence of the drying time has no distinct influence. The trends of each test are very similar in exception of the 10 minutes drying procedure.

Furthermore, it is generally claimed that a dried gravure cylinder prints less layer thicknesses. On this account the layer thickness was measured again on 16 measuring points of two electrodes for 5 following impressions for 2.5, 5 and 10 minutes. An average mean was calculated for each impression and plotted in Figure 13.

It is surely observable that a drying time of 2.5 minutes does not affect the layer thickness, the same for 5 minutes drying procedure. The decreasing average means of the 5 minutes plot are mainly caused by the high standard deviation. Much more significant are the results of the 10 minutes drying experiment, it is verifiable that the layer thickness is low at the beginning of the printing test. With every new impression and a fresh refilling of the gravure cells the layer thickness increases. After 9 impressions an almost comparable thickness is achieved like in the 2.5 minutes experiment.

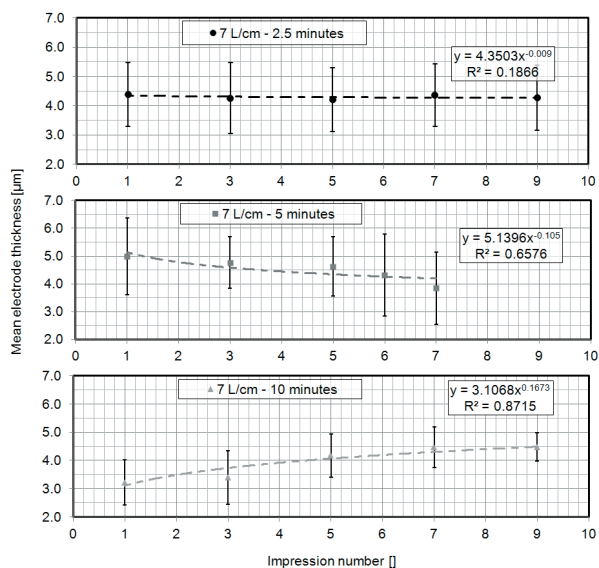


Figure 13:
Layer thickness of the printed electrodes for five impressions depending on the waiting time (2.5, 5 and 10 minutes)

5. Conclusions

The results of the presented experiments are showing that the main disturbance factors for the gravure printing process applying rough line screens are (I) the blade abrasion and (II) the nip pressure. The electrode quality is increasing significant when the lamella-tip is abraded and the tip is metering an ink film at the engraved parts of the printing cylinder. Due to this effect, an ink bulge at the nip entrance is growing caused by the insufficient doctoring. This leads to a flooding of the non-printing areas and an additional filling of the engraved areas. A negative effect of this ink bulge is a blooming effect on the non-printing areas. Further on, the increase of the nip pressure is improving the layer quality concerning amounts and sizes of defects and layer thickness without a heavy adverse effect on the electrode geometry.

Due to the model-ink composition the drying during the printing process has less relevance, nevertheless in case long drying times are occurring the amounts of defects are increasing heavily. The layer thickness will be affected only at large waiting and drying times of more than 5 minutes and is nearly recovered after 9 impressions.

Based on these results a bounding parameter set is found to fix parameters for future research applying rough line screens for printing carbon electrodes and electrochemical active electrodes for PEM fuel cells. Approaches to reduce the influence of the doctor blade abrasion should be investigated like applying more rigid blades or alternative geometries of the blades. Finally, these results are showing that the present state of the printing process requires further research and investigations to build up an industrial production like it is needed for equipping the required amount of automobiles with fuel cells.

References

- Bois, C. et al., (2011): *Characterisation of catalyst layers for fuel cell printed by flexography*, *Proceedings of Advances in Printing and Media Technologies*, 38th International Research Conference iarigai, pp. 237-245.
- Siegel, F. et al., (2011): *Gravure Printing of thick film electrodes for PEM fuel cell production*, *Proceedings of Advances in Printing and Media Technologies*, 38th International Research Conference, iarigai, pp. 247-252.
- Siegel, F. et al., (2011): *Thick Film Gravure Printing Process for the Production of Catalyst Layers*, *Proceedings of Large-area and Organic Printed Electronics Convention, LOPE-C*, 315-317
- Taylor, A. et al., (2007), *Inkjet printing of carbon supported platinum 3-D catalyst layers for use in fuel cells*, *Journal of Power Sources*, No. 171, 101-106.
- Unknown, 2011: *Facts, Figures and Data about the German Automotive Industry, Annual Report 2011*, *Verband der Automobilindustrie*, 13-50, <http://www.vda.de/en/publikationen/jahresberichte> (last request: 11.07.2012).
- Yilmaztürk, A. et al., (2012), *Fabrication and performance of catalyst-coated membranes by layer-by-layer deposition of catalyst onto Nafion for polymer electrolyte membrane fuel cells*, *Journal of Power Sources*, No. 201, 88-94.



Advantage of customized battery integration as self-sustaining and embedded device within print products

*Michael Espig¹, Sebastian Heinz¹, André Stark¹, Frank Siegel¹,
Andreas Willert², Reinhard R. Baumann^{1,2}*

¹ Chemnitz University of Technology

Straße der Nationen 62, D-09111 Chemnitz, Germany

E-mails: michael.espig@mb.tu-chemnitz.de; sebastian.heinz@mb.tu-chemnitz.de;

andre.stark@mb.tu-chemnitz.de; frank.siegel@mb.tu-chemnitz.de;

reinhard.baumann@mb.tu-chemnitz.de

² Fraunhofer ENAS, Printed Functionalities

Technologie-Campus 3, D-09126 Chemnitz, Germany

E-mails: andreas.willert@enas.fraunhofer.de; reinhard.baumann@mb.tu-chemnitz.de

Abstract

In recent years the field of large-area, organic and printed electronics has demonstrated various applications of functional devices. For most of the applications, a reliable supply with electric energy tailored with respect to functional devices and applications is a mandatory, making thin-film battery a challenging area of research. Among a variety of manufacturing concepts printing technologies and their established workflow provide interesting opportunities to fully integrate the battery in a product by customizing its size and shape regarding the device to be driven by that battery. Hence, these printed electronics applications will contribute a new momentum in the packaging market. Out of the common battery concepts for thin-film batteries, the well understood zinc manganese dioxide battery system is very promising due to its simplicity and its environmental sustainability. Therefore it has been chosen to study appropriate fabrication opportunities based on printing technologies. In this paper, we report on the development of a process workflow and the setup of a pilot manufacturing line, taking into account the requirements to adapt the energy content, the size and the shape to the powered product. The overall manufacturing procedure is divided into single process steps, following the traditional printing workflow which is used in the printing and media industries consisting of Prepress, Press and Post Press.

Keywords: printed battery, embedded device, ZnMnO₂

1. Introduction

For graphic communication the most important challenge is to draw the addressee's attention, particularly in the field of packaging, advertising and greeting cards. The quality of information perception attests the success for a printed product. Since the matter of mobile power is ubiquitous, starting from transportation aspects up to light weight portables, the main focus is often set upon power supply and its storage. But instead of using standardized power sources, contacting them conventionally to a device, a new approach is to apply just the appropriate amount of energy, which is necessary due to the consumer load. Based upon a greeting card example this paper describes the customization of a flexible printed battery and an illuminating device towards an assimilated system that highlights the given theme. Therefore the aim was not to attach a giveaway battery sample to a card; furthermore the ambition was to create a fully integrated device that represents the potential of printing technologies. To meet this expectation several approaches have been developed previously to manufacture electronic devices via printing (Liu et al., 2009).

Printing of electrical energy sources as part of the manufacturing process offers numerous advantages. So is printing itself considered to be a technology with extraordinary throughput, reproducibility and the applicability for highly efficient mass production. Therefore the use of this technique opens a high flexibility. This is not only related to the applied substrates, which can be paper, plastic foil or textiles as well. But also shape, size and layout of printed structures are variable likewise and may be exchanged very quickly. Hence the promising connection of printing and manufacturing of electrical energy sources identifies many opportunities to optimize production technology, reduce production costs and avoid special waste. The highest potential is most likely the development of new applications, e.g. smart cards and tags, lab-on-chip systems or even 3D smart objects that are powered with printed energy sources (Willert et al., 2009). The focus of this paper is to distinguish between standard batteries compared to printed smart systems in which an energy source has already been embedded.



Figure 1: Greeting card

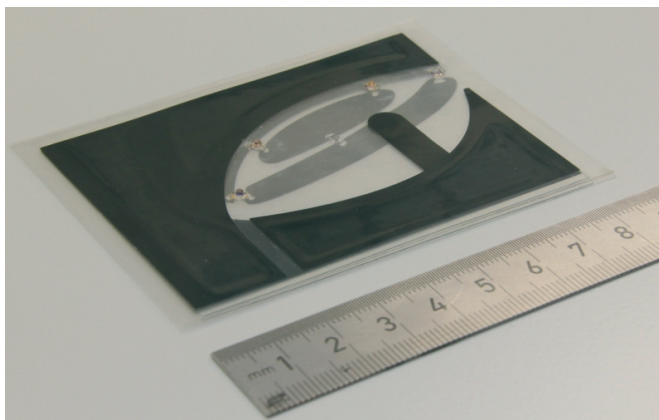


Figure 2: Custom designed battery

2. Manufacturing

Printed batteries are available in the market for a few years e.g. Enfucell, Power Paper, blue spark. They are sold as a single device that has to be connected to external electrical circuitry by the customer. In contrast to this traditional business model we demonstrate a fully integrated product consisting of a shape-adapted battery, a push-button, wiring and commercial SMD LEDs. The devices are sequentially manufactured on the same substrate and finished by lamination; giving an autonomic flexible, 1 mm thin product that can easily be integrated in an otherwise produced greeting card.

To achieve such a printed smart system the central idea was to join the adaptable power source with the card theme by using the LED-array, representing the headlights of the E-Mobile on top. In order to seamlessly fit within the final product an electrical circuitry was conceived for the LED alignment and the eco-friendly battery. Due to the use of printing technologies it was possible to customize its size and shape just to the requirements in terms of voltage and capacity.

In this way the battery is merging into the circuitry, which can be seen in figure 2. The manufacturing of the custom design was accomplished by using semi-automatic, sheet-to-sheet screen-printing and blading processes. Among others this technology enables coating application of highest layer thicknesses and makes the imprint of almost every material with special inks possible (Kipphan, 2000). Thus, the application of screen-printing for processing electrode materials appears to be reasonable. The different battery components were applied layer by layer as shown in the third figure.

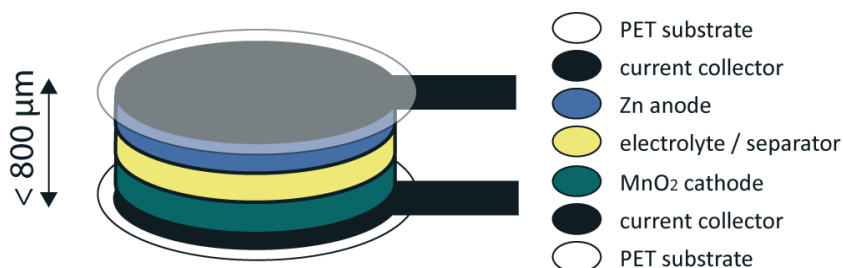


Figure 3: Assembling scheme of printed batteries

As a first step current collectors were printed onto PET foil of $100 \mu\text{m}$ thickness utilizing the table top screen printer Ekra E1-XL. After drying the first coat by the help of a continuous-flow dryer 3D Micromac microDRY, positive and negative electrode materials need to be layered. For the appliance within the staple articles like greeting cards an environmentally friendly chemical system was analyzed. The use of zinc and manganese dioxide prevents the final smart system from being classified as special waste. The chemicals, formulated with high amounts of solid matter, were printed by the same technology and dried afterwards comparably.

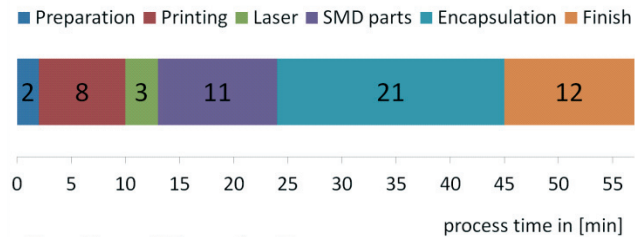
Subsequently all remaining parts for the LED array were added to the so-called half-cells. Consisting of two yellow and green SMD LEDs, respectively, and one resistor all pieces were positioned in the circuitry, applied to electrical contact and glued to the substrate. Afterwards the electrolyte, which is based on zinc chloride, was added to both electrodes (positive and negative) using the doctor blade process. The batteries were sealed afterwards by using a proprietary assembling technique and high performance adhesive tape.

The printed and fully integrated devices are very thin and lightweight, including a battery with nominal voltage of 4.5 V and weighing in total less than 5 g. Since the inlays are printed onto a plastic foil substrate, the advantage of being flexible leads to diverse scopes. Due to its design, the manufacturing of series connections of printed batteries is possible as well. Thus, integer multiples of the nominal voltage of 1.5 V are realizable and batteries up to 6 V were already produced. The nominal capacity of the manufactured zinc manganese batteries is 2 mAh/cm².



Figure 4: Integration of the smart system to a card demonstrator; including a zinc-manganese battery, a push-button and assembled components

smart system card demonstrator



allocation of times for the separate work steps

Σ = 57 min/card

Figure 5: Comparison of major steps in smart card demonstrator manufacturing regarding its time consumption

4. Process development

After approval of function and device integration the next step was to develop a process sequence to raise the quantity number from lab scale up to a volume of 500 demonstrators. Therefore quite some changes had to be taken in account beginning with redesigning the printing screens, split and change the order of intermediate steps like laser treatment up to parallelization of semi-finished parts in printing and assembling.

The constructive steps differ very strong regarding to its up scaling opportunities. To give an impression, the table at the next page shows their allocation among each other, indicating that printing actually takes less than 15% of total time consumption.

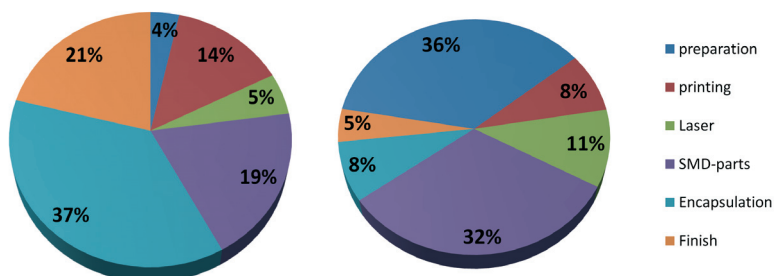


Figure 6: Comparison of major steps in relation to lot size 1 and 500 pieces of manufacturing

With process development and parallelization it was possible to reduce the cycle time down to one fifth of the default value. By integrating in-process inspections to every intermediate manufacturing step the total amount of waste dropped significantly. Furthermore also the battery performance could be stabilized due to a more reproducible assembling process. In this way the durability of the smart system lasts for approximately 1500 flash ups over a two seconds period. The result can be seen in the last figure on the bottom.



Figure 7: Printed smart system as a luminescent greeting card

5. Conclusion

With the help of the investigations on printed primary batteries a basis for the development of smart integrated systems towards a roll-to-roll production has been established. Manufacturing techniques comprising the direct integration of products have been demonstrated with this greeting card. Furthermore, the transformation of all device components into printable elements is one of the next steps in the further development. A connection of printed batteries with consumers, e.g. sensors or RFID applications should be aspired as well or approached in an embedded way.

References

- Kipphan, H.: *Handbuch der Printmedien - Technologien und Produktionsverfahren*, Springer Verlag Berlin, 2000, p. 401 et seq.
- Liu, J., Engquist, I., Berggren, M., Norberg, P., Lögdlund, M., Nordlinder, S., Sawatdee, A., Nilsson, D., Gold, H., Stadlober, B., Haase, A., Kaker, E., König, M., Klink, G., Bock, K., Blaudeck, T., Geyer, U., Baumann, R. R., *Integration of Two Classes of Organic Electronic Devices into One System*, Proceedings of Large-Area, Organic and Polymer Electronics Convention 2009 (LOPE-C 09), Frankfurt/M., June 2009, paper No. 3.8
- Willert, A., Kreutzer, A., Geyer, U., Baumann, R. R., *Lab-manufacturing of batteries for smart systems based on printing technologies*, Smart Systems Integration 2009 - 3rd European Conference & Exhibition on Integration Issues of Miniaturized Systems, March 10-11, 2009, Brussels, Heidelberg: AKA Verlag, 2009, pp. 556 - 559

Investigation in the homogeneity of gravure printed polymer films for printed electronics

Simon Stahl, Hans-Martin Sauer, Edgar Dörsam

University of Technology Darmstadt
Institute of Printing Science and Technology
Magdalenenstrasse 2, D-64289 Darmstadt, Germany

E-mail: stahl@idd.tu-darmstadt.de; doersam@idd.tu-darmstadt.de; sauer@idd.tu-darmstadt.de

Abstract

Functional printing and printed electronics became very important parts of the printing industry over the last years. The requirements on the quality of the functional printed films according to graphical printing can differ. Quality standards for graphic printing consider errors in other orders of magnitude than it is required in printed electronics. For example small deviations in the thickness of the emitting layer in an OLED lead to an inhomogeneous lighting of the device.

In gravure printing several parameters affect the printed film. One of the most important fluid properties is its viscosity. The effect of this parameter with consideration of the parameters of the gravure printing form on the homogeneity of the printed film is a key feature to produce even layers for functional printing.

In this article we present a method to detect the homogeneity of printed polymer layers. The method is applied to a set of test patterns, printed using fluids of different viscosities to investigate their printability. In the first part the fluids and their parameters are presented, followed by a brief description of the printing setup. Subsequently the evaluation method and some results are shown.

Keywords: printed electronics, gravure printing, homogeneity

1. Introduction

Functional printing and printed electronics became very important parts of the printing industry over the last years. The requirements on the quality of the functional printed films according to graphical printing can differ. Quality standards for graphic printing consider errors in other orders of magnitude than it is required in printed electronics. For example small deviations in the thickness of the emitting layer in an OLED lead to an inhomogeneous lighting of the device.

In gravure printing several parameters affect the printed film. One of the most important fluid properties is its viscosity. The effect of this parameter with consideration of the parameters of the gravure printing form on the homogeneity of the printed film is a key feature to produce even layers for functional printing.

In this article we present a method to detect the homogeneity of printed polymer layers. The method is applied to a set of test patterns, printed using fluids of different viscosities to investigate their printability. In the first part the fluids and their parameters are presented, followed by a brief description of the printing setup. Subsequently the evaluation method and some results are shown.

2. Experimental setup

For the investigation in the printability of different fluid viscosities a reference material is needed. The fluid must offer the opportunity to make formulations of different viscosities without a large change in surface tension. This can be essentially achieved using polymer solutions. These materials are relevant for nearly any application in printed electronics. For the present purpose we considered Polystyrene (PS, 197000 g/mol) dissolved in toluene, as we were not interested in electric functionality. Moreover, PS is used as an insulating material for various applications. As PS layers are almost optically transparent we improved the visibility and optical contrast by adding a small-molecule dye, were we restricted to small concentrations of 0.5 wt%. Almost no influence of this additive could be detected on the rheological parameters or the surface tension. The parameters of the formulations are shown in Table 1.

Table 1: Fluid properties of the used polystyrene formulations

Concentration [wt%] Polystyrene 197000g/mol	5%	8%	10%	12%	15%	Toluene, pure
Viscosity at 23°C [mPas]	5 ± 0,25	11 ± 0,5	19 ± 0,5	28 ± 0,5	58 ± 1	0,6 ± 0,05
Surface Tension at 23°C [mN/m]	25 ± 2	25 ± 2	23 ± 2	22 ± 2	20 ± 2	25 ± 2

For the measurement of the fluid parameters standard testing equipment was used. The viscosity values were determined by measurements with a cone-plate-geometry at a Haake MARS rotational rheometer. The measurement specifications were developed earlier (Stahl, 2010). Measurements at different shear rates show that the fluids can be assumed to be Newtonian at these concentrations. For the surface tension measurements a Krüss DSA 100 contact angle measuring system using a pendant drop method was utilized. The density, which is needed for the measurement was obtained by calculation.

The printing substrate were PET sheets (Hostaphan GN4600 by Mitsubishi). This material exhibits a one-side-coating which is intended to improve adhesion. Measurements of the contact angle yield a surface tension of 50 mN/m (polar: 47 mN/m, disperse: 3 mN/m), with water and diiodmethane as polar and non-polar testing fluids. For printing tests we used a RK Printing Proofer (cf. Figure). This is a gravure printing testing machine with a flat gravure plate with a printing size of 220x130mm. Contrast to the usual gravure process the substrate is fixed on a compressible roller, which rolls over the flat printing plate to transfer the fluid. Various studies have already been performed with such printing proofers, using a variety of printing fluids (Bornemann, 2011; Neff, 2009; Reddy, 2011).

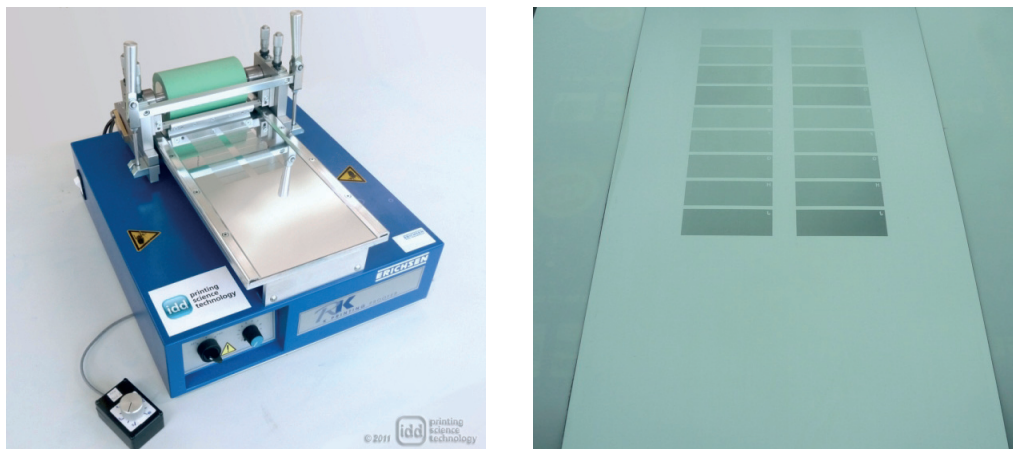


Figure 1: left: RK- Printing Proofer, right: gravure plate with different patterns

The gravure printing plates for the experiments were manufactured by electromechanical engraving, using a Ballard shell. We used screenings of 40 to 140 lines per cm. To achieve different cell volumes the depth of the cells is varied at a constant screen width creating varying halftone patterns.

The cell volume is a very important factor to evaluate the fluid transfer in gravure printing. The measurement of the exact volume is very complex and requires special equipment. Several devices with different methods are currently at the market. The reflecting surface of the chromium and the sharp geometry of the cells takes most of them to their limits. Bornemann, et al give a detailed description of a confocal microscopic measurement process of gravure cells (Borneman, 2012). However, the values of the cell volume used in this paper are calculated using the information given by the manufacturer of the printing plates.

3. Evaluation

One goal of this research is to investigate the effect of different fluid viscosities on the homogeneity of the printed film. In this work, a homogeneous film is defined as a layer with as few variability in the film thickness as possible. Thickness deviations can easily be detected by optical inspection as they correlate with light absorption of the printed layer. The polymer itself does not significantly contribute to light absorption. Rather, this feature is related to the added dye.

For relative absorption measurements we used an Epson V750 Pro scanner, which was controlled by a standard TWAIN scanning software. Images were captured in the through-light mode. For this setup, the detector and the light source are located at opposing positions of the substrate. Image resolution was 6400 dpi with 16-bit grayscale color depth. We thus obtained a luminance value of every pixel in the image. The reproducibility of the scanner measurement is quite good, as the average luminescence values of the pictures differ only about 1 % between several measurement.

In order to get a distinct value of the homogeneity for every picture, the thickness deviations are cumulated over the whole image. To create these "average homogeneity" the standard deviation of all pixels is calculated. One unavoidable difficulty of scanner measurements is the particle contamination of the foils. Because of electrostatic charge accumulation the foils tend to attract dust to their surface. The dust particles appear as black dots on the images, because they are absorbing the light in the through-light measurement almost completely. This leads to significant systematical errors in the measurements. To minimize these effects an automatic error correction is implemented in the image processing. The black dots are detected because their luminance value p_{ij} is considerably lower than the mean value of all pixel in the $(m \times n)$ image-matrix P. The mask-parameter m_{ij} is calculated for every pixel:

$$m_{ij} = \begin{cases} 0 & \text{if } p_{ij} < \bar{p} - \sigma_p * C \\ 1 & \text{else} \end{cases} \quad [1]$$

The threshold for the detection of the dark pixels depends on the standard deviation σ_p and the mean value \bar{p} :

$$\sigma_p = \sqrt{\frac{1}{m * n - 1} \sum_{i=1}^m \sum_{j=1}^n (p_{ij} - \bar{p})^2} \quad \text{and} \quad \sigma_p = \sqrt{\frac{1}{m * n - 1} \sum_{i=1}^m \sum_{j=1}^n (p_{ij} - \bar{p})^2} \quad [2]$$

The constant C has to be defined by creating test-images. The masked pixels are removed from the image-matrix, creating the matrix used for the calculation:

$$a_{ij} = m_{ij} * p_{ij} \quad [3]$$

Then the standard deviation of the corrected matrix A is processed. To get a comparable value for the homogeneity of the picture the coefficient of variation (CV) is used:

$$CV = \frac{\sigma_A}{\bar{a}} \quad [4]$$

In theory the values of CV can range between 0 and 1, with 1 as totally inhomogeneous and 0 as a uniform image. For the analyzed images the spread is between 0.0015 and 0.03. The whole image-processing is computed using Matlab.

4. Results

The input variables of the printing experiment with polystyrene are the parameters of the gravure form (screening R, halftone x) and the fluid viscosity η . As parameter characterizing the printing process we considered the cell screening and volume. The data plots in Figure 2 display the coefficient of variation (CV) as a function of cell volume and screening, for different fluid viscosities.

One observes that the polymer film becomes less homogeneous (CV increases) when polymer solutions with lower viscosity are used. Furthermore the most homogeneous prints are made with the smallest cell volumes. With the highest fluid viscosity (see diagram 5), prints with a relatively good homogeneity can be made even with higher cell volumes in order to get larger film thicknesses. For very low viscous fluids (see diagrams 1, 2) the choice of a high screening with small cell volumes is needed to get homogeneous layers which can be used for printed electronics.

One observes that the polymer film becomes less homogeneous (CV increases) when polymer solutions with lower viscosity are used. Furthermore the most homogeneous prints are made with the smallest cell volumes. With the highest fluid viscosity (see diagram 5), prints with a relatively good homogeneity can be made even with higher cell volumes in order to get larger film thicknesses. For very low viscous fluids (see diagrams 1, 2) the choice of a high screening with small cell volumes is needed to get homogeneous layers which can be used for printed electronics.

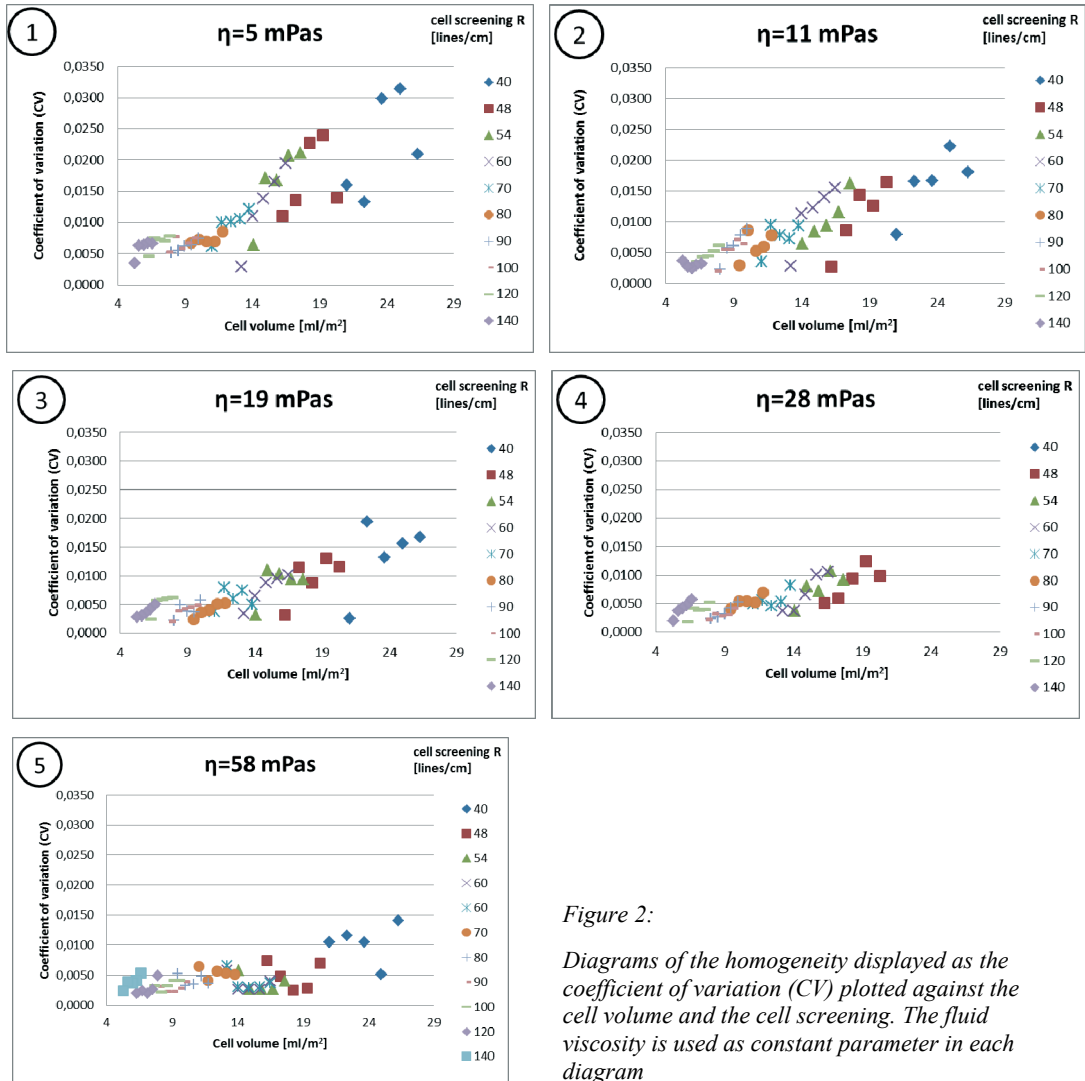


Figure 2:

Diagrams of the homogeneity displayed as the coefficient of variation (CV) plotted against the cell volume and the cell screening. The fluid viscosity is used as constant parameter in each diagram

To demonstrate the visual impression of different CV-values, two pictures of scanned printed films are shown in Figure 3. On the left side, a sample with a low CV-value of 0.005 on the right side a sample with CV=0.012 is displayed. One can obtain, that the size of the errors is scaling with the CV-values, although the cell patterns are identical. In this case, the size of the errors is only depending on the viscosity of the printed ink (left 58 mPas, right 5 mPas).

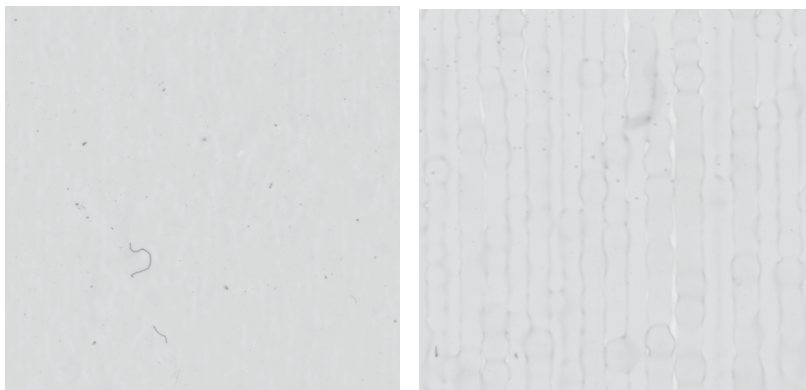


Figure 3: Two pictures obtained by the scanning of printed polymer films. The CV-values of the films are 0.005 (left) and 0.012 (right). One can see, that the dimensions of the thickness deviations scale with the CV-values. Other parameters are: screening of 70 lines/cm, ink viscosity left 58 mPas, right 5 mPas. The size of the pictures is approximately 10x 10 mm

Due to the high amount of testing fields and fluid formulations we were only able to print two samples of each parameter combination and took only one sample for the evaluation. It is clear, that this could lead to errors, due to the limited reproducibility of the printing proofer. So not every value in this evaluation is absolute but the trends shown in the evaluation are considered to be significant.

5. Conclusion and outlook

In this paper we present a method to investigate the homogeneity of gravure printed polymer films. The measurement setup is relatively simple and fast to use. Also, an error correction algorithm has been integrated. In this way we obtained a rapidly working measurement tool to calculate standard thickness deviation of printed samples on even large areas, with extremely nice reproducibility of the results. A parameter which describes the average homogeneity of a printed pattern (coefficient of variation CV) was used to characterize them. The printing tests with fluids of different viscosity indicate a systematic relation between gravure cell patterns, cell volume, and fluid viscosity. The measurements could serve as a reliable data base for checking and verifying theoretical models on layer formation from e.g. Bornemann et al. (2011), and drying of polymer solutions, a problem which is presently under intense investigation in scientific field far beyond printing research.

In our following work, we will apply the measurement setup on other materials. The correlation of fluid parameters to the homogeneity of gravure printed films will be investigated in detail in further work. Additionally it is possible to calibrate the measured thickness variations to obtain an effective thickness value. This can be done using well-defined reference layers which is currently a part of our research.

Acknowledgements

The authors want to thank the German BMBF for the founding of this work. Furthermore we appreciate the very helpful collaboration with Heidelberger Druckmaschinen AG and the Innovation Lab GmbH, Heidelberg.

References

- Bornemann, N., Sauer, H. M., Dörsam, E., (2011), Gravure Printed Ultrathin Layers of Small-Molecule Semiconductors on Glass, *Journal of Imaging Science and Technology* 55(4): 040201-1-040201-8
- Bornemann, N., Guck, T., Bitsch, T., Dörsam E., (2012), Determination of gravure cells using confocal microscopy, accepted to *iarigai* 2012
- Neff, J. E., (2009), Investigation of the effects of process parameters on performance of gravure printed ITO on flexible substrates, Master Thesis, Georgia Institute of Technology
- Reddy, A. S. G., Narakathu, B. B., Atashbara, M. Z., Rebros, M., Rebrosova, E., Joyce, M. K., (2011), Fully Printed Flexible Humidity Sensor, *Procedia Engineering* 25 120 - 123
- Stahl, S., Sauer, H. M., Dörsam, E., (2010), Development of measurement specifications for rheological tests on fluids for printed electronics, *Proceedings of LOPE-C*



Graphene inks for printed electronics

Veronika Husovska¹, Alexandra Pekarovicova¹, Paul D. Fleming III¹, Mike Knox², Hiroyuki Fukushima², Kathy Roberts²

¹Western Michigan University,
Center for Ink and Printability
A-231 Parkview, Kalamazoo, MI 49008, USA
E-mails: v.husovska@wmich.edu; a.pekarovicova@wmich.edu; dan.fleming@wmich.edu

²XG Sciences, Inc.,
815 Terminal Road, Lansing, MI 48906, USA
E-mails: m.knox@xgsciences.com; fukushima@xgsciences.com; k.roberts@xgsciences.com

Abstract

Conductive inks based on graphene nanoplatelets of particle size 5, 15 and 25 μm and surface area 60-300 m^2/g were formulated into inks based on dispersions made with/without commercial acrylic resin. Inks were deposited in dry ink film thicknesses from 2 to 25 micron. Sheet Resistivity of these inks was in the range of 8-60 Ohms/sq. Sheet resistivity was positively correlated with increasing ink film thickness. At specific ink film thickness, further improvement in sheet resistivity can be achieved by introducing a conductive polymer into the ink formulation, such as PEDOT: PSS. Inks can be tailored for specific application, such as electrical or heat conductive inks. It was also found that smaller particle sizes, such as 3-5 micron ones with low surface area resulted in inks with higher carbon particle to resin ratio, leads to lowest electrical resistance.

Keywords: graphene, conductive ink, acrylic resin, sheet resistivity

1. Introduction

Functional inks represent a very large and rapidly growing product family. They may possess electromagnetic, thermal, chemical, and/or optical properties, and can be classified into four categories, i) conductive, ii) semiconductive, iii) dielectric, and iv) resistive inks. The application areas for these functional inks have been expanding rapidly in the recent years, including touch screens (Lee, 2010), printed circuit boards (Lee, 2010), display panels (Zhu, 2011), RFID (Radio Frequency Identification) tags (Kattumenu, 2011), and sensors (Reddy, 2011). The market for printed electronics is predicted to rise from \$1.18 billion in 2007 to over \$300 billion in 2027. Silver-flake based (Kattumenu, 2011), nano-metal particle based (Lim, 2012), conductive polymer based (Hrehorova, 2007), and carbon-based inks (Joshi, 2010) are expected to be used for these applications. The silver-flake based inks often contain high loading (Kattumenu, 2011) of silver-flakes, requiring high cost, difficulty in the printing process, and reduced stability upon storage. Mainly its expensive price has led to interest in the development of solution processable copper inks for printing. New developments in copper ink technology have resulted in the commercial availability of copper inks, which can be applied by different printing processes (Lim, 2012). Other nano-metal particle based inks are becoming popular due to advancement in nano-metal particle production and lower sintering temperatures in print process. The key point in formulating nanometal based inks is to prevent agglomeration by adding stabilizers to form stable inks. The cost of the nanometal based inks is still high. The conductive polymer based inks have limitations due to lower conductivity, typically three orders lower than other conductive inks. Also, it is more difficult to formulate conductive polymers into inks because of their limited solubility, stability, and processability. The concentration of conductive polymer is often low, typically from 1 to 6%, leading to longer drying time and relatively thin films. Recently, nano-size carbon materials have been used in the conductive inks. Two of the major materials used in this area are carbon nanotubes (Mustonen, 2007) and nano-size graphene/graphite (Husovska, 2012). When carbon nanotubes are produced, the resulting material is a mixture of conductive and semi-conductive nanotubes (Lu, 2005), and thus, it is necessary to separate these two types of nanotubes, which increases the cost of the material. Both conductive and semi-conductive nanotubes are used to make conductive and semi-conductive inks, respectively. The semi-conductive inks can be used to make printed transistors and solar cells. Graphene, which is a single sheet of graphite, is actually a semimetal, due to a linear dispersion structure of π - π^* orbital, which leads to an overlapping between the valence and conductance bands at two discrete points, the so-called Dirac points (Neto, 2008; Albanin, 2011). This material has very high carrier mobility (200 000 $\text{cm}^2/\text{V}\cdot\text{s}$), optical transmittance (98%),

stiffness (1TPa), and thermal conductivity (5 000 W/mK), yet the resistivity is limited (370 (Güneş, 2009)-2100 (Li, 2009) ohm/sq). Graphite, which has multi-layer structure of graphene sheets, is a conductor due to parabolic dispersion structure of π - π^* orbital, which creates overlap between valence and conductance bands, forming a semi-metal conductor. Generally, one to two layers of graphene sheets (with thickness less than 1 nm) are considered semimetals while 3 or more layers of sheets (thickness more than 1nm) are considered conductors (Geim, 2011). Graphene inks would have a high potential if sufficient levels of conductivity could be achieved. This would open many applications in the field of printed electronics. Such applications range from the printing of circuits and antennae, or supercapacitors (Kossyrev, 2012) to the production of coated films for EMI (electromagnetic interference) shielding, or touch screen devices (Jacoby, 2011). There is tremendous potential for modification and/or improvement of electrical properties of graphene, and the estimates for potential market size range into the billions of dollars annually. Graphene nanosheets can be efficiently used alone, or as nanocomposites with different materials for modified electrical properties (Yang, 2012), in combination with Ag (Zheng, 2012), or carbon nanotubes (Jang, 2012; Kossyrev, 2012) or PEDOT:PSS (Karuwan, 2012; Sriprachubwong, 2011) for improved conductivity. Graphene nanoplatelets can be anionically-modified in order to enhance conductivity of fully printed batteries (Wei, 2011). Conductive inks based on graphene nanoplatelets are significantly less expensive than inks with metallic fillers such as silver, gold, or silver coated copper. The aim of this work was to assess the resistivity/conductivity of graphene inks made of graphene nanoplatelet conductive particles to come up with the most efficient ink formulations.

2. Materials and methods

Graphene

In this project, stand alone graphene nanoplatelets (short stacks of graphene sheets) made through a proprietary manufacturing process by XG Sciences were used to formulate conductive inks. Graphene nanoplatelets, with several different particle sizes (1, 5, 15 and 25 μm), surface area, and thickness (Table 1) were used in all experiments. Atomic composition of graphene measured by XPS (X-ray photoelectron spectroscopy XPS) showed 95.85% C, 4.10% O, 0% N and 0.05% S.

Ink formulation

Graphene nanoplatelets with particle sizes 5, 15 and 25 μm and thickness around 7 nm were employed to formulate water based fluid dispersions. Individual particle size flakes or their mixes were employed in ink formulations. Also, two types of graphene dispersions were made: resin-free and resin based. Dispersions of the powders were made via 130 Watt Ultrasonic Processor with Thumb Actuated Pulser in order to more thoroughly process dispersions, which were then formulated into inks with or without conventional styrene-acrylic resins using an air mixer @ 6000RPM for 30 minutes. Formulation of resin free dispersions followed resin free ink, and conductive polymer was introduced to the formulation (PEDOT:PSS, Clevios FE by H. C. Starck).

Substrate

127 μm PET film Melinex ST505 (DuPont Teijin Films) and SBS board were used. PET film was washed with acetone, and isopropyl alcohol before printing.

Printing/Deposition

An RK laboratory gravure proofer was used to print inks on the PET substrate. In order to use a 4-point probe Keithly multimeter for resistivity measurement, solid rectangle 7" x 2" was printed. Engraved solid image on a plate had 145 lpi resolution. Another deposition method used was Meyer rod (Fig. 1) drawdowns. Wire wound rod #6 was employed, which deposited a wet ink film thickness 15.4 microns. Dry film thickness was calculated according to the formula:

$$\text{Dry film thickness} = (\text{wet film thickness} * \text{Vol \% solids}) / 100 \quad [1]$$

One or multiple layers of ink were applied to achieve different ink film thicknesses. Oven drying (70°C, five minutes) was employed between multiple draw downs.

Rheology

The rheology of inks was monitored using a Brookfield viscometer with spindle #5. Measurement temperature was 25 °C.

Resistance measurement

Hand held Gardner Bender digital multimeter GDT -311 was used for preliminary measurements of resistance on prints. For accurate measurements, a 4-point probe Keithly Multimeter, OH 2602 System Source Master was used. Voltage and Current of solid prints were acquired, and used as basic data to calculate sheet resistivity according to formula:

$$R/\square = 4.53 (V/I) \quad [2]$$

where: V- voltage (V)
I - current (A)
 \square - square area

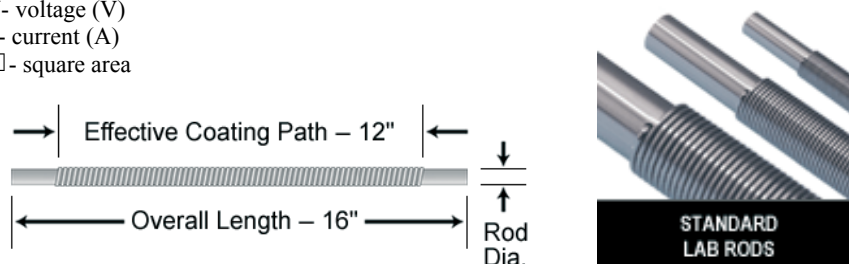


Figure 1: Meyer rod bars for ink application mimic gravure process

Table 1: Graphene particles from XG Sciences used in ink formulations (Anon, 2012)

Surface Area [m ² /g]	Thickness [nm]	Particle size [μm]
60-80	12	5, 15, 25
120-150	6	5, 15, 25
300-750	2	< 2

3. Results and discussion

Ink formulation using conductive carbon flakes had multiple phases. Inks were formulated with multiple carbon grades, containing flakes with aldehydic and acidic functional groups on the edge, causing decreased pH of their dispersions, which dropped to pH 3, and caused problems when blending with acrylic resins for formulations of water based inks. The chemistry and morphology of these particles negatively affected the blending ability, and ultimately contributed to low conductivity of finished inks (data not shown). Work had been done to reduce the amount of carbonyl and carboxyl functional groups, and change the morphology of conductive carbon flakes. Flakes had different particle sizes and they differed also in surface area, which affected their dispersability. Their blends with water were formed in different pH environments (Table 2). Smaller particle size created dispersions close to pH 6, larger particles had pH around 3, most likely due to more acidic functional groups around the edge of the flakes (Table 2). Their slurries with water with higher pH were much easier to handle, but they foamed. Thus, defoamer had to be added, but that was another factor, hindering electrical conductivity. The results demonstrate that the conductive inks would give best electrical properties, when they contain minimum foreign ingredients except the conductive particles. Preliminary experiments with particles of 5-25 micron showed that the ink resistivity is lower when using smaller parti-

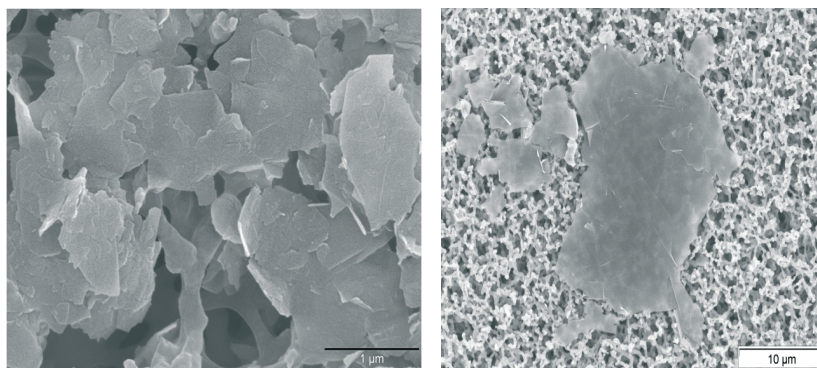


Figure 2: Micrographs of graphene nanoplatelets

cle size of conductive carbon flakes. Scanning electron micrographs of graphene nanoplatelets are shown at the Figure 1. The graphene grades (Table 1) used in this work exhibited improved processability into dispersions. New graphene dispersions were made using an ultrasonic probe, which also contributed to increased solids content of dispersions. It increased from 15% to 30-35%, which allowed for more flexibility in the formulation of final ink. The level of the resin/binder had to be established in order to maintain good adhesion of ink to the substrate and at the same time to conserve maximum electrical conductivity.

Table 2: pH of graphene dispersions

pH of Graphene Dispersions				
Grade	120-5	120-15	60-5	60-15
pH	5.09	3.17	6.17	3.43

Again, it was found that the resin choice and its amount dramatically influences electrical performance of the ink film. Resistivity is proportionally dependent on the pigment to binder ration (Table 3). Higher pigment loading will result in higher conductivity. Resin with lower molecular weight (MW) will result in significantly lower resistance than the ink made out of resin with high molecular weight (Table 3). The carbon flake properties affect viscosity of pigment dispersions. Smaller flakes with lower surface area give dispersions with lower viscosity, which is preferable for ink formulation (Figure 3 and 4). Overall, it was found that the flakes with smaller surface area and smaller particle size are more suitable for formulation of conductive inks, because they give lower viscosity dispersions, and thus higher pigment loading is possible.

Table 3: Comparison of electrical properties of graphene based ink using low and high molecular weight resin

Graphene Grade	Resin	Pigment: Binder	Resistance
120-5	Low MW	1:2.5	38 Ohms/Sq/mil
120-5	High MW	1:2.5	240 Ohms/Sq/mil

Table 4: Sheet resistivity of graphene grades (comparisons at the same graphene loading)

Graphene Grade	Resistivity [Ohm/sq]
60-5	37
60-15	88
120-5	60
120-15	105

Table 5: Viscosity of graphene based dispersions (using the same pigment loading)

Viscosity [cP]					
Speed	20 RPM	40 RPM	60 RPM	80 RPM	100 RPM
Grade					
120-5	266	180	133	113	98
120-15	3500	2300	1900	1848	1350
60-5	180	140	115	97	88
60-15	2500	1390	1290	1010	780

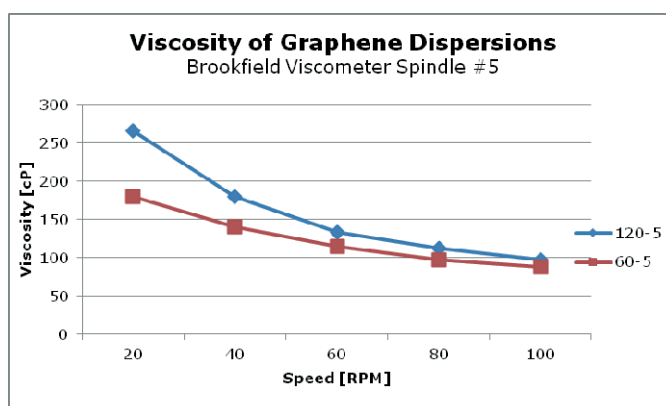


Figure 3: Viscosity of 5 micron graphene dispersions of various surface area (same pigment loading)

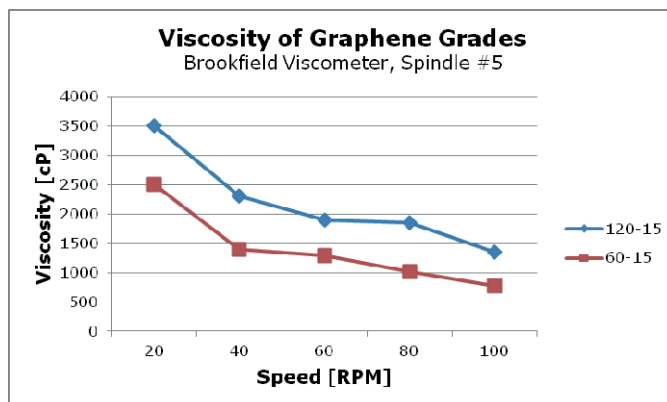


Figure 4: Viscosity of 15 micron graphene dispersions (same pigment loading, different surface area)

In further work, resin free and resin based aqueous dispersions were made. The advantage of resinous dispersions was, that they are compatible with numerous commercially available acrylic letdown resins for water based ink formulations. On the other hand, it was necessary to neutralize water slurries of carbon flakes prior to adding acrylic resins to avoid their precipitation. The example of ink formula based on resin dispersion is given in the Table 6. Different ink film thicknesses were deposited. Sheet resistivity data of these films are given in the Table 7. They were in the range of 10-25 Ohm/square, depending on the thickness of the ink film, which was in the range of 10-25 micron (Table 7). Sheet resistivity decreases with increasing ink film thickness, and thus with the printing process.

Carbon dispersions were also made without acrylic dispersion resins. In that case, a dispersion aid was used instead of resin. The advantage of such a process is that only a small amount of powerful dispersant is used in the process, but on the other hand, such dispersion would have limited compatibility with a few let down resins, e.g. polyester resins. The hyperdispersants exhibited pH around 2, and therefore the pH of carbon flakes slurry in the water did not need to be adjusted, because its pH 6 was compatible with the rest of the formulation. Another advantage of hyperdispersant was that it allowed for higher graphene loading in the dispersion than acrylic resin did. Inks were formulated with conductive polymer PEDOT: PSS, an example of the formulation is given in the Table 8. Similarly, as in the case of resin containing dispersion, increasing ink film thickness decreased sheet resistivity (Table 9). Also, PEDOT: PSS reduced the sheet resistivity, which can be seen from comparison of 10 micron ink films, where PEDOT: PSS/graphene exhibited sheet resistivity of 8 Ohms/square, and the graphene ink with acrylic resin had sheet resistivity of 40 Ohm/square (Tables 7 and 9).

Table 6: Ink formulation based on resin containing dispersion

Ingredient	[%]
DI Water	60.0
Graphene	13.0
Water-Based Resin (@ 36% solids)	18.0
Additive A	8.0
Antifoam	1.0
Total	100

Table 7: Sheet resistivity of ink films based on resin containing dispersion

Thickness of dry film (μm)	10	25
Sheet Resistivity (Ohm/sq)	40	15
M-grade / Water- Based Resin Dispersion		

Table 8: Ink formulation based on resin free dispersion

Ingredient	(%)
DI Water	75
Dispersant	3
Graphene	7.8
Conductive polymer	13.5
Additive	0.7
Total	100

Table 9: Sheet resistivity of printed ink films based on resin free dispersion

Thickness of dry film (μm)	2	4	6	8	10
Sheet Resistivity (Ohm/sq)	85	32	20	13	8
Graphene /Resin Free dispersion/Conductive Polymer					

4. Conclusions

Conductive graphene particles were formulated into water based inks. It was found that the surface area and particle size of the flakes affect the dispersability of the flakes. The particles, which are able to create dispersions with the highest solids content and lowest viscosity, are most preferable, because they allow for higher degree of freedom during final ink formulation. The conductive particle to resin ratio affects the final resistivity. The higher the ratio is, the better is the conductivity. Selection of acrylic resin affects ink conductivity. Low molecular weight resins are more preferable. Also, thicker ink films result in lower sheet resistivity. Sheet resistivity can be significantly lowered by incorporation of commercially available conductive polymers, such as PEDOT: PSS.

References

- Abanin, D. A., Morozov, S. V., Ponomarenko, L. A., Gorbachev, R. V., Mayorov, A. S., Katsnelson, M. I., Watanabe, K., Taniguchi, T., Novoselov, K. S., Levitov, L. S., Geim, A. K., "Giant Nonlocality Near the Dirac Point in Graphene", 1 Science VOL 332 5 April 2011.
- Anon, <http://www.xgsciences.com/products.html>, Accessed 7/13/ 2012
- Geim, A. K., Random Walk to Graphene, International Journal of Modern Physics, B 25 (30), 2011, pp. 4055-4080.
- Güneş, Fethullah, Gang Hee Han, Ki Kang Kim, Eun Sung Kim, Seung Jin Chae, Min Ho Park, Hae-Kyung Jeong, Seong Chu Lim, Young Hee Lee, "Large-area Graphene-based Flexible Transparent Conducting Films", NANO: Brief Reports and Reviews, Vol. 4, No. 2 (2009) 83-90.
- Hrehorova, E., Rebros M., Pekarovicova A., Fleming P.D, Bliznyuk V., "Characterization of Conductive Polymer Inks based on PEDOT: PSS", Presented at the 59th TAGA Annual Technical Conference, Pittsburgh, March 2007.
- Husovska, V., Pekarovicova, A., Knox, M., Fukushima, H., Roberts, K., Conductive Graphite Inks, Presentation given at 2012 Flexible Electronics Displays Conference and Exhibition, February 6-9, 2012, Phoenix, Arizona
- Jacoby, M., Graphene moves toward applications: As composites and inks become commercial products, advanced electronics remain a long way off, Chemical and Engineering News, Vol. 89, 47, 21, 2011, 10-15.
- Jang, W. S., Chae, S. S., Lee, S. J., Song, K. M., Baik, H. K., Improved electrical conductivity of a non-covalently dispersed graphene-carbon nanotube film by chemical p-type doping, Vol. 50, 3, 2012, 943-951
- Joshi, S., "Evaluation of Silver/Graphite Ink Blends for Use in Printed Electronics", Masters Thesis, Western Michigan University, 2010.

- Karuwan, C., Sriprachuabwong, C., Wisitsoraat, A., Phokharatkul, D., Sritongkham, P., Tuantranont, A., Inkjet-printed graphene-poly(3,4-ethylenedioxythiophene):poly(styrene-sulfonate) modified on screen printed carbon electrode for electrochemical sensing of salbutamol, *Sensors and Actuators*, In Press, 2012.
- Kattumenu, R., Rebros, M. Joyce, Hrehorova, E., Fleming, P. D., "Evaluation of Flexographically Printed Conductive Traces on Paper Substrates for RFID Applications", *TAGA J.*, **4**, 219, 2011.
- Kossyrev, P., Carbon black supercapacitors employing thin electrodes, *J. Power Sources*, Vol. 201, 1, 2012, 347-352.
- Lee, Youngbin, Sukang Bae, Houk Jang, Sukjae Jang, Shou-En Zhu, Sung Hyun Sim, Young Il Song, Byung Hee Hong, Jong-Hyun Ahn, "Wafer-scale synthesis and transfer of graphene films", *Nano Lett.*, 2010, 10 (2), pp 490-493.
- Li, Xuesong, Yanwu Zhu, Weiwei Cai, Mark Borysiak, Boyang Han, David Chen, Richard D. Piner, Luigi Colombo, Rodney S. Ruoff, "Transfer of Large-Area Graphene Films for High-Performance Transparent Conductive Electrodes", *Nano Lett.*, Vol. 9, No. 12, 2009.
- Mustonen, Tero Krisztián Kordás, Sami Saukko, Géza Tóth, Jari S. Penttilä, Panu Heliö, Heikki Seppä, Heli Jantunen, "Inkjet printing of transparent and conductive patterns of single-walled carbon nanotubes and PEDOT-PSS composites", *phys. stat. sol. (b)* 244, No. 11, 4336-4340 (2007).
- Neto, A. H. C., Guinea, F., Peres, N. M. R., Novoselov, K. S., Geim, A. K., "The Electronic properties of graphene", *Rev. Mod. Phys.* 81, 109 (2009).
- Lu, Xin and Zhongfang Chen, "Curved Pi-Conjugation, Aromaticity, and the Related Chemistry of Small Fullerenes (<C60) and Single-Walled Carbon Nanotubes", *Chem. Rev.* 2005, 105, 3643-3696
- Lim, S., Inkjet printability of Electronic Materials Important to the Manufacture of Fully Printed OTFTS, Dissertation, Western Michigan University, Kalamazoo, MI, June 2012, 140 pp.
- Reddy, A. S. G., Atashbar, M. Z., Rebros, M., Hrehorova, E., Bazuin, B., Fleming, P. D., Joyce, M., "Printed capacitive based humidity sensors on flexible substrates" *Sensor Letters*, 9, pp. 869-871, (2011).
- Sriprachuabwong, C., Karuwan, C., Phokharatkul, D., Sritongkham, P., Wisitsoraat, A., Tuantranont, A., Enhancing electrochemical sensitivity of screen printed carbon electrode by inkjet printed graphene-PEDOT/PSS Layers, ECTI-CON 2011 - 8th Electrical Engineering/ Electronics, Computer, Telecommunications and Information Technology (ECTI) Association of Thailand Conference 2011 , Article number 5947769, 54-57.
- Wei, D., Andrew, P., Yang, H., Jiang, Y., Li, F., Shan, C., Ruan, W., Han, D., Niu, L., Bower, C., Ryhänen, T., Rouvala, M., Amaratunga, G. A. J., Ivaska, A., Flexible solid state lithium batteries based on graphene inks, *J. Materials Chemistry*, Vol. 21, 26, 2011, 9762-9767
- Yang, X., Zhan, Y., Zhao, R., Liu, X., Effects of graphene nanosheets on the dielectric, mechanical, thermal properties, and rheological behaviors of poly(arylene ether nitriles), *J. Appl. Polymer Sci.*, Vol. 124, 2, 2012, 1723-1730.
- Zheng, L., Zhang, G., Zhang, M., Guo, S., Liu, Z.H., Preparation and capacitance performance of Ag-graphene based nanocomposite, *J. Power Sources*, Vol. 201, 1 2012, 376-381.
- Zhu, Yu, Zhengzong Sun, Zheng Yan, Zhong Jin, James, M. Tour, "Rational Design of Hybrid Graphene Films for High-Performance Transparent Electrodes", *ACS Nano*, 2011, 5 (8), 6472-6479.



Thermochromic composition on the base of cyanine dyes as smart packaging element

Irina Nagornova, Evgeny Bablyuk

Moscow state Ivan Fedorov University of Printing Arts
2A, Pryanishnikova str.
RU-127550 Moscow, Russian Federation
E-mails: irine.nagornova@yandex.ru; bablyuk.evgeny@yandex.ru

Abstract

This study describes the research that has been completed for the application of carbocyanine dyes as time-temperature indicators of smart packaging. The new sensors were developed for polymer packaging film (PET and PP). Film activation is performed by corona discharge. Spectral properties of the thermochromic films were characterized by reflectance spectroscopy. Morphology and chemical structure of thermochromic films were investigated by SEM and XPS.

Keywords: smart packaging, thermochromism, cyanine dyes, PET, PP, corona discharge, SEM, XPS

1. Introduction

The thermochromic systems attract much attention due to their numerous industrial application. The great scientific and practical interest of thermochromic systems is related to protection against falsification of securities, pharmaceutical and food product by latent image development. There are also quality product inspections for correct temperature control, improving food industry process efficiency, especially in the field of food supply chain management.

The improvement of smart packaging for better food safety directly benefits the end-consumer, but there may also be direct benefits for food retailers and suppliers with this technology. Sustainability of food supply chains is a topic of considerable political interest and these acts as another driving force for the development of this technology.

It should be noted here that most of known time-temperature indicators of smart packaging are micro-encapsulated systems. Manufacturing process of such systems is expensive and not efficient. Therefore, the development and study of new time-temperature indicators including thermochromic systems are important today.

In this paper, we applied polymethine (cyanine) dyes as heat-sensitive compounds of thermochrome compositions. This class of dyes has been the object of continuous interest in the scientific community because of their application in the spectral sensitization of photographic emulsion and wideband semiconductors, information recording materials, nonlinear optical materials and as fluorescence indicators in biological systems.

A feature of polymethine dye molecules is ability to self-organize so-called J-aggregates (molecular crystals). The degree of dye crystallinity depends on the environments (temperature, humidity), resulting in shift and change of a spectral curve of a visible absorption band (from wide to narrow, and conversely). Phase transition induces a large bathochromic or hypsochromic shift. This effect forms the basis of the principle using polymethine dyes as the main component of the thermochromic sensor. (Wurthner et al., 2001; Bradley, 2006)

2. Methods

The commercially available fusing polymer films of PET and PP are explored as substrates. Two type of cyanine dyes were used as thermochromic base: pyridine salt of 3,3-di- γ -sulfopropyl-9-ethyl-4,5,4',5'-di-benzotiacarboyaninbetain and three-butylammony salt of 3,3'- di- γ -sulfopropyl-9-ethyl-5-methyl-5'-phenyl-tiacarboyaninbetain.

Spectral reflectance and CIE Lab values were measured by using SpectroEye spectrophotometer (X-Rite), using D65 illuminant and 2° standard observer. Standard deviation of the measurements did not exceed 5 %.

The surface treatment of polymer films was carried out high-frequency (40 kHz) corona discharge at room temperature. The corona current value were changed from 50 to 100 mA. The distance between the grounded plate electrode with samples and the grid was 0.5-0.7 mm.

The surface morphology was investigated using Jeol JSM 7500F field emission SEM. To avoid destruction of samples low acceleration voltages (from 0.3 to 0.8 kV) was applied. Chemical structure of surfaces were analyzed by XPS using Jeol JPS-9200 in monochromatic AlK_{α} excitation source under a base pressure of 5×10^{-8} Pa. The spectra of C1s, O1s (also N1s and S2p for dyes) lines were recorded. All recorded lines were calibrated to the C1s line at 285 eV.

Thermochromic effects were estimated by using origin device at temperature intervals ranging from $-20^{\circ}C$ to $+80^{\circ}C$ with an accuracy of measurement of $\pm 3^{\circ}C$.

Conditions for the formation of containing polymethine dyes layers with necessary optical properties on a surface of initial and modified PET and PP are the subject of the study. Polymethine dyes were purchased from Moscow State University of Fine Chemical Technology and used without further purification. Dyes were dissolved in distilled water, ethanol and polymer solutions (PMMA). The concentration of dyes was of the order of 10^{-3} - 10^{-2} M. The layers were prepared using different method: by spin coating, by ultrasonic-dewetting, by flexographic (using Flexoproof100).

3. Results and discussion

3.1. Thermochromic properties of polymethine dyes layers

We have founded thermally induced color transition of composition on base investigated polymethine dyes. Temperature-caused color changes in investigated layers can easily be seen by naked eye.

Figure 1 shows reflectance spectra of the pyridine salt of 3,3-di- γ -sulfopropyl-9-ethyl-4,5,4',5'-dibenzotiacarbocyaninbetain films on activated by corona discharge and nonactivated PET surface before and after heating.

The pyridine salt of 3,3-di- γ -sulfopropyl-9-ethyl-4,5,4',5'-dibenzotiacarbocyaninbetain films have irreversible contrasting color transition after heating at temperature up to $70^{\circ}C$. The as-deposited film is blue in color associated with a J-band located at 660 nm. After heating, the 660-nm band disappears, but violet color appears, indicating that the J-aggregates are destroyed. The color difference value ΔE is 50.3.

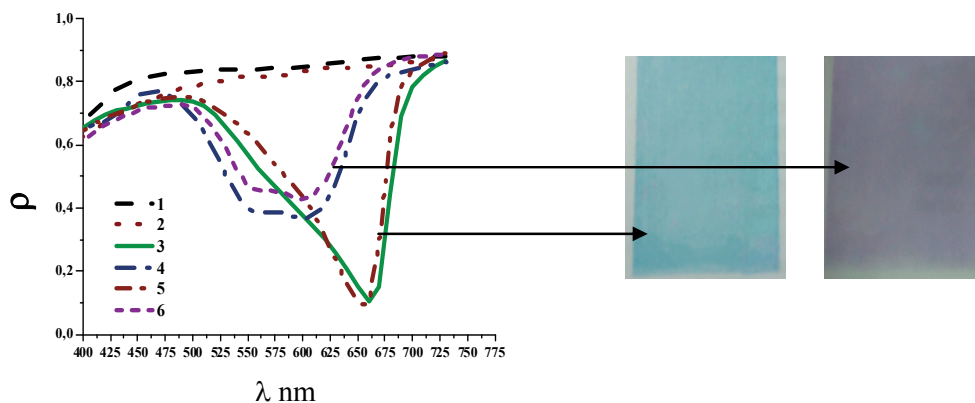


Figure 1:

Reflectance spectra and visual images of the pyridine salt of 3,3-di- γ -sulfopropyl-9-ethyl-4,5,4',5'-dibenzotiacarbocyaninbetain films, where 1 - substrate, 2 - polymer film, 3 - dye layer on initial polymer film at room temperature, 4 - dye layer on initial polymer film after heating, 5 - dye layer on modified polymer film at room temperature, 6 - dye layer on modified polymer film after heating

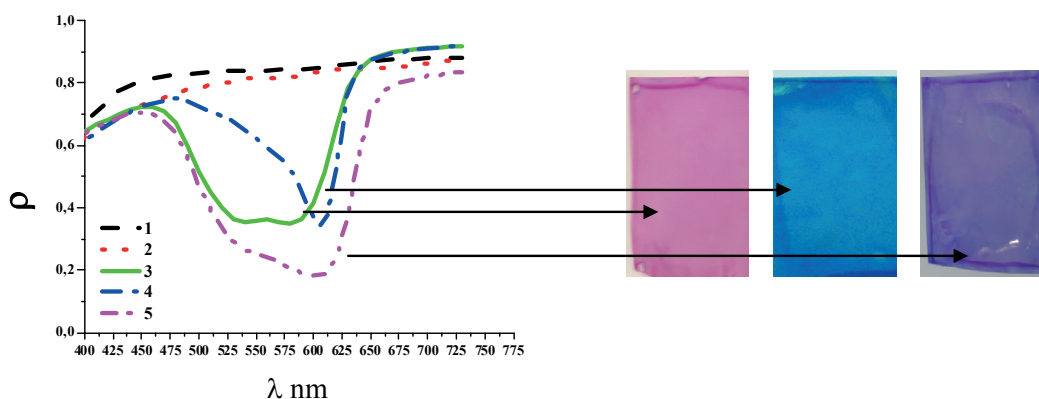


Figure 2:- Reflectance spectra and visual images of the three-butylammonium salt of 3,3'- di- γ -sulfopropyl-9-ethyl -5-methyl-5'-phenylthiacarbocyaninbetain films, where 1 - substrate, 2 - polymer film, 3 - dye layer at room temperature, 4 - dye layer after freezing, 5 - dye layer at above 0 °C

Figure 2 shows reflectance spectra of three-butylammonium salt of 3,3'- di- γ -sulfopropyl-9-ethyl -5-methyl-5'-phenylthiacarbocyaninbetain films. One can observe a reversible double contrasting color transition after coating at $T = 20^{\circ}\text{C}$, followed by samples freezing at the temperature lower $T = -20^{\circ}\text{C}$ and later heating up to 0°C and higher with discoloration after 4-5 cycles. Visual color changes from pink to blue at frozen and to violet at heating. The color difference values ΔE are 62.8 and 39.9, recently. The curve 3 of the graphic (Figure 2) associates with a J-band of second dye type located at 610 nm.

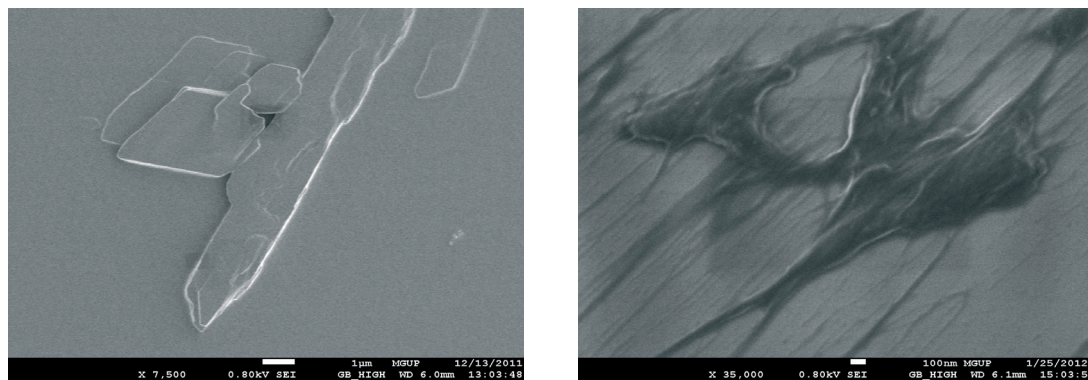


Figure 3: SEM images of pyridine salt of 3,3-di- γ -sulfopropyl-9-ethyl-4,5,4',5'-dibenzothiacarbocyaninbetain films as prepared (left) and after heating (right)

According to SEM and XPS studies, we consider that the change of optical properties based on thermally induced structure transitions dye layers (reorganization to form another crystalline phase of rather than a result of the monomers forming as it describes at literature) and partial destruction of first type dye (figure 3). As we suggested also, the quasithermochromic effect of three-butylammonium salt of 3,3'- di- γ -sulfopropyl-9-ethyl -5-methyl-5'-phenylthiacarbocyaninbetain films is based on the dye recrystallization due to partial dissolution of the surface dye composition with moisture condensed on the surface of the layers during its cooling and subsequent heating. It should be mentioned that if excluded the influence of condensed moisture on the surface layer of thermochromic effect disappears.

It should be note also, the preparation of cyanine dyes films in J-aggregated form usually involves the necessity of additional preparation of the surface by coating on a substrate so-called counter ions (metal ions), polyelectrolyte, amphiphilic substances, etc. (Bradley, 2006; Passier et al., 2010; Miyata et al., 2006).

As it is well known, the polymer film surface from PET and PP is hydrophobic. So, one of a pre-printing process steps is surface modification of polymer films, in most cases, by corona discharge. During the study, the great effect of polymer surface modification by corona discharge on optical and, accordingly, thermochromic properties of compositions based on cyanine dyes has been determined in addition to increasing adhesion to polymer.

3.2. Effect of pre-treatment of polymer films by corona discharge on the optical properties of thermochromic layers

The results of SEM and XPS studies of polymer surface treatment by corona discharge can be summarized as follows:

- the new areas of the inhomogeneous structure (Figure. 4) due to the etching of the amorphous phase and the surface layer of the polymer appears;
- the additional carboxyl and carbonyl groups founds on the surface layer of PET.

Mechanism of corona discharge treatment of a PP is similar.

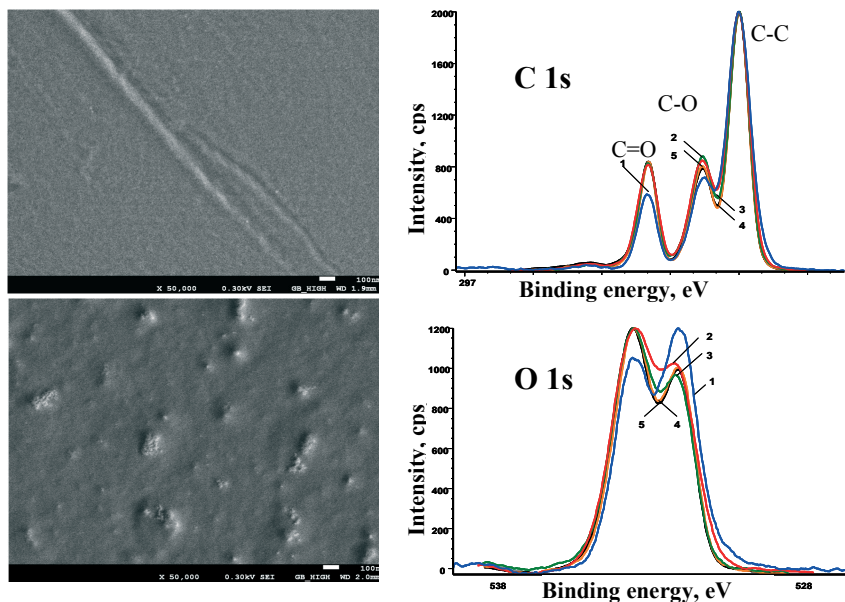


Figure 4: SEM images (left) and XPS-spectrum (right) of a initial (a) and corona modified (b) PET, where (for XPS-spectrum) 1 - initial film, 2 - treated by 50 mA of corona current, 3 - by 70 mA, 4 - by 90 mA, 5 - by 110 mA. Curves are normalized according to the maximum intensity

It has been found, that the formation of J-aggregated forms of dyes occurs only in case of corona discharge modification of a PP surface. In case of PET film the formation of J-aggregated forms occurs anyway. (Figure 5).

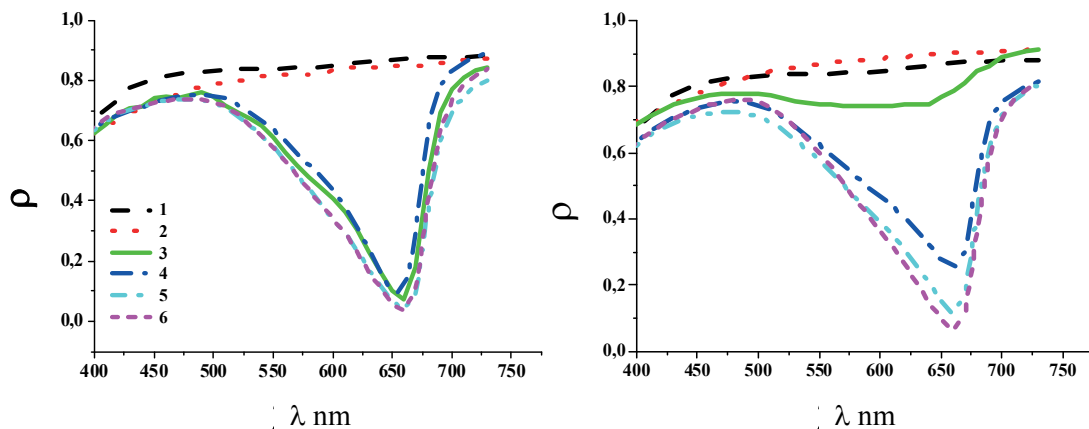


Figure 5:
Reflectance spectra of the pyridine salt of 3,3-di- γ -sulfopropyl-9-ethyl-4,5,4',5'-dibenzotiacarbo-cyaninbetain films on a PET (left) and on a PP (right), where 1 - substrate, 2 - polymer film, 3 - dye layer on initial polymer film, 4 - dye layer on polymer film treated by 50 mA of corona current, 5 - by 70 mA, 6 - by 90 mA, 7- by 110 mA

Our results suggest that the formation mechanism of polymethine dye layers in the J-aggregate form determined appearance of interaction between anions and cations of the dye and the charged surface modified polymer films. Appearance of new structural elements and defects of modified polymer surface probably also leads to the formation of the ordered structure of the dye as new centers of crystallization.

This explanation agrees with observation of morphology changes of layers on base pyridine salt of 3,3-di- γ -sulfopropyl-9-ethyl-4,5,4',5'-dibenzotiacarbo-cyaninbetain after heating (Figure 6).

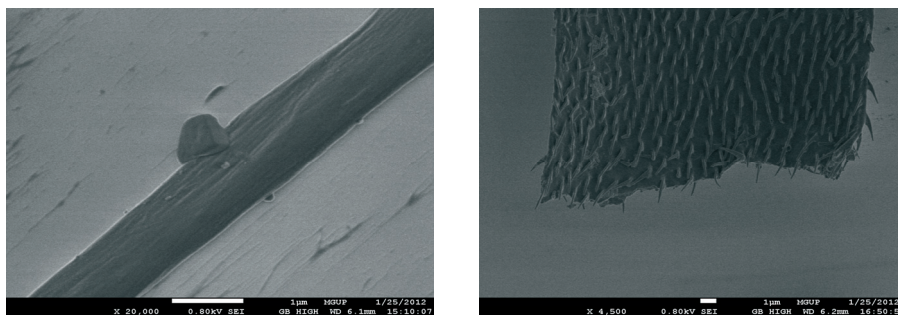


Figure 6: SEM images of a polymethine dye layers on initial (left) and corona modified (right) PET after heating

The role of preparation method of thermochromic composition should be emphasized as the important factor of forming required optical properties of layers. So, most effective methods are flexographic printing and spin coating (Figure 7). Depending on composition, the layer thickness is typically from about 300 (for dye layers, preparing from solution) to 700 nm (for dye layers, containing PMMA), relative viscosity is 16-24 seconds (DIN 53211). The printing speed is 90 m/min, the lineature is 200 lpi.

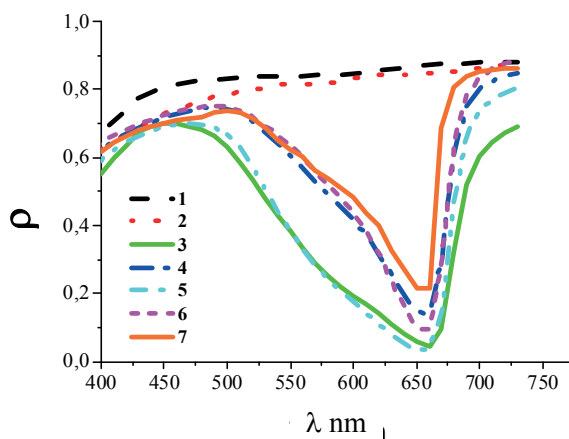


Figure 7:

Reflectance spectra of the pyridine salt of 3,3-di- γ -sulfopropyl-9-ethyl-4,5,4',5'-dibenzotiacarbo-cyaninbetain films on a PET (left) and on a PP (right), where 1 - substrate, 2 - polymer film, 3 - by simple dewetting, 4 - by ultrasonification dewetting (within a short time), 5 - ultrasonification dewetting (within a long time), 6 - by spin coating, 7 - by flexographic printing

3.3 Photochemical stability of thermochromic layers

We have also examined the photochemical stability of thermochromic layers, resistance to moisture and different solvents.

The layers on base of the pyridine salt of 3,3-di- γ -sulfopropyl-9-ethyl-4,5,4',5'-dibenzotiacarbo-cyaninbetain are stable as-prepared (before heating) for about 2 months storage in light and for a year - storage in dark. The after-heated states photochemical stability is lower. The discoloration occurs after 1-2 weeks storage.

The layers on base of three-butylammonium salt of 3,3'- di- γ -sulfopropyl-9-ethyl -5-methyl-5'-phenyltia-carbo-cyaninbetain are stable for 3 months at light storage and was kept during 12 months without direct sunlight exposure.

It is noted that all of the thermochromic layers are slightly resistant to water and relative humidity above 80%, and are resistant to some organic solvents, in particular to acetone.

To increase the photochemical stability of thermochromic layers has been preliminary investigated methods of dye layers protection by me-tallization and growing of dye crystals inside pores of track etched membranes.

Figure 8 shows reflectance spectra of the pyridine salt of 3,3-di- γ -sulfofpropyl-9-ethyl-4,5,4',5'-dibenzotiacarbocyaninbetain - metal (Pt). The metallization was carried out using Jeol FineCoater 1600. The metal film thickness is about 4-5 nm. As it can be seen, the band intensities is reduced, however thermochromic properties is presented. Also, the resistance of dye layers to moisture and different solvents are increased. We suggest that the problem can be solved by using aluminum coating due to a optical properties of aluminum. It should be mentioned that the metal coating layer protects the thermochromic composition from the action of both oxygen and moisture of the air and water.

In addition, the use of such a composition extends the technological possibilities of polymethine dyes application in various industries.

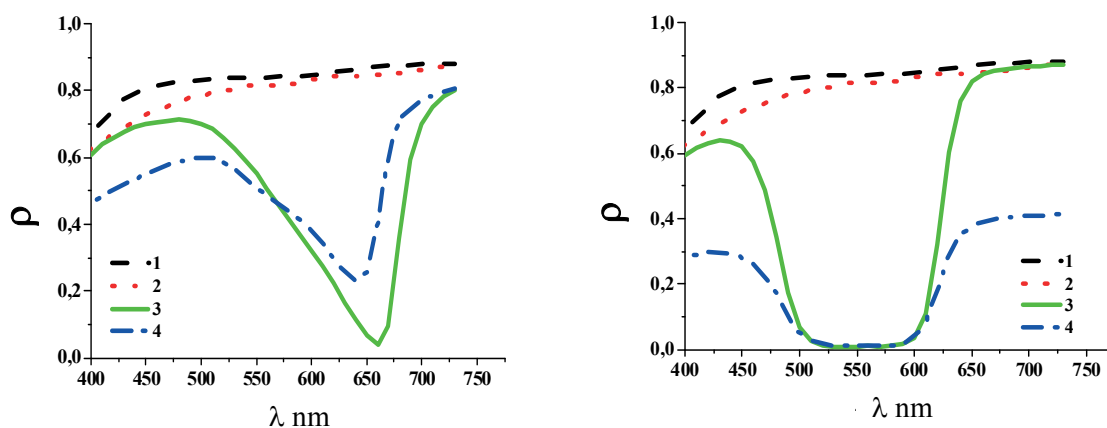


Figure 8: Reflectance spectra of the pyridine salt of 3,3-di- γ -sulfofpropyl-9-ethyl-4,5,4',5'-dibenzotiacarbocyaninbetain films (left) and three-butylammonium salt of 3,3'- di- γ -sulfofpropyl-9-ethyl-5-methyl-5'-phenyltiacarbocyaninbetain films (right) on a PET, where 1 - substrate, 2 - polymer film, 3 - as-prepared, 4 - coating platinum protect layer

Second method of thermochromic effect protecting can be growing of dye crystals inside pores of track etched membranes from dye solution using centrifuge. It was determined that the thermochromic properties of compositions in the pores of track-etched membranes (pore diameter is 1 μ m, Figure 9) retained even after immersion in water.

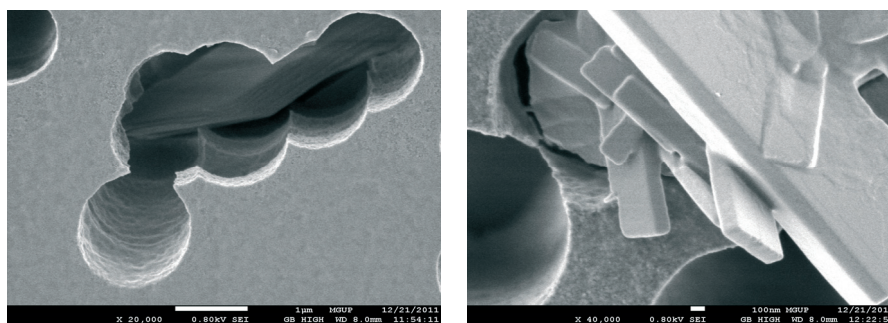


Figure 9: SEM images of a dye crystals inside pores of track etched membranes

4. Conclusions

The main aim of this study is to investigate the development of a thermochrome sensor for smart polymer packaging for possible future commercialisation.

1. We have developed two types of thermochromic systems for different temperature ranges. We have obtained stable thermochromic layers on polymer surface activated by corona discharge.
2. We have investigated morphological and chemical structure changes of thermochromic layer depending on temperature treatment.
3. We have developed methods for protection thermochromic layers during storage.
4. We have demonstrated effectiveness of flexographic for thermochrome layers deposition.

The thermochromic sensors developed in this study could be used for manufacturing of time-temperature indicators of smart polymer packaging.

The advantages of the developed thermochromic compositions are that there is no need to manufacture multicomponent microencapsulated systems, as in traditional technologies of such indicators production, and the possibility of their application to food packaging in-line with packaging equipment.

References

- Bradley, M. S., Highly absorptive thin films for integrated photonic device: thesis ... for degree of Master of Engineering. - Massachusetts : Massachusetts Institute of Technology, 2006
- Miyata, J., Thermally induced J-band narrowing in merocyanine LB films / J. Miyata, S. Morita, Y. F. Miura, M. Sugi // *Colloids and Surfaces A: Physicochem. Eng. Aspects.* - Vol. 284-285. - 2006.
- Passier, R., Thermally controlled preferential molecular aggregation state in a thiocarbocyanine dye / R. Passier, J. P. Ritchie, C. Toro, C. Diaz, A.E. Masunov, K. D. Belfield, F. E. Hernandez // *Journal of Chemical Physics* - Vol. 133 (13), 2010
- Wurthner, F. J, Aggregates: From Serendipitous Discovery to Supramolecular Engineering of Functional Dye Materials / F. Wurthner, T. E. Kaiser, C. R. Saha-Muller // *Angew. Chem. Int. Ed.* - Vol. 50. - 2011.



Hot stamping technology for functional printing

Alexandra Lyashenko, Larisa Salun, Edgar Dörsam

University of Technology Darmstadt
Institute of Printing Science and Technology
Magdalenenstr. 2, D-64289 Darmstadt, Germany
E-mails: lyashenko@idd.tu-darmstadt.de

Abstract

Hot stamping is another printing technique that may be interesting for printed electronics. In this work, we studied the suitability of hot stamping foils with a thin metal layer for printing electronics. For this purpose, several hot stamping foils were examined for processing parameters and reproducibility of the electrical properties.

All stamping experiments were carried out on a Baier GEBA 6 hot stamping machine. We varied the working temperature, the pressure, the stamping time and the position of the work table to determine the process parameters for the hot stamping foils to be analyzed. 16 different hot stamping foils produced by different manufacturers were tested.

After first research and experiments, it was determined that the selected metalized hot stamping foils with the classic layer construction have good conductive properties and they can thus be used to produce functional structures.

Keywords: functional printing, hot stamping foils, hot stamping technology

1. Introduction

The aim of research in the field of printed electronics is to simplify the low-cost mass production of printed electronic components (Hec11). Similar to conventional image printing, functional thin films are printed to produce multilayer structures. Mass printing techniques such as screen, gravure, offset, flexographic printing and inkjet are used to produce functional components (Bla05). Already successfully produced are strain sensors by screen printing (Rau11), OLEDs by inkjet (Bha98) as well as other functional elements.

Depending on the printing process and printed materials, functional layers may differ in their electrical properties (Rot01). Therefore, a central point in the further development of printed electronics is the adaptation and adjustment of the printing process and printed materials. The big challenge in manufacturing functional elements is the reproducibility and reliability of electrical properties of the printed layers. In graphical arts, variations in the layers are relevant, if and only if they can be sensed by the human eye. In contrast, a detailed reproduction of structural features is essential for the functionality of the printed elements in printed electronics (Fue06).

The second challenge is the resolution of the printed functional elements. Feature sizes of less than 20 microns are highly desired in functional printing, e.g. when creating source and drain electrodes in OFETs, but they are difficult to produce by conventional printing processes (Bla05).

Hot stamping is another printing technique that may be interesting for printed electronics. To achieve a metallic surface effect in the printing products, hot stamping foils with a thin aluminum layer (Pra05) are very common. The metal is evaporated on the polyester foil, so that the metal particles form a homogeneous film in the nm range with a certain electrical conductivity. In practice, not only aluminum but also other metals like gold, silver, copper and chromium (Kip01) can be used to increase the quality of the printed products. It seems reasonable to assume that these foils could also be used for printed electronics to increase the performance and reliability of printed functional components and to allow low-cost mass production of electronic parts.

In this work, we studied the suitability of hot stamping foils with a thin metal layer for printing electronics. For this purpose, several hot stamping foils were examined for processing parameters and reproducibility of the electrical properties.

2. Experiments

All stamping experiments were carried out on a Baier GEBA 6 hot stamping machine. We varied the working temperature, the pressure, the stamping time and the position of the work table to determine the process parameters for the hot stamping foils to be analyzed. 16 different hot stamping foils produced by different manufacturers were tested. The process parameters were determined by a series of preliminary tests for each foil. To evaluate the adhesion of the foils on the substrate and the differences of the stamped layers in optical quality due to process parameter variations (Figure 1), we examined the layers using a microscope by the company Leica.

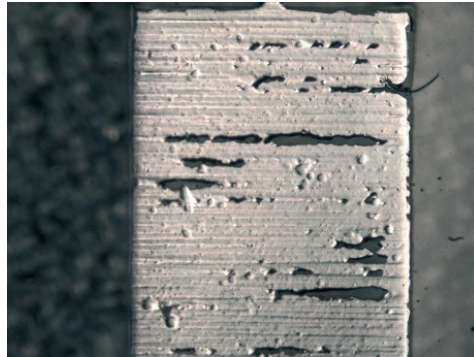


Figure 1: Microscopic survey of the stamped structures (left - poor quality, right - good quality)

As mentioned before, 16 hot stamping foils commonly used in graphical printing were chosen for the experiments. The layer composition of hot stamping foils is shown in Figure 2. The basic layer is a 12-19 microns polyester foil on which an approximately 0.01 micron separation layer is applied. On the separation layer, three layers are deposited: a protective varnish layer of 1.0-1.5 microns in thickness, a 0.02-0.03-micron-thick metal layer and, at last, an adhesive layer (Pra05).

The substrate we used for the experiment series was a 125-micron-thick Hostaphan PET film manufactured by Mitsubishi.

As a hot stamping form, we used a steel stamp. The surface layout was applied by CNC engraving. We controlled the shape, the quality of machining, the width of the elements and the quality of the edges optically using the Leica microscope.

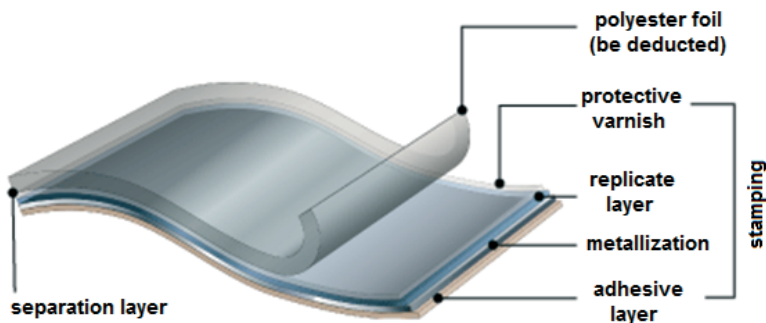


Figure 2: The layer composition of a hot stamping foil (Kur11)

2.1 Plasma etching

Most hot stamping foils have a protective varnish layer to prevent the abrasion of the metal layer. Depending on the application, the protective varnish layer may have different thicknesses (Pra05). To allow the sheet resistance measurements, we removed the protective varnish layer by plasma etching. For this purpose, we employed the semi-automatic low-pressure plasma system Nano by Diener Electronic (Die09; Egi90). The working pressure was 0.4 mbar by power of 100 %, the distance from the upper electrode to the samples was 14 cm and oxygen was used as a gas.

The optimal time of treatment was determined separately for each stamped foil. The samples were treated in the plasma system up to a total exposition time of 120 minutes. We measured the sheet resistance of the samples in 10-minute increments. The optimal duration of plasma treatment was determined by the stability of the measured values of sheet resistance and by measuring the loss of thickness.

2.2 Sheet resistance measurement

The sheet resistance measurements were performed at a four-point measuring station according to the van der Pauw method (Van58).

To perform the measurements, we stamped all 16 examined foils with specific process parameters detected in preliminary experiments. After that, the protective varnish layer as well as the residuals of the separation layer were etched away by plasma.

The sheet resistance was determined on 2×2 cm full solid areas as shown on Figure 3.

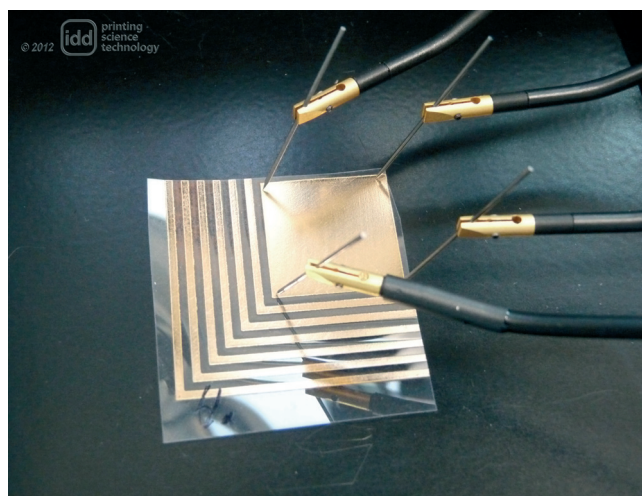


Figure 3: Measurement of a gold sample at the four-point measurement station

2.3 Reproducibility

The reproducibility of the measured sheet resistance values due to the processing was verified by using gold and aluminum foil. A cardboard sheet and a thicker blanket of the company CONTI AIR were used as a base for the stamping machine table in these two cases.

20 samples were stamped to control the reproducibility due to the processing. The process and the plasma treatment parameters remained constant and the measurements of the sheet resistance were performed as ever.

3. Results and discussion

3.1 Sheet resistance measurement and plasma etching

Table 1 shows the sheet resistance values. As described above, the values are measured by the four-point measurement method.

Eight out of 16 classic hot stamping foils (first eight foils in the Table 1) have sheet resistance of less than $1000 \Omega/\square$ and can thus be described as good conductors. Concerning the other six foils, the values are in the $k\Omega/\square$ range (foils number 9 to 14). The remaining two foils (foils number 15 and 16) were considered to be non-conductive.

Apart from the resistance values, the optimal treatment times in the plasma system could be determined for each foil. The time in the system depends on the thickness of the protective and separating layers of the foils. The course of the experiments is already described in subchapter 2.1.

Figure 4 and Figure 5 show the resistance values of two foils in the long run of the plasma etching graphically. For the example, a 24-carat pure gold foil HS 19-3 and a classic hot stamping foil PF100G with a carbon base layer were chosen.

Table 1: Sheet resistance values and optimal plasma treatment times of the examined hot stamping foils

#	Foil name	Optimal treatment time in the plasma system in minutes	Sheet resistance in Ω/\square
1	HS 19-3	70	2,95
2	ALUFIN SH	70	4,73
3	Baier J 615	80	9,45
4	HS 12-110	120	53,77
5	HS 121-110	80	124,40
6	Luxor GTS 355	40	309,97
7	Luxor SH 220	90	316,15
8	ALUFIN SFX	80	413,19
9	Baier J 916	70	1.060,00
10	Luxor SFX 220	80	1.420,00
#	Foil name	Optimal treatment time in the plasma system in minutes	Sheet resistance in Ω/\square
11	6110 LC	70	1.650,00
12	Baier F-3	80	23.160,00
13	HS 45-110	90	28.660,00
14	PF100G	20	38.800,00
15	Baier F-5	90	205.500,00
16	Baier C620	-	>200 M Ω/\square

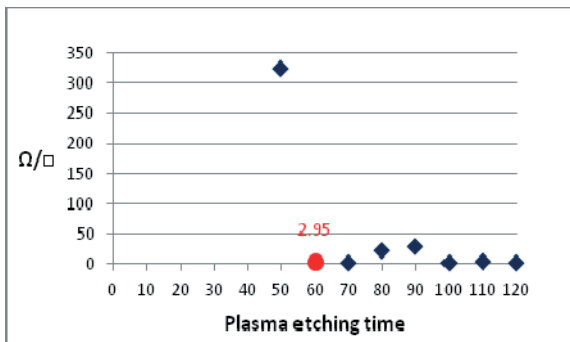


Figure 4: Connection of the plasma etching times and sheet resistance values for the gold stamping foil HS 19-3

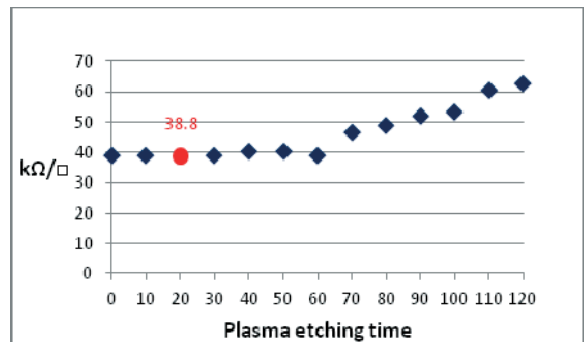


Figure 5: Connection of the plasma etching times and sheet resistance values for the hot stamping foil PF100G

As long as the protective and separation layers were relatively thick, no sheet resistance could be determined for the measured foils. As soon as the additional layers became thinner, the surface resistance was measured in the $M\Omega/\square$ and, in some cases, in the $k\Omega/\square$ range. These values are not shown in Figure 4. However, when the etching lasted too long, the metal layers were partially removed, so that the resistance increased. The duration of plasma treatment, in which the lowest point of the resistance values was achieved in the fastest way, was defined as the optimum treatment time for each foil (highlighted on the diagrams). The tendency for the distribution of values is similar for most of the foils.

A precise removal of the layers could not be determined by using optical technique due to the glossy surfaces of the stamping foils. Since the experimental effort in carrying out the plasma treatment is large, this was done only in 10-minute increments. For a better understanding of the foils, a series of measurements done in smaller increments would be necessary.

3.2 Reproducibility

A 24-carat pure gold foil HS 19-3 and a classic aluminum foil 6110 LC were used for the experiments. Both foils were tested for reproducibility of the sheet resistance values under the same conditions. Figure 6 and Figure 7 show the results graphically.

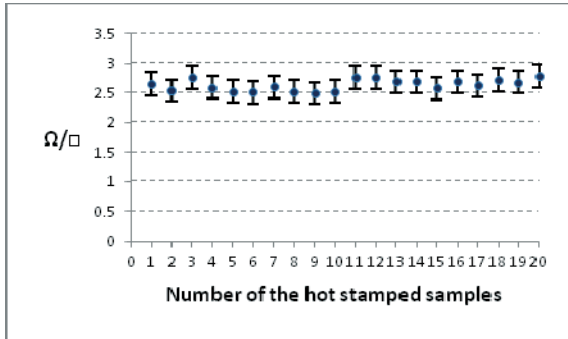


Figure 6: Reproducibility of the sheet resistance values for the 20 samples of the gold stamping foil HS 19-3

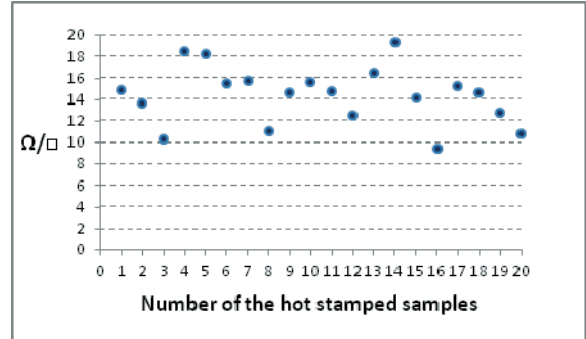


Figure 7: Reproducibility of the sheet resistance values for the 20 samples of the aluminum stamping foil 6110 LC

The sheet resistance measurements on the gold samples (Figure 6) show small variations in the measured values. For this foil, the standard deviation is 0.098 and the average value - 2.64 Ω/\square (full line in Figure 6). The measurements point at good conductive properties of the gold foil which are stable and reproducible. The measurement procedure with the four needles in the four-point measurement was also suitable for the thin gold layers. A measurement of the resistance values repeated after one month showed that the properties of the foil remained stable.

As the aluminum foils were measured, the values fluctuated relatively strongly, which can be seen by the results shown in Figure 7. A possible reason for this could be the diffusion of the adhesive in the metal layer (Bau85). This has the consequence that the metal layer is inhomogeneous and, in some cases, the sharp measuring needles have no connection to each other. In addition, the thin aluminum layers could possibly be pushed through the needles. The oxidation of aluminum, no exact positioning of the measuring needles, a measurement error or deviation of the device may be a reason as well. Error bars for the resistances values of the aluminum foil were not shown, since the error is more than 50%. The standard deviation for the values is 2.69 Ω/\square and the average value is 14.43 Ω/\square (full line in Figure 7).

Despite fluctuations, the good conductivity of the aluminum foils could also be proven. It also remains constant in time. For future measurements, other types of needles should be used for resistance measurements of fine embossed structures. Another type of measurement or a different approach is even possible in this case.

4. Conclusion

After first research and experiments, it was determined that the selected metalized hot stamping foils with the classic layer construction have good conductive properties and they can thus be used to produce functional structures.

It could be shown that various parameters affect the properties and the quality of the embossed structures. Primarily, the method and the accuracy of the layer application in producing the foils are important. The thickness of the vapour-deposited metal layers plays a crucial role as well. In addition, stamping adjustments such as pressure, temperature and stamping time as well as the quality and resolution of the used tools are important.

Eight out of 16 foils that were investigated for their conductivity have sheet resistance less than 1 000 Ω/\square . Regarding the remaining six foils, the sheet resistance was in the $k\Omega/\square$ range. Only two of the studied foils were categorized to be non-conductive. The reproducibility measurements showed that the surface resistance is reproducible and it remains stable for a long time. Therefore, it is possible to use the foils in the field of printed electronics and to produce various components currently permitted by law. The resolution desired in

functional printing is not currently reached by using the conventional method and the tools. However, the method has a high development potential. For further investigation of stamping foils, it is recommended to use more accurate measuring methods which are more suitable for the measurement of thin layers than the method used in this work.

Acknowledgments

Part of the present and still ongoing research in this field is funded by the German federal state of Hesse in the project "LOEWE-Zentrum AdRIA". This financial support is gratefully acknowledged. In addition, we thank to the following companies for donating their products: LEONHARD KURZ Stiftung & Co.KG, Baier GmbH & Co.KG, HS Strambach Neuffer GmbH.

References

- (Bau85) Bauser, H., Kurz, E., Schindler, B., Zerweck, K., Bolch, T., Haller, A., Mager, T., EP00000063347B1, Praegefolie zum Aufbringen von Leiterbahnen, 1985.
- (Bha98) Jayesh Bharathan, Yang Yang, Polymer electroluminescent devices processed by inkjet printing: I. Polymer light-emitting logo. In: Applied Physics Letters, 72, Nr. 21, 1998, pp. 2660-2662.
- (Bla05) Blayo, A., Pineaux, B., In: Joint sOC-EUSAI Conference, Grenoble, 2005.
- (Die09) Diener electronic GmbH + Co. KG, Plasmatechnik, 3. Auflage, 2009.
- (Egi90) Egitto, F. D., Plasma etching and modification of organic polymers. In: Pure & Appl. Chem., Vol. 62, No. 9, pp. 1699-1708, 1990.
- (Fue06) Fuegmann, U., Kempa, H., Preissler, K., Bartzsch, M., Zillger, T., Fischer, T., Schmidt, G., Brandt, N., Hahn, U., Huebler, A. C., Printed Electronics is Leaving the Laboratory. In: mst news, Nr. 2, 2006, pp.13-16.
- (Hec11) Hecker, K., Major Investments into Mass Production of Organic and Printed Electronics. In: Organic electronics association press release. 29.06.2011.
- (Kip01) Kipphan, H., Handbook of print media: technologies and production methods. Berlin; Heidelberg; New York; Barcelona; Hongkong; London; Milan; Paris; Singapore; Tokyo: Springer, 2001.
- (Kur11) Kurz, L., Stiftung & Co.KG online, <http://www.kurz.de/de/> from 31.01.2011.
- (Pra05) Arbeitskreis Praegefoliendruck e.V., Praegefoliendruck: Verfahren, Technik und Gestaltung; ISBN 3-7785-2968-4, Huethig Verlag, Heidelberg, 2005.
- (Rau11) Rausch, J., Salun, L., Griesheimer, S., Ibis, M., Werthschuetzky, R., Printed resistive strain sensors for monitoring of lightweight structures. In: Smart Structures / NDE. Smart Sensor Phenomena, Technology, Networks and Systems 2011, San Diego, US. Proceedings of SPIE, 2011.
- (Rot01) Roth, K., Sensfuss, S., Schroedner, M., Stohn, R. I., Clemens, W., Bernds, A., Organische Funktionsschichten in Polymerelektronik und Polymersolarzellen. In: Materialwissenschaft und Werkstofftechnik, 32, Nr. 10, 2001, pp. 789-794.
- (Van58) Van der Pauw, L. J., A Method of Measuring the Resistivity and Hall Coefficient on Lamellae of Arbitrary Shape, Philips Tech. Rev. 20, 1958.

Photoacoustic characterization of a printed electroluminescent panel

Markéta Držková, Tomáš Syrový, Nikola Peřinka, Martin Roch

University of Pardubice, Faculty of Chemical Technology

Department of Graphic Arts and Photophysics

Studentská 95, Pardubice CZ- 53210, Czech Republic

E-mails: marketa.drzkova@upce.cz; tomas.syrový@upce.cz; nikola.perinka@student.upce.cz;
martin.roch@otk.cz

Abstract

The aim of this study was to extend recent research employing the photoacoustic measurements to multilayer samples of a printed electronic device. For this purpose, samples of the electroluminescent source based on a light emitting capacitor, consisting of up to six layers (including flexible substrate), were produced by the screen-printing. The samples with four combinations of different luminescent and insulating layer thicknesses were prepared and examined both with respect to their performance and to the possibility of the photoacoustic characterization of the finished panel as well as of individual intermediate products. The examination of the functionality of prepared electroluminescent panels showed that both the luminance and its homogeneity within the active area are significantly influenced by the thickness of the active layer. The study proved that all samples, ranging from the unprinted substrate with ITO layer over the prints of individual functional layers to the complete panels, are measurable by means of the photoacoustics using excitation sources with visible wavelengths and with intensity modulation in the range between 10 Hz and 1 kHz. The capability of the photoacoustics to depth-profile the samples with varying multilayer structure was shown.

Keywords: electroluminescence, light emitting capacitor, screen printing, luminance, photoacoustics

1. Introduction

Electronic engineering belongs to the fields which have seen significant development over the last decades. Recently, besides the ongoing miniaturization and increasing of performance, the attention is paid also to the production of flexible components and development of alternative production technologies. Advances in printing techniques combined with development of new materials and ink formulations play an important role in both of these aspects. Together they enable the patterning of various functional layers with thickness in the micro- or nanometer range and with the resolution sufficient for many selected applications. The printing production can be realized at low costs and high speed. Printed electronics comprises e.g. sensors utilized on packaging to record and indicate storage and transport conditions (Tudorache, 2007), RFID tags (Subramanian, 2005), memories and transistors (Wöll, 2009), photovoltaic cells (Kopola, 2011; Luque, 2011; Green, 2012), batteries (Choi, 2010; Wendler, 2010; Wendler, 2011; Kopola, 2011; Braam, 2012), electroluminescent light sources and displays (Jabbour, 2001; Johnston, 2005; Ko, 2011).

For effective implementation of new technologies developed for production of flexible printed electronics, it is necessary to be able to control the quality of the whole production process, preferably at early manufacturing stages instead of testing the final product. Since the properties of materials vary in wide range (covering both inorganic and organic, from homogeneous to composite, from transparent to opaque, from conducting to isolating), with individual layers forming less or more complicated structure of the resulting product, it is usually needed to combine more characterization methods and, in some cases, it is still not possible to acquire all parameters in question. For this reason, photothermal methods, which have already found applications in a number of fields, represent the prospective solution. They are not limited by strict requirements on sample properties, and enable to measure optical and thermal properties as well as to study the subsurface structure of the sample, for instance to evaluate the layer thickness or component distribution (e.g. Rosencwaig, 1980; Stegge, 2001; McClelland, 2002). Equally important is their potential for non-destructive examination in an inline configuration. However, the number of detectable parameters depends on particular experimental setup, namely the radiation source used for excitation of the photothermal effect and the principle and sensitivity of detection.

Recently, the photoacoustic apparatus in a gas-microphone configuration with visible excitation and front detection of the photoacoustic signal (Rosencwaig, 1980) has been successfully used for measurement of single electrically conductive functional layers formed by two diverse materials - PEDOT/PSS based transparent conductive polymer and silver based conductive composite ink (Peřinka, 2011). The aim of this study was to

extend the research to multilayer samples of printed electronic device. Screen-printed electroluminescent source based on light emitting capacitor (LEC; Ono, 1993), consisting of up to six layers, including flexible substrate, was chosen for this purpose. The functionality of this type of an electroluminescent panel is influenced mainly by the material, layout and thickness of individual layers, especially the luminescent and insulating ones. During the production, both the materials used and the arrangement are given, whereas the achievement of required thickness of all printed layers is the objective of quality control. Therefore, samples with four combinations of luminescent and insulating layer thicknesses were prepared and examined both with respect to their performance, namely the luminance and its homogeneity within the active area of the electroluminescent panel, and to the possibility of the photoacoustic characterization of the finished panel as well as of individual intermediate products.

2. Materials and methods

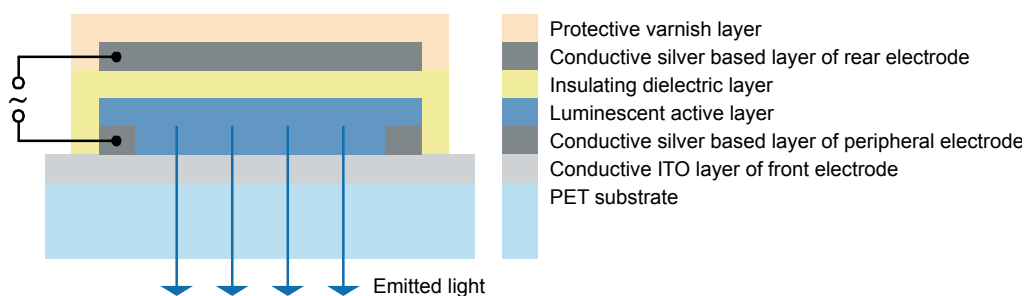


Figure 1: Schematic cross-section of the electroluminescent panel

The structure of the prepared electroluminescent panel (Metalor, 2005; Heraeus, 2010) is presented in Figure 1. The peripheral electrode bounding the luminescent active layer ensures sufficient current density for uniform power supply of the entire conductive layer of front electrode, which is in contact with the active layer. Both the peripheral electrode and the active layer were overprinted by the insulating dielectric layer, preventing arc discharge between the electrodes. Finally, the transparent varnish layer was applied to avoid the oxidation of silver particles and to mechanically protect the functional layers. The active area of the resulting panel had dimensions of 47×24 mm.

The PET foil with thickness of $120 \mu\text{m}$ and conductive layer of ITO (Indium Tin Oxide) on printed side was used as a substrate (supplied by Metalor). The samples of the electroluminescent panel were made on semi-automatic screen-printing machine S 200 HF using the set of Briflex printing pastes (Metalor, 2008) and other materials:

- Briflex Paste Active S Blue - electroluminescent paste containing encapsulated ZnS phosphor particles with active luminescent centres, solid content of 71-75 % (active layer)
- Briflex Dielectric GD1001 - solid content of 70-74 % (dielectric layer)
- Entouch S190A Flexible Silver Ink - conductive composite ink with silver particles, solid content of 70-76 % (layers of rear and peripheral electrode)
- Polyplast PY 383 (Sericol) - solvent-based varnish with approximately 20 % of retarding solvent ZV 552 (protective layer)
- Diethylene Glycol Monobutyl Ether (DGBE) - solvent for electroluminescent paste

Printing conditions and parameters were optimized to achieve uniform layers. The screen-printing machine was equipped with the aluminium float bar and the rectangular 95 mm wide triple polyurethane squeegee (durometer of 75/90/75 Shore A). The type of mesh used for printing of individual layers followed the recommendation of the producer of printing inks, with the exception of electrode printing using conductive composite ink with silver particles, for which the mesh with higher mesh opening was used to ensure sufficient thickness of the conductive layer. The increase in thickness provides higher electrical conductivity whereas it should not have impact on other tested parameters. The summary of used and recommended mesh types is given in Table 1. Prior to the printing, the substrate was cleaned in an ultrasound bath, first in re-distilled water and then in methanol (in each bath for at least ten minutes). Likewise, the electroluminescent paste was thoroughly stirred and redispersed, followed with ultrasound bath treatment in order to break up ZnS particles agglomerates. Individual layers were printed wet on dry; each printed layer was dried at conditions given in Table 2.

Table 1: Used mesh and stencil parameters (recommended parameters (Metalor, 2008) are given in parentheses)

	Active layer	Dielectric layer	Electrode layers
Mesh count [1/cm]	77 (77)	120 (120)	77 (120)
Nominal thread diameter [μm]	55 (55)	34 (34)	55 (34)
Open area [%]	28 (26.5)	29 (29.6)	28 (29.6)
Fabric thickness [μm]	90 (88)	54 (55)	90 (55)
Theoretical ink volume [cm^3/m^2]	25 (23.3)	16 (16.3)	25 (16.3)
Number of emulsion layers (squeegee/print side of screen)	1/2 (2/3)	1/2 (2/3)	1/2 (2/3)

Table 2: Drying conditions

	Active layer	Dielectric layer	Electrode layers	Protective layer
Temperature [$^{\circ}\text{C}$]	100	100	100	21
Time [min]	10	10	5	8–15

Four variants of electroluminescent panels were prepared: first one with single active and single dielectric layer (S11), second with single active and triple dielectric layer (S13), third with triple active and single dielectric layer (S31), and fourth with triple active and triple dielectric layer (S33); other layers were the same for all variants. Together with each electroluminescent panel, targets for characterization of individual functional layers and intermediate products were printed. In each case, from two to three sheets were prepared. The thickness of functional layers was measured by means of a thickness gauge (Schroeder, the resolution of $1\ \mu\text{m}$).

For the evaluation of the luminance and its homogeneity, each sample of the electroluminescent panel was connected to the linear AC power source APS-9301 (GW INSTEK, sine wave, 45-500 Hz). The absolute values of the luminance of individual electroluminescent panels were determined by means of the spectrophotometer X-Rite Eye-One XT (2° observer, measurement at five spots within the sample). Further, the active area of the panel was captured by the Pentax K-10D digital camera equipped with the Pentax 18-55 SMC DA lens in the darkroom at fixed exposure conditions to ensure objective comparison of the luminance achieved with individual panels. All images were converted from DNG to TIFF format (16-bit sRGB) in UFRaw software with constant conversion parameters. Subsequently, the images were converted to the Yxy colour space and the Y channel (lightness), which represents the changes of the luminance within the active area of the panel, was analysed in ImageJ.

For each variant of the electroluminescent panel, two sets of samples were prepared and studied by the photoacoustics. Each set contained seven multilayer samples comprising the individual functional layers and intermediate products as well as the complete panel and unprinted substrate with ITO layer, as illustrated in Figure 2.

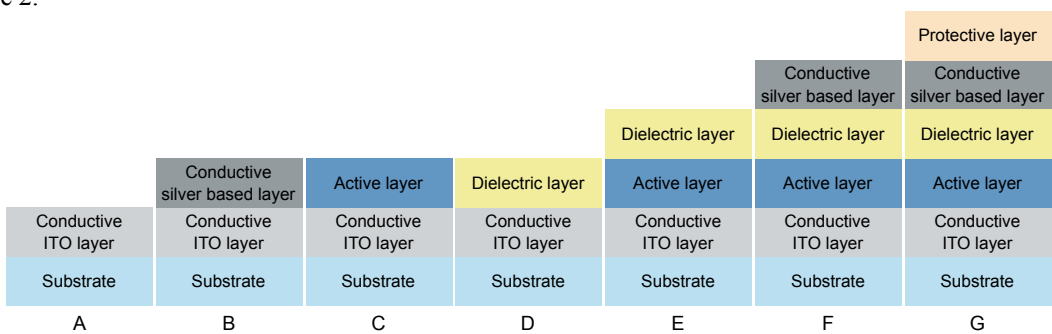


Figure 2: Schematic illustration of multilayer samples measured for each variant of the electroluminescent panel by the photoacoustics

The circular samples with the diameter of 10 mm were cut from the sheet and fixed on the poly(methyl methacrylate) backing using thin layer of medicinal white oil (MBO 46, STN 65 7310). The samples were placed to the front-detection cylindrical photoacoustic cell with the $1/2''$ condenser microphone (Brüel & Kjaer, type 4137). As the excitation source, the externally modulated diode pumped solid-state laser modules

emitting at 473 nm (Photop Suwtech, DPBL 9020), 532 nm (Suwtech, DPGL 3020T) and 655 nm (Laser Components, Flexpoint Minilaser FP 65/20ADF AV) were used, respectively. Their intensity was modulated with acoustic frequencies between 10 Hz and 1 kHz. The detected photoacoustic signal was pre-amplified and fed to the digital signal processing lock-in amplifier SR830 (Stanford Research Systems), which was also used for the modulation of excitation sources using the internal oscillator pulses. All measurements were controlled and processed by the tailored software for PC platform. The polypropylene foil with thin gold layer deposited via evaporation in high vacuum was used as a reference sample for signal normalization. The interpretation of the results was based on the generalized theory of the photoacoustic effect in a multilayer material (Hu, 1999).

3. Results and discussion

The printed electroluminescent panels can be switched on immediately after drying of the last layer by connecting the AC power supply to the electrodes of the panel. The producer recommends for the Briflex printing pastes the voltage of 110 V at the frequency of 500 Hz (Metalor, 2008). Coupling this voltage to the panel with single dielectric layer caused the electrical breakdown of this layer between the peripheral and rear electrode near the contacts resulting in sparking, which made it impossible to evaluate the luminance of respective panel. Therefore, the voltage had to be decreased below 75 V; for further testing of all prepared panels, the voltage of 60 V (at 500 Hz) was used.

The values of average luminance measured by the spectrophotometer are given in Table 3. The results show that significantly higher efficiency was achieved using the panels with single active layer. Comparing the panels with the same thickness of active layer, higher luminance was measured for samples with single dielectric layer.

Table 3: The average luminance of the electroluminescent panels and the percentage of the luminous active area determined at the voltage of 60 V, 500 Hz (the thickness of the active and dielectric layers is given in parentheses)

Electroluminescent panel	S11	S13	S31	S33
Active layer	single (40 μm)	single (40 μm)	triple (94 μm)	triple (94 μm)
Dielectric layer	single (10 μm)	triple (30 μm)	single (10 μm)	triple (30 μm)
Luminance [cd/m ²]	17.6	13.5	0.7	0.3
Luminous active area [%]	100	100	20	34

The homogeneity of the luminance within individual panels was evaluated using image analysis based on the distribution of lightness values. The percentage of luminous active area was determined as the area coverage from binary black-and-white images defined by thresholding of Y component. The threshold value was chosen on the basis of subjective visual perception during the observation of luminous panels as $Y = 0.31$ and then kept constant for all samples. Examples of colour images of luminous panels and corresponding thresholded binary images are in Figure 3, with highest lightness and its homogeneity in case of the samples with single active layer. The resulting values of percentage of luminous active area (Table 3) confirm that the quality of samples with triple active layer is insufficient; the influence of dielectric layer thickness is ambiguous.

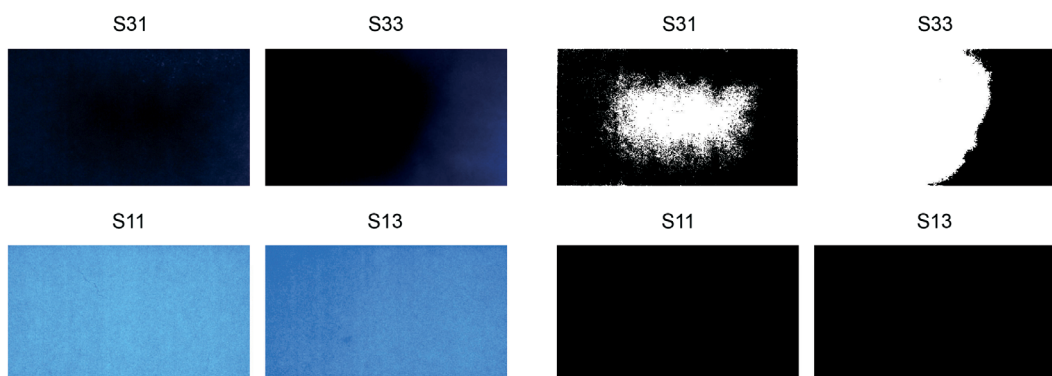


Figure 3: Examples of colour images captured at the voltage of 60 V, 500 Hz (left) and thresholded binary images of Y component (right)

The photoacoustic measurements showed that all samples are measurable at given conditions, i.e. in the modulation frequency range between 10 Hz and 1 kHz at the wavelength of 473, 532 and 655 nm, respectively. For all four variants of the electroluminescent panel (S11, S13, S31, S33), each type of the multilayer sample (A-G, see Figure 2) is discernible either in the amplitude or in the phase of the photoacoustic signal and most of the samples are discernible in both of these parameters.

Figure 4 shows the averaged results of the photoacoustic measurement for the electroluminescent panel S11 at the wavelength of 532 nm.

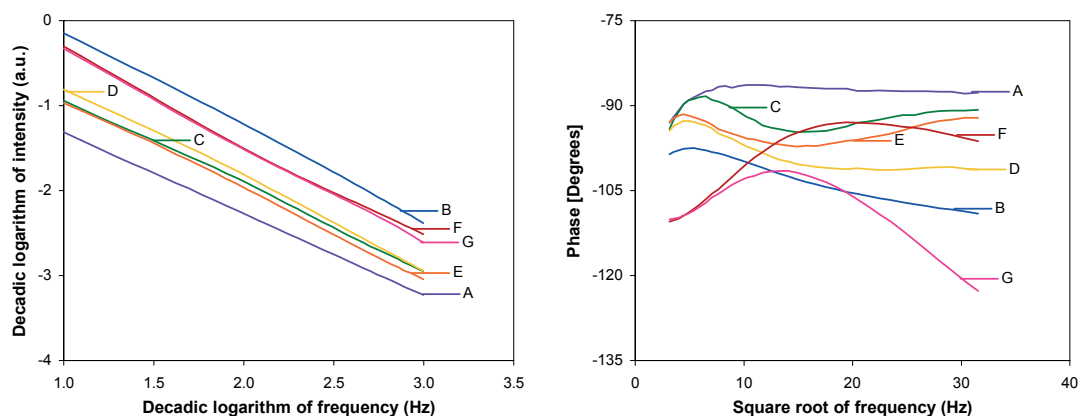


Figure 4: Modulation frequency dependence of the intensity (left) and phase (right) of the photoacoustic signal for the electroluminescent panel S11 measured at the wavelength of 532 nm

The lowest intensity and phase delay of the photoacoustic signal in the whole modulation frequency range had the unprinted PET substrate with thin ITO layer (A). The highest intensity was measured for the sample B (printed with conductive silver based paste); when comparing the samples with individual functional layers (samples B, C, and D), the phase delay of B was highest too.

The values of both the photoacoustic intensity and phase delay for the samples C, D, and E (prints of active and dielectric layer and their overprint) lie between these extremes and show dependence on the thickness, i.e. the course of the curves differs for single and triple active or dielectric layer as well as for their combinations. It means that the photoacoustics can be used for the control of quality of intermediate products in terms of proper thickness of printed layers. However, the photoacoustic signal of these samples is weaker in comparison to the samples containing the layer of conductive silver based paste, which implies lower signal-to-noise ratio and thus worse repeatability and reliability. Therefore, care must be taken to ensure satisfactory results.

The remaining two samples with the most complicated structure, F and G, differ in the intensity of the photoacoustic signal only at higher modulation frequencies, when the photoacoustic signal of sample G is more attenuated by the protective varnish layer, because it originates closer to the sample surface than at lower modulation frequencies. Also the course of the phase delay is similar at low modulation frequencies, however, it significantly changes with the increase of modulation frequency and at 1 kHz the difference reaches approximately 25° , thus the sensitivity to the thickness of protective layer is very high.

As already mentioned, the photoacoustic depth-profiling of samples of complete panels (G) allowed to distinguish individual variants with differing thicknesses of active and dielectric layer. Figure 5 shows the averaged results of the photoacoustic measurement of the samples G for all four variants of the electroluminescent panel (S11, S13, S31, S33) at the wavelength of 532 nm. The logarithmic dependence between the intensity of the photoacoustic signal and the modulation frequency is approximately linear, however, the slope changes within the given range of modulation frequency; the curves measured for the individual variants of panels intersect at modulation frequencies ranging approximately between 25 and 75 Hz. The modulation frequency dependence of the phase shows the maximum, which shifts to the lower frequencies with the increase of the overall sample thickness (approximately from 200 Hz for S11 to 40 Hz for S33). As can be seen in Figure 5, the more pronounced differences between the four combinations of active and dielectric layer thickness were measured in case of the phase of photoacoustic signal, especially at lower frequencies, making the phase information more suitable for the examination of complete electroluminescent panels.

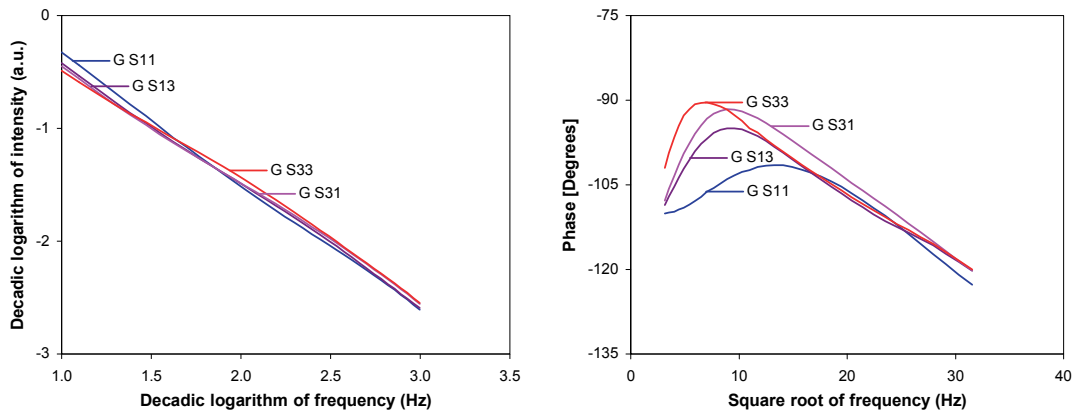


Figure 5: Modulation frequency dependence of the intensity (left) and phase (right) of the photoacoustic signal for the electroluminescent panel S11 measured at the wavelength of 532 nm

4. Conclusion

The examination of the functionality of prepared electroluminescent panels showed that both the luminance of the panel and its homogeneity within the active area of the panel are significantly influenced by the thickness of the active layer. The measurability of all samples ranging from the unprinted substrate with ITO layer over the prints of individual functional layers to the complete panels by means of photoacoustics as well as its capability to depth-profile the samples was proved. Generally, higher repeatability was achieved in case of the samples containing the layer of conductive silver based paste - both when comparing different measurements of the particular sample and measurements of the same type of sample taken from different sheets with the same variant of the electroluminescent panel. The photoacoustic signal of the samples containing the layer of conductive silver based paste is also less dependent on the wavelength of the excitation source.

Currently, the study continues with the extended number of variants of electroluminescent panels with nine combinations of single, double and triple active and dielectric layers. Further, the influence of modified formulation of the active layer and the use of the conductive polymer layer instead of the ITO layer as the front transparent electrode is examined. The luminance homogeneity within the active area and luminance distribution of each prepared panel will be measured using spectrophotometry, colorimetry and image analysis with an appropriate statistical evaluation. The photoacoustic measurements are performed in the extended range of modulation frequencies, which will increase the distinctiveness of individual multilayer samples. The topology and structure of layers with the modified formulation will also be inspected by means of scanning electron microscopy, atomic force microscopy and x-ray diffraction methods. This should make it possible to describe the dependence between the performance of the panel and the composition and thickness of respective layers as well as to test the limits and resolution of photoacoustic characterization in more detail.

Acknowledgments

This work is financially supported by the Arbeitsgemeinschaft industrieller Forschungsvereinigungen "Otto von Guericke" e. V. (AiF). The authors thank Mr. Grumbach, Mr. Lawrenz, Mr. Euler and Mr. Kurmakaev for experimental assistance. In addition, we thank the following companies for donating their products: Sensient Technologies Corporation, BASF, Clariant, Huntsman, Sun Chemical and Carl Stahl.

References

- Braam, K. T., Volkman, S. K., Subramanian V., (2012), *Characterization and optimization of a printed, primary silver-zinc battery*, *Journal of Power Sources*, no. 199, pp. 367-372.
- Green, M. A., Emery, K., Hishikawa, Y., Warta, W., Dunlop, E. D., (2012), *Solar cell efficiency tables (version 39)*, *Progress in Photovoltaics: Research and Applications*, vol. 20, No. 1, pp. 12-20. DOI: 10.1002/pip.2163
- Heraeus, (2010), *Clevios S V3: Printing of Electroluminescence Lamp, Processing Guide*, Heraeus, Hanau, 13 p.
- Hu, H., Wang, X., Xu, X., (1999), *Generalized Theory of the Photoacoustic Effect in a Multilayer Material*, *Journal of Applied Physics*, vol. 86, no. 7, pp. 3953-3958.

- Jabbour, G. E., Radspinner, R., Peyghambarian, N., (2001), Screen printing for the fabrication of organic light-emitting devices, *IEEE Journal of Selected Topics in Quantum Electronics*, vol. 7, no. 5, pp. 769-773.
- Johnston, D., Barnardo, C., Fryer, C., (2005), *Passive multiplexing of printed electroluminescent displays*, *Journal of the Society for Information Display*, vol. 13, no. 6, pp. 487-491.
- Ko, S. H., Ed., (2011), *Organic Light Emitting Diode - Material, Process and Devices*. InTech. ISBN 978-953-307-273-9
- Kopola, P., Aernouts, T., Sliz, R., Guillerez, S., Ylikunnari, M., Cheyns, D., Välimäki, M., Tuomikoski, M., Hast, J., Jabbour, G., Myllylä, R., Maanien, A., (2011), *Gravure printed flexible organic photovoltaic modules*, *Solar energy materials and solar cells*, vol. 95, pp. 1344-1347.
- Luque, A., Hegedus, S., Eds. (2011), *Handbook of Photovoltaic Science and Engineering*, 2nd ed., John Wiley & Sons, Delaware, 1210 p. ISBN 978-0-470-72169-8
- McClelland, J. F., Jones, R. W., Bajic, S. J., (2002), *Photoacoustic Spectroscopy*, In *Handbook of Vibrational Spectroscopy*, vol. 2., Chalmers J. M., Griffiths P. R., Eds., John Wiley & Sons, Chichester, pp. 1231-1251. ISBN 978-0-471-98847-2
- Metalor, (2008), *Electroluminescence Pastes Briflex: Product Data Sheet, 1.1*, Metalor Technologies SA, Neuchatel, 5 p.
- Ono, Y. A., (1993), *Electroluminescence*, In *Encyclopedia of Applied Physics*, vol. 5, Trigg G. L., Ed., VCH, Weinham, pp. 295-325. ISBN 1 - 56081 - 064 - 5
- Peřinka, N., Syrová, L., Držková, M., Syrový, T., (2011), *Photoacoustic Measurement of Screen-printed Conductive Layers*, *Printing Future Days 2011, 7-10 November 2011, Chemnitz, Germany, Proceedings 2011*, pp. 237-242. ISBN 978-3-86135-623-3
- Rosencwaig, A., (1980), *Photoacoustics and Photoacoustic Spectroscopy*, *Chem. Analysis V57*, John Wiley & Sons, New York, 309 p. ISBN 0-471-04495-4
- Stegge, J. M., Urban, M. W., (2001), *Stratification processes in thermoplastic olefins monitored by step-scan photoacoustic FT-IR spectroscopy*, *Polymer*, vol. 42, no. 12, pp. 5479-5484.
- Subramanian, V., Frechet, J. M. J., Chang, P. C., Huang, D. C., Lee, J. B., Moles, S. E., Murphy, A. R., Redinger, D. R., Volkman, S. K., (2005), *Progress Toward Development of All-Printed RFID Tags: Materials, Processes, and Devices*, *Proceedings of the IEEE*, vol. 93, no. 7, pp. 1330-1338.
- Tudorache, M., Bala, C., (2007), *Biosensors based on screen-printing technology, and their applications in environmental and food analysis*, *Analytical and Bioanalytical Chemistry*, vol. 388, no. 3, pp. 565-578.
- Wendler, M., Hübner, G., Krebs, M., (2011), *Development of Printed Thin and Flexible Batteries*. *International Circular of Graphic Education and Research*, no. 4, pp. 32-41.
- Wendler, M., Krebs, M., Hübner, G., (2010), *Screen Printing of Thin, Flexible Primary and Secondary Batteries*, In *Advances in Printing and Media Technology*, Vol. 37, Enlund N. and Lovreček M., Eds., Iarigai, Darmstadt, pp. 303-312. ISBN 978-3-9812704-2-6
- Wöll Ch., Ed., (2009), *Physical and Chemical Aspects of Organic Electronics*, Wiley-VCH, 634 p. ISBN 978-3-527-40810-8
- Metalor, (2005), *Briflex - Our Electroluminescence Range*, Metalor Technologies SA, Neuchatel, 6 p., <http://www.metalor.com/en/content/download/506/8760/file/metalor-electroluminescence-EN-01-06.pdf>, (accessed January 2011)

Web sources

- Metalor, (2005), *Briflex - Our Electroluminescence Range*, Metalor Technologies SA, Neuchatel, 6 p., <http://www.metalor.com/en/content/download/506/8760/file/metalor-electroluminescence-EN-01-06.pdf>, (accessed January 2011)



Printed UHF RFID antenna on coated cardboard

*Tadeja Muck*¹, *Matej Pivar*¹, *Miloje Đokić*¹, *Diana Gregor-Sveteć*¹, *Urška Bogataj*²,
*Marijan Maček*³, *Leon Pavlovič*³, *Boštjan Batagelj*³

¹ University of Ljubljana

Faculty of Natural Sciences and Engineering
Chair of Information and Graphic Technology
Snežniška 5, SI-1000 Ljubljana, Slovenia

E-mails: tadeja.muck@gmail.com, matej.pivar@gmail.com, miloje.djokic@gmail.com, diana.gregor@ntf.uni-lj.si

² Valkarton d.d.

Production of Corrugated Board and Packaging d.d.
Tržaška c. 1, SI-1370 Logatec, Slovenia

E-mail: urska.bogataj@gmail.com

³ University of Ljubljana

Faculty of Electrical Engineering
Tržaška cesta 25, SI-1000 Ljubljana, Slovenia

E-mails: marijan.macek@fe.uni-lj.si, leon.pavlovic@fe.uni-lj.si, bostjan.batagelj@fe.uni-lj.si

Abstract

In the recent years a growing number of smart packaging applications have appeared, main of them are based on radio frequency identification (RFID) technology. Mentioned technology contributes remarkably to the progress by providing data transmission opportunity.

The passive RFID tags are mostly used because of their low production price. Recently, an increasing number of tags include sensors to monitor various parameters on the life cycle of packaging.

In this paper the optimization of the printing process conditions for screen printing of passive UHF RFID tags on different coated packaging cardboards are presented. The antennas were printed with two conductive inks using semi-automatic screen printer. Drying conditions have been varied to obtain good print quality and relevant electrical parameters measured on the printed antennas. Two different designs for UHF RFID antennas were used regarding two different chips. The first chip is meant just for EPC encoding, the second one includes temperature sensor besides EPC encoding. On both printed antennas full measurement characterizations were performed. Finally both above mentioned chips were integrated each to the appropriate antenna. Response of the final UHF RFID tags was verified by reader.

We proved that the main influence on finally working tag has the conductive ink itself and the quality of antenna to chip contact.

Keywords: silver conductive ink, cardboard, UHF RFID, image analysis, antenna simulation

1. Introduction

Radio frequency identification (RFID) is rooted in discoveries made by Faraday and discoveries in radio and radar technologies. The RFID tags can be subdivided into active and passive tags; active tags have a longer reading/writing range and passive tags a shorter one. The latter are much simpler and cheaper than active tags and are more widely used (Bolić et al., 2010).

The RFID system can work at low (LF, 125/134kHz), high (HF, 13.56MHz) or ultrahigh (UHF, 860-960 MHz) frequency ranges (Bogataj et al., 2011). The LF and HF tags operate with inductive coupling and have short reading range, on the other hand the UHF tags use radiative coupling and have longer reading range (Merilampi et al., 2010). The integration of electronics, such as RFID tags in different applications is important in order to gain greater functionality in the products. With traditional manufacturing techniques the integration of RFID tags may not be technically and economically competitive in mass production. Etching is typically used in RFID tag manufacturing to produce conductive antenna pattern. Although it is an efficient process, it has a few drawbacks. It contains many process phases and uses different chemicals which are not environmentally friendly and are expensive (Merilampi et al. 2010).

Nowadays investigations are focused on the use of conventional printing technologies for mass production of printing electronics directly on different materials. Among the printing technologies, the most popular are screen printing (Słoma et al., 2011; Janeczek et al., 2010; Jakubowska et al., 2011), inkjet (Futera et al., 2010), flexography (Blayo et al., 2005) and gravure (Pudas et al., 2005). The performance of printed RFID antennas was characterized by many researchers (Shin et al., 2009; Syed et al., 2007; Nikitin et al., 2005; Merilampi et al., 2007; Rida et al., 2007; Yang et al., 2007).

In the investigations mentioned before, photo quality papers or foils were mainly used as printing materials.

The goal of our research was to optimize the printing process conditions for screen printing of passive UHF RFID tags on different coated cardboards - for box tracking in logistics. The antenna was printed with two conductive inks using semi-automatic screen printer. Drying conditions have been varied in order to obtain good print quality and also to achieve the relevant electrical parameters measured on the printed antennas. Two different designs for UHF RFID printed antennas were used. The first design was taken from the commercial antenna from company Avery Dennison. This design is adapted to integrate NXP chip. After that a new antenna design was made for integration the IDS chip with temperature sensor. On both printed antennas full measurement characterizations were performed. Finally both above mentioned chips were integrated each to the appropriate printed antennas on different cardboards. Response of the final UHF RFID tags was verified by the reader.

2. Materials and methods

2.1 Materials

Printing materials

Nine coated cardboards (C-1 to C-9) of different smoothness and grammage (230-350 g/m²) were chosen as printing materials. Printing was performed with a semi-automatic screen printing machine. Monofilament polyester plain weave mesh with 120 T/cm was applied.

Printing inks

For printing two different conductive inks were applied:

- CRSN2442 SunTronic Silver 280 - (SunChemical) and
- DuPont 5064H - (DuPont).

Both of them are thermal drying silver conductive inks recommended for hand, semi-automatic or fully automatic screen printing machines.

SunChemical is suitable for printing conductive tracks onto flexible materials. Monofilament meshes of 49 to 120 T/cm can be used. For a moving belt drier, a suitable profile is 100-130 °C over 30-90 seconds in the hot zone. The ink has 69%-71% of solids and the viscosity in 20-30 poises at 25 °C. Dry film thickness at 100 T/cm is 4-8 µm.

DuPont ink was developed for printing HF and UHF RFID antennas. It has excellent adhesion to various materials. Typical drying conditions are 130 °C for 10-20 min in static box oven or 140 °C for 2 min at reel-to-reel applications. The ink has 63%-66% of solids and the viscosity 10-20 poises at 25 °C. Dry film thickness at 200 T/cm is 9 µm.

Chips

To produce the final UHF RFID tags, two types of chips were used:

- NXP - SL3S1202AC0, plastic flip chip strap, 240-bit of EPC memory, EEPROM, broad international operating frequency from 840 to 960 MHz, impedance (915 MHz) Z = 22 - j195, for supply chain management - (NXP chip).
- IDS - SL900A EPC Class 3 Sensory Tag Chip, works in semi-passive mode as well as in fully passive mode, 9k-bit EEPROM, frequency: 860 to 960 MHz, data logging from on-chip temperature sensor, for applications where beside identification (item tracking), temperature monitoring is needed - (IDS chip).

2.2 Methods

For printing with two different conductive inks the optimal drying conditions to achieve the lowest resistivity of the conductive printed layers were determined. Besides hot zone drying, the Heat & Press system was used.

After successfully drying, resistance of conductive printing layers was measured using the digital multimeter DT-890G. Resistances of all samples were measured on printed test element (Figure 1, left) between points 1 and 2 with normal length $L = 22$ mm and width $W = 3$ mm. The nominal number of squares $N_{sq} = L/W = 10.3$. The final results are given as value of conductive printed layer resistivity in $m\Omega/sq$.

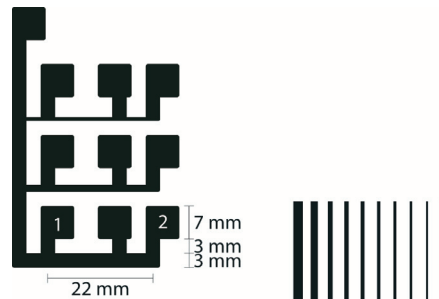


Figure 1: Test elements for resistance measurements (left) line gain determination (right)

The print quality of printed conductive layers on all different cardboards was determined with image analysis by measuring line gain and print mottle on printed test elements (Figure 1, right). Print mottle and line gain were determined using ImageJ software. The print mottle was determined under traditional STFI method by calculation of coefficient of variation, CV. ($CV = \sigma/R$; σ - standard deviation of the grey values, R - the mean grey value) (Fahlerantz et al., 2003).

The line gain, ΔL (%) was determined by measuring the area of 10 ideal lines LA_{id} - digital test element (Figure 1, right) in comparison with area of printed lines LA_p on nine different cardboards.

$$\Delta L (\%) = (\sum_1^{10} LA_p * 100 / \sum_1^{10} LA_{id}) - 100.$$

When the analysis of print quality was completed and the resistance of printed conductive layers was measured, the printing of UHF RFID antennas started. Because the antenna design must comply with the characteristics of chip two different antenna designs were printed separately for NXP and IDS chips.

- The first design was taken from the commercial antenna from company Avery Dennison. This design is adapted to integrate NXP chip - (commercial antenna).
- After that a new antenna design was made regarding to chip specification SL900A EPC Class 3 Sensory Tag Chip (Figure 2) - IDS chip - (new designed antenna).

The main requirements, for the new antenna design were the IDS chip impedance (approx. $Z = 20 - j325 \Omega$), the size and the materials used for the printed antenna. New UHF antenna was designed as a resonant planar structure at the operating frequency of 868 MHz. The antenna properties (impedance and radiation pattern) were first simulated with a commercial 3D numerical solver (Ansoft HFSS) and then also evaluated by a measurement. The relative permittivity of the base of the printed antenna cardboard used for the simulation was 3.2 with a loss tangent of 0.003. The simulated impedance $Z = 20 + j270 \Omega$ and the radiation efficiency of 87% were obtained.

On cardboards full measurement characterizations of printed UHF RFID antenna using Agilent 4284A precision LCR meter at 1 MHz was performed. An outdoor antenna measuring polygon was used for the radiation pattern measurements in the H (magnetic field) and E (electric field) plane. Measurements of antenna's radiation pattern were done for simulated and printed antennas for both antennas with different design.

At the end both above mentioned chips were integrated each to the appropriate antenna to get the finally working UHF RFID tags with printed antennas on cardboards. NXP chip integration on commercial designed antenna was easy because it is designed as a strap. The second chip with temperature sensor IDS chip was integrated manually. The response of both UHF RFID tags was verified by the reader.

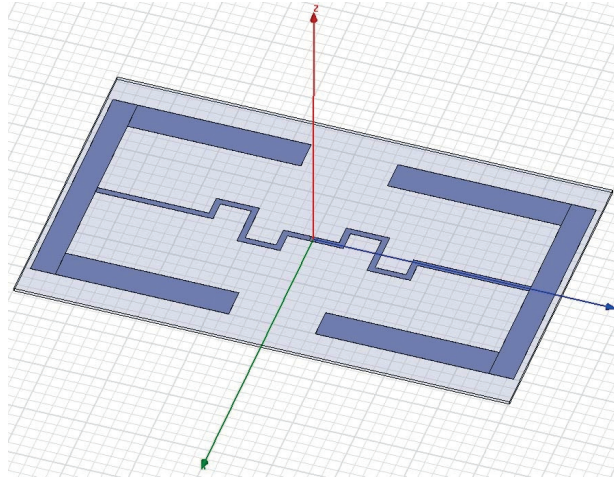


Figure 2: New designed antenna for sensory tag chip

3. Results and discussion

3.1 Drying conditions

Cardboards were dried under different conditions in order to determine optimal drying process. Drying was performed in hot zone at different temperatures, starting from 100 °C till 170 °C with 10 °C step. The drying time was extended by 45 seconds. While the resistance of prints between the points 1 and 2 (Figure 1, left) were still high (around 3 Ω), the prints on all cardboards were dried under Heat & Press. As an optimal conditions drying for 90 seconds in hot zone at 115 °C, followed by 10 seconds drying at 150 °C under pressure (3 bar) were determined (Figure 3).



Figure 3: Schematic representation of two stages combined drying process

3.2 Electric properties

After the two stages drying process the resistance of the test structure measured on nine cardboards was nearly the same (Figure 4). But SunChemical ink yields a little bit lower final resistivity. From the number of squares the final resistivity is below 100 mΩ/sq.

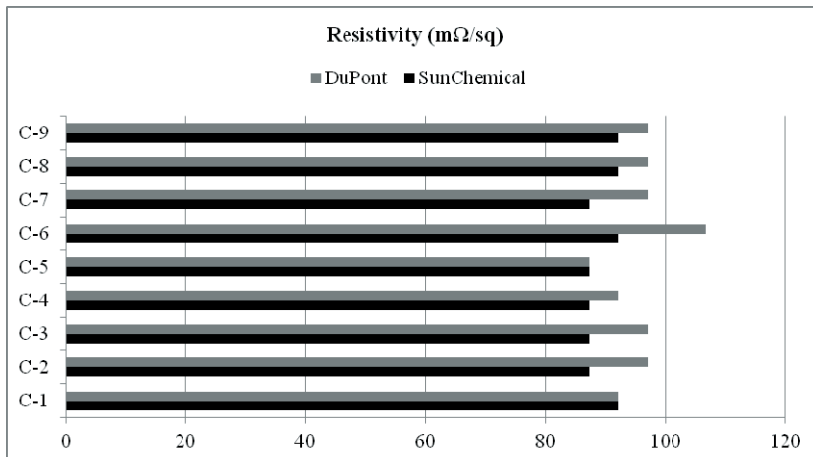


Figure 4: Resistivity on nine different cardboards printed by two conductive inks

3.3 Image analysis

Image analysis was done at all different printed samples.

From the Figure 5 one can see that the SunChemical ink gives smaller CV - smaller print mottle (Figure 5) on all printed cardboards. The reduction of print mottle is similar on all nine printed cardboards.

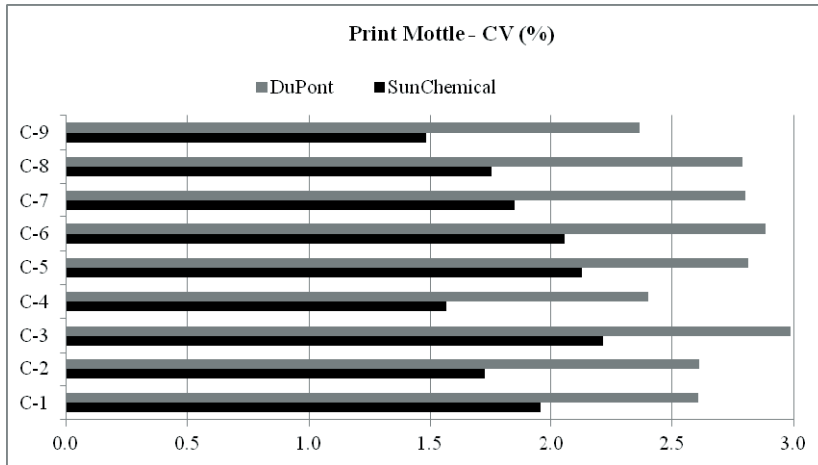


Figure 5: Print mottle on nine different cardboards printed with SunChemical and DuPont inks

On the basis of resistance measurements and print mottle results, samples printed with SunChemical printing ink were selected for further research. The ink shows lower resistivity and smaller print mottle in comparison to DuPont printing ink.

Measurements of line gain show differences between nine cardboards (Figure 6). For further research two cardboard samples were selected, the first one from the four samples with the highest (C-1) and the second with the smallest line gain (C-8). With such selection the effect of line gain on results of antenna simulation was determined.

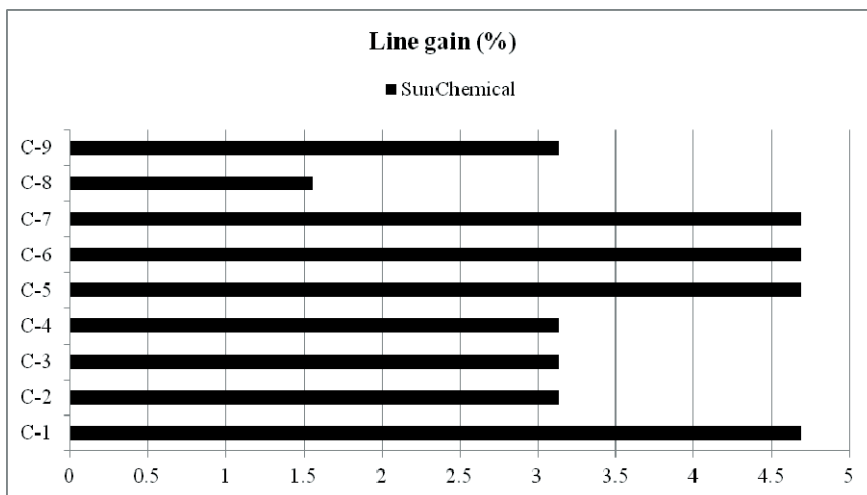


Figure 6: Line gain measured on nine cardboards printed with SunChemical ink

3.4 Measurements of radiation pattern and tags readability

The radiation pattern was evaluated by measurements of commercial and new designed antennas on two selected cardboards C-1 and C-8. The radiation pattern for both antennas is similar in the E and H planes for the simulated UHF antenna and also for printed antennas on both cardboards C-1 and C-8. The results revealed that the patterns are nearly the same no matter which printing material was used. On the Figure 7 the radiation pattern for commercial antenna is shown.

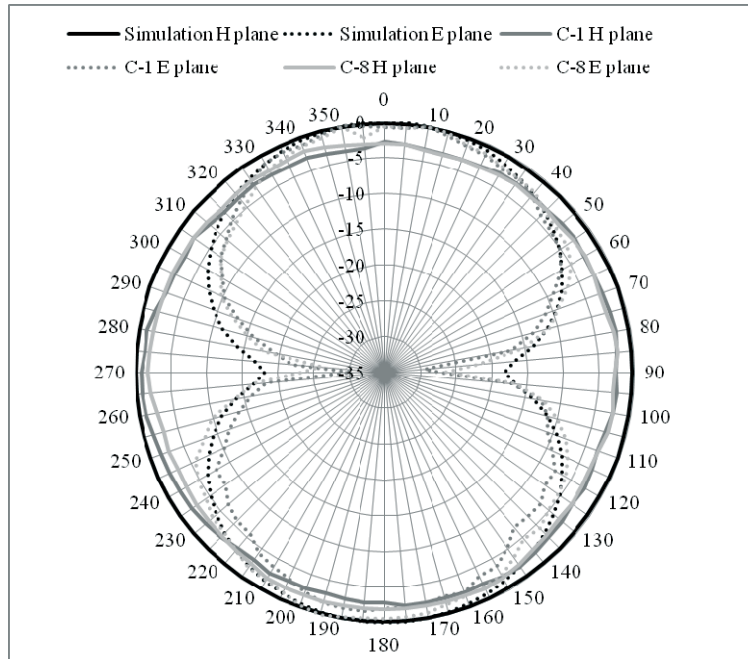


Figure 7: The radiation pattern for simulated commercial UHF antenna and printed ones on both cardboards, C-1 and C-8

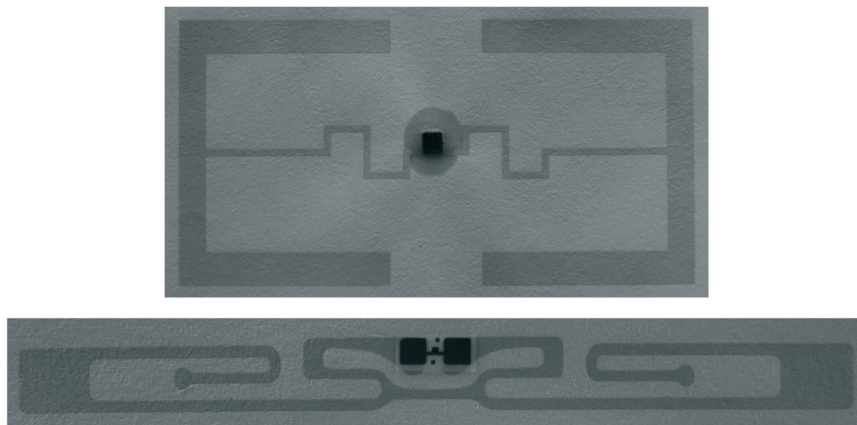


Figure 8: UHF RFID tags - new designed antenna with SL900A EPC Class 3 Sensory Chip (above), antenna with commercial design with NXP "strap" chip (below)

The response of both UHF RFID tags (first with NXP chips and another with IDS Chip) (Figure 8) was evaluated by IDS R-902 reader. On the first tag with NXP chip the power diminishes with the distance of reading from around -50 dBm to almost -70 dBm at one metre distance. The largest measured distance where the tags still worked was a little bit more than 1 m on both coated cardboards, C-1 and C-8. The manual integrated IDS chip on the new designed UHF antenna was also read with the same reader. The tag responded, but the reading distance was no more than twenty centimetres. The reason for bad reading can be the insufficient contact between chip and antenna or antenna impedance mismatch.

4. Discussion

Besides print quality the low resistance of prints is a crucial requirement for printing the RFID antennas. It is important to choose such drying conditions, which can reduce the resistance to a minimum value. In our study the drying conditions were changed in order to achieve the lowest resistance. It was found that besides drying at different temperatures in the hot zone, the pressure to which the samples were exposed after drying had an impact and results in lowering the resistance. The optimal drying conditions for printing RFID antenna were determined. The purpose of print mottle was determined to select the most appropriate printing ink for

printing RFID antennas. A minor lower print mottle was obtained at cardboards printed with the SunChemical ink (Figure 6). Two cardboards, one with the lowest and one with the highest line gain (Figure 7) were selected for measurements of radiation pattern. The measurements mentioned at last were done in order to find out how the antenna works regarding to printing material.

The design of UHF antenna is proved to be appropriate for both cardboards - no differences on radiation pattern were observed on antennas printed on different coated cardboards.

At the end we found out that the main influence on finally working tag has the quality of conductive ink itself and the quality of contact between the antenna and chip.

In our further research with the help of the company IDS chip with temperature sensor will be modified to allow easier integration. In this way directly temperature monitoring on the packages will be possible.

Acknowledgment

Authors express their gratitude to Ralf Zichner, Fraunhofer, to company IDS and company RLS. Thank to Avery Dennison for permission to use their antenna design. Urška Bogataj acknowledges the Slovenian Technology Agency for young researcher support; "Operation part financed by the European Union, European Social Fund".

References

- Blayo, A., Pineaux, B., (2005), *Printing processes and their potential for RFID printing, Proc. of the 2005 Joint Conference on Smart Objects and Ambient Intelligence: Innovative Context-Aware Services: Usages and Technologies, Grenoble, pp. 27-30.*
- Bogataj, U., Maček, M., Muck, T., Klanjšek Gunde, M., (2011), *Readability and modulated signal strength of two different ultra-high frequency radio frequency identification tags on different packaging. Packag. technol. sci., pp. 1-12.*
- Bolić, M., Simplot-Ryl, D., Stojmenović, I., (2010), *RFID Systems - Research Trends and Challenges, Wiley.*
- Fahlerantz, C. M., Johansson, P. A., Aslund P., (2003), *The influence of Mean Reflectance on Perceived Print Mottle, Journal of Imaging Science and Technology, vol. 47, (1), pp. 54 - 59.*
- Futera, K. et al., (2010), *Printed electronic on flexible and glass substrates, Proc. of SPIE, vol. 7745, (77451B).*
- Jakubowska, M. et al., (2011), *Printed transparent electrodes containing carbon nanotubes for elastic circuits applications with enhanced electrical durability under severe conditions, Materials Science and Engineering: B, vol. 176, (4), pp. 358-362.*
- Janeczek, K. et al., (2010), *Screen printed UHF antennas on flexible substrates, Proc. of SPIE, vol. 7745, (77451B).*
- Merilampi, S. et al., (2007), *Analysis of Silver Ink Bow-Tie RFID Tag Antennas Printed on Paper Substrates, International Journal of Antennas and Propagation, ID 90762, p. 9.*
- Merilampi, S. L., Bjorninen, T., Vuorimaki, A., Ukkonen, L., Ruuskanen, P., Sydanheimo, L., (2010), *The Effect of Conductive Ink Layer Thickness on the Functioning of Printed UHF RFID Antennas. Proceeding of the IEEE, vol. 98, (9), pp. 1610 - 1619.*
- Nikitin, P. V. et al., (2005), *Low cost silver ink RFID tag antennas, Proc. of IEEE Antennas and Propagation Society International Symposium, vol. 2B, pp. 353 - 356.*
- Pudas, M. et al., (2005), *Gravure printing of conductive particulate polymer inks on flexible substrates, Progress in Organic Coatings, vol. 54, (4), pp. 310-316.*
- Rida, A. et al., (2007), *Design and Integration of Inkjet-printed Paper-Based UHF Components for RFID and Ubiquitous Sensing Applications, Proc. of 37th European Microwave Conference, (<http://users.ece.gatech.edu/~etentze/EuMC07.pdf>).*
- Shin, D. Y. et al., (2009), *Performance characterization of screen printed radio frequency identification antennas with silver nanopaste, Thin Solid Films, vol. 517, (21), pp. 6112-6118.*
- Śloma, M. et al., (2011), *Investigations on printed elastic resistors containing carbon nanotubes, Journal of Material Science: Materials in Electronics, published on line 9.02 2011-04-01.*
- Syed, A. et al., (2007), *Effects of Antenna Material on the Performance of UHF RFID Tags, Proc. of IEEE International Conference on RFID, Grapevine, 26-28, pp. 57 - 62.*
- Yang, L., Tentzeris, M. M., (2007), *Design and Characterization of Novel Paper-based Inkjet-Printed RFID and Microwave Structures for Telecommunication and Sensing Applications, Proc. of IEEE/MTT-S International Microwave Symposium, pp. 1633 - 1636.*



Introducing a new anaglyph method: compromise anaglyph

Jure Ahtik

University of Ljubljana, Faculty of Natural Sciences and Engineering
Chair of Information and Graphic Technology
Snežniška 5, SI-1000 Ljubljana, Slovenia
E-mail: jure.ahtik@ntf.uni-lj.si

Abstract

Anaglyph photography is one of the stereo photographic techniques. Anaglyphs consists of two stereo pairs, which are based on complementary colour separations. The most known and used pair is red-cyan. Main advantage of anaglyph method is, that it can be rendered using any presentation technique.

Different methods of making digital anaglyphs can be found, and each of them has its advantages and disadvantages. We decided to compare true, grey, colour, half-colour, Dubois and optimised anaglyph techniques and to develop improvements to the process of making anaglyphs.

Keywords: anaglyph, stereo photography, compromise anaglyph, conversion matrix, colour difference

1. Introduction

Stereo photography is one of the photographic techniques, with the possibility to influence photography, videography and digital media in the future the most. Some of stereographic methods are almost as old as photography itself and one of them is called anaglyph photography.

Stereo photography is based on capturing images that can be seen with each human eye separately in the same moment, combining them into one stereo image and looking at them in a way, that only one stereo pair can be seen with each eye. Anaglyphs are made of two stereo pairs, which are based on complementary colour separations (Valzus, 1966). The most known and used pair is red-cyan, but there are also others, such as amber-blue. Main advantage of anaglyph method is, that it can be rendered using any presentation technique, and it can be printed and used on a paper and certainly the best one for doing so. The other great advantage is its price, because no electronic equipment is needed for its use and distribution (Vierling, 1965).

Procedure how to make an anaglyph is, first capture photographs of both stereo pairs, than to make colour separations out of them, and last, to combine them into a final anaglyph. Using colour filters, that are usually fitted in a special pair of glasses, healthy human can see stereo effect. There are different techniques of how to make a red-cyan anaglyph using different conversion matrices in the process (Wimmer, 2010).

The research was based on comparison of different known techniques of producing anaglyphs using colour matrices, colour measurement and transformations, visual evaluation and on development of possible improvements (Ahtik, 2011).

2. Methods

2.1. Measuring colour filters

First we needed to analyse the colour filtered anaglyph glasses that are available on the market. Using spectrophotometer X-rite EyeOne Pro, series of spectral measurements of light emitting through four samples of red-cyan filters, were performed. Converting spectral measurements to $CIEXYZ$ and $CIELAB$ colour spaces, colour differences ΔE_{ab}^* between average and single $CIELAB$ values were calculated.

2.2. Making of stereo pairs

Digital photographs of stereo pairs had been made with Nikon D700 digital camera and AF-S NIKKOR 24-70mm f/2.8G ED lens. ColorChecker test chart fields (Gardner, 2011) were embedded into stereopairs for better colour comparison and measurements. The final images can be seen on Figure 1.

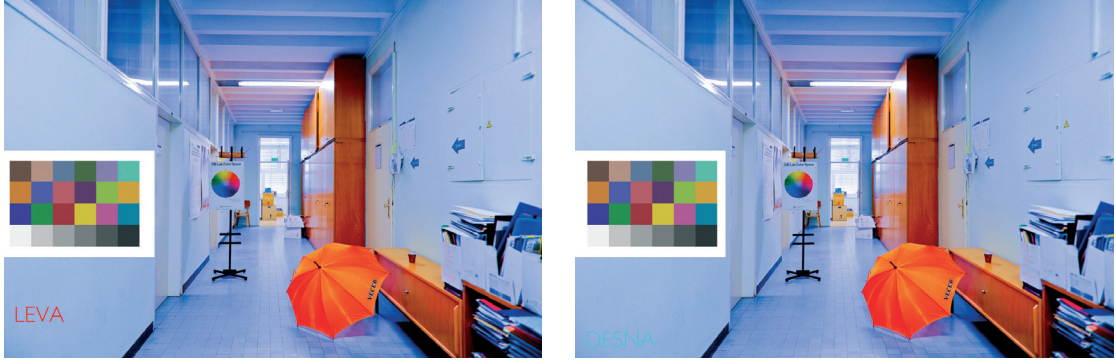


Figure 1: Left and right stereopair with embedded ColorChecker test chart

2.3. Comparing known conversion methods

The next step in the research was to compare different techniques of making anaglyphs. All colour conversions in the research had been calculated with conversion matrices, one matrix per one colour separation. This technique works with digital *RGB* images, where we multiply image, as an 3-by-1 matrix, with 3-by-3 conversion matrix, effecting each *RGB* separation on all three *RGB* channels. That way the very precise conversion is possible. For each of the conversion techniques, pair of conversion matrices is known: true anaglyph [1], grey anaglyph [2], colour anaglyph [3], half-colour anaglyph [4], Dubois anaglyph [5] and optimised anaglyph [6] (Dubois, 2010&2011; Glesson, 2010; Wimmer, 2010).

$$\begin{bmatrix} r_a \\ g_a \\ b_a \end{bmatrix} = \begin{bmatrix} 0,299 & 0,587 & 0,114 \\ 0 & 0 & 0 \\ 0 & 0 & 0 \end{bmatrix} \times \begin{bmatrix} r_1 \\ g_1 \\ b_1 \end{bmatrix} + \begin{bmatrix} 0 & 0 & 0 \\ 0 & 0 & 0 \\ 0,299 & 0,587 & 0,114 \end{bmatrix} \times \begin{bmatrix} r_2 \\ g_2 \\ b_2 \end{bmatrix} \quad [1]$$

$$\begin{bmatrix} r_a \\ g_a \\ b_a \end{bmatrix} = \begin{bmatrix} 0,299 & 0,587 & 0,114 \\ 0 & 0 & 0 \\ 0 & 0 & 0 \end{bmatrix} \times \begin{bmatrix} r_1 \\ g_1 \\ b_1 \end{bmatrix} + \begin{bmatrix} 0 & 0 & 0 \\ 0,299 & 0,587 & 0,114 \\ 0,299 & 0,587 & 0,114 \end{bmatrix} \times \begin{bmatrix} r_2 \\ g_2 \\ b_2 \end{bmatrix} \quad [2]$$

$$\begin{bmatrix} r_a \\ g_a \\ b_a \end{bmatrix} = \begin{bmatrix} 1 & 0 & 0 \\ 0 & 0 & 0 \\ 0 & 0 & 0 \end{bmatrix} \times \begin{bmatrix} r_1 \\ g_1 \\ b_1 \end{bmatrix} + \begin{bmatrix} 0 & 0 & 0 \\ 0 & 1 & 0 \\ 0 & 0 & 1 \end{bmatrix} \times \begin{bmatrix} r_2 \\ g_2 \\ b_2 \end{bmatrix} \quad [3]$$

$$\begin{bmatrix} r_a \\ g_a \\ b_a \end{bmatrix} = \begin{bmatrix} 0,299 & 0,587 & 0,114 \\ 0 & 0 & 0 \\ 0 & 0 & 0 \end{bmatrix} \times \begin{bmatrix} r_1 \\ g_1 \\ b_1 \end{bmatrix} + \begin{bmatrix} 0 & 0 & 0 \\ 0 & 1 & 0 \\ 0 & 0 & 1 \end{bmatrix} \times \begin{bmatrix} r_2 \\ g_2 \\ b_2 \end{bmatrix} \quad [4]$$

$$\begin{bmatrix} r_a \\ g_a \\ b_a \end{bmatrix} = \begin{bmatrix} 0,456 & 0,500 & 0,176 \\ -0,040 & -0,038 & -0,016 \\ -0,015 & -0,021 & -0,016 \end{bmatrix} \times \begin{bmatrix} r_1 \\ g_1 \\ b_1 \end{bmatrix} + \begin{bmatrix} -0,043 & -0,088 & -0,002 \\ 0,378 & 0,734 & -0,018 \\ -0,072 & -0,113 & 1,226 \end{bmatrix} \times \begin{bmatrix} r_2 \\ g_2 \\ b_2 \end{bmatrix} \quad [5]$$

$$\begin{bmatrix} r_a \\ g_a \\ b_a \end{bmatrix} = \begin{bmatrix} 0 & 0,7 & 0,3 \\ 0 & 0 & 0 \\ 0 & 0 & 0 \end{bmatrix} \times \begin{bmatrix} r_1 \\ g_1 \\ b_1 \end{bmatrix} + \begin{bmatrix} 0 & 0 & 0 \\ 0 & 1 & 0 \\ 0 & 0 & 1 \end{bmatrix} \times \begin{bmatrix} r_2 \\ g_2 \\ b_2 \end{bmatrix} \quad [5]$$

where:

$r_a, g_a, b_a \dots$ red, green and blue values of the final anaglyph image;

$r_1, g_1, b_1 \dots$ red, green and blue values of the first stereopair;

$r_2, g_2, b_2 \dots$ red, green and blue values of the second stereopair.

Using *Adobe RGB* to *CIEXYZ* and *CIEXYZ* to *CIELAB* colour conversions, *CIELAB* values of ColorChecker test chart fields were calculated.

In the area of stereo photography judgement cannot be based on a colour measurements that can be compared to normal human vision, only. Good anaglyph is a synthesis of two things: good colour reproduction and good stereo effect. According to this, visual comparison of all known techniques has been made and two parameters were observed: quality of stereo effect and ghosting. Stereo effect represents quality of three-dimensional presentation and ghosting represents an effect, when both stereo pairs can be seen at the same moment through the same filter, producing double image. The proper way of seeing anaglyphs is just one image through one corresponding filter. Visual evaluation has been made on LCD screen Eizo CE240, LED screen on Apple MacBook Pro and on digital print made with Canon imagePRESS C1+.

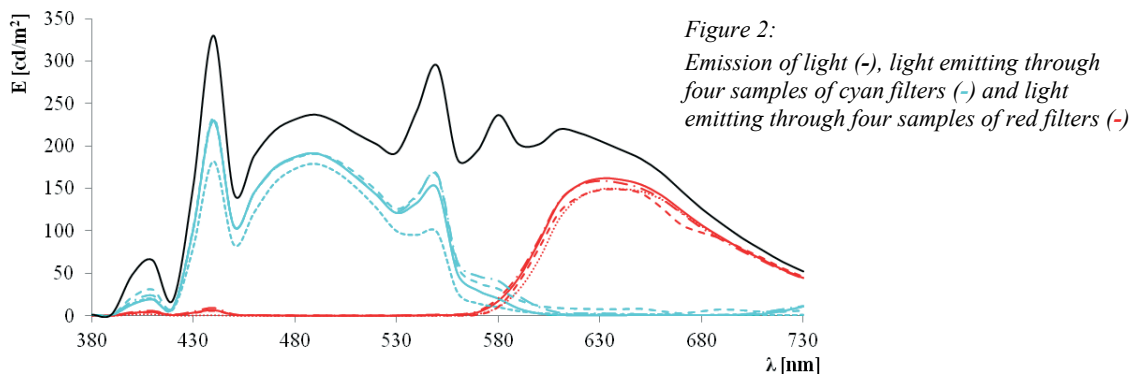
2.4. Creating a new conversion method

New conversion methods had been developed with calculating average conversion matrix out of different known conversion matrices and with adjusting them.

3. Results and discussion

3.1. Measurements of colour filters

Measuring all four filter samples has shown a great similarity between them (Figure 2). Calculated colour differences ΔE^*_{ab} between average and single *CIELAB* values were calculated and they are all lower than 6,49.



Based on the analysis of the measurements, conclusion has been made, that colour differences between different colour filters are not high enough to influence stereo effect dramatically. We believe that colour filter adaptation or correction is not needed in the process of making colour separations. Observation has been made, that anaglyph technique is indeed very suitable for wide market use, mainly because is easy to produce anaglyph glasses.

3.2. Comparison of known conversion methods

Application of different conversion matrices on prepared stereo pairs, gave us a results that can be seen on Figures 3 to 8. ColorChecker test chart has been used to measure the results. The average ΔE^*_{ab} between original and anaglyph ColorChecker test chart values were calculated and the results showed, that colour anaglyph, with ΔE^*_{ab} value 0.00 was far the best, following by half-colour anaglyph 12.09, Dubois anaglyph 17.64, optimised anaglyph 19.38, grey anaglyph 33.69 and true anaglyph 77.21.



Figure 3: True anaglyph

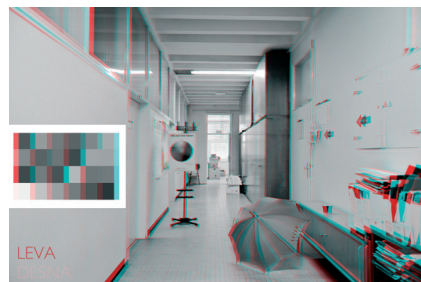


Figure 4: Grey anaglyph



Figure 5: Colour anaglyph

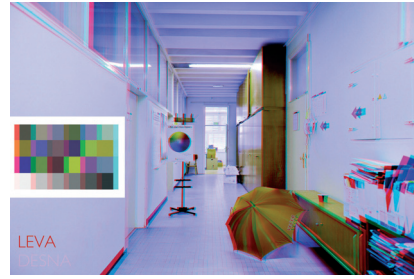


Figure 6: Half colour anaglyph

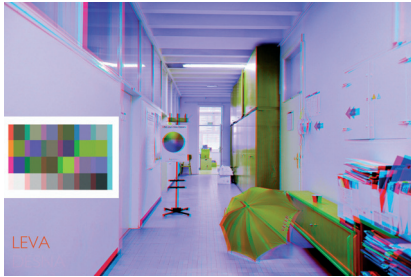


Figure 7: Dubois anaglyph

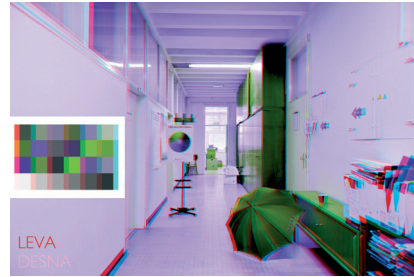


Figure 8: Optimised anaglyph

The analysis of visual comparison of different techniques showed, that the best results are produced with grey anaglyph, Dubois anaglyph and optimised anaglyph conversion techniques. On the other hand, colour anaglyph, half colour anaglyph and true anaglyph gave worst results - colour anaglyph especially.

3.3. Creation of a new conversion method

In the experiment, trying to develop better way of creating anaglyphs, an average of all conversion matrices has been made [7], producing so called experimental average anaglyph. Calculated average colour difference for ColorChecker test chart fields was 24.08 and visual evaluation was concluded as an average one (Figure 9).

$$\begin{bmatrix} r_a \\ g_a \\ b_a \end{bmatrix} = \begin{bmatrix} 0,392 & 0,494 & 0,136 \\ -0,007 & -0,006 & -0,003 \\ -0,003 & -0,004 & -0,003 \end{bmatrix} \times \begin{bmatrix} r_1 \\ g_1 \\ b_1 \end{bmatrix} + \begin{bmatrix} -0,007 & -0,015 & 0,000 \\ 0,113 & 0,720 & 0,016 \\ 0,088 & 0,177 & 0,742 \end{bmatrix} \times \begin{bmatrix} r_2 \\ g_2 \\ b_2 \end{bmatrix} \quad [7]$$



Figure 9: Anaglyph calculated with average matrix

The next step was to exclude two of the worst conversion techniques, according to colour difference. This time an anaglyph has been made with average conversion matrices calculated from matrices for producing colour anaglyph, half-colour anaglyph, Dubois anaglyph and optimised anaglyph. For the purpose of preserving grey shades in the final result, the red component values in cyan conversion matrix were corrected to zero values [8]. The reason for making so was to preserve complementary channels in each colour separation intact. Only doing so, producing perfect reproduction of grey shades when combining both, red and cyan colour separations, is possible. Calculated colour difference from the final anaglyph was 11.53 which is second best, only behind colour anaglyph that gives perfect, 0.00, result. Visual evaluation, which has been made on LCD screen, LED screen and on digital print, was the best, even better than Dubois anaglyph and optimised anaglyph (Figure 10).

$$\begin{bmatrix} r_a \\ g_a \\ b_a \end{bmatrix} = \begin{bmatrix} 0,439 & 0,447 & 0,148 \\ 0 & 0 & 0 \\ 0 & 0 & 0 \end{bmatrix} \times \begin{bmatrix} r_1 \\ g_1 \\ b_1 \end{bmatrix} + \begin{bmatrix} 0 & 0 & 0 \\ 0,095 & 0,934 & -0,005 \\ -0,018 & -0,028 & 1,057 \end{bmatrix} \times \begin{bmatrix} r_2 \\ g_2 \\ b_2 \end{bmatrix} \quad [8]$$

Calculated colour difference of 11.53 is however still very high difference, but it is compensated by the good result from the visual evaluation.



Figure 10: Anaglyph calculated with modified matrix

4. Conclusion

The development of the new, better way for accomplishing something as old as an anaglyph, was not expected, but with a help of new technologies it was not surprising. Used developed methods were not only mathematic but they also involved precise handmade corrections of the equations. Colour measurement and visual evaluation showed better result in comparison to other known techniques. The reason, why compromise anaglyph is better than other methods is in a perfect combination of viewing anaglyphs with or without anaglyph glasses. This is very important because anaglyph has to attract viewer while he is not wearing anaglyph glasses and it has to offer good stereo effect for viewers satisfaction. Having that in mind we can conclude that, this research and development of new anaglyph method is a success. Name "compromise anaglyph" has been given to the new developed technique for producing digital colour anaglyphs.

Based on correlation analysis between both comparisons (colour differences and visual evaluation) it has been concluded, that Dubois and optimised anaglyphs are the best techniques of producing good anaglyphs. Those two techniques are also most recent and most developed ones.

References

- Ahtik, J., *Techniques of Rendering Anaglyphs for Use in Art - Master thesis*. Ljubljana : University of Ljubljana, Faculty of Natural Sciences and Engineering, 2011.
- Dubois, E., *Generation of anaglyph stereoscopic images*. School of Information Technology and Engineering, University of Ottawa, Ottawa, Canada, 2000.
- Dubois, E., *A projection method to generate anaglyph stereo images*. IEEE International Conference on Acoustics, Speech, and Signal Processing, Proceedings. (ICASSP '01). Salt Lake City, UT, ZDA, 2001, Vol. 3, pp. 1661-1664.
- Gardner, R., *GretagMacbeth Color Checker Numeric Values* [online]. <<http://www.rags-int-inc.com/PhotoTechStuff/MacbethTarget/>>, 10 January 2011.
- Gleeson, S., *Wimmer's Optimised Anaglyph on Club Penguin* [online]. <<http://www.swell3d.com/2008/07/wimmers-optimised-anaglyph-on.html>>, 27 December 2010.
- Gleeson, S., *Color anaglyph methods compared* [online]. <<http://www.swell3d.com/color-anaglyph-methods-compare.html>>, 27 December 2010.
- Lindbloom, J. B., *RGB/XYZ Matrices* [online]. <<http://www.brucelindbloom.com/>>, 21 October 2009.
- Valzus, N. A., *Stereoscopy*. London : The Focal Press, 1966.
- Vierling, O., *Die Stereoskopie in der Photographie und Kinematographie*. Stuttgart : Wissenschaftliche Verlagsgesellschaft Mbh., 1965.
- Wimmer, P., *Grundlagen der Stereoskopie* [online]. <<http://pwimmer.gmxhome.de>>, 27. 12. 2010.



Printing Braille with inkjet

*Manfred Schär*¹, *Urs von Arx*², *Fritz Bircher*¹, *Reinhold Krause*¹,
*Pascal Bernet*², *Karl-Heinz Selbmann*¹

¹ Institute of Print Technology
Bern University of Applied Sciences
Engineering and Information Technology
Pestalozzistrasse 20, CH-3400 Burgdorf, Switzerland
E-mail: manfred.schaer@bfh.ch

² Bern University of Applied Sciences
Architecture, Wood and Civil Engineering
Solothurnstrasse 102, CH-2504 Biel, Switzerland

Abstract

Even today, Braille and tactile graphics for the blind are mostly printed with Braille embossers. The embossing process is rather noisy and the embossed dots are crushed easily.

In this paper, a solution for Braille printing with inkjet is presented. Thereby, the Braille dots are printed in a single shot. The dots should comply with the Braille dimensions according to the Marburg Medium standard in which the dot base diameter is 1.6 mm and the dot height is 0.5 mm. The inkjet printing system uses similar types of solenoid valves that are also used in large character inkjet markers. To print one line of Braille three valves are combined in a printhead. To print more than one line of Braille at once the printheads are stackable.

Two types of low toxic viscous Braille inks based on epoxy were formulated. Firstly, a blue light curing ink for home Braille printers and secondly a UV curing ink for library or industrial printers. The cured Braille dots are easy to read. The surface gives a solid, glass-like and low friction tactile sensation. The printed Braille was validated by a test group with the result that the achieved readability is similar to that of standard embossed Braille.

The system is particularly suited for printing Braille books for libraries or printing Braille on pharmaceutical containers since the printed Braille is robust and convenient to be read by the blind.

Keywords: Braille, inkjet, micro valve, light curing, blind

1. Introduction

History

At the Bern University of Applied Sciences (BUAS), R. Krause und F. Bircher worked on a large format inkjet printer to print on ground areas with viscous acrylic paint. The printed dots were quite big and showed interesting tactile properties. Roughly at the same time U. von Arx worked on formulations for UV curable varnishes. While discussing the results they realized that the potential of the UV curable ink and the tactile dots in combination are usable to print Braille. It was then decided to start a research project for an inkjet Braille printer.

The research project

With the start up company Touch'ink SA an implementation partner was found for the later commercialisation of the Braille printer. Together a R&D research project was submitted and later allotted by the Commission for Technology and Innovation CTI in Switzerland.

Louis Braille and Braille standards

Louis Braille (1809-1852) developed the well known Braille in 1825 as a 16 year old. A Braille character is represented by a cell of six possible tactile dots. The dot distances and the dot heights are chosen in such a way that the characters can be felt clearly by the tactile sense of the reading fingers. Historically, several Braille versions emerged worldwide due to various needs of the users. It means that the dot distances and the dot heights are different (Tiresias, 2012). In Europe the Marburg Medium standard is usually used for the Braille dimensions and common by most of the blind (Deutsche Blindenstudienanstalt e.V., 2005).

The Braille characters, according to the Marburg Medium standard consists of six possible Braille dots with a base diameter of 1.6 mm and a dot height of 0.5 mm each. The dots are arranged in a 2×3 matrix with a dot to dot distance of 2.5 mm.

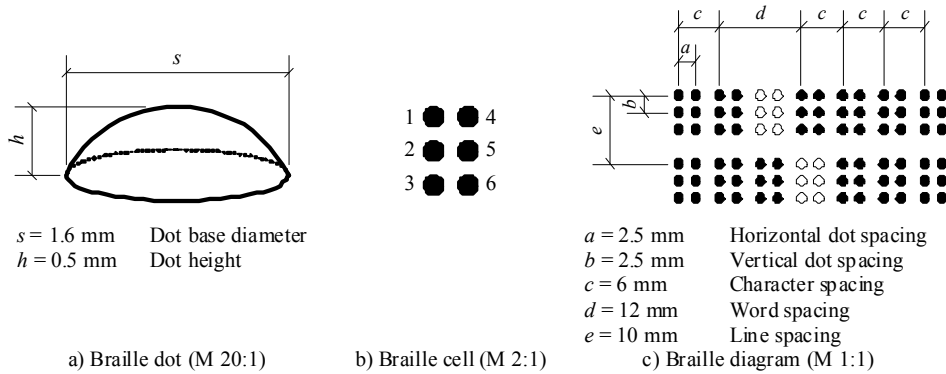


Figure 1: Braille dimensions according to the Marburg Medium standard

Braille printing with embossers

Today, Braille and tactile graphics for the blind are mostly printed with embossers, which are available in many types, e.g. for the home and personal use, for schools and for libraries. Braille printers are notorious for their loudness and annoying sound during the printing process. Additionally, embossed dots are crushed easily by applying excessive external pressure. Also, embossed Braille is worn out after some reading cycles. Usually, continuous Braille paper is needed for durable printouts.

Braille printing with inkjet

To overcome the drawbacks of the embossed Braille, the R&D project was carried out at the Institute of Print Technology with the objective to develop a silent non-impact digital Braille printing system that generates solid Braille using the inkjet technology, and is applicable for private use, and libraries. Further, it is scalable for industrial printers.

Although inkjet printing is widely used and accepted at home, at small offices and in the printing industry to produce printed media, it has not become a common alternative print system for the blind yet. The benchmark for readability is Braille embossed on Braille paper and cardboard paper rendering excellent tactile feedback.

Mass produced Braille for industrial applications

A special application of Braille is the printing on pharmaceutical cartons to comply with the Community code relating to medicinal products for human use (EU directive 2004/27/EC, 2004), which has been a mandatory regulation in 31 countries since November 2010. Braille on pharmaceutical cartons is mostly embossed with die-plates. This printing method is expedient for mass production and, further, causes no additional costs for consumers. However, the main disadvantages are the limited long term stability and the limited height of the Braille on the carton. Further, it offers only fixed text information and it is inefficient for short runs. Screen printing is another approach to print Braille but also only efficient for a long run print. Braille on packaging for medical products has been standardized and the use of the Marburg Medium standard is recommended (DIN EN 15823, 2010).

2. Methods

Screening and evaluation of the light curing ink

Generally, the ink is required to be a light curing synthetic resin. For safety reasons a blue light curing system is preferred over a UV-curing system. A laboratory screening process is used to evaluate acrylate and epoxy based resins. Also fillers and dyes are intended. The formulated inks should be evaluated for their properties before and after the printing and curing process. For the printing process the important properties are the

jetability, the viscosity of the ink and the maintaining of the dot shape until the ink is cured and solid. For the curing process a short curing time is needed and no deformation or shrinking is allowed. When cured, a good adhesion on paper, an excellent tactile sensation for readability and a low toxicity is required.

During the screening process a multivariate analysis and design of experiments software (The Unscrambler) is used to optimize the formulation of the ink for short curing times and to minimize the number of experiments. All used chemicals should be available as high-volume commodity goods too.

Calculation of the ink consumption

Braille is very voluminous compared with ordinary prints. For this reason books printed in Braille are very thick, e.g. a 10-page booklet printed on both pages measures 6.5 mm. It is also obvious that the ink consumption is considerable. Eventually, the dots have to be adapted to save ink and space but still maintaining readability.

The shape of a Braille dot is approximately a spherical segment. Therefore, the volume of a Braille dot is calculated according to equation [1].

$$V = \frac{\pi}{6} h \left(\frac{3}{4} s^2 + h^2 \right) \quad [1]$$

With the Braille dimensions according to the Marburg Medium standard the dot volume is.

$$V = \frac{\pi}{6} 0.5 \left(\frac{3}{4} 1.6^2 + 0.5^2 \right) = 0.568 \text{ mm}^3 \quad [2]$$

For an A4 cut sheet paper with the dimensions of 210 mm × 297 mm we assume a printable region of 192 mm × 270 mm on the page. With the Marburg Medium standard the page is divided into 32 characters per line and 27 lines. This means 864 characters per page or 5184 Braille dots. For an ordinary article roughly 36% of the dots are set.

Table 1: Calculated ink volume of Braille dots according to the Marburg Medium standard on an A4 cut sheet paper

Print	Dots set in %	Dots set	Volume per single page in mm ³	Volume per 100 pages in ml	Volume per 500 pages in ml
Article	36%	1866	1060	106	530
Test print	100%	5184	2945	295	1473

Screening droplet generators

Braille can be printed using the single pass or multipass method. In the single pass method the Braille dot is generated by ejecting one single drop of ink equivalent to the volume of the Braille dot which is about 500 nl. In the multipass method the Braille dot is generated by ejecting multiple droplets to build up the required dot volume of about 500 nl.

In this project the Braille dots are to be printed in a single shot to gain process speed. They are not to be built up layer for layer as in rapid prototyping machines, because the printing of a page would consume several minutes. The droplet generators should allow a printing frequency of several hundred Hertz and a dosing volume accuracy of about 10%. Also, there should be a good droplet separation from the nozzle and no satellite droplets with the use of the new high viscous ink. Available inkjet valves have to be evaluated in a laboratory test stand printing the new ink formulations. The ideal combination between inks and valves has to be determined. A high speed camera is used to study the droplet ejection and for the optimization of the nozzle geometry and printing parameters.

Curing light source

The full curing of the printed Braille dots is challenging because of the large dot height. The irradiation has to penetrate the full dot volume. Generally, UV-light has a lesser penetration depth than blue light. For the UV-curing ink a Hönle Bluepoint 4 lamp with light guide spot lamp is tested. Very promising for the blue light curing ink is also the use of high power blue LEDs as they could be integrated very easily and space saving in a printer. To prevent eye and skin irritation a blue light curing system is preferred over an UV curing system.

Printing test samples

The first printing tests of a new combination of Braille ink and printhead is usually done on substrates with a format up to 210×297 mm on a small flat bed test bench. A standardized text is printed and the resulting Braille is evaluated by the research group and the Braille test group. The printed Braille is examined for deviations in the Braille dot shapes, blisters in the dots, adhesion of the dots on different substrates, colour alterations of the cured ink, etc. The main examination tool is the sliding calliper, the measuring microscope and the Laser Scanning Microscope.

Test group

Throughout the project a test group with blind people, teachers for the blind, and representatives of organisations for the blind were invited to validate the quality of the printed Braille and to consider specifications for improvements. The test group received test samples printed on A4 cut sheet paper with different sizes of the Braille dots.

3. Results

Braille inkjet system

The projected Braille inkjet printing system mainly consists of the Braille ink, the ink container, the printhead and the curing unit which would have to be developed together in an iterative process to obtain optimal printing results.

Ink formulation

The liquid Braille ink can be formulated either as a UV or blue light curable system, using radical polymerization for acrylates or cationic polymerization for epoxies and oxetanes. Attention must be given to the O_2 inhibition of the acrylates during the curing process. UV-curing is preferred in an industrial environment since strong UV-Hg-lamps are available, and the UV shielding in a printing machine is easily implemented. In a home- and office environment a blue light curing system is preferred for safety reasons. Depending on the printing task the ink must be crystal clear or pigmented. For pharmaceutical containers a crystal clear ink is required to maintain the appearance of the container. For visually handicapped readers a pigmented ink is important to find orientation on the Braille text. In inkjet printing the viscosity of the ink is between 1...20 mPa·s. For printing Braille a viscosity up to 100 mPa·s is required to minimize ink penetration and dot spreading on the substrate. Usually, the ink is a Newtonian liquid, but with the addition of a shear thinning agent the ink will keep the shape of the Braille dot for an extended period of time without spreading. All the ingredients of an ink formulation are usually dispersed in a three roll mill.

Table 2: Formulation of the blue light curable ink

Component	Product	Producer
Monomer / Oligomer	Araldit CY 179	Huntsman
	Cyrcure UVR-6000	Dow
Initiator	Irgacure 250	Ciba
Sensitizer	(+/-)-Campherchinone	City Chemical
Accelerator	Ethyl-4-dimethylamino-benzoat	Fluka
Dyestuff	Sandoplast Blue 2B	Clariant
Rheological agent	AEROSIL R7200	Degussa

Table 3: Formulation of the UV-curable ink

Component	Product	Producer
Monomer / Oligomer	Araldit CY 179	Huntsman
	Cyrcure UVR-6000	Dow
Initiator	Irgacure 250	Ciba
Sensibilisator	CPTX	City Chemical
Co-initiator	Irgacure 127	Ciba
Dyestuff	Sandoplast Blue 2B	Clariant
Rheological agent	AEROSIL R7200	Degussa

The blue light curable ink is prone to gelling induced by ambient stray light from fluorescent lamps and sun light. The risk of clogged printheads is quite big. The printhead must be protected well from stray light. The UV curable ink is less sensitive against stray light. Usually, in closed rooms is no UV-light.

Rheological behaviour

To have a reliable droplet ejection with inkjet valves the critical value of the viscosity is about 50 mPa·s. At a temperature of 20°C the viscosity of the ink is 180 mPa·s but decreases to below 20 mPa·s at a temperature of 60°C. This is also the selected processing temperature of the ink in the printer. With temperatures above 60°C the ink starts smelling and becomes unprintable due to bubbling. The shelf life of the ink is 3...6 months. With time the ink gels and the viscosity increases. Then, reliable droplet ejection is not possible anymore, and the ink has to be disposed.

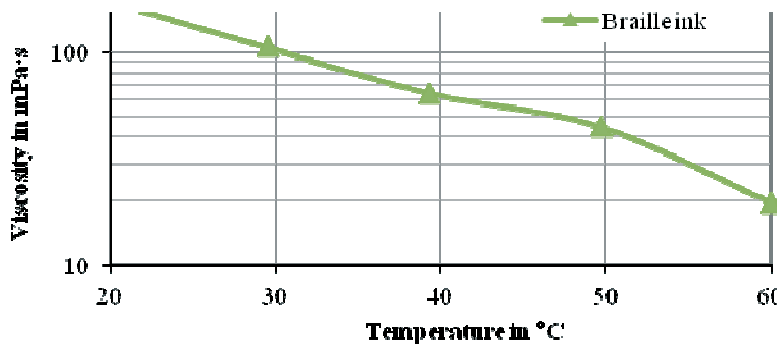


Figure 2: Viscosity vs. temperature of the Braille ink

Inkjet printing system

The single pass method is preferred, because it is assumed to have a better output performance. Thus a printhead is designed accordingly. In a first step the appropriate droplet generator is chosen among many types of micro dosing valves, piezo valves and common solenoid valves. Each droplet generator must be provided with a high speed electronic driver.

The inkjet principles, as known in home- and industrial inkjet printers, are not suited for printing Braille, because the piezo inkjet, the thermo inkjet (bubble jet) and the continuous inkjet (CIT) generate droplets which are too small. Piezo dosing valves were tested and are ideal regarding the droplet volume and printing frequency but are very expensive and wear out fast. In the end, solenoid dosing valves were chosen to generate the droplets. The droplet frequency is adequate for printing Braille. Also solenoid valves are available in larger lots and the electronic driver is easier to implement than in the other technologies. Ideally suited would be the valves from large character inkjet printers because the generated droplets are practically in the required size.

Table 4: Selection of possible droplet generator principles for printing Braille dots

Technology	Properties
Solenoid valve	Simple driver electronics, robust technology, low print frequency, low viscous fluids.
Piezo valve	Low printing frequency, also higher viscous fluids, expensive technology, high voltage driver electronics required, mechanical wearing.
Piezo inkjet	High kHz-printing frequency, generates pl-droplets.
Thermo inkjet (bubble jet)	High kHz-printing frequency, generates pl-droplets, aqueous inks.
Continous Inkjet (CIT)	High kHz-printing frequency, generates pl-droplets, conductive inks required, very expensive.

The key to success is to develop the best combination of the droplet generator and the Braille ink. This is done by using a high speed camera and/or a drop watcher to study the droplet ejection process on the nozzle. Usually, droplet ejection time is between 500 ... 5000 microseconds, and with an additional reset time the resulting droplet frequency is between 200...400 Hz.

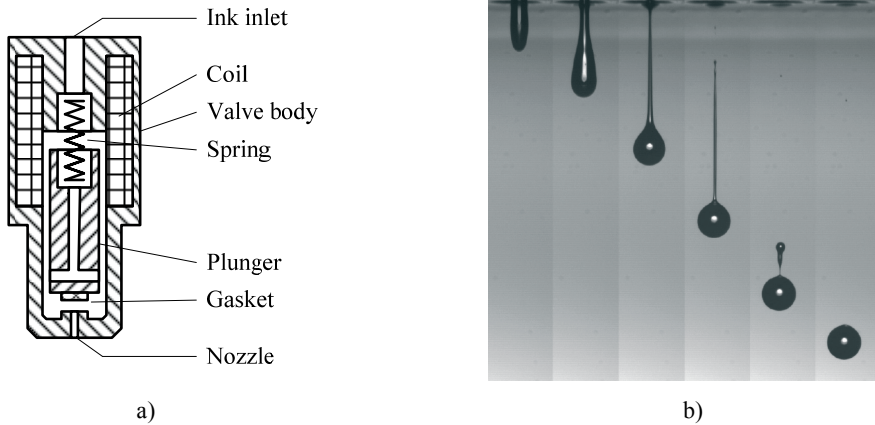


Figure 3: a) Section of a solenoid valve, b) High speed camera recording of an ejected ink droplet

The flow of the ink and the droplet volume accuracy depends on the viscosity of the ink, which is a function of the ink temperature as shown in figure 2. Therefore, a heating and temperature control system with an accuracy of $\pm 1^\circ\text{C}$ is essential.

The final printhead module for printing a single line of Braille text mainly consists of three micro valves that are arranged in a nozzle line. The ink is ejected through ceramic nozzles with 0.3 mm diameter. Before printing the ink is heated up in a flow heater at the inlet port, and the whole printhead is temperature controlled. The printhead contains the complete valve driver electronics to drive the three micro valves individually and is connected via a field bus to a Braille print server. The printhead modules are stackable. With 1...5 modules a printhead suited for pharmaceutical containers is feasible. With 32 modules an A4-format page printer for libraries could be realised for up to 60 pages per minute.

The ideal printing distance of the nozzle to the substrate is 0.5 ... 2 mm. For unevenly formed substrates an increased printing distance is required. This leads to distorted Braille with deformed and misaligned dots.

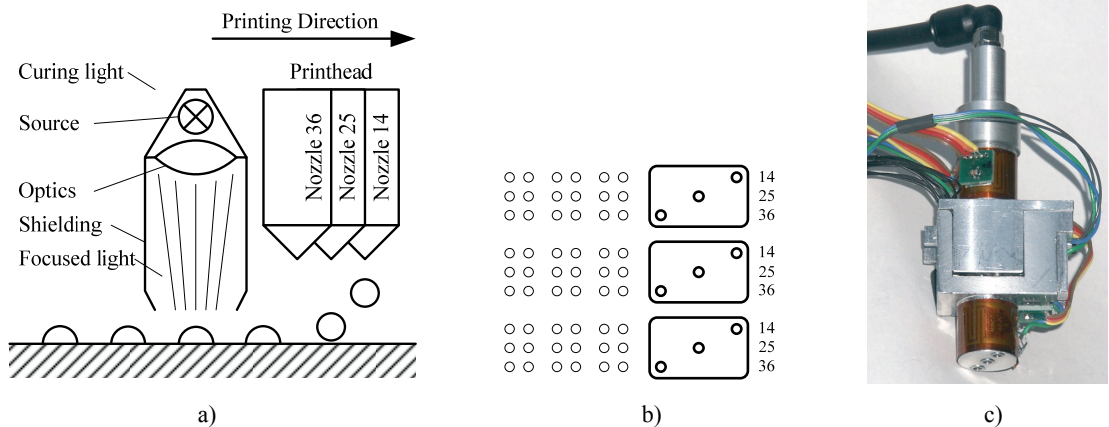


Figure 4: a) Printhead with three nozzles and the precuring light, b) The printheads can be stacked to print more than one line of Braille text at a time, c) Printhead for the home Braille printer

Curing of the printed Braille dots

For the curing of UV-ink in a roll-to-roll printer a 6 kW Hg-lamp or a 6 kW Hg-Fe-lamp is used. To cure blue light ink a 100 W blue-LED-Lamp is used. Although the layer thickness of the printed ink is up to 0.5 mm a full curing is possible. Acrylic ink cures significantly faster than epoxy ink, which shows a distinct dark curing process for some hours. Until fully cured the Braille dots are deformed by applying external forces.

The Braille dots require lamps with a curing intensity of more than 4 W/cm^2 otherwise there is not enough energy to cure the full height of the dot even at an extended period of time. Attention has to be given to the focusing effect of transparent dots that are like micro lenses.

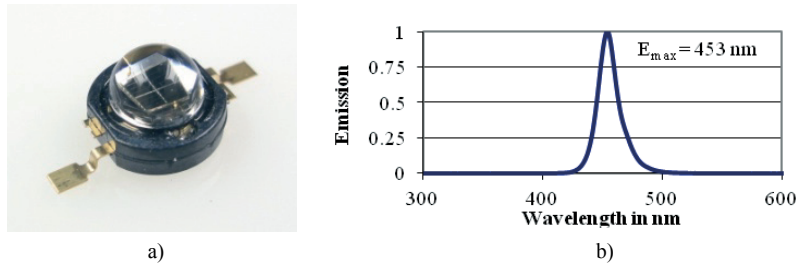


Figure 5: The blue LED lamp for the curing is made of several single LEDs, a) the used LED type is a Lumileds Luxeon LXHL-PRO2, b) the diagram shows the spectral emission of the LED with a peak wavelength at 453 nm

Printed Braille dots

The uniformity of the Braille dots depends mainly on the structure of the substrate. Fibrous substrate, such as plain paper leads to a strong deformation of the dot mainly in the direction of the fibres, but the cured ink develops a very strong adhesion with the fibres. On the other hand, polymeric substrates like polyester, polypropylene, etc. ensure an almost ideal geometrical dot shape, while the adhesion can be poor, especially when the substrate is convolved.

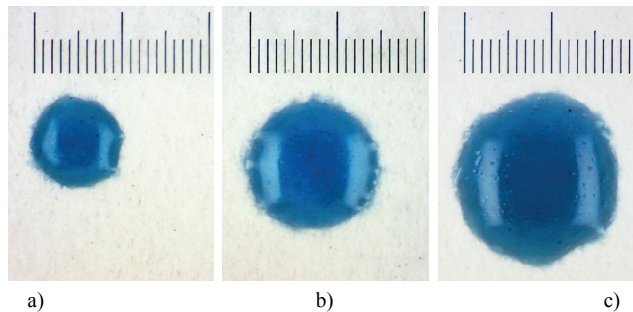


Figure 6: The Braille dots can be printed in desired sizes just by changing the printhead parameters. The shown dots were printed for the test group (scale unit = 0.1 mm), a) $s = 1.0$ mm, b) $s = 1.5$ mm, c) $s = 1.8$ mm

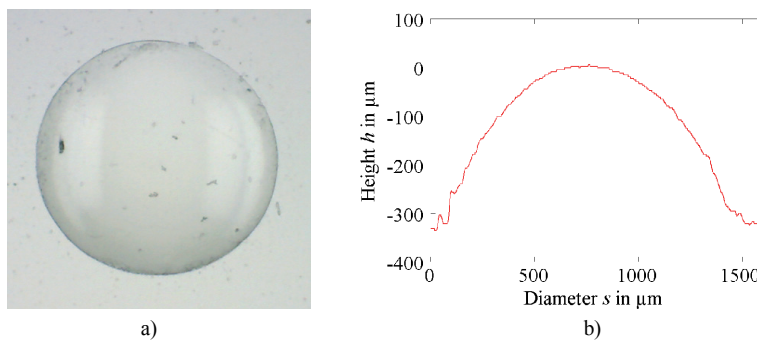


Figure 7: a) Example of a clear Braille dot printed on polyester foil, $s = 1.6$ mm, b) Section of a clear Braille dot with $s = 1.5$ mm and $h = 0.3$ mm

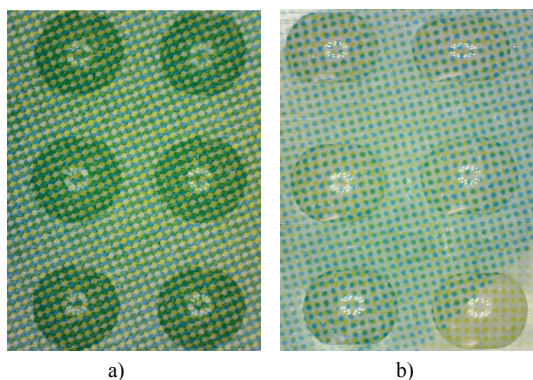


Figure 9:

Effect of the printing speed and the printing distance on the shape of the Braille dots, a) The printing speed is constant and lower than 100 mm/s and the printing distance is lower than 2 mm. The dots are spherical and well placed, the vertical dot spacing is ± 0.05 mm, b) The printing speed is more than 500 mm/s and varies more than 10%. The printing distance is more than 2 mm. The dots are elongated and misaligned

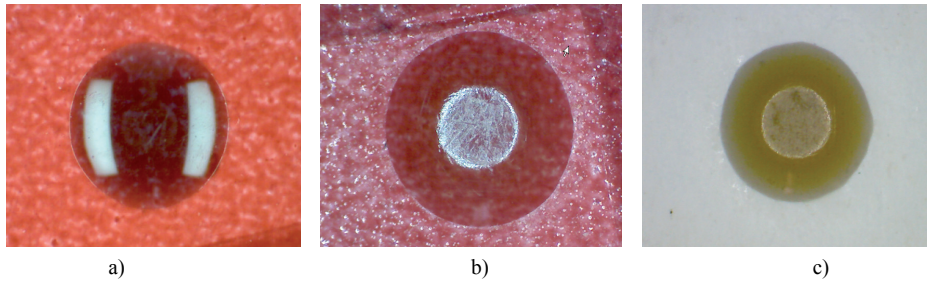


Figure 9: Durability of Braille printed on labels, a) New dot with $s = 1.6$ mm, b) Polished dot with $s = 1.9$ mm after one year of use, c) Polished dot with $s = 1.5$ mm after one year of use. The dot is slightly yellow

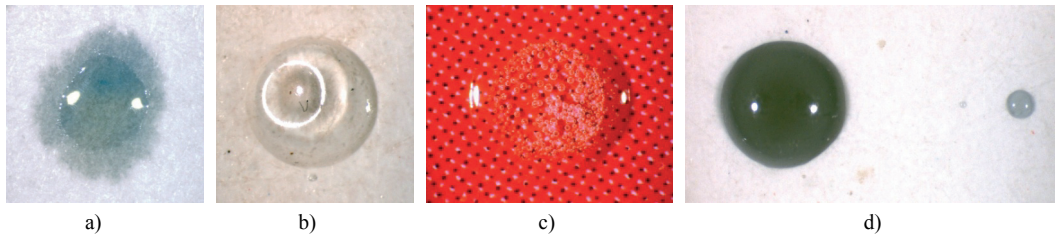


Figure 10: Examples of faulty dots, a) Without curing the ink penetrates into the paper following the fibrous structures, b) If only the surface of a dot is cured the uncured ink penetrates into the substrate leaving a sunken dot, c) Gas bubbles inside a transparent dot distort the impression of the underneath print, d) At higher print speeds satellite droplets may occur.

Evaluation by the test group

The printed test samples have been tested by 35 persons. The evaluation was done by a research office. Only un-contracted Braille was printed. As substrates were used plain A4 cut sheet paper in laser/inkjet quality with 80 g/m² and satined A4 cut sheet paper in laser/inkjet quality with 160 g/m².

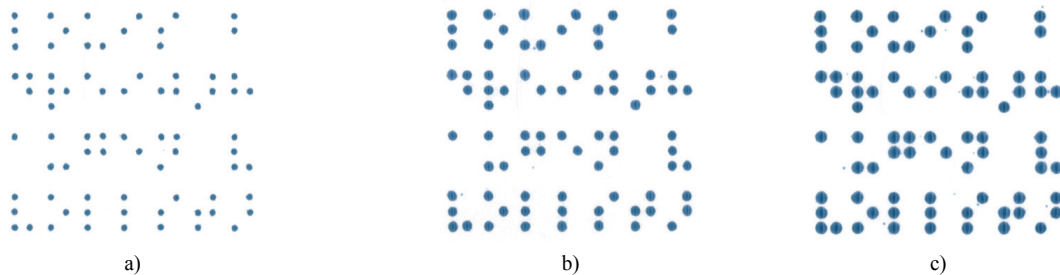


Figure 9: Pictures detail of the printed test samples (M1:1), a) sample 1, b) sample 2, c) sample 3

The conclusion of the test group is that solid Braille dots with a height < 0.2 mm are difficult to read and as well as tiresome. The optimal height of solid Braille dots for readability and long texts is 0.2...0.3 mm. Braille dots with a height > 0.3 mm are best for labels and short texts but will cause pain in the reading fingers when reading a long text. Also the plain paper is preferred over thick satinated paper.

The best Braille ink is based on epoxy. The fully cured Braille dots are easy to read, the surface gives a solid, glass-like and low friction tactile sensation which is similar to standard embossed Braille. The tactile quality of Braille printed with acrylates is currently not as good as the results with epoxy. If O₂ inhibition is not avoided, there is a layer of poorly cured ink remaining on the surface and the dots are of a soft texture. The reader has the tactile impression of a sticky surface and is disturbed in the reading flow.

Table 5: Evaluation of the Braille test prints

Sample	Dot size s in mm	Dot height h in mm	Readability	Remarks of the test group
1	1.0	0.18	poor	Dots are too small and the reading is tiresome.
2	1.5	0.25	good	Tactile feeling of the dots is equal compared with embossed Braille. Preferred for longer texts.
3	1.8	0.30	excellent	Ideal for short texts or labels.

Developed printer prototypes

At the end of the project a home Braille printer was realized. A Hewlett Packard HP Business 2600 Series Printer was taken as the base model. Then the original electronics and inkjet system was replaced by the developed Braille printhead, a blue light curing system, new driver electronics and printer driver software. Braille text is sent via a PC to the home Braille printer.

Then a roll-to-roll Braille printer was realized to print Braille labels with three lines of Braille text. Here, three Braille printheads were combined in a printer module. The ink is of a clear colour and UV curable. The Braille dots are cured immediately after printing with a standard UV-lamp from Hönle.

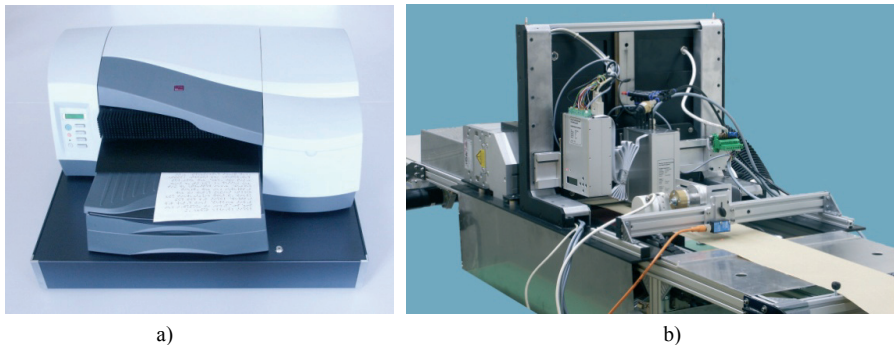


Figure 12: Realized prototypes, a) Home Braille printer, b) Roll-to-roll Braille printer for industrial applications



Figure 13: The text "Brailleprint" printed with blue light ink (M2:1)

4. Discussion

The formulation of a blue light curable Braille ink based on epoxy for home and office and the formulation of a clear UV curable Braille ink based on epoxy for industrial purposes is available. The developed printing system produces Braille according to the Marburg Medium standard but can also be adjusted to other standards of Braille. The printed Braille was validated by a test group. Braille dots with a diameter $s = 1.5$ mm and a height $h = 0.25$ mm were preferred for their good readability by the test group. The solid Braille dots show little wearing and ensure a long endurance of the printed media.

5. Conclusions

A system for printing Braille with inkjet using UV ink and blue light ink was developed and patented (WO2007/065287A1, 2007). The system is particularly suited for printing Braille on pharmaceutical containers or printing Braille books for libraries since the printed Braille is robust and convenient to be read by the blind.

Acknowledgments

QuestX, L.+R. Vicari Consulting for the evaluation of the test group and the members of the test group. The project was partially funded by the CTI (Commission for Technology and Innovation, Switzerland).

References

- Deutsche Blindenstudienanstalt e.V., (2005), *Braille-Dimensions, Marburg, Germany.*
- DIN EN 15823, (2010), *Packaging - Braille on packaging for medicinal products.*
- Directive 2004/27/EC, (2004), *Directive 2004/27/EC of the European Parliament and of the council of 31 March 2004 amending Directive 2001/83/EC on the Community code relating to medicinal products for human use.*

- Douglas, G., Weston, A., Whittaker, J., Morley Wilkins, S., Robinson, D., (2008), *Braille dot height research: Investigation of Braille Dot Elevation on Pharmaceutical Products*, University of Birmingham.
- Golob, G., Rotar, B., Šulc, D., (2011), *Braille dot height impact on the functionality and legibility of the pharmaceutical packaging*, *Advances in Printing and Media Technology*, 38, 293-299.
- Tiresias.org, (2009), *Braille cell dimensions*, http://www.tiresias.org/research/reports/braille_cell.htm
- WO2007/065287 A1, (2007), *Device and method for producing Braille script and three-dimensional structures*, *Berner Fachhochschule*, von *Arx U.*, *Bircher F.*, *Krause R.*, *Bernet P.*, *Schär M.*, filed 07. 12. 2006, published 14. 06. 2007.

Understanding graphic protection methods in print production

Branka Morić Kolarić¹, Ivan Budimir², Jana Žiljak Vujić³

¹ Narodne Novine Corp.
Savski gaj, XIII. put 6, HR-1020 Zagreb, Croatia
E-mail: bmorice@nn.hr

² Faculty of Graphic Art Zagreb
Getaldićeva 2, HR-10000 Zagreb, Croatia
E-mail: ivan.budimir@grf.hr

³ The Polytechnic of Zagreb
Vrbik 8, HR-10000 Zagreb, Croatia
E-mail: janazv@tvz.hr

Abstract

The aim of this investigation was to find out the public perception of different graphic protection methods, as well as differences in the perception of visible and invisible methods. The results obtained, as well as similar investigations, can serve as a guideline to the printers and publishers and end-users in for the security printing, thus developing methods that will be more efficient in production and application. The investigation was carried out by a poll, conducted on examinees of a control group and different experimental groups, consisting of students and experts with skills and background in printing technology.

Graphic variables describe knowledge and implementation of different types of graphic protection: for special types of print, special inks and papers. Optical variables of graphic protection describe sizes which define quality. It was necessary to examine which elements of the graphic protection the target groups are best acquainted with and which they trust the most.

The most recognized graphic protection methods on the paper are watermark and UV fibers. In print it is hologram, while on inks they are UV and IR inks. The most efficient anti-counterfeiting methods of graphic protection considered by examinees are: UV fibre, Hologram and IR ink.

It can be concluded that the awareness of graphic protection methods on paper in print and on ink is highly positively correlated with the reliability in their efficiency (Spearman's coefficient of range correlation). It is therefore necessary to develop awareness and specific knowledge's of graphic protection.

Keywords: protection of print products, security elements and technologies, UV fibre, Hologram, IR ink

1. Introduction

Graphic protection development emerged from the technology of making security and identification documents. This investigation has the aim of directing printers and publishers towards appropriate degree of required protection. In mass print production, improvement of the presses with a new design of security elements, which in a different way approaches the issue of top quality document, is being ensured in the ever growing range. The security design is applied to an expanded range of products such as bills, passports, bank cards, packaging, documents and IDs by introducing a blend of ultra-violet and infra-red technologies (Žiljak V. et al., 2009).

A plan is being developed about how to completely change the way the complete conventional printing methods is working. The level of the new individual protections creates a document designed in a unique shape of raster elements (Žiljak I. et al., 2009). At the same time, publishers, printers and end users have a secure insight in the importance and functionality of graphic protections technologies. The design has been updated on the graphic products which are made on official state level, with a goal to achieve an actual modern state of security printings.

Through this research, classification of protective elements has been carried out so as to determine which of them are desirable, necessary or required and by doing so assessment of graphic protection was carried out.

Hierarchy of values of graphic protection serves as an orientation to the graphic experts. Within this, first investigation on knowledge and perception of the methods of protection has been carried out.

2. Methods

A scale of values for printed products was determined using a system of questioning and data processing. The questionnaire was carried out among the examinees from a control group and other groups comprising of students that are oriented to graphic technology. Results showed that the examinees better acquainted with graphic protection were more aware of the importance of implementing it, which explains why a higher level of awareness should be induced. For instance, along with printing specimens, brochures which specify each installed protection are issued to help the users recognize protection implemented into a product.

Graphic variables describe knowledge and implementation of different types of graphic protection: for special types of print, special inks and papers and special types of printing machinery that are not present in standard graphic environment. Optical variables of graphic protection (Žiljak, 1994) are: UV fluorescent invisible security ink, infrared ink, iridescent OVI (Optical Variable Ink), magnetic, electrical and metallic ink; on paper: watermark, UV Fibre & Fluorescence Fibre, optical data fibres, protective metallic thread; and in print: iris print, intaglio, offset printing method, screen-printing method, gravure printing method, kinegram, hologram, miniprinting/microtext, holographic stripe, latent picture (Table 1). They describe sizes which define quality.

Table 1: Optical variables of graphic protection methods offered in the poll

Graphic protection		Number of graphic protection methods
On paper	Watermark, UV Fibre & Fluorescence Fibre, Optical data fibres, Protective metallic thread	5
In print	Iris print, Intaglio, Offset printing, Screen-printing, Gravure printing, Kinegram, Hologram, Miniprinting/Microtext, Holographic stripe, Latent image	10
In ink	UV fluorescent invisible security ink, Infrared ink, Iridescent OVI (Optical Variable Ink), Magnetic, electrical and metallic inks	6

It was necessary to examine which elements of graphic protection the target groups are best acquainted with and which they trust the most.

Analysis of graphic protection understanding and its applications was conducted by questioning 643 examinees (Table 2). Examinees were divided into two groups: control and experimental group. Experimental group consisted of students oriented to the field of graphic arts.

Table 2: Groups of examinees

Groups of examinees		Number of examinees
Group 1	Control group (general public)	198
Experimental groups:		
Group 2	Undergraduate students of the Polytechnic of Zagreb (TVZ), 1 st term	157
Group 3	Undergraduate students of TVZ, 3 rd term	43
Group 4	Undergraduate students of the Faculty of Graphic Arts Zagreb (GRF), 1 st term (design + technology)	94
Group 5	Undergraduate students of GRF, 3 rd term (design + technology)	79
Group 6	Graduate students of GRF, 1 st term	10
Group 7	Graduate students of GRF, 3 rd term	30
Group 8	Employees of printing companies dealing with the protected forms	22
Group 9	Forensic experts & scientists in the field of graphic security technology	10
Total		643

Knowledge and perception of protected printed products was determined with all the examinees.

3. Results and analysis

The analysis of knowing the graphic protection and its applications has been made by a poll carried out over 643 examinees. The experimental group consisted of students who are oriented towards the graphic trade. The control group consisted of 107 examinees (Group 1), while the experimental group contained six groups with 414 examinees in total (Group 2 had 157; Group 3 had 43; Group 4 had 94; Group 5 had 79; Group 6 had 10; Group 7 had 30; Group 8 had 22 and Group 9 had 10 examinees). Examinees were divided into control and experimental groups. The level of knowledge about graphic protection has been established with all the examinees. Most of the examined persons have a very clear concept of graphic protection and most of them are familiar with all the most important types of graphic protections. Each examinee, in average, knows about three protections on paper, four protections in print and two protections in ink (Table 3).

Table 3: Average number of graphic protection methods that the examinees, divided into groups, are acquainted with

Group	Average number of graphic protection of paper known to individual examinee	Average number of graphic protection of print known to individual examinee	Average number of graphic protection of ink known to individual examinee
	Max. = 5	Max. = 10	Max. = 6
Group 1	2.21	1.88	1.71
Group 2	1.93	1.77	1.84
Group 3	2.21	1.79	1.23
Group 4	2.12	2.33	1.93
Group 5	1.95	2.81	2.04
Group 6	2.00	4.60	2.00
Group 7	3.17	5.60	3.27
Group 8	3.27	3.73	2.27
Group 9	4.80	10.00	5.60

It was determined that most examinees have a clear apprehension of graphic protection. Most examinees are acquainted with the most significant types of graphic protection (Table 4).

Table 4: The percentage of graphic protection that knows one examinee

Groups	The percentage of graphic protections known by individual examinee		
	On paper	In print	In ink
Group 1	44.20%	18.80%	28.50%
Group 2	38.60%	17.70%	30.67%
Group 3	44.20%	17.90%	20.50%
Group 4	42.40%	23.30%	32.17%
Group 5	39.00%	28.10%	34.00%
Group 6	40.00%	46.00%	33.33%
Group 7	63.40%	56.00%	54.50%
Group 8	65.40%	37.30%	37.83%
Group 9	96.00%	100.00%	93.33%

Table 5: The most popular types of graphic protection of paper, print and ink.
Data shown below represent the best known protection among examinees

Groups	The most popular types of graphic protection on paper		The most popular types of graphic protection in print		The most popular types of graphic protection in ink	
	Protection method	% of examinees	Protection method	% of examinees	Protection method	% of examinees
Group 1	Watermark	85%	Hologram	48%	UV ink	55%
Group 2	Watermark	81%	Hologram	35%	UV ink	60%
Group 3	Watermark	88%	Miniprinting/microtext	37%	UV ink	42%
Group 4	Watermark	84%	Method of gravure print	45%	UV ink	60%
Group 5	Watermark	92%	Hologram	43%	UV ink	84%
Group 6	Watermark	90%	Hologram	100%	Infrared ink	70%
Group 7	Watermark	93%	Hologram	87%	UV ink	93%
Group 8	UV fibre	95%	Hologram	95%	UV ink	68%
Group 9	UV fibre, watermark, security thread	100%	Intaglio printing, iris printing, gravure print, offset printing, screen printing miniprinting, kinogram, metallic thread, latent picture, hologram	100%	Iridescent OVI (Optical Variable Ink), UV ink, Infrared ink	100%

The first group, the control group, is well acquainted with graphic protection, which is visible from percentages shown in the Table 5 (85% examinees of the control group is familiar with watermark). Most examinees from all groups are acquainted with the following: paper watermark, UV fibre (fluorescent threads or granules) on paper, UV ink, infrared protection (Pap et al., 2010) and holograms (Table 5).

Answers of examinees professionally oriented towards the graphic protection (forensics and researchers) show that they are acquainted with the protection much better than the other groups of examinees (Figure 1).

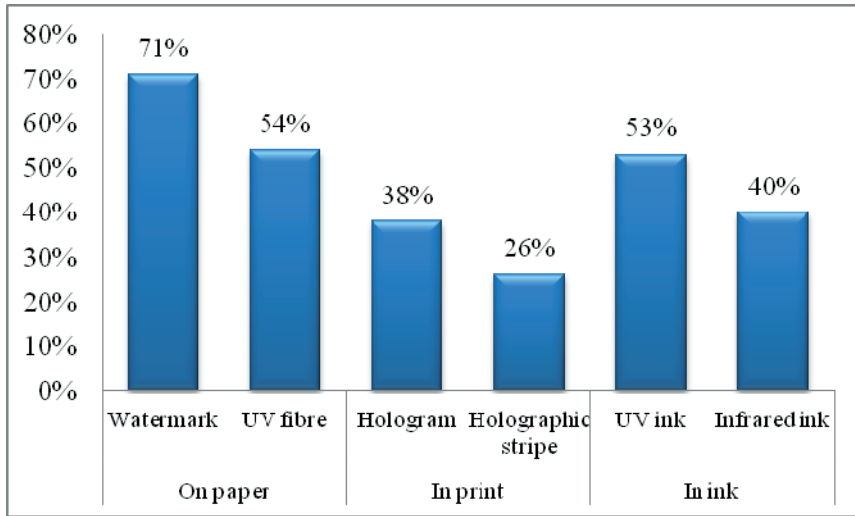


Figure 1: Recognition of graphic protection (643 examinees = 100%)

The most recognized graphic protection methods on the paper are watermark and UV fibers. In print it is hologram, while on inks they are UV and IR inks.

Examinees from Group 8 are working in print and post-print, in a printing house producing protected forms. It was proved that Group 8 is better acquainted with visible protections: (holograms and UV fibres), but less with hidden methods (mini characters, microtext).

4. Application of anti-counterfeit protection

The examinees consider the application of UV fibre on paper, holograms in print, and UV ink, to be most efficient anti counterfeit types of protection (Table 6).

Table 6: Types of anti-counterfeit protection that the examinees think are most efficient are shown in percentages/per group in the table

Group	The most efficient anti counterfeit paper security		The most efficient anti counterfeit print security		The most efficient anti counterfeit security of ink	
	Protection method	% of examinees	Protection method	% of examinees	Protection method	% of examinees
Group 1	UV fibre	42%	Hologram	44%	UV ink	31%
Group 2	UV fibre	39%	Hologram	32%	UV ink	29%
Group 3	UV fibre	44%	Hologram	23%	Optical Variable Ink (OVI)	33%
Group 4	UV fibre	40%	Hologram	29%	Optical Variable Ink (OVI)	31%
Group 5	UV fibre	39%	Hologram	27%	Infrared ink	30%
Group 6	UV fibre	30%	Hologram	30%	Infrared ink	20%
					Optical Variable Ink (OVI)	20%
					UV ink	20%
Group 7	UV fibre	33%	Hologram	53%	Infrared ink	40%
Group 8	UV fibre	68%	Hologram	45%	UV ink	41%
Group 9	Fibers with text	44%	Iris print	50%	Infrared ink	40%

These methods of graphic protection are considered by examinees as the most efficient anti-counterfeiting (Figure 2).

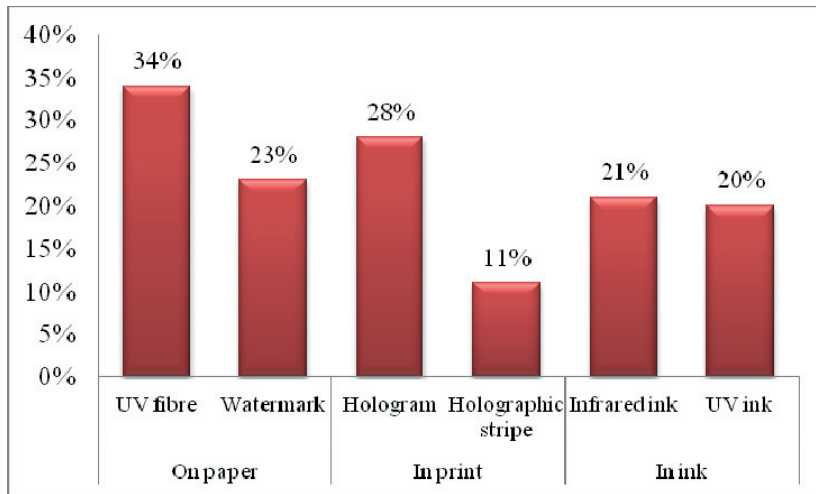


Figure 2: The most efficient anti-counterfeit graphic protection methods (643 examinees = 100%)

It was determined that the recognition of graphic protection methods on paper, in print and on ink is proportional with the confidence in their efficiency (Figure 3). It is therefore, necessary to introduce education and develop specific knowledges on these methods.

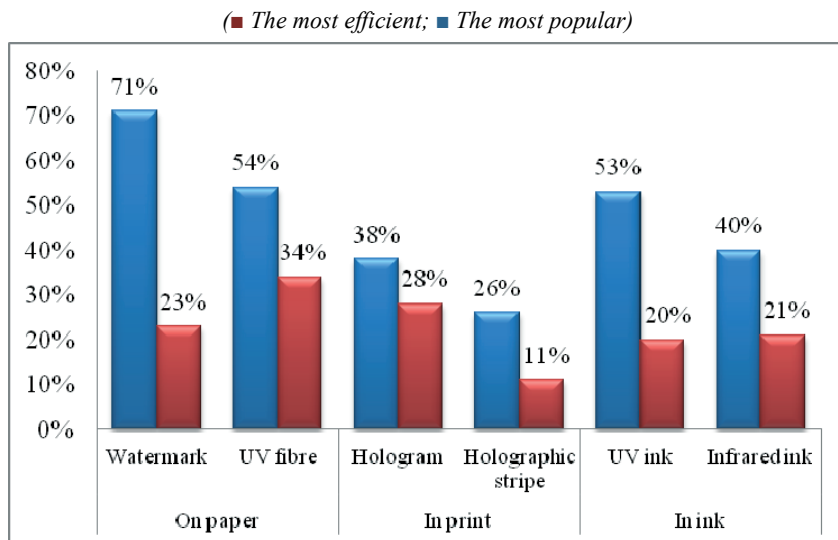


Figure 3: Relation between the most popular and the most efficient methods

With correlation coefficients (Asimov, Maxwell, 2010) the relation was determined between knowledge of all kinds of graphic protections offered to the examinees (Table 7).

Table 7: Correlation coefficients among variables, showing number of known graphic protections according to groups, with the level of significance $p < 0.05$

Average number of protection methods known to examinees by groups in:	On paper	In print	In ink
On paper	1.00	0.62	0.71
In print	0.62	1.00	0.84
In ink	0.71	0.84	1.00

Results in Table 7 are showing high to very high positive correlation among observed variables, which represent an average number of known protection methods on paper, in print and ink for examinees according to the groups.

By the means of statistical double-sided test of proportions (Vining, 2011) (Table 8), it was examined which groups are differing among each other in relation to those groups whose proportions are mutually not different. A hypothesis was examined that the proportion shares - generally marked as P_x and P_y - are equal. If their common value is marked with P_0 , the statistics used here is linked to the normal distribution of random variable Z :

$$\hat{Z} = \frac{\hat{p}_x - \hat{p}_y}{\sqrt{\frac{P_0(1-P_0)}{n_x} + \frac{P_0(1-P_0)}{n_y}}}. \quad [1]$$

Estimation of common unknown proportional share noted in Eq. 1, is calculated with its estimator of the form:

$$\hat{p}_0 = \frac{n_x \hat{p}_x + n_y \hat{p}_y}{n_x + n_y}. \quad [2]$$

Empirical p value of this test was obtained by the equation calculated with the program package Statistica 7:

$$p\text{-value} = 2P(Z > \hat{z}) \quad [3]$$

For this double-sided test the zero hypothesis is:

H_0 : proportions of knowledge of all graphic protections by groups are equal

contrary to the alternative hypothesis:

H_A : proportions of knowledge of all graphic protections by groups are different.

Hypothesis is confirmed or rejected according to the calculation of p value (Šošić, 2004), or more precisely, proportion of number of graphic protection methods, known to examinees, statistically is significantly different if p - value < 0.05 .

Table 8: Double-sided test of statistical significance, i.e. of differences of p -value between two proportions of knowledge of all graphic protections by groups of two independent samples

Group	Group 1	Group 2	Group 3	Group 4	Group 5	Group 6	Group 7	Group 8	Group 9
Group 1	1	0.1226	0.0974	0.1751	0.0014	0.0001	0.0000	0.0000	0.0000
Group 2	0.1226	1	0.8283	0.0016	0.0000	0.0000	0.0000	0.0000	0.0000
Group 3	0.0974	0.8283	1	0.0058	0.0002	0.0000	0.0000	0.0000	0.0000
Group 4	0.1751	0.0016	0.0058	1	0.1928	0.0011	0.0000	0.0000	0.0000
Group 5	0.0014	0.0000	0.0002	0.1928	1	0.0090	0.0000	0.0002	0.0000
Group 6	0.0001	0.0000	0.0000	0.0011	0.0090	1	0.0001	0.5204	0.0000
Group 7	0.0000	0.0000	0.0000	0.0000	0.0000	0.0001	1	0.0006	0.0000
Group 8	0.0000	0.0000	0.0000	0.0000	0.0002	0.5204	0.0006	1	0.0000
Group 9	0.0000	0.0000	0.0000	0.0000	0.0000	0.0000	0.0000	0.0000	1

(red figures indicate groups that are not differing)

Examinees from Group 9 - forensic experts and scientists with the background of graphic protections - are showing knowledge of all methods offered in the poll, that is far overcoming the knowledge of all other groups. It can be concluded that statistically, from Group 1 proportions are not different for Groups 2, 3 and 4, from Group 2 proportions of the Group 3. There are no significant differences of Groups 4 and 5, as well as Groups 6 and 8. That means that the same level of knowledge of graphic protection is determined for general public in control group, as well as for students from Groups 2, 3 and 4. Equal level of knowledge is found for undergraduate students of 1st and 3rd term of TVZ. Graduate students of 1st term at GRF are showing the same levels of knowledge as workers in printshops producing protected documents. Of all compared, Groups 6, 7, 8 and 9 are standing out, i.e. employees in printing business and students of 1st and 3rd year of GRF, as well as forensic experts and scientists in the field of graphic security technology. If the latter group is left out, which is - with knowledge of 96% of all offered methods far above all other groups, the total highest level of knowledge are showing graduate students of GRF (Figure 4). Out of them, the most complete knowledge of 57% of all offered methods, have the students of the 3rd year of GRF. This is the result of a

number of courses students are taking during their studies. Examinees of this group have shown better knowledge than examinees of all other groups, including workers in printing companies, except examinees from Group 9.

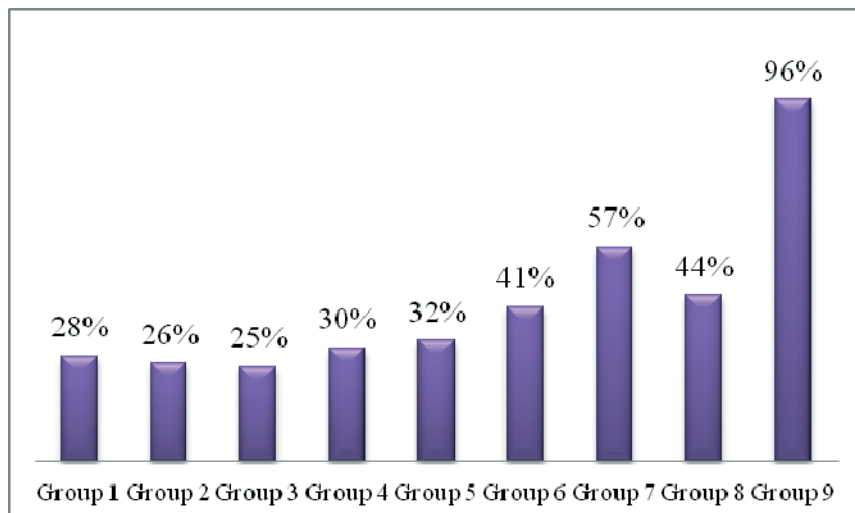


Figure 3: Percentage of all graphic protection methods recognized by examinees

Since it was confirmed that Group 7 showed the highest level of knowledge on all methods of graphic protection (except forensic experts), their knowledge will be furthermore compared with the remaining groups, specifically in recognizing protections in paper, print and ink. Analysis was conducted by a double-sided test of statistical relevance, with the results presented in Tables 9a to 9c.

Table 9a: Double sided test of statistical relevance, i.e. p-values of differences of two proportions of knowledge of graphic protections on paper between Group 7 and all other groups

Group	Group 1	Group 2	Group 3	Group 4	Group 5	Group 6	Group 8	Group 9
Group 7	0.0001	0.0000	0.0004	0.0000	0.0000	0.0049	0.7404	0.0000

It can be concluded from the above table that examinees from Group 7 know a higher number of graphic protection methods on paper than all other groups, except Group 8, with equal level of knowledge of these methods. Forensics are showing more knowledge than the examinees from Group 7.

Table 9b: Double sided test of statistical relevance, i.e. p-values of differences of two proportions of knowledge of graphic protections in print between Group 7 and all other groups

Group	Group 1	Group 2	Group 3	Group 4	Group 5	Group 6	Group 8	Group 9
Group 7	0.0000	0.0000	0.0000	0.0000	0.0000	0.0833	0.0000	0.0000

Table 9b shows that Groups 6 and 7 are not much differing in knowledge of graphic protection in printing, while in all other cases examinees from Group 7 are showing more comprehensive knowledge of protection methods in printing than examinees from other groups, except forensics.

Table 9c: Double sided test of statistical relevance, i.e. p-values of differences of two proportions of knowledge of graphic protections in ink between Group 7 and all other groups

Group	Group 1	Group 2	Group 3	Group 4	Group 5	Group 6	Group 8	Group 9
Group 7	0.0000	0.0000	0.0000	0.0000	0.0000	0.0035	0.0032	0.0000

Similar results as in previous two tables can be observed in Table 9c, where it is shown that the most comprehensive knowledge on protection methods in ink have the examinees of Group 7, excluding Group 9, which shows the most complete knowledge on this kind of graphic protection.

With a double-sided test of statistical relevance, i.e. *p-values* of difference between two proportions of knowledge of all graphic protection by groups of two independent samples, it was shown that the best knowledge of all methods of protection on paper, in print and in ink have the examinees of Group 7, that is graduate students of the 3rd term of GRF, not considering forensic experts, which - as could have been expected - have the greatest knowledge on graphic protections.

In the Table 10 Spearman's coefficients of range correlation (Soong, 2004) are calculated between knowledge of graphic protections and confidence in the efficiency of specific methods on the paper, in print and in ink.

Table 10: Spearman's coefficients of range correlation between knowledge of graphic protections on the paper, in print and in ink and confidence in the efficiency of specific methods. Coefficients are calculated for examinees of the control group, with the level of relevance $p < 0.05$

	Paper	Print	Ink
Spearman's coefficient r_s of range correlation	0.800	0.147	0.771
Degree of correlation	Very highly positive	Low positive	Very highly positive

It was confirmed on the examinees from the control group that very high positive correlation is existing between knowledge of graphic protections on the paper and in ink and confidence in their efficiency, but low positive correlation between knowledge of graphic protection in print and confidence in its efficiency.

Table 11: Spearman's coefficients of range correlation between knowledge of graphic protections on the paper, in print and in ink and confidence in the efficiency of these protection methods. Coefficients are calculated for examinees for the experimental group, which includes groups from 2 to 9, with the level of relevance $p < 0.05$

	Paper	Print	Ink
Spearman's coefficient r_s of range correlation	0.798	0.628	0.850
Degree of correlation	Very highly positive	Very highly positive	Very highly positive

Measured by the Spearman's coefficient of range correlation, a very high positive range correlation is existing between the level of knowledge of graphic protections on the paper in print and in ink and confidence in their efficiency. Based on this method, it was confirmed that the examinees have greater confidence in the protection methods they know better.

5. Conclusion

The direction of a decision about the type of printing technology for the security graphics has been established on being familiar with this issue in the circulation of documents. Results about the users' readiness on the efficiency of protections from the new printing technologies are being evaluated. Already known elements of protection, as well as those elements of protection that can be recognized and that the users trust the most are mostly applied.

The importance of introducing the graphic structure and the hierarchy of graphic protection evaluation has been pointed out, which presents a guideline to the quality of applying the graphic elements of protection. This contributes to the implementation of advanced protective graphic elements and methods. Design and choice of graphic protection is set according to the product which is to be protected and the method the protection is applied. The advantage is given to the solutions that are implemented in in-site production such as: watermark, applying holograms, UV printing ink, infrared printing ink, miniprinting, microtext. It is necessary to frequently explore and develop all kinds of graphic protection so that innovations and innovative solutions can be developed and to stay ahead of potential counterfeiters.

For that reason it is necessary to develop specific knowledges on graphic protections, which are to a great extent given at GRF. This was verified with a double-sided proportion test, which showed that the examinees of this group poses the highest level of knowledge on all involved graphic protection methods, with the exception of professional forensic experts and scientists oriented towards this field. The aim is to increase awareness on the importance of graphic protections and the level of knowledge in a part of the student

population, which would additionally improve the confidence in the efficiency of protection methods, thus enabling the real security of the aforesaid methods.

It is obviously necessary that printing companies should secure and monitor the development of protection and continue introducing new protective programs by routing the production towards more efficient protection of their printed products. In addition, scientific and technological development of graphic protection should be introduced in appropriate graphic-oriented study programmes.

References

- Asimov, L. A., Maxwell, M. M., (2010), *Probability and Statistics with Applications: A Problem Solving Text*, ACTEX Publications, Winsted, CT
- Pap, K., Žiljak, I., Žiljak Vujić J., (2010), *Image reproduction for Near Infrared Spectrum and the Infrared Theory*, The Journal of Imaging Science and Technology, Vol. 53, No. 1, pp. 1-9
- Soong, T. T., (2004), *Fundamentals of Probability and Statistics for Engineers*, John Wiley Sons Ltd., Chichester
- Šošić, I., (2004), *Primijenjena statistika (in Croatian)*, Školska knjiga, Zagreb (in Croatian)
- Vining, G., Kowalski, S., (2011), *Statistical Methods for Engineers*, Third Edition, Brooks/Cole, Cengage Learning, Boston
- Žiljak, I., Pap, K., Žiljak Vujić, J., (2009), *Infrared security graphic*, FotoSoft, Zagreb
- Žiljak, V., (1994), Kuna. *Papirnati novac Republike Hrvatske (in Croatian)*, Zagreb
- Žiljak, V., Pap, K., Žiljak, I., (2009), *CMYKIR security graphics separation in the infrared area*, Infrared Physics and Technology, Vol. 52., No. 2-3, Elsevier B.V. pp. 62-69



Accelerated light aging of digital prints

Ákos Borbély, Csaba Horváth, Rozália Szentgyörgyvölgyi

Óbuda University
Doberdó út. 6, H-1034 Budapest, Hungary
E-mail: akos.borbely@rkk.uni-obuda.hu

Abstract

Products exposed to sunlight will fade, and loose color contrast apparently. Resistance to fading is a crucial problem especially in the case of high quality products. A close match is desired between the optimum and the target lifetime of printed products placed outdoors or in a store window. Most if not all the components of the printing ink (e.g. pigments, solvent) are responsible for the resistance against irradiation, temperature and other weathering conditions.

Accelerated aging devices simulate environmental parameters reliably, they provide stable irradiation, temperature and measurement conditions. While weathering instruments are popular laboratory devices, the effects of aging on the color quality of prints are less studied.

Our research work was aimed at the investigation and understanding of the parameters and processes of aging in case of prints produced by digital printing technologies. The study focused on the changes in visual quality of test prints on different substrates. We used Atlas Suntest XLS+ weathering instrument to investigate the resistance of digital prints against filtered sunlight. The analysis of the results revealed how the parameters of print optical quality gradually deviated from the original values.

Keywords: accelerated aging, artificial weathering, digital printing, color quality

1. Introduction

Weathering is the adverse response of material or products to climate, often causing unwanted and premature product failures. Customers spend billions of Dollars or Euros every year to maintain products that inevitably degrade and to replace products that fail as a result of exposure to outdoor environment account for a significant portion of the total cost. There is opportunity to prevent deterioration and premature product failure through chemical and mechanical stabilization and through weathering tests (static weathering, laboratory accelerated weathering, natural accelerated weathering) to assess a material's durability. Many different testing options are available. The best option depends on the applications and objectives. For product development, it is vital to understand how to properly design and conduct these tests. The three factors that cause degradation are solar radiation (light energy), temperature, and water (moisture). But not just "how much" of each of these factors ultimately causes degradation to materials, because different types of solar radiation, different phases of moisture, and temperature cycling have a significant effect on materials on exposure. These factors, in conjunction with secondary effects such as airborne pollutants, biological phenomena, and acid rain act together to cause "weathering" (Atlas Weathering Testing Guidebook, 2004; Rahauser, Schönlein, 2011).

The solar radiation that reaches the earth's surface consists of wavelengths between 295 and 3000 nanometer. This terrestrial sunlight is commonly separated into three main wavelength ranges: ultraviolet (UV), visible (VIS) and infrared (IR). Wavelengths between 295 and 400 nm are considered the ultraviolet (UV) portion of the solar spectrum, making up between 4-7% of the total radiation. Ozone in the stratosphere absorbs and essentially eliminates all radiant energy below 295 nm. Extremely sensitive instruments may detect radiation below 295 nm, but this amount is considered negligible by most experts. The discussion of direct and diffuse radiation is important when considering radiant energy received at different orientations to the sun.

The result of the degradation characteristics of a material as a result of radiation depends on:

- the quality and quantity of radiant energy the material is exposed to,
- the wavelengths of radiation absorbed by the material,
- whether or not the absorbed radiation has enough energy to cause a chemical change, which could lead to material degradation.

The *temperature* of materials exposed to solar radiation has an influence on the effect of the radiation. Also, the temperature of material exposed to natural sunlight is determined by number of factors. Specimen surface temperature is a function of ambient temperature, specimen solar absorptivity, solar irradiance, and surface conductance.

Water is one of the substrates in our environment that is everywhere, whether in the form of humidity, rain, dew, snow, or hail. All materials used outdoors are exposed to these influences. Water also can be directly involved in the degradation reaction in a chemical sense (Zielnik, 2004; Bond, 2011).

The apparent sign of degradation in case of products exposed to sunlight is fading, loss of color contrast. Resistance to fading is a crucial problem especially in the case of high quality printed products, fading should be minimal during the target lifetime of products placed outdoors or in a store window. Most if not all the components of the printing ink (e.g. pigments, solvent) are responsible for the resistance against irradiation, temperature and other weathering conditions (Goudie, Viles, 2008). Therefore it is important to collect correct information on the weather resistance and aging properties of a certain product. There are numerous reliable methods regarding artificial aging and weathering of different products. Controlled outdoor testing is the most common, during which the simultaneous effect of the environment, weather and exposure to sunlight is investigated. The disadvantage of this method is the dependence on local climate and changing measurement conditions. Accelerated aging devices simulate environmental parameters more reliable, they provide stable irradiation, temperature and measurement conditions. While weathering instruments are popular laboratory devices, the effects of aging on the color quality of prints is less studied.

Our research work was aimed at the investigation of the changes of parameters that describe visual quality during aging in case of prints produced by digital printing technologies.

2. Experimental

We used an Atlas Suntest XLS+ weathering testing instrument for the aging of the specimen, the device monitored irradiance, temperature and relative humidity of the test chamber. A window glass filter was applied to simulate terrestrial sunlight entering through the glass window of a display compartment. Average irradiance on the sample plane was 50 W/m^2 in the 300 nm - 400 nm range, and 765 W/m^2 in the 400 nm - 800 nm range.

In order to investigate colour changes, we designed the test chart (figure 2). We included in the test image color control patches of primary and secondary colors, tonal scales and 400 patch test chart for profiling and calculations of the reproducible gamut.

Two test prints made with different digital printing techniques, they were subjected to measurement in view of the changes occurring due to radiant exposure. A Canon Pixma MP650 inkjet and a Canon Imagepress C1 electrophotographic press was used to print test samples. Two types of self-adhesive substrates were used: matte (Ritrama 70 g/m^2 face, 110 g/m^2 backing) and semi-gloss (JAC Duro 2000 70 g/m^2 face, 110 g/m^2 backing). Samples were printed under normal everyday conditions at room temperature.

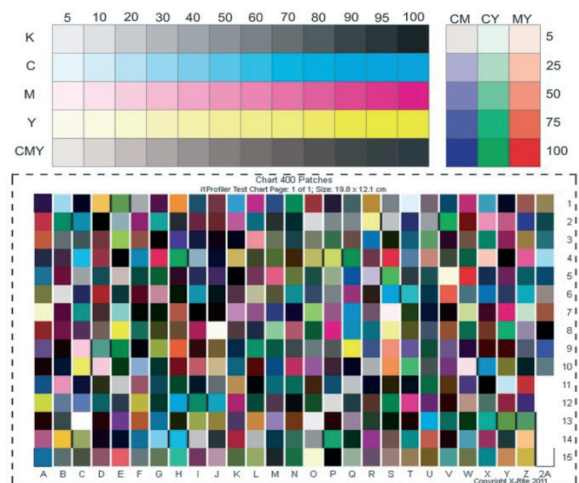


Figure 1:
Test chart printed by inkjet and electrophotographic technologies on two types of substrates. Optical properties were measured at stages of the aging process

We studied the test prints in the weathering equipment under the conditions of the ISO 4892-2 method B6 standard to investigate the resistance of digital prints against filtered sunlight, in this case without wetting. Initially the temperature of the test chamber was 24 °C, and then during the test, the thermometer inside the test chamber measured a temperature increase up to 65 °C. After completed stages of the accelerated aging process we measured parameters of the optical quality of the prints. Specimen were aged in steps of 48 hours, inkjet prints were aged for 144 hours, electrophotographic prints were aged for 192 hours altogether. After the 48 hour aging optical density, tone value increase and color differences and color gamut of the specimen were measured. For the evaluation of optical density and tone value increase (TVI, %) a Gretagmacbeth D19C reflection densitometer, for color measurement a Gretagmacbeth X-Rite Spectroeye spectrophotometer and Eye-One IO automated scanning table were used. Intensive irradiation alters color quality and the quantities of the corresponding properties. Before placed into the instrument, both samples were subjected to the measurement of the density of the primary colors and the tone value increases of all the tone scales. The L*a*b* color coordinates of the primary and secondary colors properties as well as color gamut were determined again after every 48 hours of exposure.

3. Results and discussion

As a natural consequence of the irradiation we expected the samples to fade. However, fading was not visually observable at a first glance after the first 48 hour aging period. Optical density values were de-creasing (figure 2) with radiant exposure, mostly affected were the magenta and yellow inkjet process colors. In order to obtain information on the magnitude of the changes on a visual scale, we measured the CIELAB values of the full tone process and secondary colors and calculated color differences between the original and the aged specimen in CIE 1976 ΔE^*_{ab} units. The results are shown in figure 3 for the process colors of the inkjet and electrophotographic press on the two substrates. The highest color difference values were found with the yellow and magenta inks in every case. We also investigated the secondary colors (R, G, B) together with chromatic black (CMY).

Figure 4 shows that the magnitudes of color differences are in the same ranges for every substrate-technology combinations. The largest color shifts occurred in case of the red, caused by the high level deviations of magenta and yellow. Color shifts were above threshold level already after the first 48 hours of exposure in all cases.

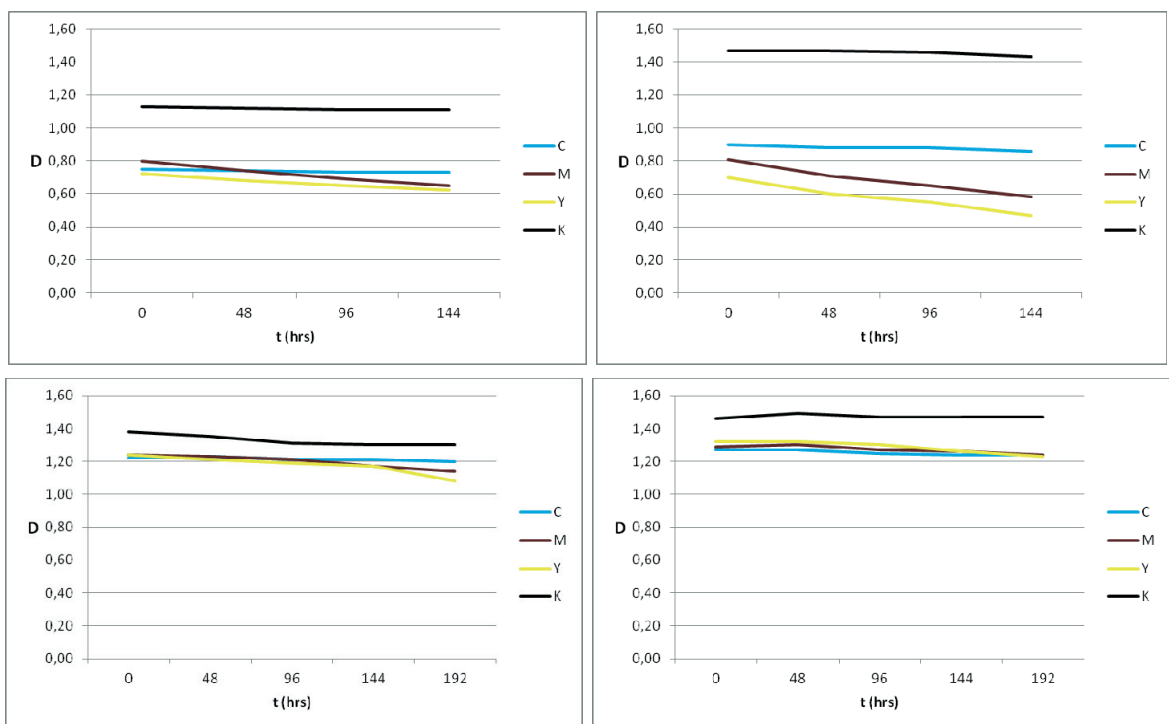


Figure 2: Optical density values of full tones of process colors (C, M, Y, K) during the 144 and 192 hours aging process. The diagrams show test prints on substrate 1 (left) and substrate 2 (right) printed using inkjet (upper row) and electrophotographic technology (lower row)

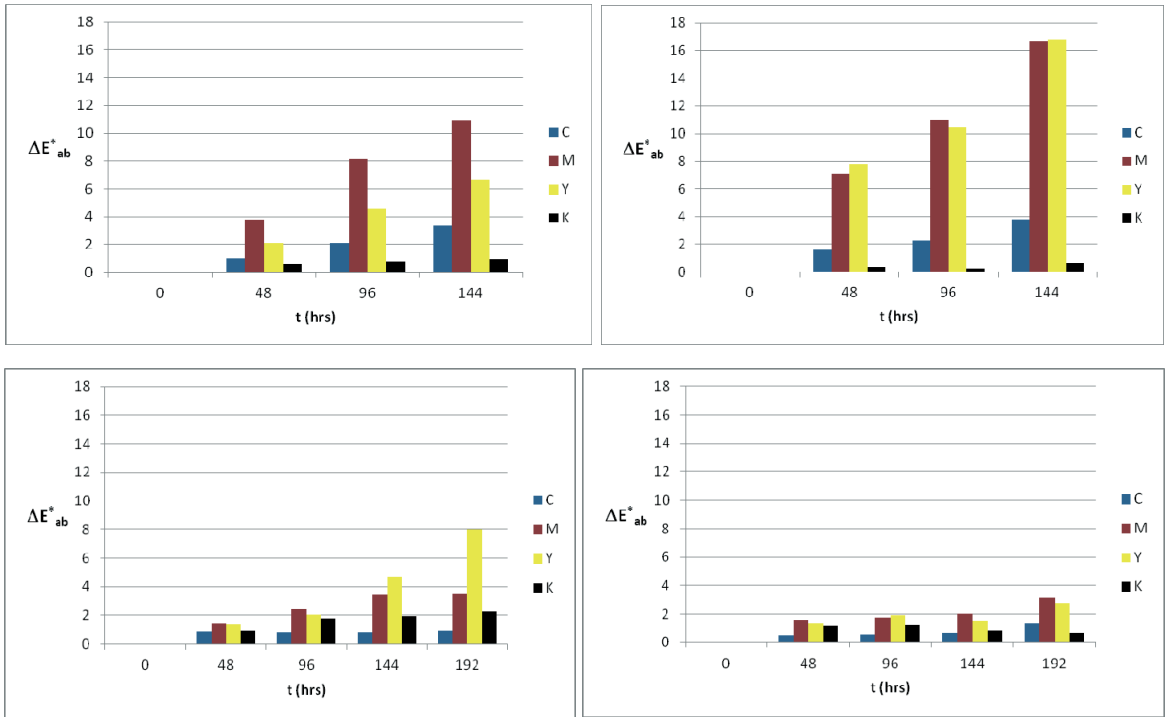


Figure 3: Color differences of solid patches of process colors (C, M, Y, K) at 48 hour steps of aging. The diagrams show test prints on substrate 1 (left) and substrate 2 (right) printed using inkjet (upper row) and electrophotographic technology (lower row)

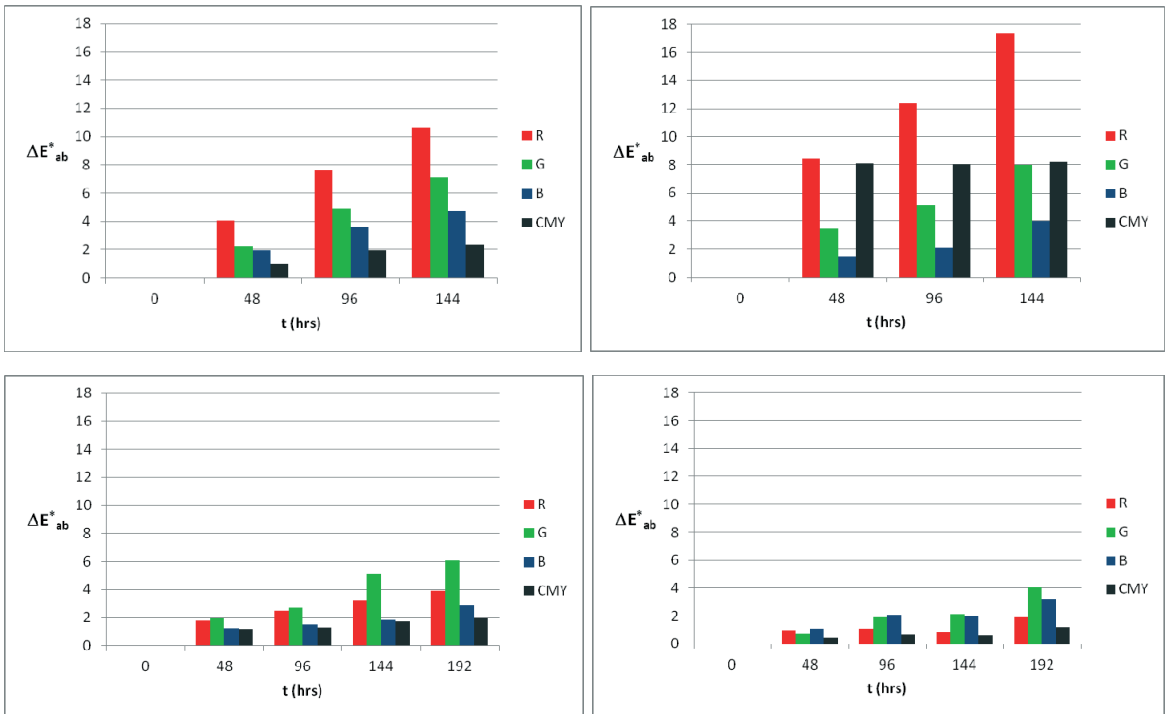


Figure 4: Color differences of solid patches of secondary colors (R, G, B) and chromatic black (CMY) at 48 hour steps of aging. The diagrams show test prints on substrate 1 (left) and substrate 2 (right) printed using inkjet (upper row) and electrophotographic technology (lower row)

We computed the range of reproducible colors (gamut) using a software tool commonly applied in proofing color workflows to visualize and compare color gamut volumes. Standard ICC printer profiles were generated based on measurements of a CMYK chart with 400 patches, which was part of our test chart. We used an X-Rite EyeOne Pro measurement device and profiling software together with an i1 iO scanning table. The

obtained profiles were loaded to a gamut visualization software, to calculate printable gamut in CIELAB color space volume units. The gamut sizes are shown in table 1, as relative values, the initial value before the aging process is taken as reference. The reproducible color gamut decreased by more than 40% in case of inkjet prints, while with electrophotographic technology gamut volume shrinking remained within 10%.

Table 1: Relative values of computed printable gamut volumes on self-adhesive substrates (s1 and s2) printed using inkjet and electrophotographic technologies

exposure time	Inkjet		Electrophotographic	
	s1	s2	s1	s2
0 h	1,00	1,00	1,00	1,00
48 h	0,90	0,79	0,96	0,98
92 h	0,78	0,71	0,95	0,98
144 h	0,70	0,59	0,94	0,98
192 h			0,93	0,98

4. Conclusions

In our discontinuous light aging experiment we tested prints produced using inkjet and electrophotographic technologies on two types of self adhesive substrates. Our samples were irradiated by window filtered sunlight in a weathering testing instrument for 48 hour terms, after each such term optical properties were measured. We experienced, that 48 hours of standard window filtered solar irradiation was enough to change optical characteristics significantly. The largest color deviations were found in case of the magenta and yellow process colors. We experienced 2% - 7% decrease of the reproducible color gamut in case of electrophotographic prints, while inkjet gamut shrinking was 30% - 40%.

References

Atlas Weathering Testing Guidebook. Atlas Electric Devices Company, 2001.

Bond, L. F., (2011): *Natural Outdoor Weathering*, "Időjárásállóság vizsgálat" (Investigation of weather resistance) conference. 2011.10.18. Budapest

Goudie, A. S., Viles, H. (2008). "5: *Weathering Processes and Forms*". In Burt T.P., Chorley R.J., Brunson D., Cox N.J. & Goudie A. S., *Quaternary and Recent Processes and Forms*. Landforms or the Development of Gemorphology.4. Geological Society. pp. 129-164. ISBN 1-86239-249-8

Rahauser, O., Schönlein, A., (2011): *A look at Accelerated Photostability Testing for Packaging Food and Drink*. SunSpots, ATLAS Material Testing Solutions. Material Testing Products and News. Vol 41. Issue 89. pp. 1-4.

Zielnik, A. F.,: *Weather Testing* (2004): Why You Need It More Than Ever. *Plastic Technology*, March 2004 <http://www.ptonline.com/articles/weather-testing-why-you-need-it-more-than-ever> (accessed: Jan 10. 2012.)



Reproduction of art paintings with their status in the near infrared spectrum

Jana Žiljak-Vujić¹, Ivana Žiljak Stanimirović², Ana Hoić³

¹ The Polytechnic of Zagreb
Vrbik 8, HR-10000 Zagreb, Croatia
E-mail: janazv@tvz.hr

² Faculty of Graphic Art Zagreb
Getaldićeva 2, HR-10000 Zagreb, Croatia
E-mail: ivana.ziljak@grf.hr

³ Museum Mimara, Zagreb
Rooseveltov trg 5, HR-10000 Zagreb, Croatia

Abstract

Each work of art has its own specific response in the infrared spectrum. An artist's paints have different response characteristics in the infrared spectrum. Process inks in printing reproduction also have different properties in the infrared spectrum. The initial assertion in this paper is that the infrared status of a work of art can be reproduced with RGB / CMYKIR separation. The target is to have the reproduction and the original work be equated to the utmost extent in the visual and infrared spectrum. This initiates discussion on the necessity to extend "conventional color management" to the range of 400 to 1000 nanometers.

The RGB experience of reproduction extends the zero separation rules with the addition of Z separation. Each RGB picture pixel is calculated in the CMYK conversion respecting the independent pixel value in the Z picture. CMYK become mutually dependent values but with the goal for carbon K to be closest to the Z status of the work of art's infrared value. Channel K acquires a new meaning. It is a separate picture, the picture observed by the infrared camera. In future artists will deliberately paint double pictures, one for the visual and the other for the infrared area. Printers and graphic designers will face a new task: to interpret a work of art in such a way that the reproduction has separate states in the visual and infrared spectrum.

Keywords: infrared technology, art reproduction, CMYKIR separation, Z value of infrared, safety in painting, hidden painting.

1. Introduction

Let us name it as the Z status. We distinguish the RGB image, the conventionally scanned status for the visual spectrum. The reproduction by printing procedures is into the CMY space, but without using UCR, GCR or UCA methods. Channel K is empty, i.e. the separation is in "non" conditions.

We scan the infrared status of the painting with a ZRGB (Žiljak et al., 2011) camera. Separation with an external picture is proposed according to the CMYKIR (Žiljak et al., 2010) theory that will determine the coverage in channel K. The goal is reducing coverage in channels C,M,Y with the Z data as the value of the future K channel.

The requirement is set for channels C, M, and Y that the reproduction should be of the same quality as that of conventional graphic separation. Channel K is carried out with carbon black colorant because it has a response in the infrared spectrum (Pap et al., 2010). A reproduction is obtained that has light absorption in the form of the Z picture, observed after applying the ZRGB scanner.

Artists have not been aware of their works of art having different states in some other spectrum such as: the ultraviolet, X-rays, gama or infrared spectrum. The most highly estimated works of art are studied today in the said sunlight wavelengths. Artists did not have instruments to measure this. They were very far from the idea to take advantage of colorants in other wavelengths and to paint a double picture on purpose. The future of painting art will change, as well as the future of reproduction photography. Such artistic and printing activity was demonstrated for the first time at IARIGAI in Budapest in 2011: a reproduction that contains two different states of a work of art; one that is observed by the human eye and the other by an instrument in the infrared spectrum.



Figure 1 a, b: The painting's visual status (a) and infrared status (b-Z0)

2. CMYKIR separation and reproduction of artistic works

The near infrared status of the original was planned by the artist Nada Žiljak. She forced out the invisible picture, Figure 1 b, hidden in picture, Figure 1 a. Reproduction with merging of the two pictures was carried out with the ZRGB program. Reproduction with the CMYKIR (Žiljak et al., 2009) method resulted with the picture that has CMYKIR channels - Figure 2.

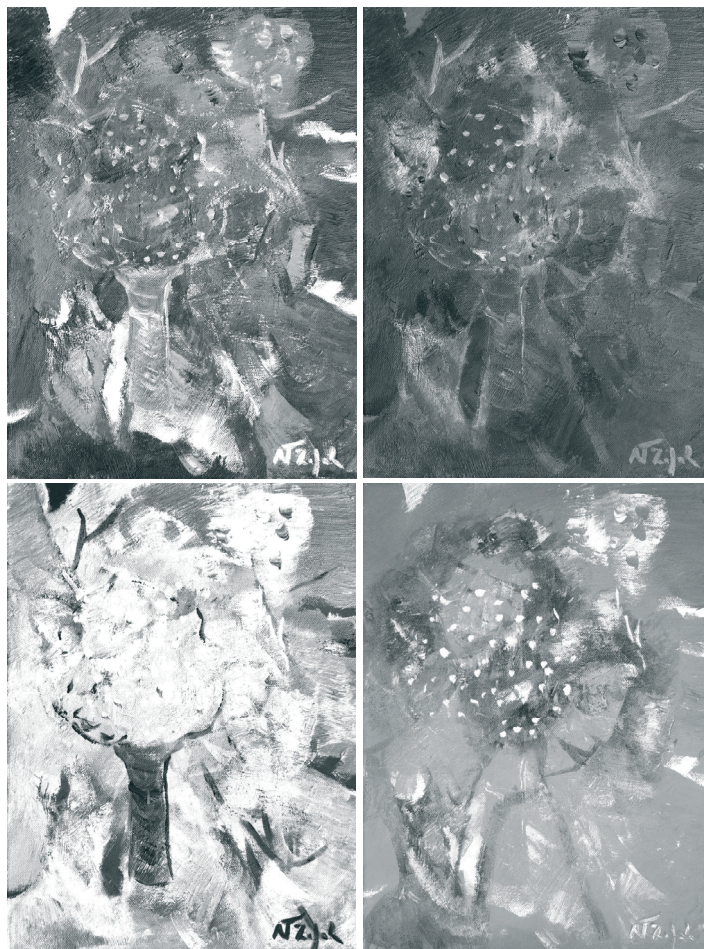





















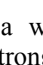
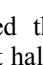
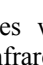


Figure 2: Channels C, M, Y, and K, after CMYKIR separation

The K_{IR} channel differs from the Z_0 state of the IR picture. This is explained by the fact that painting colors used are different in respect to the CMYK colorants for conventional graphic reproduction. A painter's colors are not cyan, magenta or yellow. Artists use dozens of different colors, they mix them further to obtain more colors, and they do not use screening technology. These colors are reproduced by the printing industry using C, M, Y printing inks, with the help of additive and subtractive technology. C, M, and Y process inks generally do not have positive absorbing properties in the near infrared spectrum. Their Z value (Žiljak et al., 2012) is zero. Carbon black is also used in InfraredArt interpretation. It is a colorant that acquires a new meaning in graphic reproduction. It becomes the carrier of the infrared component of the artist's original work of art. CMYKIR (Žiljak et al. 2009) separation is applied. With the help of this technology an endless number of hues is simulated on the painting's canvas.

There are painting colors of light shades that have absorption in Z space, and those colors that do not have the characteristic of absorbing infrared light.

Table 1: Painting colors in the visible and infrared spectrum

WINSOR & NEWTON, Harrow, Middlesex, GALERIA COLORS				
ACRYLIC	Lab	RGB VS (0 - 2 ⁸)	Gray (%) VS	Z (%) 1000 nm IR
Ultramarin	35,46,-93	 47,59,231	 85	 52
Prussian Blue Hue	1,0,0	 9,10,12	 99	 88
Cobalt Blue	27,39,-80	 32,48,187	 82	 14
Deep Turquoise	22,-9,-25	 30,61,90	 90	 65
Olive Green	38,23,18	 72,98,63	 78	 62
Silver REEVES	83,-1,4	 207,207,199	 32	 56
Burnt Sienna Opaque	39,46,38	 141,55,38	 77	 34
Burgundy	27,36,13	 100,40,50	 87	 9

The artist mixed the colors in such a way that she obtained the same shades with the following characteristics: firstly, they also have a strong response in the first half of the near infrared spectrum Z (800 to 1100 nanometers), as well as in the visual spectrum (V; 400 to 700 nm), and secondly: they have a strong response only in the V and not in the Z area.

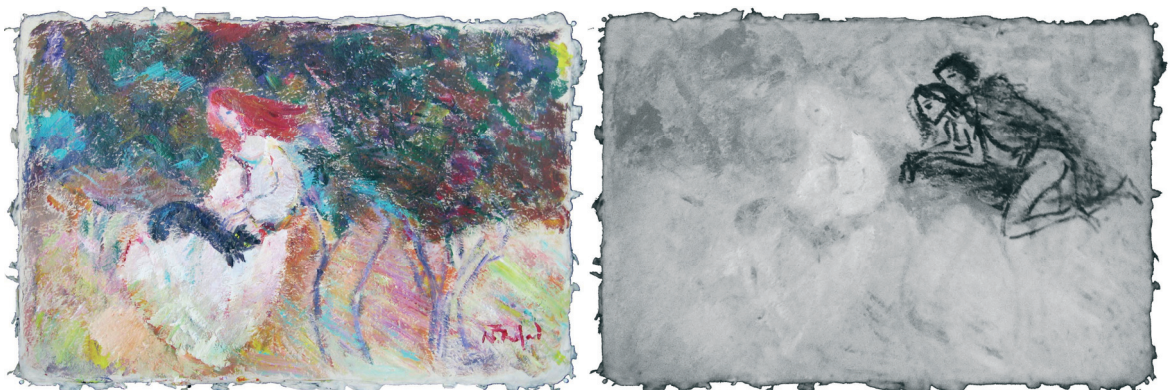


Figure 3. a, b: Portrait and a cat, acrylic on paper, Inks and control of Z from Table 1

The artist has created a work of art that has two different stories. She has hidden part of her intimate emotions from the public eye. Her collection posed a question to graphic and fiscal experts: can a reproduction be made that contains two pictures in the same way as the original does? Any attempt at forgery becomes infinitely difficult, almost impossible. Such an expert should paint the picture observed in the V space, but also the other picture that is seen in Z space. Therefore, only dual painting becomes "security painting", secured by the painting's author.



Figure 4: Visual and Z (NIR) state of art colors

The final reproduction (by merging C,M,Y and K channels) is good quality interpretation of the initial picture. The CMYKIR separation requires precise knowledge of the colorsetting for determining which colorants will be used for printing the reproduction. In Figure 2 the channels are separated for SWOP colorsetting. This means that the reproduction will hide the Z picture completely only if SWOP colors are used. If other colorants are used, the hidden Z picture will show through. CMYKIR separation must be repeated for them with parameters and the mathematical model for printing conditions determined by the other colorsetting. The algorithms for the digital Xeikon printing have been published (Pap et al., 2010), as well as several other analytical CMYKIR separation procedures.

Checking separation results can be carried out by the conventional procedure of joining CMYK channels in Photoshop. For channels in Figure 2 it is necessary to load the SWOP colorsetting. If this picture is transposed into the RGB status, then once again into the CMYK status, - the graphic display of the Z status disappears.

The second experiment in respect to the CMYKIR status sensitivity is checked by only changing the colorsetting in the Photoshop program. The Z separation status begins to show through. It becomes visible. Also, a wrong choice of process dyes, an inadequate printing technology and unplanned choice of substrate material for color printing become evident.

The graphic production dual status has a deeper background in respect to the graphic product security. Printings, especially those on wrapping material, acquire new value. They are also checked in a new manner as to authenticity. Z cameras have been developed for this purpose and they can recognize the infrared component of the solar spectra. Checking is carried out in daytime or under artificial light that has at least a small part of the Z component. Of course, all this is also possible with control security cameras in the nighttime recording mode: with cameras that have their own source of IR light.

3. Conclusion

We are setting a new method for reproducing paintings that contains the original painting's status both in the V and the Z spectrum. The book, monograph, the exhibition catalogue acquire new value. The original painting's status in the near infrared spectrum has been introduced into the reproduction, together with the status in the visual wave length of color recognition. With each copying of the graphic print with VZ statuses, the Z status disappears. Thus a new method for securing graphic reproduction has been set.

The painter Nada Žiljak creates a picture with the target being a double status of her work of art; two dependent pictures that are at the same time independent. They are linked and separated by their contents. Because of this double meaning, printing reproduction is also faced with the task to have two versions, two stories. The reproduction will be observed in two ways, in the same way as the original: with the eye and with the camera.

Reproduction inks may be spot inks, such as Pantone inks, for example. For them it is necessary to measure Z values of light absorption at 1000 nm (Žiljak et al., 2012). The artist also carries out this procedure of measuring Z values for her artistic colors. This is a new target in printing color reproduction.

References

- Pap, K., Žiljak, I., Žiljak-Vujić, J., Image Reproduction for near infrared spectrum and the infraredsign theory. // The Journal of Imaging Science and Technology. 54 (2010) , 1; 10502 -1-10502 -9
- Žiljak, V., Pap, K., Žiljak, I., CMYKIR security graphics separation in the infrared area. // Infrared Physics and Technology. 52 (2009), 2-3; 62-69
- Žiljak, V., Pap, K., Žiljak, I., Infrared hidden CMYK graphics. // Imaging Science Journal. 58 (2010) , 1; 20-27
- Žiljak, V., Pap, K., Žiljak-Stanimirović, I., Development of a prototype for ZRGB infraredsign device // Technical Gazette. 18 (2011) , 2; 153-159
- Žiljak, V., Pap, K., Žiljak-Stanimirović, I., Žiljak-Vujić, J., Managing dual color properties with the z-parameter in the visual and NIR spectrum. // Infrared Physics & Technology. 55 (2012) ; 326-336





2

*Determinators of quality
in printed products*

Towards a fully digital computer-to-screen workflow for an improved product quality and quality assurance in screen printing

Janko Jesenko¹, Bojan Petek²

¹ Etiketa Tiskarna d.d.
Industrijska ulica 6, SI-4226 Žiri, Slovenia
E-mail: janko@etiketa.si

² Interactive Systems Laboratory
Faculty of Natural Sciences and Engineering
University of Ljubljana, Slovenia
E-mail: bojan.petek@ntf.uni-lj.si

Abstract

This paper investigates how to use the Esko prepress workflow automation engine to support the Etiketa printing house recent investment in new Computer-To-Screen (CTS) technology. Esko software is primarily applicable to packaging industry. Our main motivations are the improved product quality, the reduced response time, and the faster overall design time. In order to address these issues we analyzed the obsolete workflow using films and considered it as the baseline for further comparisons. The to date analyzed Esko setups were: (i) the default software settings, (ii) the modified Esko SmartMarks, and (iii) the inclusion of JDF technology. We measured the average durations of each individual process in workflows. Our motivation was to efficiently exploit the Esko SmartMarks. This was one of the reasons why Esko software has not been optimally applied to the stencil production. The next research issue was to investigate the possible use of SQL language to collect the data from our MIS system. We investigated ways to use the modern JDF technology that requires efforts in standardization of data and represent the reference point for the ROI analysis of our CTS investment. Since there are many ways to obtain the improved results we assessed numerous workflow efficiencies.

Keywords: workflow analysis and automation, computer-to-screen printing, Esko packaging print prepress tools, signtronic stencilmaster

1. Introduction

Etiketa, tiskarna, d. d., is a printing company with 180 employees and represents one of the major printing houses in Slovenia. Its screen printing division contributes $\frac{1}{2}$ of the total turnover with high quality products mainly exported to foreign countries, of which a major proportion targets the European market. For several years, Etiketa devotes nearly 10% of its annual turnover to new investments, education and human resources. It is dedicated to use of the environmentally friendly materials, efficient energy consumption, improved health care for its employees, and has been certified with the standards ISO 9001, ISO 14001, BS OHSAS 18001, and EN 16001.

It exclusively uses colours with the ECO certificates (1).

Etiketa acquired the Esko packaging print prepress software to provide support for the packaging products that predominantly includes labels and tags (2).

Most recently, the investment in computer to screen technology (CTS) provided an emerging new opportunity for digitalization of the screen printing division. Motivation for this investment is multi-layered:

- The shortage of films for screen printing on the market;
- A substantial increase in price of films;
- Optimization of the manufacturing costs;
- Dedication to permanent increase in quality.

Figure 1 shows the recently introduced CTS imaging technology that aims to significantly improve the screen printing workflow efficiency (3).

The expected key advantages are (4):

- Workflow optimization: the reduced number of workflow processing steps leads to faster turnaround times, higher process reliability and fewer remakes;
- Improved workflow transparency: fully digital CTS workflow provides an improved control and higher transparency that are beneficial to the product quality and quality assurance;
- Potential quality improvement: the CTS stencils provide wider tonal ranges, easier printability of halftones, and improved rendering of detail;
- Improved printing press setup: the accuracy of image placement on the screen shortens the setup times on press and improves the color consistency;
- Elimination of films: significant savings in labor and materials.

The research addressed in this paper is how to optimize and use the already acquired Esko workflow tools for label production in the area of screen printing. Recently, stencil making has been improved by the introduction of SignTronic StencilMaster that enables highly automated, environment and operator-friendly production. Additional Grünig equipment is applied for developing, automatic final drying and stencil storage processes. The introduction of CTS is going to raise the level of digitalization of our workflow. Continuous improvements of processes by using the Esko SmartMarks tool will enable an improved introduction of the Job Document Format (JDF). The SmartMarks is a tool that links the data and introduces the JDF - MIS connectivity.

Our main targets are better product quality, reduced response times, faster overall design time, and improved economy. By reducing and minimizing the repetitive tasks we want to shift the operator's focus on product quality. Another research issue is how exploit standardization in the selected and optimized individual workflows.



Figure 1: The newly acquired SignTronic StencilMaster

In summary, our main objective is to explore various ways to optimally integrate the existing Esko workflow tools to the Etiketa screen printing division. Specifically, we want to verify the adequacy of Esko tools in controlling the screen printing workflow. Based on the workflow process time measurements, we want to estimate the expected benefits and remaining limitations of each proposed screen printing workflow solution.

2. Research methods

Performance parameters of the obsolete workflow using films are taken as the baseline reference for comparisons. Since the SignTronic equipment is rather recent we could only to date identify the benefits of the following software setups:

- with the default Esko software settings;
- with the modified Esko SmartMarks (5);
- with possible upgrades to include the JDF technology.

Esko software tools we used in the workflow optimization research include:

- Automation Engine - server program;
- Automation Engine Viewer - quality control tool that enables to process PDF, AI, PS, EPS file data formats;
- PackEdge - packaging preproduction editor for personal computers;
- Plato - creates print-ready layouts for the packaging and label industries;
- FastImpose - the imposition module that is added to the Esko BackStage workflow automation server;
- DeskPack - turns Adobe Illustrator and Photoshop into full-fledged packaging applications;
- FlexRip - RIP solution for all output;
- Bitmap Viewer - quality control tool that digitally verifies RIPPed data for content and printability before output.

Suitability of the selected workflow can be estimated by time measurements of individual processes in stencil production. Figure 2 shows the organizational chart that represents a typical workflow with individual operations and required human interventions.

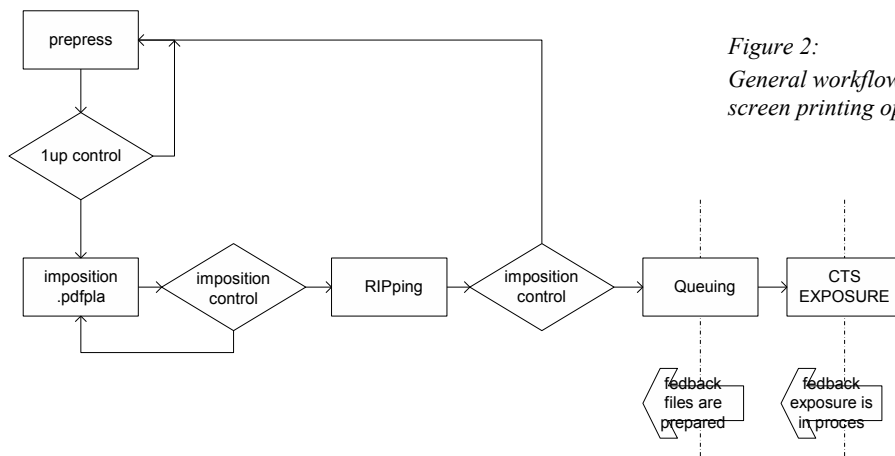


Figure 2:
General workflow for screen printing optimizations

In particular, we analyzed several workflows with a direct impact on screen production in terms of logistics with the already prepared files. We also analyzed and compared the obsolete workflow using films with the workflows aiming to efficiently support the recently installed SignTronic CTS equipment.

The workflow in Figure 2 offers the possibility of influencing digital data just before illumination. Stencils are in general washed after each use and are reclaimed. This brings a possibility of some level of "personalization" by different distribution of individual products during the final joint imposition. We now have the option of upgrading the Esko workflow in a more automated way. As a reference point, we took the measurements of times of individual operations in the workflow using films and calculated the average time spent on each operation.

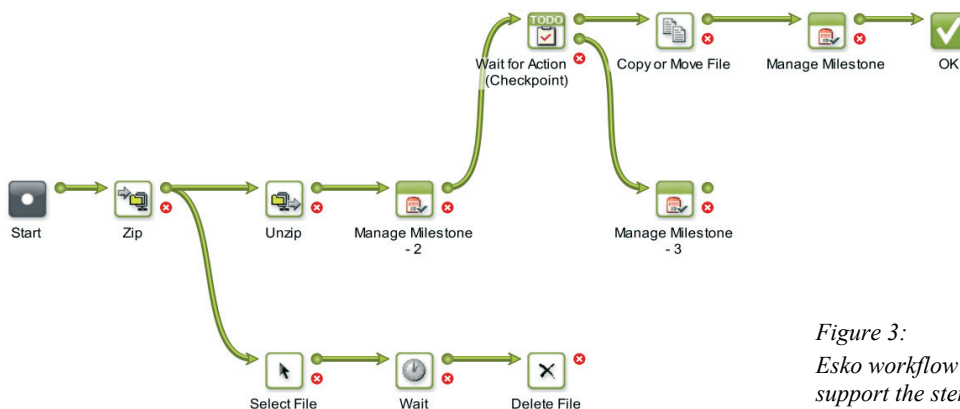


Figure 3:
Esko workflow proposed to support the stencil making

The workflow in Figure 3 is actually very similar to the previous one except that we removed all logistics and control that we had with films. This figure shows the modular structure of the workflow. It is used to send 1-bit TIFF files to the screen printing department and includes checkpoints that require the human control intervention. After this the stencil is illuminated and developed. Note that the softproof is performed with the BitmapViewer (Figure 4). Initial IUP files and imposition controls have already been performed in the pre-press stage using the Automation Engine Viewer with similar tools such as the Bitmap viewer but with suitability to PDF, AI, PS, EPS file data formats. The 1-bit TIFF files may be processed with minor adjustments as well.

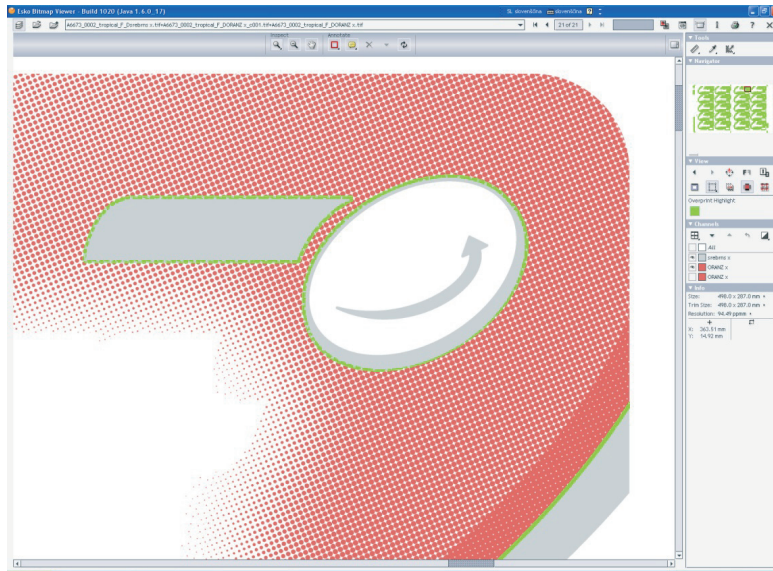


Figure 4: Esko BitmapViewer tool for visual control of 1-bit .tiff files

The Figure 5 illustrates the final stage of workflow where the operator at Stencil Master checks a list of work orders and decides for the final approval of job transfer to the SignTronic Stencil Master.

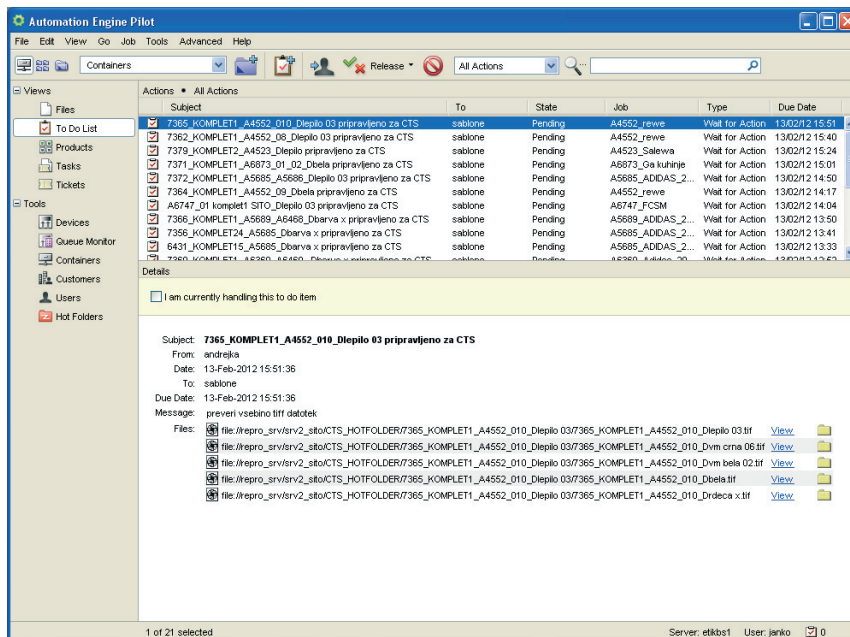


Figure 5: Dialog box for monitoring and certifying files in the workflow transferred to the StencilMaster

We compared times of the individual processes in the selected workflows that used different levels of automation in the Esko supported workflows. In order to analyze for possible workflow optimizations we introduced the number of baseline and modified Esko SmartMarks. We evaluated the possible reduction of time spent on each workflow operation. Our tracking workflow is shown Figure 6.

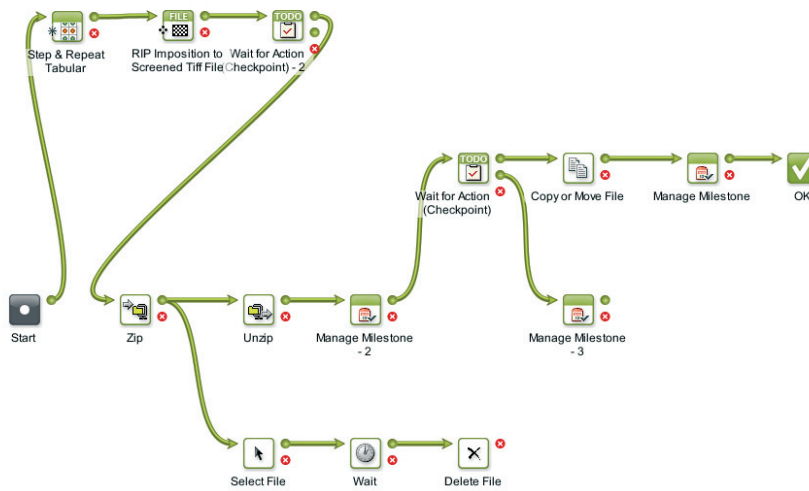


Figure 6: Modified workflow for file transfer to stencil making

In this case the workflow included the automated imposition and the ripping of files. All data were obtained directly from the database or from the Esko SmartMarks. A thorough understanding of the SmartMarks is essential when introducing the JDF technology. The SmartMarks enable more flexible workflows by allowing an efficient exchange of data with the external databases using the JDF. For example, Figure 7 shows a script that enables calculation of the predicted use of ink.

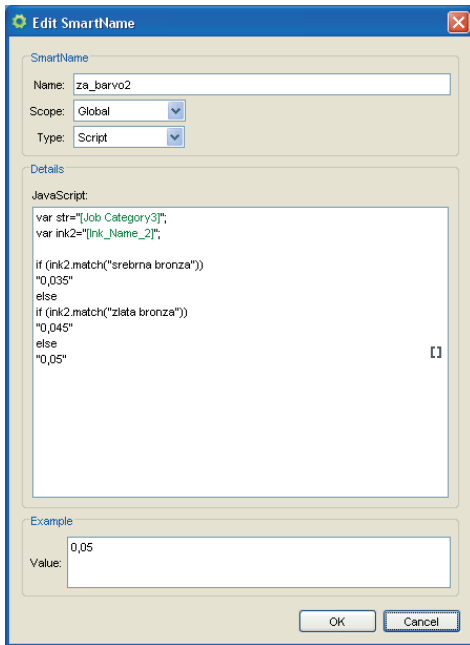


Figure 7: Example editing window for SmartMarks

The Figure 7 also demonstrates some additional options enabled by, e.g., the String Extract procedure. In general, the JDF technology allows for quite efficient addition of the selected data into the Esko JOB structure that results in an improved and automated workflow.

3. Results

The first column labeled "film" in Figure 8 highlights the average time per workflow operation measured on the existing workflow using films (6). The next column "signtronic" represents the improvement with minimal change due to the introduction of additional Esko workflow tools. Automation in this case included only the file transfer from workstation location to the CTS StencilMaster and of course the big improvement, elimination of films.

The last three columns in Figure 8 represent the to-date estimated times obtained on the number of Esko workflow alternatives we considered. We compared the results depicted in column "signtronic" to the selected modified Esko workflows. In all experimental setups only the workflow processes after the imposition were considered. These columns in Figure 8 are labeled "esko", "esko smartmark" and "MIS connection".

The "esko" column shows the case where we still perform the imposition according to the established procedure but are already using the Esko workflow without SmartMarks.

The "esko smartmark" column represents the case where the individual entries through SmartMarks require less manual interventions. This requires a degree of standardization where we also applied the SQL transfer of data needed for electronic imposition.

The column "MIS connection" represents the case where we connected the management information system (MIS) by using the Job Document Format (JDF) where the XML language is used to transmit JDF and JMF messages. In this case, the project specification data entered only once are automatically transferred using SmartMarks to all relevant workflow stages. This implies the improved workflow efficiency in prepress as well as in stencil production.

In summary, in addition to time gained by not using films we have now the opportunity to acquire different degrees of standardization that are expected to support an increased product quality while decreasing the costs.

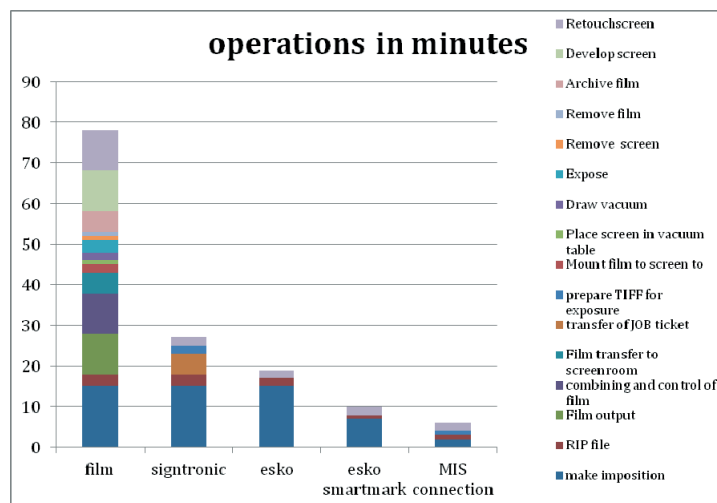


Figure 8: Average time per operation in the considered workflow variants

4. Discussion

Given the target requirements that have to be economic, a good starting point represents the proposed exploration on the efficient use of Esko SmartMarks. We argue that the SmartMarks represent an effective tool for an improved Esko supported workflow. This approach, however, requires a larger degree of standardization since we do not want to end up with an abundance of SmartMarks but with the qualitative and quantitative links among the relevant and selected workflow data.

In addition, the current economic situation requires from us to take advantage of the existing resources. Only on the basis of thorough insights into the use of the already acquired technology we can decide on further investments. Based on the experience to date it makes sense to invest into the JDF technology that automates the data flow relevant for various entities, e.g., from the Sales Department up to the Technology Service. This paper discussed a part of this workflow chain, the prepress.

5. Conclusions

The study assessed the individual workflow efficiency and how complex the optimal screen printing workflow using Esko tools needs to be. We also investigated when the human operator intervention is really required and which workflow processes can be carried out automatically using the Esko SmartMarks. Future

work will address the potential benefits of upgrading to a more modern JDF-based system. In particular, we want to understand and remove the remaining workflow bottlenecks and improve the opportunities brought by further standardization.

References

(all accessed and cited on 15 February 2012)

- (1) <http://www.etiketa.si>
- (2) <http://www.esko.com>
- (3) http://www.signtronic.com/pdf/Technical%20Specifications_StencilMaster.pdf
- (4) <http://www.kiwo.com/Product%20pages/Computer%20to%20screen.html>
- (5) <http://www.esko.com/en/Products/overview/plato/features>
- (6) http://www.kiwo.com/Downloadable%20CTS%20documents/2010_5%20ScreenSetter2%20LT_engl.pdf



Leaner and better

How can the setup time and waste at the sheet-fed presses be reduced?

Csaba Horváth

Óbuda University
Rejtő Sándor Faculty of Light Industry and Environmental Engineering
Doberdó u. 6, H-1034 Budapest, Hungary
E-mail: horvath.csaba@rkk.uni-obuda.hu

Abstract

On commission of a packaging printing company, the author has launched a research work in order to find a methodology by which the necessary steps can be explored to turn the application of this modern technology into a business success.

The lean manufacturing studies have primarily focused on the human-machine environment, analyzing all the activities that are connected with the operation and servicing of the machines. Step by step, the research has tried to expose those hindering factors, superfluous or less efficient organizational and management process elements that now increase costs.

Keywords: packaging printing, lean management, SMED in the printing industry, spaghetti mapping

1. Objectives of the research

Even the procurement of brand new equipment or the provision of base materials of the highest standards is not a guarantee for the printing business to produce printed products of consistently outstanding quality at a profit. The struggle against electronic communication, the global economic crisis and the sharp competition with the existence of excess capacities put a pressure on printers. One should ensure quicker lead times for the products, offer regulated and cheap prices, and besides steadily excellent quality is to be maintained.

Printers tend to see the source of the growth of production and profit in new investments, which is mostly not true. It is not enough to buy modern printing machines, but they are to be operated with high efficiency in order to see the return of the investment. In the conventional approach, if the printing machine features high printing speed, then it will necessarily boast of significant efficiency and utilization rate. In fact, however, additional parameters should also be considered when the utilization rate and efficiency of a printing machine is examined. Such parameters include the setup time, the time loss, the generation of rejects, the competence level and certainly the speed of the machine.

It is a legitimate question how a favourable situation can be achieved, how we can generate more profit from the given production process?

Recently, a company manufacturing packaging materials (cardboard boxes) has purchased and commissioned new sheet-fed presses with state-of-the-art accessories. However, the expected profit has not been pocketed. On commission of this company, we have launched our research work in order to find a methodology by which the necessary steps can be explored to turn the application of this modern technology into a business success.

Our studies have primarily focused on the human-machine environment, analyzing all the activities that are connected with the operation and servicing of the machines. Step by step, we have tried to expose those hindering factors, superfluous or less efficient organizational and management process elements that now increase costs.

2. Research methods

The exploration of the human-machine environment principally calls for the methods of organizational studies. *Lean management* is a systemic methodology that identifies, eliminates all forms of losses, as well as all such activities that do not represent any added value for the customer, client. Its aim is to provide the

product with ongoing drift and continuous added value. It perfects the process with which the business is able to satisfy the client’s demands; it improves production efficiency, and thus opens the way to the generation of further profit. In the past few years, the *lean* work methodology has been applied by several companies involved in graphic communication. As these companies have had hardships and witnessed varied successes in adopting the system, just little published experience is available.

At our printer client manufacturing packaging materials, we got down to implement the *lean* work methodology back in 2010. First, we structured the necessary knowledge base. We elaborated a system for the company as based on the *lean* work methodology, and called it the *SBS (step-by-step) way*. This method basically follows the *lean* thinking, but in a substantially simpler design. We considered the simplification of the system to be justified, because the company had not relied on such organizational methods before that would have at least been slightly similar to the *lean* system. We deemed the leap from the actual situation of the company to the desired position to be too large, and therefore we wanted to walk this considerable distance in smaller steps in order to avoid failure.

The *SBS way* program aims at the optimization of the printing process. The goal of the project is to improve the utilization rate of the printing machines, minimize time losses (faults, setup times), enhance performance (printing speed) and reduce reject sheets generated in production. First, the reduction of the setup time and the number of the reject sheets generated in production was targeted. These were the fields where the necessity to transform the human-machine environment seemed to be the most obvious. In the framework of the investment, the company purchased such state-of-the-art technology whose application allowed the fastest possible setup times. Still, the system failed to operate with sufficient efficiency.

To cut setup times, the SMED (Single Minute Exchange of Die) method has been applied. When the setup process is optimized, in fact the following actions are taken:

- reduction of the number of steps/components to be completed,
- reduction of the number of setups,
- improvement of the accuracy of setups,
- reduction of the generation of rejects.

To clarify the setup time and unveil the processes, causes of the excess time demand, the Fishbone/Ishikawa Diagram was used (Figure 1).

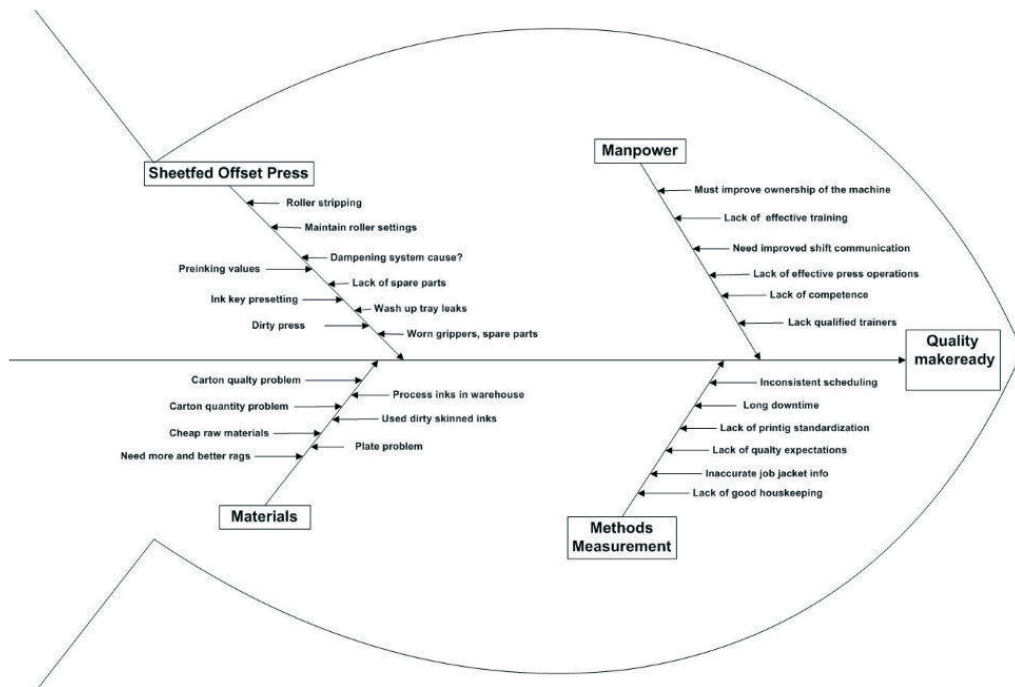


Figure 1: Makeready Fishbone diagram

The SMED makes a distinction between so-called external and internal operations that jointly form the setup process. Internal operations can be executed when the press is in standstill, for instance during the repla-

cement of the die plate. External operations can be completed in the course of the printing of the actual copies, when the printing machine generates marketable products, for example during the preparations for the replacement of the die plate.

The optimization of the setup time consists of three main phases.

- Phase 1: Separation of internal and external operations;
- Phase 2: Conversion of internal operations into external operations;
- Phase 3: Harmonization of all the elements of the setup operations.

To *separate internal and external operations*, the process of changeover was subjected to value stream analysis by way of making and evaluating a video recording. After the making of the recording, the video shots were replayed in the presence of the work team, each of the operations performed was identified, and they were also determined quantitatively (in terms of time). In addition to the video recording, a motion diagram was also compiled (Figure 2) in order to visualize and easily recognize losses.

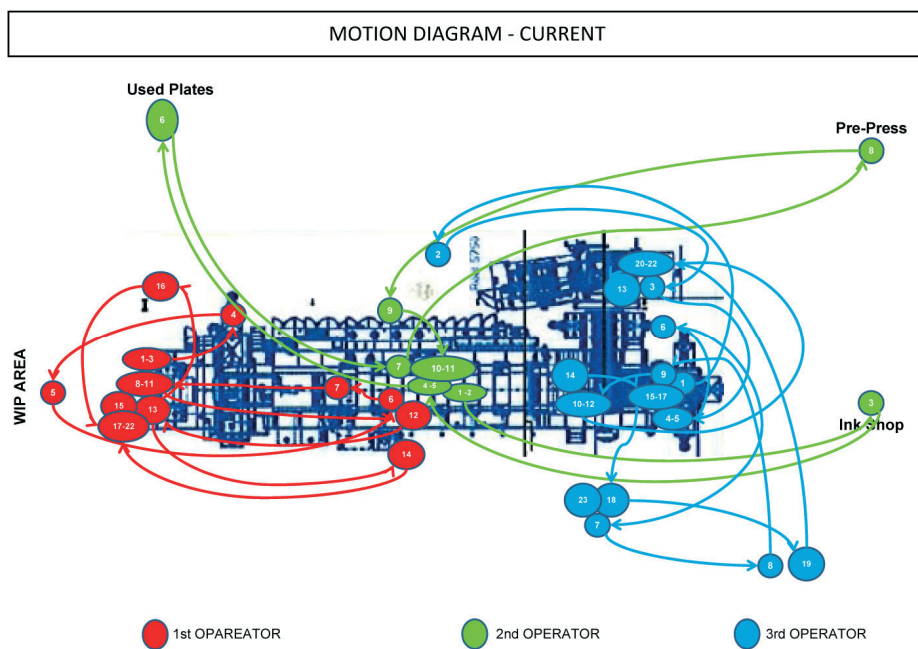


Figure 2: Spaghetti map - current

During the conversion of internal operations into external operations, the following questions need to be answered in the light of the steps that have already been identified.

- ⇒ What is the purpose of the operation?
- ⇒ Why should the machine be in standstill to perform the actions?
- ⇒ Is the operation convertible from internal setup to external setup?

We tried to form the largest possible number of operations in the external setup, as irrespective of the weight of the operation, thereby minimizing the time loss. The steps included here are:

- documentation steps (completion of the work dossier),
- preparation of the die plate, bending, checking, preparations for the replacement of the plate,
- uploading, checking CIP3 data,
- interpretation of the work dossier,
- preparation of the lacquer form,
- preparation, unwrapping of the print carrier,
- preparation of detergents, materials,
- preparation of printing colours, etc.

Once we had a clear view as to which operations should be performed when and where, we started to *harmonize the operations* and simplify more complex steps. Conventional tasks, such as the development of the die plate and the machine washing process, did not result in considerable challenges, because the printing presses included in the target group feature a significant level of automation. On the other hand, the synchronization of the work steps of printing engineers proved to be a more difficult task. It brought about changes, and initially they were hardly accepted. Nevertheless, they recognized that if they were working as a team, more steps could be performed concurrently, in parallel. As they also watched the video recording, i.e. how they had been working, it was easier to convince them. The losses were shown before their own eyes. During the SMED project, merely joint team work contributed to the success, because the workers themselves planned work processes, and optimized their operations. Such difficulties were experienced as the differing competence levels. Certain printing engineers were capable of performing only certain steps, thereby deteriorating flexibility, but within the framework of the lean training program the differing competence levels could also be resolved. We tested the newly framed work processes in practice, with success. The same steps were taken by the printing engineers, but in a different order, and thus materially cut the time demand of setup (Figure 3).

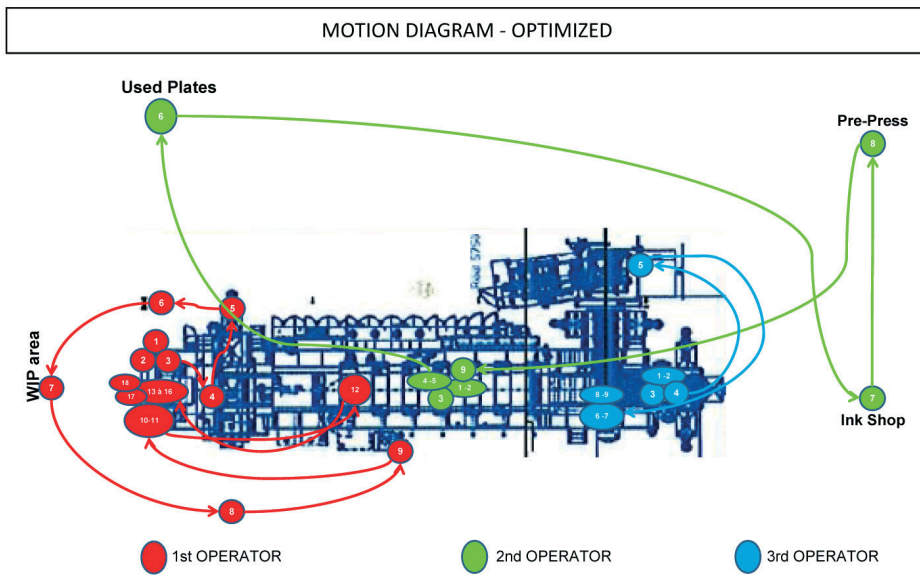


Figure 3: Spaghetti map - optimized

3. Summary of results

In 2011, the optimization of the printing process proved to be the key achievement in the life of the plant. Our aim has been accomplished, as the setup times and the number of reject sheets have been substantially reduced and permanently minimized (Figure 4).

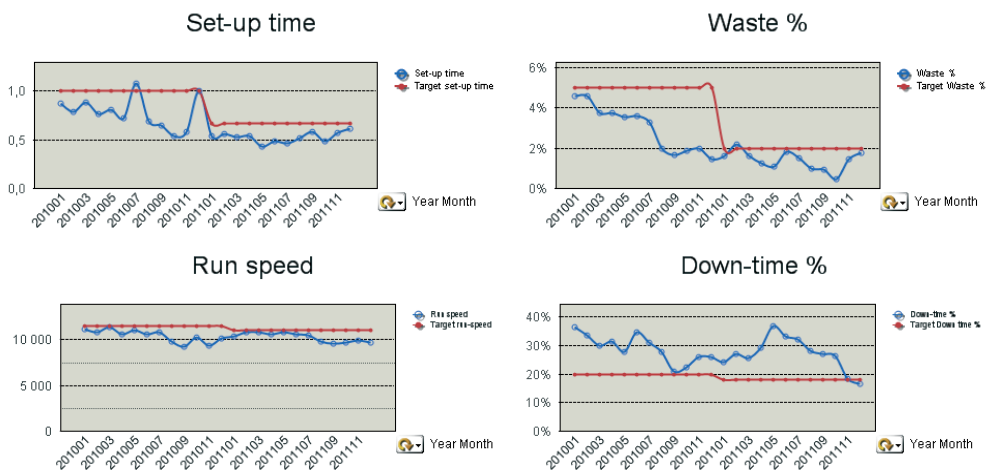


Figure 4: Utilization properties of the printing presses taken as the target group

This Figure also shows that the problems associated with the speed of the machine and time losses are still to be tackled. However, it is again an outcome corresponding to our step-by-step approach. For the upcoming year, we should make progress in this latter field, as well. Our successes so far underline the efficiency of the application of *lean management*, and as a consequence there is rising trust in our researches and the related, practical organizational work.

4. Conclusion

Today, profitable printing production is not feasible by means of price increases; the only expedient way to follow is to cut costs. In this respect, *lean management* can be supportive.

The *lean* simplification we have elaborated, i.e. the SBS (Step by Step) way method has proved its efficiency in making the first achievements, which demonstrates that the printing business is a proper scene for the application of the method, and further cost-cutting solutions can be expected from the continuation of the work.

References

- Behringer, R., Sustainability as a Success and Competitive Factor (presentation), Lean & Green, International Environment Conference, DRUPA, Düsseldorf, May 12, 2012.
- Cooper, K., Keif, M. G., Macro, K. L., Jr., Lean Printing: Pathway to Success PIA/GATFPress, Pittsburgh, 2007, ISBN: 0-88362-586-5.
- Cooper, K., Lean Printing: Cultural Imperatives for Success, PIA/GATFPress, Pittsburgh, , 2010, ISBN: 9780883626887.
- Rizzo, K. E., Total production Maintenance: A guide for the printing industry, PIA/GATFPress, Pittsburgh, (3rd ed.), 2008, ISBN: 0883626209.
- Rothenberg, S., Cost, F., Lean Manufacturing in Small- and Medium-sized printers, RIT Printing Industry Center, 2004.
- Weather, J. P., Lean & Green, Economic and Environmental benefits of Lean (presentation), Lean & Green, International Environment Conference, DRUPA, Düsseldorf, May 12, 2012.
- Wells, N., Leaner & Greener, Value Chain (presentation), Lean & Green, International Environment Conference, DRUPA, Düsseldorf, May 12, 2012.



Digitisation of old printed typeface

Klementina Možina, Tanja Urbanc

University of Ljubljana
Faculty of Natural Sciences and Engineering,
Chair of Information and Graphic Arts Technology
Snežniška 5, SI-1000 Ljubljana, Slovenia
E-mails: klementina.mozina@ntf.uni-lj.si; tanja@urbanc.org

Abstract

The aim of this study was to create a new font based on the oldest Slovenian printed cookery book, *Kuharske bukve*, which is very important for the Slovenian cultural heritage. The goal was to investigate its contemporary usability and some design changes in the form of its letters. The digitisation of a typeface is a well-known process, unless a new font has to be created on the basis of an old printed metal or wooden typeface. The process is an exact piece of work if the original typeface is missing and we only have prints of different quality at our disposal. Especially, as the digitised typeface should be as applicable in conventional as in digital media.

The steps of the digitisation process were as follows: taking photos of all book pages, analysing the design properties of the typefaces, cutting a larger number of individual characters, selecting the least deformed characters, comparing the characters and defining different properties, making a handmade draft, designing the characters in a computer program, defining the spacing. The presentation of the practical application of the *Metelka* typeface and its typographic tonal density were made as well. During the digitisation, some legibility improvements in the typeface design had to be made, although the question arose regarding how many and which improvements to make, for the typographic cultural heritage not to be dismissed.

Keywords: type design, type digitisation, cultural heritage, Jožef Blaznik, *Kuharske bukve*

1. Introduction

Typography is an extremely wide field with numerous open questions, possibilities for research and new creations. The aim of this study was to make a new typeface based on the typeface used in the oldest Slovenian printed cookery book, *Kuharske bukve*, which is of extreme importance for the Slovenian cultural heritage.

A goal was to investigate the contemporary usability and some design changes in the letter form of the new typeface. By digitising the old printed typeface, we wanted to create a typeface that retains the historical spirit of the first half of the 19th century. We tried to preserve the appearance of the originally printed letters to the greatest extent possible. Therefore, we accurately analysed the letter structures and tried to approach them typographically as much as possible, taking into consideration that the reading habits changed from loud to silent reading in the late 18th century (Gabrič, 2011) and especially in the second half of the 20th century when different media (for presenting text) came into use (Jury, 2004; Kipphan, 2001).

The first legibility research was conducted in 1790 (Spencer, 1969). A number of studies on the legibility in conventional printed (Možina, 2001; Reynolds, 1988; Spencer, 1969; Tinker, 1966), digital printed (Možina, Medved, Rat, Bračko, 2010; Rat, Možina, Bračko, Podlesek, 2011) and digital media (Dyson, Haselgrove, 2001; Ling, Schaik, 2006; Pušnik, Možina, 2009) highlight its importance. There are some typeface characteristics to be taken into consideration to make a text more legible, i.e., distinctive character features (counter shape), x-height, ascender, descender, serifs, contrast (stroke weight) etc (Gautley, 2001; Možina, 2001; Reynolds, 1988; Tracy, 2003).

For the body typography, the difference in stroke width and typographical tonal density (or typographic tonality) are of importance (Možina, Medved, Rat, Bračko, 2010; Rat, Možina, Bračko, Podlesek, 2011), influencing text legibility. Typographic tonal density was taken into account as it refers to the relative blackness or shades of grey of type on a page. It can be expressed as the relative amount of ink per square centimetre, pica or inch (Keyes, 1993). The changes in various type features can create variations in typographic tonal density (Možina, 2001; Možina, Černič, Demšar, 2007; Reynolds, 1988).

The digitisation of a typeface is a process where a new digital typeface is created, based on written or engraved letters or printed metal or wooden typefaces. The process of digitisation of a typeface is well known, especially in the field of taking photos, the process of digitisation and typeface format (Baines, Haslam, 2002; Felici, 2003; Gordon, 2001). There is a lack of studies about the digitisation of an old type-face, i.e., they have not been preserved (Berry, 2002; Will, 2001), the design adaptation of linguistic culture of typography (Bringhurst, 2004) or a global typographic evolution, where the preservation of linguistic properties in the use of typography is required for the national cultural heritage (Medved, Možina, 2007).

From the above mentioned studies, some typographic changes have been made, i.e., word spacing is nowadays smaller - width of a small letter *i* (Cheng, 2005; Felici, 2003; Jury, 2004) - as it was suggested until the beginning of the 1980s, one half of an *em* or one third of an *em* for narrower typefaces, respectively (Blejec, 1957; Možina, 2011), x-height is nowadays higher, especially if a typeface is designed for digital media (Gatley, 2001; Jury, 2004). Therefore, the aim of the study was to create a typeface that could be used in different media with respect to cultural heritage.

2. Historical background

Professional and educational books in the Slovenian language were very rare in the second half of the 18th century. At that time, mostly religious and linguistic books were printed. Valentin Vodnik (1758-1819), the author of the first cookery book, *Kuharske bukve* (1799), in the Slovenian language, wrote numerous educational and linguistic books and prepared the material for a Slovenian-German dictionary (Mahnič, 1997; Šifrer, 1981; Vuga, 2004; Žvanut, 1998). He realised that the Slovenian language could grow with literature for professional and daily purposes (Ilich, 2006). Therefore, he started collecting recipes which were in use, regardless of the fact that he was not a culinary expert. The recipes were in German and Vodnik translated them into Slovenian. Unfortunately, the originals have not been found and it is hence not known whether Vodnik merely translated the recipes or also modified them to suit the Slovenian cooking of that time. In the preface, he wrote that "he tried to provide his fellow-countrywomen with the beginning of the Carniola culinary". Nevertheless, the first Slovenian cookery book was written in an understandable and uniform Slovenian language. This was not easy, as at that time, the Slovenian cookery terminology was not uniform and different parts of the country used different expressions. Therefore, Vodnik had to be very careful to use the correct language (Šifrer, 1981; Zlobec, 2006).

The cookery book was very popular among people. In consequence, 15 years after the author's death, a very important printer and publisher in Ljubljana, Jožef Blaznik (1800-1872), reprinted it. The book was slightly altered when reprinted for the second time in 1842 by the same printer. Blaznik's printing office was known as the best of that time. He bought a cylinder printing machine and was up-to-date in the typographic and lithographic technology. His works were known for their good quality. He is also important as he was supporting young Slovenian writers and printed Slovenian contemporary literature, e.g. Prešeren's poems (one of them is now the national anthem). Blaznik also printed some Slovenian magazines and the newspaper *Slovenec* (Berčič, 1969; Horvat, 1989; Jurač, 1989; Mikeln, 1990; Možina, 2003).

Since the second and third edition of the first Slovenian cookery book were printed in the best printing office of that time, the owner of which also played an important role in the growth of the Slovenian language, we decided to digitise the used typefaces. Especially, as the letters did not survive and we did not have any information where the matrix and the typefaces were bought.

3. Experimental

The process of digitisation is an exact piece of work if the original typeface is missing and we can only deal with prints of different quality. (Particularly, as the digitised typeface should be as useful in conventional as it is in digital media.) In the digitisation process, an exact typographic analysis of original printed types should be conducted. The analysis of the proportion between the height and the width of letters, between the height of letters and the stem or thick strokes, and between the thick and thin strokes should be performed. According to the data, a grid from a referential unit could be made. The referential unit is a small square the side of which is as long as much as the letter *I* is wide. The grid is used for sketching the new shapes forming a typeface and is later designed in a computer program for designing typefaces. During the digitisation, some improvements in the type design should be made to get recognisable letters and therefore the possibility for a legible text.

The original books are to be found in the Slovenian National and University Library. The digitisation of typefaces was developed through many different phases:

- taking photos of all pages in the books;
- cutting in Adobe Photoshop CS5 computer program a larger number of the same characters for the roman and italic typeface;
- enlarging the photos into a larger size than 7 and 8 pt;
- selecting four the most preserved and the least (during printing) deformed, respectively, characters for each small and capital letter, and figures;
- comparing the characters and defining different proportions;
- sketching a grid and positioning the letters, figures, punctuation marks, missing letters, missing figures for the italic typeface and some special characters for the roman and italic typeface in the grid;
- designing the letters, figures, punctuation marks, missing letters and some characters for the roman and italic typeface in the FontLab Studio 5 computer program, and
- defining the spacing and kerning pairs for the roman and italic typeface.

The differences in the typographic tonal density of the original and the redesigned typeface, called *Metelka*, were measured with an image analysis (ImageJ). This software gives the opportunity to measure, analyse and provide output values, e.g., area, number of particles, circularity and percentage of coverage (National Institutes of Health, 2011).

3.1 Results and discussion

Table 1: Average values of height and width measurements of roman typeface from original books (1834 and 1842)

	Height of small letters (pt)	Width of small letters (pt)		Height of capital letters (pt)	Width of capital letters (pt)
a	18.56	17.46	A	27.97	23.81
b	29.35	20.40	B	28.37	26.16
c	/	/	C	/	/
d	29.83	20.69	D	29.57	30.82
e	18.19	16.06	E	30.21	26.94
f	28.99	14.92	F	28.74	24.75
g	30.66	21.00	G	30.94	28.05
h	30.14	21.41	H	28.94	29.20
i	17.37	11.25	I	28.04	13.10
j	30.47	9.88	J	30.21	17.58
k	29.62	20.44	K	28.08	28.38
l	30.07	9.70	L	28.59	29.75
m	17.46	34.39	M	29.38	37.70
n	16.78	21.29	N	30.02	29.81
o	18.50	18.19	O	31.05	27.50
p	30.04	22.65	P	30.48	22.94
q	/	/	Q	/	/
r	17.33	17.16	R	29.60	27.50
s	18.21	11.41	S	30.40	18.75
ss	30.25	15.54	SS	/	/
t	25.18	11.24	T	29.71	31.50
u	17.90	22.23	U	/	/
v	17.89	18.69	V	28.25	28.17
z	17.19	15.31	Z	28.51	26.60
x	/	/	X	29.93	32.75
y	/	/	Y	/	/
w	/	/	W	/	/

From the measurement results (cf. Table 1), it can be seen that the height of roman capital letters is between 28.04 and 30.94 pt, while the height of roman small letters with ascender is between 28.99 and 30.14, the x-height of roman letters is between 17.19 and 18.56 pt, the height of roman small letters with descender is

30.04 pt for letter p, 30.47 pt for letter j and 30.66 pt for letter g. It can also be observed that the letters with flat upper and bottom strokes (i.e. H, I, L, Z, X, h, k, l) are smaller and the letters with rounded upper or/and bottom strokes (i.e. G, O, P, R, S, a, e, j, g, o, s) are larger.

Italic capital letters are slightly smaller (cf. Table 2), as their height is between 27.27 and 30.70 pt, while the height of italic small letters with ascender is more coherent, i.e. between 29.48 and 30.01 pt. The x-height of italic letters is between 18.58 and 20.87 pt and is higher than at roman letters. The height of italic small letters with descender is the lowest for letter p (30.28 pt) and the highest for letter g (31.83 pt), as it can be seen at the roman letters. An exception is small letters f and ss; the bottom part of the stroke of these goes into descender. As it is already seen at the roman as well as italic letters, the letters with flat upper and bottom strokes are mostly smaller, and the letters with rounded upper or/and bottom strokes are larger. The measurements indicate the difference in the letter width between the roman and italic typeface (cf. Tables 1 and 2). Italic capital letters are wider than roman letters, while a minor width difference between the small letters of the roman and italic typeface can be observed.

Table 2: Average values of height and width measurements of italic typeface from original books (1834 and 1842)

	Height of small letters (pt)	Width of small letters (pt)		Height of capital letters (pt)	Width of capital letters (pt)
a	18.81	22.35	A	28.88	38.42
b	30.00	18.36	B	29.29	31.44
c	/	/	C	/	/
d	29.99	23.37	D	29.79	37.62
e	20.87	15.38	E	/	/
f	46.23	42.00	F	/	/
g	31.83	26.94	G	30.70	27.08
h	29.48	22.06	H	27.27	36.13
i	18.58	9.44	I	/	/
j	30.28	24.59	J	30.11	30.00
k	30.01	22.39	K	29.85	36.31
l		31.52	L	30.07	32.92
m	19.53	33.75	M	29.67	47.75
n	18.38	22.94	N	30.31	38.58
o	19.52	18.63	O	31.87	29.38
p	30.56	23.59	P	29.60	31.22
q	/	/	Q	/	/
r	19.40	20.13	R	29.39	31.31
s	20.11	17.13	S	30.49	24.34
ss	45.41	36.19	SS	/	/
t	26.67	13.50	T	30.11	36.57
u	19.25	21.85	U	/	/
v	20.24	18.63	V	29.42	36.81
z	19.30	16.06	Z	28.69	28.00
x	/	/	X	/	/
y	/	/	Y	/	/
w	/	/	W	/	/

According to the measurements, the proportion between the stem and height of a capital letter is 1:6.78. After the first sketches, the proportion changed into 1:6 (cf. Figure 1). Later, at the designing of letters in the computer program, we realised that the changed proportion between the x-height and ascender or descender could increase legibility. It was also noticed that a slightly thinner stem would improve legibility. Therefore, the proportion between the stem and height of a capital letter was changed into 0.9:6.2, and the proportion among the x-height, ascender and descender was finalised into 4.3:1.9:2.0.

The width of digitised roman letters was changed into slightly wider as it was at the originals (cf. Figure 2). The only exceptions are the capital letters T and M, and the small letter m. For small letters, slightly higher x-height and larger counter size were designed. The ascender stroke at letters f and t is shorter. Figures underwent the most substantial changes, especially 3 and 4, while the non-lining form was preserved. The slope into the right at the digitised italic typeface is smaller. The proportions between the letters' width and height are uniform. All capital letters, with the exception of S, are slightly narrower from the original typeface, whe-

reas the width of some small letters (i.e. *b*, *d*, *e*, *g*, *h*, *p* and *s*) is slightly wider (cf. Figure 3). The ascender stroke at letters *f* and *t* is shorter. Not only the figures for the italic typeface, but also the missing letters, diacritics and special characters had to be designed for contemporary use (cf. Figure 4).

The typographic tonal density (TTD) of the body typeface from the original books and digitised typeface was measured (cf. Figure 5, Table 3). The results show a slight difference in TTD between the originally printed books, which is a consequence of the printing pressure and used papers. The digitised typeface has lower TTD from the originally printed typeface, since the counter size and proportion of the stem and the height of the capital letter and among the x-height, ascender and descender were changed.

The digitised typeface is still the same style, i.e. modern (Možina, 2003; McLean, 1996), as originally printed in 1834 and 1843, respectively. Due to some changes during the digitisation, the digitised modern typeface *Metelka* becomes uniform, enables better legibility and is useful in contemporary use.



Figure 1:
First sketches of roman typeface

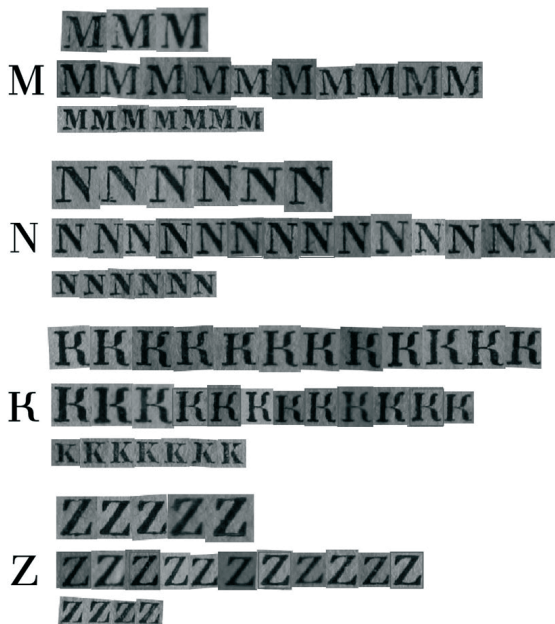


Figure 2:
Some original and digitised capital
letters of roman typeface

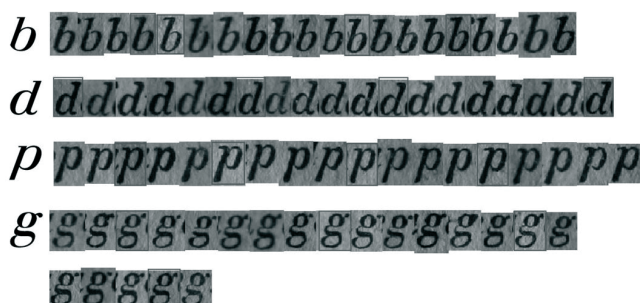


Figure 3:
Some original and digitised small letters
of italic typeface

ABCČDEFGHIJKLMN *ABCČDEFGHIJKLMN*
 OPQRSŠTUVWXYZŽ *OPQRSŠTUVWXYZŽ*
 abcčdefghijklmno *abcčdefghijklmno*
 pqršstuvwxyzž *pqršstuvwxyzž*
 01234567789 *01234567y89*
 ÁĆÉÍĹŃÓŔŚÚÝŽ *ÁĆÉÍĹŃÓŔŚÚÝŽ*
 áćéíńóŕśúýž *áćéíńóŕśúýž*
 ÄËÏÖÛÿäëïöü *ÄËÏÖÛÿäëïöü*
 ČĎĚĽŃŔŠŤŽčďěňŕšž *ČĎĚĽŃŔŠŤŽčďěňŕšž*
 ÀÈÌÒÙàèìòù *ÀÈÌÒÙàèìòù*
 ÂÊÎÔÛâêîôû *ÂÊÎÔÛâêîôû*
 ŦđŕŕŐŰŐűŹžĐđĎĽ *ŦđŕŕŐŰŐűŹžĐđĎĽ*
 &@€%/'-'“-” „-… ê@€%/'-'“-” „-…
 !?¿:÷×{|}—i”±`´Ń *!?¿:÷×{|}—i”±`´Ń*
 ^"#S%&(*)+,-./:;<=> *^"#S%&(*)+,-./:;<=>*
 ÆæĒēŊŋŪŵzēŪŷĶĴĴ
 3zHhNnŦŵéžóĪ

Figure 4: All digitised and newly design characters of roman and italic typeface Metelka

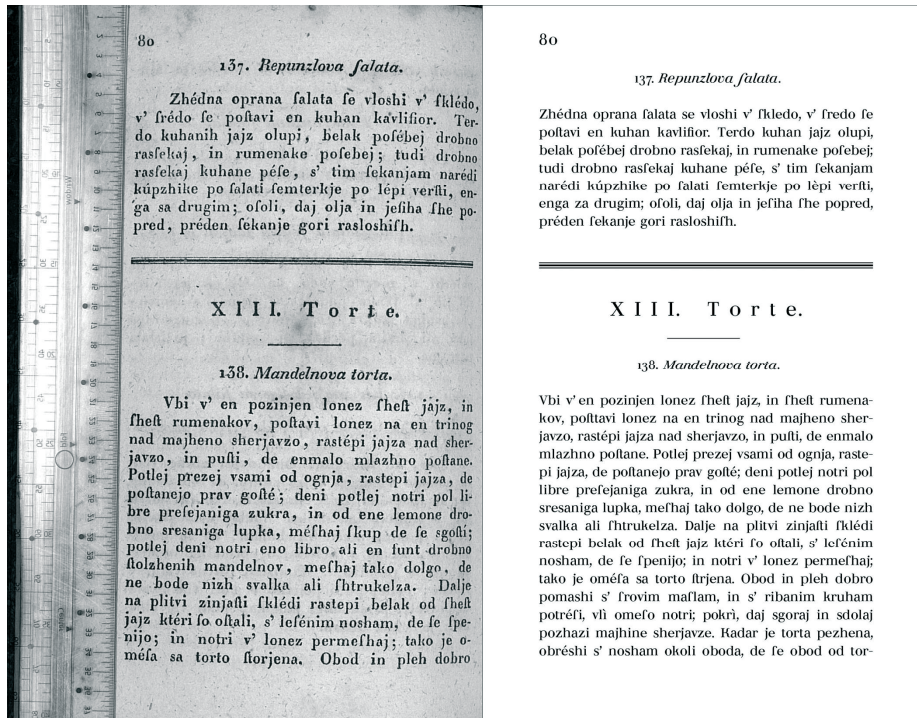


Figure 5: Originally printed text in 1834 (left) and digitised typeface Metelka (right)

Table 3: Average typographic tonal density (TTD) of body text from original books and digitised text

	Body text from 1834	Body text from 1842	Digitised text
TTD (%)	15.49	16.13	14.64

4. Conclusions

The digitised typefaces are not identical copies of the originals. The type style is still the same, i.e. modern. Generally, modern typefaces have the poorest legibility among the typefaces with differences between thick and thin strokes. With some minor changes in the letter form, the proportion between the stem and height of a letter, higher x-height and softer transition between strokes, the digitised modern typefaces become uniform and enable better legibility. The practical use of digitised typefaces showed that they are appropriate for contemporary use.

In the digitisation of an old typeface, very precise decisions about some improvements in the type design should be taken into consideration to get recognisable letters and therefore the possibility for good legibility in different media, although the typographic cultural heritage should not be dismissed.

References

Print sources

- Baines, P., Haslam, A., (2002), *Type & typography*, London, Laurence King Publishing, pp. 93-101.
- Berčič, B., (1968), *Tiskarstvo na slovenskem: zgodovinski oris, Ljubljana, Odbor za proslavo 100-letnice grafične organizacije na Slovenskem*, pp. 124-131.
- Berry, J. D., (2002), *Language Cultural Type - International type design in the age of Unicode*, New York, Association Typographique Internationale.
- Blejec, M., (1957), *Priročnik za ročne stavce, Ljubljana, Združenje grafičnih podjetij Jugoslavije, sekcija za LRS v Ljubljani*, pp. 91, 92, 184-190.
- Bringhurst, R., (2004), *The Solid Form of Language: An Essay Form of Language*, Kentville, Gespereau Press, pp. 9, 15-19, 27, 37, 41, 44, 55.
- Cheng, K., (2005), *Designing Type*, New Haven, Yale University Press, pp. 218-226.
- Dyson, M. C., Haselgrove, M., (2001), *The influence of reading speed and line length on effectiveness of reading from screen*, *International Journal of Human-Computer Studies*, Vol. 54, pp. 585-612.
- Felici, J., (2003), *The Complete Manual of Typography*, Berkeley, Peachpit Press, pp. 61-65, 145-150.
- Gabrič, A., (2011), *Reading from the pleasure of the elites to the common good*, *Knjižnica*, Vol. 55, No. 4, pp. 49-67.
- Gaultney, V., (2001), *Balancing Typeface Legibility and Economy: Practical Techniques for the Type Designer*, research essay, Reading, University of Reading, pp. 23, 24.
- Gordon, B., (2001), *Making digital type look good*, London, Thames & Hudson, 2001, pp. 26-35.
- Horvat, J., (1989), *Jožef Blaznik, tiskar - in še več: pozno a od srca*, *Delo*, No. 282, p. 5.
- Ilich, I., (2006), *Pota knjige, Ljubljana, Društvo Bralna značka Slovenije - ZPMS*, pp. 128-132.
- Jurač, J., (1989), *Vonj tiskarskih barv, Ljubljana, Splošno združenje grafične, grafičnopredelovalne industrije, časopisne in založniške dejavnosti ter knjigotrštva Slovenije*, pp. 46-59.
- Jury, D., (2004), *Reviving the rules of typography*, *Hove, RotoVision*, pp. 56-75, 78-80, 92-93, 128-131.
- Keyes, E., (1993), *Typography, color, and information structure*, *Technical Communication*, Vol. 40, No. 4, pp. 638-654.
- Kipphan, H., (2001), *Handbook of Print Media: Technologies and Production Methods*, Berlin, Springer, pp. 6-13, 983-992, 995-997, 1013-1019.
- Ling, J., Schaik, van P., (2006), *The influence of font type and line length on visual search and information retrieval in web pages*, *Displays*, No. 64, pp. 395-404.
- Mahnič, J., (1997), *Valentin Vodnik: Koprivnik in Gorjuše*, *Delo*, No. 104, p. 14.
- McLean, R., (1996), *The Thames and Hudson Manual of Typography*, London, Thames and Hudson, pp. 58-62.
- Medved, T., Možina, K., (2007), *Typeface Praetoria: from V-cut to digital media*, *ATypI Conference 2007: September 12-16, Brighton, University of Brighton and Association Typographique Internationale*.
- Mikeln, M., (1990), *Zaljubljen v črko: Ob ljubileju Blaznikove tiskarne*, *Delo*, No. 38, p. 14.
- Možina, K., (2001), *Zgodovinski razvoj knjižne tipografije*, doctoral thesis, Ljubljana, University of Ljubljana, pp. 244-254.
- Možina, K., (2003), *Knjižna tipografija, Ljubljana, University of Ljubljana*, pp. 100, 101, 169-178.
- Možina, K., Černič, M., Demšar, A., (2007), *Non-destructive methods for chemical, optical, colorimetric and typographic characterisation of a reprint*, *Journal of Cultural Heritage*, Vol. 8, pp. 339-349.

- Možina, K., Medved, T., Rat, B., Bračko, S., (2010), *Influence of Light on Typographic and Colorimetric Properties of Ink jet Prints*, *Journal of Imaging Science and Technology*, Vol. 54, No. 6, pp. 060403-1-060403-8.
- Možina, K., (2011), *Typography of Jože Plečnik*, *Knjižnica*, Vol. 55, No. 4, pp. 147-161.
- Pušnik, N., Možina, K., (2009), *TV programme typeface legibility*, *13th International conference on printing, design and graphic communications: Blaž Baronič 09: September 30-October 2, proceedings*, Zagreb, *University of Zagreb, Faculty of Graphic Arts*, pp. 145-149.
- Reynolds, L., (1988), *Legibility of Type, Baseline*, *International Typographic Journal*, No. 10, pp. 26-29.
- Rat, B., Možina, K., Bračko, S., Podlessek, A., (2011), *Influence of Temperature and Humidity on Typographic and Colorimetric Properties of Ink Jet Prints*, *Journal of Imaging Science and Technology*, Vol. 55, No. 5, pp. 050607-1-050607-8.
- Spencer, H., (1969), *The visible word*, London, *Royal College of Art, Lund Humphries*, pp. 12-14, 16-27, 31-35.
- Šifrer, J., (1981), *Vodnikove kuharske bukve: priloga*, Ljubljana, *Cankarjeva založba*.
- Tinker, M. A., (1966), *Bases of Effective Reading*, Minneapolis, *University of Minnesota Press*, pp. 125-127, 135-146.
- Tracy, W., (2003), *Letters of Credit: A View of Type Design*, Boston, *David R. Godine*, pp. 30-32.
- Vuga, D., (2004), *Spomin na Valentina Vodnika v Ljubljani*, *Rodna gruda*, Vol. 51, No. 1-2, p. 48.
- Will, G., (2001), *Genzsch Antiqua*, *ATypI Conference 2001: Copenhagen*, *Association Typographique Internationale*.
- Zlobec, M., (2006), *France Prešeren na žlici*, *Delo*, No. 55, p. 24.
- Žvanut, M., (1998), *Vodnikova domačija: Kulturni in naravni spomenik Slovenije*; Ljubljana, *Ministrstvo Republike Slovenije za kulturo, Uprava za kulturno dediščino*, pp. 7-19.

Web sources

National Institutes of Health, (December 2011), Research Services Branch, <http://rsb.info.nih.gov/ij/>

Surface patterning of flexo plates for improved ink transfer

Anja Hamblyn, Davide Deganello, Timothy C. Claypole

Welsh Centre for Printing and Coating
College of Engineering, Swansea University
Singleton Park, Swansea, SA2 8PP, United Kingdom
E-mail: 594674@swansea.ac.uk

Abstract

Flexography is being developed to improve process quality for new printing products such as printed electronics and biomedical applications. One of the causes for poor performance in flexography are hydrodynamic instabilities occurring during the ink transfer. The introduction of surface patterning to printing elements on the flexo plate is claimed to be a possible method to address the issue. This paper investigates the performance of several in-house surface patterns under a range of printing conditions. The test prints were produced on an IGT-F1 printability tester, and their digitised images analysed for optical density and print uniformity. Strong interactions between surface patterns and printing parameters were found which, depending on the printing conditions, could be beneficial as well as detrimental to the print quality. Therefore, surface patterns are not a universal remedy and have to be well-matched to the process parameters. If this is the case, not only the position of flexography in comparison to other printing processes will improve, but the flexo printer will be able to achieve better print quality at lower cost.

Keywords: flexography, ink transfer, print uniformity, surface patterning

1. Introduction and objective of research

The performance and quality of printing and coating processes is hampered by hydrodynamic instabilities occurring during the ink transfer between the rollers and to the substrate. One manifestation of the phenomenon is the well-known ribbing of viscous liquids usually associated with the lithographic printing process (Pearson, 1960; Reuter et al., 2007; Claypole et al., 2009). More recently it was documented under different names for gravure and flexographic printing (Voß, 2002; Bornemann et al., 2010, Bornemann et al., 2011). The result in all cases is an uneven ink film thickness which meets neither the aesthetic criteria for graphical products, nor the functionality of printed electronics or biomedical applications.

The introduction of surface patterning for solid printing areas is gaining popularity in flexographic printing as it appears to be leading to fewer visual artifacts in the printed areas, higher optical density of the solids, reduced ink built-up along the printing edges and therefore less dot gain. However, very little is known about the underlying mechanisms which counteract the occurrence of hydrodynamic instabilities.

This paper reports an investigation of the effects of surface patterns on print uniformity in flexography using a range of different plate materials, inks, substrates and printing conditions. The aim was to explore the underlying science in order to make the process of ink transfer more predictable and controllable.

2. Methodology

Two flexo plate materials (differing in surface energy and roughness) were imaged with 12 printing patches each. One of these remained without surface patterning and served as a solid reference patch. The other eleven patches had track and gap, grid, checkerboard, tile, positive and negative dot patterns (Figure 1). The nominal area coverage for the surface patterns varied between 50 and 95%. The nominal size of the macro features was 50 µm depending on the pattern.

An IGT-F1 laboratory printability tester was used to produce images under different printing conditions according to a full-factorial experimental plan. The following printing parameters were varied at two different levels: substrate, ink, printing pressure (50 and 150 N), printing speed (0.2 and 0.8 m/s) and anilox volume (8 and 12 cm³/m²). Representative for graphics printing, standardised coated paper APCO by Scheufelen (low surface roughness and absorptivity) and UV-curing ink (FlexoCure Gemini by Flint) were used as printing materials. With regards to biomedical applications, Ford's Gold Medal by Arjo Wiggins Fine Papers

(high surface roughness and absorptivity) and an in-house model biological ink (containing water, low-molecular PVA, surfactant and dye) were chosen for the investigation. A total of 64 different parameter combinations was examined.

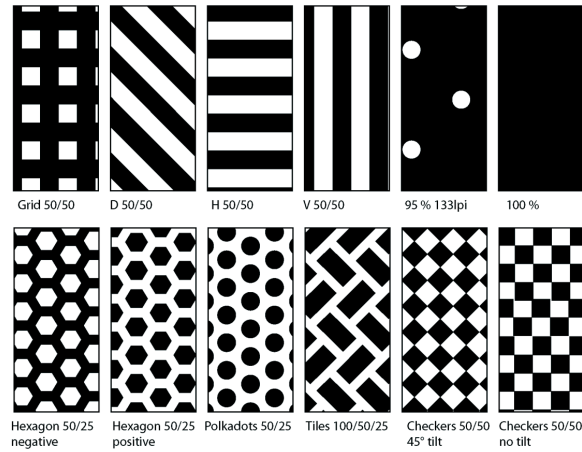


Figure 1: Illustration of plate images - (from top right to bottom left) reference solid, negative dot, track and gap, grid, checkerboard, tile, positive dot, positive and negative hexagon pattern

For the evaluation of print uniformity and optical density the prints were scanned at 8-bit greyscale and a resolution of 2000 dpi on an EPSON Perfection V700 Photo flatbed scanner and then analysed using the public domain image processing software ImageJ. The histogram of greyscale levels, mean greyscale level of the distribution and standard deviation of the mean were calculated for an area of 10x10 mm per patch and experiment.

Examples of the different types of distributions can be found in Figure 2. The shape of the greyscale level distribution provided information of the print uniformity. A narrow band with a single peak (unimodal, short-tail distribution) indicated a very uniform print. Wider, skewed distributions with several peaks and long tails could be seen for uneven prints. For this investigation the inverse correlation between the standard deviation of the mean greyscale level and the visually perceived uniformity of the print was sufficient to allow the use of the standard deviation as a measurand for print uniformity. The mean greyscale level was inversely proportional to the optical density of the prints. The correlation between the two has been confirmed through spectrophotometry. The lower the mean greyscale level, the darker is the printed image perceived.

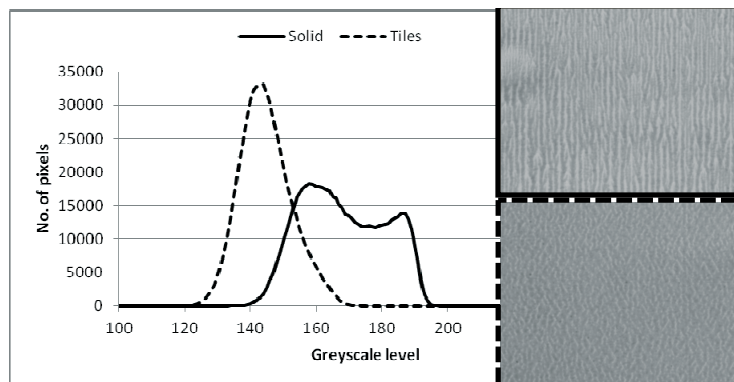


Figure 2: Example for the distribution of greyscale levels for the prints of a reference solid and tile pattern patch (water-based ink on APCO, 150 N pressure, 8 cm³/m² anilox volume, 0.8 m/s speed, rough plate)

3. Results and discussion

The mean values of all 64 experiments suggest that surface patterning can be used to improve optical density when printing with water-based ink (Figure 3). However, the print uniformity declines (Figure 4). In the case of UV-curing ink both, optical density and print uniformity are negatively affected by surface patterns in comparison to the reference solid.

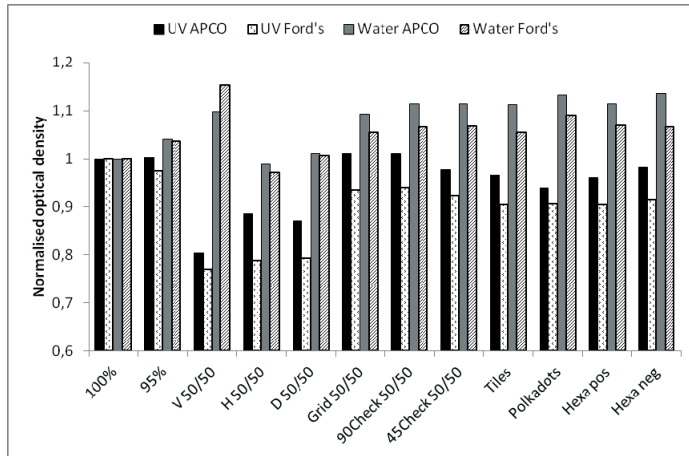


Figure 3: Mean optical density of all experiments normalised to the reference solid (higher values = higher density)

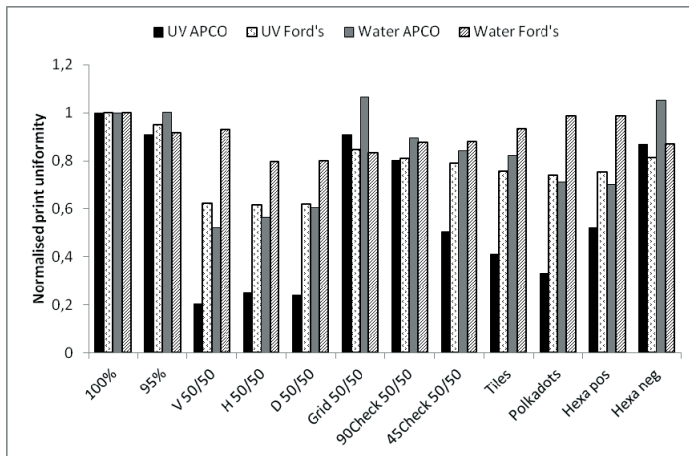


Figure 4: Mean print uniformity of all experiments normalised to the reference solid (higher values = more uniform)

Tables 1 and 2 compare the optimum surface pattern resulting in the best print uniformity at any given parameter combination on APCO substrate. For the smaller anilox volume of $8 \text{ cm}^3/\text{m}^2$, the reference solid produced some of the most uniform prints, while pattern patches dominated the higher volume range. The best pattern for print uniformity did not necessarily correlate with the one for highest optical density.

Table 1: Surface pattern providing highest print uniformity for a given parameter combination for printing with water-based ink on APCO

		Rough plate material		Smooth plate material	
		50 N	150 N	50 N	150 N
$8 \text{ cm}^3/\text{m}^2$	0.2 m/s	Reference solid	Grid	Reference solid	Reference solid
	0.8 m/s	Grid	Tiles	Grid	Reference solid
$12 \text{ cm}^3/\text{m}^2$	0.2 m/s	Tiles	95% halftone	Negative hexagons	Reference solid
	0.8 m/s	Checkerboard at 90° angle	Checkerboard at 45° angle	Negative hexagons	Negative hexagons

Table 2: Surface pattern providing highest print uniformity for a given parameter combination for printing with UV-curing ink on APCO

		Rough plate material		Smooth plate material	
		50 N	150 N	50 N	50 N
$8 \text{ cm}^3/\text{m}^2$	0.2 m/s	Reference solid	$8 \text{ cm}^3/\text{m}^2$	0.2 m/s	Reference solid
	0.8 m/s	Grid		0.8 m/s	Grid
$12 \text{ cm}^3/\text{m}^2$	0.2 m/s	Checkerboard at 45° angle	$12 \text{ cm}^3/\text{m}^2$	0.2 m/s	Checkerboard at 45° angle
	0.8 m/s	Checkerboard at 90° angle		0.8 m/s	Checkerboard at 90° angle

Several different sources of the print non-uniformities were identified by the nature of their appearance (Figure 5):

- substrate roughness;
- plate patterning and
- hydrodynamic instabilities.

The substrate roughness led to uneven contact between printing plate and substrate, thereby leaving valleys in the paper structure unprinted. This decreased optical density as well as print uniformity. Increasing the printing pressure levelled out some of the differences in surface height. That improved the optical density and print uniformity for all the ink systems and surface patterns examined. There was also an interaction of ink and printing plate particularly with the smoother substrate. At the lower pressure mainly the raised parts of the printing patterns made contact with APCO. The nominal surface patterning was identifiable in the prints. The ink squeeze at higher printing pressure led to a more contiguous ink film.

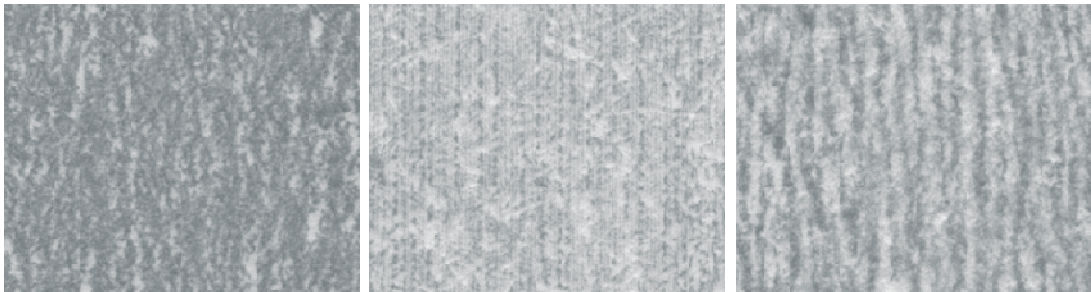


Figure 5: Uneven prints for water-based ink on Ford's Gold Medal caused (from left to right) by paper structure, plate patterning of vertical lines and hydrodynamic instabilities (the latter two superimposed with paper structure)

An increase in optical density for all ink-substrate combinations was also achieved by increasing the anilox volume. More ink provided on the anilox increased the ink transfer to the printing plate and ultimately to the substrate. This improved the area coverage for the rough blotting paper and was beneficial for forming a coherent film during ink squeeze, thereby improving the print uniformity. Only the water-based ink on APCO resulted in a significant decline in print uniformity for increased anilox volume. The reason for this were hydrodynamic instabilities during the ink transfer which manifested themselves as visual artefacts resembling tree bark. These structures were less pronounced at lower anilox volume, but the higher ink transfer increased the contrast in the prints by increasing the amplitude of the undulations of the ink film thickness. Due to its higher viscosity the UV-curing ink was less prone to such effects under the given printing conditions.

The increase in printing speed led to decreased ink transfer of the UV-curing ink, thereby printing from the tops of the surface patterns only and leaving areas of the substrate uncovered. This reduced the optical density and print uniformity. The opposite was achieved for water-based ink leading to better print results.

The printing plate with higher surface roughness and apparent contact angle transferred more coherent ink films to the substrate. The rough features on the plate surface possibly acted as an additional micro texturing to the macro pattern. The exact implications this has on the prints will have to be investigated separately.

4. Conclusions

A comprehensive investigation of the influence of plate surface patterning on the ink transfer of solids has been undertaken. There is a strong interaction between the plate pattern and the process parameters. Under some conditions the patterning was found to have an adverse effect on the amount and consistency of the ink transferred. Therefore surface patterns are not a universal remedy against visual artefacts and low optical density.

However, if plate pattern and process parameters are well-matched, the traditional boundaries of the flexographic operating regime will be pushed allowing a wider range of ink-substrate combinations to be printed under otherwise challenging printing conditions. This might provide flexographic printing with a vital advantage over the other competing printing processes with regards to functional printing. Graphics printers could also benefit with higher print quality, greater production efficiency, and therefore reduced cost, by being able to run faster printing speeds and to print high quality halftones and solids using the same printing plate.

Future work will see the confirmation of this small-scale print trial on an industrial-size printing press, as well as the inclusion of commercially available surface patterns in the investigation.

Acknowledgments

This research was funded through the Knowledge Economy Skills Scholarship (KESS) Project. KESS has been made possible by the EU's Convergence European Social Fund through the Welsh Government. The authors wish to thank Lorraine Leung for her assistance in printing, digitising and measuring the samples.

References

- Bornemann, N., Sauer, H. M., Dörsam, E., 2010. Thin film behavior after ink transfer in printing processes. In: LOPE-C (Large-area, Organic & Printed Electronics Convention), Frankfurt a. M., Germany, 31 May - 2 June 2010.
- Bornemann, N., Sauer, H. M., Dörsam, E., 2011. Gravure printed ultrathin layers of small-molecule semiconductors on glass. *Journal of Image Science and Technology*, 55(4), Article 040201.
- Claypole, T. C., Vlachopoulos, G., Bould, D. C., 2009. Ink ribbing in printing nips. In: *Advances in Printing and Media Technology*, IARIGAI 2009 Proceedings, Vol. 36, Stockholm, Sweden.
- Pearson, J. R. A., 1960. The instability of uniform viscous flow under rollers and spreaders. *Journal of Fluid Mechanics*, 7, p. 481-500.
- Reuter, K., Kempa, H., Brandt, N., Bartzsch, M., Huebler, A. C., 2007. Influence of process parameters on the electrical properties of offset printed conductive polymer layers. *Progress in Organic Coatings*, 58(4), p. 312-315.
- Voß, C., 2002. Analytische Modellierung, experimentelle Untersuchungen und dreidimensionale Gitter-Boltzmann Simulation der quasistatischen und instabilen Farbspaltung. Doctorate thesis, Bergische Universität Gesamthochschule Wuppertal, Studiengang Kommunikationstechnologie Druck.



Effects of solvents on flexographic printing plates

Alexandra Theopold, Jann Neumann, Daniel Massfelder, Edgar Dörsam

Technische Universität Darmstadt
Institute of Printing Science and Technology
Magdalenenstr. 2, D-64289 Darmstadt, Germany
E-mail: theopold@idd.tu-darmstadt.de

Abstract

High reproduction accuracy is a significant aspect in printed electronics. Small deviations can decide on the functionality of printed electronic devices. An undefined change of process parameters can have a negative effect on the printing results.

Aggressive solvents in functional fluids for printed electronics have an influence on the material properties of flexographic printing plates. We characterized the influences of solvents on material properties of flexographic printing plates. Differences in material characteristics before and after incubation with inappropriate solvents were analyzed.

We created a test bed to determine the effect of solvents on flexographic printing plates in a dynamic printing process. This dynamic solvent resistance tester allows us to perform solvent resistance tests under almost realistic printing conditions.

We analyzed characteristics of dynamic solvent resistance tests compared to static solvent resistance tests. We determined differences in material parameters of flexographic printing plates with and without mechanical stress.

Keywords: printed electronics, flexographic printing plates, solvent resistance, dynamic solvent resistance test

1. Introduction

The flexographic printing process plays a crucial role in printed electronics. Soft and elastic flexographic printing plates are well suited for printing on sensitive materials such as silicon wafer for solar cells or glass for organic light-emitting diodes (OLEDs). For printing electronic devices, high reproduction accuracy is very important. Small changes in material properties of flexographic printing plates during the printing process could limit or prevent the functionality of a printed electronic device.

Flexographic printing plates consist of photo-polymeric and elastomeric materials. These materials are often not compatible with solvents used in fluids for printed electronics. Toluene is a typical solvent which is used in functional fluids. Fine structures of flexographic printing plates tend to swell or shrink when they contact inappropriate solvents (Massfelder, 2012), (Theopold et al., 2012). The latter cause leaching of substances of the elastomeric and photopolymeric materials (Theopold, Dörsam, 2011) and material properties such as the viscoelasticity of the flexographic printing plates may be influenced. We analyzed the effects of solvents on flexographic printing plates under static and dynamic conditions. As illustrated in Figure 1, we compared the effects of solvents on the material properties such as swelling behavior and viscoelastic properties after static and dynamic solvent resistance tests.

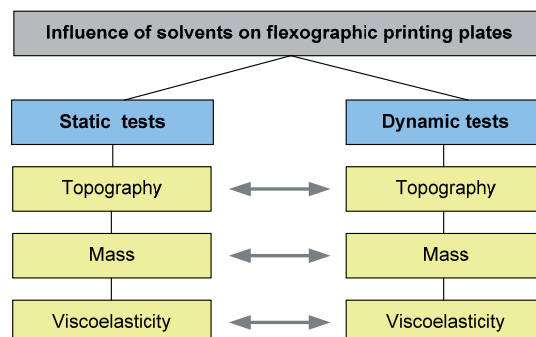


Figure 1: Influence of solvents on flexographic printing plates after static and dynamic solvent resistance tests

2. Experiment

For static and dynamic solvent resistance tests in the context of printed electronics, we used flexographic printing plates with test elements consisting of fine structures and solid areas. The printing plates were produced by different manufacturers with a resolution of 4 000 dpi for photopolymeric materials, and 2 540 dpi for elastomeric materials. The plate thickness was 1.14 mm. Solvents such as toluene and ethanol were used as test fluids. Toluene is a typical solvent for functional fluids which are used for printed electronics. Ethanol is a common solvent for the flexographic printing process for graphical printing. To ensure comparability, the materials were exposed to the solvents for an equally long time in static and dynamic tests.

Flexographic printing plates consist of viscoelastic materials. The increase in volume and the leaching of substances of the photo-polymeric and elastomeric materials may have an effect on the viscoelastic properties. We analyzed the viscoelastic properties of flexographic printing plates before and after solvent exposure.

2.1 Static solvent resistance tests

The solvent resistance of flexographic printing plates was tested with different solvents. In static solvent resistance tests, the tests are applied without exerting mechanical pressure. The samples of the different flexographic printing plates were placed into glass vessels, which were filled with the test solvents. The samples were completely covered with the solvent (Figure 2). The tests were absolved for a defined time period at constant ambient temperature of 23°C and humidity of 50%.



Figure 2: Test sample in a glass vessel at static solvent resistance test

To determine the solvent resistance of flexographic printing plates, static tests are common. However, these standard resistance methods do not perfectly reflect the actual conditions of the flexographic printing process (Theopold, Dörsam, 2011). Frequential mechanical loads of the material during exposure to solvents are not considered. In most cases, standard resistance tests do not reflect the printing conditions, in which only the surface of a flexographic printing plate comes into direct contact with the solvents.

2.2 Dynamic solvent resistance tests

To have a test method that corresponds to the actual printing conditions better, we developed a dynamic solvent resistance tester called *IDD rolling test rig*. This *IDD rolling test rig* simulates loads of the printing process such as abrasion and periodic compression by the rotation of printing plates.

Figure 3 shows the design drawing of the *IDD rolling test rig*. The design of the dynamic solvent resistance tester is based on the flexographic printing process. An ink supply is realized with a solvent trough. An anilox roller is used as a dosage. The printing plate can be mounted on a form cylinder. The printing pressure can be realized by means of an impression cylinder. The form cylinder is driven by a speed controlled motor. The anilox roller and the impression cylinder can be placed on the form cylinder. The fluid level is kept constant and controlled by a sensor.

For the comparison of the influence of static and dynamic solvent resistance tests on flexographic printing plates, the static and dynamic tests were absolved with the same time period, shown in Table 1.

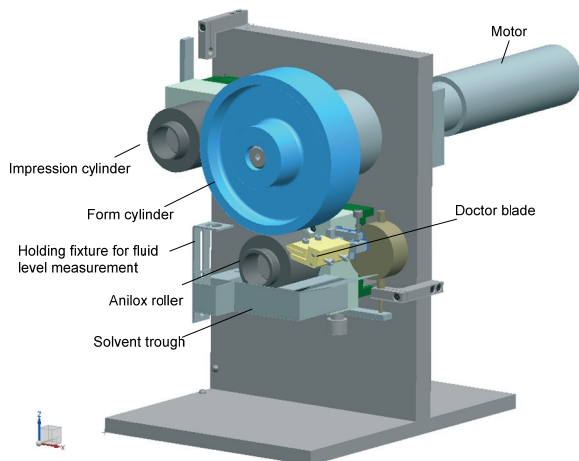


Figure 3:
Design drawing of the IDD rolling test rig for dynamic solvent resistance tests

Table 1: Incubation times of the static and dynamic solvent resistance tests

Test method	Incubation time	
	Toluene	Ethanol
Static test	45 minutes	360 minutes
Dynamic test	45 minutes	360 minutes

2.3 Characterization of viscoelastic properties

To characterize the viscoelastic properties of flexographic printing plates, *Zwick Z050* was used as a testing machine. This machine can be used for strain, shear and bending tests of various materials. By using this machine, we performed compression tests of elastomeric and photo-polymeric printing plates. The elastic deformation behaviors of the samples were measured with special compressive stress equipment (Figure 4). We developed that device especially for compression tests on thin material like paper (Kaulitz, 2009), (Desch et al., 2011), or flexographic printing plates. For the measurement of minor deformations, a high-precision digital gauge with a 50 nm resolution and an accuracy less than 1µm was integrated. The hardened cylinder that applies the load on the surface of the sample has a diameter of 6mm. The spherical calotte adjusts axial derivations.

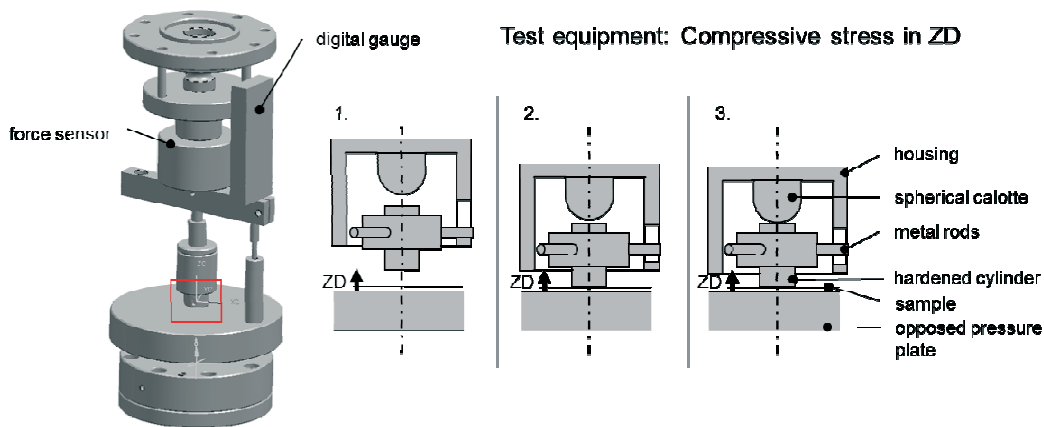


Figure 4: Picture of the function principal of the compressive test, designed at IDD (Kaulitz, 2009)

The elastic properties of various flexographic plate materials were compared before and after the exposure to solvents. As test elements, solid areas of the printing plates were selected. To simulate the stress of the flexographic printing plates in a printing process, a cyclic load was used. The cyclic load was determined on three cycles because of the evaporation of the solvents during the testing time. For evaluation, the first cycle was not considered. In printing processes, the plates are also loaded several times to get the printing result. All tests were performed at the same temperature of 23 °C because of the temperature dependence of the viscoelastic properties. A maximum surface pressure of 2.12 N/mm² was set. Limited by the machine characteristics, a velocity of 1 mm/s was chosen.

3. Comparison of the effects of static and dynamic solvent resistance tests

In flexographic printing processes, the printing plate materials are exposed to mechanical stress. However, in common static solvent resistance tests these mechanical loads are not considered. In this investigation we compared the effects of static and dynamic solvent resistance tests on elastomeric and photo-polymeric flexographic printing plates.

3.1 Influence on topographical properties of flexographic printing plates

To analyze the influence of solvents on topographic properties, the light microscope Leica DM 4000M was used. We compared the differences of fine positive structures after static and dynamic solvent resistance tests. Figure 5 shows a micrograph of an untreated elastomeric ethylene propylene diene monomer (EPDM) flexographic printing plate before the incubation with solvents. For the positive line of the untreated plate we measured $266\ \mu\text{m}$. For the negative line width, $365\ \mu\text{m}$ was measured.

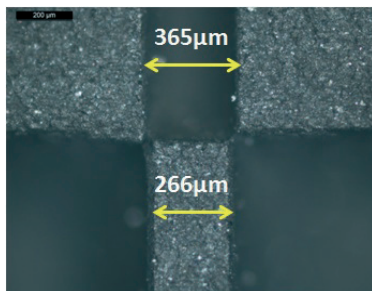


Figure 5:
Micrograph of an elastomeric printing plate before the incubation with solvent

A comparison of an elastomeric printing plate after static and dynamic solvent resistance tests with toluene is shown in Figure 6. In the positive line, there was a greater shrinkage after the static solvent resistance test compared to the dynamic test. For the positive line, after static tests, we measured $19\ \mu\text{m}$ shrinkage (Figure 6a). After the dynamic test, the positive lines showed no reduction of line width, but they exhibited defects as shown in Figure 6b. Negative lines tend to broaden after static and dynamic tests.

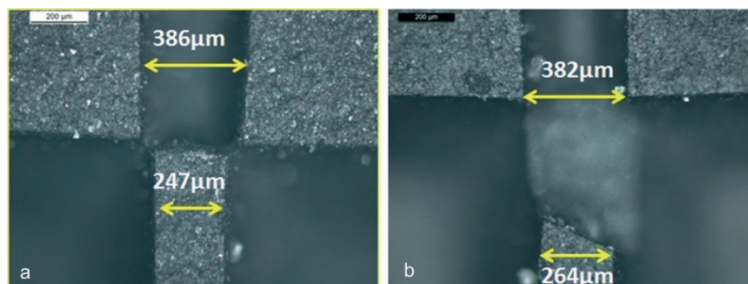


Figure 6: Micrograph of elastomeric printing plate after static (a) and dynamic (b) solvent resistance test with toluene

Figure 7 shows a micrograph of the photo-polymeric printing plates after static and dynamic solvent resistance tests with toluene. The photo-polymeric material was greater damaged after treatment with toluene in combination with mechanical load (Figure 7b), compared to solvent exposure without mechanical stress shown in Figure 7a.

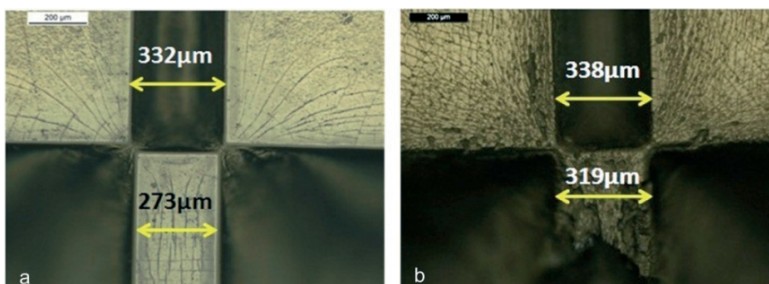


Figure 7: Micrograph of photopolymeric printing plates after static (a) and dynamic (b) solvent resistance test with toluene

Figure 8 shows white light interferometry measurements of positive lines of elastomeric flexographic printing plates.

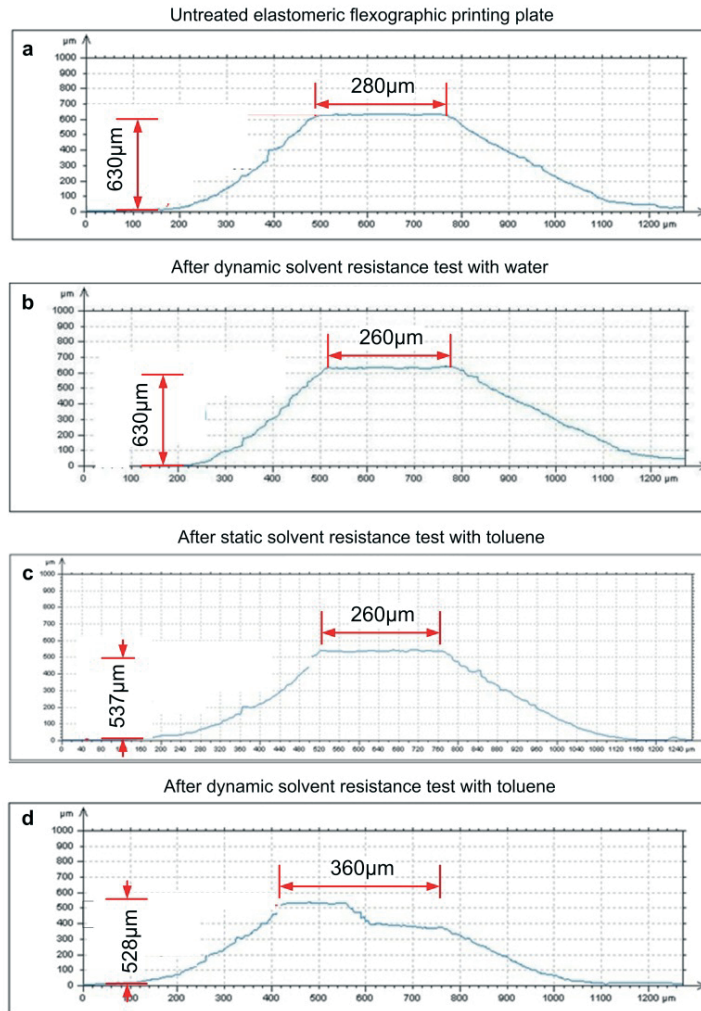


Figure 1: Pictures of optical profilometry measurements of an elastomeric flexographic printing plate relief before (a), after a dynamic solvent resistance test with water (b), after a static solvent resistance test with toluene (c) and after a dynamic solvent resistance test with toluene (d)

Figure 8a maps the profile of an untreated line of an elastomeric flexographic printing plate. The relief of the printing plate after the dynamic test with water (Figure 8b) showed no defects and no loss of height. After the static solvent resistance test method with toluene (Figure 8c), the relief had lost height, but it did not show any defects. After the treatment with toluene by using the *IDD rolling test rig* (Figure 8d), the relief height of the line decreased and showed defects. The combination of chemically treatment and mechanical stress cause a damage of the printing plate material.

3.2 Swelling properties of flexographic printing plates

We investigated the swelling of printing plates with gravimetric methods. The printing plates were weighed before and shortly after the exposure to solvents. To quantify the swelling, we used the swelling degree (Stachetzki, 2002) based on the change of mass q_0 , which is defined in equation [1].

$$q_0 = \frac{m_s + m_{pp}}{m_{pp}} \left[\frac{g}{g} \right] \quad [1]$$

with: q_0 : swelling degree based on change of mass
 m_s : mass of solvent that migrates into the printing plate
 m_{pp} : mass of the printing plate before solvent exposure

Comparing the swelling degree q_0 of different printing plates in static and dynamic tests (Massfelder, 2012) using toluene as a solvent, we found a discrepancy between the two methods. As shown in Table 2, static swelling tests cause higher swelling degrees.

Table 2: Swelling degrees of different printing plates in static and dynamic swelling tests with toluene

Printing Plate	Static tests	Dynamic tests
Photopolymer	1.8	1.7
Elastomer (EPDM)	1.4	1.3
Photopolymer p.el.	1.0	1.0

This gravimetric test method is not meaningful for the swelling behavior of the printing areas such as fine structures of flexographic printing plates (Theopold et al., 2012). However, it can serve as an indicator of the different changes in material properties after static and dynamic solvent resistance tests.

3.3 Effects of solvents on viscoelastic properties of flexographic printing plates

Previous investigations (Theopold, Dörsam, 2011) resulted, that inappropriate solvents cause leaching of substances out of the flexographic printing plates. A size exclusion chromatography (SEC) analysis showed that different types of substances are dissolved out of the material during the suspending in tetrahydrofuran (THF) as a test solvent (Theopold, Dörsam, 2011). A loss of substances could change the viscoelastic properties of the printing plates.

A common approach for the description of linear elastic deformation behavior of materials is the elastic modulus or young's modulus. The elastic modulus is defined by the slope of its stress-compression curve that can be measured by the universal testing machine *Zwick Z050*. Unfortunately, all flexographic printing plates show nonlinear stress compression behavior (hysteresis). Strictly observed, the assumption of elastic modulus E (Equation [3]) cannot be applied. Regardless, for the comparison of printing plates the linearized assumption is very helpful and therefore the hysteresis was approximate with a linear function.

$$\varepsilon = \frac{\Delta l}{l_0} \cdot 100 [\%] \quad [2]$$

$$E = \frac{\sigma}{c} = \frac{\Delta \sigma}{\Delta c} \left[\frac{N}{m^2} \right] \quad [3]$$

The compression ε is based on the deformation Δl with respect to the sample thickness l_0 (Equation [2]). The slope $\frac{\Delta \sigma}{\Delta c}$ of the deformation caused by stress was selected of each function $\sigma(\varepsilon)$ in the linear part between 0.5 N/mm² and 1 N/mm².

The comparison of the printing plates after static and dynamic solvent resistance tests with toluene and ethanol and without any treatment, showed differences in the stiffness. Table 3 shows the stiffness of the tested flexographic printing plates. For the evaluation, the second cycles of the measurements of each printing plates were considered.

Table 3: Comparison of the stiffness [N/mm²] of untreated printing plate materials and printing plates after static and dynamic solvent resistance tests with ethanol and toluene

Printing plate		PP		EPDM		PP p.el.	
Solvent		Ethanol	Toluene	Ethanol	Toluene	Ethanol	Toluene
Untreated	Stiffness [N/mm ²]	53		80		147	
Static test		44	7	79	32	138	112
Dynamic test		50	6	89	23	125	165

The behavior of photo-polymeric printing plate (PP) after static and dynamic solvent resistance tests with ethanol do not differ significantly. The slopes in the linear parts of the functions $\sigma(\varepsilon)$ vary minimally only. The stiffness between 0.5 N/mm² and 1 N/mm² for the untreated photo-polymeric material is 53N/mm². The material after the static solvent resistance test with ethanol has the stiffness of 44 N/mm². After the dynamic solvent resistance test with ethanol, the elastic modulus is 50 N/mm². In contrast, the material stiffness after the incubation with toluene differs significantly from the untreated photo-polymeric printing plate.

A stress-compression diagram of a photo-polymeric printing plate (PP) after static and dynamic solvent resistance tests with toluene, and without any treatment as well, is shown Figure 9. The untreated photo-polymeric printing plate is about a factor 8 stiffer than the material after the exposure to toluene. The stiffness after static and dynamic solvent resistance tests do not differ essentially.

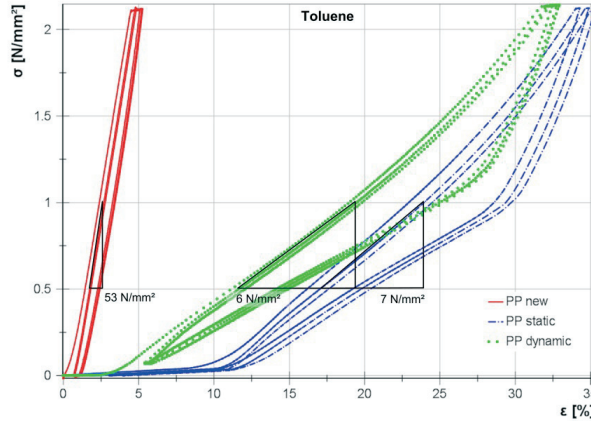


Figure 9: Comparison of photo-polymeric printing plate (PP) without any treatment (new) and after static and dynamic solvent resistance tests with toluene

The ethylene-propylene-diene monomer (EPDM) printing plates also showed no significant change in viscoelastic properties after the exposure ethanol, as shown in Figure 10. In contrast, the stiffness of the elastomeric material after static and dynamic solvent resistance tests with toluene decreased approximately by factor 3 (Figure 11).

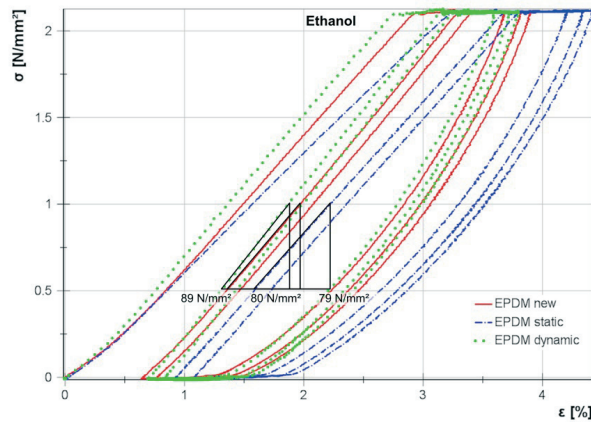


Figure 10: Comparison of an elastomeric printing plate (EPDM) without any treatment (new) and after static and dynamic solvent resistance tests with ethanol

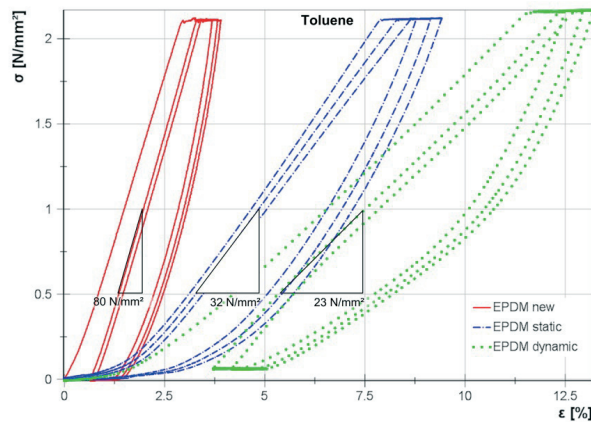


Figure 11: Comparison of an elastomeric printing plate (EPDM) without any treatment (new) and after static and dynamic solvent resistance tests with toluene

The material stiffness of a photo-polymeric printing plate for printed electronics does not vary essentially from the untreated material properties after the incubation with ethanol as well. In contrast to the other tested materials, the elastic modulus before and after any treatment with toluene also caused small differences only. The stiffness of the photopolymer for printed electronics (PP p.el.) increased after the contact with toluene. Figure 12 shows stress-compression- diagram of a photo-polymeric flexographic printing plate for printed electronics (p.el.). One striking feature is that the printing plate for printed electronics is stiffer than the photo-polymeric and elastomeric printing plates for graphical industries.

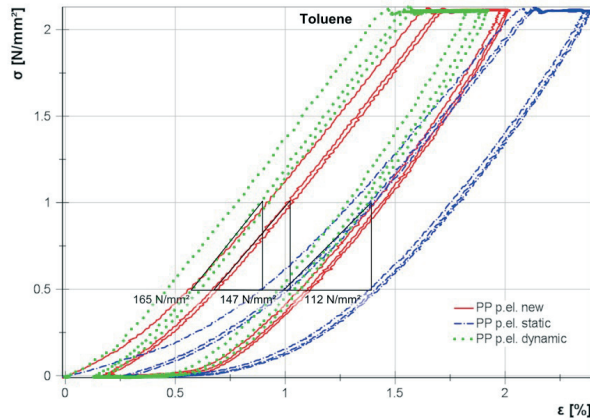


Figure 12: Comparison of a photopolymeric printing plate for printed electronic (PP p.el.) without any treatment (new) and after static and dynamic solvent resistance tests with toluene

4. Conclusion

The investigation of fine structures after the incubation with toluene shows, that the solvent has an important impact on the accuracy of the structures. Fine structures tend to swell or to shrink by contact with toluene. The comparison of the printing plates after static and dynamic solvent resistance tests shows, that a combination of chemically treatment and mechanical stress cause damage on the printing plate material. A chemically treated flexographic printing plate material is not stable under mechanical stress. In contact with the solvent during the printing process, the stability of the fine printing areas may be affect. Usual static solvent resistance tests do not consider the influence of mechanical loads on the flexographic printing plates. A damaged flexographic printing plate influences the printing results and the functionality of the printed electronic devices essentially.

The viscoelastic properties of photo-polymeric and elastomeric flexographic printing plates are not affected significantly by the test solvent ethanol. The printing plate materials are well adapted for graphical applications. In contrast, the elastic material properties changed essentially in contact with toluene. The stiffness of the photo-polymeric and elastomeric printing plates decreased significantly. The usual flexographic printing plates are well suited for graphical printing, but not for applications for printed electronics. Only the photo-polymeric printing plate for printed electronics showed no significant changes in elastic properties after the contact with toluene. Differences were found between the stiffness after static and dynamic solvent resistance tests. The stiffness of the material for printed electronics decreased after static solvent resistance tests with toluene. However, the material stiffness increased after dynamic solvent resistance tests. The tested printing plates for printed electronics are suited for functional fluids. It is conspicuous, that this printing plate is stiffer than usual printing plates for graphical applications. This has to be considered during the printing process.

Flexographic printing is interesting for applications for printed electronics. However, the flexographic printing plate materials have to adapt for the solvents in functional fluids. The usual printing plates for graphical printing are not suited for printing of electronic layers without problems. If the flexographic printing process would stay competitive in the field of printed electronics, the printing plate materials have to be adapted to the new conditions. The printing plate manufacturers and printing fluid manufacturers have to closely work together. For the production of functional printing fluids, the manufactures have to consider that the plate materials are negatively influenced by the solvents usually used in fluids for printed electronics.

Acknowledgments

This work is funded by the BMBF (Federal Ministry of Education and Research) under grant no. 13N12128. Special thanks go to the companies Asahi Photoproducts Europe n.v./s.a., DuPont de Nemours GmbH, Felix Böttcher GmbH and Co.KG and Flint Group Flexographic Products for sponsoring the flexographic printing plates and the nice cooperation.

References

- Desch, M. et al., (2009), Industrial Use for the "nip-induced effect" to separate sheets, Stillwater.
- Desch, M. et al., (2011), Determining the amount of sheets in a stack of paper by using a pressure stamp, Stillwater.
- Kaulitz, T., (2009), Bilden von Schneidlagen unter Ausnutzung des Nipinduzierten Effekts für die Druckweiterverarbeitung, Dissertation, Institut für Druckmaschinen und Druckverfahren Technische Universität Darmstadt.
- Massfelder, D., (2012), Solvent resistance of flexographic printing plates for printed electronics, Seminar paper at Technische Universität Darmstadt.
- Mirle, S. K. et al., (1988), Viscoelasticity of photopolymer plates and ink hydrodynamics in modeling flexographic printing, *Mathl. Comput. Modelling*, Vol.11, pp.1162-1165.
- Stachetzki, (2002), Untersuchung der mechanischen Eigenschaften und Quellung von mit Schwefelverbindungen vernetzten Stärkemaleaten, pp.32-53.
- Theopold, A., Dörsam, E., (2011), Characterization of flexographic printing plates with regard to the field of printed electronics, LOPE-C 2011, pp.330-334.
- Theopold, A. et al., (2012), Influence of solvents on flexographic printing plates, LOPE-C 2012.



Permanent flexographic plate changes through nip contacts

David Beynon, Timothy C. Claypole

Welsh Centre for Printing and Coating
School of Engineering, University of Swansea
Swansea, SA2 8PP, UK

E-mails: d.g.beynon@swansea.ac.uk; t.c.claypole@swansea.ac.uk

Abstract

In flexographic printing the image is carried on a relief surface that is deformed in the printing nips. It is not known if the pressures applied cause any permanent changes in plate dot geometry which is crucial for image quality. Any change in the shape of the plate dot could have an affect on phenomena such as dot gain and non-uniform ink spread. In this work white light interferometry has been used for accurate measurement of a conventionally produced photopolymer plate pre and post printing. Printing was conducted at full press scale with varied anilox volumes printing UV curing ink onto polypropylene substrate at 150 ft/min. The plate contained tonal strips from 5-80% coverage at line rulings of 65 lpi, 120 lpi and 175 lpi therefore a wide range of dot geometries were investigated.

The plate dots were found to increase in surface area (coverage) and decrease in circularity. There was however no correlation between coverage increases and dot height indicating that the increases in coverage are due to permanent stretching of the dot surface. There is also no correlation between circularity and coverage changes, the stretching is therefore due to contact in the anilox to plate nip.

Keywords: flexography, plate deformation, geometry

1. Introduction

In the flexographic printing process the image is carried on a flexible deformable relief surface (Kipphan, 2001). The raised dots of the halftone areas carry the image and are fundamental to the print quality therefore measurement of the plate has been crucial in previous research (Warford, 1997), (Liu, 2004), (Hamblyn, 2004). In the normal course of printing a positive engagement is added to the plate in the nip formed between the plate and the anilox roll and the nip formed between plate and substrate (impression cylinder) (Bould, 2004), (Bould, 2007). This engagement must be taken up by deformation of the printing plate, it is however unknown if this deformation has any permanent effect on the plate dots. Should the pressure exerted on the plate dots in the printing nips permanently alter the plate dot geometry this would impact current understanding of the role of plate deformation in phenomena such as dot gain and non-uniform ink spreading. For example an elongation of the dots would indicate that non-symmetrical ink spreading is not only a result of directional ink squeeze but also a result of permanent plate dot deformation. In this investigation measurement of an unprinted plate is followed by measurement of the plate post printing in order to determine changes in the plate dots through the print run.

2. Experimental procedure

The trial plate was a previously unused 1.14mm thick conventionally produced photopolymer plate containing three identical bands. These bands correspond to volumes of 1.63 (band1), 4.18 (band 3) and 5.49 cm^3/m^2 (band 4) of a banded anilox roll. All bands of the anilox roll were engraved at 500 lpi line ruling with a cell size of 50 μm . Within each band of the printing plate were coverage strips of 5, 20, 40 and 80% nominal coverage (coverage specified in PDF data) with line rulings of 65 lpi, 120 lpi and 175 lpi. The trial therefore investigated a wide range of dot shapes and geometries.

This work forms part of a wider trial investigating ink transfer in flexographic printing (Claypole, 2008), therefore the printing of the plate was subject to short runs with different plate to substrate engagement of 3thou (76.2 μm), 4thou (101.6 μm) and 5thou (127 μm). The force applied at the three plate to substrate engagements used was measured on solid areas of the plate using thin film sensors, the force applied was 30 N, 45 N and 83 N respectively for the 3, 4 and 5 thou engagements. The force between anilox and plate was measured as 92 N.

The UV curing ink used was first applied to the plate during set up and remained in contact with the plate throughout the trial with no cleaning of the plate between runs. At completion of print trials the anilox was backed away and excess ink printed from the plate surface. Finally the plate was removed from the backing tape (3M 1015 soft tape) and cleaned on a flat surface using IPA solvent, a cleaning brush and gentle patting with low lint cloth. In total the ink was in contact with the plate for approximately 5 hours.

Printing was conducted at full press scale printing UV ink onto polypropylene substrate using a Timsons T-Flex 508 press at speeds of 150 ft/min.

3. Measurement methodology

The new plate was measured before printing, the same patches were then measured after printing having allowed 64 hours for any remaining cleaning solvent to evaporate. Plate measurement was conducted using white light interferometry, measuring the full depth of a single dot cell (Figure 1). Surface area of the dots was determined by isolating the surface and the dot height measured using a 2-D profile across the dot surface and depth marks. 20 dots within each coverage patch were measured and the average calculated.

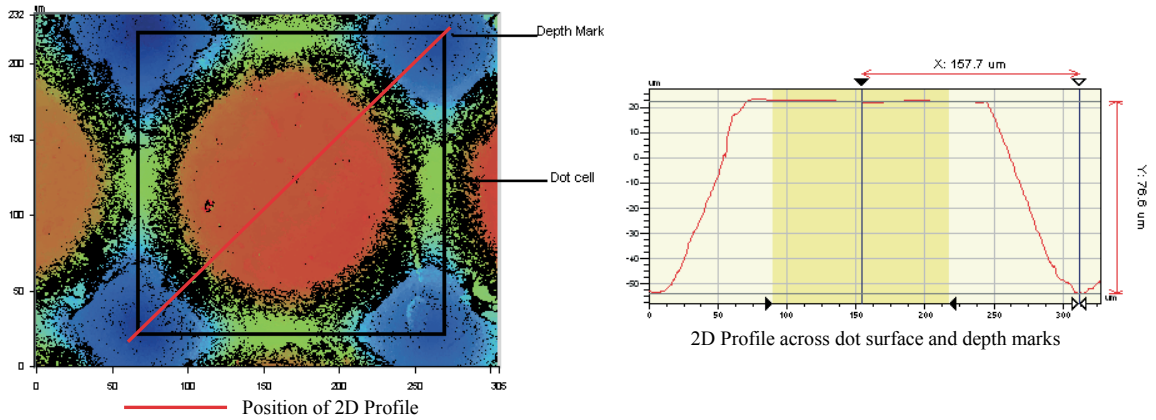


Figure 1: Measurement of a 50% coverage dot

The printed dot circularity has been used as a measure of the print quality (Galton, 2006) and can also be used to characterize the geometry of the plate dot. This method uses Vision 32 software to remove the dot shoulder roughness and isolate the dot surface, the measurement is then exported as a TIFF image. Image analysis software is then used to determine the circularity of the dot. The circularity is calculated according to equation 1 where a circularity of 1 represents a perfect circle and decreasing circularity value represents an increasingly elongated polygon (Image J manual, 2007).

$$Circularity = 4\pi \left(\frac{Area}{Perimeter^2} \right) \tag{1}$$

4. Results

4.1 Coverage

The plate deformation is plotted against pre-printing coverage in Figure 2 for the 120lpi tonal strips, the 120lpi data is representative of the trends seen for all line rulings. The plate deformation through the printing nip has been calculated according to equation 2. The percentage plate deformation is the percentage increase in dot size from the pre-print measurement to the post print measurement.

$$Plate\ Deformation = Post-Print\ Coverage - Pre-Print\ Coverage \tag{2}$$

The only coverage patch to show coverage increase for band 1 is the 5% coverage. The band 3 and 4 patches show a gain in coverage that gets larger from 5 to 40% coverage, decreasing from 40% to 80%. The percentage plate deformation (Figure 3) is largest for the 5% coverage patches and decreases from 5% to 80% with the highest coverage gain seen for the band 3 dots followed by the band 4 dots.

The increase in stretch from 5-40% is observed because the dots are larger and therefore can stretch by a larger amount, the decrease in stretch from 40-80% is due to increased rigidity of the dots preventing stretching as the dots become joined.

The dots of band 3 have the largest stretch through the printing nips however, the tonal strip had the lowest coverages pre-printing, this is thought to be due to a lower exposure due to bulb positioning during manufacture. A reduced exposure could lead to a lower degree of hardening of the photopolymer therefore leading to a larger degree of stretching through the printing nips.

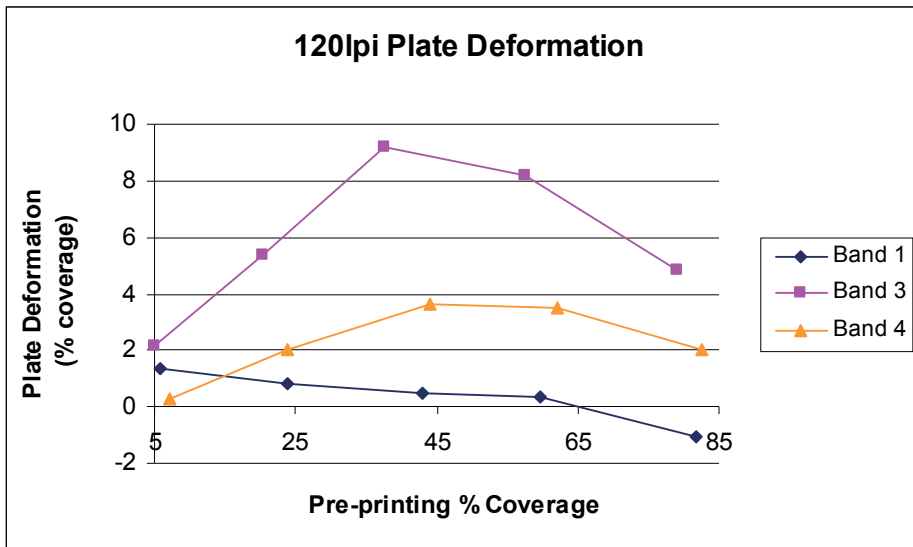


Figure 2: 120 lpi plate deformation

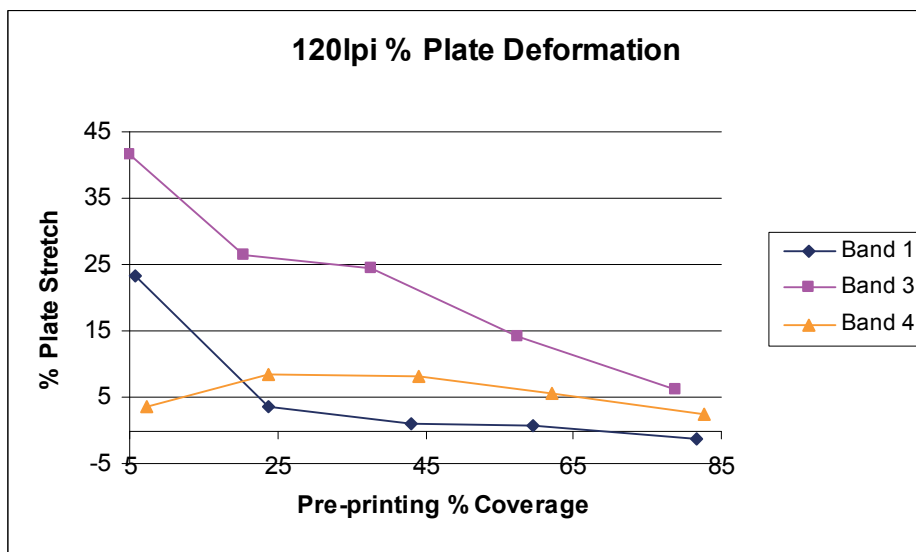


Figure 3: 120 lpi % plate deformation

Figure 4 shows the measured coverages both pre and post printing. It would appear that the variation between the bands is reduced through the printing nip, especially for band 3. There are still however significant differences between the bands for the post print data.

The coverage changes observed through the printing nip could be caused by 2 mechanisms, permanent barrelling of the shoulder or permanent stretching of the dot surface (5). If the source of dot growth is the permanent barrelling of the dot shoulder the change in coverage would have an associated dot height reduction. There is however no correlation between dot height change and plate stretch therefore the plate stretch through the printing nips is due to a permanent stretching of the surface of the dot.

4.2 Circularity

The circularity changes through the printing nips are presented in Figure 5, the circularity decreases through printing however there is no trend observed for this circularity change. The reduction in circularity indicated that the coverage changes are not equal around the circumference of the dots. There is however no correlation between the circularity changes and coverage changes. Therefore the changes in dot shape and size are being created in the anilox to plate nip. The contact between the anilox cell walls and the plate dot could occur at many different positions, some of which are shown in Figure 6. As in the anilox to plate nip contact between the dots and anilox cell walls occurs over narrow bands (compared to the entire dot at the plate to substrate nip) a larger pressure is exerted over this part of the dot resulting in permanent stretching of the dot surface, increasing the coverage and decreasing the circularity. As the position of contact with the anilox cell walls will be different for each plate dot within a coverage patch the degree of stretching and circularity change will be different for each dot therefore no correlation will be observed between the coverage and circularity changes.

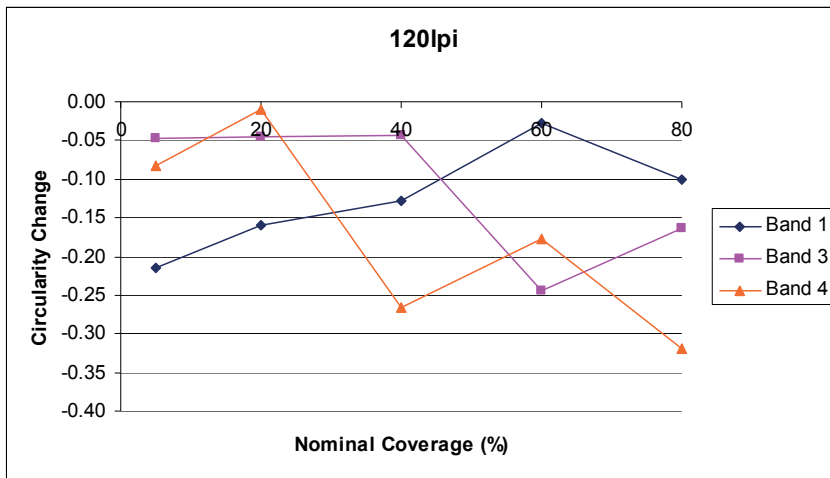


Figure 5: Change in plate dot circularity through printing

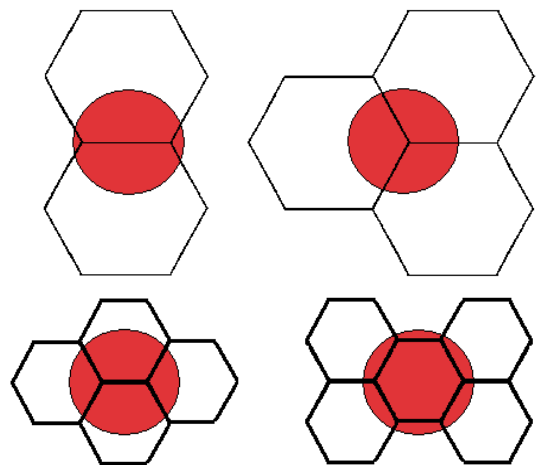


Figure 6: Possible contact points between anilox cells and plate dots

5. Conslusions

Significant increases in coverage have been found through the printing nips. The largest increase in coverage was found for the band with the lowest initial coverage. This acted to reduce deviation between nominally identical bands however significant differences between the bands still existed. The reduction in deviation between nominally identical bands suggests that an initial pre-load on the plate may act to reduce non-uniformity across the print area.

No correlation was found between the coverage increase and height change therefore the increased coverage is due to permanent stretching of the plate surface and not permanent barreling of dot shoulders.

Significant circularity decreases occurred through the printing nips therefore coverage changes are not equal around the circumference of the dots. There is however no correlation between coverage increases and circularity decreases therefore permanent plate dot deformation is caused in the plate to anilox nip.

References

- Bould, D. C., Claypole, T. C., Bohan, M. F. J (2004) An investigation into plate dot deformation in flexographic printing. Proc. Instn Mech Engrs Vol 218 Part B: J. Engineering Manufacture p1499-1511.
- Bould, D., Hamblyn, S., Cherry, J. , Claypole, T (2007). Modelling the anilox-plate micro contact. Advances in Printing and Media technology Vol 34, p69-76.
- Claypole, T. C., Beynon, D. G., Hamblyn, S. M. (2008) Ink transfer during flexographic printing to paper. Advances in printing and media technology, Vol 35, p181-188.
- Galton, D., Rosenberger, R. (2006) A novel solution to the evaluation of flexographic print quality. TAGA proceedings.
- Hamblyn, S. (2004) The Role of the Plate in the Ink Transfer Process in Flexographic Printing, PhD Thesis, University of Wales Swansea.
- Image J manual (2007), <http://rsbweb.nih.gov/ij/docs/guide/userguide-27.html#sec:Analyze-Menu>
- Kipphan, H. (2001) Handbook of Print Media, Springer-Verlag
- Liu, X., Guthrie, J., Bryant, C. (2004) A study of the relevance of plate quality and print quality to UV flexographic folding carton printing. Surface coatings international Part B: Coatings transactions Vol 87.
- Warford, M. (1997) Shoulder Angle determination with Flexographic Photopolymer Plate Material. TAGA Proceedings, p906-929.



Ink splitting: The influence of structured surfaces on the contact angle in flexo printing

Stefan Griesheimer, Edgar Dörsam

Technische Universität Darmstadt
Institute of Printing Science and Technology
Magdalenenstr. 2, D-64289 Darmstadt, Germany
E-mails: griesheimer@idd.tu-darmstadt.de; doersam@idd.tu-darmstadt.de

Abstract

Surface tensions of contacting surfaces play a central role in the ink splitting process. A structured roll surface may have both positive and negative effects on the liquid surface tension, on the adhesion and, ultimately, on the ink splitting process. Due to the cavitation in highly dynamic ink splitting processes, viscous fingering instability may occur after the printing process, depending on the viscoelastic properties of the fluid. The printing results show how this viscous fingering supports the increase of filament spinning. The development of these filaments and the transmission behavior from roll to roll has not yet been adequately investigated. The application of knowledge of structured surfaces and characteristics of the inks to the highly dynamic printing process is a broad field of research. In this paper, contact angle measurements were performed on flexible plates to observe the behavior of liquids on structured surfaces. In a further step, a simple experiment demonstrated in that a structured surface has an influence on the filament formation. This research is the approach to find the scientific relations of dynamic separation and contact angle measurements. It could be the approach to understand the ink splitting better.

Keywords: surface tension, contact angle, ink splitting

1. Introduction

During flexo printing, ink is transferred from the chambered doctor blade onto the anilox cylinder, from there onto the plate cylinder and then onto the substrate. Older studies show that the increase in surface tension of the contact partners with the main flow of ink has a positive effect on the transmission (see Figure 1). The surface tension of solid surfaces depends on their structure and the respective material properties (DEU99), (WAG64).

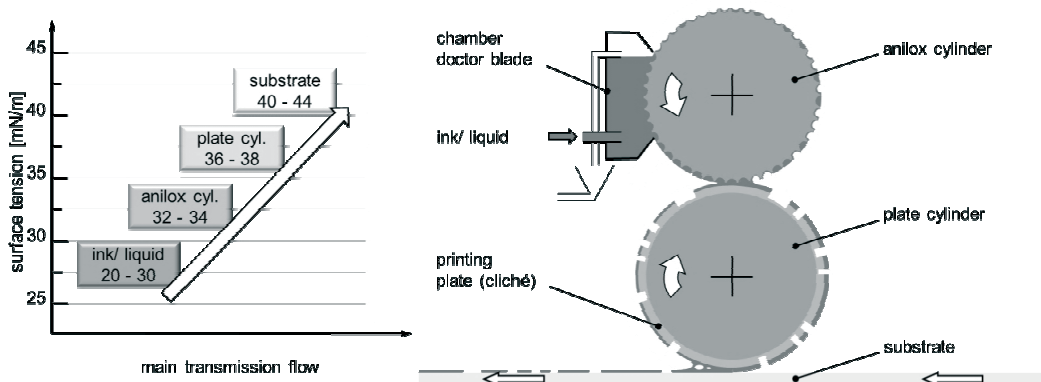


Figure 1: Surface tension of contact partners with the main flow and total flexo printing process (DEU99), (KIP00)

When using flexo printing for "functional printing", new very complex functional liquids are used. Depending on the surface tension of these liquids, the whole ink transfer can change. As a consequence, new questions arise. In particular, structured surfaces and characteristics of the inks in the highly-dynamic printing process generate a broad field of research. There are two conditions in ink transfer: "film splitting" (large ink volume) and "split of dots" (small ink volume) (BEH93), (BER99), (HÜB91).

In the manufacture of functional layers, the aim is to produce full tone areas with a printing plate or a flexible plate (cliché). For the further development of functional flexo printing, it is important to understand the transmission phenomena better. Moreover, the surface tension depends on the geometry and the direction of the structuring of the printing plate (BIC01), (CHU10).

2. Characterization of the printing plate

A printing form is defined by the angle of orientation, the number of lines per centimeter and the percentage of the transfer surface. As an example, only one type of printing plate with 48 lines/cm is presented here. It is a digital printing plate manufactured by "reproform" and prepared by means of the film exposure and commercially available LAMS (laser ablative mask solution) layer. The height profile of the surface was measured by means of white light interferometry (Sensofar Plμ Neox) very accurately from 0 to 100% of printing areas (see excerpts in Figure 2 (a)). Generally, it is assumed that the ink is transmitted through the printing areas on the substrate. However, there is a relationship between the printing and the non-printing areas. Upon contact of the plate cylinder and the anilox cylinder, the structuring of the total area has a significant influence on the ink transfer. Depending on the structuring of the printing form, more or less ink is transferred. In the ink transfer to the substrate, the non-printing areas also have an indirect influence on the amount of ink to be transferred. The stored ink from the non-printing areas flows across the contacting areas and it is transferred. According to the rheological properties of the ink and the behavior of the structured surface, the desired ink transfer may increase or decrease. The surface structure of the non-printing areas changes as soon as the printing areas increase. The fact that the dots meld together has a huge impact on the structure of the total surface. The storage volume of the non-printing areas decreases with the increase of the printing area. The reduction of the possible storage volume is not constant because the structure changes (see Figure 2 (a)).

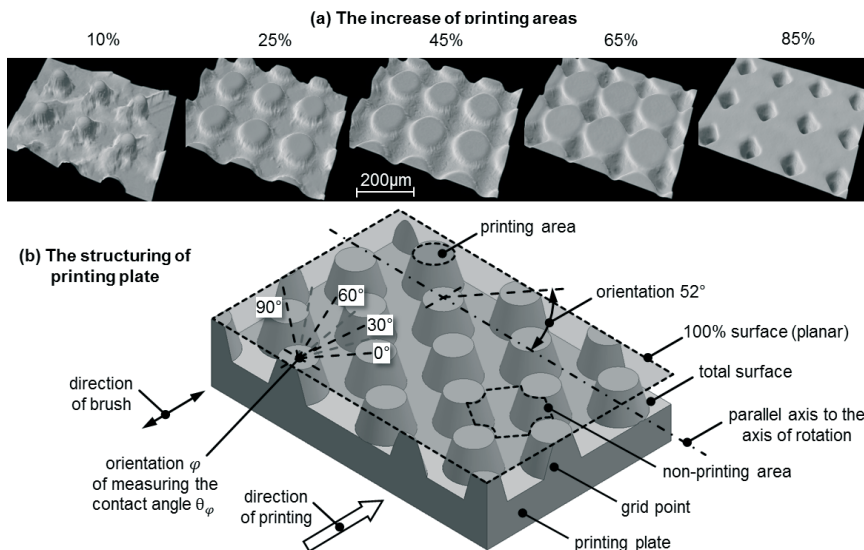


Figure 2: A conventional printing plate measured by white light interferometry (a) and a sketch of the surface to illustrate the orientation of the structuring (b)

A variable structure of the non-printing areas has a direct influence on the adhesion effect and thus on the fluid intake. Depending on the type of wetting of the surface, there are air bubbles in the capillary to reduce the adhesion effect. The influence of the adhesion effect is directly related to the surface tension and the contact angle θ_φ (see Figure 3). To determine the pending size of the surface tension, the increase in area of the printing plates at a contact angle measurement system (KRÜSS DSA 100) was examined more closely. The method of determining the contact angle of the structure surface is not new. However, it is necessary to characterize the printing plate and compare it with phenomena in the printing process. The investigations of the contact angle were considered only statically. The contact angle θ_φ was measured at different angles of the orientation φ to analyze the influence of the orientation of structuring. Figure 2 (b) shows the appointed angle of the direction of orientation that was investigated in the contact angle measurement. Distilled water, a glycerol-water mixture and water-based flexo ink were investigated. The amount of liquid in the static measurement was 3 μl and the printing surface raised by 45% printing area (see Figure 3).

It was found in experiments that there is a direct correlation between the orientation of the printing plate and the contact angle. Thus, we rotated the plate in steps of 30° and determined the contact angle. The results of the three fluids that we used are shown in Figure 3. The curves are polynomials and they show only one possible cause. In fact, the contact angle should be the same at 0° and 90°. This can be caused by applying the liquid manually or from washing out phenomena in the manufacturing process such as scratches from the

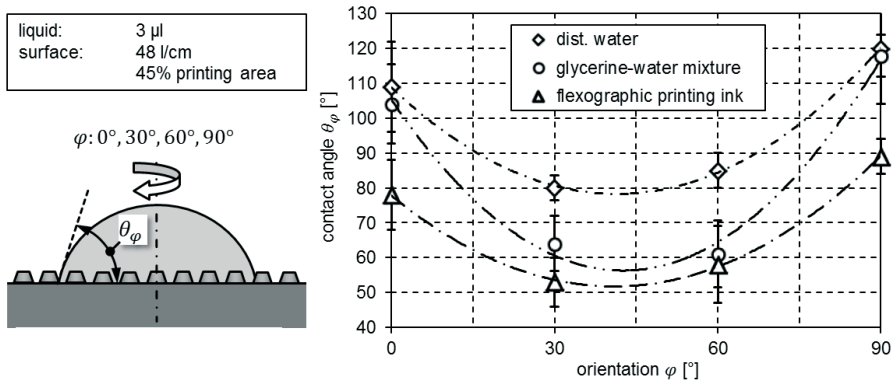


Figure 3: Influence of the orientation of a printing plate on the contact angle

the liquid manually or from washing out phenomena in the manufacturing process such as scratches from the brush. Not all fluids have the same behavior at a rotation of 90°. Depending on the rheological properties of a fluid, the contact angle varies during rotation. The measurements that were repeated several times were reproducible. An orientation of surface would have an influence on the fluid behavior and the ink transfer regardless of the quantity of ink. In a further step, the influence of the amount of liquid was examined. The following example shows the behavior of the glycerine-water-mixture in steps of 15° (see Figure 4).

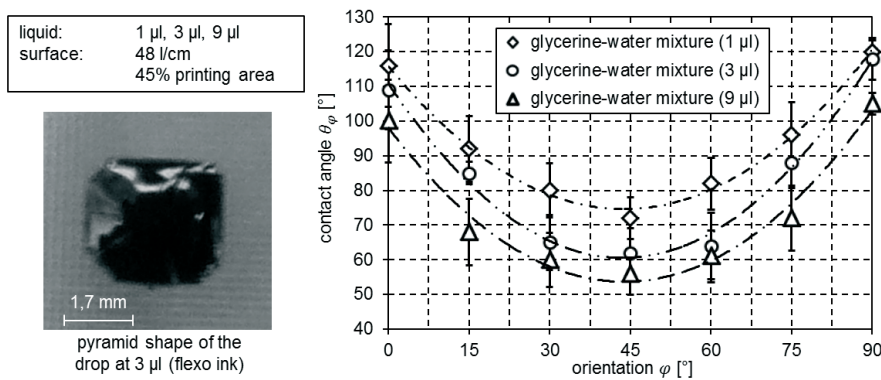


Figure 4: Influence of the orientation and liquid dimension of a printing plate on the contact angle.

Decreasing the amount of liquid, the drop takes a pyramid shape more and more (see Figure 4). This is due to the increase of the influence of surface. The drop is oriented on the flanks of the surface structure. There are few studies and models of contact angle on structured surfaces such as WENZEL or CASSIE-BAXTER (DAL11), (MAR03), (OKU08), (WHY08), (ZIM10). However, the behavior of liquids on printing plates or polymer surfaces is very complex and it is still subject of research. The wetting behavior of the fluid depends on the size scale of the surface structures in relation to the fluid volume. Capillary forces act in a certain amount of liquid. This behavior also shows liquid bridges between two structured surfaces. Chapter 4 deals with this subject.

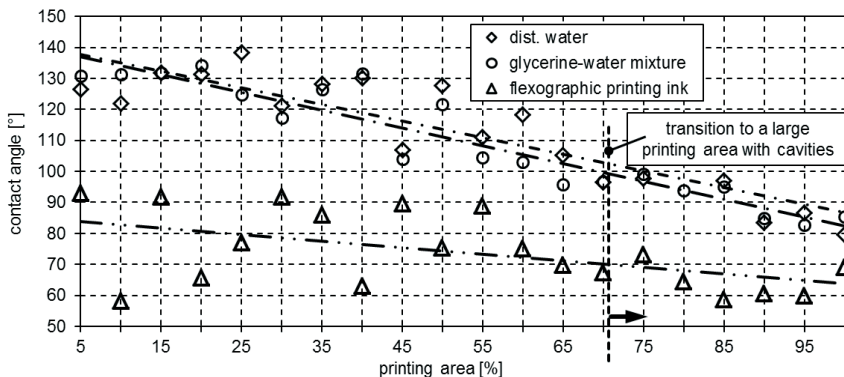


Figure 5: Maximum contact angle depending on the increase in printing area

Further studies of the contact angle examined the influence of the increase of the printing area. The respective contact angles were determined for an increase in area between 5% and 100%. The maximum contact angle during the rotation at 90°, depending on the increase in area, is shown on Figure 5. The amount of liquid here is also 3 μl and 48 l/cm at the surface.

By using a simple straight line, the contact angle decreases from all liquids with increase of the printing area. It shows that the structure changes with the increase of the printing area and that it has a direct effect on the surface tension. However, reducing the contact angle, the curves undergo a fluctuation. The fluctuation occurs in all three liquids. The straight lines reflect a fundamental trend but not the direct influence of geometry on the fluctuation.

3. Discussion

It is unclear whether there are air bubbles under the drop (model CASSIE-BAXTER) (MAR03), (OKU08), (WAG64). It is also not known what impact the air bubbles have to the wetting. The examination of the fluid dimension must be continued. It was observed that the pyramid flattens with less and less liquid and wets the surface. Nevertheless, the contact angle measurements do not agree with the actual amounts of fluid in the match process. Thus, it is possible that, in a smaller dimension, the surface is a sum of several areas. Each area has its own surface tension. The basic properties of the total surface result from the summation of the individual areas. This will be investigated in further experiments, as well.

Investigation with white light interferometry show that scratches are formed when washed out by means of a brush. These scratches are between 5 and 20% at most (see Figure 2 (a) at 10%). However, this may be caused by a reduced cross-linking of polymers in the manufacturing process, by a lower energy input between 5 and 20%. Between 70% and 75% due to the transition from the individual printing areas to a total area with small cavities (see Figure 2(a)). These cavities may have the consequence that the contact angle decreases at the flexo ink between 75% and 95% (see Figure 5). This connection must be examined in more detail in future studies.

With the increase in surface, the adhesion effect increases as well and thus the printing process is affected (see Figure 6). In a further step, the surface can be analyzed numerically to evaluate surface profiles more accurately and identify dependencies of the surface tension. An open question deals with the effect of the adhesion in the dynamic printing process. The dynamic behavior of various amounts of fluid on the printing form is unknown. A dynamic measurement of the contact angle should be done.

4. First investigation of ink splitting with structured surfaces

Separation experiments of structured surfaces were used to understand the influence of the surface more precisely. The influence of the orientation of the printing plate should also be analyzed. Figure 6 shows a sketch of instability of drops which are separated between two surfaces highly dynamically. The left side with plain surfaces shows a circular contour of the liquid with instabilities (see Figure 6 (a)). The right side with structured surfaces shows a boundary structure on the interface with instabilities as well (see Figure 6 (b)). On the right side, the influence of the structure can directly be seen. The liquid complies with the pattern of the surface.

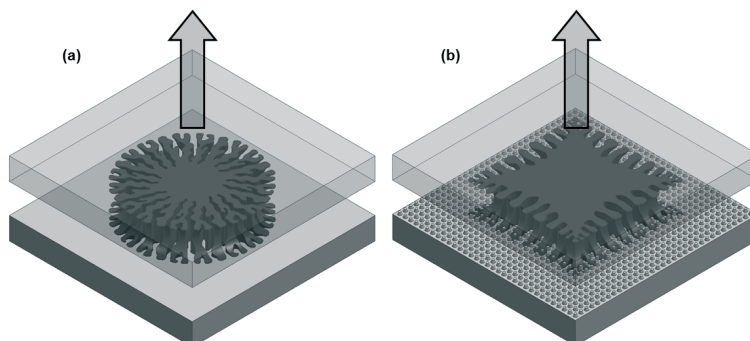


Figure 6: Sketch of viscous fingering instability without structuring from the experiments of BEHLER (BEH93)(a) and with structuring from the experiments of WEICKGENANT (WEI12) (b)

The sketch in Figure 6 (a) shows a section from the PhD thesis of BEHLER [BEH93]. First experiments with structured surfaces were made on the experimental setup of WEICKGENANN (WEI12) in cooperation with the Center of Smart Interfaces (CSI) of the Darmstadt University of Technology. It is assumed that, rotating the screening, the ink splitting changes and thus the ink transfers. In a further step, tests were conducted at the Institute of Printing Science and Technology (IDD). The experimental setup is a modified extensional rheometer (HAAKE CaBER). A distance measuring system and a high-speed camera were added as well. Further investigations are currently running. First results show that there is a direct correlation between the structuring and orientation of the printing plate and the filament formation. There could be a relationship between the dynamic and static studies which can be expressed in a formula.

5. Conclusion

It was shown that fluids behave differently depending on the printing plate. This behavior primarily depends on the surface tension, structuring and the adhesion effect. It was also shown that there is an influence of the orientation of the printing form. The dynamic behavior of liquids has been demonstrated on structured surfaces as well. Problems and research potential were also demonstrated. Planned studies in this field of research were also presented. These approaches may give a better understanding of the printing process and the collected knowledge can be used for functional printing.

References

- (BEH93) Behler, H., (1993). *Die Randstruktur von Druckpunkten - eine experimentelle Untersuchung der Farbspaltungsströmung*. Dissertation, Technische Hochschule Darmstadt.
- (BER99) Berg, M., (1999). *Untersuchungen zur Erzeugung und Dosierung dünner Flüssigkeitsschichten auf Walzen*. Dissertation, Technische Universität Chemnitz.
- (BIC01) Bico, J., Tordeux, C. & Quéré, (2001). *Rough wetting*. *Erophysics letters*, 55 (2), pp. 214-220.
- (CHU10) Chu, K.-H., Xiao, R., Wang, E. N., (2010). *Uni-directional liquid spreading on asymmetric nanostructured surfaces*. *Nature Materials*, Vol. 9, pp. 413-417.
- (CLA08) Claypole, T. C., Beynon, D. G., Bould, T. C., (2008). *Ink Transfer during flexographic printing to paper*. 35th IARIGAI Conference, Valencia.
- (DAL11) Dallmann, S., (2011). *Reinigung superhydrophober Oberflächen*. Dissertation, TU Dortmund.
- (DEU99) Deutschsprachige Flexodruck-Fachgruppe e.V. [DFTA] & Meyer, K.-H., (1999). *Technik des Flexodrucks* (4. neu bearbeitete Auflage). St. Gallen: Coating-Fachbücher.
- (GAL10) Galton, D., Bould, D. C., Claypole, T., (2010). *The effect of surfact properties on the printability of flexographic printing plates*. IARIGAI 2010 proceedings: Advances in Printing and Media Technology, Vol. 37, Montreal.
- (HÜB91) Hübner, G., (1991). *Ein Beitrag zum Problem der Flüssigkeitsspaltung in der Drucktechnik*. Dissertation, Technische Hochschule Darmstadt.
- (KIP00) Kipphan, H., (2000). *Handbook of Print Media*. Berlin: Springer Verlag.
- (MAR03) Marmur, A., (2003). *Wetting of Hydrophobic Rough Surfaces: To be heterogeneous or not to be*. *Langmuir* 19 (20), pp. 8343-8348.
- (OKU08) Okumura, K.; Okumura, K., (2008). *Wetting transitions on textured hydrophilic surfaces*. *European Physical Journal*, 25 (4), pp. 415-424.
- (THE11) Theopold, A., Dörsam, E., (2011). *Characterization of flexographic printing plates with regard to the field of printed electronics*. In: Large-area, Organic & Printed Electronics Convention (LOPE-C), Frankfurt.
- (ÜCÜ12) Ücücü, M., (2012). *Grundlagenuntersuchung der Fluidspaltung zwischen zwei strukturierten Oberflächen*. Unveröffentlichte Bachelorthesis. Technische Universität Darmstadt.
- (WAG64) Wagenbauer, K., (1964). *Studien zum Farbübertragungsprozess im Druckwerk*. Habilitation, Technische Hochschule Darmstadt.
- (WEI12) Weickgenannt, C. M., Roisman, I. V., Tropea, C., (2012). *Experimental investigation of liquid ligament fragmentation*. ICLASS 2012, 12th Triennial International Conference on Liquid Atomization and Spray Systems, Heidelberg.
- (WHY08) Whyman, G., Bormashenko, E., Stein, T., (2008). *The rigorous derivation of Young, Cassie-Baxter and Wenzel equations and the analysis of the contact angle hysteresis phenomenon*. *Chemical Physics Letters*, 450 (4-6), pp. 355-359.
- (ZIM10) Zimmer, L., (2010). *Dreidimensionale nanostrukturierte und superhydrophobe mikrofluidische Systeme zur Tröpfchengenerierung und-handhabung*. Dissertation, Karlsruher Institut für Technologie.



The influence of engagement on the flexographic printing of fine lines

*Timothy C. Claypole*¹, *Glyn R. Davies*¹, *Simon M. Hamblyn*¹,
*David Galton*², *Richard Hall*³

¹Welsh Centre for Printing and Coating
College of Engineering, Swansea University
Singleton Park
Swansea, SA3 4LL, UK

E-mails: s.m.hamblyn@swansea.ac.uk; t.c.claypole@swansea.ac.uk; g.r.davies@swansea.ac.uk

²Asahi Photoproducts UK
1Prospect Way, Shenfield
CM13 1XA, UK

E-mail: dg@asahi-photoproducts.co.uk

³Timson Ltd
Perfecta Works
Bath Road, Kettering, Northants
NN16 8NQ, UK

E-mail: richard.hall@timsons.com

Abstract

In flexography, the ability to print fine lines of consistent width and height with a well defined narrow gap is the key to realising the printable polymer electronics. This paper describes a study of the effect of engagement on printed fine lines. A novel image carrier technology was developed to minimise the out of roundness of the image carrying surface. The plate cylinder was coated with photopolymer and then ground while rotated in its bearings. The image was then laser engraved into the surface. This approach eliminates the varying engagement due to out of roundness of the image carrier. An image with features representative of those required with flexible electronics (fine lines, grids etc) was repeated cross the width of the image carrier. The ink level was varied using 5 bands of a banded anilox roll. In this initial investigation, a black UV graphics ink was used to access the effect of varying the engagement at constant speed. Successful printing was achieved across the whole image with a minimum engagement of 25 μm above "kiss" contact. Engagements of 50 μm and 75 μm were also evaluated.

Three generic forms of contact could be identified. A minimum engagement where the ink film on the image carrier contacted the surface, but there was little squeezing of the ink. The line produced was less than the nominal dimensions of the feature. At slightly higher engagement, a squeeze film was created between the image carrier and the substrate. The line reproduced had little gain compared with the nominal line dimensions and the print was consistent across the width of the line. At higher engagement the image carrier was impressed into the surface, forcing the ink to spread sideways creating line gain. There was a tendency for there to be an uneven distribution of the ink with less in the middle and heavy deposits on the edges, particularly with the wider lines. The ink having been forced to the side by the contact of the image carrier with the substrate was not then drawn back into the centre of the line by the negative pressure as the plate and substrate separate. This phenomenon is frequently seen on flexographic prints. The quality of the line was affected by the thickness of the ink on the plate. At low inking levels, then the local ink transfer from the cells on the anilox roll was carried through to the printed image. However, under the optimum conditions of engagement and ink film thickness the lines were reproduced evenly in all directions.

Keywords: flexography, fine lines, pressure

1. Introduction

Flexography has the potential for the volume additive manufacture of flexible polymer electronics. The ability to print fine lines of consistent width and height with a well defined narrow gap is the key to realising electronic circuits and devices such as transistors. The quality of the line and the gap is a function of the image carrier, ink, substrate and process parameters. This paper describes a study of the effect of engagement on printed fine lines.

The flexography image carrier is usually a photopolymer which is exposed in the flat to create the raised features. This is then mounted on a plate cylinder that has been accurately ground, to enable minimal run out between the image carrier and the substrate. The polymer image carrier is wrapped around the cylinder and attached with adhesive cushion tape. Thus intrinsically this is producing local distortion of the plate and forces that will distort unsupported fine features such as high resolution fine lines. This results in low spots, out of roundness and inconsistent run out. The nett effect is that from the first contact with the substrate, the plate has to have an inference engagement of at least $100\mu\text{m}$ before the image will print across the full width and further engagement to ensure print consistency. The move towards fibre glass sleeve technology to improve changeover times in graphic production, introduces further errors due to the out of roundness of the sleeve. Also, the cantilever layout of the rolls with bearings at one end reduces the rigidity. The fibre glass sleeve does afford the potential for it to be directly coated with polymer, ground to size and imaged in the round. However, the manufacturing tolerances of the glass fibre sleeves and the distortion they undergo during mounting on the mandrel negate this potential advantage. Recently, some suppliers have introduced aluminium sleeves which could potentially afford a more precise arrangement. One possibly way to overcome these issues would be to coat, grind and image the sleeve on the mandrel. However, one would have to ensure if the sleeve was removed that it went back onto the same mandrel at precisely the same location.

In this study, an alternative approach to creating the image carrier based on directly coat the plate cylinder grind and engraving the image in the round was used. An image with features representative of those required with flexible electronics (fine lines, grids etc) was repeated cross the width of the image carrier. The ink level was varied using a banded anilox roll. In this initial investigation, a black UV graphics ink was used to access the effect of varying the engagement at constant speed.

2. Methodology

A bespoke cylinder was produced in this manner by Asahi using the "Adless" system (Figure 1).

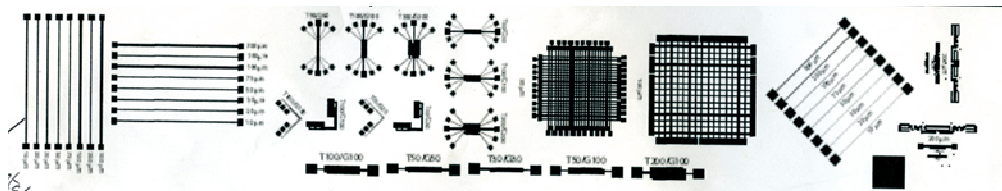
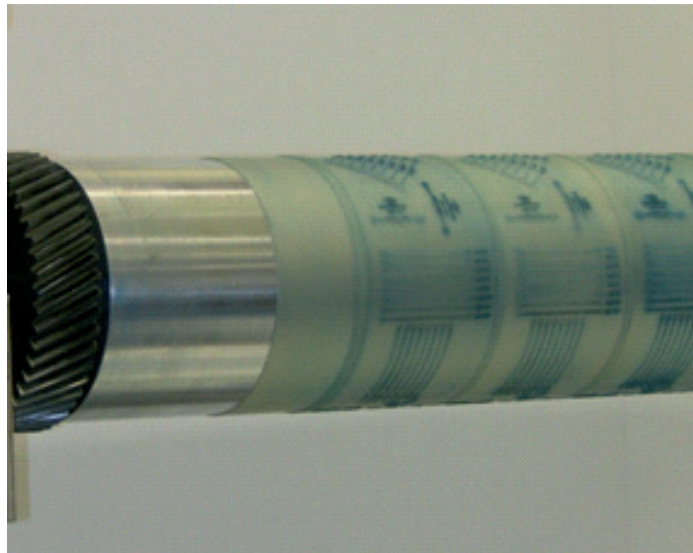


Figure : The Asahi Adless direct coated and engraved cylinder

The plate cylinder was coated and ground while rotating supported in its own bearings. The image was then created in the polymer using direct laser engraving. This was to ensure the highest point of the images regardless of the feature size would be at the same radial height. The use of direct laser engraving also affords the potential to control the profile of the different features so as to ensure the most effective ink trans-

fer. The image contained a series of features representative of those required in the printing of polymer electronics. The profile of each of the features was evaluated using white light interferometry. The image was repeated five times across the cylinder, corresponding to the bands in the Anilox used in this trial. The anilox had a constant line ruling (500LPI) with varying volume in each band (Table 1). A black UV graphics ink was printed onto 2 clear BOPP substrates. Successful printing was achieved across the whole image with a minimum engagement of 25 μm above "kiss" contact. Three levels of engagement were study, 25 μm, 50 μm and 75 μm above "kiss" pressure. The experiments were run at a constant speed of 17m/min. The features were evaluated optically using a microscope with 400x magnification, calibrated with a reference plate.

Table 1: Anilox specification

Band	2	3	4	5	6
Volume (cm ³ /m ²)	3.04	4.18	5.49	6.59	8.31
Screen angle (Degrees)	60	60	60	60	60
Screen count (LPI)	500	500	500	500	500

3. Results and discussion

A comparison was made of the individual fine lines printed in the direction of print, cross print and diagonal to the direction. There is an increase in printed line width compared to the nominal (Figure 2).

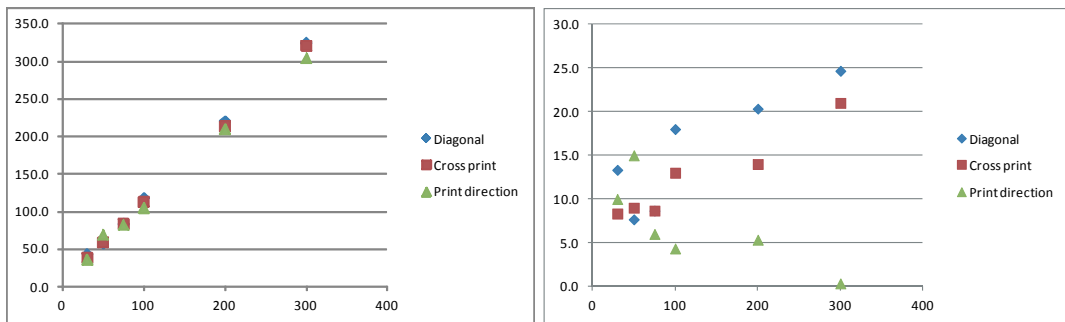


Figure 2: Printed line width (left) and line gain against nominal line width (75 μm engagement and 3.04 volume anilox band)

There is more gain with the diagonal lines. Both the cross print and diagonal lines show an increase in gain with width, but this is not in proportion to the width so the percentage line gain falls. The slight increase for all lines suggest that the gain is the result of the ink spreading at the edge of the feature. There is a fall in the line gain with width for the lines in the direction of printing suggesting that process is interacting with the local ink transfer. For printed electronics, there is a need to reproduce fine lines. The effect of engagement for the 75 μm line is shown in Figure 3.

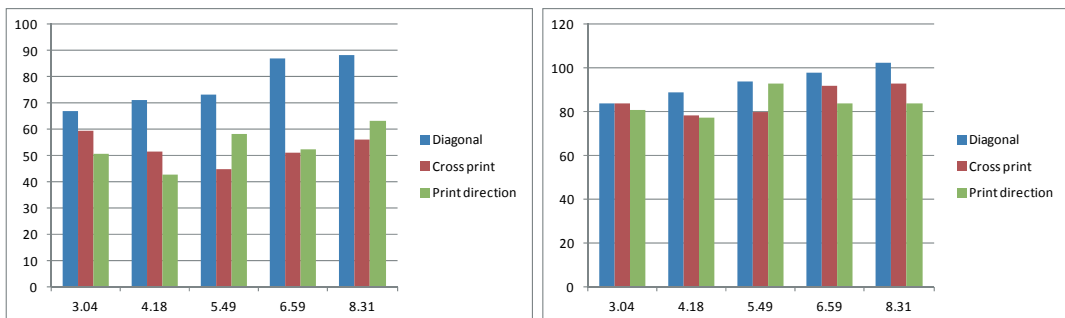


Figure 3: Printed width of 75 μm nominal lines for varying anilox volume (25 μm engagement left and 75 μm engagement right)

At the lowest engagement, the line gain is negative as a line of approximately 50 μm in the cross direction and in the direction of print. Only the diagonal line shows any line gain. However, the quality of the lines suggests that incomplete transfer was occurring. It is likely that at this engagement the ink is being trans-

ferred with minimal if any contact pressure. Increasing the engagement causes all the lines to increase in width and exhibit similar gains. For the lowest anilox volume, the printed line width is similar in all directions. This contrasts with the recent study of flexo printing silver conductive inks sponsored by Flextech Alliance and presented at Flextech Conference 2012 (Kahn, 2012), where the line gain was strongly dependent on orientation.

Increasing the engagement has a similar effect on the 300 μm lines (Figure 4).

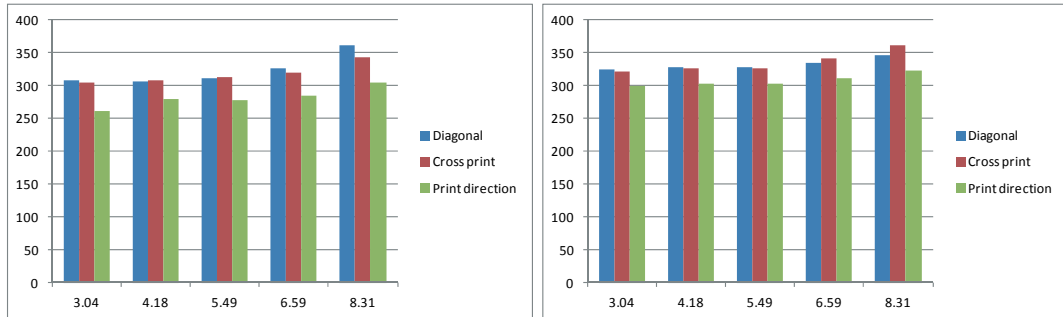


Figure 4: Printed width of 300 μm nominal lines for varying anilox volume (25 μm engagement left and 75 μm engagement right)

As well as the overall width, examination of the prints indicated there was quite frequently a lighter area in the middle of the line, as illustrated in Figure 5.

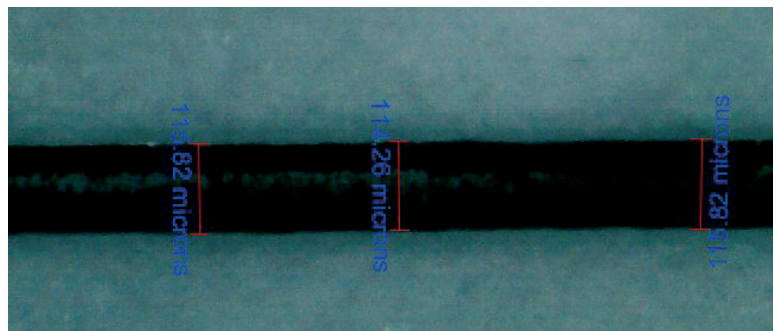


Figure 5: 100 μm line in the cross print direction with 75 μm engagement

This would indicate, there is less in the centre of the line. A possible scenario is that the plate is forced into contact with the substrate and displaces the ink to either side of the line. As the plate and substrate separate, then there is insufficient tensile force to draw the ink back into the centre and the ink splits on both edges of the line.

This effect was also observed by Kahn, where the profilometry measurements of the lines showed that there was an influence of speed, the printed ink film in the centre of the line becoming flatter at higher speeds. This would support the hypothesis that it is the negative pressure as the substrate and plate separate that draws the ink into the centre. At higher speeds the inertia of the ink will counter this action.

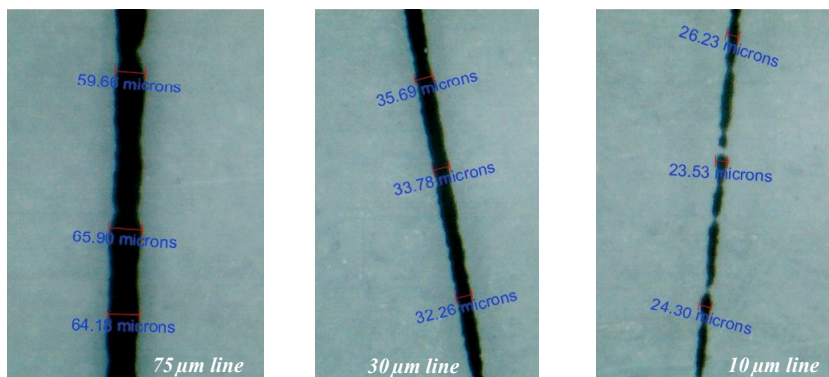


Figure 6: Lines in the direction of print direction with 25 μm engagement

Another feature of the lines sometimes observed, particularly with low engagement, is the rippled edge of the lines (Figure 6). Although it could be argued that this is a reticulation effect, the frequency indicates that it is more likely to be the reproduction of the anilox pattern in the ink film.

4. Conclusions

The study has shown the potential of flexography to print consistent fine lines that would be conducive to the manufacture of printable electronics and smart packaging. However, to achieve consistent lines both in all directions of print and across the full width of the feature, there is a need to ensure the plate impresses into the substrate forming a consistent squeeze film to control the dimensions of the feature. Sufficient time has to be allowed for the ink to flow as the plate separates, to create a cross section with an even cross section. This has implications for the speed at which printable electronics and smart packaging can be produced. This will be highly dependent on the nature of the ink and is likely to be more of an issue for high viscosity inks.

Acknowledgments

The authors wish to acknowledge the financial support of the UK Technology Strategy Board for this work. The authors would also like to thank David Beynon for his assistance in running the press trials and Christopher Claypole, Swansea Printing Technology Ltd who measured the prints and plate features.

References

Kahn, B. H., "The race to the finish: Considerations for the commercial scale flexographic printing of Electronics", Presented at the 2012 Flextec conference, Tempe, Arizona



Effect of flexographic press parameters on the reproduction of colour images

Timothy C. Claypole, Eifion H. Jewell, David C. Bould

Welsh Centre for Printing and Coating
College of Engineering, Swansea University
Singleton Park, Swansea, SA3 4LL, UK

E-mails: t.c.claypole@swansea.ac.uk; d.c.bould@swansea.ac.uk; e.jewell@swansea.ac.uk

Abstract

There is a tendency to evaluate the impact of press parameters either quantitatively on tone strips or qualitatively by subjective assessment of images. This paper presents a quantitative assessment of the impact of flexo press parameter changes on the gamut of four colour images compared with the measurement of the tone strip and a detailed evaluation of the dot shape. The prints were produced on a 500 mm wide narrow web flexo press. The test print contained a range of half tone strips and also a number of four colour process images designed to address a range of different image types. The printing speed, the impression pressure and anilox to plate engagement were varied independently. The colour profile of the individual ink dots can provide qualitative information with regard to the physics of the printing process, the colour being a metaphor for local ink transfer. The complex fluid dynamics of the ink transfer process can be inferred from these measurements. The dot spread and recession, particularly in the low and mid tones are affected by the local surface energy. In the single colour tone strips, the relative surface energy is a function of the ink and substrate only. However, in areas of overprinting, such as the grey balance patches and the four colour image, then this relationship becomes more complex.

Keywords: flexography, half tone, tone gain, impression pressure, speed

1. Introduction

Understanding the relationship between printed image, dot area, tone value increase and coverage on the plate is one of the keys to being able to predict the flexographic printing process. There is a tendency to evaluate the impact of press parameters either quantitatively on tone strips or qualitatively by subjective assessment of images. Prints were produced on a 500 mm wide narrow web flexo press. The printing speed, the impression pressure and anilox to plate engagement were varied independently. The test print image contained half tone strips and also a number of four colour process images designed to address a range of different image types. A quantitative assessment of the impact of press parameter changes on the gamut of four colour images was undertaken and compared with the measurement of the tone strip. The colour profile of the individual ink dots was also measured as it provides qualitative information with regard to the physics of the printing process, the colour being a metaphor for local ink transfer. The complex fluid dynamics of the ink transfer process can be inferred from these measurements.

2. Printing trials

The printing trials were performed on a Timson T-Flex 508 press in temperature controlled clean room. The clean room was achieved by placing a polymer tent around the press and lightly pressurising it with filter air to achieve class 7 conditions. The design of the press allowed the anilox to plate pressure and the plate to substrate pressure to be varied independently. While the plate to substrate pressure could be varied in measured amounts, the anilox to plate could only be varied between two settings, high and low.

The image was printed with a conventional four colour UV ink (Flint ink Xsys) on a white, high gloss, two side coated, biaxially oriented polypropylene film with enhanced UV stability, and intended for graphic art or label applications (Innovia Rayoart WGS92). The plates were conventionally imaged, with an imposed gamma curve correction so that the four colour images produced would be visually correct. High resolution conventionally engraved anilox were used as specified in table 1. Six images (original WCPC or ISO standard) were included on the print to cover a full range of categories of image, including flesh tones, predominantly highlight and shadow (Figure 1). Half tone test strips, grey balance, solid over prints and fine lines were included. The coverage in the tone strips on the plate was measured with whitelight interferometry.

Table 1: Anilox specifications

	Ruling lpi	Vol (cm ³ /m ²)
C	1200	2.39
M	1200	3.32
Y	1200	3.10
K	1200	3.73



Figure 1: Test Image

The press parameters were systematically and independently varied in seven experiments. The effect of effect of plate to substrate was investigated at a constant speed (46 m/min) and low anilox to plate setting. These were varied to produce four levels for magenta ink and two levels for the other three colours (Table 2). Experiment C was the best print condition. The speed was increased to 92 m/min (experiment E) and 122 m/min (Experiment F) keeping all other settings as for experiment C. A further experiment (G) was run at the same settings as experiment C but with the anilox to plate pressure set to high.

Table 2: Variation of plate substrate engagement (μm)

Experiment	A	B	C	D
C	76	76	102	102
M	76	127	102	178
Y	76	76	102	102
K	76	76	102	102

The images in the prints were scanned with semi - professional A4 scanner (Epson perfection Photoscanner) at a resolution of 300 lpi. These were analysed using Swansea Printing Technology "Digital eye glass" software to obtain gamut, lightness distribution and a*b* plots. The density of the patches in the half tone strips were measured using a calibrated scanning spectrophotometer (Gretag/Macbeth spectroscan). The area of the dots in the half tone strips was measured so the tone gain during the printing process could be evaluated. The individual dot areas were scanned using the semi - professional A4 scanner at it's highest non interpolated resolution (9600 lpi). This enabled the features of a field of dots to be evaluated (Figure 2). The percentage colour distribution of each patch in the tone strip was evaluated using bespoke software. The original concept was to divide the dot image into printed and non printed areas, using a binary threshold. This was thought would equate to the dot area used to establish percentage tone value, as used in other processes such as offset. Thus, these measurements should equate to tone value calculated from the measured density. However, the initial measurements revealed that the darkest areas of each half tone patch increased with coverage and that there were distinct areas of different density. Initially this was attributed to optical effects and light scatter in the substrate. However, this could not explain some of the distinct regions, particularly lighter areas in the solid and a concentric pattern around some dots. Therefore, the image for each half tone patch was threshold image processed to calculate the percentage coverage for five increasing amounts of density - substrate, light, medium, dark and solid. The substrate colour and the solid were set by measurement of the unprinted substrate and the darkest area of the solid. The others threshold levels were set subjectively to correspond to features on the prints.

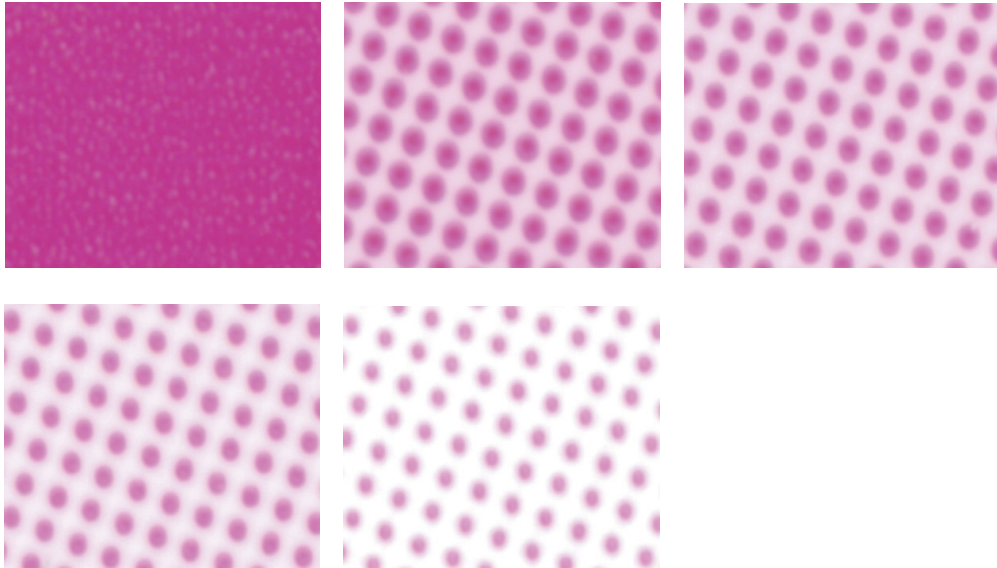


Figure 2: Magenta dots images obtained by photo scanner

3. Results

There is a fall in the L^* distribution of the prints when the plate to substrate engagement is increased by $25\mu\text{m}$ for all colours to obtain the best print condition (Figure 3). This is as expected as there is an increased amount of ink transferred. There are negligible changes in the maximum gamut given by the a^*b^* plot on the left. This plot represents a view looking down along the L^* axis, so it only reveals the maximum, not whether there has been any expansion of the total gamut volume. However as the speed is increased, a^*b^* plot becomes smaller suggesting a reduction in gamut (Figure 4).

All of the systematic changes impact on the magenta ink transfer. Therefore, the impact on these on half tone ink transfer is presented in more detail. In most cases the "Best print" condition is used as the reference setting. Altering the plate-substrate engagement by $\pm 25\mu\text{m}$, has an almost equal affect across the whole half tone range (Figure 5). This has more impact on the highlight TVI, thus altering the pressure around the best print conditions would cause a change of highlights compared to shadows. However, increasing the engagement by a further $25\mu\text{m}$ causes a disproportionate increase in the ink transfer in the mid tones and shadows. The effect is seen beyond the point at which the dots on the plate would start to coalesce, providing lateral support increasing the stiffness of the dot. At lower coverage, the dots would have more opportunity to flex. This produces a non linear response from the TVI. Thus, over engagement will have an adverse effect on the balance of the image.

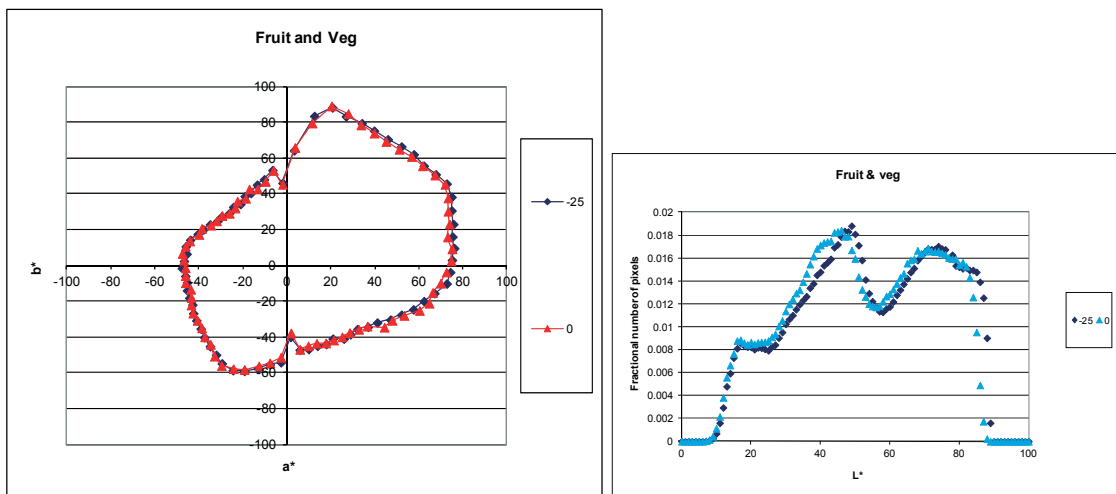


Figure 3 Effect of increasing engagement on plate to substrate on image gamut

Increasing the anilox to plate pressure produced an increase in the midtone ink transfer, but a fall in the solid, which ecentuates the impact on TVI (Fig. 6). The initial rise in speed to 92 m/min produced a drop in ink transfer, particularly in the highlights (Fig. 7). However, the further increase in speed to 122 m/min produced a slight increase in ink transfer, although still less than the best print, causing the density and TVI to rise slightly (Fig. 8).

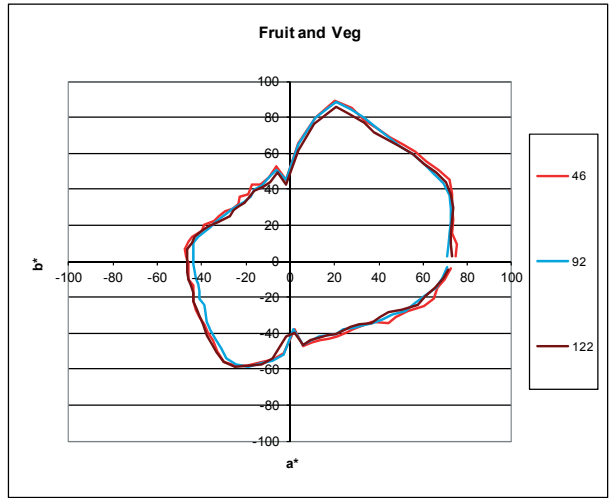


Figure 4: *a*b* plots for increasing print speed*

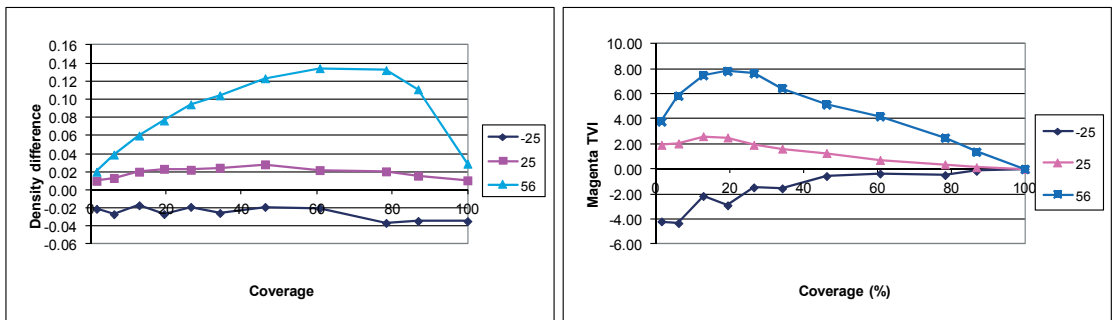


Figure 5: *Effect of plate engagement on magenta density relative to best print conditions*

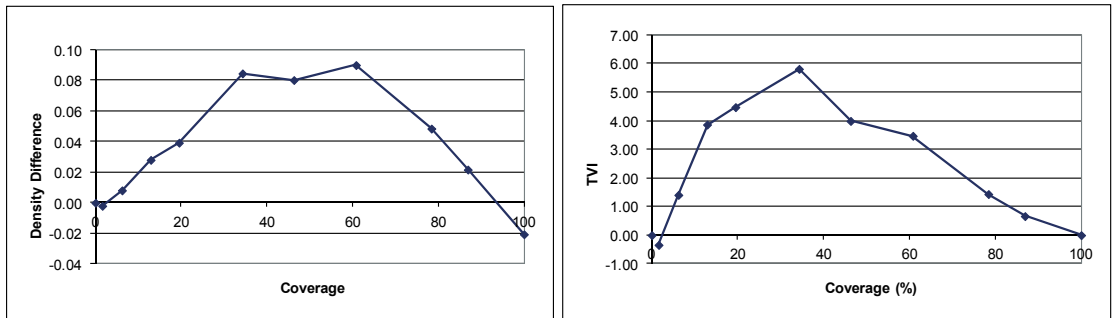


Figure 6: *Increase in density and TVI with anilox to plate engagement*

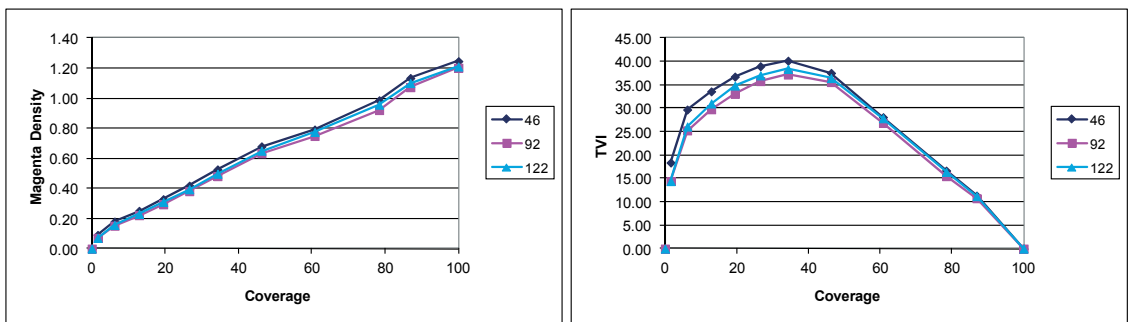


Figure 7: *Density and TVI for varying printing speed*

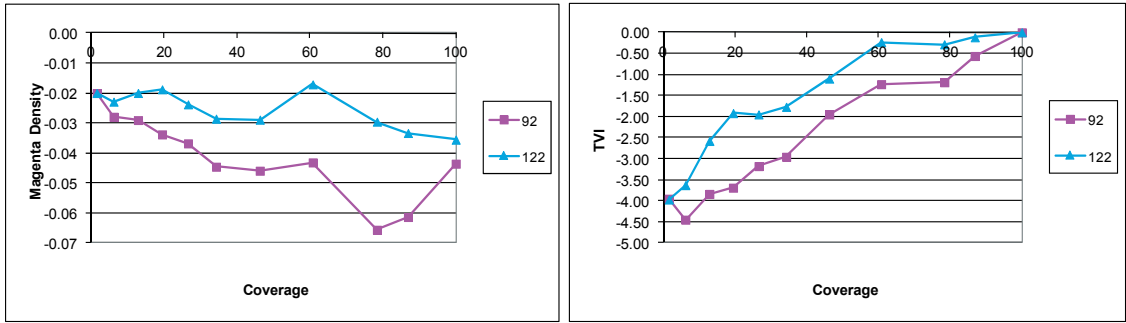


Figure 8: Density and TVI change with speed relative to best print conditions

The intention was to measure dot areas and compare these with the TVI obtained using Murray Davies from the density measurements of the half tone. The scanner offered the advantage of a stabilised light source compared to a dedicated microscope and using a professional grade scanner intended for the commercial photographers had both the stability and the un-interpolated resolution to resolve the dot features. Initially, it was planned to use a simple threshold algorithm to separate the half tone strips into printed and unprinted areas. These would be a direct analogy for TVI. However, this did not prove a good match to the notational tone value. It became apparent during the analysis of the first test strip that during the printing process the ink was separating in a dark and a light phase during the half tone printing process, producing some dots with distinctive halos. Therefore, it was decided to use multiple thresholds, selected from each image for the darkest and mid colours on the image. However, as these were set for each image, there was an initial darkest area that was then superseded by the further dark area. The net effect was a mid lightness value which was found predominantly between 20% and 60%, initially at the expense of the area of the darkest part of the print. However, the sum of these two areas was almost equivalent to the coverage (Figure 9). One of the issues with this initial setting of measurements was the assumption that the darkest area on the print would be representative of the solid ink transfer and could be used to set the thresholds. A revised approach was adopted of establishing the thresholds based on the solid, mid and highlights of the print and using these thresholds to analyse all of the half tone patches. Also, to cover the full range seen in the initial measurements, the image was split into 5 bands corresponding to unprinted substrate and the solid, plus three intermediate levels which were observed on the print. This approach is reliant on the colour stability of the scanner. Tests were made based on repeat scans to test the validity of this assumption.

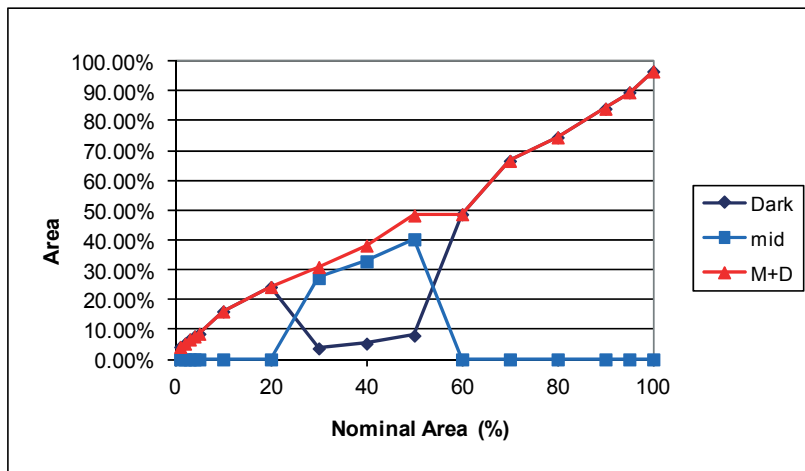


Figure 9: Magenta half tone test strip separated into three lightness regions

The impact of varying the plate to substrate engagement on the printed dots in the tone strip is shown in Figure 10. Untinted substrate is only present up to a maximum of 35% coverage. At the lowest engagement (A) the substrate is visible between the dots up to 60% coverage, the points at which the image inverts from being dots to being a solid with holes. Beyond this point, there is an ink film over the whole of the image. As the engagement is increased so the amount of substrate visible at each printed dot area becomes less. The point at which it becomes zero is difficult to estimate as there is only a coarse 10% gradation whilst it is most likely that the effect of engagement is continuous. The next level of light coverage is present at the lowest

engagements The amount of the light colour in the image increases in the low coverage area and decreases in the higher coverage. The majority of this could be an optical effect caused by scatter of light in the substrate, particularly at the lower coverage. It could also be due to transfer of the ink film from the land areas on the anilox, held suspended between the dots on the plate, once they become sufficiently close. To provide an approximation, to the unprinted substrate, the substrate and light bands were combined into a single substrate level (Figure 11). This is more effective than the previous threshold method as it produces a sharper cut off.

The medium corresponds to the hallow around the dots (Figures 10 and 11). This represents a distinctly lighter density or colour of ink. This colour is seen at the lowest coverages and rising to a peak at approximately 40%, but despite falling is still present in the solid area.

The solid (darkest part of the print) increases with engagement, but only reaches a maximum of just over 55% in the solid patch (Figure 10). The dark area decreases in the solid. If both are combined to give an approximation to the solid colour, then there is a linear but not one to one relationship with coverage. Therefore, the TVI cannot be considered to represent the actual dot area produced in flexo printing.

While the density measurement can give information on the tone value increase and empirical corrections such as Yule-Neilsen made so the formula gives an approximation to the dot area, it is only by examining the detailed dot density that a better understanding can be obtained of the ink transfer mechanisms. Using a microscope with a 400x magnification, a detailed study of the dot structure was also undertaken to correspond to the scanner study (Figure 12). The density can be used as a measure of the local cured ink thickness indicative of the ink transfer and subsequent distribution during the printing process. The solid patch (top left) shows that the during separation of the plate from the substrate, the ink has formed filaments, drawing the ink away from areas of the print to leave less dense areas of print. In the 40% coverage area there is lighter halo printed around each dot. This suggests that as the dot initially made contact with the substrate, pushing the ink to a larger diameter. However, as the filament formed when the plate withdrew from the plate, the tensile forces were sufficient to overcome the local surface energy and the majority of the ink was pulled back into the centre, creating a dark centre while leaving a lighter halo. There is some evidence of this in the 30% coverage (bottom left), the tensile forces are insufficient to completely overcome the surface energy, and therefore the ink remains as a discrete fairly uniform dot. This could also be a function of the amount of ink carried on the dot and related to the anilox coverage. The bottom right shows a nominally 4% coverage, where the dot on the plate has made contact with the surface and has displaced the ink in some cases to form a doughnut shaped dot with the centre missing. In these detailed images there is also evidence of the dots elongating in the direction of print. Whether this is due to the printing process or plate mounting is difficult to evaluate.

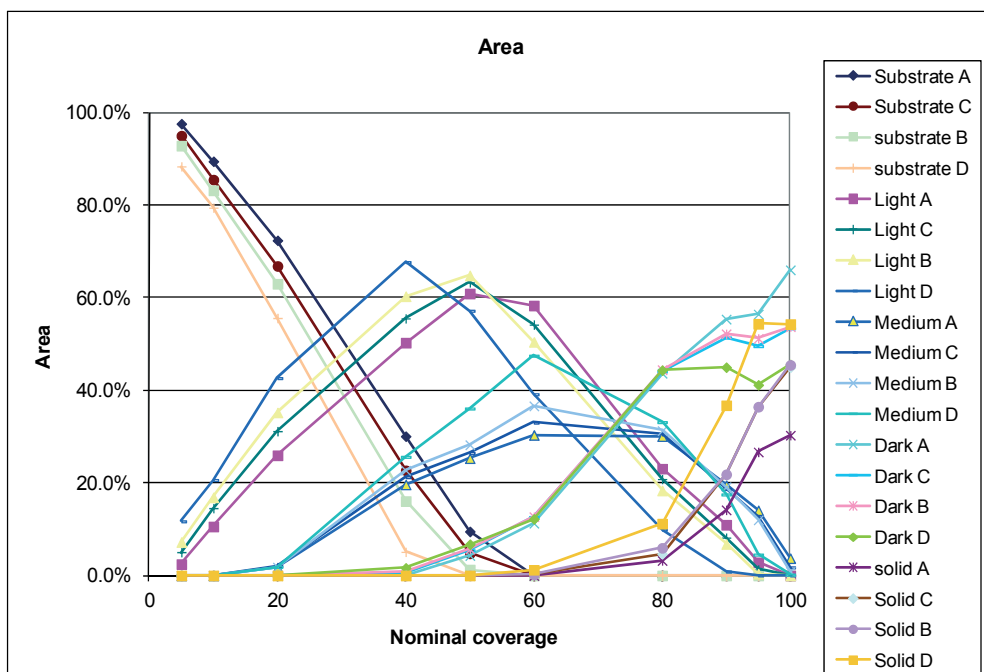


Figure10: Magenta percentage coverage for increasing engagement (C=4, B=5, D=7)

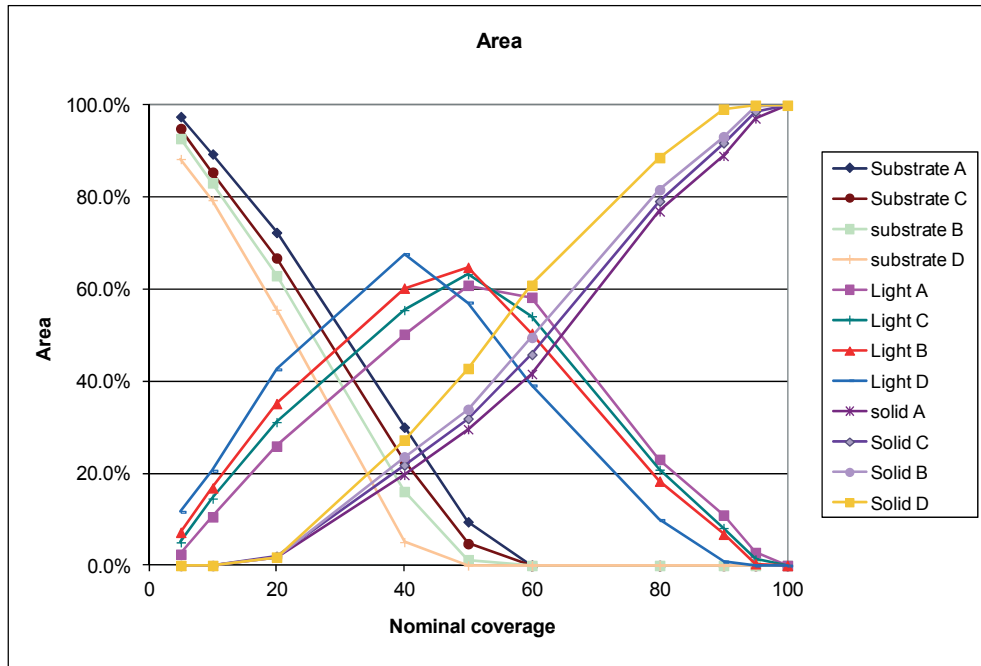


Figure 11: Magenta percentage coverage for increasing engagement (A= 3, C=4, B=5, D=7) - revised threshold groups

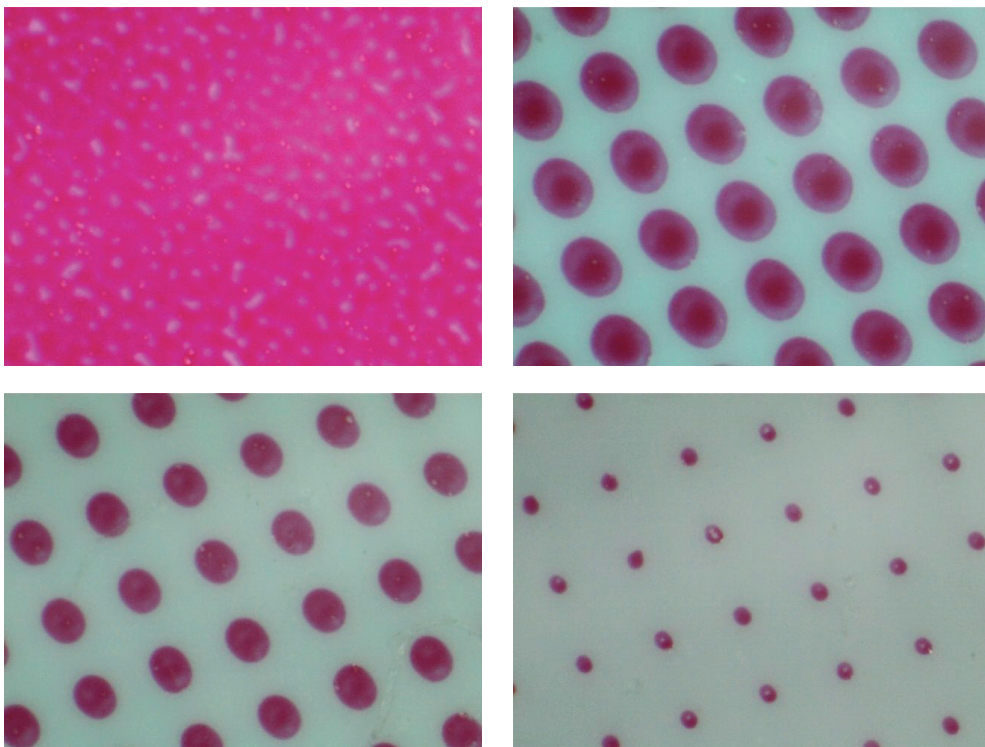


Figure 12: Magenta dots (solid through to 4% nominal) - 400x magnification

The colour profile of the individual ink dots can provide qualitative information with regard to the physics of the printing process, the colour being a metaphor for local ink transfer. The dot spread and recession, particularly in the low and mid tone coverage is effected by the local surface energy. In the single colour tone strips, the relative surface energy is a function of the ink and substrate only. However, in areas of over-printing, such as the grey balance patches and the four colour image, then this relationship becomes more complex. Thus, the amount of ink transfer, dot density and the dot shape are affected in a complex manner which influences the printed colour.

4. Conclusions

A study of the impact flexo process parameter on the printing half tone images. Specifically the plate to substrate engagement, anilox to plate pressure and speed have been varied independently. While the direct measurements from the printed four colour image have revealed little about the process, the study of the half tone test strips has shown the complex nature of flexographic printing. Previous studies have focused on the use of density to obtain TVI as a means of evaluating the impact of these process parameters. However, the detail measurements of the printed dots has revealed the effect of plate feature stability and the physical characteristics of a multi phase ink. The impressing and splitting of the ink film is almost certainly the key to a fuller understanding of the flexographic process. Understanding the mechanisms involved is a necessary step both to a practical solution of press stability issues and essential to the development of predictive algorithms.

Acknowledgments

The authors wish to acknowledge financial support of the ERDF and the practical support of Asahi Photoproducts UK for this project. They also wish to acknowledge the measurement work carried out by Andrew Claypole of Swansea Printing Technology.

Developing a laboratory simulation of tail edge pick

*Eveliina Jutila*¹, *Cathy J. Ridgway*², *Patrick A. C. Gane*^{1,2}

¹ School of Chemical Technology
Department of Forest Products Technology, Aalto University
P.O. Box 16300, FI-00076 Aalto, Finland
E-mails: eveliina.jutila@aalto.fi; patrick.gane@omya.com

² Omya Development AG
CH-4665 Oftringen, Switzerland
E-mails: cathy.ridgway@omya.com; patrick.gane@omya.com

Abstract

The development of a laboratory scale test method to simulate the tail-edge picking effect is described. Adopting the commonly used rotational nip methodology applied on many laboratory print testing devices, exemplified here using the Ink Surface Interaction Tester (ISIT), the method depends on the development of an impact pulse and subsequent pressure drop in order to simulate the release effect at the tail edge of a solid print area where fountain solution will also be concentrated due to the rolling action of the nip. Image analysis of the edge regions provides the measure of pick intensity developed. By combining this information with the number of passes required to induce pick, a logarithmic relation was devised to bring lab evaluation into correlation with visual ranking of the commercially printed papers, but with a lack of sensitivity in respect to differentiating relatively good papers. This extra required sensitivity of separation has subsequently been increased by optimising the pulse development design and test parameters, including ink amount, ink-on-paper tack response, contact force and speed of printing/passes. The new resulting analysis of the pick area together with knowledge of the new number of passes provides a linear correlation, having $R^2 > 0.9$.

Keywords: tail-edge pick, laboratory pick testing, visual ranking of print quality, ink tack, piling, wet pick

1. Introduction

Today's requirements for print-press runnability and print quality demand an optimised absorption from, and adhesion of, printing ink on the paper surface. When printing coated papers, it is the interactions between the ink and the coated paper that largely determine the efficiency of the printing operation and the quality of the final printed product. Aspler and Lepoutre (1991) have reviewed a number of past studies concerning offset ink and coated paper interactions. Xiang and Bousfield (1998, 1999, 2000; Xiang et al., 2000) have studied the effects arising from the application of fountain solution, the ink tack development and the print quality dependency when using emulsified ink, which, when compared to pure ink, was suggested may lead to a higher print gloss. Together with Donigian et al. (2004) they also looked at the relationship between offset ink setting rates, back trap piling and micro-picking on a series of coatings. They showed that a back trap mottle pattern can occur in offset printing due to a micro-picking type mechanism, linking the results to picking and piling issues. The relations between pore structure, ink setting, ink tack development and print gloss have been reported in several studies (Bluvol et al., 2008; Burri et al., 2004; Donigian et al., 1997; Gane and Seyler, 1993; Gane et al., 2003a, 2003b; Karathanasis et al., 2001, 2003; Rousu et al., 2000; Ström and Karathanasis, 2008; Schoelkopf et al., 2003a, 2003b).

There are a number of techniques for predicting the printability of papers, such as the ink tack build on the printed surface, the wet pick or wet repellence, print mottle etc. These measurement methods are covered in a review paper by Wygant et al. (1995), and include laboratory tests, such as, the Ink Surface Interaction Tester (ISIT) (Gane and Seyler, 1993), the LodCell development by Concannon and Wilson (1992), latterly promoted as the P&I test by Plowman Associates (Nancy Plowman Associates, Inc., 30-32 Ray Ave., Burlington, MA 01803, USA), which was more recently reduced to a lab-bench scale equipment (Deltack) by Prüf-bau (Prüfbau, Dr. Ing. H. Dürner GmbH, Werk Peissenberg, Aich 17-23, D-82380 Peissenberg, München, Germany). Despite the plethora of lab test methods for pick strength, including other direct methods, such as the IGT (IGT Testing Systems, Keienbergweg 25, 1101 EX Amsterdam Z.O., The Netherlands), correlation with experience directly on the offset press is at best frequently missing, and at worst contradictory. This was recently illustrated to good effect in the study made by Dahlvik et al. (2011) on a sheet fed offset press, in

which the concentration of picking occurring at the tail edge of a solid print area in multicolour printing was shown to depend on ink tack, press speed, configuration, paper quality and press setting, including fountain solution pre-application. Although some degree of correlation was achieved between the "passes to fail" in the P&I test results, there remained, nonetheless, outliers which would still require the expense of a full-scale trial to remove potential doubt.

Establishing a prototype more realistic laboratory method for determining tail-edge wet picking is the focus of interest in this study. It is recognised that the method needs to encompass the relation to fountain solution and print dynamic interactions with the printing ink and coated paper surface, and so these effects are further investigated. We provide an introduction to a continuing "work in progress" to develop such a new lab-scale method to improve the reproduction of the phenomenon, and so save the costs of full scale offset print trials. The aim of the work is to reproduce the tail edge geometry, and to see if this improves on the general testing offered by repeat revolution methods for paper surface destruction, e.g. NPI method of passes to failure. This paper goes on to show the progress toward increased sensitivity, especially in the differentiation of high quality papers.

1.1 Background

A previous study was undertaken to look at the factors influencing the surface strength of coated papers (Dahlvik et al., 2011), and this forms the in-practice correlation basis for our lab test development. The papers were sheet fed offset papers topcoated on mill-precoated woodfree basepaper with formulations differing in solids content, the type, fineness and particle size distribution of the pigment(s) and the binder level. The focus here is not on the details of the papers, but, for completeness, the specific formulations are shown in Table 1. Four different ground calcium carbonate (GCC) pigments are used, including one with a narrow particle size distribution (NPSD) and two using high glossing clay, initially in a blend with GCC and secondly at 100% clay.

Table 1: Topcoating formulations of trial programme - mill blade precoated base paper (modified from (Dahlvik et al., 2011))

Coating colour formulation	1	2	3	4	5	6	7	8	9	10	11
GCC 95 (80 % < 1 µm)	100	100	100	100	100	100	50				
Clay (high glossing)							50	100			
NPSD GCC (75 % < 1 µm)									100		
GCC 60 (60 % < 2 µm)										100	
GCC 90 (90 % < 2 µm)											100
Latex SBR	7.5	7.5	7.5	5.0	5.0	5.0	7.5	7.5	7.5	7.5	7.5
Synthetic thickener	0.10	0.15	0.20	0.10	0.15	0.20	0.25	0.15	0.15	0.30	0.20
Solids content	71	68	65	71	68	65	65	65	68	68	68

Calendering conditions were adjusted to obtain a sheet gloss of 75% for trial point 1. The same calender parameters were used for the remaining trial conditions. The focus of the study was in terms of sensitivity toward tail-edge picking, i.e. picking at the trailing edge of a full tone image area. The samples were printed at full scale using a tailor made printing layout/method using a specially designed printing plate, Figure 1, and high-tack inks (Ink tack values: standard = 7.5 - 10; high = 9.5 - 10.8) to accentuate this phenomenon. The papers were ranked on a scale of 0 to 100 in terms of increasing quality, Figure 2, based on the visual evaluation of the print tests. Full details of the printing trial and the ranking of the samples can be found in Dahlvik et al. (2011).

The discussion of which formulations gave the greater tendency toward tail-edge picking has already been reported in detail by Dahlvik et al. (2011), and is not considered further here. The aim is to retain the rankings offered by the previous workers and to use the same sample papers, but separately reconsider the ink behaviour, in the lab-scale test development being reported here by the authors. Further details of the pigments in question and the overall trial rationale can be found in Dahlvik et al. (2011).



Figure 1: Layout developed for evaluation of edge picking in commercial offset printing trials (Dahlvik et al., 2011)

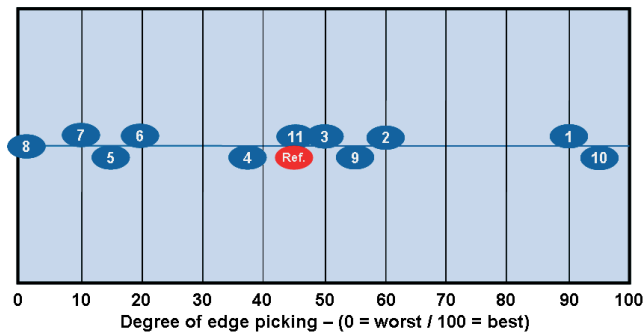


Figure 2: Visual observer ranking according to the degree of tail-edge picking (Dahlvik et al., 2011)

1.2 Previous laboratory testing

The coated samples described above were evaluated by standard lab test methods commonly used in the industry. The Nancy Plowman passes to failure (NPA Paper and Ink Stability Test, i.e. P&I Test) were measured, and compared to the visual ranking values of the commercial offset printing trials, Figure 3. The number of passes until coating failure is normally determined by visual inspection of the test strips.

The points in the lower left region of Figure 3 show good correlation between the P&I test method and reality of the printing trial. Nonetheless, we see significant outliers present destroying the correlation in several cases, either being regarded as "bad samples" by the P&I test method as they show picking after a relatively low number of passes, whereas on the commercial printing scale they are of a medium ranking and are equivalent to the reference sample or vice versa. So, although a relatively strong 'trend' can be seen in many cases a more robust and tighter measurement technique for wet pick in respect to tail-edge failure still needs to be developed.

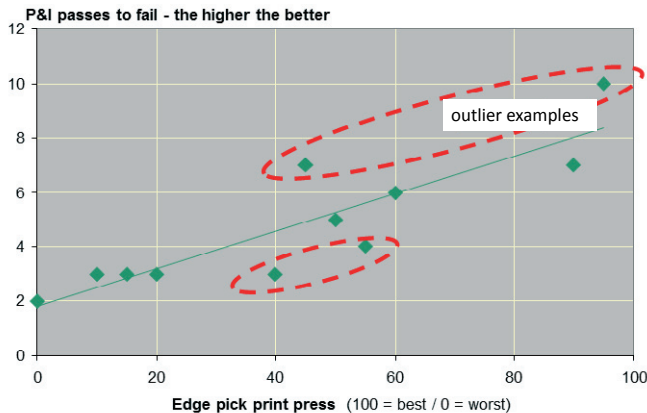


Figure 3: P&I passes to failure against tail-edge pick ranking - commercially printed papers - showing the significant outliers in the correlation (modified from (Dahlvik et al., 2011)

2. Method

2.1 Developing a novel laboratory method

Purfeerst and van Gilder (1991) correlated tail-edge picking with tack build using a prototype Ink Surface Interaction Tester (Gane and Seyler, 1993). Their work studied a range of binder types (binder ratio mixes), and correlation with print press trials was established. However, although tack rise was found to match reasonably well in the work of Dahlvik et al. (2011) using the LodCell device (Concannon et al., 1992), in the form of the P&I test, exceptions were found when the pore structure of the coating differed greatly in respect to the fine pore volume component as induced by changes in coating pigment between GCC and fine glossing clay.

Tail-edge picking relates to the combination of concentration of transported dampening solution (fountain solution), ahead of either the subsequently applied ink layer or in the later colour printing station(s) as the film split of an existing ink layer is established, and the ink film split force at the transition between image and non-image area. The transported fountain solution acts under pressure to weaken the coating surface as a function of hydraulic impregnation in the printing nip. The contact edge between the newly applied or secondary split ink layer and the transported fountain solution leads to a non-wetting ink-fountain solution liquid-liquid interface, such that the film split on the trailing edge of the image occurs under impulse dynamics, i.e. the application of the separation force occurs over a time span $\Delta t \rightarrow 0$. This pulse effect transmits an effectively enhanced pick force to the coating surface directly at the point of greatest coating surface weakening. Simultaneously, an interface water layer may lead directly to ink adhesion failure. By introducing a film split pulse, as might be expected to occur at the tail edge of the image area under press dynamics, the picking tendency should in principle be able to be assessed. The pulse is effected by inserting a semi-rigid thin packing between the sample under test and the mounting sector, Figure 4 and Figure 5. This packing may be either a chosen thin substrate as we further developed, or even crudely, as a first approximation for testing less good papers, double-sided adhesive tape as used, for example, on the interaction tester to attach the sample to the rotating sector. As the print roller applies ink onto an already pre-damped coated paper or board surface, the pressure step function encountered as the printing roller impacts at the point of profile elevation and depression, induced by the inserted packing, effectively reproduces the tail-edge pick pulse. Thus, opposite analysable effects are seen at the point of positive pressure impulse, and at the pressure drop pulse region at the rear of the packing insert.

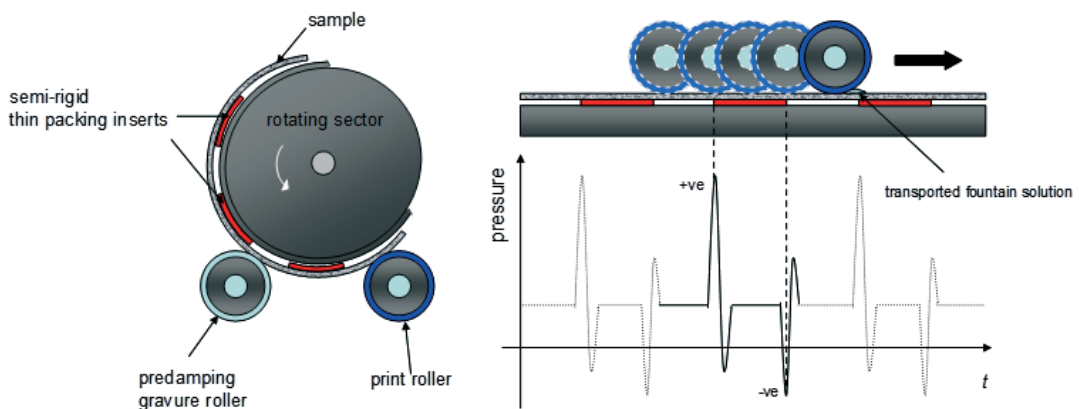


Figure 4: Schematic of the printing setup on the ISIT to mimic tail edge pick, and pressure pulse generated under the printing nip

3. Proof of principle - using first crude test parameters

The trial papers were first measured using the same high tack ink, Sun cyan 38100, as used in the practice commercial print test. The papers were prepared by placing five pieces of doubled sided sticking tape (tesa[®] 4961) spaced conveniently along a 29 cm strip of the sample to be measured. The tape used is a hard rubber adhesive set and has extremely high shear strength. It is, therefore, non-splitting and could be removed readily from surfaces after use. The tape pieces were adhered to the paper strip such that there were four 1 cm gaps left between the taped regions, and the sample strip was then adhered by the tape to the rotating sector of the underlying tape regions.

Water was used to imitate the fountain solution; this was applied using a gravure roller applying $0.2 \text{ cm}^3\text{m}^{-2}$ of water at a speed of 0.5 ms^{-1} and at a pressure of 300 N. After 5 s the sample was printed at a speed of 0.5 ms^{-1} at a pressure of 500 N applying 0.3 cm^3 of the high tack cyan ink to the roller. The gravure roller had a width of 3.8 cm and print rollers a width of 2.0 cm. The print roller was kept in place and single passes were made until there was visual evidence on either/both the print roller and/or the printed strip of pick, or more importantly any edge picking. It was noted how many of these post print passes it took until failure occurred, i.e. until white marks could be seen on the roller or on the printed strip. A series of repeat tests were performed at three different pressures: 100 N, 50 N and 5 N. The edge pick areas were then evaluated microscopically using image analysis.

3.1 Analysis method and initial results

Using transform image analysis to characterise the print density distribution across the impact region (Figure 5), the degree of tail-edge ink-surface adhesion failure, together with any pick when present, could be assessed.

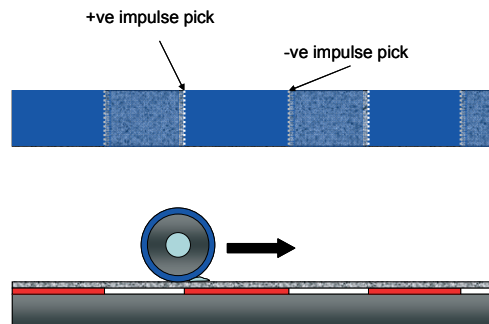


Figure 5: Schematic representation of the test strip after printing

For one strip measured on the interaction tester, four edge pick areas were created that could be measured and averaged. The strips were scanned with an HP Scanjet 8300 scanner at a resolution of 300 dpi adopting full colour mode. The image was then filtered to reduce the noise, and the intensity part of the full colour image was copied into a black and white image, Figure 6.

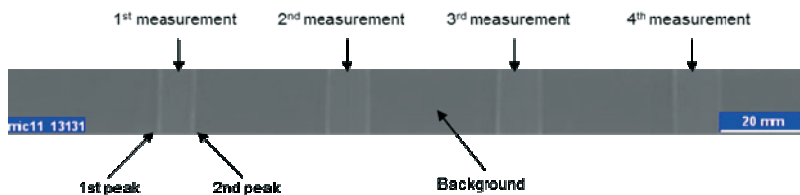


Figure 6: Test paper 1, 100 N, 1 pass, grey level intensity image showing measurement points

This gave an image having 180×2020 pixels. The grey levels of the 180 pixels in the y direction of the strip (cross/sample width direction) were averaged to give the intensity trace for that sample, and it was clearly identifiable where the four measurement points were for the tail-edge and front-edge pick areas, Figure 7. The curves were standardised such that the first peak was at the 500 pixel point.

The difference between the noise filtered grey level peak and the background was calculated, and this value was normalised to the background grey level intensity and inversely weighted according to the number of passes to pick initiation, $n_{\text{passes to picking}}$, to give comparable edge pick values according to the following formula, which, due to the inclusion of the image analysis, smoothens the result and improves upon the previously digitised "on-off" characterisation resulting from the traditional numbers of passes to failure.

$$\text{Edge Pick} = \frac{I_{\text{peak}} - I_{\text{background}}}{n_{\text{passes to picking}} \times I_{\text{background}}} \quad [1]$$

Figure 6 and Figure 7 show the intensity scan and intensity curve for Paper 1, one of the best ranking papers. In contrast, Figure 8 and Figure 9 show the intensity scan and intensity curve for Paper 8, the paper with the worst ranking in the commercial print trials.

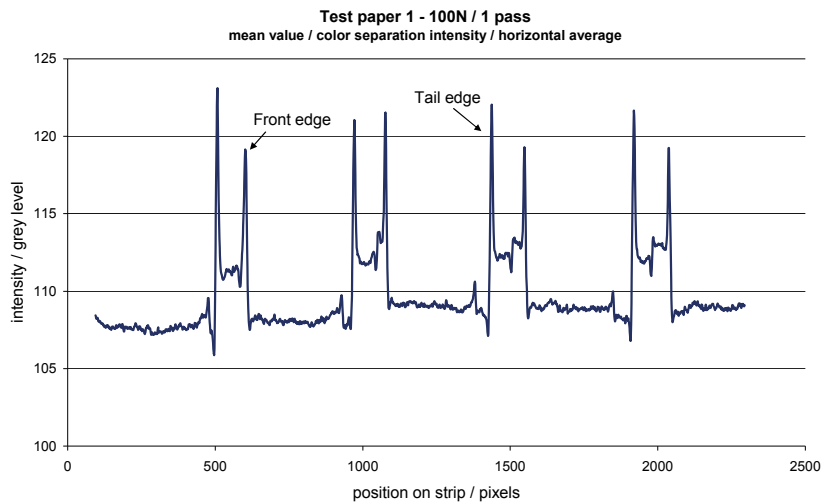


Figure 7: Intensity curve for Paper 1: one pass at 100 N, showing the statistical advantage of collecting four regions of tail edge behaviour

Figure 6 and Figure 7 show the intensity scan and intensity curve for Paper 1, one of the best ranking papers. In contrast, Figure 8 and Figure 9 show the intensity scan and intensity curve for Paper 8, the paper with the worst ranking in the commercial print trials.



Figure 8: Test paper 8, 100 N, 1 pass, colour separation, intensity black and white image showing measurement points

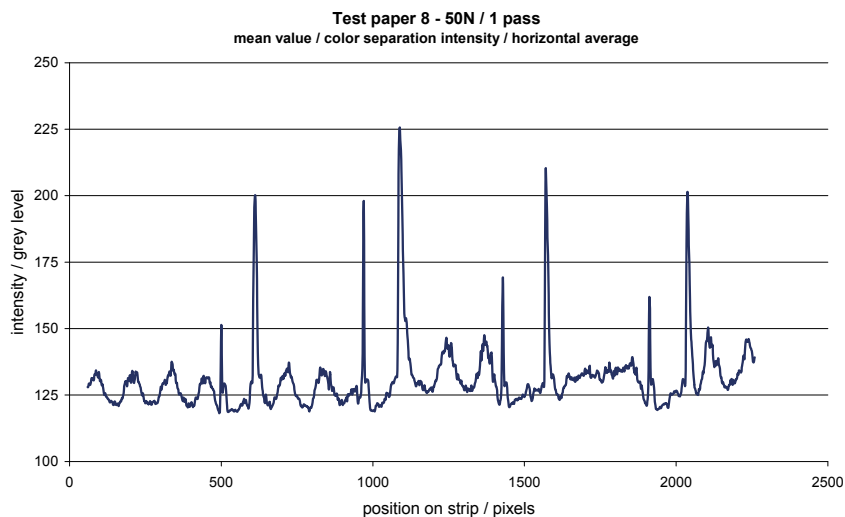


Figure 9: Intensity curve for Paper 8, one pass at 100 N - again showing the statistical advantage of the four repetitive regions of tail edge pick

It is obvious that there is a higher noise level with Paper 8, even after filtering, and this reflects the pick onset already appearing between the edge study areas. The scale of the curve in Figure 9 is now eight times greater compared to that for Paper 1 in Figure 7.

It is still, however, possible to see where the peaks are that represent the front and tail edge peak regions. This indicates that the test in this form is somewhat too severe for this badly picking paper. As will be seen by altering the set-up parameters and impulse backing material design, a finer separation can be established between the numbers of passes to pick initiation.

For all samples analysed, the highest points in the pick black and white intensity traces are determined, and an average of the four points used to give a value for the front-edge pick or tail-edge pick for each sample at each of the three pressures measured. A summary of the values calculated according to the formula given in Eqn [1] is given in Table 2 for the tail-edge pick. The standard deviation values are also shown, and are in the range of ~ 10 % of the average pick value for all the papers except Paper 8, which has the most unstable surface.

Table 2: Tail-edge pick data

Sample	100 N			50 N			5 N		
	Pass(es)	average	std. dev.	Pass(es)	average	std.dev.	Pass(es)	average	std.dev.
Paper 10	2	0.058	0.004	2	0.086	0.003	2	0.091	0.004
Paper 1	2	0.058	0.007	2	0.079	0.001	2	0.104	0.001
Paper 2	2	0.066	0.003	2	0.094	0.005	1	0.162	0.011
Paper 9	2	0.067	0.007	1	0.163	0.004	2	0.109	0.006
Paper 3	2	0.086	0.007	2	0.085	0.003	1	0.151	0.008
Paper 11	2	0.069	0.002	2	0.090	0.003	2	0.110	0.004
Paper 4	2	0.059	0.004	1	0.148	0.007	1	0.156	0.006
Paper 6	1	0.127	0.016	1*	0.150	0.006	1	0.155	0.007
Paper 5	1	0.139	0.005	1	0.149	0.006	1	0.145	0.007
Paper 7	1*	0.132	0.009	1	0.155	0.005	1	0.173	0.009
Paper 8	1*	0.256	0.095	1*	0.314	0.159	1*	0.110	0.016

* evidence of pick already at the print stage prior to the test passes

Plotting the edge pick value calculated via Eqn [1] against the number of passes shows that the data fall into four regions, shown by the coloured (and labelled) circles in Figure 10. The upper left region shows samples where the edge picking and final print quality are both very bad, red circle. The number of passes to pick is very low and picking occurs almost immediately. As a result, the intensity value calculated from the picked image area is very high showing a high contrast from the background printed area. The lower right region of the graph shows the samples that are very good, green circle, i.e. the samples requiring a higher number of passes until wet pick occurs and with a lower measured intensity difference between the peak area and the background area, once the image analysis formula has been applied to the data. The upper right and lower left regions show sample evaluations of medium quality, orange circles.

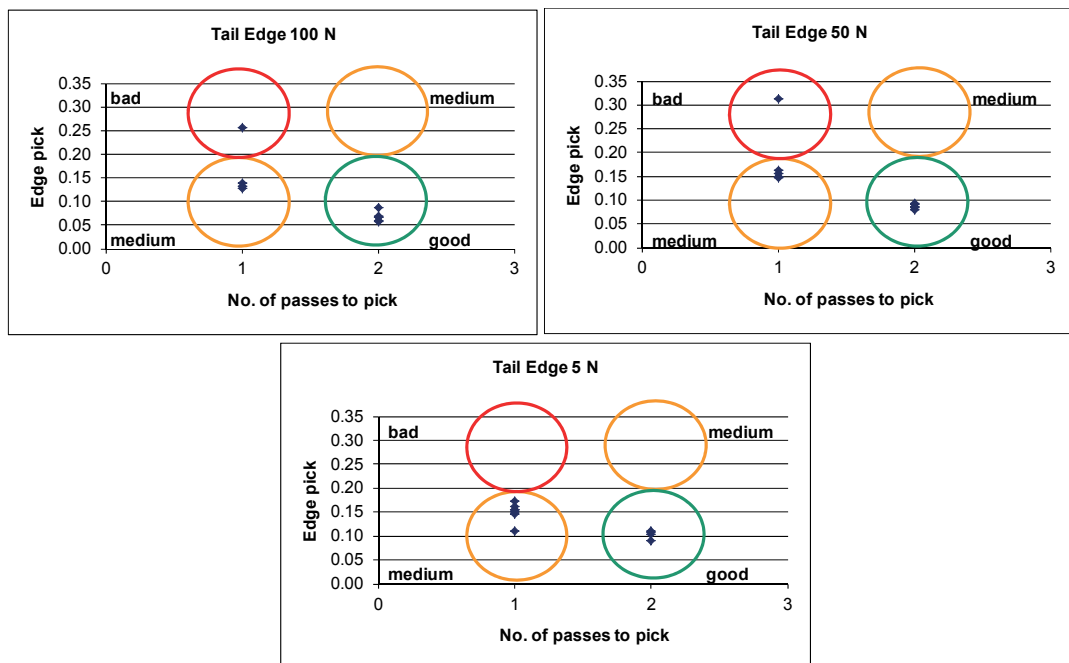


Figure 10: Edge pick intensity against number of passes with coloured circles indicating whether the samples are of good (green), bad (red) or medium quality (orange)

The recurring sample in the 'very bad' top left corner throughout Figure 10 is Paper 8. It is also of interest to note from these graphs that even after a high number of passes there are no samples with a high edge pick intensity value, top right corner. This means the samples don't suddenly break down, the edge pick occurs gently and slightly over time when the paper surface is strong. The tail edge pick at low pressure is also showing an apparently greater sensitivity, i.e. all the intensity values are in the lower half of the graph. Once again, given the lift effect on the paper of the tacky ink roll in the non-adhered regions (between the adhesive tapes) it suggests that low pressure at the tail edge leads to a stretching of the paper, and the mechanical strength is again stressed as at the front edge, i.e. stretch versus compression having similar effect on rupture.

4. Further development to enhance sensitivity

The test method is improved by using a flexographic polyester backing, designed to replace the initially used pieces of double-sided tape. This gives some improved reproducibility as well as introducing a compressible backing as would better represent the rubber backing roll and the deformation properties of the print system in reality. The green polyester film has a 570 µm relief formed as five raised areas, (nyloflex® ACE 076 D produced by Flint Group Flexographic Products, Sieglestrasse 25, D-70469 Stuttgart, Germany) which is used to replicate the pulse dynamic for the edge pick. The backing is attached to the sample carrier of the rotating sector with double-sided tape. The paper strip is subsequently held by 2.5 cm of tape at each end onto the rotating sector of the ink-surface-interaction tester, as can be seen in Figure 11.

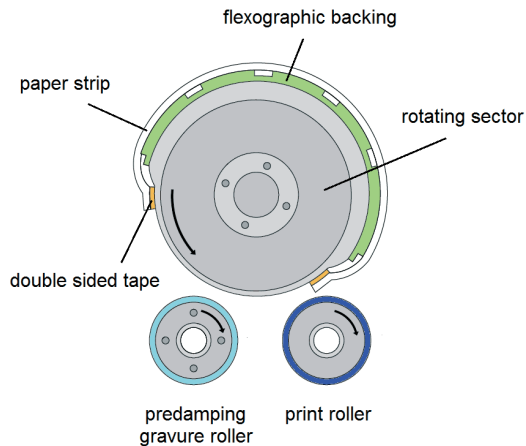


Figure 11: Schematic of the improved printing/picking setup on the interaction tester to mimic tail edge pick

The initiation of edge pick was evaluated visually in two ways so as to ease the work of evaluating the adjustment of parameters to increase sensitivity. The main evaluation method was by monitoring the appearance of white specks on the print roller. It seemed that edge pick occurred earlier on the tail-edge and also more white specks appeared on the tail-edge areas than on the front-edge areas. A distinction was also made based on the degree of edge pick, and edge pick was divided into two categories: little picking and picking, as seen in Figure 12. Little picking refers to a situation in which only few individual white marks appear onto the edge areas of the print roller, and picking refers to a situation in which the white marks form a line on the edge areas. The second evaluation method was based on paper strip appearance, and it was mainly used to compare papers which exhibited edge pick after the same number of passes.

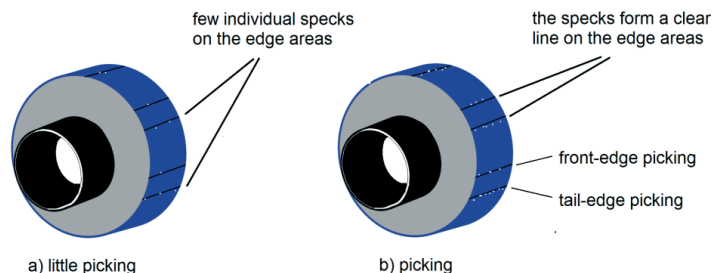


Figure 12: The two visual categories of edge pick initiation used to adjust parameters to increase sensitivity:
a) little picking and b) picking

4.1 New test parameters

A detailed laboratory study was made in order to increase the number of successful passes before tail pick occurred during the developed test so as to improve the differentiation of good papers. The parameters studied were the type of fountain solution, time delay between wetting and printing, ink type and amount, force and speed of printing, contact force and speed of passes and delay between passes. The most influential parameters on the number of passes were found to be the ink amount and the force and speed of printing. When lower amounts of ink were applied the number of passes to edge pick was reduced. This is because when a thinner ink film is transferred onto the paper the tack development rate is faster than when compared to that of a thicker ink film. The solvents are also absorbed into the coating more easily with a thinner ink film than with a thick ink film (Keiter, 1998). Therefore, a higher ink amount was chosen to be applied such that the number of passes until edge pick occurred would be increased.

Edge pick increased when higher printing pressures were used. Higher printing forces place higher demands on the paper and were found to cause cracking at the edge areas during ink application, resulting in increased edge pick. Lower printing forces increase the subsequent number of passes to edge pick. The number of passes to edge pick also decreased when higher printing speeds were used. This was expected as higher speeds make the release more challenging for the paper. Lower speeds also seemed to give a better register in terms of edge pick areas. Therefore, a lower printing force and a slower printing speed were selected for the application of the ink.

Water was again used to imitate the fountain solution in the new test set up. It was found that additional use of wetting agents or alcohol led to increased edge picking, presumably due to increased surface wetting - a topic that will be more fully addressed elsewhere. The water was again applied using the gravure roller applying $0.2 \text{ cm}^3 \text{ m}^{-2}$ at a speed of 0.3 ms^{-1} at a pressure of 300 N. After 11 s the sample was printed at a speed of 0.3 ms^{-1} , a pressure of 300 N, applying 0.4 cm^3 of the previously used high tack cyan ink to the roller. An ink with a lower intrinsic tack was also tested, but since it developed a higher ink-on-paper tack, it led to faster edge picking - an important point to be noted when choosing the test ink, i.e. do not expect to rank pick severity simply by intrinsic tack alone! The print roller was kept in place and single passes were made until there was visual evidence of edge pick on the print roller. It was noted how many of these post print passes it took until failure occurred, i.e. until white marks could be seen on the roller (or on the printed strip). A series of repeat tests were performed at a pressure of 100 N, a pressure shown to provide best differentiation. The edge pick areas were then evaluated microscopically using image analysis. A fuller reporting of the range of test parameters will be made in an upcoming Masters thesis by E. Jutila, Aalto University, Helsinki.

4.2 Results analysis for the new test setup

A summary of the values calculated according to the formula given in Eqn [1], i.e. applying the more detailed image analysis to the pick areas, is given in Table 3 for the tail-edge pick. The standard deviation values are also shown, and are in the range of $\sim 12\%$ of the average tail-edge pick values for all the papers, except for Paper 11, which was $\sim 25\%$.

Table 3: Tail-edge pick data

Sample	100 N		
	Passes	Tail-edge Pick	
		average	std.dev.
Paper 10	8*	0.017	0.003
Paper 1	4*	0.037	0.003
Paper 2	4*	0.048	0.007
Paper 9	4*	0.062	0.004
Paper 3	4	0.054	0.006
Paper 11	6*	0.019	0.005
Paper 4	3*	0.097	0.017
Paper 6	3	0.099	0.007
Paper 5	3*	0.119	0.016
Paper 7	3	0.101	0.011
Paper 8	2	0.132	0.014

* evidence of little picking on the print roller

Figure 13 shows the relationship between the formulation edge pick values for the tail edge picking against the commercial ranking of the samples. It can be seen that there remains one distinct outlier, paper 11, which either has another reason for its practice ranking or is a statistical failure of that ranking. Personal observation of the strip after the test would have ranked this sample higher following these laboratory test. Excluding this sample when fitting the data results in an R^2 value of 0.92, when using a linear function.

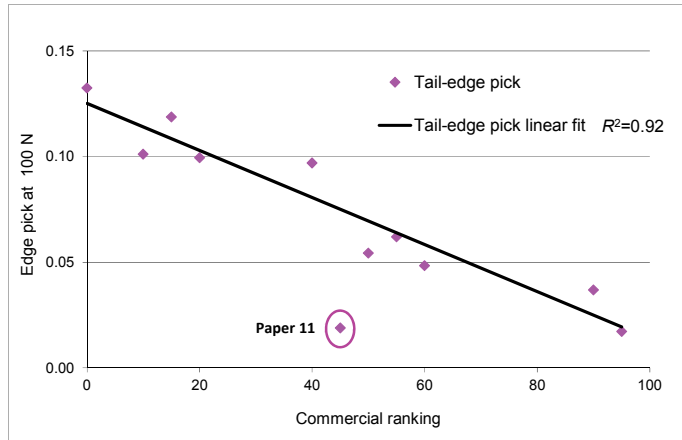


Figure 13: Formulation edge pick at 100 N against commercial ranking with new test setup

The new test method was able to increase the number of passes until edge pick occurs from a range of one to two passes up to a range of two to eight passes. Previously, when comparing the edge pick data with the commercial ranking data, it was seen that there was a very low sensitivity between the higher commercially ranked papers in terms of edge pick. With the new experimental setup, the differentiation between the edge pick values for all samples is more evenly distributed and the data can be viewed on a linear scale.

5. Conclusions

A laboratory test method is able to establish correlation with tail-edge pick as visualised from a commercial sheet fed offset printing press. The method adopts a typical rotational print test apparatus (in this case the ink-surface-interaction tester). The technique applies a pressure impulse and subsequent depression within the print nip as it passes over the coated paper surface, so as to mimic the tail edge separation of ink following a solid tone print area in the presence of fountain solution. The test has been developed adopting a specially designed flexographic polymer backing. The test has been further developed to increase the sensitivity of separation between good papers by increasing the number of passes from an initial maximum of two to a maximum of eight for the best papers. This was achieved by investigating the effect of parameters, such as fountain solution, delay between wetting and printing, ink type and amount, force and speed of printing, contact force and speed of passes and delay between passes, on edge pick and by developing a new test set up based on the investigations. The most influential parameters on the number of passes were found to be the ink amount and the force and speed of printing. The image analysis of the pick area together with knowledge of the new number of passes required to induce pick provides a linear correlation, having $R^2 > 0.9$.

Acknowledgments

The authors gratefully acknowledge the contribution of our colleague Silvan Fischer of Omya Development AG in developing the microscopic image analysis method used in this work. Omya Development AG is also gratefully acknowledged for funding the Masters study by E. Jutila at the Omya Laboratories and at Aalto University, Helsinki.

References

- Aspler, J., Lepoutre, P., "The Transfer and Setting of Ink on Coated Paper", *Progress in Organic Coatings*, 19(4), 1991, p333-357.
- Bluvol, G., Dahlvik, P., Hipp, A., Salminen, P. J., Welsch, G., "Cost saving concept for production of high quality double coated papers - Part 2: Blade-blade coating systems", *Tappi PaperCon '08 Coating Conference*, Dallas, TAPPI, Atlanta, 2008.

- Burri, P., Bluvol, G., Gane, P. A. C., Carlsson, R., "Optimising ink setting properties on double coated woodfree papers", *Tappi Coating and Graphic Arts Conference, Baltimore, Tappi, Atlanta, 2004*.
- Concannon, P. W., Wilson, L. A., "A method for measuring tack build of offset printing ink on coated paper", *TAGA Conference Proceedings, Rochester 1992, p282-301*.
- Dahlvik, P., Bluvol, G., Kagarer, K.-H., Arnold, M., "Factors influencing the surface strength of coated papers", *PaperCon 2011, Covington, Kentucky, TAPPI, Atlanta, 2011, p374-392*.
- Donigian, D. W., Ishley, J. N., Wise, K. J., "Coating Pore Structure and Offset Printed Gloss", *Tappi Journal, 80(5), 1997, p163-172*.
- Donigian, D. W., Vyörykkä, J., Xiang, Y., "The relationship between ink setting rates, backtrap piling and micro-picking", *TAPPI Coating Conference, TAPPI, Atlanta, 2004*.
- Gane, P. A. C., Schoelkopf, J., Matthews, G. P., "Offset Ink Tack and Rheology Correlation Part 1: Ink Rheology as a Function of Concentration", *Tappi Journal, 2(6), 2003a, Online Exclusive*.
- Gane, P. A. C., Schoelkopf, J., Matthews, G. P., "Offset Ink Tack and Rheology Correlation Part 2: Determining in Real Time the Solids Content of Ink-on-Paper Using the Ink Tack Force-Time Integral", *Tappi Journal, 2(7), 2003b, Online Exclusive*.
- Gane, P. A. C., Seyler, E. N., "Some aspects of ink/paper interaction in offset printing", *TAPPI Coating Conference, TAPPI, Atlanta, 2004, p243-260*.
- Karathanasis, M., Carne, T., Dahlvik, P., Haugwitz, B., Ström, G., "Importance of Coating Structure for Sheet-Fed Offset Print Quality", *Wochenblatt für Papierfabrikation (7), 2001, p426-432*.
- Karathanasis, M., Fogden, A., Dahlvik, P., "The Concept of Critical Ink Setting Time and Its Relation to Print Gloss - Influence of Latex Binder", *Nordic Pulp and Paper Research Journal, 18(2), 2003, p145-149*.
- Keiter, S., "Haftung und Aufnahme von Druckfarben auf gestrichenen Papieroberflächen", 1998, *Diploma Thesis of the University of Dortmund and Private Communication*.
- Purfeerst, R. D., van Gilder, R. L., "Tail-Edge picking, back-trap mottle and fountain solution interference of model latex coatings on a six-color press predicted by laboratory tests", *Tappi Coating Conference, Montreal, Tappi Press, Atlanta, 1991, p461-472*.
- Rousu, S. M., Gane, P. A. C., Spielmann, D. C., Eklund, D. E., "Differential absorption of offset ink components on coated paper", *International Printing and Graphic Arts Conference, Savannah, Georgia, Tappi Press, Atlanta, 2000, p55-70*.
- Schoelkopf, J., Gane, P. A. C., Ridgway, C. J., Spielmann, D. C., Matthews, G. P., "Imbibition Behaviour of Offset Inks: I Gravimetric Determination of the Imbibition Rate of Oil into Pigmented Coating Structures", *Tappi Journal, 2(6), 2003a, p9-13*.
- Schoelkopf, J., Gane, P. A. C., Ridgway, C. J., Spielmann, D. C., Matthews, G. P., "Imbibition Behaviour of Offset Inks: II Gravimetric Determination of Vehicle Separation Rate into Pigmented Coating Structures", *Tappi Journal, 2(7), 2003b, p19-23*.
- Ström, G., Karathanasis, M., "Ink setting on coated media - Importance of pores structure and latex content", *2nd International Papermaking & Environment Conference Proceedings, Tianjin, China 2008, p894-900*.
- Wygant, R. W., Pruett, R. J., Chen, C.-Y., "A review of techniques for characterizing paper coating surfaces", *1995 TAPPI International Paper Coating Fundamentals Symposium, Dallas, Texas, TAPPI, Atlanta, p1-15*.
- Xiang, Y., Bousfield, D. W., "The influence of coating structure on ink tack development", *Tappi International Printing and Graphic Arts Conference 1998, p93-101*.
- Xiang, Y., Bousfield, D. W., "Effect of fountain solution on ink tack development and print quality", *Tappi Coating Conference, May 2-5, 1999, Toronto, Canada, Sheraton Centre, Tappi Press, 1999, p179-189*.
- Xiang, Y., Bousfield, D. W., "Influence of Coating Structure on Ink Tack Dynamics", *Journal of Pulp and Paper Science, 26(6), 2000, p221-227*.
- Xiang, Y., Bousfield, D. W., Hayes, P. C., Kettle, J., Hultgren, L., "Effect of latex swelling on ink tack build and ink gloss dynamics of coatings", *2000 International Printing & Graphic Arts, October 1-4, 2000, Hyatt Regency Savannah, GA, Tappi Press, 2000, p139-151*.



Control of the breakup of ink filaments in offset printing

James Claypole¹, Phylip R. Williams¹, Davide Deganello²

¹ College of Engineering,
Swansea University, UK

E-mails: 480704@swansea.ac.uk; p.r.williams@swansea.ac.uk

² Welsh Centre for Printing and Coating
College of Engineering, Swansea University, UK

E-mail: d.deganello@swansea.ac.uk

Abstract

In the printing processes, ink filaments are commonly formed during the ink splitting between separating rollers and between rollers and the substrate. As these filaments break, satellite droplets are often produced due to the rapid extension of the ink. These droplets produce an effect referred to as the 'misting' phenomenon, which is a major cause of problems with print quality (1) as well as health and safety problems (2, 3). In this paper, we evaluated the potential for using a blade or wire held parallel to the rollers to control the misting formation by promoting a controlled early failure of the liquid filaments. The proposed approach was tested for an offset ink and was shown to be extremely effective with reductions of the misting by 1-2 orders of magnitude when compared to control experiments.

Keywords: offset, ink, misting, ink filamentation, rollers

1. Introduction

In the printing processes, ink filaments are commonly formed during the ink splitting between separating rollers and between rollers and the substrate. As these filaments break, satellite droplets are often produced due to the rapid extension of the ink. These droplets produce an effect referred to as the 'misting' phenomenon, which is a major cause of problems with print quality (1) as well as health and safety problems (2)(3). Hence any reduction in the misting levels can have significant benefits on the health and safety of the printing industry.

The level of misting is affected by different aspects of the printing process, such as roughness of roller, printing speed, ink film thickness and the properties of the ink. In offset printing the combination of high viscosity non-Newtonian inks (15-25 Pa s) with high printing speeds (100-400 m/min) (4) is the underlying cause of high levels of misting.

In a previous work by M. Decre et al (5), a length of string was held inside the meniscus of a fluid suspended between separating rollers. The aim was to control the ink separation between the rollers without any reference to misting or filaments formation. The previous work was also conducted using only low viscosity Newtonian silicon oils and low speeds, up to 30 m/min.

This paper evaluates the potential for using a blade or wire held parallel to the rollers to control the misting formation by promoting a controlled early failure of the liquid filaments. The idea is to cause the filaments to break earlier than they would normally have done, by imposing a mechanical force on them, and so stopping the formation of long filaments, cause of misting. In order to validate the feasibility of the proposed approach, the method was evaluated for a high viscosity offset ink at simulated press speeds of up to 200 m/min.

2. Methodology

The experimental tests were performed on an IGT tack tester 450. A diagram of the experimental set-up is presented in Figure 1. The system consists of three rollers, one of which can axially oscillate to improve the distribution of the ink.

Two different approaches were designed to induce the early failure of the filaments. In the first instance, a blade, with a thickness of 0.20 mm at its thinnest point, was attached to the edge of a metal plate.

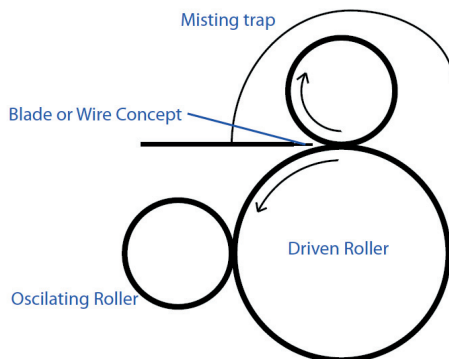


Figure 1:
Diagram showing the experimental setup

The plate stopped the blade from flexing and allowed it to be held between the rollers using a clamp stand. The equipment was set up as shown by Figure 2 (a). In the second instance, a wire, with an average thickness of 0.4 mm, was used suspended between the rollers and held at a tension of 0.6 kg (Figure 2 (b)).

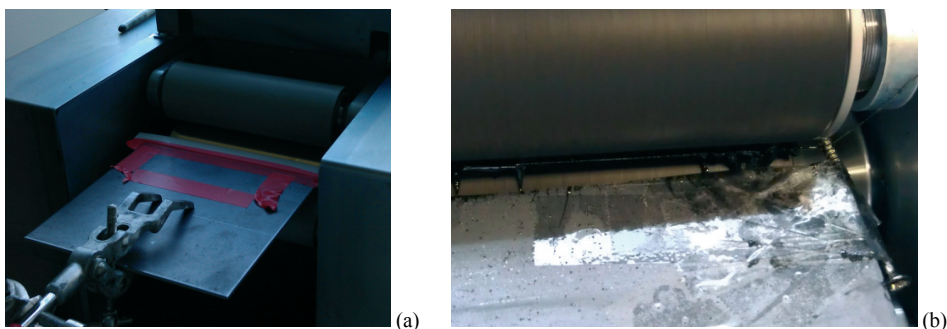


Figure 2: (a) Experimental set up for blade concept (b) Experimental setup for wire concept

For the experimental trials, Vanson VS110 Black Offset ink was used. The ink rheology was characterised on a Bohlin Gemini 150/200 HR shear rheometer. The ink presented a shear thinning behaviour with a viscosity varying from 250 Pas at 1 1/s to 10 Pas at 10 1/s. The ink showed almost no electric properties when subjected to strain tests.

For each experiment 7 ml of ink was deposited on the rollers using a 2 ml IGT ink pipette for accurate measure. The blade and wire were tested at a range of speeds with or without the distribution roller oscillating. Control tests were performed by running the system with the same parameters but without either the blade or wire.

Each of the experiments was run over 20 mins to show any significant difference in the observed levels of misting and any significant time effect.

The effectiveness of the proposed approaches was qualitatively observed using a Kodak high speed camera and accurately measured by analysing the level of misting produced. For the measurement of the misting, a paper sheet was placed around the rollers, acting a trap to catch the misting droplets during the experiments (Figure 1). After the test, the paper was removed and optically scanned with an EPSON PERFECTION V700 PHOTO at 1200 dpi and 24 bit colour. The images were then analysed measuring the misting droplets distribution and total area coverage using the particle analysis tools in ImageJ software (Figure 3).

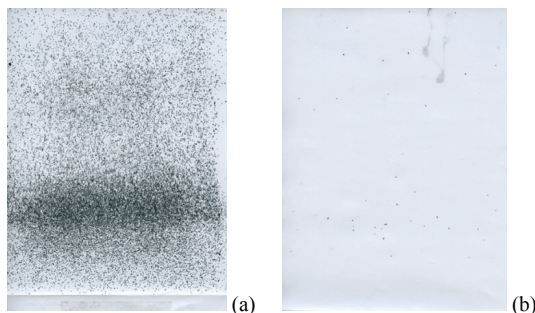


Figure 3:
Scanned images of the misting trap
(a) 100m/min control experiment without oscillation
(b) 100m/min string concept without oscillation

By blocking the oscillation of the distribution roller, it was also possible to analyse the effect of our approach on the formation of ribbing on the rollers. This was measured by taking pictures of the rollers at the end of the experiments, counting the number of formed ribs.

3. Experimental results and discussion

During the experiments, the blade or wire was positioned at the "edge" of the meniscus. The higher forces caused by the increase in printing speeds and viscosity meant that the wire could not be placed inside the meniscus as in (5). The blade and wire was being used to cut the liquid filaments rather than control the flow between rollers. The high speed camera observations showed this process where the filaments cut while coming into contact with the edge of the blade or wire.

To more clearly see the effect caused by the wire on the ink filaments a numerical model was produced using the level set method in PHYSICA. The results from this model show that the wire causes the early breakup of the filament. The starting conditions were the same for both models as can be seen in Figure 4 (a) and Figure 5. The wire caused the filament to break up early at a time of $t = 0.24$ s. Compared to the control test took a time of $t = 0.36$ s before the filament broke.

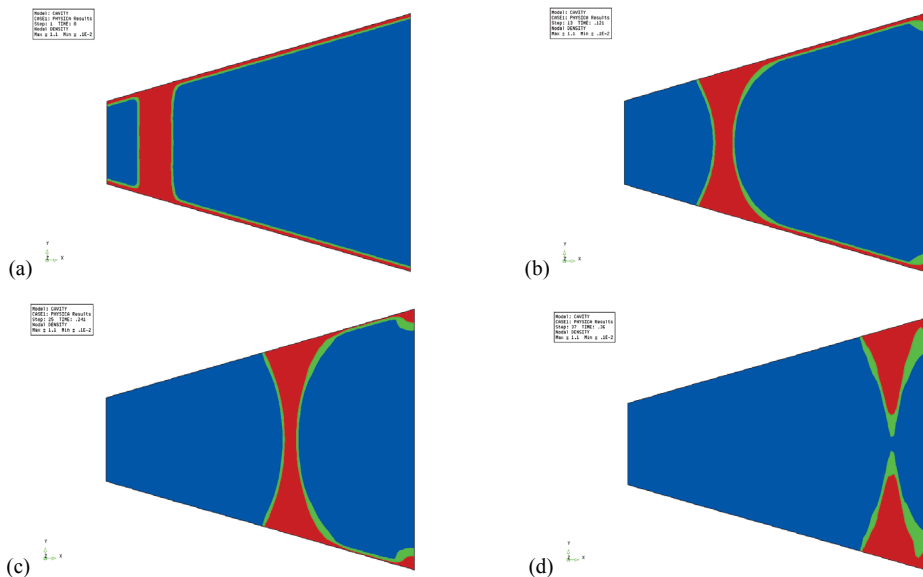


Figure 4: Numerical model results without either the blade or wire being imposed (a) $t = 0$ s (b) $t = 0.12$ s (c) $t = 0.24$ s (d) $t = 0.36$ s

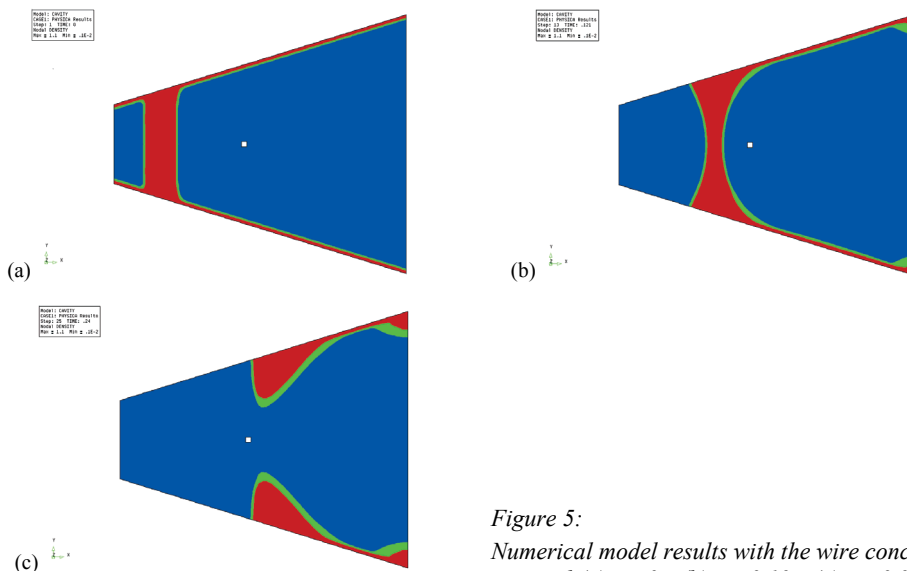


Figure 5: Numerical model results with the wire concept imposed (a) $t = 0$ s (b) $t = 0.12$ s (c) $t = 0.24$ s

Optical analysis of the resulting misting is presented in Figure 6. The presented results are normalised for the control sample at 100 m/min. In the test control samples, increasing speed or blocking the oscillation of the distribution roller resulted in an increase of misting as expected. For all the conditions, the blade and wire both significantly reduced the misting observed. The blade reduced the level of misting by an average of 92% over all 3 testing conditions. The wire reduced the level of misting by an average of 94% over all conditions.

The wire tended to perform better at lower speed than the blade. At higher speeds the vibration in the wire caused by the increased forces meant that it could not be placed as far into the break-up point, resulting in the wire being less effective at these speeds.

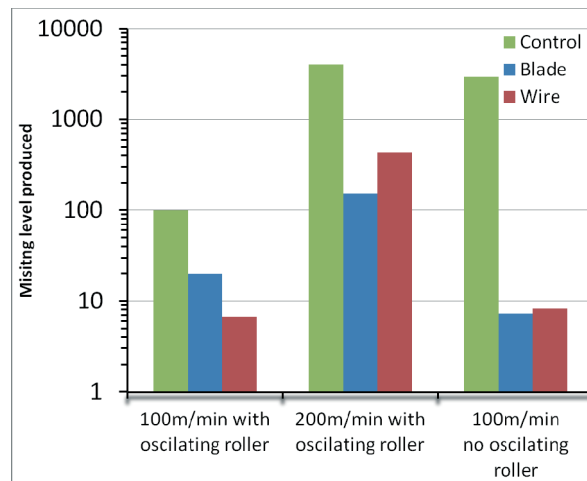


Figure 6: Optical analysis of the misting trap experiment. The results are normalised against the control experiment at 100m/min with the "oscillating" roller. A logarithmic scale was used due to the large difference in results

At the end of the experiments any long term effect on the wire and blade were observed. The blade showed a significant build up of ink on the edge as shown in Figure 7(a). This problem was not present in the wire where only a finite volume of ink built up on the downstream area as shown in Figure 7 (b).

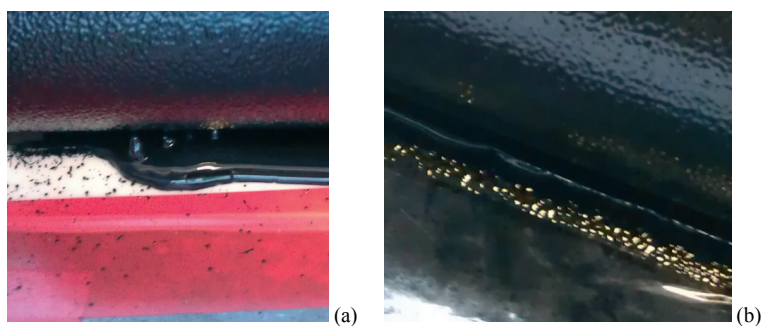


Figure 7: (a) Build up of ink on the back of the blade after 20 min run at 100 m/min
(b) Wire after 20 min run at 100 m/min

The analysis of the ribbing (with oscillation of distribution roller blocked) showed that the number of ribs increased from an average of 17 on the test control samples to 39 and 45 bands for the blade and wire respectively. By avoiding the formation of long filaments, our approach appears to avoid the concentration of ink in ribs allowing ultimately a better distribution of the ink.

4. Conclusions

In this paper, we evaluated the potential for using a blade or wire held parallel to the rollers to control the misting formation by promoting a controlled early failure of the liquid filaments. The proposed approach was tested for an offset ink and was shown to be extremely effective with reductions of the misting by 1- 2 orders of magnitude when compared to control experiments. Together with misting, the proposed approach was effective also on the ribbing formation by improving the ink distribution.

The marked difference in the levels of misting produced shows that the development of the proposed approach for commercial offset presses could significantly reduce the level of ink misting and flinging, leading to improved health & safety and print quality.

References

- (1) Decre, M., Gailly, E., Buchlin, J., *Meniscus Control by String in Roll Coating Experiment*. 1996, AIChE Journal, Vol. 42(6), pp. 1583-1589.
- (2) HSE Books. *The Printers Guide to Health and Safety*. 2002. ISBN 978 0 7176 2267 2.
- (3) Leach, R. H., *The Printing ink manual*. s.l.: Springer, 1993.
- (4) Luce, D., Landre, M., Clavel, T., Limousin, I., Dimerman, S., Moulin, J., *Cancer mortality among magazine printing workers*. 1997, Occupational and Environmental Medicine, pp. 264-267.
- (5) Vlachopoulos, G, Claypole, T., Bould, D, *Ink mist formation in roller trains*.. 2010. IARIGAI 2010 proceedings: Advances in Printing and Media Technology. Vol. 37, pp. 119-123.



Hardness and electric conductivity of copper in gravure form production

Armin Weichmann, Matthias Galus, Tim Wolber

Hochschule der Medien

Institut für Angewandte Forschung (IAF)

Nobelstr. 10, D-70569 Stuttgart, Germany

E-mails: weichmann@hdm-stuttgart.de; galus@hdm-stuttgart.de; tw047@hdm-stuttgart.de

Abstract

The electromechanical gravure of gravure cylinders demands specific characteristics of the copper to be engraved especially regarding the brittleness of the metal. The brittleness is correlated to the hardness and therefore the measure is usually the hardness according to Vickers. As the ductility is correlated to conductivity also, alternatively the conductivity can be a measure. If the brittleness is too low, parts of the edges are pressed back into the cell and deteriorate the shape of the cell leading to poor print results. It was shown, that the recently available device for measuring the conductivity of the copper surface does measure the relevant copper layer (1/10 mm) and that the conductivity, the hardness and the brittleness, measured by the bending angle of the copper layer before break, correlate nicely. A threshold for good engraving quality could be defined.

Keywords: gravure printing, copper, electric conductivity, hardness, electromechanical engraving

1. Scope of work

In gravure printing the most important element is the print form cylinder, which holds small cells according to the image wise necessary amount of ink. The manufacturing of this cylinder is a multi step process including copper and chromium galvanic, grinding, polishing and engraving of the copper. Today the generation of the cells is mostly done by electromechanical engraving. A diamond stylus vibrates with a frequency of up to 12 kHz, cuts out of the copper chips with lengths between some 10 μm and some 100 μm and forms cells with typical depths in the range of some micrometers up to 50 μm , leaving edges at the boundaries of the cells. After the grinding a diamond scraper removes these edges. The chips and the edges are withdrawn by suction. When the scraper abrades them, the edges should break away completely. Otherwise parts of the edges are pressed back into the cell and deteriorate the shape and the volume of the cell (see Figure 1). This could lead to a different tone reproduction in the printing process and therefore to unacceptable colour deviations.

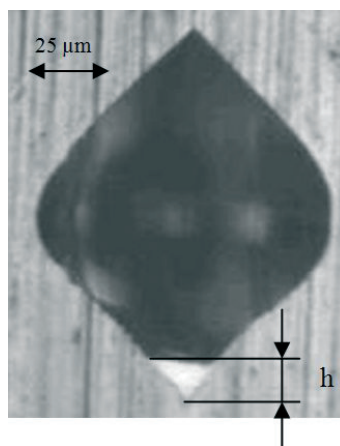
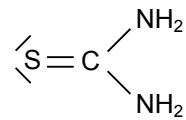


Figure 1: Cell with edge pressed back into the cell with height h

To avoid this, the copper, which is going to be engraved, has to be sufficiently brittle. The brittleness or ductility of copper on the other hand is directly related to its hardness. The hardness of metals can be specified according to Vickers. For good quality of the electromechanical engraving it is said, that the hardness has to be in the range of 240 HV (220 HV - 250 HV).

The copper is plated in a galvanic bath, using copper as anode, the gravure cylinder as cathode, CuSO_4 as electrolyte and H_2SO_4 to adjust the conductivity. To reach the necessary hardness additives are used. The main ingredient of these additives is thiourea with its chemical formula:



Thiourea works in two ways. Firstly it works as an inhibitor. The effect of an inhibitor can be explained by the theory of Kardos (1974). At a micro protrusion the field strength of the magnetic field is higher and therefore more copper would be deposited than at lower areas leading to a faster growth of the protruding areas and a more and more uneven surface. On the other hand over a micro protrusion the thickness of the diffusion layer is smaller and this leads to a higher adsorption of thiourea at the protruding areas. Thiourea now hinders the deposition of copper and therefore leads to a leveling out of the surface.

Secondly, after decomposing, its sulphur is incorporated into the copper layer presumably in form of sulphide (Bindschädler, 1980; Turner and Johnson, 1962). Therefore the additive is consumed and has to be replenished during the plating. The sulphide ions cause defects within the crystal matrix, which hinder the atom layers to slide on each other. The copper gets harder (Turner and Johnson, 1962; Walker and Bridges, 1974) and its brittleness is increased (Javet and Hintermann, 1964). Also these defects represent barriers to the conduction electrons and reduce their relaxation time within the metal. The relaxation time of the conduction electrons and the electric conductivity are related. If the relaxation time decreases, the electric conductivity decreases accordingly. Therefore the conductivity should be connected with the brittleness of the copper. A measurement of the conductivity should give relevant information about the brittleness and therefore the engravability of the copper for the stylus of an electromechanical engraving device.

Helmut Fischer GmbH has developed a measuring device for this purpose, the Sigmascope SMP 10 with sensor ES40HF. This device is based on eddy current and is able to measure the conductivity of the surface layer of the copper according to DIN EN 2004-1 and ASTM E 1004. The measurement is fast and convenient and therefore could supplement the hardness measurement according to Vickers.

Within the project we firstly wanted to prove that the thickness of the layer, which is measured, fits with the thickness of the layer to be engraved. Secondly we investigated the correlation between ductility, hardness and conductivity of the engravable copper.

2. Determination of the thickness of the influencing layer

2.1 Measurement principle

The principle of the measuring device is shown in Figure 2.

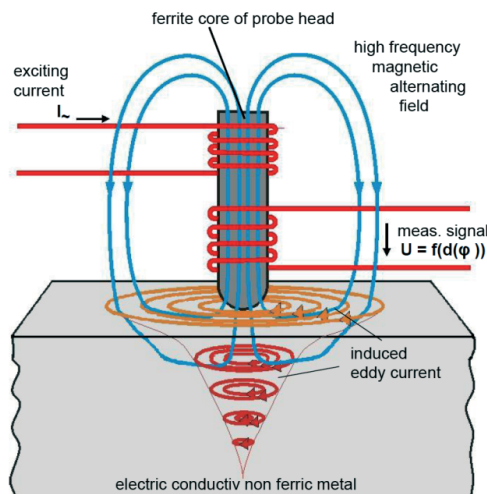


Figure 2: Schema of conduction measurement based on eddy current (Fischer, 2012a)

A ferrite core has a coil wrapped around. Exciting current generates a high frequency alternating magnetic field which induces through the ferrite core eddy current within the electric conductive non ferric material, which is in our case copper. The current resp. the voltage induced in a second coil wrapped around the ferrite core is measured.

The phase angle ϕ between the exciting current and the current induced in the measurement coil is a measure of the conductivity of the copper (see Figure 3). The higher the conductivity the more eddy current is induced. This leads to a higher reactive part of the impedance and to a bigger ϕ . An advantage of using the phase angle is its independency to a small lift of the probe head, which eases the use of the device.

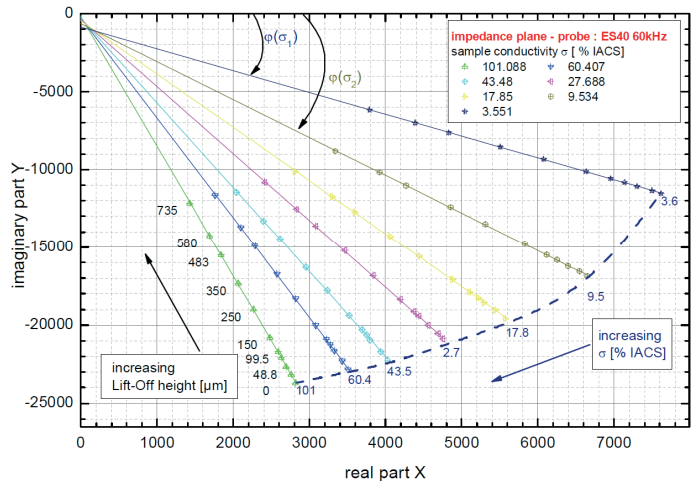


Figure 3: Impedance plane for different conductivities and varying lift off heights. The phase angle is independent of the lift off height. (Fischer, 2012b)

The eddy current J induced by an alternating electromagnetic field decreases exponentially with the depth.

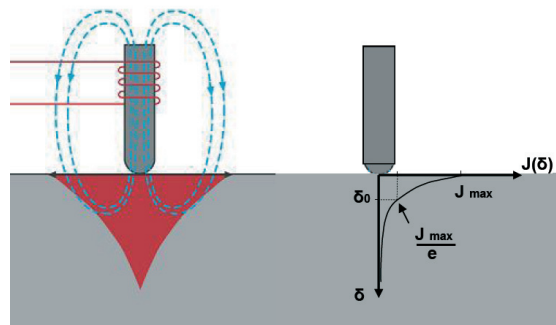


Figure 4: Schema eddy current depth (Helmut Fischer, 2012a)

The eddy current depth δ_0 , at which the current is decreased to $1/e$ of the current J_{max} at the surface, depends on the electric conductivity σ of the material and the frequency f of the alternating electromagnetic field according to [1] with μ_0 the vacuum permeability.

$$\delta_0 = \frac{1}{\sqrt{\pi \cdot f \cdot \sigma \cdot \mu_0}} \tag{1}$$

For gravure copper at a typical electric conductivity of 41 MS/m with the used frequency of 1.25 MHz an eddy current depth of 70 μm results.

The maximum depth of a gravure cell for coloured inks is about 50 μm . For layers of white or special technical applications it could be up to 100 μm . In cylinder plating the layer to be engraved is galvanized upon a basic copper layer and is normally about 100 μm thick. In general the electric conductivity of the basic layer is unknown. Therefore to get the value of the relevant layer for engraving, the topmost 100 μm only should influence the measurement. To be certain to have no influence of the basic layer in theory a depth of 3 times the eddy current depth would be necessary, which is about 200 μm .

2.2 Measurements

To answer the question, up to which layer thickness an influence of the basic copper layer is visible in reality, a cylinder was plated. We used a very soft basic copper with an electric conductivity of 53.5 MS/m and a hardness of 107 HV. The conductivity of the gravure layer was 43 MS/m with a hardness of about 240 HV.

The plating was interrupted regularly 16 times after each 10 μm of plating and every time an additional small area was masked with a patch, so that no further copper growing was possible there (see Figure 5).



Figure 5: Copper cylinder with patches of reduced layer thickness

The resulting thicknesses were evaluated against their electric conductivity as is shown in Figure 2.

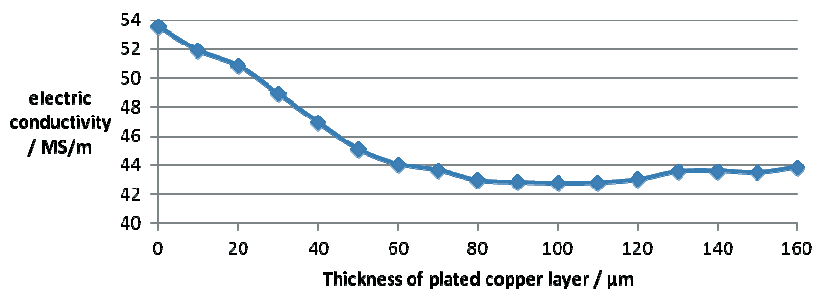


Figure 6: Conductivity versus thickness of copper layer with top layer significantly less conductive as base layer

2.3 Results

As expected at the eddy current depth of 70 μm a small effect of the basic copper was visible, but it disappeared at 90 μm already. A copper layer in the range of 100 μm , as it is often plated for the electro-mechanical engraving, is therefore sufficient, to be measured by the device without significant influence of the basic copper. If the time for the galvanic process has to be optimized and the copper layer is significantly thinner, like 60 μm , then a significant part of the signal results from the basic layer. If the conductivity of this layer deviates much from the gravure layer, misleading numbers could result to some extent.

3. Correlation of ductility, hardness and electric conductivity

3.1 Methods

To investigate the dependency of ductility, hardness and conductivity of the to be engraved copper, the cylinders were manufactured using the so called Ballard skin process. Prior to galvanising a silver layer, a couple of nanometres thick, is metalized onto the surface of the base copper. This layer diminishes the bond between the base copper and the newly galvanized copper. Thus after printing, the image carrying copper layer can be removed completely with ease. For that reason the plated copper layer can be investigated directly regarding ductility in particular.

Starting with an electrolyte without hardening additive, 24 cylinders were produced, increasing the concentration of hardening additive from cylinder to cylinder.

The bath parameters were:

Volume:	600 l
Concentration CuSO_4 :	220 g/l
Concentration H_2SO_4 :	60/l
Temperature:	30°C

Rotocopper HS of IPT International Plating Technologies GmbH thinned 1:14 to the ready to use dilution was used as hardening additive. 100 ml dilution after each produced cylinder were added for the first 13 cylinders, 200 ml for the next five, increasing to 300 ml, 500 ml and 1000 ml, to get to the limit value of the hardness, which can be reached with this additive. 70 ml of the additive (0.125 ml/Ah) were dosed continuously during the galvanic process to replace the consumption of the additive.

After plating the hardness and the conductivity were measured at 40 predefined points around the cylinder mantle, the mean value and the confidence interval were calculated.

To get the copper surface ready for engraving, it has to be grinded to the specified diameter and provided with a surface roughness of typically $0.4 \mu\text{m} R_z$. This ready to be engraved copper was then measured again at the 10 points regarding hardness, conductivity. Additionally the ductility together with the microscopic investigation of the engraved cells and its edges after engraving were determined.

The cells were engraved with an electromechanical engraver K500 from Hell using Hell screen 70 lines per centimetre with angle 4. For each cylinder a microscopic picture was taken of cells with the dot gain values of 1%, 5%, 10%, 20% to 90%. The pictures were evaluated within Photoshop and the edges were measured (see Figure 1). The mean value out of these 11 cells was taken as the measure of the size of the pressed back edges for this cylinder. After removing the Ballard skin a bending test was performed, using a bending measuring device from Lorentzen & Wettre, where a strip of the Ballard skin is flatly clamped on one end and loaded with a weight on the other end. The clamping then bends 90° to one side, then back and 90° to the other side. The numbers of 90° bends until the strip breaks was counted.

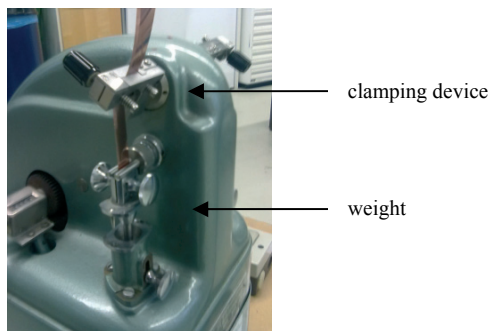


Figure 7:
Clamping device from Lorentzen & Wettre to determine the ductility of the Ballard skin

3.2 Results

As expected we found a negative linear dependency between hardness and conductivity (see Figure 7).

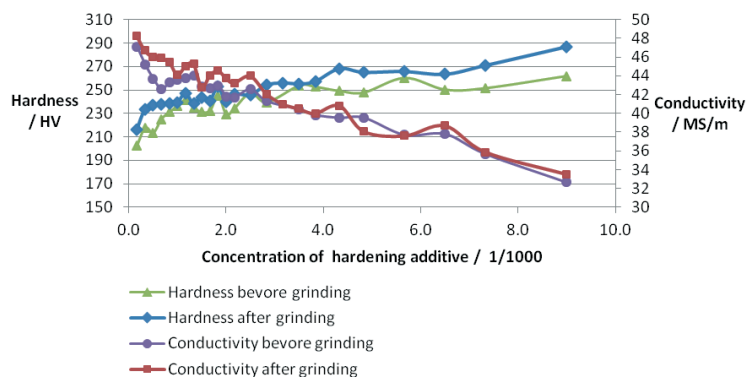


Figure 8: Hardness and conductivity versus concentration of hardening additive. Measurement directly after the galvanic process and after grinding to roughness

The hardness increases by grinding by more than 10 HV, as the metal structure is compacted at the surface. Interestingly this is not directly reflected by the conductivity. At lower hardness, i.e. higher conductivity above 42 MS/m the conductivity increases with the grinding, below 42 MS/m no significant change can be seen. With a value of $-0,81$ the correlation between conductivity and hardness for the copper measured directly after plating was somewhat weaker than the correlation after grinding with a value of $-0,94$. Figure 3 illustrates this correlation, whereupon the error bars mark the 95% confidence interval.

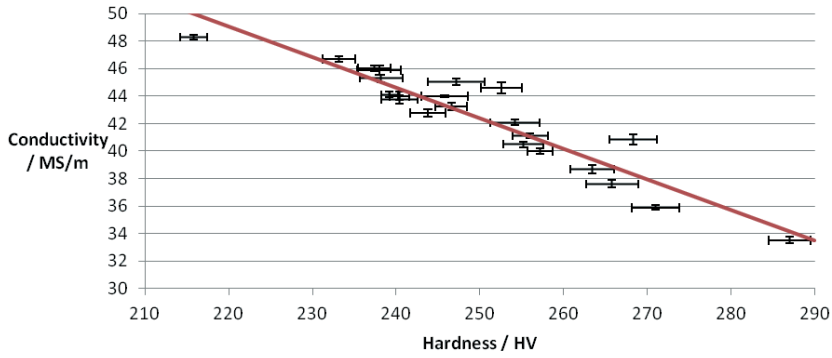


Figure 9: Negative linear dependency between hardness and conductivity. The measurements after grinding are shown. The error bars mark the 95% confidence intervals

The microscopic evaluation of the engraved cells showed a continuous decrease of the size of the pressed back edges with increased hardness.

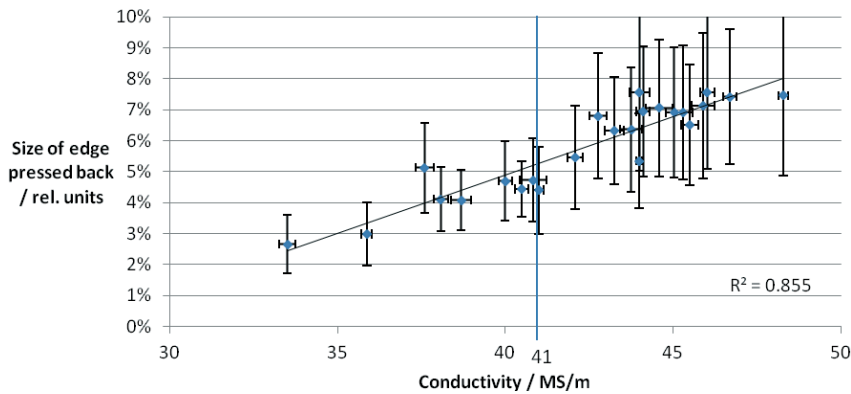


Figure 10: Dependency between conductivity and size of the pressed back edges. The error bars mark the 95% confidence intervals. R^2 is the coefficient of determination

The ductility was determined by counting the number of 90 degree bends before breaking. This number correlated to the conductivity shows Figure 11.

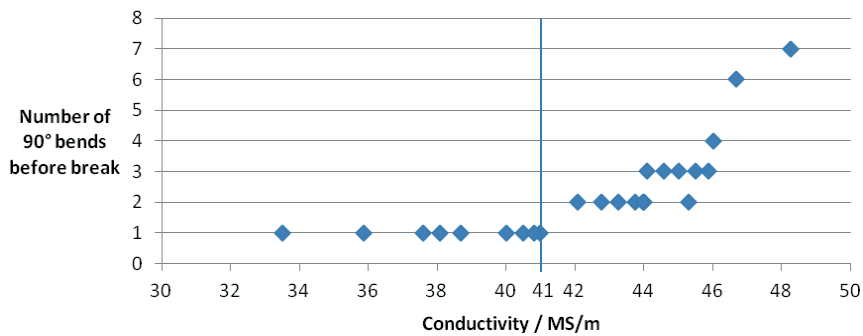


Figure 11: Number of 90° bends of the Ballard skins before break versus the conductivity

4. Discussion

It can be seen, that the size of the pressed back edges decrease nearly linearly with the conductivity.

If one defines as threshold for an acceptable quality at a size of the pressed back edges of 5% of the maximal cell cross diagonal, this corresponds to a conductivity of 40.5 to 41 MS/m together with a hardness of 250 HV. Together with a small safety zone a number of less than 40 MS/m should guarantee a good engraving quality.

We were able to verify this threshold by investigating the production of a gravure cylinder manufacturer, even if the galvanic baths there presumably have somewhat different parameters than our lab bath.

The somewhat inconsistent behaviour of the curves in Figure 8 especially in the low hardness area seem to be related to the specific circumstances in our lab. As we have only one galvanic bath, the bath was used for teaching purposes during the investigation, which took some weeks. After the sixth, ninth, thirteenth and eighteenth cylinder other cylinders were plated in between and this led to slight deviations of the additive concentration. It is highly probable that without these interruptions a smoother curve would have resulted.

The above defined threshold of conductivity for good quality corresponds with bends of less than two times 90° before break. This is consistent to the consideration that if an edge is thrown up by the stylus and after that pressed back again, it undergoes two times a bend in the range of 90° . If the copper is brittle enough that these two bends lead to a break, the edge should break when the scraper reaches the edge and it can be removed successfully.

5. Conclusion

It could be demonstrated that measuring the electric conductivity by eddy current for determining the quality of engravable copper layer is applicable and that there is a direct dependency of the conductivity to the ductility and the size of the edges pressed back into the cells. A conductivity of less than 40 MS/m has been found to give good engraving quality.

A descriptive model regarding the connection of ductility and removability of the edge could be verified. If an edge is not able to bend two times 90° before break, it too breaks after scraping and the remaining small parts, which might be pressed back, do not negatively, influence the engraving quality.

As the measurement of conductivity is fast and the requirements for placement accuracy are low, its application is simple and it can easily be incorporated in an automatic line, therefore securing the quality of the engraved cells. This adds another brick to the high reliability of the now 50 year old method of electro-mechanic engraving, which will presumably stay the most economic technology for cylinder making for another couple of years.

References

- Andrä, K., (1992); Untersuchungen zur Bewertung der Wirksamkeit organischer Badzusätze in schwefelsauren Kupferelektrolyten mittels potentiostatischer Einschaltbelastungen. Dissertation TH Iimenau.
- Bindschedler, D. P., (1980); Der Einfluß von Thioharnstoff auf die elektrolytische Kupferabscheidung. Daniel Philipp Bindschedler. - 214 S. - Hochschulort: Zürich. - Zürich, ETH, Dissertation.
- Fischer, H., (2012); Prospekt Sigmascope SMP 10 [pdf] Available at <http://helmut-fischer.de/globalfiles/DE_SMP10_DE_0901.pdf> [Accessed 2012-02-28].
- Javet, P., Hintermann, H. E., (1964); Verhalten des Thioharnstoffs bei der Kupfer-Abscheidung aus sauren Kupfersulfat-Bädern. Chemie Ingenieur Technik, Vol. 36 (6.1964), p. 679 - 681.
- Kardos, O., (1974); Plating 61, p. 129, 229, 316.
- Turner, D. R., Johnson, G. R., (1962); J. Electrochem. Soc. 109, p. 798, 918.
- Walker, R., Bridges, C. E., (1974); Plating 61, p. 1125.



Characterization of gravure cells using confocal microscopy

Nils Bornemann, Tim Guck, Thorsten Bitsch, Edgar Dörsam

Technische Universität Darmstadt
Institute of Printing Science and Technology
Magdalenenstr. 2, D-64289 Darmstadt, Germany
E-mail: bornemann@idd.tu-darmstadt.de

Abstract

Gravure printing is a promising technology to be utilized for organic electronics. It has the potential of strongly reducing productions costs compared to vacuum deposition techniques. On the contrary, demands on inks, substrates and printing conditions are very different in comparison to graphical applications. Therefore, conventional printing techniques such as gravure printing are under intense re-investigation to be applicable to OLEDs or OPVs. In this context, we found that physical parameters of a gravure cylinder are often not exactly known. Usually, gravure cell parameters are defined by optical tonal values or optical proof prints obtained with color inks. Those methods do not reflect the exact physical dimensions of the gravure cylinders. We adapted an optical scanning system that is based on confocal microscopy to acquire topographic data sets of the gravure cylinder surface.

We present a data analysis method to extract important gravure cell parameters like cell depth, cell volume and pick-up volume. We applied the method to different electro-mechanical engraved cylinders from different suppliers and found strong deviations between measured and manufacturer values. We motivated a linear calibration model for the cell depth and identified confocal microscopy as a reliable method for gravure cell determination.

Keywords: gravure printing, confocal microscopy, cell depth

1. Introduction

Gravure printing is a promising technology to be utilized for organic electronics. It has the potential of strongly reducing productions costs compared to vacuum deposition techniques (Huebler, 2002). On the contrary, demands on inks, substrates and printing conditions are very different in comparison to graphical applications. Therefore, conventional printing techniques are under intense re-investigation, e.g. (Hrehorova, 2011; de la Fuente Vornbrock, 2010; Bornemann et al., 2011a). For example, organic light emitting diodes (OLEDs) require constant layer thicknesses of around (50-100) nm and it has been shown that gravure printing is capable of producing these layers (Kopola 2009; Bornemann 2011b). However, obtaining a stable, reliable process for this application is very difficult because of different hydrodynamic instabilities that may occur for these nanometer thick layers (Bornemann, 2011b).

Understanding these issues require a deep understanding of the gravure printing process itself. In this context, we found that physical parameters of a gravure cylinder are often not exactly known. Usually, gravure cell parameters are defined by optical tonal values or optical proof prints obtained with color inks. Those methods do not reflect the exact physical dimensions of the gravure cylinders. However, it has been shown that white light interferometry is capable of determining gravure cell topography (Hrehorova, 2007). Instead, we adapted an optical scanning system that is based on confocal microscopy to acquire topographic data sets of the gravure cylinder surface.

We presented a data analysis method to extract important gravure cell parameters like cell depth, cell volume and pick-up volume. We applied the method to different electro-mechanical engraved cylinders from different suppliers and found strong deviations between measured and manufacturer values. We motivated a linear calibration model for the cell depth and identified confocal microscopy as a reliable method for gravure cell determination.

The paper is organized as follows. We introduce the measurement procedure consisting of the confocal scanning system in section 2 followed by the description of the data analysis method to extract the gravure cell properties in section 3. The fabrication technique for electro-mechanical engraved gravure cylinders is shortly introduced and the gravure cylinders used in the present study are described in section 4. The results of the proposed gravure cell determination method applied to the test cylinders are presented in section 5 and concluding remarks are given in section 6.

2. Measurement procedure

The measurement setup consists of a state-of-the-art optical profiler (Sensofar Plu Neox) and an in-house designed gravure cylinder stage, shown in Figure 1. The cylinder stage allows us to rotate and translate a gravure cylinder to find the optimal position for the gravure cell measurements. The optical system is capable of using interferometric and confocal microscopy to acquire a three-dimensional data set of the topography. Dealing with length scales of microns we found that the confocal mode is more robust and faster than the interferometric one. The optical objectives used in this study range from 10x to 50x which results in fields of view (FoV) from (1270 x 950) μm^2 to (255 x 192) μm^2 .

The crucial part of the topographic measurement is to resolve the gravure cell flanks. They might enclose high angles to the cylinder surface depending on the angle of the cell openings. Optically, successful measurements are limited by the numerical aperture (NA) of the objective. We adapted a 50x objective with a NA of 0.95 that results in a maximum viewing angle of 71 degrees which was suitable for all measurements of this study. A drawback of a high NA is the reduced working distance between objective and sample, in the present case 300 μm .



Figure 1: Measurement setup: Confocal microscope (Sensofar Plu Neox) equipped with an adjustable stage for the gravure cylinders

In standard confocal microscopy the depth of focus (DoF) is extremely reduced by implementing pin-hole like apertures in front of the illumination and the photo detector. Alternatively, a laser can be implemented for the spot-like illumination. By scanning the sample laterally and vertically the optical sensor measures the highest intensity when the surface is positioned within the DoF (Bass, 1995). The topography is reconstructed by correlating the brightest signal to the xyz position of the DoF.

Unlike common confocal profilers, the present system is equipped with a reflective micro display, a LED (light-emitting diode) illumination and a camera to perform the lateral scanning without mechanical movement (Bertran et al., 2009). The optical setup is sketched in Figure 2.

The light from the LED is directed to the reflective micro display by a beam splitter. The reflective micro display only reflects light from pixels that have been switched on. The switching is controlled by the computer to enable the lateral scanning through the display. A second beam splitter guides the lateral structured illumination through the objective onto the sample. The system allows us to acquire topographic measurements in less than ten seconds that makes it suitable for fast cylinder characterization. We measured each type of engraving at least two times with the 10x objective and three times with the 50x objective.

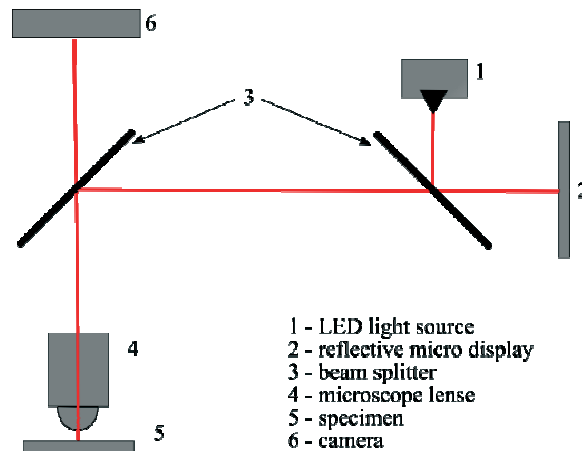


Figure 2: Optical setup of the confocal scanning microscope used in this study. The reflective micro display enables the lateral scanning without mechanical movement

3. Data analysis

The data analysis was performed using the commercial software package Mountains Map 5.1 (Digital Surf). It is equipped with a range of standardized evaluation procedures. However, according to the parameters of interest - like cell or pick-up volumes - we had to apply several different analysis steps.

We determined parameters that define gravure cell orientation like screen angle, screen ruling and cell density by analyzing images which were captured with the 10x objective. We removed the deviations due to the cylindrical form of the cylinder by a convolution of a second order polynomial. For the cell density we related a number of cells to their spanned unit area. Acquiring data and analyzing parameters with the 10x objective ten times for the same sample resulted in a standard deviation of less than 1%.

To determine the volume and shape parameters of single gravure cells we analyzed the data set obtained with the 50x objective. Figure 3 shows a typical three dimensional representation of the obtained topography that was further evaluated. We neglected the curvature of the cylinder since the side lengths ($\approx 2 \cdot 10^{-4}$ m) of the scanned square areas are small compared to the radius of the gravure cylinder ($\approx 2 \cdot 10^{-1}$ m).

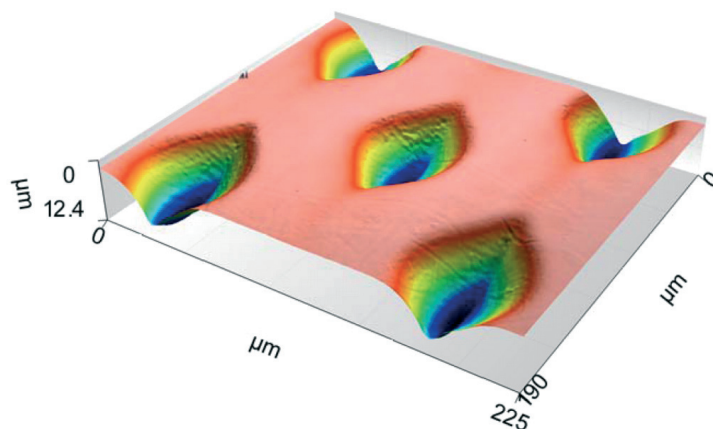


Figure 3: Typical confocal image of an electro mechanical engraved gravure cylinder using a 50x objective

The procedure to obtain volumes, cell footprint area and cell depth consists of four steps. First, the topography was leveled along the wall faces between the gravure cells to define a horizontal reference plane. Secondly, using an Abbott curve representation we set the z -position of this plane to define the upper boundary of the cell. Thirdly, we evaluated the confined single cell volume, the opening area and the cell depths with a built-in procedure for island parameter determination. And fourthly, the pick-up volume was obtained by multiplying the single cell volume and the cell density. The standard deviation of fifteen times acquiring and analyzing the same sample was below 2% for all parameters.

4. Samples

We focused our measurements on electro-mechanical engraved cylinders. Electro-mechanical engraved gravure cylinders are fabricated by several process steps. The important ones are described in the following. The steel core of a gravure cylinder is plated with a thin copper layer. This copper layer is engraved with a diamond styles to obtain the negative image on the cylinder surface in form of small pyramid-like cells. After a polishing step chromium is plated to establish a hard and resistant surface that is finally also polished. Important parameters to describe a gravure cylinder are diamond stylus angle, screen angle, screen ruling, gravure cell depth and pick-up volume. For graphical applications the tonal value is also of interest.

We measured three electro-mechanically engraved gravure cylinders from three different manufacturers (MF 1, MF 2, MF 3). The cylinder MF 1 possessed 32, cylinder MF 2 possessed 8 and cylinder MF 3 possessed 10 different engravings. The main parameters given by the suppliers are listed in Table 1.

Table 1: Manufacturer information of the three different electro-mechanical engraved cylinders from three different manufacturers analyzed in this study

Cylinder	Stylus angle	Screen angle	Screen ruling	Cell depth
MF 1	140°	45°	60 l/cm - 120 l/cm	6.4 μm - 29.5 μm
MF 2	125°	37°	60 l/cm	24 μm - 40 μm
MF 3	140°	37°	70 l/cm	11 μm - 33 μm

5. Results and discussion

With our method we determined screen angle, screen ruling, cell depth, single cell volume and pick-up volume for all different engravings of the three cylinders. For the screen angles and screen rulings we could confirm the manufacturer information within less than 2% deviation. However, the measured cell depths strongly differ from the ones specified by the manufacturer. Figure 4 a) - d) shows the difference for the cylinder MF 1 depending on the screen ruling of the different fields.

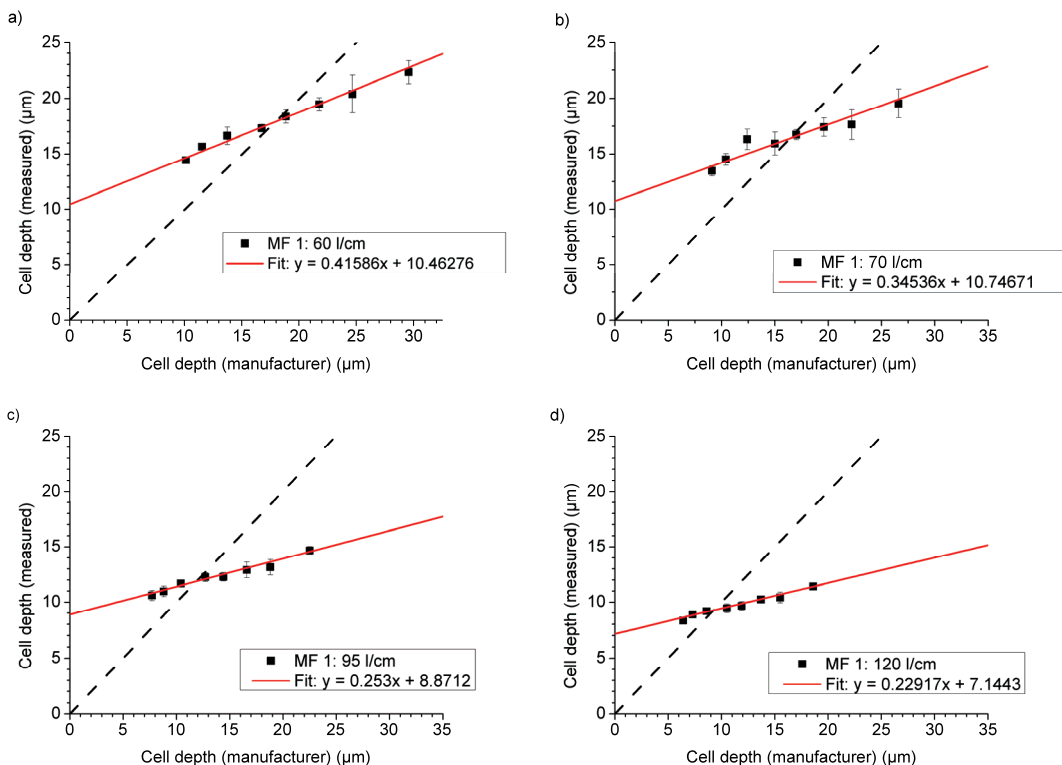


Figure 4: Measured cell depths versus cell depth supplied by the manufacturer MF 1. The dashed line through the origin depicts the manufacturer values and the solid line the fit through the measured ones. a) -d) illustrate the results for screen ruling of 60 l/cm, 70 l/cm, 95 l/cm and 120 l/cm

The dashed line through the origin depicts the manufacturer values. We observed that measured small cell depths of MF 1 were up to 48% above and measured large cell depths up to 39% below the manufacturer values. The line fittings in Figure 4 a) - d) show deviations in slope and offset from the line through the origin. Smaller slopes for all the screen rulings might indicate that during the manufacturing process of the cylinder the polishing step at the end abraded material differently. The contact area of larger gravure cells is smaller because the distance between walls is smaller so that the grindstone removes more material here. This can result in the smaller slope of the line fittings and the cell depth dependent deviation.

Measured versus manufacturer cell depths of the cylinders MF 2 and MF 3 are depicted in Figure 5 a) and b). For cylinder MF 2 the line fitting also differs by an offset and a smaller slope compared to the line through the origin. This indicates a depth dependent deviation. We found the maximal difference of 42% for the smallest cell depth.

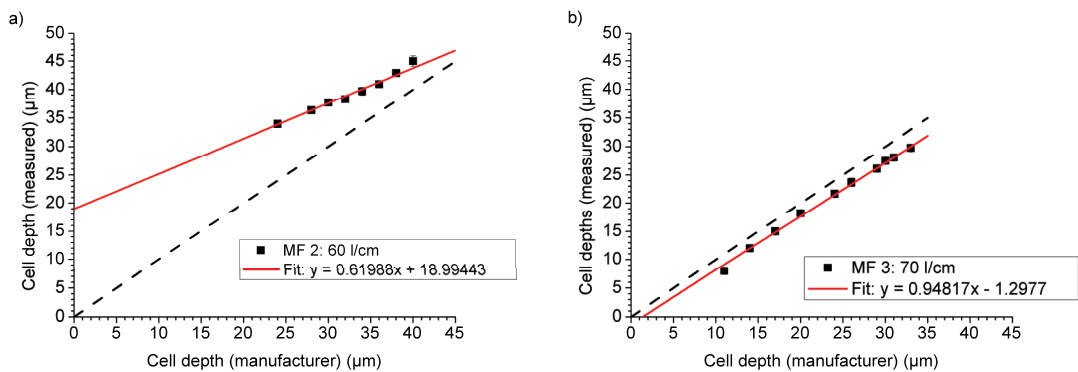


Figure 5: Measured cell depths versus cell depth supplied by manufacturer MF 2 a) and manufacturer MF 3 b). The dashed line through the origin depicts the manufacturer values and solid line the fit through the measured ones. Measured cell depths in b) for MF 3 show good agreement with the manufacturer values

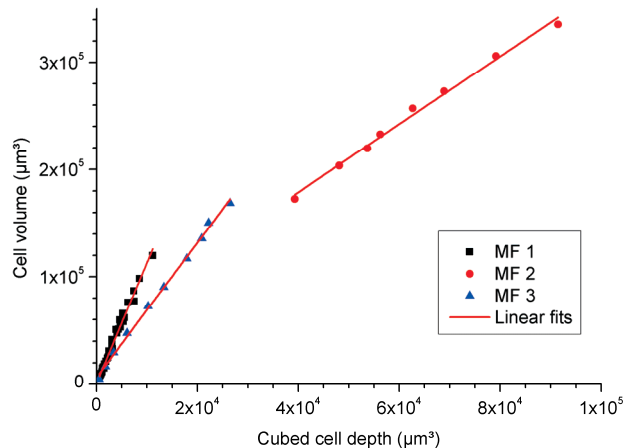
For cylinder MF 3 we evaluated only a very small cell depth dependent variation between measured and given values by the manufacturer, see Figure 5 b). The line fitting yields a slope of $0.95 \mu\text{m}^{-1}$. The offset of $1.3 \mu\text{m}$ is small compared to the ones found for the other manufactures. Hence, cylinders MF 3 reveals the best match between measured and manufacturer values.

The equations of the line fittings shown in Figure 4 and Figure 5 can be used to calibrate between measured and manufacturer values. In principle, the comparison that is described above for cell depths can also be applied to parameters like tonal values or pick-up volumes. Whereas the latter is proportional to the cell depth cubed. We measured the pick-up volumes of all engravings and found a maximum deviation of 647%, or a factor of 7.5 for cylinder of MF 1.

Furthermore we compared the measured single cell volumes of the different engravings to the cell depth. Assuming that the gravure cells are perfectly scale-invariant formed pyramids we would expect the ratio of cell volume (V_c) and cell depth (d_c) to the power of three to be constant for varying cell depths, $V_c/d_c^3 = \text{const}$. The constant is dependent on the opening angle of the pyramid. Figure 6 shows this ratio of measured values versus the measured cell depth for all engravings of the three cylinders.

Indeed, in Figure 6 we observe that $V_c/d_c^3 = \text{const}$. The different slopes for the different manufactures can be qualitatively related to the opening angles of the cells. These angles might differ for engraved cells not only according to the stylus angle but also to direction of the single cell. In direction of the rotation axis the opening angle is equal to the stylus angle. In printing direction the opening angle is usually affected by the screen angle. If the latter equals 45° the opening angle in printing direction is comparable to the stylus angle. For larger screen angles the opening angles in printing direction are larger because the cells are stretched in printing direction and for smaller screen angles vice versa. In Figure 6 steeper slopes of the line fittings are related to wider overall opening angles of the cells. We identify the largest slope for the cylinder MF 1 that was engraved with a stylus angle of 140° and a screen angle of 45° . Manufacturer 3 fabricated the cylinder with 140° and 37° which results in a slightly larger overall opening angle than MF 2 with 125° and 37° . This circumstance reflects the decreasing slopes of the different line fittings in Figure 6. As shown, the comparison sketched in Figure 6 is very sensitive against gravure cell deviations and can also be related to aging effects of the cutting diamond stylus.

Figure 6:
 Measured single cell volumes V_c as a function of the measured cell depths to the power of three d_c^3 . The line fits prove the linear relation but with different slopes. Larger slopes indicate gravure cell shapes with wider opening



6. Conclusion and outlook

Although the knowledge of detailed gravure cell geometry might be negligible for graphical applications, it is of great importance for the proper implementation of functional printing. We identified important aspects of confocal microscopy to gain reliable information on the geometry of electro-mechanical engraved gravure cells in a reasonable time frame. We presented a data analysis method to extract important gravure cell parameters from the topography measurements. Furthermore, we measured and analyzed three different gravure cylinders of three different suppliers and found strong deviations between manufacturer information and measured values up to 48% for cell depth and 647% for pick-up volume. According to cell depths we demonstrated that the deviation between measured and manufacturer values can be calibrated using linear fitting curves. We also discussed the relation between single cell volumes and cell depths that allows us to compare and evaluate the quality of engravings. In order to further increase the reproducibility we would like to provide a fully automated system not being subject to manual interference in the data analysis process. Furthermore, the application range of the analysis process in particular, should be adapted when using other geometries, e.g. line engravings (hachure).

Acknowledgments

We thank Robert Thieme, Nils Lawrenz and Hans Martin Sauer for useful discussions. The research was financially supported by the German BMBF under Grant No. 13N10760.

References

- Bass, M., 1995. Devices, measurements, and properties. Optical Society of America., ed., New York: McGraw-Hill.
- Bertran, F. L., Pursals, R. A., Artigues, C. C., 2009. Dual technology optical profilometer. Available at: <http://www.freepatentsonline.com/7636167.html> [Accessed February 13, 2012].
- Bornemann, N., Sauer, H. M., Dörsam, E., 2011a. Evaluation and Determination of Gravure Cylinders for Functional Printing. In Large-area, Organic & Printed Electronics Convention (LOPE-C). Large-area, Organic & Printed Electronics Convention (LOPE-C) 2011. Frankfurt, Germany, pp. 309-313.
- Bornemann, N., Sauer, H. M., Dörsam, E., 2011b. Gravure Printed Ultrathin Layers of Small-Molecule Semiconductors on Glass. *Journal of Imaging Science and Technology*, 55(4), p. 040201.
- de la Fuente Vornbrock, A. et al., 2010. Fully gravure and ink-jet printed high speed pBTTT organic thin film transistors. *Organic Electronics*, 11(12), pp. 2037-2044.
- Hrehorova, E., Kattumenu, R.-C., 2007. Evaluation of Gravure Print Forms for Printed Electronics. Available at: <http://www.gravurexchange.com/gravurezine/0702-ezine/hrehorova.htm> [Accessed February 16, 2010].
- Hrehorova, E. et al., 2011. Gravure Printing of Conductive Inks on Glass Substrates for Applications in Printed Electronics. *Journal of Display Technology*, 7(6), pp. 318-324.
- Huebler, A. et al., 2002. High volume printing technologies for the production of polymer electronic structures. In *Polymers and Adhesives in Microelectronics and Photonics, 2002. POLYTRONIC 2002. 2nd International IEEE Conference on. POLYTRONIC 2002 2nd International IEEE Conference on Polymers and Adhesives in Microelectronics and Photonics*. Piscataway, N.J.: IEEE, pp. 172-176.
- Kopola, P. et al., 2009. Gravure printed organic light emitting diodes for lighting applications. *Thin Solid Films*, 517(19), pp.5757-5762.

Adhesive strength of surface coatings on digital printed products

Dragan Milosavljević, Johannes Backhaus

Bergische Universität Wuppertal

Rainer Gruenter Straße 21

D-42119 Wuppertal, Germany

E-mails: dm@uni-wuppertal.de; jbackhaus@uni-wuppertal.de

Abstract

For about 20 years digital printing technology has become increasingly important for the printing industry. Simultaneously it became more efficient. Nowadays there is a demand on the market for digitally printed packaging. Most of the packaging have to be laminated. It is not much known about laminating digitally printed products. This field is studied in this paper.

Some tests are made with different kind of digital printing systems which use different kind of ink. Then the adhesion force of the laminating is compared and some conclusion are made, if these digital printing systems can be used for laminated products or if there can occur problems.

Keywords: packaging, paper and ink interaction, print quality and measurement

1. Introduction

For about 20 years digital printing technology has become increasingly important for the printing industry. At the same time it has become more efficient. In addition to new - individualised and on-demand-products - digital printing is substituting the small volume production print. Figure 1 shows that digital printing has increasingly developed over the last 15 years. The number of firms has increased more than five times and the annual payroll has increased even more than 8 times since 1998. The figures of the entire printing industry remain constant or even shrink. This shows that digital printing has become more and more important for the industry and that we must keep a close eye on this technology. (USC11).

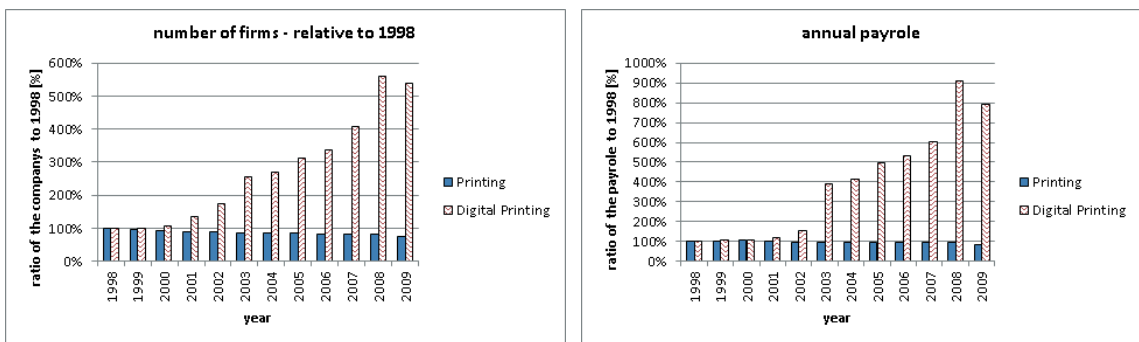


Figure 1: Development of digital printing (USC11)

Against this background, the reorganization of the technology used in finishing and postpress machines and the finishing processes of digitally printed products are to be studied. Printing is becoming digital but postpress is staying analogue. Postpress is still optimized on conventional printing systems (offset, flexo, gravure print) and works fine in combination with them. But in the case of digital printing systems there are only a few scientific studies. In this context laminating and coating of printing products is one significant item.

The need for laminating and coating printed products exists mainly in the field of labels, food grade and pharmaceutical packaging. Printing packaging, with digital printing machines, is still not well established, but there is a demand in the market. Packaging-producers have to observe the legal regulations and the often very high quality standards of the customers. Particularly with regard to food packaging, pharmaceuticals, and cosmetics are subject to strict hygiene requirements and must also be hermetically sealed concerning light and diffusion. In many cases light, oxygen, water vapor and aromas are not allowed to pass through the packaging, neither from the outside to the inside nor from the packaged goods to the outside. Of course, no

components of the packaging itself should contaminate the packed goods. This protection is achieved by UV-coating, or lamination with films which have special barrier properties. (Nab09, DIN09)

Because of all that, it is important to be able to coat and laminate products which are printed digitally. Only then can the afore-mentioned required barrier properties be guaranteed. An article in "Deutscher Drucker" refers to a case where a salesman had labeled packaging which was printed digitally and afterwards laminated. During a sale period he had removed the price labels and replaced them with new ones. However, by doing so, the laminating was released from the substrate. The adhesion between the laminating glue and the toner was not strong enough for the requirements (Sta12).

This paper researches the adhesion of coatings and lamination of printing products of typically used digital printing systems.

2. Research methods

The laminating quality, or rather the laminating adhesion, was exemplarily assayed for two different kinds of digital printing processes: One with powdery toner (Xerox iGen3) and one with liquid toner (HP Indigo E-Print). Therefore typical cartons, certified by the machine manufacturers, were used as substrates. "Ensocoat" from "Stora Enso", for the Xerox iGen digital press and "Invercote" from "Iggesund Paperboard" for the HP Indigo digital press (Pae09, Pai09).

For the above mentioned substrates a specialised test-chart was developed and printed. This test-chart contains the following sample-areas:

- full tone fields of the primary printing colours (CMYK)
- a typical two colour overprint solid (C+M)
- a four colour overprint solid (C+M+Y+K)
- two halftone-samples (K 60 % & K 80 %)

All areas are large enough to cut out a specimen for the mechanical tests (cf. Figure 2).

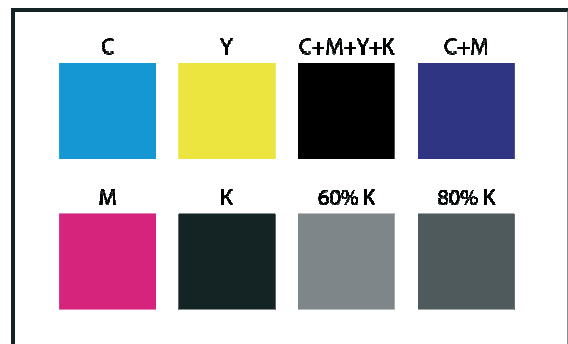


Figure 2: Testchart

In a second process step, the printed carton was laminated with a bi-oriented polypropylene foil (BOPP). Therefore a dispersion-glue of the "JOWAT AG" was used. Further samples were UV-coated instead of being laminated. The adhesive force of the composite material was determined by a universal-pull-testing-machine (Frank). According to DIN EN ISO 8510-2, a strip is adhered to a steel-plate. Then the lamination is peeled off from the substrate, at an angle of 180° and with a specified speed of 200 mm/min.

The measured line-force describes the adhesion of the composite. Preliminary experiments showed that components of the glue (two component epoxy resin) for fixing the specimen on a metal plate, penetrates the carton up to the BOPP film. Contrary to the norm, the metal plates were left and the specimens were directly fixed by the clamps of the pull-testing machine (DIN10).

3. Results

The destruction of the composites can occur in different forms. Adhesion fracture: the bond dissolves completely from the substrate; cohesion fracture: one of the layers is destroyed, while the composite sustains; mixed fracture: cohesion and adhesion fracture occur side by side.

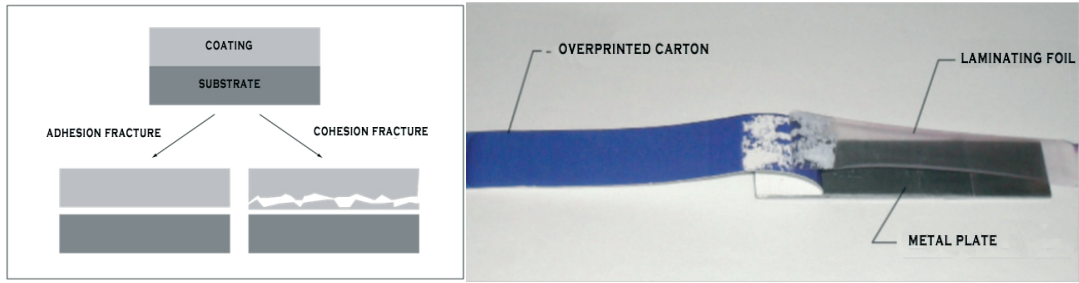


Figure 3: Different types of fracture (left: adhesion fracture and cohesion fracture; right: example of mixed fracture)

The author's research shows that not only the adhesion of the coating material on the carton needs to be taken into account, but also the adhesion of the ink to the coating material. The adhesion of the ink on the carton and also the adhesion of each ink layer to each other have a significant influence. "Weak spots" in each of these boundary layers have direct effects on the cohesion of the assemblage.

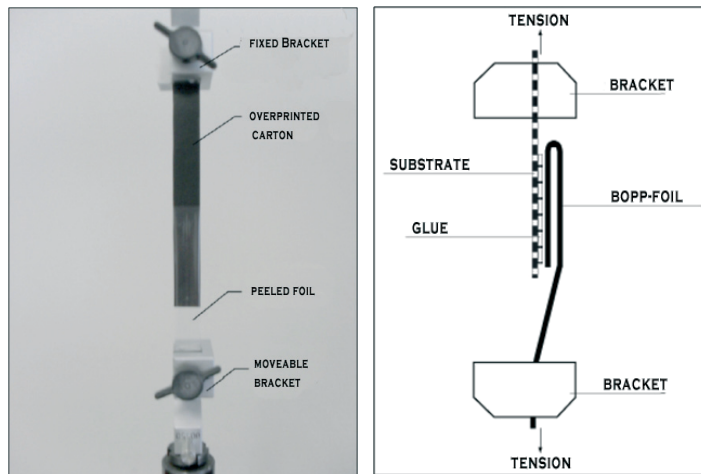


Figure 4: Different types of fracture (left: adhesion fracture and cohesion fracture; right: example of mixed fracture)

Following up, this is shown in the results, which will now be illustrated:

3.1 Single test

Every pattern of the pull test shows the same typical shape (c.f. Figure 5): first a small adjusting section. The pull-force increases while the sample is getting adjusted and the BOPP film is stretched to the yield strength. By reaching the yield point, the composite then gets separated. The peel force applied for the separation remains constant during the experiment. This force is a complex feature for the cohesion of the composite system consisting out of carton, toner, adhesive and laminating film.

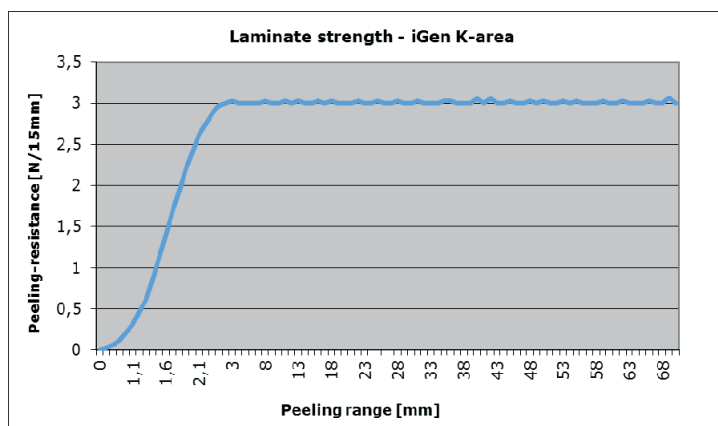


Figure 5: Typical peeling shape

3.2 Comparison of the different composites' strength

In order to compare the single test results, the delamination strength (i.e. the constant section of the pattern) is shown in Figure 6. Each bar represents the average of five pull-tests.

The blank substrate, without any ink-layer, shows the strongest adhesion for both used carton-types. For increased area coverage the adhesive strength of the composite is reduced for both the powder and the liquid toner. The adhesive strength of the full tones, compared to the half tones, is at least less. The adhesive strengths of all full tones of each toner type have nearly a constant value. Furthermore it can be shown that the composite adhesion is significantly less for the liquid toner of the HP Indigo compared to iGen3's powder toner.

The loss of adhesive strength compared to the blank carton as well as the differences between the two printing methods probably is caused by the single technology. Along with the technology used in the iGen3, residues from the silicon-oil may be left on the ink-surface. The HP Indigo ink is previously dispersed in the so called "imaging oil". Both agents reduce the glue-bond of the composite, but with a different strength of effect.

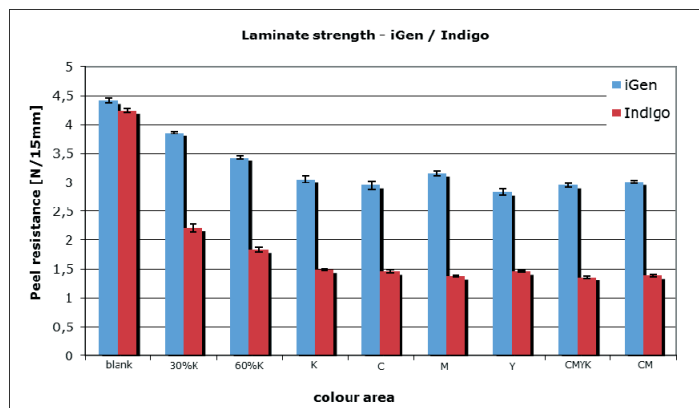


Figure 6: Comparison of the foil adhesion - iGen/Indigo

The material which was UV-coated was also tested with regard to the adhesion force of the coating. The composite material was very compact. The materials could not be separated from one another.

3.3 Correlation between area-coverage and adhesion-force

During the tests mentioned before, two different types of carton are used, each according to a digital press. From a strict academic point of view it could be said that two incomparable substrates were compared. Consequently the results would be useless.

On the other hand, there are only some certified carton substrates for each type of digital presses. Comparing test results of two digital presses based upon substrates being certified only for one of the press types would fulfill only one of the entire systems press/carton. This would fail the other entire system. Doing so misses practical relevance, because printers attend using a correct substrate.

For estimating a potential influence of different substrates, first laminated blank substrates were tested (Figure 6). Laminates of blank substrates show the highest strength of all. Also, the two types of substrate differ only minimally (2%).

The level of the laminate strength depends on the specific digital printing system and its ink. Here, iGen prints (full tone) show peeling forces of about 3 (N/15 cm) and Indigo prints show only 1,5 (N/15 cm). It may be possible that the affinity of the particular glue and ink considerably influences the strength of the laminate. This has not been investigated within the testing-series.

The comparison of blank substrate with 30%, 60% half tone, where the contact areas of blank substrate and adhesive are successively reduced, and with full tone fields of carbon ink, document that the strength of a laminate decreases to the ink coverage ratio.

The principle of different contact areas of glue, ink and blank substrate is shown in Figure 7: blank substrate (Figure 7a), partly printed substrates (Figure 7b) and totally ink-covered substrates (Figure 7c).

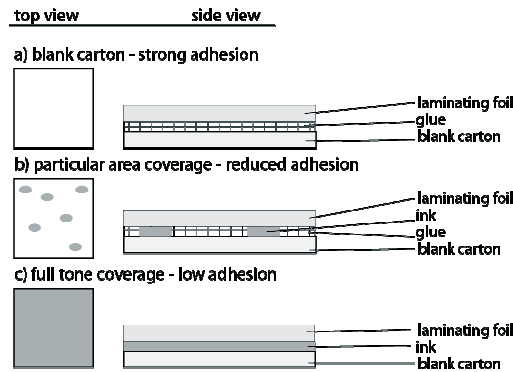


Figure 1: Correlation between area coverage and adhesion

In the full tone areas significant differences in laminate strength for the different colours of the ink could not be found. Also, single ink layers (100% ink coverage) and multi ink layers (200% and 400% ink coverage) do not differ in their laminate strength. Thus, the strength of a laminated, digitally printed compound of carton, adhesive and ink depends on the coverage ratio of the ink and - probably - on the affinity of the glue to the particular ink-system.

4. Conclusions

In contrast to conventional printing processes, i.e. offset gravure, flexo, screen e.a., the system of ink and digital press is locked. This is on the one hand because of the technical process, on the other hand due to commercial reasons (pay-by-click agreements). Printers only can purchase the ink (toner) from one single source, the machine supplier. They cannot improve the ink system and adapt it to their particular purposes. Thus, one instrument to improve the strength of laminated, digitally printed compounds is to adapt the adhesive to the particular toner. The other instrument is to optimize the laminating process. Both require further studies.

References

- (DIN09) DIN EN ISO 11607-1:2009-09.
- (DIN10) DIN EN ISO 8510-2.
- (Geo11) Georgiev, E., "Haftung von Beschichtungen auf Digitaldrucken", Bachelor thesis at the Bergische Universität Wuppertal (2011).
- (Heu11) Heuchemer, S. M., "Haftung von Beschichtungen auf digital bedrucktem Faltschachtelkarton", Bachelor thesis at the Bergische Universität Wuppertal (2011).
- (Nab09) Nabenhauer Verpackungen GmbH "Barriereigenschaften von Verpackungsfolien" <http://www.innovations-report.de/html/berichte/unternehmensmeldung/bericht-127878.html>.
- (Pae09) Pack aktuell, "Stora Enso präsentiert Digitaldrucksystem Gallop erstmals in der Schweiz".
- (Pai09) Pack aktuell, "Unbehandelter Invercote für Digitaldruck", Pack aktuell- Fachmagazin für Verpackungstechnik und - design, LZ Fachverlag AG, Schweiz (April 2009).
- (Sta12) Stadler P., 2012, "Wenn Etiketten auf veredelten Druckprodukten zu gut haften", Deutscher Drucker, Nr.10, p.27.
- (USC11) U.S. Department of Commerce, United States Census Bureau www.census.gov.



Printing ink modified with hyperbranched polymer: rheological behaviour and print quality

Zuzanna Żolek-Tryznowska, Joanna Izdebska, Maciej Szymanowski

Mechanics and Printing Institute

Faculty of Production Engineering, Warsaw University of Technology
Konwiktorska 2, PL-00-217 Warsaw, Poland

E-mails: z.tryznowska@wip.pw.edu.pl; j.izdebska@wip.pw.edu.pl; mackojns@gmail.com

Abstract

In this work flexographic printing ink Urania® was modified with commercially available hyperbranched polymer Boltorn U3000. Surface tension of printing inks were measured. Rheology behaviour of printing inks is presented. The obtained flow curves - shear stress versus shear rate - for printing inks exhibit pseudoplastic behaviour. Modified flexographic inks were laboratory printed on three different plastic films: PE, oPP and PET. The impact of small amount of hyperbranched polymer on the printing ink colour was examined by optical density, total colour difference ΔE^* ($L^* a^* b^*$ CIE) and gloss of print film. In general the addition of hyperbranched polymer improved the colour fastness and hardness resistance. The influence of hyperbranched polymer on rheological properties, optical density and CIE LAB coordinates and colour fastness is discussed.

Keywords: hyperbranched polymers, flexographic printing inks, rheology, colour measurements; print quality

1. Introduction

Flexographic printing technology is suitable for printing on paper materials (coated and uncoated), non-porous substrates including metalized and paper foils, and plastic films used in packing industry. Flexography requires low viscosity inks, lower than 0.05 - 0.5 Pa·s (Kipphan, 2001). There are three types of flexographic printing inks: water based, solvent and UV curable.

Surface tension and viscosity are the two parameters of inks, which have important influence on the ink droplet formation in printing (Kipphan, 2001) and also on print quality. It is well known that Printing process requires that surface tension of the printing ink is lower than surface energy of plastic film to allow good proper wetting and adhesion between the layers of ink film and plastic film. Surface free energy of plastic films, i.e. surface tension of PE and PP < 32 mN m⁻¹ (Rentzhog, 2006); Surface tension of printing inks mostly depends on the solvent of the ink, i.e. surface tension of ink-jet inks is higher as 21 mN·m⁻¹ (Khan, 2010; Kosolia, 2010). Rheology of printing inks has been already studied in the literature. Flexographic printing inks exhibit non-Newtonian and shear thinning behaviour (Havlíková, 1999; Rentzhog, 2005).

Hyperbranched polymers (HBSs) are a new class of polymers. They are globular and highly branched macromolecules with a large number of functional groups. HBSs exhibit polydispersity and irregularity in terms of branching and structure (Seiler, 2006). Polyester materials, such as hyperbranched polyesters from Boltorn™ family, have been recognized as the most promising family of HBPs, mostly due to unique properties, biocompatibility, biodegradability, nontoxicity, high solubility (sometimes even in water), as well as storage stability (Mallepally, 2009; Gao, 2003). A large number of possible combinations of functional end groups and the molecular weight of polymer may tailor the polymer properties for a specific purpose (Jikei, 2001). The primary appeal of HBPs is based on their unique physical properties, including the ability of solvating a wide range of materials and HBPs show a lower viscosity in comparison to linear analogs. HBPs also have a wide array of applications in the field of chemical engineering (Seiler, 2006).

The purpose of this work is to present the new application of HBPs. In this work commercially available hyperbranched polyester - Boltorn U3000 (B-U3000) is used to modify properties of the flexographic ink, colour properties and colour fastness of the overprinted ink film. The hyperbranched polymer, Boltorn™ U3000 (B-U3000), is a fatty acid modified dendritic polyester. It has a highly branched polymer backbone and in average 14 unsaturated fatty ester groups in the molecule. B-U3000 is formed in an esterification reaction of hyperbranched polyester Boltorn H30 with sunflower oil that consists of C₁₆ and/or C₁₈ fatty acids (Rolker, 2007). The full set of basic thermophysical information concerning the investigated B-U3000, including the glass transition temperature, density and viscosity of pure polymer and solubility were presented earlier (Domańska, 2009).

The surface tension and flow curves of commercially available printing ink and its modifications with hyperbranched polymer B-U3000 are presented. The impact of small amount of hyperbranched polymers on the printing ink colour was examined by optical density, total colour difference $\Delta E (L^* a^* b^* \text{ CIE})$ and gloss of the overprint ink film. The influence of hyperbranched polymer B-U3000 on the printing quality: colour properties and colour fastness, is discussed.

2. Experimental

2.1. Materials used

The hyperbranched polymers, Boltorn™ U3000 (B-U3000) was offered by Perstor AB (Sweden). Polymer was further purified by subjecting the polymer to a very low pressure of about $5 \cdot 10^{-3}$ Pa at temperature $t = 30^\circ\text{C}$ for approximately 48 h. The properties of B-U3000 is shown in Table 1.

Table 1: Properties of investigated hyperbranched polymer B-U3000

Property	
Molecular Mass ($\text{g} \cdot \text{mol}^{-1}$)	6500 ^a
Polydispersity	1.5 ^a
Glass Transition Temperature ($^\circ\text{C}$)	-44 ^b
Density at 25°C ($\text{g} \cdot \text{cm}^{-3}$)	0.9840 ^c
Dynamic viscosity at 25°C ($\text{mPa} \cdot \text{s}$)	1016 ^c
Statis surface tension ($\text{mN} \cdot \text{m}^{-1}$)	32.69 ^d

^a provided by Perstor; ^b Domańska, 2009; ^c Domańska, 2009; ^d Domańska 2010

The investigation were performed using flexographic black printing ink Urania® produced by WFFG (Poland). It is alcohol solvent ink with high resistance properties recommended for printing on plastics films. The modified inks were prepared by the drop wise addition of calculated weight of hyperbranched polymer to the pure ink Urania® upon continuous stirring. The ink was stirred for 30 min with an mechanical stirrer (Silverson, UK) as a disperser at 1 800 rpm. The mass-fraction of B-U3000 in a printing ink were: 0.01; 0.03, 0.05 and 0.07

Three popular plastic films (Kenty, Poland) were used: polyethylene (PE, white, thickness: $38 \mu\text{m}$), tarns-oriented polypropylene (oPP, transparent, thickness: $32 \mu\text{m}$) and poly(ethylene terephthalate) (PET, transparent, thickness: $12 \mu\text{m}$).

2.2. Methods

Laboratory printing was carried with K-hand roller nr 2 (RK prints, UK). The wet ink film was $10 \mu\text{m}$. The printing was performed in controlled environmental conditions (23°C an $50\% \text{ RH}$). The rheological characteristic of the flexographic printing inks were specified by the flow time in a flow cup (volume 100 ml, outlet diameter of 4 mm) according to ISO standards (ISO 2431, 2011). The kinematic viscosity was $18 \pm 0.5 \text{ s}$ for all printing inks. The non-volatile compounds of the printing ink (nVOC) was determinate by a gravimetric method using moisture analyzer Sartorius MA30 (Sartorius AG, Germany) set on 110°C . Static surface tension of inks was measured using a Sigma 701 Tensiometer (KSV Instruments Ltd, Finland) equipped with a platinum DuNoüy ring at 23°C . Reported values of kinematic viscosity, nVOC and static surface tension are the mean of two samples. Properties of investigated printing inks, i.e. nVOC and surface tension, are listed in a Table 2.

Table 2: Properties of the investigated printing inks: original printing Urania® and printing inks with addition of hyperbranched polymer B-U3000

mass fraction of HBP	nVOC (%)	surface tension ($\text{mN} \cdot \text{m}^{-1}$)
Urania®	19.95	23.85
0.01	21.30	23.80
0.03	23.13	23.66
0.05	24.02	23.58
0.07	25.84	24.36

The rheological behaviour of inks was studied using a Rheolab QC rheometer (Anton Paar, Austria) with concentric cylinder geometry CC39. The shear stress was measured during the controlled applied shear rate increasing from 0 s^{-1} to 1500 s^{-1} . The standard volume (60 ml) of sample was placed in a measuring cup. The measurements were repeated 2 times with new sampling at 23°C .

In this work flow curves were fitted by the Ostwal-de Waele using least square analysis. Flow curve model according to Ostwald and de Waele includes flow coefficient c [Pa·s] (consistency) and the exponent p (power-law index) (Mezger, 2006):

$$\tau = c \cdot \gamma^p \quad [1]$$

where p characterizes flow behaviour:

$p < 1$ for shear-thinning (pseudoplastic) flow behaviour;

$p > 1$ for shear-thickening (dilatants) flow behaviour and

$p = 1$ for ideal-viscous (Newtonian) flow behaviour.

Adhesion of the dried ink film to the board was simply performed by a tape test using a tesa-tape, firmly attached to the print was rapidly peeled off by hand. One test on two different overprinted strips were carried out for each sample 15 min after printing and 48 hours after printing. The adhesion was quantified by image analyses of the mark on the overprinted ink film and was compared to the mark on the ink film of original ink Urania®.

Spectrofotometer SpectroEye (GretagMacbeth, Switzerland) was used for the optical densities of ink layers measurements and determination of specific ink colour components L^* , a^* , b^* . The measurements of optical density were performed with following settings: D50 illuminant using 2° observer, $0^\circ/45^\circ$ measuring geometry, with polarization filter. The measurements of L^* , a^* , b^* were carried with settings: D50 illuminant, 2° observer, $0^\circ/45^\circ$ measuring geometry, without polarization filter. The reported results are average of measurements from minimum six values on two different prints. Colour differences ΔE is calculated from:

$$\Delta E = \sqrt{(\Delta L)^2 + (\Delta a^*)^2 + (\Delta b^*)^2} \quad [2]$$

where:

$(\Delta L^*) = L_{(w)} - L$; $(\Delta a^*) = a_{(w)}^* - a^*$; $(\Delta b^*) = b_{(w)}^* - b^*$ are the differences between parameter value of ink with w addition of B-H2004 and original print Urania®.

The gloss of prints was measured at 20° , 60° and 85° geometry condition with the use of glossmeter Picogloss 503 (Erichsen, Germany). Data collection was performed in six different positions of the samples, the reported values are the average of measurements.

The rub resistance of the printed films was studied at least one week after printing using Ink Rub Tester (TMI Machines, Canada). An offset paper stripe (90g, Arctic Paper Kostrzyn, Poland) was attached to a weight (1.8kg) and it was automatically rubbed 1 000 times with speed 85 cycles/min along overprinted sample. From the analysis of colour of paper stripe to the gray scale the colour fastness was quantified. The measurements were performed on two different overprinted samples. The scratch resistance of all prints was tested by pencil test using a pencil hardness tester (BYK Instruments, Germany). Pencils of various degrees of hardness (9B to 9H) were used to drawn over the coating surface to determine which pencil causes indentation. On one sample were performed five scratches. The hardness of the hardest pencil that does not mark the coating is the so-called pencil hardness.

3. Results

The viscosity and shear stress versus shear rate for investigated printing inks are given in Figure 1.

The parameters c and p along with R -squared of the fittings for investigated printing inks are listed in Table 3.

The optical density and colour values L , a^* , b^* are presented in Table 4.

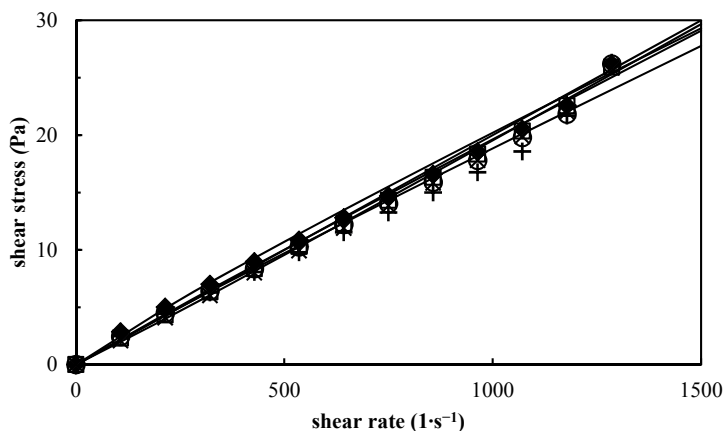


Figure 1: The shear stress versus shear rate dependencies measured for flexographic printing inks at $t = 23^{\circ}\text{C}$ for original flexographic printing ink (◆) Urania[®] and after addition of B-U3000. Polymer mass fraction: (+) 0.01; (○) 0.03; (□) 0.05; (×) 0.07

Table 3: The Ostwald model parameters along with R -squared of the fitting calculated for the flow curves of the investigated printing inks: original printing Urania[®] and printing inks with addition of B-U3000

Sample	Ostwald parameters		
	$10^2 c$ (Pa s)	p	R^2
Urania [®]	3.6	0.916	0.989
0.01	2.6	0.956	0.986
0.03	2.4	0.969	0.990
0.05	1.6	1.000	0.992
0.07	1.5	1.030	0.993

Table 4: Optical density, L^* , a^* , b^* values and colour differences ΔE of printed samples with original printing ink Urania[®] and printing inks modified with hyperbranched polymer B-U3000

Sample	Optical density	L^*	a^*	b^*	ΔE
PE					
Urania [®]	3.00	11.43	-0.58	-2.17	
0.01	2.79	13.64	-0.19	-0.53	2.8
0.03	2.33	20.75	0.31	0.52	9.7
0.05	2.08	22.61	0.71	1.50	11.8
0.07	1.96	27.08	1.16	2.85	16.5
oPP					
Urania [®]	3.05	12.28	-0.59	-2.02	
0.01	2.79	13.51	-0.37	-0.65	1.8
0.03	2.21	17.38	0.30	-0.13	5.5
0.05	1.95	21.24	0.66	1.25	9.6
0.07	1.92	24.42	0.90	2.00	12.9
PET					
Urania [®]	2.92	14.68	-0.35	-1.63	
0.01	2.72	16.50	-0.29	-1.07	1.9
0.03	2.17	16.69	0.24	0.15	2.7
0.05	1.89	21.11	0.60	1.18	7.1
0.07	1.84	23.86	0.72	1.51	9.8

Values of gloss are presented on Figure 2.

The colour fastness to rubbing and hardness according to pencil test is shown in Table 5.

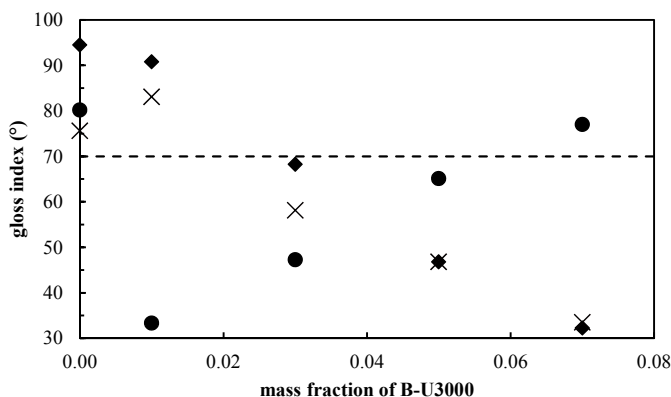


Figure 2: Dependence of the print gloss on the mass fraction of hyperbranched in printing ink for overprinted films: (●) PE, (◆) oPP and (×) PET

Table 5: Colour fastness to rubbing and pencil hardness of flexographic printing inks: original printing ink Urania[®] and printing inks modified with hyperbranched polymer B-U3000

Sample	Grey scale rating for colour change			Pencil hardness rating for film hardness		
	PE	oPP	PET	PE	oPP	PET
Urania [®]	1	3/4	5	2B	6H	6H
0.01	3/4	1/2	3	F	6H	6H
0.03	3	2	3	H	6H	6H
0.05	4	3	3/4	H	6H	6H
0.07	4/5	3/4	4	F	6H	6H

4. Discussion

All investigated inks after addition of HBPs were tested using flow cup. Addition of HBP to the printing ink Urania[®] have no impact on flow time - 18 ± 0.5 s for all investigated inks.

The static surface tension of inks decreases with increasing mass fraction of B-U3000 from $w = 0$ (original Urania[®]) two $w = 0.05$. The surface tension for original printing ink Urania[®] is slightly lower than surface tension of modified printing inks containing 0.01, 0.03 and 0.05 B-U3000. The highest value of static surface tension was observed for printing ink containing 0.07 of B-U3000, 24.36 mN m^{-1} . The change in surface tension with the increasing polymer mass fraction in printing ink is not linear. Indeed, the surface tension in polymer solutions is nearly constant up to the polymer concentration of about 0.05 mass fraction. It could be concluded that higher concentration of HBP than $w = 0.07$ in printing ink increases considerably static surface tension. A similar behaviour was observed previously in the solution of B-U3000 with alcohols and ethers (Domańska, 2010).

As expected, shear stress increases when shear rate increases, what is observed for shear-thinning or pseudoplastic materials and also many printing inks (Rentzhog, 2005; Havlínová, 1999). The viscosity of original printing ink Urania[®] is insignificantly higher than for other inks. The presence of HBPs have a very small effect on viscosity and flow curve behaviour. According to the Ostwal-de Waele model $p < 1$ as expected, investigated printing inks exhibit pseudoplastic flow behaviour. The addition of B-U3000 have an effect on p parameter: p increases when mass fraction of B-U3000 in printing ink increases. Similar impact of water addition on p parameter was observed for yellow water-reducible flexographic printing ink (Havlínová, 1999).

Before optical density, L^* , a^* , b^* , gloss colour fastness to rubbing and scratch resistance measurements the adhesion of the ink film to the base - plastic film PE, oPP or PET was examined. Generally, the adhesion on PE was much better then adhesion on PET and oPP film. There was no difference between the adhesion of original printing ink Urania[®] and ink with of addition of the B-U3000 polymer to the PE. However, the adhesion to the PET board changes in series:

$$\text{Urania} > 7\% \text{ B-U3000} > 5\% \text{ B-U3000} \approx 3\% \text{ B-U3000} \approx 1\% \text{ B-U3000}.$$

Analysis of the results of testing investigated prints showed that optical density is decreasing, when mass fraction of the B-U3000 in the printing ink is increasing for all investigated plastic films (Table 4). Optical density is higher for original ink Urania[®] than for modified inks. The colour parameters: L^* , a^* and b^* are linearly increasing when mass fraction of B-U3000 is increasing. The highest values of L^* , a^* and b^* parameters are observed for overprinted PE film. In generally, the colour differences ΔE linearly increases, when mass fraction of B-U3000 increases for all investigated plastic films. For the oPP and PET and ink with 0.01 addition of B-U3000 the colour difference ΔE are lower than 2, which means that the colour matching is good and the differences are low, invisible for human naked eye. For other systems ΔE is higher than 2. Differences may occur because of aggregation and cross-linking of the polymer macromolecules.

Gloss is a property of materials responsible for light reflection on a surface. The methods for gloss measuring depends on the kind of base. Values of gloss using measuring geometry 60° are given on Figure 2. The measuring geometries of the angle 20° and 60° were used. According to ISO standards geometry of 20° is recommended when gloss index is exceeding 70 units at measuring of geometry angle 60° (ISO 2813, 1994). The gloss index for prints overprinted with original printing ink Urania[®] and printing ink containing 0.01 of B-U3000 (except overprinted PE) are higher than 70 units. The experimental studies have pointed out that the print gloss is decreasing when mass fraction of B-U3000 is increasing for overprinted PET and oPP. For the overprinted PE opposite dependence is observed - print gloss is increasing when mass fraction of B-U3000 is increasing.

In this work, print quality is defined as a adhesion the printed ink film to the base, colour fastness to rubbing and printed ink film hardness. The overprinted PE with originally printing ink Urania[®] shows slightly better colour fastness to rubbing then overprinted oPP and PET. However, the best colour fastness to rubbing was observed for the printing ink containing $w = 0.01$ of B-U3000 for oPP and PET films. The small addition of B-U3000 have a great impact on the rub resistance. The colour fastness to rubbing have changed of two units: from 3/4 for Urania[®] into 1/2 for printing with $w = 0.01$ B-U3000 for oPP and from 5 into 3 for PET. The film hardness according to pencil test of printing ink containing $w = 0.01 \div 0.07$ B-U3000 is better for overprinted PE. For other prints, the addition of HBPs have no effect on scratch resistance. In generally, the small addition of B-U3000 ($w = 0.01$) to the printing ink increased the colour fastness to rubbing and the film hardness.

5. Conclusions

For the first time the use of hyperbranched polymers, such as hyperbranched polyester from Boltorn[™] family: B-U3000 as performed additive to printing inks is widely discussed. It can be concluded that the small addition of B-U3000 (0.01) to the printing ink improves the print quality of overprinted plastic films. On the other hand, the results obtained reveal that the addition of B-U3000 does not have any significant impact on the surface tension and the flow behaviour. The investigated inks represents pseudoplastics fluids and the rheological behaviour can be described using Ostwald flow model. A comparison of colorimetric parameters of overprinted samples with printing ink containing $w = 0.01$ B-U3000 shows acceptable differences in the L^* , a^* , b^* values. The overprinted samples with printing ink containing $w = 0.01$ B-U3000 have better colour fastness to rubbing and film hardness then original printing ink Urania[®].

Experimental tests and analysis of the results have showed the possibility of using hyperbranched polymers as a performed additives improving the mechanical properties of the prints. Hyperbranched polymers have good possibilities to find commercially applications on the large scale and acceptance into to the print market.

Acknowledgments

Funding for this research was provided by the Ministry of Science and Higher Education in the years 2010-2011 from the budgetary means for science (project nr IP2010 050570).

References

- Domańska, U., Żolek-Tryznowska, Z., (2009), *Temperature and composition dependence of the density and viscosity of binary mixtures of (hyperbranched polymer, B-U3000 + 1-alcohol, or ether)* *J. Chem. Thermodyn.* 41, 6, 821-828.
- Domańska, U., Żolek-Tryznowska, Z. (2010), *Effect of temperature and composition on the surface tension and thermodynamic properties of binary mixtures of Boltorn U3000 with alcohols and ether.* *J. Solution Chem.* 39, 864-876.
- Domańska, U., Żolek-Tryznowska, Z., Pobudkowska, A., (2009), *Separation of hexane/ethanol mixtures. LLE of ternary systems (ionic liquid or hyperbranched polymer + ethanol + hexane) at T = 298.15,* *J. Chem. Eng. Data* 54, 3, 972-976.
- Gao, C. et al., (2003), *Water-Soluble Degradable Hyperbranched Polyesters: Novel Candidates for Drug Delivery?* *Biomacromolecules* 4, 3, 704-712.
- Havlíková, B. et al., (1999), *Water-reducible flexographic printing inks - rheological behaviour and interaction with paper substrates.*, *J Mat. Sci* 34, 8, 2081-2088.
- ISO 2431:2011 *Paints and varnishes - Determination of flow time by use of flow cups.*
- ISO 2813:1994 *Paints and varnishes - Determination of specular gloss of non-metallic paint films at 20 degrees, 60 degrees and 85 degrees.*
- Jikei, M., Kakimoto, M., (2001), *Hyperbranched polymers: a promising new class of materials* *Prog. Polym. Sci.* 26, 8, 1233-1285.
- Khan, M. S. et al., (2010), *Biosurface engineering through ink jet printing,* *Colloid Surf. B: Biointerfaces* 75, 2, 441-447.
- Kipphan, H., (2001), *Handbook of Print Media: technologies and production methods.* Springer-Verlag, Heidelberg.
- Kosolia, C. T., Tsatsaroni, E. G., (2010), *Synthesis and characterization of hetarylazo disperse colorants: Preparation and properties of conventional and microemulsified inks for polyester ink-jet printing.* *J Appl. Polym. Sci* 116, 3, 1422-1427.
- Mallepally, R. et al., (2009) *Enzymatic degradation of hyperbranched polyesters,* *J. Appl. Polym. Sci.* 112, 4, 1873-1881.
- Mezger, T. G., (2006), *The rheology handbook For Users of Rotational and Oscillatory Rheometers,* Vincentz Network, Hannover.
- Perstorp, *Product Data Sheet: Boltorn™ U3000.*
- Rentzhog, M., Fogden, A., (2005), *Rheology and surface tension of water-based flexographic inks and implications for wetting of PE-coated board,* *Nordic Pulp Paper Res. J* 20, 4, 399-409.
- Rentzhog, M., Fogden, A., (2006), *Print quality and resistance for water-based flexography on polymer-coated boards: Dependence on ink formulation and substrate pretreatment.* *Prog Org Coat* 57, 3, 183-194.
- Rolker, J. et al., (2007), *Potential of Branched Polymers in the Field of Gas Absorption: Experimental Gas Solubilities and Modeling,* *Ind. Eng. Chem. Res.* 46, 20, 6572-6583.
- Seiler, M., (2006), *Hyperbranched polymers: Phase behavior and new applications in the field of chemical engineering* *Fluid Phase Equilib Fluid Phase Equilib.* 241, 1-2, 155-174.



Printing quality characteristics of rich mineral paper for offset commercial printing

Yung-Cheng Hsieh, Kuo-Kun Lee, Ssu-Yi Cheng, Chih-Cheng Kao

Department of Graphic Communication Arts
National Taiwan University of Arts
59, Section 1, Ta-Kuang Rd., Pan-Chiao City
Taipei County, Taiwan R.O.C.

E-mails: t0308@mail.ntua.edu.tw, masterw@ntua.edu.tw, cindy9518183@gmail.com; jkaolh@gmail.com

Abstract

Rich mineral paper (RMP) has the advantage of being energy efficient, clean and creating no pollution during its production processes, with low production costs, and enjoying naturally complete biodegradability, fully compatible with the emerging demands for energy efficient carbon reducing features and the trend for environmentally green solutions, so if this media can replace traditional paper uses to become a new print media, tremendous environmental efficacy can be expected. So this study aims to discuss the print quality performance characteristics of RMP applications in large print run offset printing operations. The study deploys True Experimental Study methodology, with use of the digital printing test target of Graphic Arts Technical Foundation (GATF), with flat offset printing on traditional coated paper and eco-friendly RMP, printing 800 sheets of each, with systematic random sampling of 35 samples for the study. Quality determinations rely on X-rite i1 Pro for elucidation of the printing quality characteristics for solid ink density, TVI, contrast, gray balance, and color gamut measurement.

The results of this study indicate the KCMY solid ink density and contrast of the eco-friendly RMP were less than traditional coated paper; TVI value was higher than traditional coated paper; color gamut performance was less than the traditional coated paper. Optimal gray balance combination for RMP was determined as follows: 7% tone with C7M3Y4, 30% tone with C30M28Y26, 60% tone with C60M58Y5, and 80% tone with C80M76Y66.

Keywords: rich mineral paper, offset printing, print quality

1. Introduction

As global raw materials prices reach unprecedented new heights, with global print pulp prices in 2011 surpassing the highest levels since the 2008 financial tsunami, traditional fiber based paper is no longer the most energy efficient, carbon reducing, environmentally friendly reading medium.

Rich Mineral Paper was first developed in 1960 by Japan and Germany, with technological enhancements achieved on Taiwan in the 1990s, the emergence of environmentalism has witnessed its revival as a new trend. RMP is produced from inorganic powder (pulverized rock) and minute quantities of plastic resin, yielding a new paper similar in functionality to wood pulp paper. RMP does not require any forest resources, and can be produced without water, eliminating the traditional pulp-based papermaking processes of steaming, washing and bleaching, which produce massive pollutant streams, thereby eliminating much water pollution, gas waste and waste at the source, through production processes delineated in Figure 1.

Additionally since RMP relies in inexpensive mineral rock powder, production overhead is 20-30% less than for traditional paper. Moreover as the RMP is produced primarily from inorganic mineral powder and polyethylene, RMP is water resistant and fire resistant, while burning does not generate toxic fumes, and the finished medium remains naturally biodegradable.

Encountering this emerging environmentally-friendly print medium, with its surface tactility similar to paper, though composed of quite dissimilar material with unique physical characteristics, one notes that complete replacement of traditional paper will require further investigation of RMP use in printing production lines and post-production processing for similarity or better performance for print quality than traditional paper in comparable uses.

Thus this study explores RMP print quality performance in typical large print run offset printing.

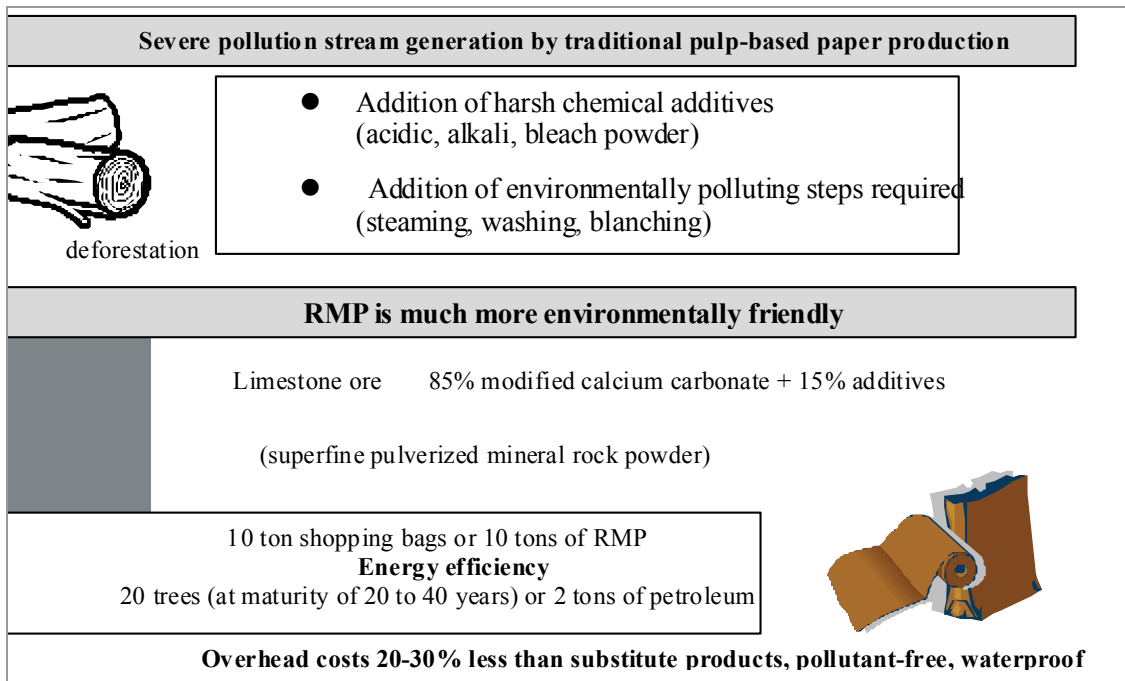


Figure 1: RMP and traditional paper production process comparison

2. Methods

This study relies on a True Experimental Study, conforming to the GATF Digital the Test on Form 5.0 designed electronic originals, with offset printing on traditional coated paper and Rich Mineral Paper for the printed media. 800 sheets of each of the two materials were printed, deducting the first and last 50 sheets due to ink instability, then we systematically random sampled every other 20 extracted sheets, yielding a total of 35 sheets of each material in the total sample.

Each sample was then analyzed using X-rite i1 Pro / X-rite i1iO with the GretagMacbeth Spectrolino / SpectroScan reflective spectrophotometer to determine print quality characteristics across the dimensions of solid ink density, TVI, contrast, gray balance, and color gamut. The measurements obtained were then analyzed using the SPSS 18.0 and Minitab 16.0 statistical software packages to determine print quality characteristics. Then these values were input into the X-Rite ProfileMaker 5 to generate 3D simulated color space diagrams.

The traditional coated paper selected for the study, Yungfeng premium coated paper, conformed to the ISO 12647-2:2004 (E) recommended specifications, with a basis weight of 158GSM. The Rich Mineral Paper selected was Taiwan's Lung Meng RP140 from an 85% natural inorganic mineral powder, with a base weight of 168GSM. The ink selected was Tokyo Ink Company's SOY-CERVO environmentally friendly printing ink. Printing processes were done on the German FOGRA PSO (Process Standard Offset), and conforming to the ISO 12647-2 standard to ensure the experimental print process stability.

3. Results

This study deployed the traditional coated paper standard values suggested by the General Requirements for Applications in Commercial Offset Lithography (GRACoL) color reproduction Specification for sheetfed offset lithography, ensuring that the investigational printing process and ink characteristics conform to the best international professional standards.

In terms of Solid Ink Density and contrast, the RMP KCMY values were less than for traditional coated paper. Optimal gray balance for RMP indications were: 7% tone C7M3Y4, 30% tone C30M28Y26, 60% tone C60M58Y5 and 80% tone C80M76Y66, as shown in Table 1.

Table 1: Values of solid ink density, contrast and gray balance for RMP and traditional paper

Solid Ink Density			Contrast			Gray balance		
	Coated paper	RMP		Coated paper	RMP		Coated paper	RMP
K	1.7234	0.9126	K (75%)	41.309	19.598	7%	C7M4Y4	C7M3Y4
C	1.5689	0.8609	C (75%)	41.303	19.642	30%	C30M18Y20	C30M28Y26
M	1.4217	0.8131	M (75%)	33.805	16.686	60%	C60M52Y48	C60M58Y52
Y	1.2249	0.7609	Y (75%)	32.642	23.799	80%	C80M74Y72	C80M76Y74

As Figure 2 indicates, RMP with CMYK 50% tone value increase had greater values than traditional coated paper, indicating ink absorbency uptake was greater for RMP than coated papers, but less subject to control in the printing process.

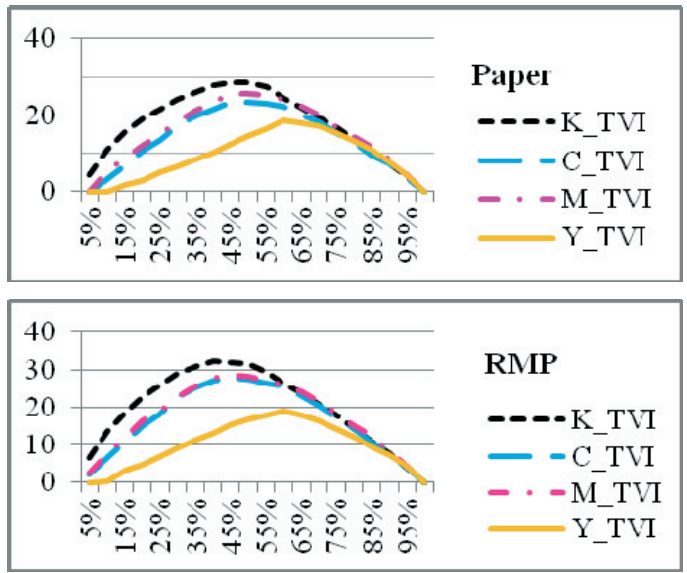


Figure 2: Traditional coated paper and RMP TVI curves

Figure 3 indicates, color gamut analysis 3D Lab value and 2D ab values, with yellow indicating traditional coated paper and blue for RMP. In terms of 3D Lab value color gamut, the RMP values were less than for traditional coated paper. For the 2D ab value color gamut analysis one can see that the blue-violet gamut for RMP exceeded that for traditional coated paper color gamut in some respects, but most of the RMP color gamut was within the color gamut parameters of the traditional coated paper.

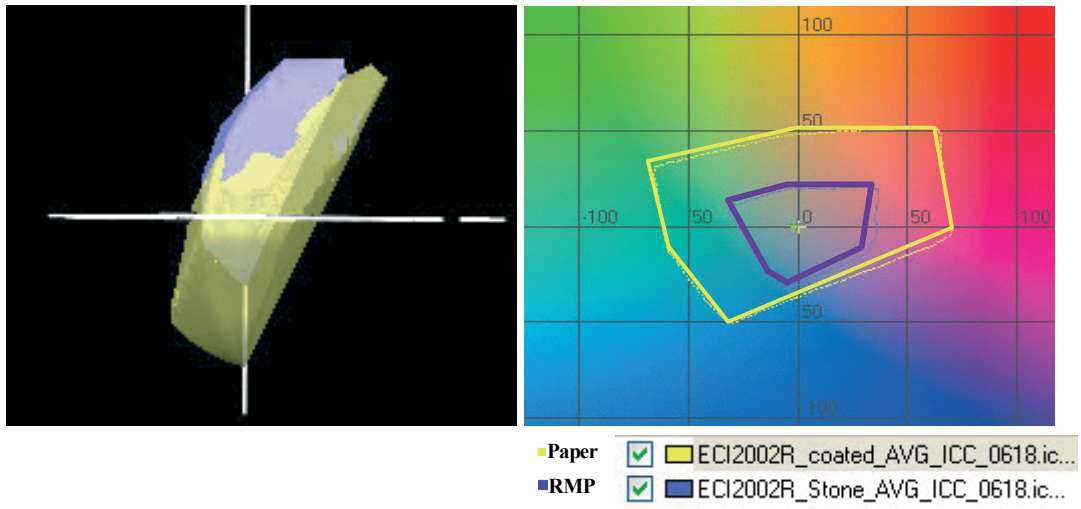


Figure 3: Analytical comparison of 3D Lab values and 2D ab values for color gamut in RMP and traditional coated paper

4. Discussion

The results of this study indicate the KCMY solid ink density and contrast of the eco-friendly RMP were less than traditional coated paper; TVI value was higher than traditional coated paper; color gamut performance was less than the traditional coated paper. Optimal gray balance combination for RMP was determined as follows: 7% tone with C7M3Y4, 30% tone with C30M28Y26, 60% tone with C60M58Y5, and 80% tone with C80M76Y66.

The study suggests that ink particularly suitable for RMP uses remains in need of development. Additionally, the study found that use of RMP in the paper machinery indicated transverse and longitudinal tensile strength is slightly inferior to the traditional coated paper, resulting in unsmooth surfaces post-printing, for which it is recommended that RMP makers should consider paper machinery structural aspects when pursuing future research on modifying solutions for greater printing efficacy with RMP.

5. Conclusions

RMP used for standard commercial offset printing has a number of distinguishing characteristics from traditional coated paper print quality performance, so it is suggested that GRACoL establish applicable RMP performance standards. Print contrast performance approximated that of non-coated papers in the GRACoL offset lithography standard, so initially RMP ought to be able to readily supplant use of non-coated papers in traditional offset printing.

The study found that RMP surface characteristics affected ink transfer and retention, so it is recommended that RMP producers develop RMP with a variety of surface characteristics, and compatible specialized inks, to attain optimal ink transfer capabilities and optimal gray balance performance.

Since RMP is a non-plant fiber material, which relies solely on surface absorption affects for ink absorbency, the ink is thus characteristically poorer in terms of drying. Thus it is further recommended that further studies explore UV ink and resin inks be deployed for additional print quality tests with RMP, to elucidate optimal color gamut performance.

Acknowledgments

We wish to express our profound appreciation and gratitude for the support of the National Science Council for funding this study (Research Grant: NSC 100 - 2815 - C - 144 - 001-H). We also are deeply appreciative for the assistance rendered by the Printing Technology Research Institute.

References

1. W. Venessa: Paper, Plastic, or Pebble, *Business Week*, Issue 4146 (2009), p. 56-56.
2. Graphic Communications Association: *General Requirements for Applications in Commercial Offset Lithography* (2002).
3. P. Bill, H. Fred, and S. Franz: *Color Gamut Quantified* (Switzerland 2008).
4. Heidelberg, in: *Basic principle of quality control*, edited by Heidelberg (2004).
5. Information on <http://news.syd.com.cn/index.ht>

Influence of surface free energy of biodegradable films on optical density of ink coated fields of prints

Joanna Izdebska, Halina Podsiadło, Liliya Harri

Mechanics and Printing Institute
Faculty of Production Engineering
Warsaw University of Technology
Konwiktorska 2, PL-00-217 Warsaw, Poland

E-mails: j.izdebska@wip.pw.edu.pl; h.podsiadlo@wip.pw.edu.pl; l.harri@wip.pw.edu.pl

Abstract

The paper presents the results of studies on the effect of surface free energy of polymeric biodegradable films, intended for manufacture of packages, on optical density of fields fully coated with printing ink in printing by flexographic technique. The surface free energy of biodegradable films was determined by the Owens-Wendt method.

Both polar and dispersive components of surface free energy of the films tested were calculated. It has been found the value of surface free energy of the film and its polar and dispersive components have a substantial impact on optical density of fields coated with printing ink on printed films.

Keywords: biodegradable polymer film, surface free energy, optical density, flexographic printing

1. Introduction

A dynamic development of the market of plastic packages has been observed in recent years. In the production of packages traditional materials are more and more often replaced by plastics. In 2005 in package industry of Poland the use of plastics was estimated as 36.7%, paper - 26.1%, metal - 22.2%, and glass - 9.6% (Wasiak, 2009). The use of plastics in manufacture of packages has many advantages, such as:

- possibility of considerable reduction of the mass of package;
- good mechanical properties;
- resistance to most of environment aggressive media;
- possibility of optimum protection of the packaged product by selection of optimum polymers or use of laminated materials, etc.

A drawback of the plastics consists, however, is their long time of storing on storage yard and difficulties connected with recycling due to problems of selective gathering. This drawback has become now of special importance, as the community wrestles with the problems of pollution of natural environment. The time of natural decomposition of plastics is very long. It is estimated that synthetic polymers such as polystyrene or polyethylene decompose within 500 or 1 000 years (Żenkiewicz, 2010). For this reason in recent years more and more attention has been paid to biodegradable materials.

The essential feature of biodegradable materials is their ease of degradation under natural conditions. They become degraded within the time of several months to several years (Plastech, 22.01.2009; Żakowska, 2008). The market of these materials has shown a steady dynamic growth since 2006. The mean rate of annual growth up to 2012 has been estimated to a level of about 17.3% (Plastech, 17.01.2008).

Two essential groups have been distinguished in biodegradable polymers, namely:

- polymers produced from renewable natural raw materials, such as starch, cellulose, or proteins;
- polymers based on non-renewable fossil raw materials and stocks (Żakowska, 2003; Piecyk, 2008; Florjańczyk, 2009; Duda, 2003; Lim, 2008; Nampoothiri, 2010; Siracusa, 2008; Rudnik, 2008).

Biodegradable materials based on polylactide, starch or cellulose have become the most important on the market of such materials. Their production amounted to 250,000 ton in the year 2007 to increase up to 400 000 ton a year later. Nowadays the biodegradable materials represent less than 1% of the total market of plastics, but a significant increase is anticipated (Plastech, 17.01.2008; Platt, 2006; Plastech, 12.11.2009).

In addition to their primary protective function the packages play nowadays also a marketing function: promoting the products and their distinguishing on shop shelves. For this reason the prints made on packages and their qualities are of very high importance. The colour saturation of ink deposited on the printing base is one of important features determining the quality of prints. Optical density is a measure of colour saturation of printing ink used (Kipphan, 2001).

The optical density of ink-coated fields depends i.e. on pigment concentration in the ink and on ink layer thickness on the print. In the flexographic printing technique, which is now the technique most often used in printing on packages, the thickness of ink layer on the base depends on many various factors such as: parameters of anilox cylinder depositing the ink in printing process, ink properties, printing plate, and printing base used (Panák, 2002; Czichon, 2006; Czech, 1993). In printing on non-absorbing bases, such as plastic films, the surface free energy is a very important parameter influencing the thickness of ink layer deposited on the base.

The present paper shows the results of studies on the effect of surface free energy of biodegradable package films on optical density of ink-coated fields in prints made by flexographic printing technique.

2. Experimental

2.1. Materials used

Biodegradable films of various producers, based on various polymers, differing in structure and application range, were used as the object of investigation. The bases of the films were:

- cellulose: *NatureFlex 23NVS*, *NatureFlex 23NK*, *NatureFlex 23NVR* (produced by Innovia Films);
- polylactide: *Ecovio L BX 8145* (produced by BASF);
- starch: *Mater-Bi* (produced by Novamont).

All the films used in the tests were biodegradable and compostable materials conforming to the standard EN 13432 (EN 13432, 2000). They conform also to European requirements concerning the materials intended for contacts with food.

Films NatureFlex 23NVS, *NatureFlex 23NK*, *NatureFlex 23NVR* are supplied with thermally weldable layer on both sides, owing to which packages can be produced by two-side welding. The films were transparent, with high gloss, naturally antielectrostatic, susceptible to printing and processing. They provide also good barrier properties against gases and odours and resistance to oils and fats. The film *NatureFlex 23NVS* is characterized with increased permeability to humidity. It is intended mainly for packaging fresh products, for manufacture of "window bags" and in baker's trade. The *NatureFlex 23NK* film, of high barrier properties to humidity, is used mainly for production of torsion packages, formation of packages on vertical and horizontal packaging lines, as well as an element of multilayer films. The *NatureFlex 23NVR* film, featured by medium barrier properties against humidity, is used mainly as packaging material in bakery and confectionery, for packaging of pasta, rice etc. products (Innovia). The thickness of all the cellulose foils used in the tests was 23 μm .

The *Ecovio L BX 8145* film is composed of a biodegradable polyester and polylactide. About 45% of this film originates from renewable raw materials. The film is semitransparent, white, of medium gloss, suitable both for printing and for processing. The film is intended for manufacture of carrier bags and compostable bags, for packaging food and hygiene products (BASF). The thickness of the *Ecovio L BX 8145* film was 21 μm .

The film *Mater-Bi* used in our tests has good barrier properties to aromatic compounds and high permeability to water vapour, exceeding that of polyolefin films, thus it prevents accumulation of mist. The material is semitransparent, white, and matt. According to the producer's information it can be printed with traditional inks. Carrier and compostable bags, flexible packages for fresh vegetables, fruits, processed food, and hygiene products are the main fields of its application (Novamont). The thickness of *Mater-Bi* film tested was 23 μm .

2.2 Methods

Surface free energy of the biodegradable films was determined according to the Owens-Wendt method (Rudawska, 2008; Żenkiewicz, 2000). With this aim the contact angle of diiodomethane and distilled water was measured for all the films. Distilled water is a strongly polar liquid, since the polar component of its surface free energy is high (51 mJ/m^2), and the dispersive component is low (21.8 mJ/m^2). Diiodomethane is

a nonpolar liquid, since the polar component of its surface free energy is low (2.3 mJ/m²), and the dispersive component is high (48.5 mJ/m²) (Żenkiewicz, 2000).

In order to determine the contact angle of water and diiodomethane photographs were taken of magnified drops of these liquids on the surface of each film by means of camera coupled with stereoscopic optical microscope *Olympus SZ-STU* and computer. The contact angle was measured with the aid of a special software *Iris*. The principle of determining the contact angle between the foil and the test liquid is shown in Figure 1.

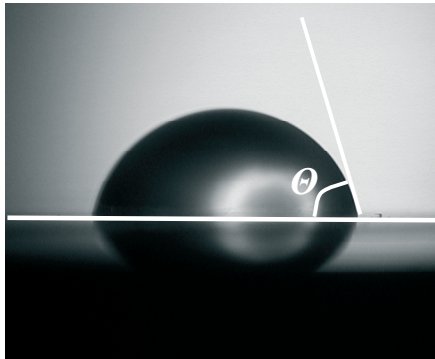


Figure 1:
 Photograph of a drop of measurement liquid on a film surface taken with the aid of optical microscope: Θ - contact angle

Following the determination of contact angle between the biodegradable films and water or diiodomethane the dispersive component γ_s^d and the polar component γ_s^p of surface free energy of the films were calculated by dissolving the following of equations [1] and [2], taking into account the fact that the values of γ_w , γ_w^d , γ_w^p , γ_d , γ_d^d , γ_d^p are known (Żenkiewicz, 2000).

$$(\gamma_s^d)^{0,5} = \frac{\gamma_d(\cos \Theta_d + 1) - \sqrt{\frac{\gamma_d^p}{\gamma_w^p}} \gamma_w(\cos \Theta_w + 1)}{2 \left[\sqrt{\gamma_d^d} - \sqrt{\gamma_d^p \frac{\gamma_w^d}{\gamma_w^p}} \right]} \tag{1}$$

$$(\gamma_s^p)^{0,5} = \frac{\gamma_w(\cos \Theta_w + 1) - 2\sqrt{\gamma_s^d \gamma_w^d}}{2\sqrt{\gamma_w^p}} \tag{2}$$

where:

- γ_s^d - dispersive component of surface free energy of the film,
- γ_s^p - polar component of surface free energy of the film,
- γ_w - surface free energy of water,
- γ_w^d - dispersive component of surface free energy of water,
- γ_w^p - polar component of surface free energy of water,
- Θ_w - contact angle of water,
- γ_d - surface free energy of diiodomethane,
- γ_d^d - dispersive component of surface free energy of diiodomethane,
- γ_d^p - polar component of surface free energy of diiodomethane,
- Θ_d - contact angle of diiodomethane.

The surface free energy of biodegradable films was then calculated with the use of the formula [3].

$$\gamma_s = \gamma_s^d + \gamma_s^p \tag{3}$$

where:

- γ_s - surface free energy of the film,
- γ_s^d - dispersive component of surface free energy of the film,
- γ_s^p - polar component of surface free energy of the film.

The prints on the biodegradable package films tested were made with the use of *Flexiproof 100* device using a flexographic technique, involving printing plate prepared by digital laser-photochemical method, from photopolymer plate Cyrel DPN 1.70 produced by DuPont. The density of anilox cylinder used for application of ink on printing plate was 200 l/cm.

The printing process was carried out with the use of water-dilutable black printing ink based on styrene-acrylic resin and organic solvent-based black ink based on nitrocellulose-polyurethane resin. The viscosity measured by Ford Ø4 cup conforming ISO standard (ISO 2431, 1993) was 18 s for the water-dilutable ink and 20 s for the solvent-based ink. Surface free energy of the inks was determined according to the tensometric Du Noye method (Pigoñ, 2009). It was measured by means of KSV Instrument Ltd. Sigma 701 with constant temperature 23 ± 0.001 . Surface free energy of the water-dilutable ink was 30.86 mJ/m^2 , and that of solvent-based ink was 23.46 mJ/m^2 .

Optical density of print fields fully coated with ink was measured by means of *Macbeth TR 927* transition densitometer.

3. Results

The collected results of measurements of contact angle of water and diiodomethane and calculated values of surface free energy are arranged in Table 1.

Table 1: Surface free energy of biodegradable films tested

N.	Film	Contact angle of water, Θ_w [°]	Contact angle of diiodomethane, Θ_d [°]	Surface free energy, γ_s [mJ/m^2]
1.	<i>NatureFlex 23NVS</i>	71,68	23,65	47,75
2.	<i>NatureFlex 23NK</i>	72,00	24,44	47,38
3.	<i>NatureFlex 23NVR</i>	106,96	45,00	37,50
4.	<i>Ecovio L BX 8145</i>	91,68	42,15	38,39
5.	<i>Mater-Bi</i>	82,22	32,47	42,86

The polar and dispersive components of surface free energy are presented on the Figures 2 and 3.

Figure 2:
Polar component of surface free energy (γ_s^p) of biodegradable films:
1 - *NatureFlex 23NVS*, 2 - *NatureFlex 23NK*,
3 - *NatureFlex 23NVR*, 4 - *Ecovio L BX 8145*,
5 - *Mater-Bi*

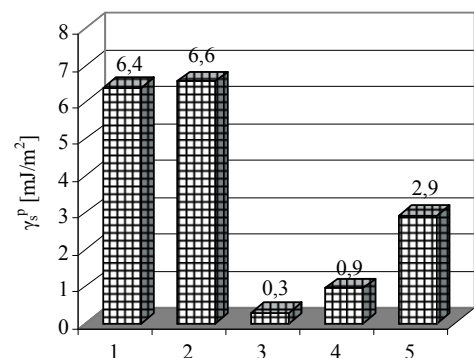
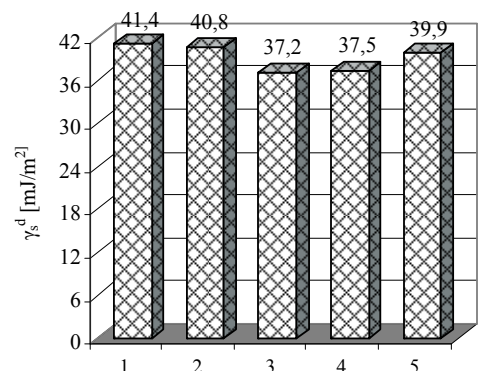


Figure 3:
Dispersive component of surface free energy (γ_s^d) of biodegradable films:
1 - *NatureFlex 23NVS*, 2 - *NatureFlex 23NK*,
3 - *NatureFlex 23NVR*, 4 - *Ecovio L BX 8145*,
5 - *Mater-Bi*



Measurements of the optical density of fully coated fields depended on the kind of ink and film are displayed in Figures 4 and 5.

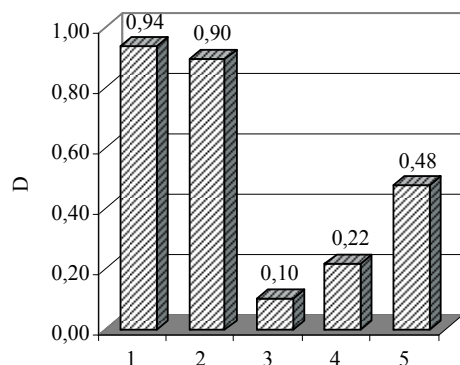


Figure 4:
Optical density of fully coated fields on biodegradable films printed with water-dilutable ink:
1 - NatureFlex 23NVS, 2 - NatureFlex 23NK, 3 - NatureFlex 23NVR, 4 - Ecovio L BX 8145, 5 - Mater-Bi

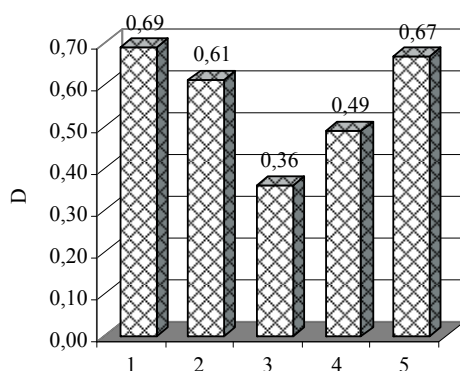


Figure 5:
Optical density of fully coated fields on biodegradable films printed with solvent-based ink:
1 - NatureFlex 23NVS, 2 - NatureFlex 23NK, 3 - NatureFlex 23NVR, 4 - Ecovio L BX 8145, 5 - Mater-Bi

4. Discussion

Analysis of the results obtained shows that individual biodegradable films tested differ in the value of their surface free energy, as well as in the polar and dispersive components of surface free energy (see Table 1 and Figures 2-3). The highest values of surface free energy was found for the films *NatureFlex 23NVS* and *NatureFlex 23NK* (Table 1). Slightly smaller values of surface free energy were found in the case of *Mater-Bi* film. The lowest values of surface free energy were found for the films *NatureFlex 23NVR* and *Ecovio L BX 8145*. The polar and dispersive components of surface free energy of the *NatureFlex 23NVR* and *Ecovio L BX 8145* films are also lower than those of the other films (Figures 2-3). It is also to be noted that the films *NatureFlex 23NVR* and *Ecovio L BX 8145* are characterized by very low values of polar component of surface free energy (see Figure 2), whereas the dispersive component of surface free energy, as compared with that of all the other films tested, is not much different (Figure 3).

Analysis of the results of testing the prints made on the biodegradable films showed that the films with lower surface free energy (Table 1) had lower optical density of the fields coated with printing ink (Figures 4-5). It should be stated, however, that a higher correlation was observed between optical density of fields coated with water-dilutable ink and polar component of surface free energy of the film as well as between the optical density of fields coated with solvent-based ink and dispersive component of surface free energy of the film. Optical density of fields coated with water-dilutable ink was the highest on *NatureFlex 23NVS* and *NatureFlex 23NK* films (Figure 4) which are featured with the highest values of polar component of surface free energy (Figure 2). The films *NatureFlex 23NVR*, *Ecovio L BX 8145* and *Mater-Bi*, which exhibit the lowest value of polar component of surface free energy (Figure 2) are characterized also by lower values of optical density of fields coated on prints with water-dilutable ink (Figure 4).

In the group of biodegradable films printed with organic solvent-based ink the highest values of optical density of ink-coated fields was observed in the films having the highest values of dispersive component of surface free energy, namely the films: *NatureFlex 23NVS*, *NatureFlex 23NK* and *Mater-Bi* (Figures 3 and 5). The films *NatureFlex 23NVR* and *Ecovio L BX 8145* exhibited lower values of optical density of fields coated with solvent-based ink, since they have lower dispersive component of surface free energy.

The difference in values of optical density of the fields coated with printing ink on individual films was smaller in the case of solvent-based films (Figure 5) than in the cases where water-dilutable ink was used (Figure 4). Also the difference in the values of dispersive component of surface free energy of the films (Figure 3) was smaller as compared with the difference in the polar component of their surface free energy (Figure 2).

The results presented above enable to state that the higher is the polar component of surface free energy of a biodegradable film, the higher is the value of optical density of fields coated with water-dilutable ink on prints, and the higher is the dispersive component of surface free energy of the films, the higher the optical density of fields coated with solvent-based ink.

The effect may be explained by the fact that the higher value of polar component of surface free energy of the film is connected with stronger adhesion of water-dilutable ink to the film surface on printing, and a higher value of dispersive component of surface free energy of a film corresponds to stronger adhesion of solvent-based ink to the film. A stronger adhesion of printing ink to the film surface enables to obtain a thicker ink layer on the prints. The higher is the thickness of a black printing ink on a transparent film, the stronger is absorption of light by the ink layer, and thus the smaller the light transmittance (τ) defined as the ratio of luminous flux (ϕ_T) transmitted by the film coated with a layer of black printing ink to a luminous flux (ϕ_0) transmitted through a transparent film non coated with the ink [4].

$$\tau = \frac{\phi_T}{\phi_0} \quad [4]$$

where:

τ - light transmittance,

ϕ_0 - luminous flux transmitted through a transparent film (in the absence of ink),

ϕ_T - luminous flux transmitted through a film coated with a layer of black printing ink.

For this reason a thicker ink layer on a film gives a higher optical density of ink coated fields, which in densitometric measurements may be calculated from formula [5] (Kipphan, 2001).

$$D = -\log \tau = \log \frac{1}{\tau} = \log \frac{\phi_0}{\phi_T} \quad [5]$$

where:

D - optical density of field coated with printing ink on the film,

τ - transmittance,

ϕ_0 - luminous flux transmitted through a transparent film (in the absence of ink),

ϕ_T - luminous flux transmitted through a film coated with a layer of black printing ink.

5. Conclusions

Experimental tests and analysis of the results obtained enable to state that the biodegradable films available on the market and intended for production packages differ in the values of their surface free energy and its both polar and dispersive components. The value of the surface free energy and the values of its components have a substantial impact on optical density of fields coated with printing ink on printed films.

In printing biodegradable films with water-dilutable inks the optical density of fields coated with printing ink depends mainly on the value of polar component of surface free energy of the film. The higher the polar component of surface free energy of a biodegradable film, the higher is the optical density of fields coated with printing ink. In printing biodegradable films with solvent-based inks the optical density of fields coated with printing ink depends mainly on the value of dispersive component of surface free energy of the film. The higher the dispersive component of surface free energy of a film, the higher is the optical density of fields coated with solvent-based printing ink.

References

- BASF, *Information materials of BASF company*.
- Czech, G. (ed.), (1993); *Technologia fleksograficzna zagadnienia standaryzacji (The standardization of flexographic technology)*, COBRPP, Warsaw.
- Czichon, H., Czichon, M., (2006); *Formy fleksodrukowe (Flexographic plates)*, OWPW, Warsaw.
- Duda, A., Penczek, S., (2003); *Polilaktyd [poli(kwas mlekowy)]: synteza, właściwości izastosowania (Polylactic [poly(acid milk)]: synthesis, properties and application)*, *Polimery* 48, 1, 16-27.
- EN13432:2000 *Packaging. Requirements for packaging recoverable through composting and biodegradation. Test scheme and evaluation criteria for the final acceptance of packaging.*
- Florjańczyk, Z. et al., (2009); *Synthetic and natural polymers in modern polymeric materials. Part I. Polymers from renewable resources and nanocomposites*, *Polimery* 54, 10, 611-625.
- Innovia, *Information materials of Innovia Films company*.
- ISO 2431:1993 *Paints and varnishes. Determination of flow time by use of flow cups.*
- Kipphan, H. (ed.), (2001); *Handbook of Print Media*, Springer, Heidelberg.
- Lim, L.-T. et al., (2008); *Processing technologies for poly(lactic acid)*, *Prog. Polym. Sci.* 33, 820-852.
- Nampoothiri, K. M. et al., (2010); *An overview of the recent development in polylactide (PLA) research*, *Bioresource Technol.* 101, 22, 8493-8501.
- Novamont, *Information materials of Novamont company*.
- Panák, J. et al, (2002); *Poligrafia. Procesy i technika (Printing processes and technique)*, COBRPP, Warsaw.
- Piecyk, L., (2008); *Biopolimery do produkcji opakowań (Biopolymers to packaging production)*, *Opakowanie* 3, 34-39.
- Pigoń, K., Różewicz, Z.: (2009) *Chemia fizyczna T.1 (Physical Chemistry Vol.1)*, PWN, Warsaw.
- Platt, D., (2006); *Biodegradable polymers: market report*, Rapra Technology, Shawbury.
- Rudawska, A., (2008); *Surface free energy and geometric structure of the surfaces of selected epoxy composites*, *Polimery* 53, 6, 452-456.
- Rudnik, E., (2008); *Compostable Polymer Materials*, Elsevier.
- Siracusa, V. et al., (2008); *Biodegradable polymers for food packaging: a review*, *Trends Food Sci. Tech.* 19, 634-643.
- Wasiak, W., (2009); *Rynek i przemysł opakowań w Polsce - wybrane problemy (Packaging market and industry - selected problems)*, Polish Chamber of Packaging, Warsaw.
- Żakowska, H., (2003); *Opakowania biodegradowalne: recykling organiczny, mechanizm biodegradacji, metody badań przydatności do kompostowania, biodegradowalne materiały opakowaniowe (Biodegradable packages: organic recycling, biodegradation mechanism, process of testing to utility to compostable, biodegradable packaging materials)*, COBRO, Warsaw.
- Żakowska, H., (2008); *Opakowania kompostowalne (Compostable packaging)*, *Opakowanie* 5, 14-18.
- Żenkiewicz, M., (2000); *Adhezja i modyfikowanie warstwy wierzchniej tworzyw wielkocząsteczkowych (Adhesion and modification of macromolecular materials surface layer)*, WNT, Warsaw.
- Żenkiewicz, M., (2010); *Proceedings of Scientific and Technical Conference: Trends in polish printing and printed packaging development*, Poznań 8-9.04.2010, 193-198.
- http://www.plastech.pl/wiadomosci/arttykul_1216_1/Analiza-rynku-polimerow-biodegradowalnych. 17.01.2008.
- http://www.plastech.pl/wiadomosci/arttykul_2319_1/Biopolimery-i-tworzywa-ulegajace-biodegradacji-biotworzywa. 22.01.2009.
- http://www.plastech.pl/wiadomosci/arttykul_3148_1/Biotworzywa-zastapia-90-proc-tradycyjnych-tworzyw. 12.11.2009.



Measuring forces appearing while cutting a stack of sheets with the aim to improve post press processes

Jann Neumann, Michael Desch, Dieter Spiehl, Edgar Dörsam

Technische Universität Darmstadt
Institute of Printing Science and Technology
Magdalenenstr. 2, D-64289 Darmstadt, Germany
E-mail: neumann@idd.tu-darmstadt.de

Abstract

The aim of this paper was to discuss the influencing parameters on the cutting forces. All experiments were carried out on a special test rig that was developed, designed and built up at IDD. To get comparable results we kept the most of the parameters like paper stack geometry and cutting speed as well as clamping force constant. The variable parameters were paper (coated and uncoated with different grammage) and the cutting angles. We showed that different cutting angles lead to different cutting forces, but nearly same cutting work. This can be explained by the dependency of work on force and distance. With increasing angles α and β the forces increase, but the cutting distance decreases and so work is nearly the same. Despite that cutting work is nearly the same for all cutting angles, it should be mentioned that higher cutting forces imply a stiffer machine frame and an actuator with more power. On the other hand an acute cutting angle leads to a larger knife travel distance what necessitates a larger machine frame. So guillotine producers need to balance between cutting forces and angles. With our test rig at the Institute of Printing Science and Technology (IDD) / Darmstadt, we have an instrument to carry out cutting test under defined and reproducible conditions.

Keywords: post-press, cutting forces, paper stack geometry, wedge edge

1. Introduction

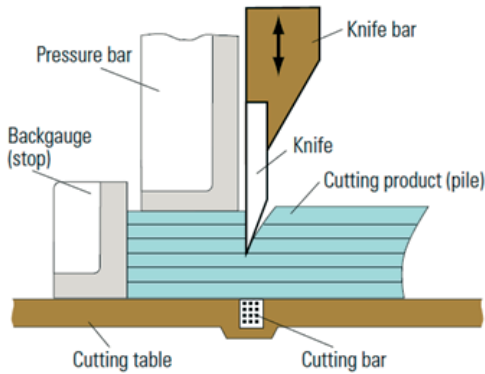
Stacks of sheets are cut with high speed guillotines within the industrial post press process. The active principles and the fundamental configuration have not been changed since the nineteen thirties. But nowadays, the requirements on accuracy, productivity, performance of a cutting machine as well as lifetime of knives are increasing. Especially in a modern industrial printing workflow a poor cutting quality is not acceptable. Because of its position at the end of the value-added chain, defective products are corresponding cost-intensive.

To adjust high speed guillotines to the increasing requirements of post press process a structured development process is essential. A trial and error method is not advisable for state of the art product engineering. The bases of a target oriented development process of a new machine design are reliable measurement data and understanding of the mechanical processes appearing while cutting a stack of paper. First of all, forces appearing during the cut are of interest. The appearing forces in conjunction with knife stroke are a measurand for the mechanical work.

Cutting is characterized as a mechanical separating of a solid using a wedge cutting edge (Feiler, 1970). The edge intrudes the solid by the use of compression. The cut generates two solids and creates two new surfaces called intersections. This cutting principle is used in guillotines for industrial use. They are needed for the printing industry in the post processes. The cutting width varies between 660 mm and 2600 mm with a maximum loading height of 165 mm.

Figure 1 shows the working principle and the main components of a cutting machine. The pressure bar clamps the pile before and during the cut. The clamping force and time is adjustable for different cutting materials. It should be adjusted proportional to the height of the pile, the compressibility of the stack (Desch et al., 2011) and the surface roughness of the sheets in the stack (Wimmer, 2004). Stress distribution inside the stack is not constant. While observing a single sheet, stress is lowering in the stack from top to bottom due to the distribution of the force to a larger area. After clamping the stack, a pull rod pulls the knife through the paper stack and cuts a pile from the stack.

The movement of the knife can be divided into four main types (Dittrich, 1965). Nowadays this movement of the knife is called knife travel and is defined by the two angles α and β shown in Figure 2.



- Pressure bar: Fix the pile during cutting
- Knife: Cut the pile
- Knife bar: Fix and guide the knife
- Cutting bar: Penetrated by the knife at the end of the cut
- Cutting table: Working area
- Backgauge: Adjust the specified size of the pile

Figure 1: Design of a guillotine cutter (Kipphan, 2001) and a list of essential components of a guillotine cutter

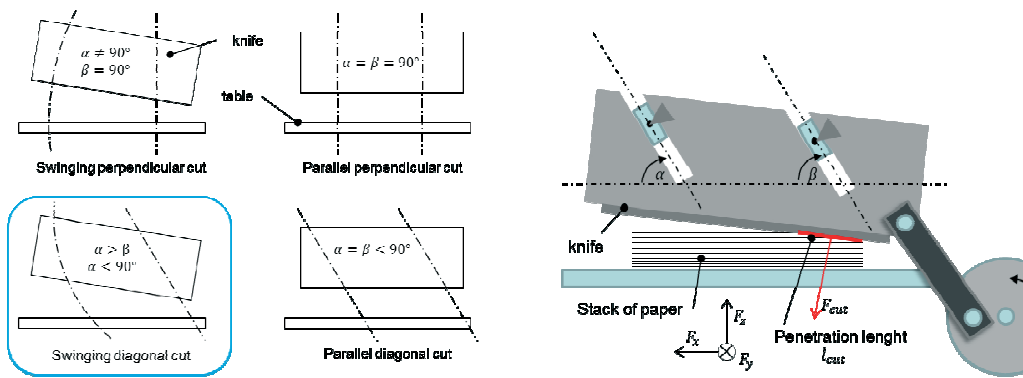


Figure 2: Left: Four different knife travels (Liebau et al., 1997) modified. Right: Function principle of an industrial high speed cutting machine with linear guide

The four different relative knife movements are shown in Figure 2 on the left side. The author Mordowin (Mordowin, 1962) claims the best cutting results, accuracy and straightness can be achieved by the swinging diagonal cut. The picture on the right side of Figure 2 shows the technical realization of a gear mechanism to achieve a swinging diagonal cut. Here the knife dips in the cutting material on one edge. The other side of the knife is above the pile at an angel of α_{cut} . During the cut the angle α_{cut} decreases and turns to 0° when the knife touches the cutting bar. This type of knife travel is the one available on the market nowadays. It is achieved by two different angles α and β of the linear guide for the knife bar. Typical values are $\alpha=45^\circ$ and $\beta=42^\circ$, what leads to a value of 0.5° to 1.5° for α_{cut} , depending on other geometrical data like knife length and distance between knife and table.

In literature plots for the mentioned cutting forces are all quite the same. Their diagrammatic laps are identical and all of them are based on mechanical plotting of the forces (Mordowin, 1962; Weyl, 1962; (Dittrich, 1965; Tiefenbach, 1960). In the 90ies the company Wohlenberg (Wohlenberg, 1990) introduced a patent (Wohlenberg, 1990) where the force is measured by a resistance strain gauge inside the knife. This gave a quite precise measurement with more details compared to literature before it. This approach only helps for quantitative monitoring of the cut. All named literature, beside the patent, is quite old and there were no new investigations in that field since the sixties. Today there are new materials in the market and these need to be cut, as well as there are new alloyed quality steels and machine components which are useable for a guillotine. Printed electronics for example are quite sensitive and can only be fixed or clamped with very low pressure forces. Here the IDD investigated and built a laboratory size guillotine. This is equipped with high accurate measurement technique for tracing value and direction of the forces applied to the cutting material by the knife and the pressure bar.

2. Experimental setup

The laboratory guillotine at IDD is a small size model of a high speed industrial guillotine. Its design is very stiff and all the needed components are included.

3. Experiments

The aim of this paper is to discuss the influence parameters on the appearing forces while cutting a stack of sheets. Therefore we selected four different types of paper. To reduce the number of experiments, we investigated only swinging diagonal cuts. Because of the present day industrial cutting machine design, we agree that this knife travel is most significant. To investigate the influence of different angles, we varied the angles α and β . To receive comparable results the geometrical parameter of the paper stack and the pile were always the same. The dimensions of the paper stacks were: height = 26 mm, width = 75 mm and length = 50 mm (see Figure 4).

Table 1: Parameter variation

	$\alpha = 35^\circ, \beta = 30^\circ$	$\alpha = 45^\circ, \beta = 42^\circ$	$\alpha = 80^\circ, \beta = 77^\circ$
P1, matt coated, 135g/m ²	3	3	3
P2, office paper, 80g/m ²	3	3	3
P3, matt coated, printed, 170g/m ²	3	3	3
P4, full embossed and printed, 75g/m ²	3	3	3
Number of experiments:			36

For investigation of the influence of paper, we tested four different types of paper. P1 is a silk-mat coated paper with a grammage of 135 g/m² and a thickness of 110 μm , P2 is a normal office paper with a grammage of 80 g/m² and a thickness of 104 μm , P3 is a matt coated paper with a grammage of 170 g/m² and a thickness of 155 μm , in contrary to P1 and P2, P3 is printed on both sides, P4 is a packaging paper that is printed and fully embossed on the entire surface. The grammage of P4 is 75 g/m² and the thickness is 58 μm . The cutting speed is another influencing parameter whose investigation would exceed the framework of this paper. So we decided to execute all experiments at the same cutting speed, 2000 mm/min.

4. Evaluation

This paper aims to show the correlation between knife travel and cutting forces. Figure 4 shows the association between the angles α , β , knife length l_{length} , measured length s and α_{cut} . With the measurement technique implemented in the experimental cutting machine at IDD, it is not possible to measure the cutting angle α_{cut} directly. Actually, that is not necessary because the correlation between all geometric quantities is bijective so the cutting angle α_{cut} can be calculated with:

$$\alpha_{cut} = \arctan\left(\frac{h_k}{l_{knife}}\right) \quad [1]$$

with

$$h_k = \Delta l_M \cdot \tan \alpha \quad [2]$$

The length Δl_M can be determined with the equation

$$\Delta l_M = \Delta l_\beta - \Delta l_\alpha \quad [3]$$

$$\Delta l_\beta = s \cdot \cos \beta \quad [4]$$

$$\Delta l_\alpha = \frac{s \cdot \sin \beta}{\tan \alpha} \quad [5]$$

Finally, the cutting angle α_{cut} is defined by the equation:

$$\alpha_{cut} = \arctan\left[\frac{s \cdot \left(\cos \beta - \frac{\sin \beta}{\tan \alpha}\right) \cdot \tan \alpha}{l_{knife}}\right] \quad [6]$$

In our experiments the knife length l_{knife} is 105 mm. Therefore, all geometric quantities are known and the PXI-System can calculate α_{cut} as a function of the measured distance s . The cutting angle α_{cut} is the input value for the calculation of hedge h_{edge} (see Figure 4).

According to Figure 4 we derive a simple equation for the height h_{edge} :

$$h_{edge} = \Delta h_{\beta} + \Delta l_{pile} \cdot \tan \alpha_{cut} \tag{7}$$

The measurement platform detects forces in the three directions (F_x, F_y, F_z) but for the calculation of work only the force components in moving direction of knife F_x, F_z are of interest. Because of the test rig stiffness the deformation in y -direction is approximately zero. Therefore the distribution of force to mechanical work in that direction is zero, as well. The general relationship between work and force is:

$$w = \int_{s1}^{s2} \vec{F}(s) \cdot d\vec{s} \tag{8}$$

In an orthogonal coordinate system, like we have it in our test rig, the work can be calculated with a dot product.

$$W = \vec{F} \cdot \vec{s} = F_x s_x + F_z s_z \tag{9}$$

A challenging issue is the calculation of s_z because similar to the calculation of h_{edge} , s_z is a function of α_{cut} and of the contact lever point (working point of force F_y). But this length to the pivot of the lever is unknown and therefore we apply the simplification that the working point of the resultant force is on the same line as h_{edge} . Because of the small angle α_{cut} the resulting error is negligible. Additionally we apply that error on all samples so that we obtain only a small constant systematic error.

The resultant force F_{res} is defined by:

$$F_{res} = \sqrt{F_x^2 + F_z^2} \tag{10}$$

5. Results

The compositions of the next three figures are always the same. The upper diagram shows the resultant cutting force F_y vs. the distance h_{edge} and the lower diagram shows the calculated work vs. h_{edge} . The moving direction of the knife is from $h_{edge} = 30$ to 0 mm. In the first part of the diagram (number 1 in Figure 5) the knife travels down.

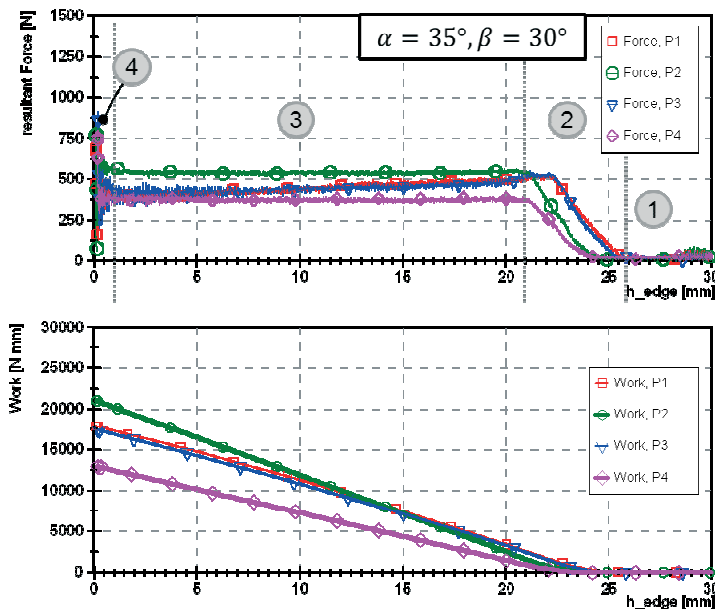


Figure 5: Forces appearing while cutting four different types of paper with an angle of $\alpha=35^\circ, \beta=30^\circ$ vs. h_{edge}

The knife has no contact to the paper, yet. In the second part (number 2), the knife hits the paper stack at the right edge. After this first contact, the force increases until the knife affects the stack over the whole length $l_{cut} = 75$ mm. In part three the knife cuts the stack of paper. Normally, in that part, the force is almost constant. At the end of the cutting process (number 4), the knife is almost parallel to the cutting bar. Sometimes, that causes fluctuation of cutting forces due to cutting like punching of the last sheets. At last, the knife hits the cutting bar, which leads to increasing forces at the end of the cut. Work is calculated as explained in the last chapter.

Figure 6 shows the resultant forces and work at the angles $\alpha = 45^\circ, \beta = 42^\circ$. In comparison with Figure 5 the average of the resultant force is a little higher but the calculated work is nearly the same. The explanation of that effect is, that an obtuse angle causes a shorter knife travel distance. The shorter knife travel distance compensates the higher forces so that the product of both represented as work are nearly the same.

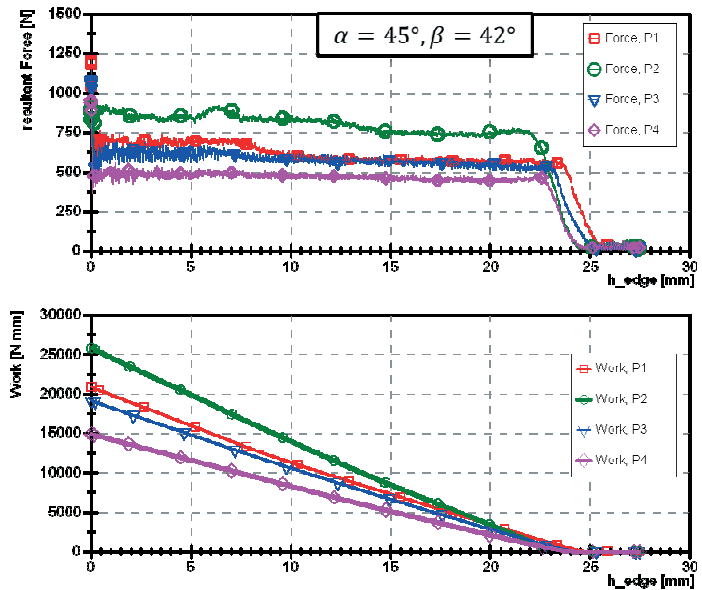


Figure 6:
Forces appearing while cutting four different types of paper with an angle of $\alpha=45^\circ, \beta=42^\circ$ vs. h_{edge}

Corresponding to Figure 5 and Figure 6, Figure 7 shows the resultant force at the maximum angle our test rig runs undisturbed. It is quite interesting that cutting force of paper 2 (Office paper, 80g/m²) is nearly twice as high as at the acute angles $\alpha = 35^\circ, \beta = 30^\circ$. However, the cutting work is constant at quite the same level. Like mentioned before, the reason can be found in the travel distance. At the angles $\alpha = 80^\circ, \beta = 77^\circ$ we have almost a perpendicular cut, which means the knife takes the shortest way through the stack of paper.

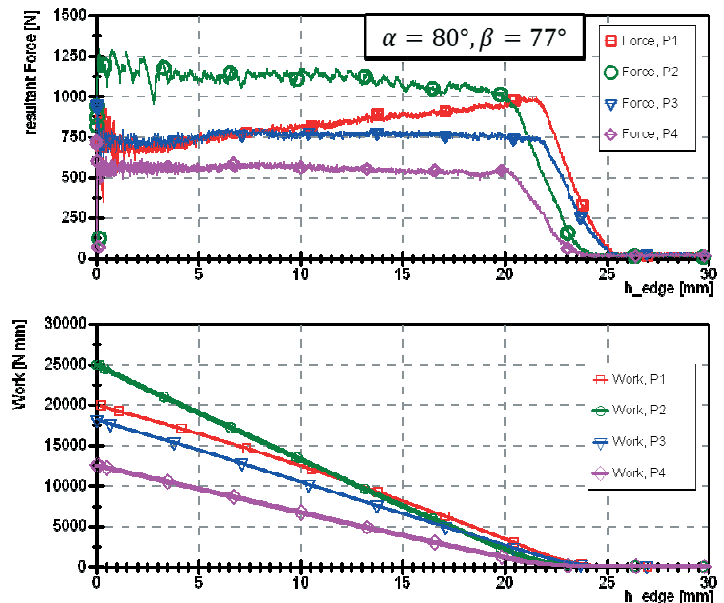


Figure 7:
Forces appearing while cutting four different types of paper with an angle of $\alpha=80^\circ, \beta=77^\circ$ vs. h_{edge}

Figure 8 shows the summarization of all above mentioned cutting experiments results. The interpolated continuous lines show the average cutting force and the dotted lines show the interpolation of the cutting work for all four types of paper at the three different angle couples.

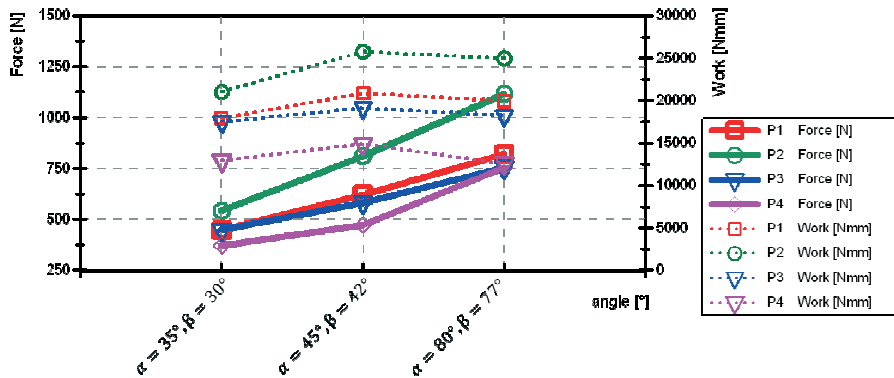


Figure 8: Summarization of cutting experiments results comparing cutting force and work for the four different types of paper

6. Conclusion and outlook

The aim of this paper was to discuss the influencing parameters on the cutting forces. All experiments were carried out on a special test rig that was developed, designed and built up at IDD. To get comparable results we kept the most of the parameters like paper stack geometry and cutting speed as well as clamping force constant. The variable parameters were paper (coated and uncoated with different grammage) and the cutting angles. We showed that different cutting angles lead to different cutting forces, but nearly same cutting work. This can be explained by the dependency of work on force and distance. With increasing angles α and β the forces increase, but the cutting distance decreases and so work is nearly the same. Despite that cutting work is nearly the same for all cutting angles, it should be mentioned that higher cutting forces imply a stiffer machine frame and an actuator with more power. On the other hand an acute cutting angle leads to a larger knife travel distance what necessitates a larger machine frame. So guillotine producers need to balance between cutting forces and angles. With our test rig at the Institute of Printing Science and Technology (IDD)/Darmstadt, we have an instrument to carry out cutting test under defined and reproducible conditions.

In future we try to describe the main cutting process including the measurements which are necessary to determine the friction during the cut of the knife vs. the stack of paper. Here especially the warming of the wedge edge of the knife is of interest.

Acknowledgments

The authors want to thank Perfecta Cuttings Systems, Bautzen for the funding of this work and for the very helpful collaboration.

References

- Desch, M., Dörsam, E., (2011), Determining the amount of sheets in a stack of paper by using a pressure stamp, Stillwater, Oklahoma
- Dittrich, H., (1965), Schneidemaschinen - Ausgewählte Beiträge, Leipzig
- Feiler, M., (1970), Ein Beitrag zur Klärung der Vorgänge beim Schneiden dünner flächiger Materialien, Dissertation, Institut für industrielle Fertigung und Fabrikbetrieb, Universität Stuttgart
- Kipphan, H., (2001), Handbook of print media : technologies and production methods ; including 92 tables, Berlin
- Liebau, D., Heine, I., Herzau, E., Wulf, J., Nestler R., Schumann, F., (1997), Industrielle Buchbinderei, Itzehoe ; Bad Langensalza
- Mordwin, B. M., (1962), Buchbindereimaschinen I: Berechnungen und Konstruktionen polygraphischer Maschinen, Berlin

- Spiehl, D., (2009), Konstruktive Umsetzung einer Vorrichtung zur Schneidkraftbestimmung in Papierstapeln, Diplomarbeit, Institut für Druckmaschinen und Druckverfahren (IDD), Technische Universität Darmstadt
- Tiefenbach, D., (1960), Kein Titel, Studienarbeit, Lehrstuhl und Institut für Druckmaschinen und Druckverfahren, Technische Hochschule Darmstadt
- Weyl, (1962), Schnittkräfte an Papierschnidemaschinen, Allgemeiner Anzeiger für Buchbindereien, 2,3,4,5, 64-65; 124; 126; 140; 240-241; 252-254; 336-339
- Wimmer, M., (2004), Grundlagen zur Bewertung von Schneid- und Falzmaschinen, Wiesbaden, München
- Vertriebs- Und Service Gmbh Wohlenberg, (1990), Verfahren zur Schnittqualitätserfassung einer Schneidemaschine für Papier, Pappe oder dergleichen sowie Schneidmaschine, DE 40 13 906 C 2, D. Patentamt

Wear of packaging during transport simulation

Peter Rättö, Thomas Trost, Erik Blohm

Innventia

P. O. Box 5604, SE-11486 Stockholm, Sweden

E-mails: peter.ratto@innventia.com; thomas.trost@innventia.com; erik.blohm@innventia.com

Abstract

A commercial board was coated with a laboratory coater using colours with differed pigments, binders and amounts of binder. The coated board was then calendered at different temperatures and printed with a standard offset ink.

The printed board was subjected to wear using a Sutherland Rub Tester or to wear during a simulated transport on an electro-hydraulic vibration table. Print disturbances were evaluated visually after both the rub tests and after the transport simulations. The print disturbances were classified into three different categories: removed ink (rub off in Sutherland), scratches and polishing.

Wear during rub-tests seemed to depend mostly on the ink adhesion onto the substrate while wear during transport simulations depended more on the abrasiveness of the surface. Ink adhesion can be improved by an appropriate pore structure where a high porosity and a large number of small pores would be favourable. Print disturbances of coated substrates after transport can on the other hand be minimized by smoothing the paper surface on a particle size scale (0.1-1 μm), either by the choice of a flat pigment (clay) or by high temperature calendering.

Keywords: abrasion, coated board, friction, print quality, transport, wear

1. Introduction

In today's manufacturing chain, packages are transported long distances. The package is usually manufactured and printed in one factory, and then transported to a packaging plant where the package is filled with its content. The final product is then transported long distances to the consumer. During transport and handling, the package is subjected to various potential causes of damage, both as scratches on the printed surface but also as physical damage on the packaging itself. This sort of wear and damage cause large economical costs and costs in good-will at the same time as large efforts are made in order to produce an appealing and selling package.

Wear of a surface is a complex phenomenon which depends both of the load onto the surface and the strength of the surface. In addition to the surface strength, the wear of the surface depends thus also on the friction, the friction mechanism and abrasiveness of the counter surface.

Paper to paper friction has been quite widely studied for uncoated papers (Back, 1990; Gurnagul et al., 1992; Fellers et al., 1998; Johansson et al., 1998; Bäckström et al., 1999; Gunderson, 2000). The contact of uncoated paper surfaces is mostly elastic (Higashijima et al., 2010; Kawashima et al., 2008). Consequently, the friction mechanisms of uncoated paper surfaces are mostly due to chemical adhesion between the surfaces (Gurnagul et al., 1992). It shall be emphasized that frictional behavior of uncoated papers also depends on weak boundary layers acting as lubricants (Garoff et al., 1999). These boundary layers usually consist of extractives but might also consist of resins used for sizing. Addition of structured particles such as precipitated silica will increase friction due to the adsorption of such resins while flat particles like talk might decrease the coefficient of friction (Withiam, 1991; Hoyland et al., 2000; Karademir and Hoyland, 2003; Holm et al., 1991).

Friction of coated paper has not been as widely studied as friction for uncoated papers but recent findings have revealed that the friction mechanisms differ between uncoated and coated papers (Higashijima et al., 2010; Kawashima et al., 2008; Higashijima and Yamauchi, 2011). The contact onto coated surfaces is mostly plastic (Higashijima and Yamauchi, 2011) and paper-to-paper friction of coated papers depend therefore mostly on mechanical interlocking (Rättö et al., 2000; Enomae et al., 2006; Rättö, 2012). Rättö et al. (2000) showed that the coefficient of friction mostly depended on the pigment particle shape. Clay based coatings

showed thus a lower coefficient of friction than GCC (Ground Calcium Carbonate) based coatings. Enomae et al. (2006) showed that the presence of sharp GCC particles lead to scratches when the two surfaces were slid onto each other during frictional measurement. They also showed that the coefficient of friction increased when clay was gradually replaced by GCC. Rättö (2012) investigated the influence of different friction mechanisms on paper to paper friction of coated papers and suggested that friction was mostly due to mechanical interlocking during sliding at moderate binder levels. Friction measurements resulted in plastic deformation and wear of the coated surface due to the abrasion of the hard pigment particles.

The wear of the surface also depend on the strength of the surface or the ability of the surface to withstand abrasion. Wear of printed surfaces causes large problems with rub off and smearing after the printing process, but also of wear of packaging surfaces during handling and transport. Smearing is usually due to the incomplete drying of ink after printing and rub off is usually due to a poor adhesion of the ink onto the surface. Several studies has shown that the ink drying depend on coated paper depend both on the type of binder and the pore structure of the coating layer (e.g. Schoelkopf et al., 2000; Ström, 2005; Ström and Gustafsson, 2005; Gane et al., 2006; Koivula et al., 2008). A higher porosity increases the drying rate, but a higher drying rate is also favored by smaller pores due to capillary absorption (Shoelkopf et al., 2000). Rub off resistance was also shown to improve with a faster ink setting rate (Gane et al., 2006; Koivula et al., 2008).

Wear of surfaces can also depend on the counter surface. Martinez (2005) showed that products might be damaged by the packaging surface. Boards containing sharp fillers were in this case the most abrasive packaging materials. Salesin et al. (2008) compared the abrasion of different printed samples with two rub testing methods, the Sutherland Rub test and the Ugra Rub test, and found that the abrasion differed between different samples. Some samples showed gloss increase while other samples showed a gloss decrease. Abrasion in forms of streaks was also observed for some combinations of printed surface and abrasive surface.

Testing the abrasion of packaging surfaces is thus not an easy task and the abrasion resistance of packaging materials can be tested with a number of methods. The most common test method today is the Sutherland rub tester where a back side of a sheet is rubbed against a printed surface. The rubbed off ink is then evaluated visually. Rub testers such as Sutherland give some information of the rub resistance of the printed surface but the loading conditions on the packaging surface during transport are also needed in order to get a proper evaluation of abrasion. Teshima et al. (1990) compared the abrasion during transport with laboratory vibration testing. They suggested that the average transport situation was equivalent with 5 min of laboratory testing and that the worst transport condition could be simulated by a 20 min vibrational test.

Wear of printed surfaces depend thus on the adhesion of the printing ink to the covered substrate and the load of the abrasive substrate onto the same surface. The mechanisms behind the ink adhesion onto the paper surface are quite well known but the knowledge behind wear mechanisms and friction of the package surface is quite limited. Also a relevant classification of defects is missing.

2. Materials and methods

For the trials, a coated board from StoraEnso, Sweden with a grammage of 190 g/m² was used as base substrate. Both carbonate and clay pigments were used together with three different latices and a potato starch binder.

The ground calcium carbonate (GCC) pigments were HC90 and CC60 supplied by Omya, Switzerland. The former had a wide particle size distribution and an average particle size of 0.70 µm and the latter had a narrow particle size distribution and an average particle of 0.60 µm. All GCC pigments were considered to have an isometric particle shape. The clay pigment was ND3090 supplied from Imerys, UK, and had an average particle size of 0.51 µm with a shape factor of 27.4.

The latices were one PVAc latex supplied by CIBA Chemicals, Finland, and two S/B latices supplied by Dow Chemical, Switzerland, denoted soft S/B and hard S/B, respectively, with different Tg giving two latex binders with different hardness. The soft S/B had a Tg of 13 °C and the hard S/B had a Tg of 55 °C. In some of the coatings using only S/B latex as binder, 0.5 or 1 pph of CMC was added. The CMC was Finnfix 5 supplied by CP Kelco, Finland. The starch was a cationic starch supplied by Solam, Kristianstad, Sweden.

The coating colour compositions are given in Table 1. The coating colours were mixed to a dry content of 65%, except for coating 3 where a dry content of 50% was used. A coat weight of 17±1 g/m² was applied in

a model K-coater laboratory coater from RK Print-Coat Instruments Ltd of Royston, England, and the papers were then oven-dried for 15 min at a temperature of 105 °C. After drying, the papers were calendered in a laboratory calender from DT Paper Science, Finland at room temperature, i.e. 23 °C. The web speed was 10 m/min and the line load 40 kN/m. The board with the last coating colour (GCC, S/B latex) was also calendered at roll temperatures of 50 °C and 70 °C. The samples were then printed in an offset laboratory printing press from IGT, Netherlands, in order to detect cracks. A standard cyan ink, Toplith from Sun Chemical, was used for the laboratory printing. All the samples were printed in full tone and the print was dried at room temperature.

Table 1. The coating colour compositions used in the trials

Coating colour	Pigment	Binder	CMC content
GCC+clay, S/B latex	60 pph ND3090/ 40 pph HC90	11 pph S/B latex	0.5 pph
GCC+clay, PVAc		11 pph PVAc latex	0.5 pph
GCC+Clay, Starch+S/B latex		10 pph S/B latex+5 pph starch	0.5 pph
Soft S/B latex	No pigment	S/B latex	0.0 pph
Hard S/B latex		Hard S/B latex	0.0 pph
40 pph soft S/B latex	90 pph ND3090/ 10 pph HC90	40 pph S/B latex	0.5 pph
40 pph hard S/B latex		40 pph hard S/B latex	0.5 pph
GCC, S/B latex, T=23,50,70°C	50 pph SC HG/50 pph CC60	20 pph S/B latex	0.5 pph

The board was then subjected to wear using a Sutherland Rub Tester during 100 cycles according to ASTM D5264-98 and during a simulated transport, horizontal direction, according to ASTM D4169-09 on an electro-hydraulic vibration table from Schenck using a randomized vibration spectrum, see Figure 1.

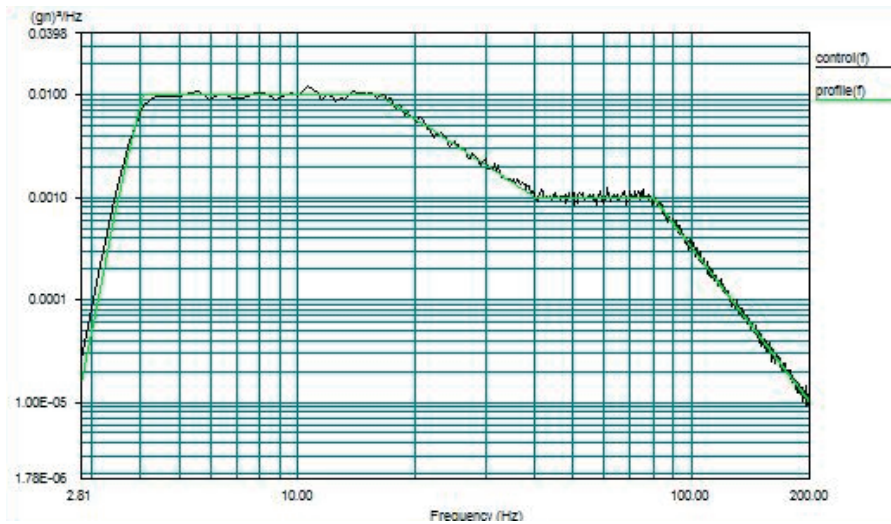
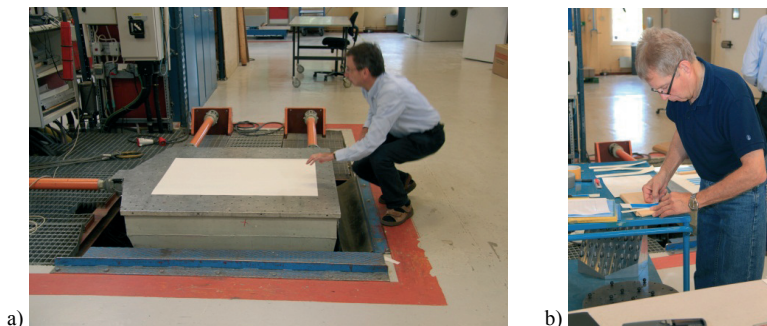


Figure 1: Randomized vibration spectrum used during transport simulations

The transport simulation tests were performed by attaching printed samples onto a large piece of carton board which was mounted on the vibration table, Figure 2a. An additional set of samples were then attached to a steel plate wrapped in paper with the weight of 7.5 kg, Figure 2b.



a)

b)



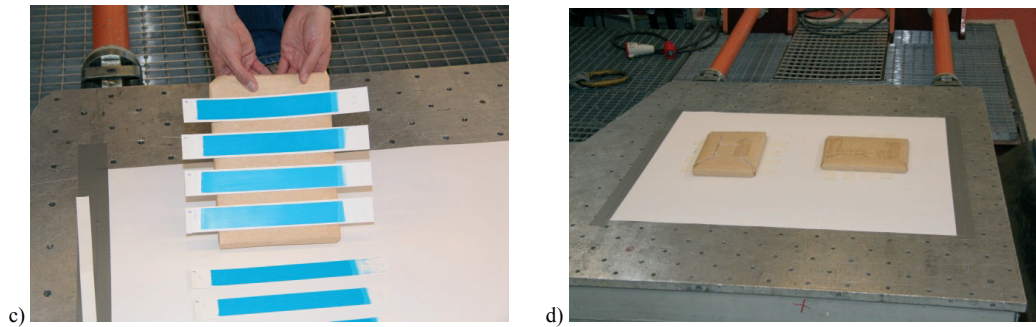


Figure 2: Pictures from the transport simulations on the vibration table: a) vibration table with solid board, b) attachment of samples on 7.5 kg steel plate, c) attached samples on steel plate and attached samples on vibration table, and d) samples on steel plate and solid board before transport simulation

The steel plate was then placed on the vibration table, Figure 2c, with the samples "rubbing" on to each other during testing, Figure 2d. Print disturbances were evaluated visually after both the rub tests with the Sutherland and the tests on the vibration table.

3.Results

Figure 3 (a) to (c) shows sample images of board surfaces after transport simulation. Figure 3 (a) shows a printed surface that was coated with only latex. After transport simulation, this surface showed mainly print disturbances in terms of removed ink, although some minor scratches were visible. Figure 3 (b) shows a sample surface that was coated with a mixture clay and GCC pigments with both S/B latex and starch as binders (10 pph S/B latex and 5 pph starch).

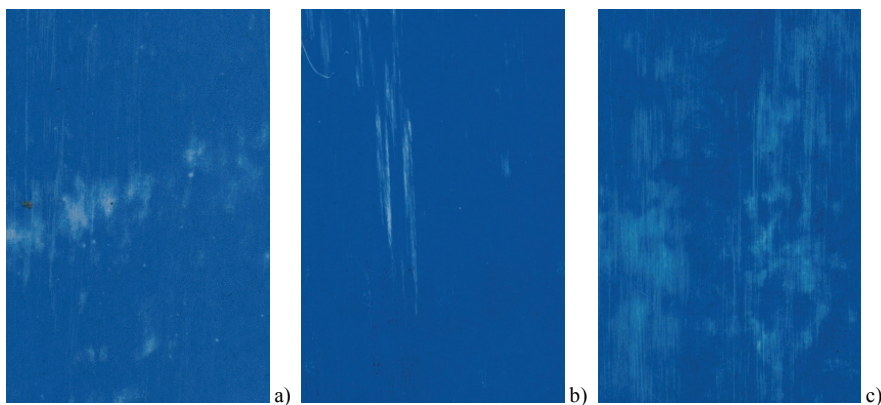


Figure 3:

Sample images of surfaces after transport simulation. (a) shows the surface of a sample coated with hard S/B latex, (b) shows a surface coated with Clay+GCC and S/B latex+Starch, and (c) shows a surface coated with GCC and S/B latex which had been calendered at 70°C

Table 2: Summary of print disturbances after rub off testing and transport simulation. The temperature given for the last three samples refer to the temperature of the heated calender roll

Sample	Rub off test, Sutherland	Transport simulation, vibration table
GCC+Clay, S/B latex	No damages, tendencies to rub off	Few scratches, some polishing
GCC+Clay, PVAc Latex	Scratches	scratches, some polishing
GCC+Clay, Starch+S/B latex	Few scratches, rub off	scratches, some polishing
Soft S/B latex	Few scratches, tendencies of rub off	Removed ink, polishing
Hard S/B latex	Lot of scratches already after 40 cycles	Removed ink, polishing
40 pph soft S/B latex	Few scratches	Polishing, scratches
40 pph hard S/B latex	Few scratches	Polishing, sharp scratches
GCC, S/B latex, T=23 °C	Few scratches	Scratches
GCC, S/B latex, T=50 °C	Scratches, rub off	Scratches and polishing
GCC, S/B latex, T=70 °C	Scratches, rub off	Polishing

This surface showed print disturbances in terms of sharp scratches of scratched. The samples surface in Figure 3 (c) was coated with a GCC pigment combined with 20 pph of S/B latex. This sample was also calendered at a temperature of 70 °C on the heated roll and showed a polished surface. All samples showed at least one of these three defects after transport simulation and print disturbances were therefore classified into these three different categories: removed ink (rub off in Sutherland), scratches and polishing.

3.1 Sutherland rub tester

Wear during rub-tests showed that coatings containing clay pigment showed less scratched and less rubbed off ink than coatings containing only GCC, see Table 1. The type of binder had a small but significant influence. Coatings containing clay and only S/B latex as binder showed no scratches and a low amount of rubbed off ink. Coatings with the same pigment composition but with PVAc latex as binder showed a higher amount of scratches but less amount of rubbed off ink. Similar coatings but with a mixture of S/B latex and starch as binder showed less scratches but more rubbed off ink than the coatings containing PVAc. Coatings containing only latex showed both scratches and a lot of rubbed off ink. When GCC particles were added (100 pph GCC and 40 pph of S/B latex), the amount of scratches decreased and less ink was rubbed off compared to the samples coated with only S/B latex. Coatings containing only GCC as pigment and 20 pph of S/B showed an increased amount of scratches and an increased amount of rubbed off ink with increased calendering temperature.

3.2. Transport simulation

The samples from the transport tests showed a slightly different pattern, see Table 1. The samples containing the mixture of clay and GCC showed a low amount of scratches, some polishing and low amount of removed ink. Samples coated with only S/B latex showed no scratches, some polishing and removed ink. When some GCC particles were added (100 pph GCC and 40 pph of S/B latex), some of the polishing was replaced by scratches. The calendering temperature had here a great influence on the type of wear. The samples calendered at room temperature showed mostly print disturbances due to scratches. When the calendering temperature was raised to 50 °C, the sample showed both scratches and polishing while a calendering temperature of 70 °C resulted in only polishing. None of these samples showed any large amounts of removed ink.

4. Discussion

An earlier study about paper-to-paper friction of the same unprinted samples suggested that the friction mechanisms differed between the samples (Rättö, 2012). Friction of the pigmented samples depended mostly on interlocking of asperities on a pigment particle size scale, i.e. 0.1-1 µm, while friction of the pure latex coatings depended on the chemical adhesion between the surfaces. It was also observed that hard pigment particles in the coating layer were necessary in order to obtain plastic deformation through polishing or scratching. The amount of plastic deformation also decreased when the surface roughness was smoothed out on a particle size scale (0.1-1 µm) by choosing a flat pigment (e.g. clay) or by high temperature calendering.

The print disturbances also depend on the other hand also on the adhesion of the ink onto the coated surface. Here, porosity is a major factor since the ink will penetrate into a porous surface and thus increase the adhesion (Gane et al., 2006; Koivula et al., 2008). Consequently, rubbed off ink was observed on the samples coated with only latex from both the Sutherland and from the vibration table. When pigment was added to the system, the tendencies between the two methods started to differ. Pigment enables for a pore structure and thus a higher ink adhesion, and the print disturbances of removed ink after the rub off tester decreased while the print disturbances after transport simulations turned into scratches and polishing.

When the calendering temperature increased, the porosity of the coating and the roughness on a particle size scale, 0.1-1 µm, decreased. The decrease in porosity decreases the adhesion of the ink onto the surface (Gane et al., 2006; Koivula et al., 2008) and consequently the rub off tendencies in the Sutherland was higher. At the same time, the print disturbances after transport simulation turned from scratches to polishing as observed on the earlier friction study (Rättö, 2012) rather than rubbed off ink. This is in accordance with the results of Martinez (2005) who showed that the abrasiveness due to presence of sharp particles at the counter surface affect wear considerably, and the results of Salesin et al. (2008) which suggest that different mechanisms might be present for different type of samples. It is therefore suggested here that the Sutherland rub-tester measures the adhesion of the ink onto the substrate while print disturbances during transport seems to depend more on friction mechanisms and plastic deformation of pigment coated surfaces.

5. Conclusions

The print disturbances due to wear during transport and handling can be classified into three different categories: removed ink (rub off in Sutherland), scratches and polishing. The occurrences of each of these categories depend to a great extent on the surface structure of the coated substrate.

Wear during rub testing with Sutherland and wear during transport simulation differ quite considerably. Rub testing measures the adhesion of the ink onto the surface while print disturbances during transport simulation depended on the plastic deformation due to friction during sliding of two surfaces onto each other. Ink adhesion can be improved by an appropriate pore structure and surface chemistry. Print disturbances of coated substrates after transport can on the other hand be minimized by smoothing the paper surface on a particle size scale (0.1-1 μm), either by the choice of a flat pigment (clay) or by high temperature calendaring.

Acknowledgments

The authors express their abundant thanks to Ångpanneföreningens forskningsstiftelse, to Vinnova and to RISE for their financial support. They also express their gratitude to Axeb AB, Falex Tribology, FrontPac, Peterson Packaging, Sony Mobile Communications and Sun Chemical for their support in this research work.

The authors also wish to thank Mrs. Jolanta Borg for preparing the laboratory-coated papers, Mrs. Anni Hagberg for performing the laboratory printing of the samples and the contact angle measurements, and Mr. Anders Herbner for performing the transport simulation tests.

References

- ASTM D4169 - 09 Standard Practice for Performance Testing of Shipping Containers and Systems.
- ASTM D5264 - 98 (Reapproved 2011) Standard Practice for Abrasion Resistance of Printed Materials by the Sutherland Rub Tester.
- Back, E. L., (1990): Paper-to-paper and paper-to-metal friction, TAPPI Int. Paper Physics Conf., TAPPI Press, Atlanta, GA, 49,1991, pp 49-65.
- Bäckström, M., Fellers, C., Htun, M., (1999): The influence of kappa number and surface energy on paper-to-paper friction, Nord. Pulp Paper Res. J., 14, 3, pp 204-208.
- Enomae, T., Yamaguchi, N., Onabe, F., (2006): Influence of coating properties on paper-to-paper friction of coated paper, J. Wood Sci., 52:509-513.
- Fellers, C., Bäckström, M., Htun, M., (1998): Paper-to-paper friction - paper structure and moisture, Nord. Pulp Paper Res. J., 13, 3, pp 225-232.
- Gane, P. A. C., Ridgway, C. J., Gliese, T., (2006): A Re-evaluation of factors controlling print rub on matt and silk coated papers, Nord. Pulp Paper Res. J., 21, 3, pp 382-394.
- Garoff, N., Jernberg, S., Nilvebrant, N.-O., Fellers, C., Bäckström, M., (1999): The influence of wood extractives on paper-to-paper friction, Nord. Pulp Paper Res. J., 14, 4, pp 320-329.
- Gunderson, D. E., (2000): Concerning the coefficient of friction, Tappi J., 83, 6, pp 39-41.
- Gurnagul, N., Ouchi, M. D., Dunlop-Jones, N., Sparkes, D. G., Wearing, J. T. (1992): Factors affecting the coefficient of friction of paper, J. Appl. Polym. Sci., 46, 5, pp 805-814.
- Higashijima, K., Sato, J., Yamauchi, T., (2010): Friction of coated and non-coated papers-Effect of real contact area, Proc. Progress in Paper Physics Sem., FPInnovations, Montreal.
- Higashijima, K., Yamauchi, T., (2011): Frictional contact of coated paper and its surface chemical analysis, Seni Gakkaishi, 67, 3, 72-75.
- Holm, M., Husband, J., Preston, J. S., (2008): Influence of fillers in the scavenging of surfactants in the fluid phase of newsprint and the resultant coefficient of friction, PTS Paper Symposium 2008, Munich, Germany, 16-19 Sept., 2008, p9.
- Hoyland, R. W., Neill, M. P., Keenan, T., (2000): Factors affecting the frictional properties of paper - the effect of ASA neutral size, Pap. Techn., 40, 10, pp 50-52.
- Johansson, A., Fellers, C., Gunderson, D., Haugen, U., (1998): Paper friction - influence of measurement conditions, Tappi J., 81, 5, pp 175-183.
- Karademir, A., Hoyland, R. W., (2003): The sizing mechanism of AKD and its effect on friction, Appita, 56, 5, pp 380-384.
- Kawashima, N., Sato, J., Yamauchi, T., (2008): Paper Friction -Effect of Real Contact Area, Seni Gakkaishi, 64, 11, pp 329-335.

- Koivula, H., Gane, P., Toivakka, M., (2008): Influence of ink components on print rub, *Nord Pulp Paper Res. J.*, 23,3, pp 277-284.
- Martinez, E., (2005): Effect of the abrasive properties of the packaging on the transport of delicate products, 22nd IAPRI Symp., Campinas, Brazil, May 22-24.
- Rättö, P., (2012): An investigation of friction mechanisms of paper-to-paper friction of coated papers, *Nord. Pulp Paper Res. J.*, 27, 1, pp 122-129.
- Rättö, P., Barbier, C., Rigdahl, M., (2000): An investigation of the friction properties of coated paper, *Nord. Pulp Paper Res. J.*, 15, 4, pp 351-356.
- Salesin, E., Scott, J., Nishimura, D., Adelstein, P., Reilly, J., (2008): Abrasion of digital reflection prints, 24th Int. Conf. on Digital Printing Techn., Pittsburgh, PA, USA, Sept 6-11, 2008, pp 232-234.
- Schoelkopf, J., Gane, P. A. C., Ridgway, C. J., Matthews, G. P., (2000): "Influence of inertia on liquid absorption into paper coating structures", *Nord Pulp Paper Res. J.*, 15:5, pp 422-430.
- Ström, G., (2005): Interaction between offset ink and coated paper: a review of the present understanding, *Adv. in Paper Sci. and Techn.: 13th Fund. Res. Symp.*, Cambridge, UK, 11-16 Sept. 2005, vol. 2, pp 1101-1137.
- Ström, G., Gustafsson, J., (2005): "Physical and chemical drying in sheet-fed offset printing on coated paper", 22nd PTS Coat. Symp., Baden Baden, Germany, 20-22 Sept. 2005, Paper 15
- Teshima, T., Kawachi, Yoshiteru, K., Kanehiro (1990): Evaluation of abrasion resistance in transport packages, *Pack. Tech. And Sci.*, 3:161-171.
- Withiam, M. C., (1991): The effect of fillers on paper friction properties, *Tappi J.*, 74:4, pp 249-256.





3

Media and the consumer

Augmented Reality as a technology bringing interactivity to print products

Anu Seisto¹, Maiju Aikala¹, Ravi Vatraru^{2,3}, Timo Kuula¹

¹ VTT Technical Research Centre of Finland

P.O.Box 1000, FI-02044 VTT, Finland

E-mails: anu.seisto@vtt.fi; maiju.aikala@vtt.fi; timo.kuula@vtt.fi

² Copenhagen Business School

Howitzvej 60 2.14, DK-2000Frederiksberg, Denmark

E-mail: vatraru@cbs.dk

³ Norwegian School of Information Technology (NITH)

Schweigaardsgate 14, N-0815Oslo, Norway

E-mail: vatraru@cbs.dk

Abstract

Augmented Reality (AR) is the technique of superimposing virtual objects in the user's view of the real world, providing a novel visualization technology for a wide range of applications. Hence, it is a user interface technology that combines the perception of real environments with digital, virtual information. AR is also a promising tool for creating playfulness connected to printed items. In this study we present one example of creating an interactive and playful advertisement for a printed magazine by innovating possible outcomes together with a publisher (Aller), an advertiser (brand owner, Sinebrychoff) and technology experts (Undo and VTT).

The whole process was carried out in close contact with the readers and their viewpoints were taken into account in several parts of the design process. Based on the results, more than the easiness of the application, the readers of the magazine studied valued the inspiration and connectedness that the use of the application offered. The overall rating of the application was positive and encouraging for the future use of the technology. It may also be concluded that the use of AR applications in conjunction with print products makes it possible to expand the scope of the traditional marketing mix.

Keywords: augmented reality, hybrid media, mobile services, technology acceptance

1. Introduction

Augmented Reality is a promising tool for creating playfulness connected to printed items. In this study we present one example of creating an interactive and playful advertisement for a printed magazine by innovating possible outcomes together with a publisher (Aller), an advertiser (brand owner, Sinebrychoff) and technology experts (Undo and VTT). The whole process was carried out in close contact with the readers and their viewpoints were taken into account in several parts of the design process. VTT was in charge of the technical implementation, Undo of providing the 3D content, Sinebrychoff of the product that was advertised and Aller of providing the media environment in the form of the ELLE magazine. The project offered a fruitful case study of using technology in a consumer application. The aim of the cooperation was to bring new dimensions into advertising and to give the readers new experiences. The approach is also an excellent example of combining printed and digital content in advertising and this way making printed advertisement interactive. At the same time, a brand can be presented in a new environment and new kind of buzz may be created around it. Video of the application may be found at:

<http://www.youtube.com/watch?v=UCH16hSCQqg>.

In this paper, we are presenting the user centric process that was chosen for the study and results from it. We are evaluating the application mainly from the viewpoint of technology acceptance. However, as we are focusing on consumer applications, it is very important to also consider their business potential.

1.1 Augmented reality

Technology for combining print with digital has been available for several years now, and different commercial applications have been tested and used since the early 2000's. The applications designed with 2D barcodes, such as QR or Upcode, to be used with mobile phones to link physical products with digital content

have been very popular in Japan, but only recently have more and more applications emerged also in Europe and North America. Recently also several applications utilizing Augmented Reality technology have been published. Augmented Reality (AR) is the technique of superimposing virtual objects in the user's view of the real world in such a way that they form one environment (Höllerer and Feiner 2004; Vallino 1989). This reality of mixed information can be interacted within real time, and it is registered in 3D (Azuma 1997; Azuma et al. 2001). One of the first applications combining printed and digital information is a printed product catalogue from 2004, on which 3D images of the products could be seen through data glasses when looking at the catalogue. After that, several examples utilizing the PC and a web camera have been published. Dibidogs Augmented reality book for children (<http://www.youtube.com/watch?v=aR-g9RbYUYs>) can be mentioned as an example. Most recently also applications where smart phones have been used as the tool combining printed and digital content.

Achieving a convincing and believable combination of the real and the virtual worlds is possible with AR technology, but the system often requires a detailed and accurate model of the real scene and the virtual information. Hence, traditionally, AR applications are only available on high-end desktop computers or notebooks as they are the devices that have enough computing power. However, with the rapid revolution of mobile devices in the recent years, smart phones nowadays are often equipped with processors and memory that makes mobile AR applications possible. Another feature of the smartphones is that they come with camera enabled, resulting in increasing popularity of mobile AR applications. Rapid development of sensor and communication technology makes mobile devices increasingly aware of the information resources and affordances nearby, the user's social network, device orientation, and other characteristics of the context. When location awareness is added to the application, mobile AR may be applied in a wide variety of situations in consumers' everyday life (Häkikilä 2006; Kaasinen 2003; Olsson et al. 2011; Oulasvirta 2004; Peng 2003). New demonstrations and commercial applications in this area appear constantly.

The growing use of smartphones and reading pads are affecting people's media use habits. Because access to web services is everywhere, consumers are more and more used to getting updated information based on their instant needs. This sets increased demands for printed products in order to compete with other media. At the same time, a sophisticated combination of media could generate benefit for both consumers and stakeholders in the production chain of traditional media.

1.2 Technology acceptance

User acceptance is crucial to the success of new technologies but it is difficult to predict. User acceptance of new technologies that are not just incremental improvements on existing ones but cause clear changes in peoples' lives, so-called disruptive technologies, is especially hard to predict because these technologies may take decades or longer to undergo the transition into everyday objects (Norman, 1998). Similarly, predicting acceptance in the case of radical innovations is challenging, since consumers are not always able to perceive or explicitly state the value of a radically new product, but instead, they need to learn the value by experimenting it (von Hippel, 1986).

Kaasinen (2005) studied the user acceptance of mobile services, in particular mobile Internet and location-aware information services targeted at consumers based on a series of field studies of different services. Her studies took into consideration e.g. the following questions: What kind of general attributes can be recognized in the services that affect user acceptance? What kinds of service entities are acceptable both by the end users and the service providers? How can we balance user needs, the service provider's interests in providing services, and the possibilities offered by the technology?

Technology acceptance models aim at studying how individual perceptions affect the intentions to use (information) technology and further the actual usage as presented in Figure 1. According to the Technology Acceptance Model for Mobile Services (Kaasinen, 2005), user acceptance of mobile services is built on three factors: *perceived value of the service*, *perceived ease of use* and *trust*. These three factors affect the intention to use a mobile service. With mobile services targeted at consumers, taking the services into use is often a major obstacle to the user. A fourth user acceptance factor, *perceived ease of adoption* becomes more prominent as the user proceeds from an intention to use to actual usage.

Olsson et al. (2011) have studied the expected user experience of mobile AR services in a shopping center context. Their results were in line with the building blocks of the user acceptance of mobile services. (Kaasinen, 2005) The user experience plays a significant role in *value perception of the service*. The results showed that the identified characteristics of user experience in mobile AR services were mostly related to pragmatic

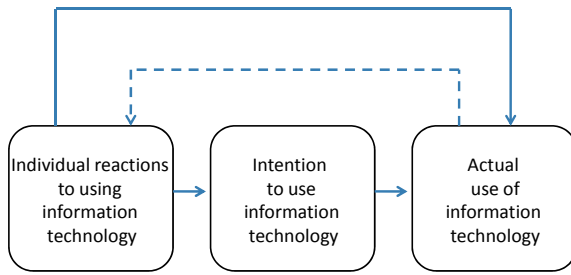


Figure 1:
The basic concept underlying user acceptance models (Venkatesh et al., 2003)

and utilitarian aspects, that is efficiency and empowerment, increased awareness and knowledge, and intuitiveness. In addition, emotional and hedonic characteristic of experience, like inspiration, liveliness, surprise, captivation and playfulness, were also expected. The aspects of *trust* were also raised in the study: the results highlighted the need for privacy management, explicit user control and feeling of having information secured. The study of Olsson et al. (2011) focused on people's expectations on experiences that mobile AR services evoke. They utilized a mock-up representation of a future mobile device without any functionalities, thus, they did not include the aspect of ease of use in their study. However, the participants anticipated the mobile AR services to be usable and offer relevant, personalized and reliable content.

1.3 Business potential

Augmented Reality offers new possibilities for designing interactive print products as the technology allows for creative linkages between the physical and digital worlds. The business potential of AR applications for print products is to be situated in two transformational developments in technology, business, and society. Internet resulted in a vertical integration of organizational channel capacities such as production, distribution, transaction, and communication; and a horizontal integration of organizational communications such as advertising, public relations, and promotion (Li & Leckenby, 2007). Social media channels that emerged from the participatory turn of the internet facilitated by developments in social computing created new opportunities for interaction and innovation within and across the different stakeholder groups in both the public and the private sectors. This had led to a "Concomitant Convergence" of technologies, terminals, touch-points, and services (Vatrapu, 2012).

AR applications enable print products to explore and exploit the business opportunities resulting from the Concomitant Convergence. As the e-Media report (Lindqvist, Bjørn-Andersen, Kaldalóns, Krokan, & Persson, 2008) points out, technological convergence and terminal convergence leads to service convergence. The evolution of touchscreen smartphones with high-speed mobile broadband, wireless internet access, and mobile apps is a good example for the concomitant convergence of technologies, terminals, and services. This is further evidenced by the slogan "there's an app for that" with regard to erstwhile standalone services often offered on unique and distinct terminals. Four particular concomitant convergences are relevant for the purposes of this paper:

- Design: Local, Social, and Mobile;
- Media: Owned, Paid, and Earned;
- Interactions: My Place, Your Place, and Our Place;
- Scorecards: People, Planet, and Profit.

1.2.1 Design: local, social and mobile

The coming together of social navigation and recommendation, local business discovery, and mobile applications and services has been hailed as "SoLoMo" (portmanteau of Social, Local, and Mobile). This concomitant convergence refers to the deployment of mobile applications in order to intertwine the online social world of the users with the local physical contexts and services of organizations. AR applications for print products operating in this design space can offer value-added services that are personalized and hyper-local.

1.2.2 Media: owned, paid and earned

With respect to the marketing communications from the organization and the customer conversations about the organization, there is a now tripartite distinction of the media world: Owned Media, Paid Media, and Earned Media. Owned Media refers to the media properties owned and controlled by the organization (e.g.

website). Paid Media refers to the purchasing of advertisements and promotional materials in media channels (e.g. TV Commercials, Search Engine Marketing in the form of Adwords on Google, Facebook advertisements). Earned Media refers to the coverage in traditional and new media channels that is not directly paid for. AR applications for print products have the potential to bridge these disparate media worlds.

1.2.3 Interactions: my Place, your place, and our place

Just as with media, a tripartite distinction can be made with respect to the Customer-Organization interactions. From an organizational point of view, My Place refers to the customer interactions located on discussion forums owned and controlled by the organization (e.g. customer support forums). Your Place refers to the customers' interactions with the organizations' goods and services at their own personal interactional sites (e.g. Facebook wall of a customer). Our Place refers to interactional spaces that engender a sense of community and co-ownership between the organizations and its consumers (e.g. a Facebook page of a brand community). AR applications for print products can facilitate novel types of online communities that include not only social engagement but also playful experiences

1.2.4 Scorecards: people, planet and profit

With the emergence of Balanced Scorecards (Kaplan & Norton, 1992) as strategic management systems, the debate on Corporate Social Responsibility (Friedman, 2007; Harrison & Freeman, 1999), and the current social media revolution, social responsibility, environmental sustainability, and economic profitability become critical dimensions of measurement and evaluation for both organizations and its stakeholders. As such the new generation of business scorecards needs to compass metrics and key performance indicators across these three critical organizational dimensions. AR applications for print products can empower the consumers to make real-time decisions in what is increasingly a complex consumer decision-making environment.

2. Methods

A user-centric approach was taken in the design process of the new mobile AR application already from the very beginning. The process was adopted from the ISO 9241-210 standard "Human-centered design for interactive systems" and is illustrated in Figure 2.

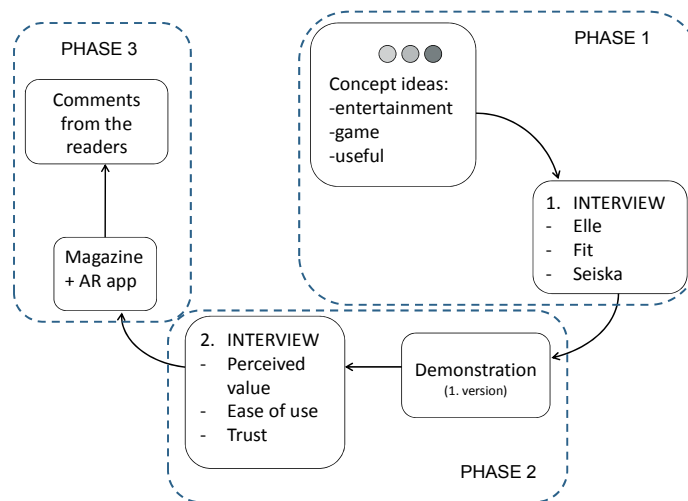


Figure 2: Structure of the design process and the different phases of user involvement for the AR application in a printed magazine

The process started with a state-of-the-art review of AR applications. Based on the review, the applications were roughly divided into three groups with applications that were purely entertaining, games and game-like applications and finally applications that intended to be useful for their focus groups. These applications were used as examples in focus group interviews carried out with the readers of three Aller Media magazines: ELLE (fashion, focus group interview: 6 female young adults), FIT (sports, focus group interview: 6 female young adults) and Seiska (gossip, focus group interview: 3 male and 2 female middle aged adults). In the first group interview the main goal was to get an understanding of the general attitudes of the users towards

mobile applications and specifically AR. Examples of mobile applications were presented to the users and they were asked to give ideas of applications that would be attractive to them. Based on the results of the interviews, the most promising focus group and application type were chosen.

In the second phase of the process the first version of the mobile AR application was built and used to demonstrate the application in a group interview for one focus group (ELLE readers, 7 female young adults). In this interview the focus was mainly on the technology acceptance of a mobile service based on the TAM for mobile services by Kaasinen (2005). Personal mobile devices are increasingly being used as platforms for interactive services, but as the approach and the technology are not well known for the consumers, it is interesting to take this viewpoint. Ease of use is important, but the applications and services should also provide clear value to the user and they should be trustworthy and easy to adopt. Themes for this group interview were determined from this starting point.

In the final phase of the process, the users were interviewed after the launch of the mobile AR application. The Golden Cap Sparkly advertisement was published in the 2011 December issue of ELLE magazine in Finland, and comments from the users were collected through a questionnaire and by phone interview at the end of 2011. Altogether 20 readers filled in a questionnaire and were invited to take part in a phone interview. In this final interview the users were asked to evaluate and rate the application from different perspectives and to explain why they would or would not be interested in using similar applications also in the future.

3. Results

3.1 General attitudes of consumers towards a mobile AR application

In the first interview, different examples of mobile AR applications were presented to the readers of three different magazines. None of the readers were familiar with the term Augmented Reality, but when looking at the examples, all of them knew some mobile applications and nearly all of them had sometimes used a mobile application. About half of the interviewees thought of themselves as active users of mobile applications. The most enthusiastic users of mobile applications said that they are interested in technical devices and would be ready to personally invest on technology. They also owned a smartphone and/or a tablet. The ones that used mobile applications the most were clearly the ones with a busy and mobile lifestyle. For example, they found it convenient to use Facebook, read e-mails or just surf the net while commuting. In addition, as they were on the move a lot, they also enjoyed having map and navigation services easily at hand. The positive attitude towards mobile applications in general aroused from this same need. That is, mobile applications were used to ease the ordinary daily routines and for achieving some personal goals. In other words, usefulness was the primary reason motivating the use of mobile applications. The results from the first group interviews are summarized in Figure 3.

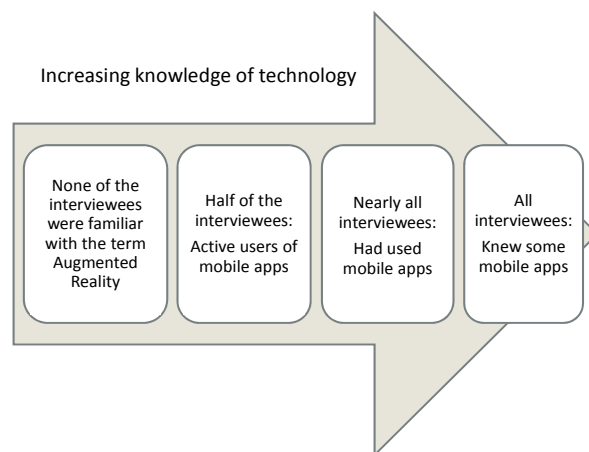


Figure 3: Summary of the results of the first group interview

The basic motivation for the use of a mobile application was very similar in all three groups interviewed. However, as the interests of the focus groups were different, also the issues they found useful were different. The ideas that the users came up with as useful applications were guided by their own interests, which deri-

ved from similar needs as their choice of a magazine and is also supported by the content of the magazine. In all three groups, the idea of achieving additional information of an article or advertisement in the printed magazine in digital form in the smartphone was well received. In addition, in all of the focus groups studied, games or game-like applications did not receive any spontaneous interest. However, competitions and discounts were found more appealing.

Based on the interviews and the specific user needs, the ELLE readers were chosen as the focus group to continue with. The attitudes of the ELLE readers were well in line with the aim of this study to make a real life case with an advertiser. Even though the readers of the ELLE magazine are mainly interested in fashion and beauty, they are also an appealing focus group for a drink such as Golden Cap Sparkly by Sinebrychoff. However, Sparkly being a mild alcohol drink, there were several legal issues and restrictions that needed to be taken into account when moving further into developing the first prototype of the application. For example, even though the general attitude towards discount coupons was positive among the readers, it is not allowed to mention a discount in an advertisement for alcohol beverages.

3.2 Acceptance of a mobile AR application in a fashion magazine

We utilized the technology acceptance approach as the main theoretical frame work when interviewing the ELLE readers again in the second and third phases of the study, i.e. before and after publishing the advertisement. In the second interview we also presented the first version of the mobile AR application that was used together with an advertisement in the ELLE magazine (Figure 4).

For brief description of the application, the user downloads it from AppStore and is then able to play a mobile AR game using the iPhone. The user points the phone to the advertisement in the ELLE magazine and sees a 3D Sparkly bottle augmented in the camera image. The bottle starts wobbling and falling. If the user manages to keep the bottle standing for fifteen seconds, he/she gets as reward a mobile discount coupon for Sparkly which he/she can utilize in the nearest restaurant, shown on the map. The user can also share the coupon with friends, read product info etc.

In the focus group interview, clearly the most important issue from the viewpoint of the readers was the perceived value of the service. It is very important that the service is well in line with the interests of the focus group. The readers were especially happy with the possibility to share the discount coupon with their friends, and found this feature even more useful than getting the coupon themselves. They would have liked an application that had more uses than just one advertisement, possibly an "ELLE app" that could be used for several advertisements and editorial content in ELLE. They also mentioned that a mobile application could make other net-based activities easier, e.g. taking part in competitions.

Ease of use was not seen as an issue by the ELLE readers. Even though the focus group is not especially technology oriented, they are familiar with several mobile services and frequent users of some. Also, the readers found the service trustworthy. They trust mobile services as much as any digital services and they are very aware of leaving information of them when using a service.



Figure 4:
Interactive advertisement utilizing AR technology in print magazine

The most important factor was, however, the high trust of the readers on the ELLE magazine. ELLE is a very strong brand, and therefore any advertisement in the magazine is highly trusted. Several dissenting opinions were received on simultaneous use of a magazine and a smart phone, some readers found it very natural while others hesitated.

Based on the focus group interview, ease of use and trust are not considered as hindrances for the use of a mobile service in combination with a printed magazine, as long as the magazine has a strong brand. In addition, perceived value of the service was clearly emphasized and the usefulness of the service in the specific focus group has to be very clear. The comments obtained from the readers after the Sparkly advertisement had been published were very well in line with the focus group interview.

Using a scale of 1 to 10, the readers gave the best scores on the application being easy to download (8.1) and fast to start (7.4). Also reading the AR marker on the magazine with the smart phone was considered easy (7.6). Even though the game was considered fairly difficult (4.2), some readers were quite happy with it. The overall rating of the app was positive (all ratings above 6). The app was considered quite pleasant and using the magazine together with a smart phone was quite inspiring. Based on this first experience, the ELLE readers' attitudes of having more AR apps in the magazine is fairly positive. The readers' comments were also mainly on the positive side:

"It was fun to find something extra in the magazine. This of course means that the phone needs to be available when reading the magazine. A very nice idea, hopefully there will be more in the future."

"...it took a while to understand how to play the game but otherwise this was nice."

In the final interview, the users were also asked to comment why they would or would not be interested in using an interactive print advertisement based on the AR technology in the future. In general, the attitudes of the users were positive:

"[I would use it] for winning prizes and for getting experiences."

"[I would use it] because it's fast and fun"

However, some doubtful comments were also expressed. In these comments, the fear of the readers was mainly that increasing amount of interactive advertisements would result in applications that are not at all interesting or that their use would not be easy enough:

"If there was a game that was completely stupid, I would not use the application"

"One could get tired of applications like this... a small amount of applications could be interesting"

"[I wouldn't use it] if, for example, downloading an application was really slow or if the instructions were poor"

4. Discussion

The experiences achieved from this first trial of utilizing Augmented Reality technology in bringing interactivity into an advertisement in a printed magazine were very promising. As a starting point, mobile applications and especially AR applications are not yet well known to the general public. It is therefore challenging to get people to notice, download and use an application. In addition, the AR advertisement was published in a magazine which has a focus group of young women, very much capable of using mobile applications but certainly not the most "tech savvy" when it comes to new devices and new technology. Taking this into consideration, the Sparkly advertisement was very well received. The readers of the ELLE magazine gave valuable comments along the design process that could be utilized not only for designing this particular advertisement but for future advertisements as well.

When considering how the intention of the ELLE readers to start using an AR app in connection with a printed advertisement would develop into actual usage, the most important factor is clearly in how valuable and useful the reader evaluates the application to be. Based on the interviews with the ELLE readers, the mobile AR application was evaluated as easy to use: it was easy to download, fast to start and reading the AR marker was easy. However, more than the easiness of the application, the interviewees valued the inspiration and connectedness that the use of the application offered. Hence, the factors that made the application feel as useful for the ELLE readers were more important than mere ease of use. Emotional experiences and the hedonic value are more subjective than the pragmatic experiences and utilitarian value and stem from consumers' fantasies, feelings and fun (Babin et al., 1994, Holbrook & Hirschman, 1982). Emotional experiences are important to consider in order to exceed user's pragmatic expectations and provide additional hedonic value and

pleasurable experiences (Desmet et al. 2007), and this way also getting a more profound understanding of what is considered as useful in a certain focus group.

In the shopping context, the hedonic aspect influences more the satisfaction with the retailer, positive word of mouth and repatronage anticipation, which have a vital role in building loyalty (Jones et al., 2006). In the context of this study, that is the mobile AR application in the printed magazine, the hedonic experiences can lead to stronger commitment and loyalty to the magazine brand. This can happen also other way around: if the magazine brand is strong, like ELLE magazine, the use of the mobile AR application linked to the brand can provide stronger emotional and more pleasurable experience. The strong brand also affected the readers being more open to start using new technology as they already had high trust in ELLE providing reliable content, including the advertisements in the magazine.

Situated within the context of concomitant convergence of design, media, interactions, and scorecards, AR applications facilitate the inclusion of print products in the emerging "Internet of Things" that seeks to seamlessly integrate real-world physical objects and the online digital worlds. One business potential of AR applications is to create innovative socio-technical interactions for the different stakeholders of print products. Particularly, AR applications for print products can create new socio-technical affordances for subscribers and users. Socio-technical affordances are "action-taking possibilities and meaning-making opportunities in a socio-technical system relative to actor competencies and system capabilities" (Vatrapu, 2010, p. 111). AR applications for print products can be used to create a mixed-reality environment of physical print and digital objects that are open to multiple meanings and actions. From a marketing perspective, AR applications for print products expand the scope of the traditional marketing mix of the 4P's (Product, Price, Place, and Promotion) to the 8P's associated with digital marketing that adds physical evidence, process, people, and partnerships to the 4P's model (Chaffey, Ellis-Chadwick, Mayer, & Johnston, 2009).

5. Conclusions

- New possibilities for designing interactive print products are offered by Augmented Reality technology as creative linkages between the physical and digital worlds become possible.
- User acceptance is crucial for the success of new technology and becomes extra critical for disruptive technologies, which cause clear changes in people's lives. User acceptance of mobile services is built on three factors: value of the service, ease of use and trust.
- Mobile applications and especially AR applications are not yet well known to the general public. It is therefore challenging to get people to notice, download and use an AR application. In this study, positive feedback was obtained from the users of an AR application in combination with a fashion magazine.
- The subjects of interest of the readers guide strongly the views and wishes for the content, i.e. it may be assumed that the application will be successful the more it is designed to take into account what is important for the focus group of the magazine and what eases the lives of this focus group the most. Hence, more than the easiness of the application, the readers of the ELLE magazine valued the inspiration and connectedness that the use of the application offered.
- AR applications facilitate the inclusion of print products in the emerging "Internet of Things" that seeks to seamlessly integrate real-world physical objects and the online digital worlds. Thus, the use of AR applications in conjunction with print products makes it possible to expand the scope of the traditional marketing mix.
- The concomitant convergence of technologies, terminals, touchpoints, and services allows for completely new kind of services to be provided by the publishers to the readers. This will be studied more closely in a Nordic co-operation project that started in May, 2012.

Acknowledgments

This study was carried out as part of the Ubimedia project that belongs to the Next Media program in Finland. Aller Media, Undo and Sinebrychoff are thanked for excellent co-operation during the project.

References

- Azuma, R., (1997) *A Survey of augmented reality. Presence: Teleoperators and Virtual Environments* 6, 1997, pp. 355-385.
- Azuma, R., Bailiot, Y., Behringer, R., Feiner, S., Julier, S., MacIntyre, B., (2001) *Recent advances in augmented reality. IEEE Computer Graphics and Applications*, Vol. 21, No. 6, pp. 34-47.
- Babin, B. J., Darden, W. R., Griffin, M., (1994) *Work and/or Fun: Measuring Hedonic and Utilitarian Shopping Value. Journal of Consumer Research*, 20 (March), pp. 644-656.
- Chaffey, D., Ellis-Chadwick, F., Mayer, R., Johnston, K., (2009). *Internet Marketing: Strategy, Implementation and Practice. Financial Times/Prentice Hall*.
- Desmet, P. M. A., Porcelijn, R., van Dijk, M. B., (2007) *Emotional Design; Application of a Research-Based Design Approach. Know Tech Pol*, Vol. 20, No. 3, pp. 141-155.
- Holbrook, M. B., Hirschman, E. C., (1982) *The Experiential Aspects of Consumption: Consumer Fantasies, Feelings, and Fun. Journal of Consumer Research*, 9 (2, September), pp. 132-140.
- Häkkinä, J., (2006) *Usability with context-aware mobile applications. Dissertation, University of Oulu*.
- Höllerer, T., Feiner, S., (2004) *Mobile augmented reality. In: Karimi, H., Hammad, A. (eds.) Telegeoinformatics: location-based computing and services. Taylor & Francis Books, London*.
- ISO, International Organisation for Standardisation (2010) *ISO 9241-210:2010 Ergonomics of human-system interaction. Part 210: Human-centred design for interactive systems*.
- Jones, M. A., Reynolds, K. E., Arnold, M. J., (2006) *Hedonic and utilitarian shopping value: Investigating differential effects on retail outcomes. Journal of Business Research* 59, pp. 974-981.
- Kaasinen, E., (2003) *User needs for location-aware mobile services. Pers Ubiquit Comput*, Vol. 7, No. 1, pp. 70-79.
- Kaasinen, E., (2005) *User acceptance of mobile services - value, ease of use, trust and ease of adoption. VTT Publications 566, Espoo 2005*.
- Li, H., Leckenby, J., (2007) *Examining the Effectiveness of Internet Advertising Formats. In D. Schumann, & E. Thorson (Eds.), Internet Advertising: Theory and Research: Lawrence Erlbaum Associates*.
- Lindqvist, U., Bjørn-Andersen, N., Kaldalóns, Ö. S., Krokan, A., Persson, C., (2008) *New Business Forms in e-Business and Media. 'e-Media'. Final Report of the NICe Project 06212. VTT WORKING PAPERS: <http://www.itu.dk/people/rkva/2011-Spring-EB2022/readings/E-Media%20FinalReport%20May2009.pdf>*.
- Norman, D. A., (1998) *The Invisible Computer. MIT Press, Cambridge, MA*.
- Olsson, T., Lagerstam, E., Kärkkäinen T., Väänänen-Vainio-Mattila, K., (2011) *Expected user experience of mobile augmented reality services: a user study in the context of shopping centres. Pers Ubiquit Comput*. 20 Dec. 2011. DOI: 10.1007/s00779-011-0494-x
- Oulasvirta, A., (2004) *Finding meaningful uses for context-aware technologies: the humanistic research strategy. In: Proceedings of CHI 2004, Vienna, Austria. ACM Press, New York, pp. 247-254*.
- Peng, Z. R., Tsou, M. H., (2003) *Internet GIS, distributed geographic information services for the internet and wireless networks. Wiley, New Jersey*.
- Vallino, J., (1998) *Interactive augmented reality. Dissertation, University of Rochester*.
- Venkatesh, V., Morris, M. G., Davis, G. B., Davis, F. D., (2003) *User acceptance of information technology: Toward a unified view. MIS Quarterly*, Vol. 27, No. 3, September, pp. 425-478.
- Von Hippel, E., (1986) *Lead Users: A Source of Novel Product Concepts. Management Science*, 32/7, 791-805
- Vatrapu, R., (2010). *Explaining culture: an outline of a theory of socio-technical interactions. Proceedings of the 3rd ACM International Conference on Intercultural Collaboration (ICIC 2010)*, 111-120.
- Vatrapu, R., (2012). *Understanding Social Business. Proceedings of the International Conference on Technology Management (ICTM), 18-20, July 2012, Bengaluru, India*.



A graphic designer's view on the interaction design for mobile application development

Klemen Vadnjaj, Ana Praprotnik, Bojan Petek

Interactive Systems Laboratory
Faculty of Natural Sciences and Engineering
University of Ljubljana
Snežniška 5, SI-1000 Ljubljana
Slovenia

E-mails: klemen.vadnjaj@gmail.com; anci.praprotnik@gmail.com; bojan.petek@ntf.uni-lj.si

Abstract

Typical workflow for the design and development of mobile applications in a user-centered way requires a close collaboration between the interdisciplinary team members. Since efficiency also implies the ability for rapid prototyping and versioning of mobile applications, it is very important to choose the appropriate tools and understand their strengths and weaknesses. It is clear that modern mobile applications design and development aim towards a good user experience (UX), originally formulated as the way a person feels about using a product, system or service.

Objectives of this paper are twofold.

First, we propose a novel mobile application that aims to improve the student and teacher communication at our department. Second, we show that by choosing the advanced interaction design tools, the graphic designer's ability to prototype and communicate with the developer significantly improves. We created a prototype using the Adobe Flash Catalyst CS5.5 that can be further refined in Adobe Flash Builder 4.5. The supported mobile operating systems are the iOS, Android and BlackBerry OS. One of the weaknesses of the current version of Flash Builder is the lack of support for the flexible way to create mobile application prototype for re-use in Flash Catalyst.

Keywords: future of graphic communication, user centered design, interaction design tools, bidirectional graphic designer-application developer workflow, mobile application design and development

1. Introduction

Typical workflow for the design and development of mobile applications in a user-centered way requires a close collaboration between the interdisciplinary team members. One of the critical challenges for efficient collaboration is the choice of tools that should enable an efficient bridge between creative expressions of the designer and programming eco-system of the developer. Since efficiency also implies the ability for rapid prototyping and versioning of mobile applications, it is very important to choose the appropriate tools and understand their strengths and weaknesses (Rogers et al., 2011).

The Global Information Industry Center at University of California, San Diego, reported that one of the trends in U.S. information consumption is the rise of interaction. Specifically, it has been estimated that in the States a third of information (in words) is received interactively (Bohn and Short, 2009; Hilbert and Short, 2011). This trend combined with the rapid increase in mobile and ubiquitous information access represents one of the major challenges for designers and developers of modern mobile applications. It is clear that modern mobile applications design and development aim towards a good user experience (UX), originally formulated as the way a person feels about using a product, system or service (Norman et al., 1995).

Objectives of this paper are twofold. First, we propose a novel mobile application that aims to improve the student and teacher communication at our department. Its main innovation is in optimized, 24/7, one-point stop, and mobile access to the selected, aggregated and personalized information.

Second, we show that by choosing the advanced interaction design tools, the graphic designer's ability to prototype and communicate with the developer significantly improves. This part also highlights the observed strengths and limitations of the selected tools in a bidirectional graphic designer-application developer workflow we experienced during this project.

2. Research methods

2.1 Interaction design

Interaction Design Association (IxDA) defines the interaction design (IxD) as the structure and behavior of interactive systems (Interaction Design Association, 2010). The five fundamental principles of Interaction Design that we followed throughout our experimental work described in the next section are:

- Consistency (implies the sensitivity to change since the changes in appearance and behavior can attract unwanted attention; the designer should strive for consistency in both the appearance and behavior).
- Visibility (implies the principle to signal the availability of interactions without the hidden ones that can hinder usability and efficiency; content hinting is used to avoid this problem).
- Learnability (represents conforming to learning theories from psychology like (i) operant conditioning (positive outcome increases the probability of return to the same activity) and (ii) observational learning (eg, similar to video learning where we repeat what we have already seen)).
- Predictability (implies applying the characteristics of consistency, dependability and reliability).
- Feedback (means conforming to the concepts like indicating the system status or action progress status, communicating the future events or possibilities, as well as the completion or closure. The feedback should not disrupt the normal user interaction; should enable to undo an action; clearly display the progress indicators; and to acknowledge the interaction).

It should be noted that prototyping and evaluation phases should always be iterative. We bear in mind that we design for the final users and not for the designers or developers.

2.2 Mobile application design example

We created a prototype using the Adobe Flash Catalyst that can be further refined in Adobe Flash Builder. The application design is stored in an FXP file that contains all files and references expressed in the MXML and ActionScript languages. The prototype designed in this way can be visualized using the Flash SWF format. This provides an efficient and elegant possibility since many operating systems support Flash. One of the main advantages is also that the prototype design can be efficiently communicated without using any target mobile device (Shorten, 2010).

The backbone of our application is programmed using the Flex environment. Our principal idea was to aggregate the selected data into a main database from different faculty information servers including VIS (the main faculty server that supports education) as well as several related web servers. This enables data categorization and personalization for individual students.

In the following we briefly describe the main functionalities of the developed mobile application.

2.2.1 User registration

Figure 1 shows the developed user registration entry window that is also used to provide the user background information. This implies that every user ID represents a query to a database containing information about students' study program, user preferences and the selected personal data.

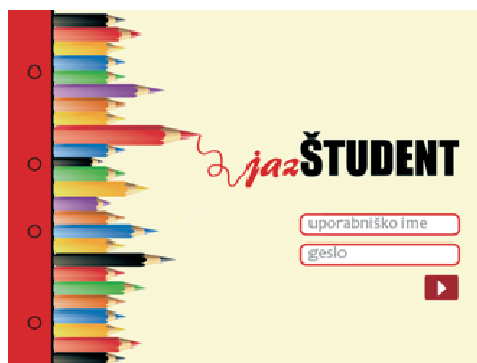


Figure 1: The user registration interface with implemented access to personalized information

2.2.2 Schedule overviews

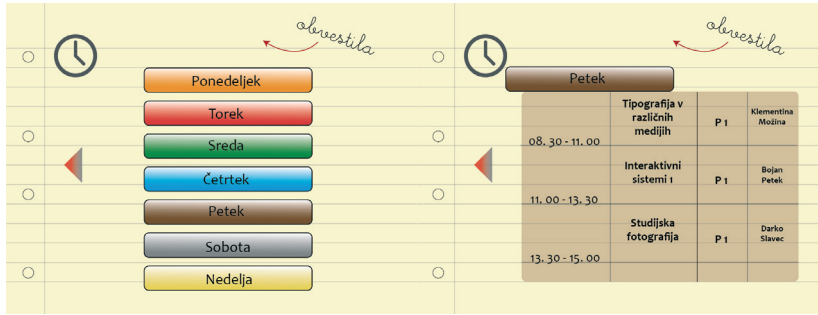


Figure 2: Weekly organized schedule overview (left), example of dynamically updated daily activities (right)

The application provides schedule overviews tailored to the specifics of a student study program. The main innovation is to establish a relationship with the users and dynamically adapt to their needs (Figure 2). The application provides only the most important data and avoids the abundance of useless information otherwise communicated by the VIS information system.

The Flex technology used in Adobe Flash Catalyst and Adobe Flash Builder allow that our application can connect live using the PHP, Adobe ColdFusion and other servers and provide the data generation in real-time. The information can be displayed in files created by Flash Catalyst using the DataList function.

2.2.3 Notifications and exam dates

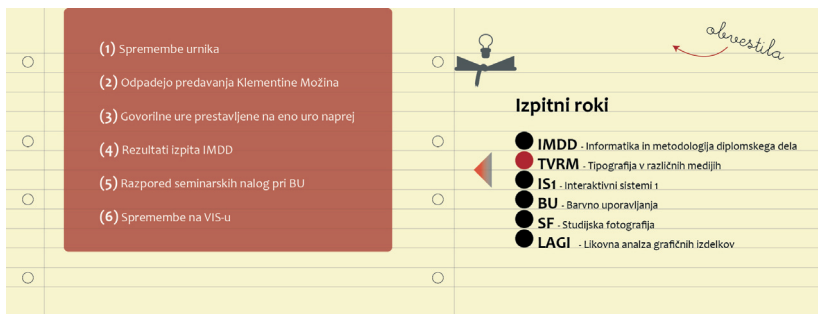


Figure 3: Short high priority notifications (left) and course specific personalized student information (right)

This functionality provides students with the updated news about their study program and other valuable information related to the study. For example, if a lesson should for any reason be cancelled just few hours before the start, the notification bar will alert the student in real-time (Figure 3). The section with exam dates helps the student to efficiently organize her or his plans. The major advantage is that all data is displayed at users fingertips. The data is transferred from the VIS server to the application server.

2.2.4 Professor information

This functionality enables the student to efficiently access any faculty professor's basic information (Figure 4).

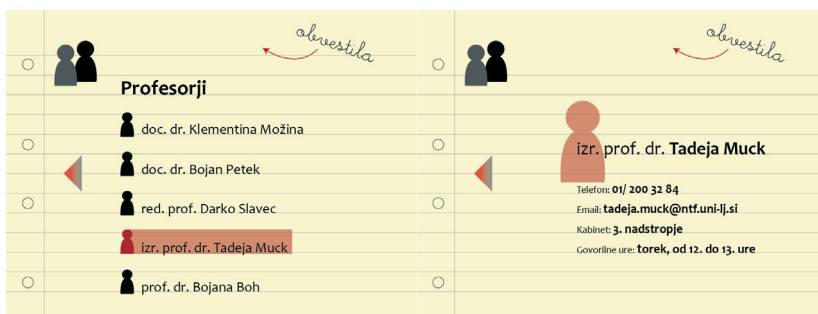


Figure 4: An example individual list of student professors (left) and the selected professor's contact data (right, updated in real time)

The provided information includes the contact information that the server will acquire from the professors database used in the VIS system. We also considered a possibility of acquiring the updated information that would change in real-time according to the professor's daily activities and obligations.

2.2.5 Parties and events

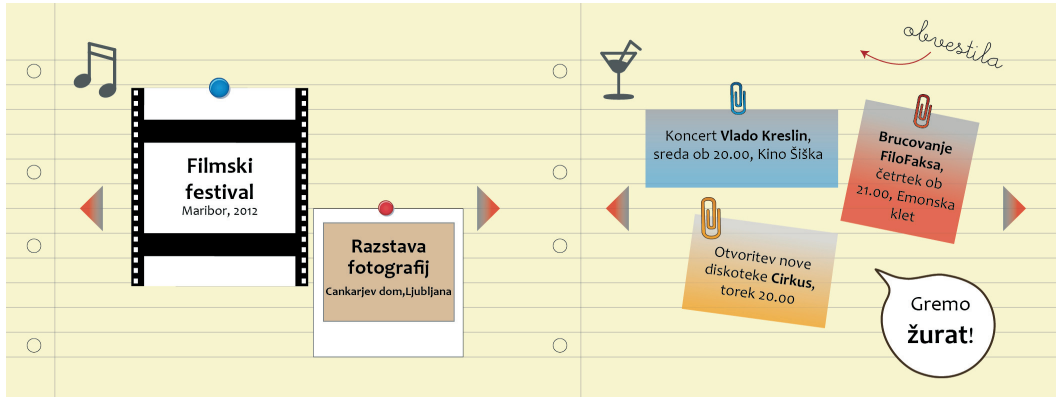


Figure 5: Selected personalized information on cultural events (left) and example short message bulletin board with students' initiatives (right)

The baseline idea for this functionality is to put the personalized information about student parties and events into the main database. This information is received by our application from servers defined by Flash Builder. The main idea is to bring to the student fresh information about student's social life that is otherwise scattered by content and location across several URLs (Figure 5).

3. Results and discussion

3.1 The Flex framework

The Adobe Flex framework resides on using two programming languages, MXML and ActionScript 3.0. Since our workflow involved efficient use of two program tools, Adobe Flash Catalyst and Adobe Flash Builder, we briefly explain their roles in the workflow as experienced from the designer's perspective during our project described in the previous section.

The design is in Flex based application described with the MXML code while the functions are implemented using the ActionScript 3.0.

The practical MXML use implies that with appropriate code and scripts we first locate the proper graphic elements in our working folder and then define the coordinates where we want to place them in our application. Using the ActionScript language we assign the proper action to the aforementioned elements.

3.1.1 Adobe Flash Catalyst

Adobe Flash Catalyst CS5.5 is a program for generating MXML markup language from the Adobe Illustrator and Adobe Photoshop design files. This program also allows the designer to define the final application elements such as buttons or text fields. The program tool was originally introduced at the Adobe Creative Suite 5 release. It provides a fast and easy way to animate and automate various elements envisioned in the project. It is not a standalone program in the sense that the project cannot be started and fully completed, since most of the projects are actually initialized using the Adobe Illustrator or Photoshop and can later be finalized in Adobe Flash Builder. The role of Flash Catalyst is therefore to define a design project into a fully programmable prototype.

3.1.2 Perceived advantages

One of the main advantages using this program is the graphic designer's ability to create the MXML documents in a very easy and efficient way. It defines a novel philosophy and design framework where also graphic designers can build standalone prototypes without the active support of a programmer during the early design stage. Understanding the ActionScript 3.0 and Flash Builder functional capabilities lead the de-

signer to build prototypes were the programmer can later very efficiently refine the baseline ideas in terms of functionality using the ActionScript language. The second advantage is the ability to create professional animations that can greatly improve the user experience.

3.1.3 Observed disadvantages

There are also many disadvantages observed during our project. The first one is the inability to add multi-touch interactivity. It can be later implemented in Flash Builder but the process is time consuming and quite complex. The second disadvantage is that there is a lack for the proper mobile support. Specifically, the prototypes developed in Flash Catalyst CS5.5 for mobile applications have to be in the form of a desktop application. Only in the later stages they can be converted into the localized mobile prototypes.

3.1.4 Adobe Flash Builder

Adobe Flash Builder 4.5 is a tool for creating applications based on the Flex framework. In addition to using the MXML and ActionScript 3.0 languages the Flash Builder also exploits and contributes to the capabilities of Adobe Flash Player, Adobe AIR platform and various backend server tools. Use of this program is primarily targeted to expert programmers. It is the successor of Adobe Flex and offers the possibility of testing, debugging and profiling the application.

The designer's knowledge of current strengths and limitations of the Flash Builder and Flex frameworks is important. It ensures that the designer who primarily uses the Flash Catalyst maintains the effective and efficient communication in providing ideas and instructions to the programmer.

3.1.5 Perceived advantages

With Flash Builder we can easily test the designer's prototype directly on the mobile device. The supported mobile operating systems are the iOS, Android and BlackBerry OS. The second advantage is the possibility to reimport the project into the Flash Catalyst without losing the code already written. This implies that we can create preprogrammed projects that can be redesigned in Flash Catalyst in the form of templates. One solution can be to use preprogrammed templates of the designer's portfolio applications for the iPad or any of the Android based tablet devices.

One of biggest benefits of the Adobe Flash technology is that using the ActionScript 3.0 we can be prototype almost everything. We can even control microcontrollers (Arduino; Phidgets). The language also supports the increasingly important 3D experience.

3.1.6 Observed disadvantages

From the designer's view there is only one important weakness. The current version of Flash Builder does not support the flexible way to create mobile application prototype for re-use in Flash Catalyst. In principle there is a way but is not supported officially by the Adobe Systems. This means that designer have to build first prototype based on the desktop application and convert it into the mobile application using Flash Builder. The action is irreversible and any further design correction cannot be made.

4. Conclusions

Mobile applications represent now one of the major trends that benefit from the rapid development of mobile phones, tablet PCs and continuous improvements in the mobile operating systems. Given that quite heterogeneous mobile devices are typically widespread across different user groups, it is necessary to provide appropriate design and development that leads to good user experience for each of them. We furthermore believe that the creation of mobile applications will evolve and will become a discipline of its own in the future graphic interactive communications.

Our principal idea was to create an application for mobile devices that will facilitate access to the aggregated information with high relevance to the student. As designers we were looking for a tool most suitable for the graphic designer. The most obvious choices at that time were the Adobe Flash Catalyst and the Flash Builder. We described their characteristics, strengths and weaknesses from the viewpoint of the specific user. In April 2012, however, Adobe decided to streamline the Flash technology in the field of mobile applications support tools. The Flash Builder has been replaced with a new workflow - the Adobe Creative Cloud.

The Adobe Creative Cloud now offers not only the tools provided in the Adobe Creative Suite but also new tools designed for web publishing and creating desktop and mobile applications. In the field of mobile application support we can find the Adobe Proto, the Adobe Muse, and the Adobe PhoneGap. The workflow philosophy is very similar to the established Flex workflow, e.g., the role of Adobe Flash Catalyst is now comparable to the role of Adobe Proto, Adobe Muse or Adobe Dreamweaver. The Adobe PhoneGap is the replacement for the Adobe Flash Builder.

The new workflow appears more flexible and well adjusted for the mobile applications development than the Flex workflow. First, we create an application using HTML, CSS and Javascript. With the Adobe Proto we can prototype it on a mobile device. Instead of Adobe Proto can also use the Adobe Muse, a very intuitive tool for designers to create the HTML-based applications. We can also create HTML applications using the Adobe Dreamweaver or in any other HTML, CSS or Javascript tools. The strongest advancement of the Adobe Flash Catalyst is the Adobe Muse, a tool for creating HTML applications and websites without hand coding.

The Adobe PhoneGap is a tool that allows creating mobile applications from the already created HTML applications. There is no need for any SDK or compiler besides the cloud ones. The main advantage of the Creative Cloud workflow is that once you write and create the mobile application you can upload it from the cloud. There is no need for further converting or rewriting. The application is provided for all major mobile platforms. In our opinion this is a very important step in the field of mobile application development. The fact is that these tools are released only a few months by now. Despite this paper was created before the new tools release the baseline philosophy remains the same.

This paper describes how we started from scratch to create our first prototype system. The scope of our paper was to complete the first out of five steps of the iterative design process. We completed the initial interface design using the Flex workflow. This step covers creation of the whole structure of the application. Usually, the designer must be very keen in the field of programming. In this paper, we have made a step forward by researching the method where the graphic designer can efficiently express ideas and creates the application without explicit hand coding. In summary, the baseline motivation for our mobile application was to provide the selected relevant information to students in a ubiquitous, fast, intuitive and simplified way. The fundamental idea was to develop a mobile application connected to a server that pools the data scattered across diverse databases and URLs. In this way, information about professor's contacts, schedules, and various curriculum and extra-curricular events is meshed up into a personalized user centered information system that can be easily accessed from the mobile devices. Further work will include a thorough usability study of the developed mobile application. The next logical step therefore is to evaluate the initial design with the users. With various methods we plan to further evaluate the efficiency of our application. The last, fifth step is the repetition of all previous steps until the system is refined to become designed in the true user-centered way. Specifically, when the GUI reaches its final form it will be handed over to the implementation specialist that will use the Adobe Flash Builder to enable the services and merge the system with the appropriate databases (e.g., VIS (UL NTF OT), ŠOU (ŠOU v Ljubljani) and the databases created by ourselves). As already mentioned the scope of our paper was to show how to achieve the first, i.e., the most important step.

References

(all URLs accessed on 26. February 2012)

- Bohn, R. E., Short, J. E., (2009). How Much Information? Report on American Consumers. Accessible at http://hmi.ucsd.edu/pdf/HMI_2009_ConsumerReport_Dec9_2009.pdf.
- Hilbert, M., Lopez, P., (2011). The world's technological capacity to store, communicate and compute information, *Science* 332(6025):60-65. Accessible at <http://www.sciencemag.org/content/332/6025/60.abstract>.
- Interaction Design Association, (2010). Definition of IxD. Accessible at <http://www.ixda.org/about/ixda-mission>.
- Norman, D., Miller, J., Henderson, A., (1995). What you see, some of what's in the future, and how we go about doing it: HI at Apple Computer. In *Conference companion on Human factors in computing systems (CHI '95)*, I. Katz, R. Mack, and L. Marks (Eds.). ACM, New York, NY, USA.
- Rogers, Y., Sharp, H., Preece, J., (2011). *Interaction Design: Beyond Human - Computer Interaction*. Wiley, 3rd edition, ISBN-10: 0470665769.
- Shorten, A., (2010). Exploring Flash Catalyst and Flash Builder workflows. Accessible at http://www.adobe.com/devnet/flashcatalyst/articles/flashbuilder_flashcatalyst_workflows.html.
- ŠOU v Ljubljani. Študentska organizacija Univerze v Ljubljani. Accessible at <http://www.sou-lj.si>.
- UL NTF OT. Prijava v študentski informacijski sistem. Accessible at <https://vis.ntf.uni-lj.si>.

Legibility on Apple iPhone 4S

Blaz Rat, Klementina Možina

University of Ljubljana, Faculty of Natural Sciences and Engineering
Department of Textiles, Chair of Information and Graphic Arts Technology
Snežniška 5, SI-1000 Ljubljana, Slovenia
E-mails: blaz.rat@ntf.uni-lj.si; klementina.mozina@ntf.uni-lj.si

Abstract

The company Apple Inc. entered in 2007 the smartphone market and their newest technological achievement of the mobile technology, introduced in October 2011, is called iPhone 4S and has numerous high-tech characteristics. One of them is Retina Display, which is the highest-resolution phone display ever launched.

Our study was conducted in the form of a research on the interdependency among typefaces and type sizes, with the purpose of drawing conclusions and making recommendations how to achieve the best possible legibility on a mobile screen. Four different typefaces were tested (one old-style, one transitional, one modern typeface and one sans-serif typeface) in four different sizes (6, 8, 10 and 12 pt) and two device positions (vertical and horizontal). The legibility research was performed with the help of readers who read the text comprised of between 120 and 130 words and the speed of reading was calculated.

The results of the study show that it is necessary to consider the chosen typeface and its size to ensure text legibility. At the type size 6 pt, the time of reading was the longest, while the text was read the fastest at 12 pt, regardless of whether in the vertical or horizontal position.

Keywords: iPhone 4S, legibility, typography, Blaznic

1. Introduction

The accessibility and usage of different mobile devices is on the increase. (Statista, 2012) The devices enable the presentation of information and contents in a special way; it is not only about the visual appearance of applications, the use of colours and animations, but also about the selection of typography, which plays a significant role in our daily lives. The reason for the increase can be found in better user experience, technologies, and appropriate use of the typeface and type size.

The company Apple Inc. entered in 2007 the smartphone market with the product called iPhone. During the last few years, five models have been produced, each with better software and hardware characteristics. Apple's newest technological achievement of the mobile technology, introduced in October 2011, is called iPhone 4S and has numerous high-tech characteristics that enable better user experience. One of them is Retina Display, which was already produced for iPhone 4 (released in 2010). It is a multi-touch screen display, which is a 3.5-inch (89 mm) liquid crystal display from scratch-resistant glass. The capacitive touch screen is designed for a bare finger or multiple fingers for multi-touch sensing. The screens of the first three iPhone generations have the resolution of 320×480 pixels (HVGA) at 163 ppi, while the display on iPhone 4 and iPhone 4S has the resolution of 640×960 pixels at 326 ppi. (Apple - iPhone 4S, 2012) This resolution is most appropriate for video calls, multitasking, HD video and, until now almost impossible on mobile phones, reading of longer texts.

Retina Display is the highest-resolution phone display ever launched. The pixel density is so high that the human eye is unable to distinguish individual pixels. The reason lies in anti-aliasing which enables the reader to experience the same feeling by looking at the screen as they would by looking at a printed page. This method is based on the description of the font outline, considering repeated colour shades that appear against background colour. The parts where the font outline united with the background were joined using middle hue values. In this way, more smooth-looking fonts are created, especially when using larger font sizes. When working with smaller font sizes, anti-aliasing influences the entire letter, which makes the letter appear soft and blurred. Nevertheless, Retina Display is able to pack four times the number of pixels into the same 3.5-inch (diagonal) display and by smoothing the jagged edges of pixels, it provides an image of quality which is higher than previously available on mobile devices. The resulting pixel density on the latest iPhones thus makes the text and graphics look smooth and continuous at any size. The effects of the display technology are

noticeable in many uses, but especially in a text where the font edges are curves which are substantially smoother than on previous display technologies. The image quality of the Retina Display derives from a number of factors (Apple - Retina Display, 2012):

- greater density of pixels,
- higher contrast ratio for brighter whites and deeper blacks,
- In-Plane Switching (IPS) technology which improves viewing angles, and
- chemically treated glass over the screen and LED backlighting to improve the image quality.

Legibility is important and according to the large number of studies on legibility (Dyson, Kipping, 1998; Dyson, Haselgrove, 2001), it should be taken into consideration.

Legibility refers to the performed process how easily the reader translates symbols into meaning (Götz, 1998; Kommer, Mersin, 2002). To enable reading, the text must have the visibility for a clear image of adequate size to be perceived in the real-time. It also has to achieve recognisability or perceptibility of letters and words which make up the text. This is affected by factors such as type style and form as well as by the person's reading skills. The third property of a text is comprehension, which is affected not only by the text content but also by its visibility and perceptibility, and by the reader's verbal capacity. (Možina, 2001; Spencer, 1969; Reynolds, 1979).

There are also some typeface characteristics to be taken into consideration to make a text more legible, i.e., distinctive character features (counter shape), x-height, ascender, descender, serifs, contrast (stroke weight), set width, type size, leading (i.e., space between lines) etc.

Our study was conducted in the form of a research on the interdependency among typefaces and type sizes, with the purpose of drawing conclusions and making recommendations how to achieve the best possible legibility on a mobile screen.

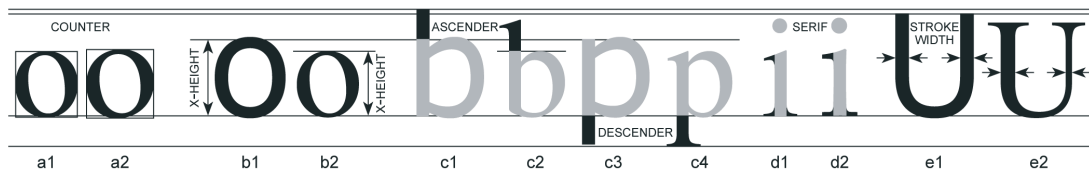


Figure 1: Some typographic characteristics which are important for text legibility, i.e., counter size (a1, a2), x-height (b1, b2), ascender (c1, c2), descender (c3, c4), shape and size of serifs (d1, d2), contrast or stroke width (e1, e2)

2. Experimental

The study was based on the results of previous researches (Možina, Medved, Rat, Bračko, 2010; Rat, Možina, Bračko, Podlessek, 2011) which led us to the typefaces and type sizes most appropriate for use in further research. The legibility research was performed according to the method "rate of work" with the help of readers who had to read a text in two different phone positions - vertical and horizontal (cf. Figure 2). The time required for the text to be read was measured, which enabled direct comparisons of text legibility in different phone positions. The study was performed by means of Tobii Mobile Device Stand and Tobii X120 Eye Tracker, which is a stand-alone eye tracking unit designed for eye tracking studies of real-world flat surfaces or video screens. The system allows substantial head movements, providing a distraction-free test environment that ensures natural behaviour and therefore valid results. The high accuracy and precision of the tracking technology ensures that the research results are reliable (Tobii, 2012). The reader distance from the device was 40 cm and the view angle was 15 degrees.

Different texts from the *National Geographic* journal were displayed in different typefaces. Four different typefaces with differences in stroke width and one with no or minor difference in stroke width were tested, i.e., one old-style (Palatino) (Možina, 2003; McLean, 1996), one transitional typeface (Times) (Možina, 2003; McLean, 1996), one modern typeface (Blaznic) (Možina, 2003; McLean, 1996) and one sans-serif typeface (Arial) (Možina, 2003; McLean, 1996), in four different sizes, i.e., 6, 8, 10 and 12 pt. The length of texts, which was the same for all readers, in a certain typeface, type size and position, amounted to between 120 and 130 words.

The speed of reading (in seconds per 600 characters) the text was calculated, based on the time required for the reading of the whole text. The pilot study was performed first and included 5 readers. No problems were encountered during the pilot testing; hence, the testing continued. The readers ($N = 35$) were aged between 22 and 45 years with normal or corrected-to-normal vision. All of them read 16 (4 typefaces \times 4 type sizes) different texts in the horizontal and 16 different texts in the vertical phone position. The texts were presented to different participants each time in a specific order to prevent any undesirable effects, influencing the final results.

The influence of the typeface, type size and phone orientation on legibility was statistically analysed with the IBM SPSS 20 software (IBM, 2012).

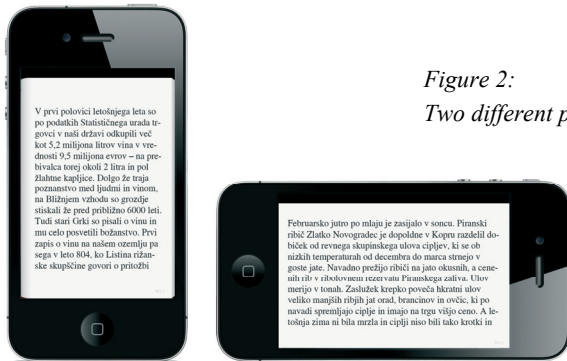


Figure 2:
Two different phone positions - vertical and horizontal

3. Results and discussion

The study was performed among a group of people, represented by both genders - 34% male, 66% female. 23% of readers were aged 22-24, 14% 25-27, 29% 28-30, 11% 34-36 and 6% 37-39 years. The remaining 6% was equally distributed into groups aged 40-42 and 43-45 years, each representing 3%. The results show (cf. Figures 3 and 4) that the text was read faster in the horizontal position.

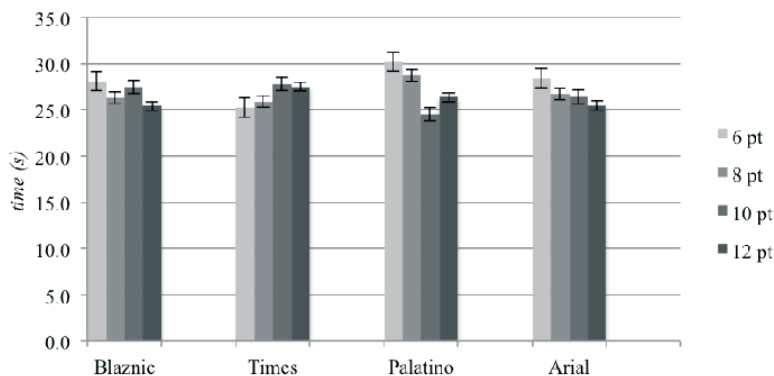


Figure 3: Time of reading 600 characters on Apple iPhone 4S in vertical position

In a more detailed analysis, it can be seen that the average time of reading 600 characters was at the typeface Blaznic 24.20 seconds, at the typeface Times 25.30 seconds, the typeface Palatino was read in 24.00 seconds and the typeface Arial in 25.00 seconds. In comparison, these measured values of reading were by 2.60 seconds faster at Blaznic, 1.30 seconds at Times, 3.50 seconds at Palatino and 1.70 seconds at Arial, followed by those measured in the vertical position. The reason is in the length of the text line, which can be described as optimal, especially at the smallest type size (6 pt), where the number of characters was approximately 65 per line. This number of characters per line is normally not optimal for displaying on screen, but the quality of Retina Display can be compared to the quality of a printed text on paper. At the largest type size (12 pt), the number of characters was approximately 40 per line. In the vertical position, the number of characters per line was approximately 35 at the type size 6 pt and 20 characters at the type size 12 pt.

Nevertheless, the wide thick stroke and higher x-height of the typeface Blaznic make it legible enough. The reason for unsatisfactory results of the typeface Palatino can be found in its (thin) strokes, which lead despite the high resolution Retina Display to worse character recognition.

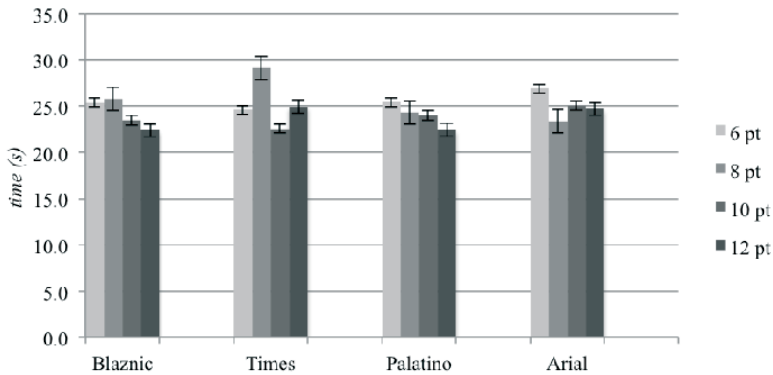


Figure 4: Time of reading 600 characters on Apple iPhone 4S in horizontal position

The text legibility was influenced by the type size (cf. Figure 5), as the results show that at the type size 6 pt, the time of reading was the longest, regardless of whether in the vertical or horizontal position. In both positions, the text was read the fastest at 12 pt, followed by the text at 10 pt and 8 pt. The difference in the time of reading between the vertical and horizontal position at the type size 6 pt was 2.40 seconds, at 8 pt 1.30 seconds, at 10 pt 2.80 seconds and at 12 pt 2.60 seconds in favour of the horizontal position. Furthermore, the longest time of reading was at the typeface Palatino, despite the typeface Blaznic being a modern typeface, i.e., a typeface style which is considered unsuitable for screens due to its very light thin stroke.

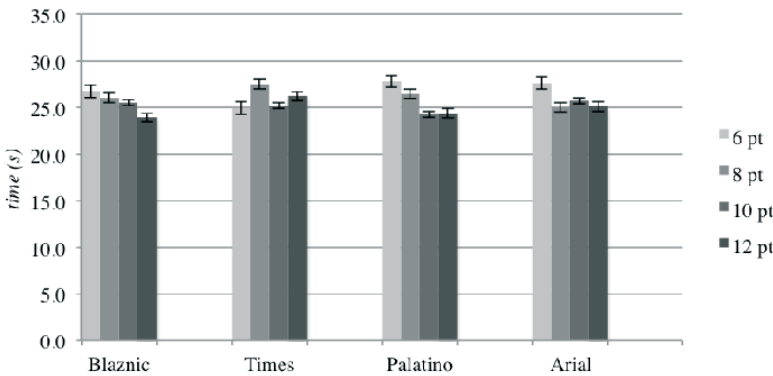


Figure 5: Average time of reading 600 characters on Apple iPhone 4S regardless of position

The analysis of text comprehension and correctness of answers shows (cf. Figure 6) that on average, most correct answers were given after reading the text written in the typeface Blaznic - 86%. In the vertical position of the device, the number of correct answers at the typeface Blaznic was escalating in dependence of the type size. On the other hand, at the typefaces Times, Palatino and Arial, the number of correct answers at different type sizes varies.

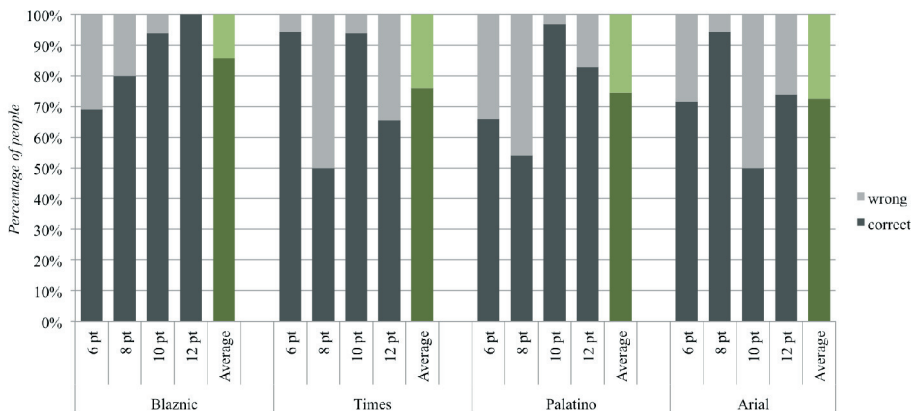


Figure 6: Percentage of people who answered correctly (vertical position of device)

The reason can be found in the text comprehension and longer time of reading; nevertheless, the average number of correct answers at all three typefaces was 74%. In a more detailed view, it can be seen that less satisfactory results were at the type size 8 pt at Times and Palatino, and at 10 pt at Arial. The highest number of correct answers at these three typefaces was achieved at the type size 10 pt at Palatino (91%); however, 100% of the answers were correct at the typeface Blaznic at the type size 12 pt. The reason lies in its widest thick stroke and the largest x-height among the tested typefaces.

In the horizontal position of the device, the results of text comprehension and correctness of answers (cf. Fig. 7) are similar to those in the vertical position. The highest average number of correct answers regardless of the type size was at the typeface Blaznic (91%), followed by the typefaces Palatino (84%), Times (81%) and Arial (79%). Again, the results vary regarding the type size, while the smallest number of correct answers was achieved at the type size 8 pt at the typeface Arial. On average, regardless of the typeface, the highest number of correct answers was at the type size 6 pt (91%), followed by 12 pt (86%), 10 pt (84%) and 8 pt (74%). Furthermore, it can be seen that at the old-style (Palatino) and transitional typeface (Times), most correct answers were given at the type size 6 pt (94%) and 10 pt (93%), at the modern typeface (Blaznic) at the type size 8 pt (97%) and 12 pt (94%), and at the sans-serif typeface (Arial) at 12 pt (100%).

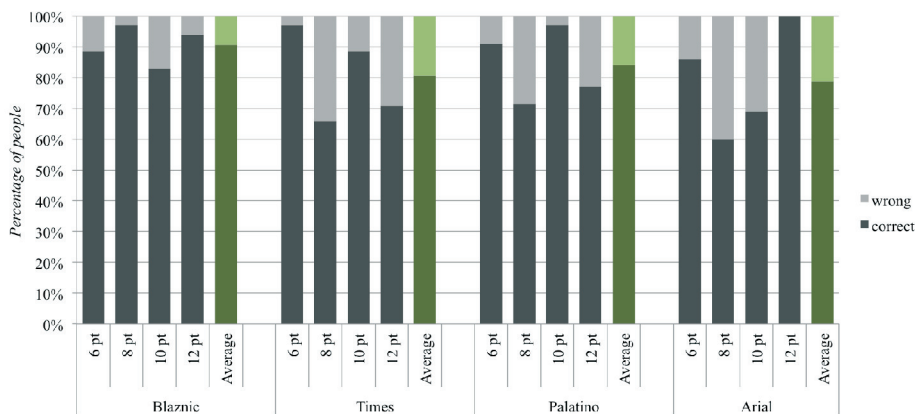


Figure 7: Percentage of people who answered correctly (horizontal position of device)

4. Conclusion

The results of the study show that it is necessary to consider the chosen typeface and its size to ensure text legibility. The obtained results reveal that the phone orientation may be of great importance. Moreover, it is important to pay attention when choosing a typeface, as a less than optimal combination of a typeface and phone orientation can lead to unsatisfactory legibility. In addition, typeface design needs to be taken into consideration to enable better legibility and text understanding.

The modern-styled typeface Blaznic has the widest thick stroke and the largest x-height among the tested typefaces, and it thus gives the best legibility results. The fact that the popularity of Apple iPhone is on the increase is a well-founded reason to continue with the research. The aim is to make Blaznic one of the most suitable typefaces for different electronic devices.

Acknowledgments

The financial support for the PhD grant from the Slovenian Research Agency for the PhD student Blaž Rat is gratefully acknowledged by the authors

References

- Dyson, M. C., Kipping, G. J., (1998), *The legibility of screen formats: Are three columns better than one?* *Computers & Graphics*, Vol. 21, No. 6, pp. 703-712.
- Dyson, M. C., Haselgrove, M., (2001), *The influence of reading speed and line length on the effectiveness of reading from screen.* *International Journal of Human-Computer Studies*, Vol. 54, No. 4, pp. 585-612.
- Götz, V., (1998), *Color and type for the screen.* *Crans : RotoVision SA*, pp. 70-99.

- Kommer, I., Mersin, T., (2002), *Typografie und Layout für digitale Medien*. München : Carl Hanser Verlag, pp. 109-143.
- McLean, R., (1996), *The Thames and Hudson Manual of Typography*, London : Thames and Hudson, pp. 58-62.
- Možina, K., (2001), *Zgodovinski razvoj knjižne tipografije : doctoral thesis*, pp. 244-290.
- Možina, K., (2003), *Knjižna tipografija*, University of Ljubljana, Ljubljana, pp. 156-169, 184-191, 254.
- Možina, K., Medved, T., Rat, B., Bračko, S., (2010), *Influence of Light on Typographic and Colorimetric Properties of Ink jet Prints*, *J. Imaging Sci. Technol.*, Vol. 54, No. 6, pp. 060403-1-060403-8.
- Reynolds, L. (1979), *Progress in documentation*. *Journal of Documentation*, Vol. 35, No. 4, pp. 307-339.
- Rat, B., Možina, K., Bračko, S., Podlesek, A., (2011), *Influence of Temperature and Humidity on Typographic and Colorimetric Properties of Ink Jet Prints*, *J. Imaging Sci. Technol.*, Vol. 55, No. 5, pp. 050607-1-050607-8.
- Spencer, H., (1969), *The visible word*. London : Royal Colege of Art in Lund Humphries, pp. 13-24.

Web sources

- Apple - iPhone 4S - See everything clearly with the Retina Display, January 2012
<<http://www.apple.com/iphone>>
- Apple - iPhone 4S - The most amazing iPhone yet, January 2012 <<http://www.apple.com/iphone>>
- Tobii - Eye tracking and eye control for research, communication and integration, January 2012
<<http://www.tobii.com>>
- IBM SPSS software, January 2012 < <http://www-01.ibm.com/software/analytics/spss>>
- Statista - Media tablets: global sales 2010–2015 (forecast), January 2012
<<http://www.statista.com/statistics/165462/forecast-of-global-sales-of-media-tablets-by-2015>>

Visualizing a content scenario for mobile devices towards inexperienced user

Chrysoula Gatsou^{1,2}, Anastasios Politis^{1,2}, Dimitrios Zevgolis¹

¹ School of Applied Arts,

Hellenic Open University, Patra, Greece

Emails: cgatsou@teiath.gr; politisresearch@techlink.gr; zevgolis@eap.gr

² Graphic Arts Technology

Faculty of Graphic Arts and Design, TEI of Athens, Greece

Abstract

The purpose of the present study concerns the examination of a scenario involving the visualizing of content at mobile devices- platforms and their respective applications. The scenario follows certain design principles that cater for interaction with inexperienced users within the interface of mobile devices. The visual design of an artifact obviously influences the way in which a user will interact with it. Gestalt laws and principles form one possible framework for the collection of helpful design guidelines. Based on field research, a prototype has been developed according to these principles. The results of a evaluation by users on the proposed visualization of content, are finally discussed.

Keywords: visual interface design, design principles, mobile interaction, inexperienced user

1. Introduction

The way in which users interact with digital artifacts is obviously of vital importance as it regards mobile devices. How to make possible interactions in a system discoverable is a significant issue in human-computer interaction and the idea of perceived affordances is sometimes used to address the problem (Miller, 1956). As Löwgren and Stolterman point out, our designed world is full of digital artifacts. Although digital artifacts rest upon on technical systems, they influence our lives at the level both of the individual and of society (Löwgren & Stolterman, 2004).

A display is a central component of a physical UI, because the interaction with a mobile device relies heavily on graphical information and visual perception. Carroll points out that "When we design systems and applications, we are most essentially, designing scenarios of interaction" (1995). Visual screen design is vital for both designers and users in their attempts to offer users the ability to interpret visual objects correctly and to interact with artefacts. More broadly, fundamental aesthetic properties, such as colour, layout, and simplicity have been found to predict correctly overall visual appeal ratings across users (Carroll, 1995).



Figure 1: The tablet application

The perceptual abilities of users vary, who therefore have different needs concerning the use of visualization (Ware, 2004). Weeimer (1995) noted that "the product's appearance can influence one's perception of how easy the product is to use and that a negative reaction to the appearance of, for example, a user interface may mean that the product is not used successfully and so not adopted" (Watzman, 2002). Lindgaard et al. (2006)

showed that impressions of the visual appeal of websites form very quickly, within 50 milliseconds. The style in which information concerning the development of some artifacts is visualized is a matter that should be considered (Hackos & Redish, 1998). Mulet and Sano (1995) argue that "good graphic design can significantly improve the communicative value of the interface, leading to increased usability". However, little research has been published on screen visual representation.

2. Visual cognition - perception

Clearly, the user's perception and interpretation of representational graphics is the key to discovering how such graphics are to be used effectively. Thus the nature of visual perception is obviously a crucial factor in the design of effective graphics. An understanding of perception can significantly improve both the quality and the quantity of information being displayed (Ware, 2004). Yet another view regarding the perception of images is given by Pettersson, who states that the perception of an image is rapid, almost immediate (Pettersson, 1999). In connection with this discovery (Pettersson, 1999) three assumptions regarding the perception of symbols can be made. First, several different symbols may convey a similar meaning and a specific message. Second, one symbol may be able to convey more than one message. Third, the user has first to learn the intended meaning of symbols. Pettersson states that the concept of "perception" is a collective designation for the processes in which an organism obtains information on the outside world. In the view of Paivio's dual coding theory, the reason why the meaning of icons are likely to be remembered better is related to the fact that the two types of information (verbal and imaginal) are encoded by separate subsystems, one specialized in the handling of sensory images and the other specialized in handling verbal language (Paivio, 1986). The visual system processes and stores more concrete information, such as images, sounds and feelings. The verbal system, on the other hand, processes and stores language and other abstract information. The two systems are independent, but connected. Furthermore, pictures are better remembered than words, because pictures are more likely to activate the image-to-word referential connections, which means that they can be coded both visually and verbally (Paivio, 1971; Moreno & Mayer, 2002).

One of the findings embodied in structural theories of perception is that certain simplified views are easier to read (Ware, 2004). This should be considered, when we want to convey information via screen design. In Miller's view, humans are capable of absorbing more information when they use their eyes, rather than any other faculty (Miller, 1956). The reasons for this have been investigated by such Gestalt psychologists as Koffka, Köhler and Wertheimer, who have argued that we constantly search for a 'good fit' between visual image and stored memories of visual objects. This process usually happens very quickly, since visual objects naturally have organised patterns and these are only minimally related to an individual's past experience (Koffka, 1935). Research into visual imagery (Kosslyn, 1980), suggests that visual recall seems to be better than verbal recall. It is not clear how images are stored and recalled, but it is clear that humans have a natural ability in the use of images. Weidemann's results regarding text-based knowledge acquisition and task performance are clearly different from his results regarding the corresponding picture-based performance (Weidemann, 1989).

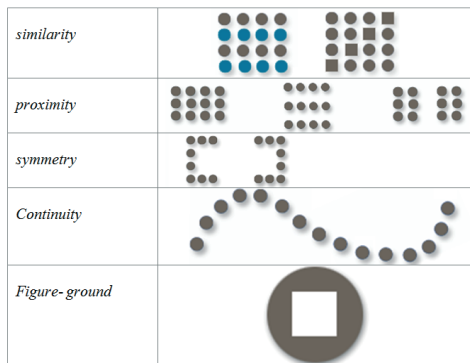
2.1 Key laws of Gestalt theory

One set of theoretical principles that can help novices construct mental models are the Gestalt laws for pattern perception used in the design of the layout of displays. Any use of a knowledge structure is dependent on users' mental models (Johnson-Laird, 1983). Most modern theories of pattern perception have their roots in the work of the Gestalt psychologists (Carroll, 2003). Gestalt theory is fundamental to visual communication design. It is generally accepted that Gestalt theory may be used to improve screen design and improve user interaction (Preece et al., 1994). In applying the theory of perception to screen design, various aspects must be considered. The Gestalt psychologists believed that perception of objects as a whole differs from the perceiving the sum its parts. They therefore focused on discovering determining principles that might explain how small elements become grouped into a whole. In Gestalt theory, context is regarded as very important to perception. Thus Gestalt laws offer guidance on how a suitable and unambiguous grouping, or division, of visual elements is to be achieved. As a general rule, spatial organization of information, i.e. page layout, must be driven by alignment and balancing criteria. These include similarity, proximity, symmetry, continuity, and finger ground. It is important to keep in mind that each principle, far from operating independently, always works in concert with every one of the others. Screens consist of both visual and interactive elements, which have gestalt properties. Furthermore, in many real-world conditions, Gestalt principles, instead of operating in separation or function independently of one another, usually interact with each other, to promote logical and meaningful perception (Quinlan & Wilton, 1998).

2.2 Gestalt principles used in this study

Similarity: Elements that look similar will be perceived as a being part of the same, which means that elements tend to be integrated into groups, if they are similar to each other. **Proximity:** Entities placed in close proximity to one another are assumed to be related. This phenomenon is a simple and powerful way of emphasizing relationships between data entities. **Symmetry:** The law of symmetry expresses the idea that, when we perceive objects, we tend to perceive them as symmetrical shapes formed around their centre. **Continuity:** Oriented units or groups tend to be integrated into perceptual wholes, if they are aligned with each other. **Figure and ground:** This is the tendency to organize perceptions by distinguishing between a figure and a background. Figure 2 illustrates the gestalt principles used in this study.

Gestalt principles of perceptual organization (Wertheimer, 1938) play a crucial role in the visual processing of graphical representations. They indicate related functionality and purpose by the use of similar properties, by grouping objects together and by separating objects from unrelated items by the use of "negative" or "white" space. Gestalt principles of perceptual organization make objects in interfaces and the relationships between them more visually striking, thus causing such objects to be interpreted, particularly by novices, in a more detailed and accurate fashion (Wertheimer, 1938).



*Figure 2:
Illustration of Gestalt principles used
in this study*

3. Study set up and methods

3.1 User analysis

Users obviously vary in terms of personal characteristics, physical abilities, cultural assumptions, education and in their expertise in interacting with artefacts. Users also vary in psychological terms, in that they present:

- Differences in perception and attention;
- Differences in short term and long term memory and
- Differences in mental models of objects.

Norman describes mental models as follows: "In interacting with the environment, with others, and with the artefacts of technology, people form internal, mental models of themselves and of the things with which they are interacting (Norman, 1983). These models provide predictive and explanatory power for understanding the interaction". Mental modes influence perception and thus the way we see and think of the world. This also holds in regard to our perception of user interfaces, our preferences, and how we generally receive and process information (Ito & Nakakoji, 1996).

There are many reasons for the problems that novice users face when using new information technologies, such as ticket vending machines, ATMs or mobile devices, on an everyday level. One problem arises from the pressures felt by designers and developers to add more features and functions. Due to perceptual abilities, users have different needs concerning the use of visualization (Ware, 2004). Another reason is that novice seem to have difficulty in articulating knowledge on which their skills rest, partly because they have little experience on which to base descriptions (Gatsou et al., 2011). Novice users feel frustrated, insecure and even frightened, when they have to deal with a system whose behaviour is incomprehensible, mysterious and intimidating (Baecker & Buxton, 1987; Buxton, 2007). Moreover, a typical user, who thirty years ago would have been a professional programmer, is now an impatient novice (Booth, 1989). Thus today the inexperienced user wants to benefit from such artefacts, as mobile tablets, which, however, are usually complex (Shneiderman & Plaisant, 2005).

3.2 Sketching a concept scenario

During this creative process, a rough and sketchy visualization style is required. Freehand design drawings like sketches have been identified as material that stimulates reflection in the early stage of design. Schön points out that drawing is crucial as a tool in this reflecting process. Designers place ideas down on paper and inspect them, during this process, they discover visual cues that suggest ways to refine and revise ideas. This situation is like having a conversation with one's self (Schön and Wiggins 1992). Storyboarding concept screen sketches constitute one effective way of exploring alternative directions while avoiding details of design. This approach allows the user to experience visualized interactions and the structure of the application by means of a creative analysis of screens that can then be designed, evaluated, and explained in more depth. Throughout this phase the preliminary designs are evaluated by means of testing, walk-through and paper mockups, in order to elicit users' comments.

Figure 3a shows the sketches of the scenario "first aid" for the four muster screens. This phase is pivotal. The scenario is as follows: the user wants to see first aid information. He selects an icon from the tablet desk top and so selects the first screen. Touching the first screen takes him to the main menu screen, where he can select the specific topic that interests him. From the second screen he can select subcategory, if he wants to enlarge photographs in order to examine details.

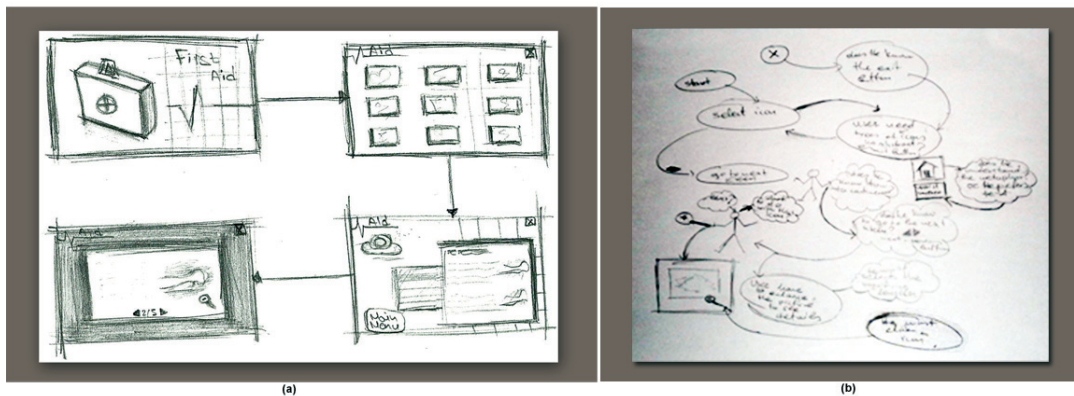


Figure 3: Storyboard paper sketches of the interaction concept

These early user observations through sketching (Figure 3b) were an invaluable experience and proved to us several important points. Firstly, we noticed that some older users had difficulty in understanding the metaphor of a home icon used on the navigation button in the main menu. Their past experiences may not have enabled them to understand the meaning of this well-known metaphor. Secondly, that menu navigation tasks could be improved in this phase. These points encouraged us to continue improving the structure and further develop our concept of 'visualising a content scenario for inexperienced users'.

3.3 Content visualization

Here we present the benefits of Gestalt laws and design principles when applied to a "first aid" content scenario for a mobile tablet application. An effort has been made for interface to accommodate the context and visual features deriving from these principles, in order to help inexperienced users. Appropriate graphic representation is a vital factor in the correct functioning of mobile applications.

For icons to evoke the desired meaning in the viewer's mind, each symbol must display a strong, direct association with the desired meaning, in the mind of both designer and user (Gatsou et al., 2011).

Icons are used here for the home screen that enables users to exploit their experience with mobile phones. To explain the layout of the visual elements in gestalt and graphic design terms: in a screen, balance occurs when all the design elements are equally distributed throughout the design (Weeimer, 1995). Menu preferences, icons and text buttons give a balance to the whole screen. In addition, the home screen uses the law of similarity to allow communication with the content. This is effected by the use of the buttons set inside red bordered boxes, which function as links to the content. This impression is then reinforced by user experience, since all these elements behave consistently. Emphasis indicates the most important element in the layout in terms of the message and is the element that stands out and is noticed first. The initial screen displays a picture of the small white first aid box (Figure 5a), which is the most emphasized visual element.

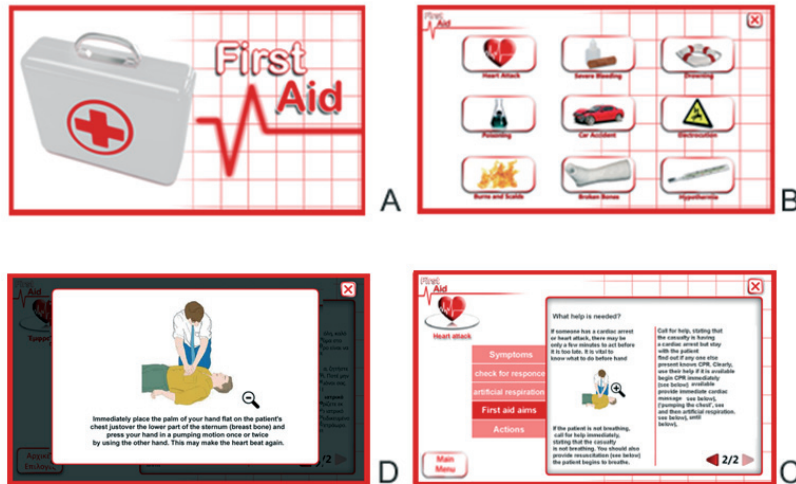


Figure 4: Visualization of content scenario. Initial screen A, home screen B, category screen C, enlargement of photo details D

Lauer notes that, if everything is emphasized, then nothing is emphasized (Lauer, 1979). Finger ground perception helps us to distinguish category headings. This is quickly perceived to be text content (Figure 5c), set on an almost imperceptible background shading (ground).

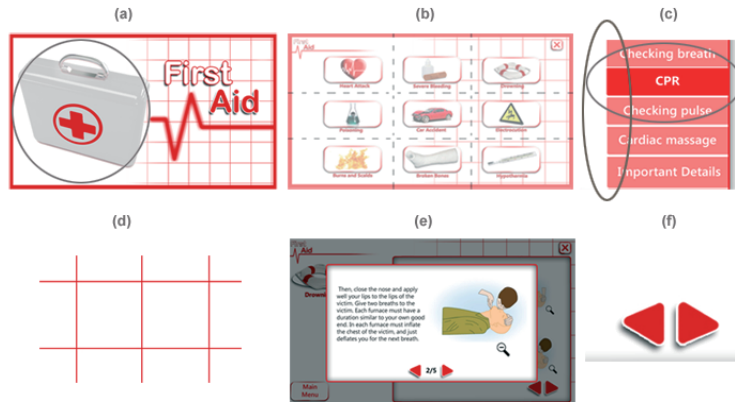


Figure 5: Screenshots of principle implementation on screen design

As for contrast is used the picture is also enlarged, which allows the details be seen more clearly. The application of the red grids to all of the screens employs the use of the principle of rhythm, as we wished to indicate sequential flow (Figure 5e) As for Symmetry, in the Figure 5f, the 'next' and 'previous' arrow buttons consist of geometrical shapes placed symmetrically. They are clearly pointing in opposite directions, so as to lead the user to next or previous screen. As regards Proximity, in the category screen design, in, for example, Figure 5c, each visual element in the subtitles is identified and clearly placed by grouping them together and by separating them from unrelated items using "negative" or "white" space. As regards Unity, a sentence conveys more information than random words on a page, whilst a paragraph conveys more information than random sentences on the page. Unity is achieved when all the design elements relate to one to another and project a sense of completeness (Resnick, 2003).

Phi (Φ - the Greek letter for "F") is the term used to represent the golden ratio. The Phi Ratio is a proportional relationship commonly accepted to possess a strong visual beauty and has a long history in the theory of aesthetics. A line can be bisected using the golden ratio by dividing its length by 1.62 (exactly 1.6180339...). A simplified version of the golden ratio is applied more commonly today in graphic arts, photography and design in the form of the "Rule of Thirds". The Rule of Thirds states that people are strongly attracted to objects placed at the intersections of hypothetical lines on a page or in a photograph divided into thirds vertically and/or horizontally (Bezanson, 2007; Lidwell et al., 2003). Phi-based proportions provide an inherent natural sense of beauty, balance and harmony, because these proportions appear so pervasively in nature.

We used the golden spiral (the Rule of Thirds) as a guide for laying out the content of the initial and the category screen. The intention was to guide the viewer's eye to the content help information and to guide him through text and pictures. The basic idea is illustrated in Figure 6.

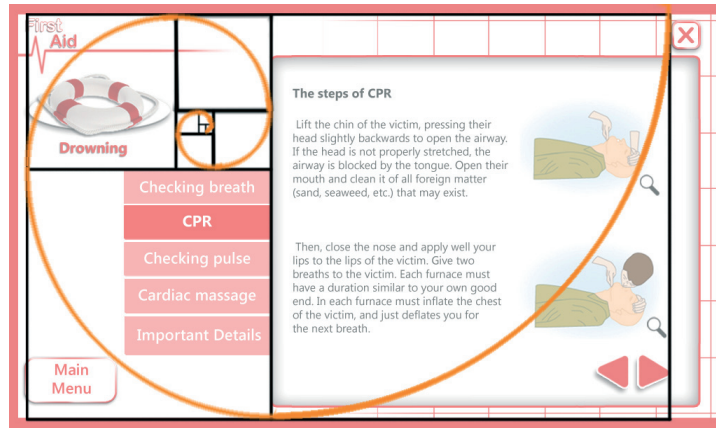


Figure 6: The use of golden ratio in screen design

4. Results of prototype evaluation

After the design phase and often the concurring with it, the iterative User Centered Design cycle continues to evaluate and test the prototype. The purpose of the experiment was to examine the effectiveness, efficiency and ease of use of prototype. Menu navigation is one of the most common interactions between user and mobile device. We required each participant to complete a mobile device task consisting of nine steps, in a specific order. According to an informal survey, these tasks are typically those first attempted by novice mobile computing users. For some of these tasks, the primary focus was on navigating or searching the menu for some application file that was required.

4.1 Participants

18 individuals (10 women, 8 men) took part in the study. Participants ranged from 15 to 74 years in age, distributed among three age groups. Participants were aged between 15-34 ($n = 6$), 35-54 ($n = 6$), 55-74 ($n = 6$) years of age, respectively. Each subject was given a brief overview of the experiment and briefed as to the purpose and procedure of the study. All participants were mobile computing novices. Participation was voluntary.

4.2 Experimental design variables

In order to evaluate task effectiveness, we measured the percentage of steps successfully solved within the set time limit (Table 1). To evaluate efficiency, we recorded the time needed to process the task, results are showed in Table 2.

In order to measure ease of use, we asked participants to rate each of the following statements on a 5-point Likert scale (1=strongly disagree, 5=strongly agree): (a) 'It was easy to complete the task'; (b) 'I felt lost in the menu'; (c) 'It was easy for me to remember how to perform'; (d) 'I did not know where to go next'; (e) 'I was satisfied with the application'; (f) 'I did not know how to reach a specific function'.

4.3 Results

The results arising from the menu navigation task show that not all users make incorrect steps. The results are showed in Table 1 and that the elder participants make more time to complete the task. More specifically, there was a significantly different operating time between age groups.

Subjects' comments regarding navigation indicate that they found the buttons self-explanatory, consistent, permitting them easily to recover from mistakes. Four participants commented that the button for carrying the user to the "next screen of heart attack" in the application menu was not clear. Figure 7 gives age groups related to time required to complete the task.

Table 1: Specific user navigation steps and user effectiveness (steps successfully solved)

Steps	Tasks	n = 18
Step 1	Turn mobile device on	94.4%
Step 2	Find the icon for the 'first aid' application	100.0%
Step 3	Select the icon and go to first screen	83.3%
Step 4	Select information for "heart attacks" via the main menu.	100.0%
Step 5	Go to screen with "heart attacks".	94.4%
Step 6	Go to next screen(menu depth: four levels)	88.8%
Step 7	Return to application main menu	88.8%
Step 8	Exit of the application	100.0%
Step 9	Turn of the mobile device	83.3%

Table 2: Mean task completion time (seconds) and Std.Dev.

Age group	Mean task completion time (seconds) and Standard deviations
15-34 (n=6)	84.2 (Std. dev. = 7.0)
35-54 (n=6)	96.7 (Std. dev. = 9.2)
55-74 (n=6)	127.7 (Std. dev. = 5.1)

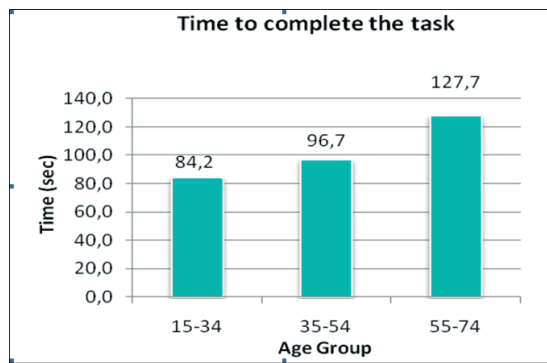


Figure 7: The interaction effect of age on operating time and mean task completion time (seconds)

Subjects' comments regarding navigation indicate that they found the buttons self-explanatory, consistent, permitting them easily to recover from mistakes. Four participants commented that the button for carrying the user to the "next screen of heart attack" in the application menu was not clear. Figure 7 gives age groups related to time required to complete the task.

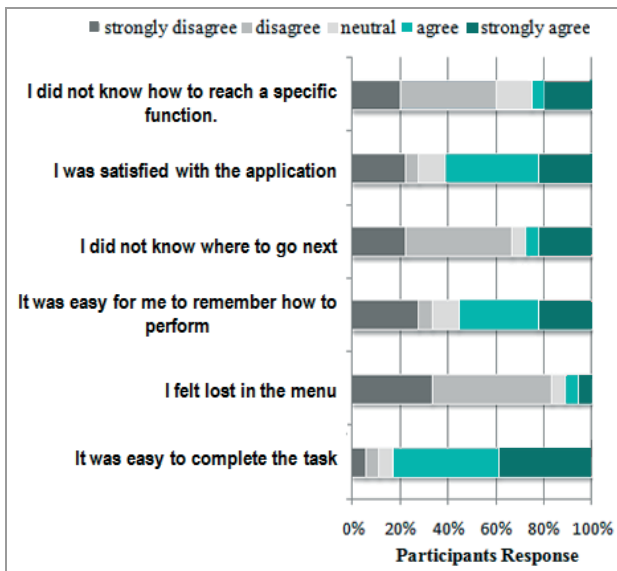


Figure 8: Participants ratings on ease of use for the application

After completing the tasks, participants rated the perceived ease of use of the mobile device. Ratings mirrored the outcomes in performance measures. Users rated the ease of use of the tablet application. The results are given in Figure 8. Participants were asked informally what the most important factor was in learning how to use the mobile device. In their view, being shown through easy, interesting applications was the most important factor, followed by the use of a hand book. Some users told us that they had never used a computer before and that they liked this approach, preferring the touch screen over other environments. Another factor that participants commented on was the ease of use of the menus. Menus are usually complicated and act as barrier between user and interface which affects user interactivity. As Lindgaard points out, user satisfaction is a complex construct that incorporates several measurable concepts and is the culmination of the interactive user experience (Lindgaard, 2007).

5. Conclusions - future work

Visualizing content information is an important process in design and a difficult skill to apply effectively in practice. Different classes of applications require different levels of emphasis of the various elements in content screens. As a first step, design teams should create storyboard sketch prototypes, to allow them to gather feedback regarding all levels of an artifact. Gestalt laws and design principles are the foundation that determines the nature of the mental representations that users generate when viewing a visual screen.

An analysis of the data shows a large increase in time across age groups. More specifically, there was a significant difference in operating time between age groups. This observation was confirmed by an analysis of the time data, which revealed that age was indeed a significant factor. In general with respect to users' interaction with mobile application strongly support the feasibility of prototype.

From this empirical study, we have learned some basic ideas on how to design effective user interfaces and present contents structurally, so that users may use mobile devices efficiently. We believe that interface design should be carefully considered for usage of the mobile devices by inexperienced users - adding communication capabilities is extremely important. Exploring the link between interaction, communication, and mobility can be a fruitful and exciting area of research for mobile computing.

We believe that developing applications to support novice user interaction is an exciting and promising area of future research for pervasive computing applications. The experience we gained will contribute to the design of future digital artefacts, since our goal is to give inexperienced users easy access to mobile devices.

Acknowledgements

This research has been co-financed by the European Union (European Social Fund - ESF) and Greek national funds through the Operational Program "Education and Lifelong Learning" of the National Strategic Reference Framework (NSRF) - Research Funding Program: Heracleitus II. Investing in knowledge society through the European Social Fund. We would also like to thank Aristovoulos Pavlakis and the participants in the study.

References

- Baecker, R. M., Buxton, W., (1987), *Readings in Human-Computer Interaction*. San Mateo CA.: Morgan Kaufmann Publishers.
- Bezanson, W., (2007), *The Life of Phi: Beauty and the Golden Ratio*. Baico Publishers, Ottawa, ON, Canada.
- Booth, P., (1989), *An Introduction to Human-Computer Interaction*. Hillsdale, N.J.: Lawrence Erlbaum Associates
- Buxton, W., (2007), *Sketching user experience: getting the design right and the right design*. San Francisco, CA: Elsevier.
- Carroll, J., (1995), *Scenario-based design: envisioning work and technology in system development*. John Wiley & Sons.
- Carroll, J. M., (2003), *HCI Models, Theories, and Frameworks: Toward Multidisciplinary Science (Interactive Technologies)*, Morgan Kaufmann.
- Gatsou, C., Politis, A., Zevgolis, D., (2011), *From icons perception to mobile interaction*. In *proceedings of the Computer Science and Information Systems (FedCSIS)*, 705-710.
- Hackos, J. T., Redish, J., (1998), *User and task analysis for interface design*. New York: Wiley.

- Ito, M., Nakakoji, K., (1996), *Impact of Culture on User Interface Design*. In: Galdo, E. M. & Nielson, J. (eds.), *International User Interfaces*. New York: John Wiley & Sons, Inc.
- Johnson-Laird PN, (1983), *Mental Models*, Cambridge University Press, Cambridge.
- Koffka, K., (1935), *The Principles of Gestalt Psychology*. New York, Harcourt Brace.
- Kosslyn, S. M., (1980), *Images and Mind*. Cambridge, MA, Harvard University Press.
- Lauer, D., (1979), *Design Basics*. New York, Holt, Reinhart and Winston.
- Lidwell, W., Holden, K., Butler, J., (2003), *Aesthetic- Usability Effect*. In *Universal principles of design*. Massachusetts: Rockport.
- Lindgaard, G., (2007), *Aesthetics, visual appeal, usability, and user satisfaction: What do the user's eyes tell the user's brain?*, *Australian journal of emerging technologies and society (AJETS)*, 5 (1), 1-16.
- Löwgren , J., Stolterman, E., (2004), *Thoughtful Interaction Design: A Design Perspective on Information Technology*, The MIT Press, Cambridge, MA
- Norman, D. A., (1983). *Some observations on mental models*. In: D. Gentner & A. L. Stevens (Eds.), *Mental models (pp. 7-14)*. Hillsdale, NJ: Erlbaum.
- Moreno, R., Mayer, E., (2002), *Verbal redundancy in multimedia learning: When reading helps listening*. *Journal of Educational Psychology*, 94, 000-000
- Mullet, K., Sano, D., (1995), *Designing Visual Interfaces*, Mountain View, CA: SunSoft Press.
- Paivio, A., (1986), *Mental representations: A dual-coding approach*. Oxford University Press, New York.
- Paivio, A., (1971), *Imagery and verbal processes*. New York: Holt, Rinehart, and Winston.
- Pettersson, R., (1999), *Graphic symbols-Design and meaning*. *Natural vistas: Visual Literacy & the World Around Us*. R. E. Griffin, W. J. Gribbs, and V. S.
- Quinlan, P. T., Wilton, R. N., (1998), *Grouping by proximity or similarity? Competition between the Gestalt principles in vision*. *Perception* 27, 417-430.
- Resnick, E., (2003) *Design for Communication: Conceptual Graphic Design Basics for John Wiley & Sons Publishers*.
- Schön, D., (1985), *The Design Studio*, RIBA Publications, London.
- Schön, D., Wiggins, G., (1992), *Kinds of Seeing and their Function in Designing*, *Design Studies*, 13(2), 135-156.
- Shneiderman, B., Plaisant, C., (2005), *Designing the user interface*. Addison-Wesley.
- Ware, C., (2004), *Information Visualization*. CA: Morgan Kaufman Publishers. Christopher North . San Francisco.
- Weidenmann, B., (1989), *When Good Pictures Fail: An Information-Processing Approach to the Effect of Illustrations*. In *Knowledge Acquisition from Text and Pictures*, Heinz Mandl and Joel R. Levin, Eds. Amsterdam, North-Holland.
- Weeimer, J., (1995), *Research Techniques in Human Engineering*, (Prentice Hall, N. J).
- Wertheimer, M., (1938), *The Syllogism and Productive Thinking*. In: W. D. Ellis (Ed.), *A Source Book of Gestalt Psychology*, 274-282. Reprint (1997): New York: The Gestalt Journal Press.



Linking physical print and digital media: opportunities and challenges of quick response codes in the face of mobile visual search technology

Natalia Lumby

Ryerson University
350 Victoria St., Toronto, Ontario, M5B 2K3, Canada
E-mail: nlumby@ryerson.ca

Abstract

This research investigates the opportunities and challenges of technologies that link print and digital media. Specifically, quick response (QR) codes and mobile visual search (MVS) are evaluated. We begin with an interrogation of the benefits and challenges of these technologies. Following, constructs from a mobile marketing acceptance model developed by Bauer et al. (2005) are used to evaluate a variety of advertisements. The value of QR code scans is compared to that of MVS given two key drivers for adoption: information and entertainment value. A total of 102 ads scanned reveal that a symbiotic relationship can exist between the two technologies. Here, QR codes have the ability to take consumers to targeted locations that have informational and entertainment capacity, while MVS is primarily informational, with a less controlled landing point. Thus, marketing professionals can plan integrated campaigns with trackable landing pages using QR codes, and extend search engine optimization concepts to their printed products for best MVS results. In addition to reflecting on the value of both technologies, the research provides some design considerations for best scan results.

Keywords: mobile visual search, quick response codes, mobile marketing

1. Introduction

Today's increasingly digital landscape is a challenge for traditional print marketing. Arguments of sustainability, measurability, and a lack of interactivity can push advertisers in the digital direction (Picard, 2003). It is important to remember however that digital and traditional print advertising should not be mutually exclusive. There is an opportunity to forge a strong relationship between the two, benefitting from the multiplier effect (Havlena et al., 2007).

Combining print and digital advertising is not unusual, however the technologies to do this are constantly changing. Research is needed as the market continues to absorb emerging combinations of online and offline advertisements (Lu, Cao, Wong, and Yang, 2011; Bauer, Barnes, Reichardt, Neumann, 2005). Commonly we identify print and digital media as being separate vehicles, which we can then combine. However, given various 2D barcode and digital marker technologies, one can start to conceptualize this combination more holistically. Terms used to describe this include hybrid media (Louho et al. 2006; Lindqvist et al., 2009) or phygital marketing (Downes, 2012). This new form of marketing combines printed advertisements such as direct mail with a digital component such as quick response (QR) codes. While the one component is physical in nature (printed) the other takes the consumer to a digital space. Due to the proliferation of mobile phones, other technologies with a similar goal, such as augmented reality (AR) and mobile visual search (MVS), are evolving in this space.

This study evaluates the benefits and challenges associated with QR, AR and MVS. While all three technologies are in the beginning stages of market acceptance in North America, it may be that not all reach maturity. Augmented reality (AR) markers for example, can deliver the same content, with a richer experience, and a stronger brand aesthetic than QR codes (Barocas, 2012). Thus the longevity of QR codes may be shortened by evolution in AR. These three technologies both augment and compete with one another, thus understanding their individual opportunities and challenges is beneficial. Further, the research investigates the value of scanning QR codes. Informed by a mobile marketing model developed by Bauer et al. (2005), we test if QR codes are entertaining or informational - two characteristics that drive adoption. Secondly, we investigate the use of mobile visual search (MVS) to capture similar information. MVS technology uses a camera to upload an image to a database and retrieve relevant search results. For example you can take a photo of a company logo and be taken to their website. Because of their vast search capabilities, Google has had a strong impact in this market with its mobile application, Google Goggles (Dredge, 2010). We use Goggles to scan ads that feature QR codes, to compare the landing results from these two technologies.

The study reveals that there is an opportunity for strong synergy between QR codes and MVS technology. While QR codes are not being used to their full potential, the research does reaffirm that they (or similar technologies) have a role to play. We conclude that QR codes are a marketing-centric tool, that can drive traffic to a particular location, while MVS is a consumer-centric tool used to find out more about a particular product or service. Thus, one can be used to augment the experience of the other.

2. Methods

This descriptive study investigates several technologies that move the reader from print to digital media using a mobile phone. Content analysis is used to gather the data. Mobile is a relatively new marketing platform in North America, and requires further research (Bauer et al., 2005). Current research in this field uses models to interrogate why and how a mobile technology is adopted. Such studies include: the technology acceptance model (TAM), innovation diffusion theory, and the theory of reasoned action (Wong & Hsu, 2008; Carlsson, Hyvönen, Repo, & Walden, 2005). In each of these models usability or usefulness is a common thread, asserting that people will use a technology if it provides them with some sort of value (Bauer et al., 2005).

Using several constructs of the framework developed by Bauer et al. (2005), we focus on the concept that users must choose to use a technology, and that they do this because of some perceived value. This is appropriate because one of the key issues with barcode technology currently, is that it is simply not being used. For example a study by comScore revealed that in 2011, only 6.2% of people who owned a capable phone in the USA, had scanned a QR code. The concept of value is distilled into a need for information and entertainment. As such we evaluate the information and entertainment value provided by the use of QR codes and MVS.

Information and entertainment value are not broken down in Bauer's model but rather treated as individual vectors. Thus, to increase the depth of understanding we catalog both of these constructs on a Likert scale. While the informational construct is derived from the definition of the word itself (providing new facts or data), the entertaining construct is more subjective. We chose to build on a previously tested scale developed by Schlinger (1979) because it is rooted in the subject of media. The informational construct consists of: not informational, few facts present, several new facts present, and a lot of additional information present. While the entertaining construct consists of: not entertaining, clever, fun and interactive, catches one's attention and stays in his/her thoughts.

This study consists of several phases. The first phase of research entailed collecting QR code advertisements for the period of one month in downtown Toronto, Canada. Two researchers scanned every code seen, and catalogued the experience to investigate how the QR code was used. The information and entertainment value of each experience was noted thus allowing us to understand how many "useful" QR codes an average individual may interact with, if they chose to actively participate with the technology.

In the second phase of the study more QR codes were gathered to investigate a greater number of scans and be able to generalize the results. Allowing for the initial one month of passive QR code gathering revealed some conclusions about the number of average interactions a person may expect to have with QR codes in a large urban North American city. We hypothesized that the number of interactions with QR codes in the period of one month would be low (H1). Further we forecasted that the value offered from scanning available codes would be low (H2). This value again, is derived from the scan being informational and/or entertaining.

The last phase of the research consisted of scanning the ads collected using mobile visual search technology. There are several competing technologies in mobile visual search such as Kooaba, SnapTell and Google Goggles. Each of these solutions offers slightly different areas of focus. For example, Kooaba focuses on interactive print ads (also providing augmented reality solutions). SnapTell (owned by Amazon) is very strong in product search, helping drive traffic to Amazon purchases. Lastly, Google Goggles, is able to leverage their powerful search technology. Given these technologies we hypothesize that MVS will be an effective method of connecting the physical advertisements with their digital counterparts (H3).

We chose to work with Goggles because Google is strong in search overall. Further, Goggles is able to scan QR codes, which allowed us to complete both phases using a single technology. Another reason for selecting Google technology was to investigate their new *print ads* functionality, which allows users to scan an advertisement from any popular magazine and redirect to the company website (though Goggles is not the only application that can do this).

MVS is a newer technology, and thus more difficult to catalogue accurately. We took several measures to improve the reliability of our results. Firstly, both Apple (iPhone 4) and Android (Samsung Galaxy 551) phones were used to scan the ads, allowing us to explore any platform/camera differences. While, mobile phone camera quality was once an obstacle for MVS technology, today most phones are sufficiently capable (Rohs & Gfeller, 2004). Further, instead of scanning each ad one time, we scanned it four times, focusing on different elements of the scan. Thus, each ad was scanned as a whole, then the logo (if present) was scanned, then text, and lastly an image (if present) was scanned. This allowed us to draw some conclusions not only about the success of MVS but also the best method of scanning. This is important, as there are no visual markers on the ads the way there would be with a QR code or AR marker.

A total of 102 codes were collected, and 1020 scans conducted (1 for the QR code, 4 for MVS, scanned on two phones). The landing pages were then catalogued and evaluated for each technology. The final results presented in the next section allow us to better understand the QR and MVS experiences as well as compare them.

3. Results

Prior to a discussion of data collected, a review of both QR and MVS technologies is discussed. We begin by looking at the advantages and disadvantages of each. Primary and secondary research reveals that QR codes, the more mature technology, offer a variety of benefits including the ability to collect, measure, and track print campaigns at a low cost. However security risks, a lack of aesthetic appeal, and value for effort are some of the challenges in the area. While MVS is more aesthetically appealing and does not suffer from security threats, its challenges include the use of proprietary technology, an inability to identify scan areas, and a more complex back end system to manage the images. Both technologies are limited by the software of the mobile device being used to scan them, however we are beginning to see standardization in this regard. Table 1 contains a list of benefits and challenges for QR, AR and MVS solutions. While AR is not a focus in this research it is important to understand, as it is often the middle ground between the two technologies of focus. It can also be conceptualized as competing for leadership with QR codes. The table may not be an exhaustive list, however it identifies some of the areas marketers would need to consider when choosing a method to link digital and printed campaigns.

Table 1: Benefits and challenges of QR, AR and MVS

QR Codes	AR Markers	MVS
Easy for marketers to track (Gao, 2007; Ebner, 2008; Girod <i>et al.</i> , 2011).	Easy for marketers to track (Hull <i>et al.</i> , 2007).	Depending on the technology, more difficult to track (SEO must be used on images).
The brand owner determines landing page.	The brand owner determines landing page.	The search engine determines landing page.
Easy to identify the scanning area on the page.	Scan area may be less obvious, depending on the marker used.	Difficult to know if the page can be scanned, and if so, which area.
Simple data management.	Complex data management.	Complex data management.
Requires a 3 rd party application to scan (most applications now work on a majority of codes) (Ramkumar, 2007)	Requires a proprietary 3 rd party application to scan.	Can be set to work with the camera application that is preinstalled. Some MVS technologies require different applications.
The printed product is not used after the scan takes place.	The printed product can be used to create an interactive experience.	The printed product is not used after the scan takes place.
Can pose a security risk by being hacked (Barocas, 2012).	No security risk for hacking as no code is present.	No security risk for hacking as no code is present (Barocas, 2012).
The barcodes can be aesthetically not pleasing.	Visual markers are typically used though are not always required.	No distracting barcodes or markers are required.
Requires a camera and WiFi (Ramkumar, 2007).	Requires a camera and WiFi.	Requires a camera and WiFi.
Relatively inexpensive for marketers to implement.	Can be expensive for marketers to implement (though costs are coming down).	Can be expensive for marketers, however free technologies (Google Goggles) also exist.
Scanned code must be flat (2D) (Barocas, 2012).	Scanned marker must be flat (2D).	3D photos can be used to extract data (Barocas, 2012).

We now move to the results of this specific study. In phase one, QR codes were gathered for the period of one month (March 2012). Two researchers scanned every code with which they came into contact. This of course is slightly artificial as a consumer would not be interested in every product, which had a code. We

hypothesized (H1) that even with this requirement, few codes would exist to be scanned. There were in fact only 22 QR codes found. This is not generalizable to other countries or cities. For example, in Japan there is a much greater proliferation of QR codes (Schmidmayr, 2008). We argue however, that Japan has always been a technology hub, with few countries advancing to the same degree. It is very unlikely that the adoption rate in North America would ever come near Japan's.

Because so few results were scanned during the test month we will offer analysis of QR codes with the overall data only. However there are a few key findings to note. Firstly, there were several types of QR codes that were not scanned due to their placement. Examples include: QR codes on the side of a moving bus, QR codes on highway billboards, and QR codes in underground tunnels where there is no Internet. QR codes outdoors in general were awkward as one had to stop walking to scan. Thus, QR codes are beneficial in two areas: where consumers linger and have time to use them, or where they require more information that is better provided digitally. This includes most printed reading materials, stores (special promotions on store signage), and shopping mall/city maps to name a few.

While most of the ads scanned in March were informational, only three of them had any entertainment value. Use case examples of these include sending consumers to videos or social media communities. A wine ad took users to a recipe on a mobile friendly website (Figure 1 left). The site also featured a link to a location where the wine can be purchased. Another example for an art exhibit, distributed across the city, featured links to a map, videos and other interesting content. The last innovative example for March included a live model posing in a special glass booth made to look like a poster case (Figure 1 right). A QR code in the bottom corner took consumers to a website with a video and some further details about the product. The premise of this last example is that you had to see the hair care product to believe it.

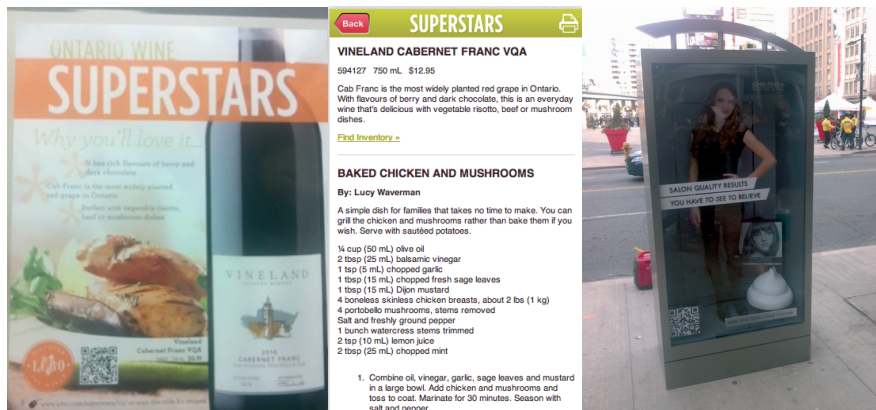


Figure 1: Print ad for wine (left), mobile site from QR code scan (center), glass booth with real model (right)

Following the month of March, more QR codes were actively collected. For this phase another 80 QR codes were scanned. The following are some findings, keeping in mind the list of advantages and disadvantages compiled previously. We begin with some design considerations. An overwhelming majority of ads (92%) used QR codes with one colour and no unique images. While marketers often complain about QR codes being unattractive, they are not using them in a visually interesting way. There are better options in this regard. Figure 2 (left) is an example of a QR code created by Qrezy Codes for a game. The code is fully functional and takes users to the App Store to buy the game.



Figure 2: Example of decorated QR code by Qrezy Codes (left), Interesting hierarchical placement of a QR code (right)

In addition to looking neglected visually, the placement of QR codes on the page was also poor - 78% of QR codes scanned were in the bottom left or right corners. This seems to be indicative of the importance of the code during planning. If marketers are going to use a code to it's fullest potential, it should be important enough that they give it better hierarchy on the page. Thus, we found that codes in the bottom corners were more likely to be less valuable for the consumer. Figure 2 (right) is an example of good placement, where it is clear that scanning the code is an important part of the initiative. Of course driving traffic to the code is beneficial for tracking purposes (which is one of the main reasons marketers use QR codes).

The placement and look of QR codes can be improved, but it is not likely they are major contributors to the lack of click through rates reported. Much like in our previous study (Gilewicz, 2011) only about half (48%) of QR codes landed on mobile friendly sites. Loading full websites on mobile devices makes the information exceptionally difficult to navigate. Secondly, 75% of the QR codes simply led to the company website. This offers very little value, as it is highly unlikely that a simple search for the product would not return the same results. It is also a missed marketing opportunity, as you forgo the potential of two-way communication with the consumer. Figure 4 identifies other landing pages of the QR codes in this study. The category of web forms includes all instances of the consumer being asked questions (be it for a coupon, contest, membership of etc.).

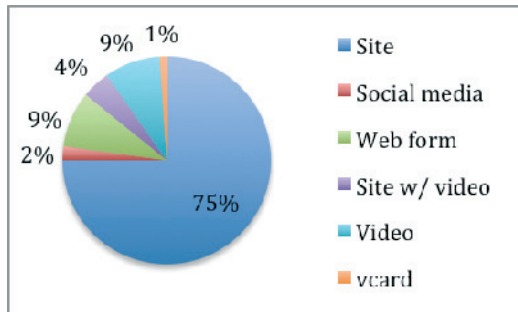


Figure 4: Landing locations for QR codes

Lastly, informed by a framework developed by Bauer (2005), we identified whether the landing pages offered informational or entertainment value. These two characteristics motivate consumers to use mobile marketing. The categories are independent of one another, thus landing pages do not have to be both entertaining and informational. The informational construct focused on additional data pertaining to the ad itself. Figure 5 shows that 28% of ads provided additional information specific to the ad, however little informational value was being offered 37% of the time. Further, 52% of all ads offered no entertainment value. Thus our second hypothesis (H2) is confirmed, with opportunity to offer much more value using QR codes. An example of a highly information and entertaining ad would be one that links to features or reviews of the specific product, with a link to comment using social media, watch a video, or play a game.

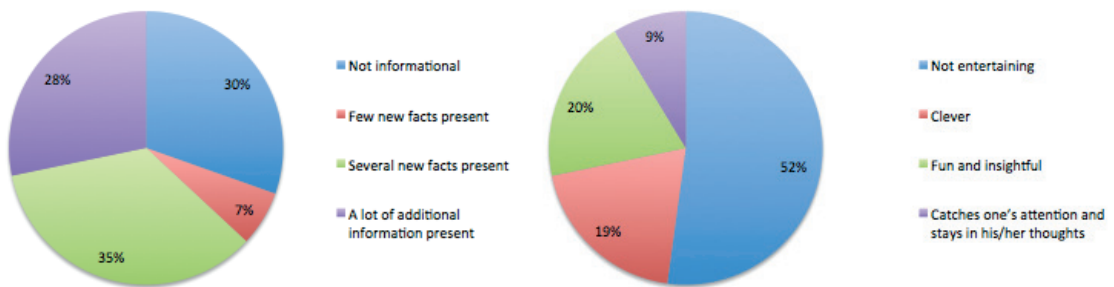


Figure 5: Scanning the QR code is informational (left), scanning the QR code is entertaining (right)

The last phase of the research involved rescanning all of the ads using Google Goggles, a mobile visual search application. MVS is being touted by the media as a possible replacement technology for QR codes (Barocas, 2012). With the many benefits listed previously, it is a promising technology. We scanned each ad 4 times using different pieces of the ad each time (text, logo, image and finally the whole ad). We also used two different devices. Figure 6 indicates which scans retrieved the best results most often for each device. It can be seen that in the case of the Android phone, the scans of the whole ad performed best, while the logos showed best results for the iPhone. In some cases ads performed equally well in multiple categories, with logo or full ad scans often retrieving good results.

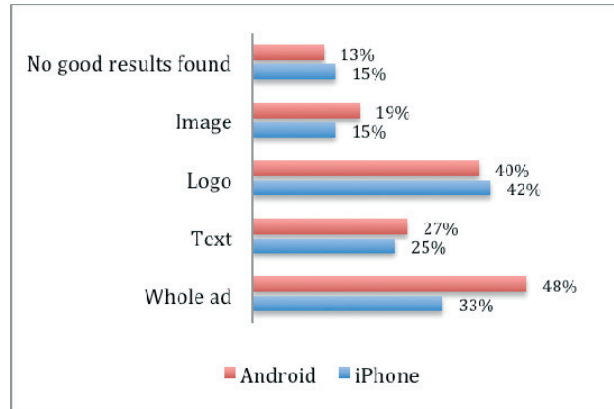


Figure 6: Best Way to Scan MVS

While Figure 6 indicates what to capture for a good scan, Figure 7 reflects on the quality of the scans themselves, in relationship to their search results. The graph shows that MVS has a long way to go to improve scan accuracy. The best categories show MVS landing successfully on topic (or better) about 50% of the time. Thus if accuracy of landing destination was vital, marketers could only count on success half the time.

The value of the MVS scans (again identified by information and entertainment value) shown in Figure 8 was lower than that of QR codes in this study. In the informational category the MVS results are not so far out, because in instances where QR codes land on websites, the MVS results are likely to also match the search. However, the entertainment category for MVS was very poor, with 90% of searches offering no entertainment value. We will interrogate the implications of this in the discussion section.

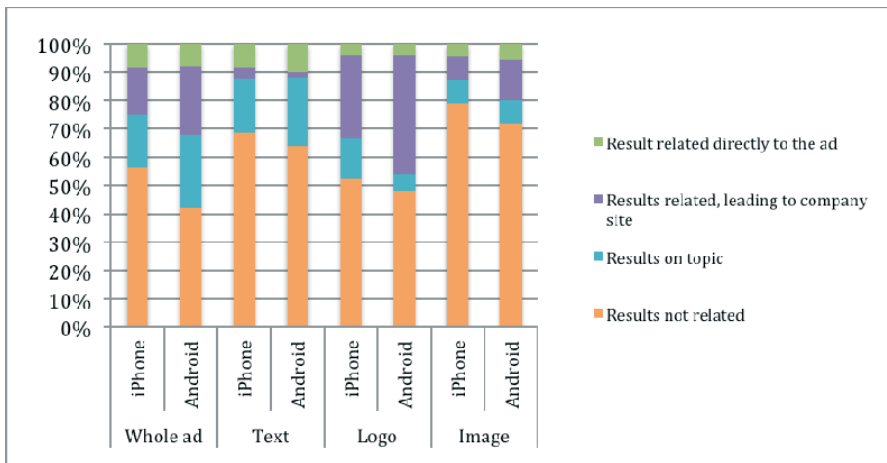


Figure 7: Landing results for MVS scans

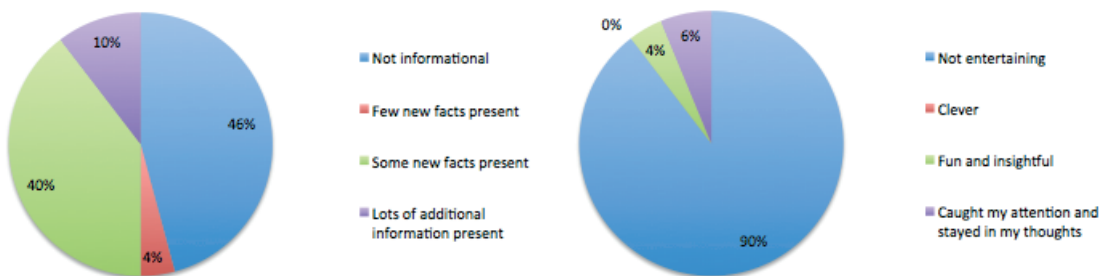


Figure 8: Scanning ad using MVS is informational (left), scanning ad using MVS is entertaining (right)

Lastly, we compared the QR results and the MVS results more directly in Figure 9. This revealed that QR codes provide more useful results (they link most closely to the ad) 59% of the time. However, in 28% of cases MVS results are comparable to QR codes. Further, comprised mostly of QR codes that failed to scan,

MVS returned superior results 7% of the time. Thus, it will likely be some time until our third hypothesis is correct - and MVS technology provides stable results. Keeping in mind that the scan data should be considered together with the benefits and challenges outlined previously, we will now move to a discussion of these results.

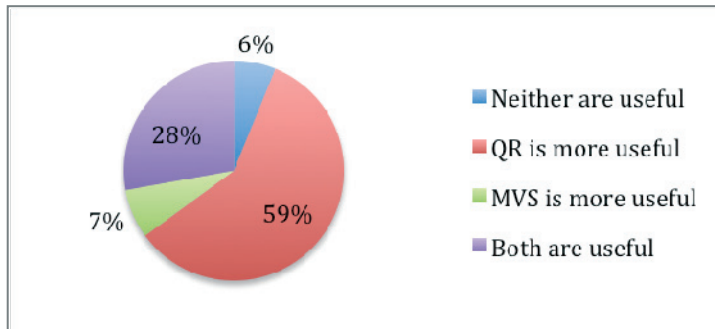


Figure 9:
QR vs. MVS comparison

4. Discussion

This paper took a descriptive look at two technologies that connect print to digital media, from a marketing-centric point of view. While a study like this does not directly report on the state of this technology, it does provide a practical insight into how a marketer may use it and how a consumer may experience it today.

The overarching insight from a discussion of the benefits and challenges of QR, AR and MVS, is not finding which technology is better but rather where each belongs. It is possible that as mobile visual search evolves, and consumers adopt searching through pictures, that QR codes will become less and less popular. However, that would also mean giving up some of the benefits that come with a barcode or marker.

Each of these technologies has a place. Unfortunately, while QR codes are excellent at taking users to a programmed destination, this study shows that not much happens when you get there. Consumers pursue activities that are valuable to them (Duncan & Moriarty, 1998). In the world of mobile media that value is most compelling when is informational or entertaining in nature (Bauer et al., 2005). There may be other ways to evaluate media "worth", but no matter what they are few would agree that launching an application and scanning a code is any easier than typing a URL (or more likely searching for a brand). The scan rates of QR codes will only go up if the content improves.

Mobile visual search is another area of opportunity for linking online and offline communication. We will focus our discussion primarily in this new area. Scanning one's surroundings with a camera to return a result is still very novel. However, MVS search providers, like Goggle Goggles, are working hard to improve the technology. The Goggles print ads initiative is a great example of this progress. In 2011 Goggles began to recognize print ads in popular magazines. In an effort to test this technology, we scanned all of the one-page ads in an issue of Wired magazine. Of the 48 ads present in the issue only 2 did not return direct results - however both still linked to their respective company websites. That is a tremendous success that provides a new way to interact with printed magazine ads.

Of course there are many printed products that do not fall into the printed ads category defined by Google - this is where MVS needs improvement. Throughout this study we developed a list of key points that would improve the success rate of MVS. The substrate and/or quality of the print have an impact. Using MVS on newsprint was more difficult than taking a photo of a higher quality print.

Other design considerations include font and colour choices. Not overcrowding the page, having enough solid contrast, and staying away from ultra fine typefaces has a positive impact. As an example, one ad we scanned had a yellow textbox with white text printed on newsprint - it did not yield desired results. Interestingly, these are all recommendations given for good quality print results, thus they are not unfamiliar to a good designer.

While the design recommendations are familiar, the content should be treated a bit differently. Firstly, the language chosen for the ad is important, particularly for a lesser-known brand. Text should describe the product/service accurately but also in a way that is unique, without too much industry jargon. As an example, an

ad for a printing company had the word "fan" on the page - this triggered sports related MVS results. In another instance, an ad returned direct competitors as results. This can happen because when similar wording is found across ads, Goggles will display the more popular search result. Even images can suffer this problem, with many small companies using stock images for their artwork. Instead of stock images, product shots were much more effective at driving good search results.

Choosing text carefully is very important, but perhaps most important of all is that in order for that text to be associated with the product, it (the text) must exist online (Girod et al., 2011). This is true for all ad elements; Goggles must have existing information in its database to be able to compare with and return appropriate results. As such search engine optimization (SEO) now needs to extend to printed ads. Elements of the ad, if not the whole ad itself, should be uploaded online, so that it is available for indexing. Descriptive text for items and images also improves search results. Lastly, publishing online in a variety of ways increases the possibility that the search will be successful. As an example, several ads scanned landed on a digital edition of a publication online (especially true for magazines using Issuu).

The lack of value offered in QR codes has already been discussed and the technology and know-how is there to improve this (as show by some use case examples). In this way, MVS is more restricted. The results above showed that 90% of MVS searches were not entertaining. This is logical because a typical MVS search simply directs users to the website. Thus, the nature of the technology is informational. While, MVS could be prompted to go to somewhere more specific by using a marketer-focused application, this approach eliminates some MVS advantages as the user must download that specific application to take the picture. QR, on the other hand, can be entertaining, with the scan results determined completely by the marketer. This is also where AR technology fits in nicely, sharing many similar advantages as previously discussed. As the cost and time to develop AR experiences decreases, and there is more standardization in AR readers, AR markers may replace unattractive QR codes.

As such, synergy begins to emerge with MVS driving to online content, and QR/AR linking the consumer to a specific destination. This destination should be well thought out by the marketer and offer some special value to the consumer. For example, a poster for a car could use a QR code or AR marker to link to a video about some special features with an option to enter contact data. If the user wants to know more about the car s/he can take a picture of the advertisement and link to search content (as well as storing those search results to his/her browser for later review). Ultimately consumers will decide which technologies to adopt, and it is likely that the most useful technologies will prevail.

5. Conclusions

This study is a comparison of two technologies that link the physical and digital worlds: QR codes and MVS. The challenges and opportunities of these types of technologies are discussed. Through this discussion it can be seen that there can exist a symbiotic relationship between the two. Ultimately, the study revealed that QR codes did not provide sufficient value. With most codes simply landing on a company webpage (which was only optimized for viewing on a mobile device half the time), there was little reward for scanning. This does not mean however that QR codes are unusable for marketing purposes. When thought out well, they can be a contributing factor to the success of printed campaigns. We provided such use case examples in the study.

Initially the study was borne out of the notion that MVS is a strong replacement technology for QR codes. However, this research shows that visual search results for ads are only as strong as the brands that are being searched. With a strong brand presence and well-known brand elements (such as logos) that exist online, MVS is a great solution. However, in situations where the images and text are new and therefore unknown to the search database, MVS does not return strong results. In fact it can even take a consumer to a competing product. Improving online presence and search engine optimization are key components in successful visual search.

Thus we conclude that marking technology (such as QR codes or AR markers) will act to direct traffic to specific places (videos, promotions, etc.) and will continue to work well for one-off promotions such as events (that are not individually branded). It can be understood as a marketer-centric technology, taking users to specific campaign locations. If marketers begin to use this technology to its full potential we may see improvements in adoption. Mobile visual search then, can be understood as a consumer-centric technology, used to research a particular product or service. It takes users to related search results, not necessarily landing in a location desired by the marketer, but similarly to internet search, returning the closest matching result,

whether it is for that product, the competitors, or a third party site that compares this product category. By planning integrated marketing campaigns that consider both QR and MVS, brand owners can use both of these technologies to drive digital traffic.

Acknowledgments

I would like to acknowledge the hard work of my research assistants Nathan Drong and Nikita Kuzmin. Thank you for your dedication to this project. Further, I'd like to thank the Faculty of Communication and Design and the School of Graphic Communications Management at Ryerson University for their support, as well as IARIGAI for the opportunity to present this paper.

References

- Barocas, J., (2012). Why QR Codes Won't Last. *Mashable*. Retrieved from <http://mashable.com/2012/02/15/qr-codes-rip/>
- Bauer, H., Barnes, S., Reichardt, T., Neumann, M., (2005), Driving Consumer Acceptance of Mobile Marketing: A Theoretical Framework and Empirical Study, *Journal of Electronic Commerce Research*, 6 (3), 181-191.
- Carlsson, C., Carlsson, J., Hyvönen, K., Puhakainen, H., Walden, P., (2006). Adoption of Mobile Devices/Services - Searching for Answers with the UTAUT. *Proceedings of the 39th Hawaii International Conference on System Sciences*.
- Downes, G., (2012). Let's get phygital. *Marketing Age Magazine*. Retrieved from <http://www.businessandleadership.com/marketing/item/27104-lets-get-phygital/>
- Dredge, S., (2010). Google reveals Goggles-enabled print ads from big brands. *Mobile Entertainment*. Retrieved from <http://www.mobile-ent.biz/news/read/google-reveals-goggles-enabled-print-ads-from-big-brands/012336>
- Duncan, T., Moriarty, S., (1998). A communication-based marketing model for managing relationships. *Journal of Marketing*. Vol. 62, No. 2, 1-13.
- Ebner, M., (2008). QR Code - the Business Card of Tomorrow? *Proceedings FH Science Day*. 431-435.
- Gao, J., Prakash, L., Jagatesan, R., (2007). Understanding 2D-BarCode Technology and Applications in M-Commerce - Design and Implementation of A 2D Barcode Processing Solution. *Annual International Computer Software and Applications Conference (IEEE Computer Society)*.
- Gilewicz, N., (2011). *Multiple platform magazine publishing: integration of print and digital content in traditional magazine advertising*. In *Advances in Printing and Media Technology*, Vol. XXXVIII. 395-402.
- Girod, B., Chandrasekhar, V., Grzeszczuk, R., Reznik, Y., (2011). Mobile Visual Search: Architectures, Technologies, and the Emerging MPEG Standard, *IEEE Multimedia*, vol. 18, no. 3, 86-94.
- Girod, B., Chandrasekhar, V., Chen, D., Cheung, N., Grzeszczuk, R., Reznik, Y., Takacs, G., Tsai, S., Vedantham, R., (2011). Mobile Visual Search: Linking the virtual and physical worlds. *IEEE Signal Processing Magazine*, Vol. 28, No. 4, 61-76.
- Havlena, W., De Montigny, M., Cardarelli, R., Eadie, W., (2007). Measuring Magazine Advertising Effectiveness And Synergies. *Worldwide Readership Research Symposium*, 233-242.
- Hull, J., Erol, B., Graham, J., Ke, Q., Kishi, H., Moraleda, J, Van Olst, D., (2007). Paper-based Augmented Reality. *17th International Conference on Artificial Reality and Telexistence*. Washington, DC. 205-209.
- Katz, E., Haas, H., Gurevich, M., (1973). On the Use of the Mass Media for Important Things. *American Sociological Review*, 38(2), 164-181.
- Lindqvist, U., Aikala, M., Federley, M., Hakola, L., Mensonen, A., Moilanen, P., Viljakainen, A., Laukkanen, M., (2009). Hybrid media in packaging. *VTT Working Papers*. 142, Espoo.
- Louho, R., Kallioja, M., Oittinen, P., (2006). Factors affecting the use of hybrid media applications. *Graphic Arts in Finland*, 3, 11-21.
- Lu, Y., Cao, Y., Wong, B., Yang, S., (2011) A study on factors that affect users' behavioral intention to transfer usage from the offline to the online channel. *Current Research Topics in Cognitive Load Theory*. 27(1), 355-364.
- Marlowe, C., (2012). Research: How QR codes could improve. *Digital Media Wire*. Retrieved from <http://www.dmwmedia.com/news/2012/01/04/research-how-qr-codes-should-improve-with-charts>.
- Picard, R., (2003). Cash cows or entrecote: Publishing companies and disruptive technologies. *Trends in communication*, 11(2), 127-136.
- Ramkumar, G., (2007). Image recognition as a method for opt-in and applications for mobile marketing. *International Journal of Mobile Marketing*.
- Rohs, M., Gfeller, B., (2004). Using Camera-Equipped Mobile Phones for Interacting with Real-World Objects. *Advances in Pervasive Computing*, Austrian Computer Society (OCG), 265-271.
- Schlinger, M., (1979). A Profile of Responses to Commercials. *Journal of Advertising Research*, 10, 37-46.

Schmidmayr, P., Ebner, M., Kappe, F., (2008). What's the Power behind 2D Barcodes? Are they the Foundation of the Revival of Print Media? - in: *Int. Conf. of Knowledge Management and New Media Technology*. (2008), 234-242.

Wong, Y., Hsu, C., (2008). A confidence-based framework for business to consumer (B2C) mobile commerce adoption. *Journal of Personal and Ubiquitous Computing*, 12. 77-84.

Legibility of offset prints after exposure to light

Blaž Rat, Sabina Bračko, Klementina Možina

University of Ljubljana, Faculty of Natural Sciences and Engineering

Department of Textiles

Chair of Information and Graphic Arts Technology

Snežniška 5, SI-1000 Ljubljana, Slovenia

E-mails: blaz.rat@ntf.uni-lj.si; sabina.bracko@ntf.uni-lj.si; klementina.mozina@ntf.uni-lj.si

Abstract

The aim of this study was to examine the influence of light on the legibility of offset prints, considering the changes in typographic and colorimetric properties. The goal was to investigate how to achieve long-term legibility of printed texts and information permanence. Under the influence of external factors, i.e., light, heat and humidity, the appearance of prints can change significantly; therefore, three different papers were used. Three different typefaces (one old-style, one transitional, and one modern) in two different sizes (6 and 8 pt) were tested. The resistance of prints to light was evaluated according to the ISO 12040 standard, the colour differences were determined spectrophotometrically and the differences in the typographic tonal density of typefaces were measured with image analysis. The legibility research was performed with the help of readers who read the printed text before and after the ageing process induced with exposure to light. It was concluded that exposure to light especially influences the legibility of 6 pt sized typefaces with thinner stroke width.

Keywords: legibility, lightfastness, typography, offset prints

1. Introduction

The goal of this study was to examine the influence of light on the legibility of offset prints, considering the changes in typographic and colorimetric properties. Despite the well-known recommendations for preserving different substrates used in the graphic arts production (Feller, 1994; IFLA, 1998; ISO 11799, 2003), there have been until now no available recommendations or standards regarding the preservation of different typeface styles and type sizes which would offer a print better quality and better fastness, ensuring legibility (Možina, 2001; Reynolds, 1988). The aim was to establish how to achieve long-term legibility of printed texts and information permanence. Under the influence of external factors, i.e., light, heat and humidity, the appearance of prints can change significantly (Černič, Bračko, 2007; Karlovič, Gregor-Sveteč, 2011; Možina, Černič-Letnar, Beškovič, Bračko, 2006; Možina, Černič, Demšar, 2007; Možina, Medved, Rat, Bračko, 2010; Vikman, 2003).

While the communication on paper requires from the reader to translate symbols into meaning, legibility refers to how easily this process is performed. To enable the reading, the text must have three properties, namely (Možina, 2001; Reynolds, 1988):

- visibility, for a clear image of adequate size to be perceived in the real-time;
- recognisability or perceptibility of letters and words which make up a text, this being affected by factors such as type style and form;
- comprehension, which is affected not only by the text content but also by its visibility and perceptibility, and by the reader's verbal capacity.

A number of studies on legibility highlight its importance (Možina, 2001; Bix, Lockhart, Selke, Cardoso, Olejnik, 2003; Reynolds, 1988). There are some typeface characteristics to be taken into consideration to make a text more legible. For a small type size, the differences in stroke weight and typographic tonal density (or typographic tonality) are significant (Možina, Medved, Rat, Bračko, 2010; Rat, Možina, Bračko, Podlesek, 2011), influencing the text legibility. The goal of our research was to establish what impact these influences really have, even though a number of other typographic characteristics need to be observed in order to make a text more legible, i.e., distinctive character features (counter shape), x-height, ascender, descender, serifs, contrast (stroke weight), set width, type size, leading (i.e., space between lines) etc (Gaultney, 2001; Možina, 2001; Reynolds, 1988; Tracy, 2003).

Moreover, typographic tonal density was taken into consideration as it refers to the relative blackness or shades of grey of type on a page. It can be expressed as the relative amount of ink per square centimetre, pica or inch (Keyes, 1993). The changes in various type features can create variations in typographic tonal density (Možina, 2001; Možina, Černič, Demšar, 2007; Reynolds, 1988).

The legibility research was performed according to the method "rate of work" (Možina, 2001) with the help of readers who read the printed text before and after the aging process induced by exposure to light. The time required for the text to be read was measured, which enabled direct comparisons of text legibility under different conditions. Furthermore, the evaluation of colorimetric properties of black prints with 50% and 100% intensity was conducted.

In the present study, we examined how the changes in typographic and colorimetric properties are related to the changes in text legibility.

2. Experimental

The prints included in the study were printed with popular text and were made with the offset printing technology on three different papers. We used two papers for which it was already established (Možina, Medved, Rat, Bračko, 2010; Rat, Možina, Bračko, Podlesek, 2011) that there are minor differences between them. We also added a matt coated paper which is normally used in the book production. Prior to the printing, the basic, surface and optical properties of paper were measured.

Paper grammage was measured according to the ISO 536 standard, while paper thickness was measured according to the ISO 534 standard. Density was calculated according to the ISO 534 standard. The measurements of specific volume were performed according to the ISO 534 standard. The paper roughness measurement was conducted with the Bendtsen method in accordance with the ISO 8791-2 standard. The porosity of paper was tested according to the Bendtsen method in line with the ISO 5636-3 standard. The water absorption of paper was measured with the Cobb method in accordance with the ISO 535 standard. The measurement of specular gloss was conducted according to the ISO 8254-1 standard. The measurement of brightness was made according to the ISO 2470 standard. Opacity was measured with regard to the ISO 2471 standard. Before determining paper characteristics, the samples were conditioned according to the ISO 187 standard. The measured properties on the felt side of the three papers (S1-S3) are presented in Table 1. Paper 1 (S1) has a matt coated paper declaration and Paper 3 (S3) has a recycled paper declaration.

Table 1: Properties of tested papers (S1-S3).

Properties	S1	S2	S3
Grammage (g/m ²)	92.30	89.30	80.15
Thickness (mm)	0.075	0.112	0.100
Density (kg/m ³)	1222.93	797.30	797.75
Specific volume (cm ³ /g)	0.82	1.25	1.26
Roughness (ml/min)	23	408	420
Porosity (ml/min)	2	698	690
Water absorption (g/m ²)	29.80	21.00	18.50
Gloss (%)	28.10	4.10	3.80
ISO Brightness (%)	96.94	99.64	82.06
Opacity (%)	88.01	88.62	78.60

Black prints were made on an offset printing machine GTO ZP 52 (Heidelberg, Germany) with Perfect black ink (Van Son, Netherlands) on three different papers.

Previous researches (Možina, Medved, Rat, Bračko, 2010; Rat, Možina, Bračko, Podlesek, 2011) showed that typefaces of smaller sizes with differences in stroke width are more affected by the external factors of light, humidity and temperature. Hence, three different typefaces with differences in stroke width were tested, i.e., one old-style (Palatino), one transitional typeface (Times) and one modern typeface (Blaznic) (McLean, 1996; Možina, 2003), in two different sizes, i.e., 6 pt and 8 pt. On each of the three papers, the 100% (K100) and 50% (K50) field intensity was printed.

The resistance of prints to light was evaluated according to the ISO 12040 standard using a Xenotest Alpha (Atlas, USA) with a xenon arc lamp. The colour temperature was between 5500 and 6500 K at the constant temperature of 35 °C and constant relative humidity of 35 %. The samples were exposed to xenon light for 144 hours.

The CIELAB parameters of prints were measured with a spectrophotometer EFI/ES -1000 (Gretag Macbeth, USA) in accordance with the ISO 13655 standard, using D50 standard illumination, 2° standard observer, black backing and instrument geometry 45/0. The colour difference (ΔE) between the nonexposed and exposed samples was calculated using the CIELAB equation for colour differences (Marcus, 1998).

The differences in typographic tonal density of the nonexposed and exposed typefaces were measured with an image analysis (ImageJ). This software gives the opportunity to measure, analyse and provide output values, e.g., area, number of particles, circularity and percentage of coverage (National Institutes of Health, 2011). All the measured samples were of the same size, i.e., 1 100 × 175 pixels (300 dpi).

Different texts from the *National Geographic* journal were printed in different typefaces on different papers. The length of the text was between 200 and 210 words for the type size 6 pt, and between 130 and 140 words for the type size 8 pt. The leading for the type size 6 pt was 8 pt and for the type size 8 pt 10 pt. The speed of reading (characters per minute) before and after the exposure of the text was calculated, based on the time required for the reading of the whole text.

The readers ($N = 300$) were people aged between 18 and 30 years with normal or corrected-to-normal vision. They were divided into 6 groups of 50 people, with each group participating in 1 of the 6 combinations of different levels of three independent-measures factors (3 samples × 2 measurements, before and after exposure). Each group read all 6 combinations of two repeated-measures factors (3 typefaces × 2 type sizes), which were presented in a random order to different participants to eliminate possible order effects. The speed of reading (100 words in seconds) before and after the exposure of the text was calculated, based on the time required for the reading of the whole text. The influence of typeface, type size, as well as papers on legibility was statistically analysed with the IBM SPSS 20 software (Field, 2005). For analysing the calculation of frequency, an average with standard deviation according to the normal distribution was derived.

3. Results and discussion

The obtained results (cf. Table 2) show that black prints exhibited low chromaticity and lightness values. This was evident especially for the prints with 100 % intensity on Sample 1. The lightness of prints with 50 % intensity was considerably higher and very similar on all three papers. The colour differences (ΔE) on paper samples and prints were calculated after the exposure to xenon light. The results (cf. Figure 1) show that on average the most substantial colour differences (ΔE) on paper (0 % intensity) were observed on Sample 1, followed by Sample 2, while the smallest differences were measured on Sample 3. Relatively high ΔE values indicate a significant visual change of all paper samples after the exposure to light. According to the results, the prints with 50 % intensity changed much more than the prints with 100 % intensity. The smallest colour differences after the exposure to light appeared on Sample 3 (recycled paper). A large colour difference after the exposure to light appeared on Samples 1 and 2, especially on the print of 50 % intensity on Sample 1, which was a matt coated paper.

Table 2: CIELAB parameters of black prints with 100 % and 50 % intensity printed on different papers (S1-S3)

		100%	50%
S1	L*	16.66	58.52
	a*	-0.16	0.40
	b*	-2.01	-3.77
S2	L*	34.36	60.09
	a*	1.23	1.25
	b*	0.09	-3.21
S3	L*	33.14	57.92
	a*	1.52	0.92
	b*	0.95	-1.39

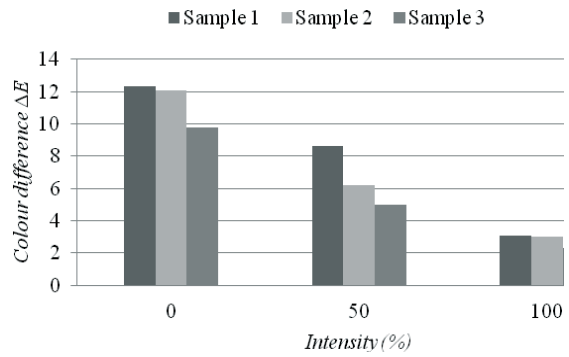


Figure 1: Colour difference (ΔE) on paper samples and prints after exposure to xenon light

The typographic tonal density (TTD) of each typeface, each in different size, was measured on nonexposed and exposed prints. The results (cf. Table 3) show a higher TTD at the modern typeface Blaznic due to its wider stroke width of letters. The lowest TTD was observed at the old-style typeface Palatino; however, the measured values were very similar to those of the transitional typeface Times. Palatino letters have a big counter size, and the difference between thick and thin strokes is not substantial, while Times letters have smaller counter size, wider thick strokes and thinner thin strokes than the old-style typefaces.

Table 3: Average value of typographic tonal density (TTD) of tested typefaces before and after exposure for prints on different papers (S1-S3)

Typefaces	TTD (%)			
	S1	S2	S3	Average
Blaznic-nonexposed	22.09	22.61	23.46	22.72
Blaznic-exposed	21.74	22.45	23.18	22.46
<i>Difference</i>	0.35	0.16	0.28	0.26
Times-nonexposed	18.50	18.69	19.96	19.05
Times-exposed	18.01	18.47	19.69	18.72
<i>Difference</i>	0.49	0.22	0.27	0.33
Palatino-nonexposed	18.23	18.61	19.52	18.79
Palatino-exposed	17.92	18.33	19.23	18.49
<i>Difference</i>	0.31	0.28	0.29	0.30

According to the results, paper selection is important, as the differences in TTD were especially seen between Sample 3 and the other two samples. All the tested typefaces in both type sizes had higher TTD on Sample 3. Comparing the printed samples, the most noticeable differences appeared above all on Sample 1.

After the exposure, the most noticeable average difference in TTD occurred on average at the Times typeface (0.33) and a slightly smaller difference at the Palatino typeface (0.30). The smallest differences were observed at the Blaznic typeface (0.26). Nevertheless, thinner thick strokes at old-style and transitional typefaces led to lower resistance to light.

The obtained results (cf. Figure 2) show the most substantial differences at the typefaces used in the 6 pt size. The typographic tonal density at smaller typeface sizes is usually higher due to a smaller counter size of letters and leading.

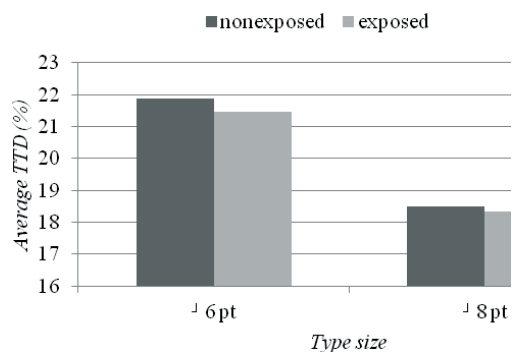


Figure 2: Typographic tonal density (TTD) of tested typefaces in sizes 6 and 8 pt

The differences were even more evident after the exposure to light. At the typefaces with lower typographic tonal density, the difference in typographic tonal density after the exposure to light influenced - due to the thin strokes, wider counter, lower x-height - legibility more than at the typefaces with wider strokes. The starting TTD value and its change during the exposure to light need to be taken into consideration.

Exposure to light affected the legibility of various typefaces differently (cf. Figure 3). While the speed of reading the typeface Blaznic did not change much from the first ($M = 30.00$) to the second measurement ($M = 31.50$), the change was much more noticeable in the case of the typeface Times (there was an increase from 32.33 to 40.83 seconds per 100 words) and the typeface Palatino (there was an increase from 27.16 to 34.83 second per 100 words), which can also be observed from a more substantial difference in TTD. The legibility of the Blaznic typeface thus seemed to be the least affected by the exposure to light; the typeface Blaznic has the widest thick stroke and the smallest decrease in TTD among the tested typefaces. The typeface Palatino has the highest reading speed before the exposure to light, thinner thick strokes were obviously more affected by the exposure to light, the reading speed hence decreasing substantially. The highest decrease in the reading speed (by 5.83 seconds per 100 words) was observed at Sample 3 (cf. Figure 4). Evidently, the contrast between the background and smaller type sized typefaces was no longer good enough.

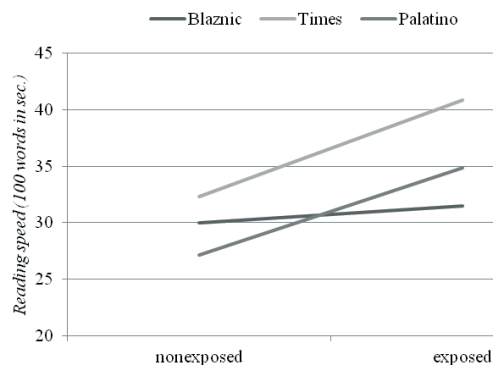


Figure 3: Speed of reading samples with different typefaces. Data are averaged across different printed samples

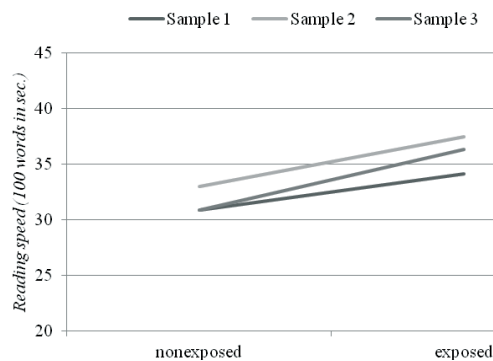


Figure 4: Speed of reading on different samples (S1-S3). Data are averaged across samples printed with different typefaces and type size

3. Conclusions

The results of the study show that it is necessary to consider the chosen typeface and its size to ensure the information permanence and legibility of a text. The obtained results reveal that there are relatively small differences in the light fastness of the used papers. Nevertheless, according to the measured CIELAB parameters and typographic properties, the typeface has the greatest impact on the legibility and speed of reading. The modern-styled typeface Blaznic has the widest thick stroke and the largest x-height among the tested typefaces, which leads to the best legibility results. Text legibility is influenced by typographical tonal density, which varies with the used typeface and its size. We need to pay attention to the starting value of typographic tonal density and its change during the exposure to light. Therefore, the typeface design (i.e., thick enough stroke width, higher x-height, distinctive counter shape) needs to be taken into consideration as well in order to enable better legibility and ensure information permanence.

Acknowledgements

The financial support for the PhD grant from the Slovenian Research Agency for the PhD student Blaž Rat is gratefully acknowledged by the authors.

References

Print sources

- Bix, L., Lockhart, H., Selke, S., Cardoso, F., Olejnik, M., (2003), *Is x-height a better indicator of legibility than type size for drug labels?*, *Packaging Technology Science*, Vol. 16., pp. 199-207.
- Černič, M., Bračko, S., (2007), *Influence of Paper on Colorimetric Properties of an Ink Jet Print*, *Journal of Imaging Science and Technology*, Vol. 51, No. 1, pp. 53-60.
- Feller, R. L., (1994), *Accelerated Aging: Photochemical and Thermal Aspects*, Los Angeles, The Getty Conservation Institute.
- Field, A., (2005), *Discovering Statistics Using SPSS*, London, Sage Publications.
- Gaultney, V., (2001), *Balancing Typeface Legibility and Economy: Practical Techniques for the Type Designer*, research essay, Reading, University of Reading.
- IFLA, Principles for the care and handling of library material*, (1998), *IFLA PAC, International Preservation Issues*, Vol. 1, pp. 23-25.
- ISO 11799-2003, Information and documentation - Document storage requirements for archive and library materials*, Geneva, ISO.
- ISO 12040-1997, Graphic technology: Prints and printing inks - Assessment of light fastness using filtered xenon arc light*, Geneva, ISO.
- ISO 13655-1996, Graphic technology: Spectral measurement and colorimetric computation for graphic arts images*, Geneva, ISO.
- ISO 187-1990, Paper, board and pulps: Standard atmosphere for conditioning and testing and procedure for monitoring the atmosphere and conditioning of samples*, Geneva, ISO.
- ISO 2470-1999, Paper, board and pulps: Measurement of diffuse blue reflectance factor (ISO brightness)*, Geneva, ISO.
- ISO 2471-1998, Paper and board: Determination of opacity (paper backing) - Diffuse reflectance method*, Geneva, ISO.
- ISO 534-1997, Paper and board: Determination of thickness and apparent bulk density or apparent sheet density*, Geneva, ISO.
- ISO 535-1991, Paper and board: Determination of water absorptiveness - Cobb method*, Geneva, ISO.
- ISO 536-1995, Paper and board: Determination of grammage*, Geneva, ISO.
- ISO 5636-3-1992, Paper and board: Determination of air permanence (medium range) - Bendtsen method*, Geneva, ISO.
- ISO 8254-1-2009, Paper and board: Measurement of specular gloss - Part 1: 75° gloss with a converging beam, TAPPI method*, Geneva, ISO.
- ISO 8791-2-1990, Paper and board: Determination of roughness/smoothness (air leak methods) - Bendtsen method*, Geneva, ISO.
- Karlović, M., Gregor-Svetec, D., (2011), *Comparison of durability between UV inkjet and conventional offset prints exposed to accelerated ageing*, *Journal of Graphic Engineering and Design*, Vol. 2, No. 2, pp. 10-15.
- Keyes, E., (1993), *Typography, color, and information structure*, *Technical Communication*, Vol. 40, No. 4, pp. 638-654.
- Marcus, R. T., (1998), *The measurement of color*, in: K. Nassau (Ed.), *Color for Science, Art and Technology*, Amsterdam, Elsevier, pp. 31-96.
- McLean, R., (1996), *The Thames and Hudson Manual of Typography*, London, Thames and Hudson, pp. 58-62.
- Možina, K., (2001), *Zgodovinski razvoj knjižne tipografije*, doctoral thesis, Ljubljana, University of Ljubljana.
- Možina, K., (2003), *Knjižna tipografija*, Ljubljana, University of Ljubljana.
- Možina, K., Černič, M., Demšar, A., (2007), *Non-destructive methods for chemical, optical, colorimetric and typographic characterisation of a reprint*, *Journal of Cultural Heritage*, Vol. 8, pp. 339-349.
- Možina, K., Černič-Letnar, M., Beškovič, B., Bračko, S., (2006), *Light fastness of ink jet colour prints*, *Professional Papermaking*, No. 1, pp. 72-77.
- Možina, K., Medved, T., Rat, B., Bračko, S., (2010), *Influence of Light on Typographic and Colorimetric Properties of Ink jet Prints*, *Journal of Imaging Science and Technology*, Vol. 54, No. 6, pp. 060403-1-060403-8.

Rat, B., Možina, K., Bračko, S., Podlesek, A., (2011), Influence of Temperature and Humidity on Typographic and Colorimetric Properties of Ink Jet Prints, *Journal of Imaging Science and Technology*, Vol. 55, No. 5, pp. 050607-1-050607-8.

Reynolds, L., (1988), *Legibility of Type, Baseline*, *International Typographic Journal*, No. 10, pp. 26-29.

Tracy, W., (2003), *Letters of Credit: A View of Type Design*, Boston, David R. Godine.

Vikman, K., (2003), *Fastness properties of ink jet prints on coated papers - Part 1: Effect of coating polymer system on light fastness*, *Journal of Imaging Science and Technology*, Vol. 47, No. 1, pp. 30-37.

Web sources

National Institutes of Health, (December 2011), Research Services Branch, <http://rsb.info.nih.gov/ij>



Brand experience as a tool for brand communication in multiple channels

Aino Mensonen, Janne Laine, Anu Seisto

VTT Technical Research Center of Finland
P. O. Box 1000, FI-02044 Finland
E-mail: aino.mensonen@vtt.fi

Abstract

The diversity of media field set new challenges to the brand owners. Media is increasingly fragmented while costs continue to increase; consumers are less attentive to mass vehicles as newer alternatives compete for consumers' time and new technologies are changing media consumption habits. The brand owners need information on how to efficiently communicate with the consumers through different media platforms. Thus there is a need to know, how the customers perceive the different platforms and the content that is provided through them. This knowledge is essential for stressing the brand owner's values in different communication platforms in a way that the customer receives the message as desired.

Our study focuses on different types of media platforms that are relevant for brand owners by presenting a case study carried out with one Finnish brand owner. In this paper we will describe how the communication messages used for brand building reach and address the customers through the different communication platforms. The results are visualized through a brand experience map. By the brand experience map we are able to indicate which brand attributes are successfully communicated and which need to be improved.

Keywords: brand communication, brand experience, magazine

1. Introduction

The diversity of media field set new challenges to the brand owners. Today's mass marketing model is under attack because it is becoming less effective. Media is increasingly fragmented while costs continue to increase; consumers are less attentive to mass vehicles as newer alternatives compete for consumers' time and new technologies are changing media consumption habits. The brand owners need information on how to efficiently communicate with the consumers through different media platforms. Thus there is a need to know, how the customers perceive the different platforms and the content that is provided through them. This knowledge is essential for stressing the brand owner's values in different communication platforms in a way that the customer receives the message as desired.

Different scales have been developed to measure brand experience. Yoo et al. (2001), for example, developed a scale for brand equity, which refers to value added by products brand name. Brand equity is defined as consumers' different response between focal brand and unbranded product, when both share same marketing actions and product values. Brakus et al. (2009) categorized the brand experience into dimensions of sensory, affective, behavioral and intellectual. They also showed that brand experience has an effect on loyalty. Zaran-tello et al. (2010), on the other hand, look at the consumers based on their brand attitudes and purchase intention, and have created five groups based on this information: hedonistic, action-oriented, holistic, inner-directed and utilitarian consumers. They showed that there is a connection between attitudes and purchase intentions, and that the strongest intention was for holistic type of consumers. Based on their findings the communication messages can be directed differently to different types of consumers.

The emotional brand attachment is an important issue in communication messages. Thomson et al. (2005) has developed a scale for measuring the strength of consumers' emotional attachment. Malär et al. (2011) have found that brands with actual self-congruence have higher impact on emotional brand attachment compared to brands with tailored to consumers' ideal self.

Our study focuses on different types of media platforms that are relevant for brand owners by presenting a case study carried out with one Finnish brand owner. In this paper we will describe how the communication messages used for brand building reach and address the customers through the different communication platforms. The results are visualized through a brand experience map. By the brand experience map we are able to indicate which brand attributes are successfully communicated and which need to be improved.

The objective in this study was to help the brand owner to direct the brand communication to meet the needs and demands their customers set them in multiple channels including print, internet, fairs etc. The objective was approached by further development of the multisensory experience map (Mensonen et al., 2010). Figure 1 presents the progress of the research. Also previous experience of the role of packaging as a tool for brand communication was used (Mensonen et al., 2012).

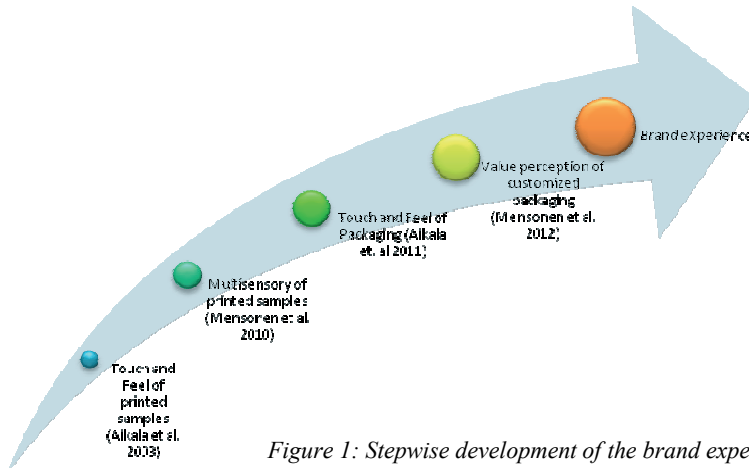


Figure 1: Stepwise development of the brand experience approach

2. Methods

The study was carried out as a case study with a Finnish brand owner, Novita. Novita is a family business in yarn industry and their customer focus is based on home knitters. They provide yarn, patterns, accessories, help-line, magazine and an internet community to their customers. They also send weekly emails to their customers and meet them at fairs, at their own deli-shop and via Facebook. The paper binder that holds the skein of the yarn (the package) has also an important role in the communication strategy. Figure 2 presents Novita's tools for the brand building.



Figure 2: Novita's tools for the brand building

The study was conducted in four phases as presented in Figure 3. The study began with deep-interviews with the top management of Novita and five end-users. The aim was to gather information of the Novita brand - on the one hand how Novita sees the brand, which values they want to emphasize and which they desire to communicate to their customers, and on the other hand how the customers see the Novita brand. The interviews were recorded and the attributes describing the brand were collected from the transcriptions. Selection of the attributes was based on grouping and in the end 16 attributes were chosen to be studied further.

The perceived strengths of attribute associations with the brand were tested in the second phase of the study, in which 40 club members of Novita were interviewed by phone. The attributes were presented as statements. The first statement covered the company brand as a whole. In addition, six communication channels were stu-

died in detail. The selection of the communication channels was based on the interviews with Novita and it included magazine, internet community, email, fairs, Facebook, and the packaging. All comments from the inter-viewees during the interview were collected. In the end of the interviews, the interviewees were asked to judge, which of the communication channels is the most important to them, and describe by their own words how loyal they are to the Novita brand.

In the third phase, principal component analysis (PCA) was used in the interpretation and visualization of the results. The company brand and the communication channels were considered as samples. Jackson (2003) describes principal component analysis in detail. The model for examining brand experience in multiple channels was created based on the results in the fourth phase of the study.



Figure 3: Phases of the study to collect information and build the brand experience map

3. Results

The chosen attributes and an example of a statement, based on Phase 1 of the study, are described in Table 1.

Table 1: Chosen attributes for the Novita case study, and an example of the statements

Attributes
Close, Trustworthy, Pleasant, High quality, Finnish, Traditional, Trendy, Visible, Big, Honest, Ethical, Availability, Expensive, Skillful, Inspiring, Joy of success
Example of the statement
Novita is close to you, the closeness of Novita comes up in the magazine/ on the packaging / at the fairs/ on the Facebook/ on the internet community/ through the email

According to the results of Phase 2, *the Novita magazine* was highly appreciated. It's inspirational and the club members save almost all issues. The lacquered cover was found fancy as well as the pictures inside the magazine. The magazine and the community were the most important channels of communication for the club members.

The internet community Neulomo is where the club members seek for direct communication with Novita. The members expect that Novita takes into account their opinions and replies to their questions and comments fast enough. They also use the community to communicate with other knitters. They share photos of their own hand made knitting and comment on other people's knitting. The community is not for discussing knitting only, as the members often come there to also discuss various matters in their ordinary, daily life.

During the phone interview, the Neulomo members commented the web-shops of different yarn companies. According to them, the threshold to buy yarn though a web-shop is lower, when the user has read comments from other users about a certain yarn. Blogs play an important role in recommending products.

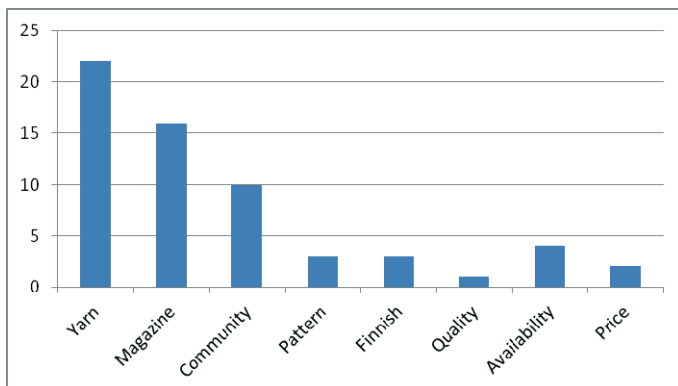


Figure 4: Number of spontaneous comments on loyalty to Novita

The Neulomo members were asked whether they feel that they are loyal to the Novita brand. Most of the members felt they are loyal and they also spontaneously explained why they feel so. They commented their relationship with the magazine, yarn, community, patterns, Finnish origin, quality, price and availability. The communication with the customers seems to strengthen the loyalty, as the members felt that unlike with other yarn brands, with Novita they have the opportunity to express their wishes and be in regular contact with the Novita people. Figure 4 presents the number of comments regarding the importance of the different factors on the loyalty of the Neulomo members.

Data obtained in Phase 2 of the study was analysed by using PCA in Phase 3. Figure 5 shows the location of the company brand and the locations of different communication channels on all mental attribute scales measured in the survey. Multivariate analysis of variance of the full data from the subjective assessments of all mental impressions of all communication channels, as well as the overall brand experience irrespective of any specific communication channel, indicated that the brand experience in the different communication channels was significantly different between all pairs of communication channels at 95% confidence level in all cases, except for the pair 'Paper around the yarn' / 'Email' and the pair 'Fair' / 'Paper around the yarn', for which the MANOVA results did not indicate statistically significant differences.

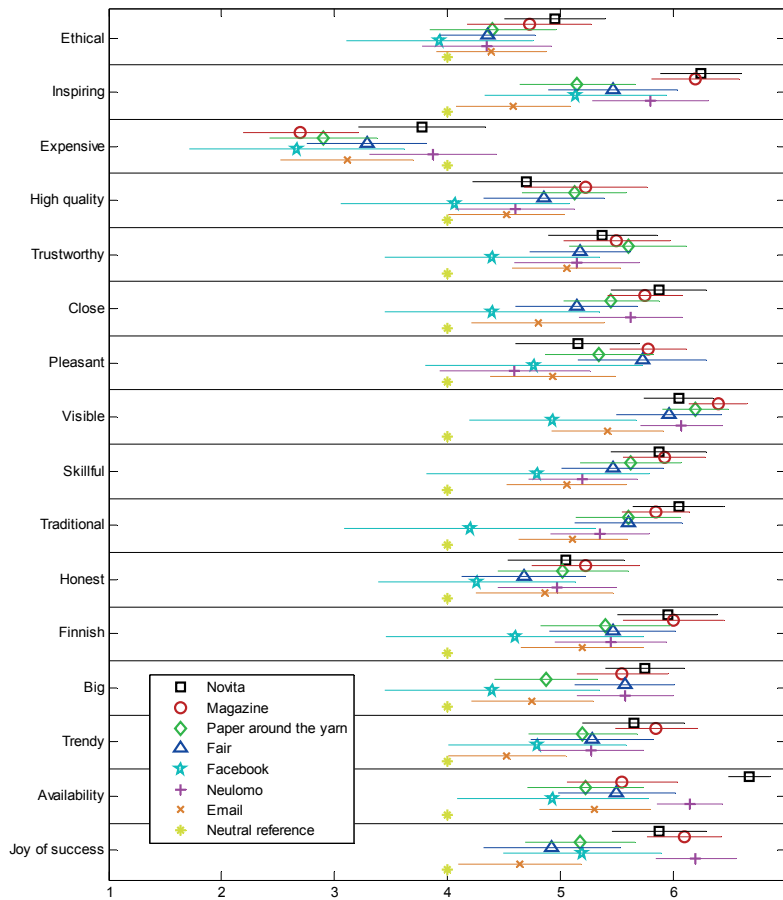


Figure 5: The locations of the communication channels on different mental attribute scales, calculated as the mean ratings across all participants. Larger the scale value of the given communication channel on the scale of given mental attribute, more strongly that attribute was associated with that communication channel. The horizontal bars indicate 95% confidence intervals for the mean values

The profiles of chosen mental attributes and the brand experience maps are presented in Figures 6-11. In the brand experience maps the multivariate observations of different media platforms on different mental attribute scales have been mapped, using a linear combination of original scale values calculated by principal component analysis, to a two-dimensional graph that visualizes the main differences between the customer perceptions of communications on different media platforms. The square mark in the Figures stands for the company or the media platform at issue, the stars inside the clouds represent the attributes that are emphasized on the platform in question and the circles represent attributes that were not emphasized. The grey circles stands for the attributes, which the company is unable to communicate through any media platform.

According to Figure 6, Novita is unable to communicate ethical values and honesty through any media platform, even though the company sees them as important issues. The Novita-brand is found to be quite positive, but the Neulomo members don't connect the attributes pleasant and high quality to the company brand. It was also found that the communication messages don't address the club members through Facebook and emails, as presented in Figure 7.

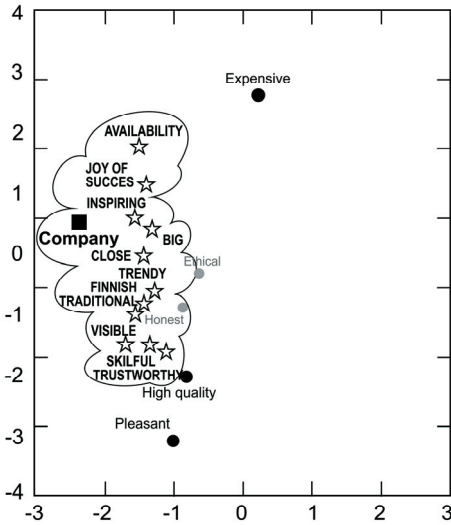


Figure 6: The brand experience map of the company

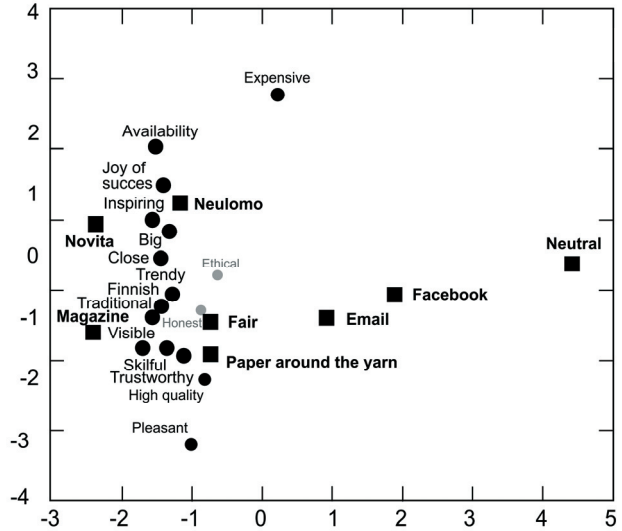


Figure 7: The brand experience map of all the communication platforms

In general, the Neulomo members find the different communication channels of the Novita-brand very positive. Club members gave the highest values to the Novita magazine for each attribute with the exception of availability (Figure 8). The highest rating in availability was given to the community (Figure 9). One explanation for that could be that the members use the community as a channel to sell yarns to each other, especially the yarns that are out of production and can no longer be found from shops. They also share the information of best yarn sales through the community. The attributes high quality and pleasant were emphasised by the magazine.

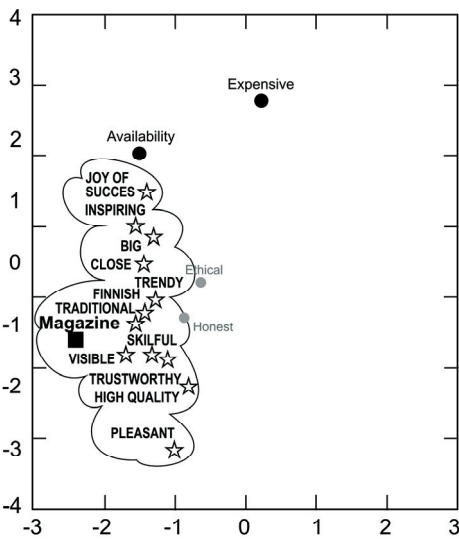


Figure 8: The brand experience map of the magazine as a tool of brand communication

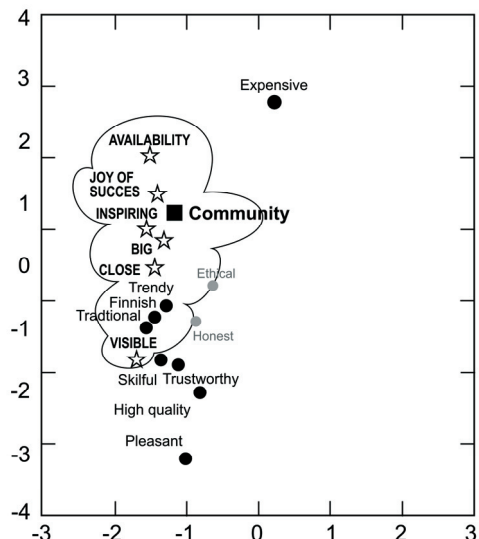


Figure 9: The brand experience map of the community as a tool of brand communication

The packaging, i.e. the paper around the yarn was described as visible, skilful, trustworthy and high quality (Figure 10). There were many comments of how few mistakes there are in this piece of paper. On the other hand, the attributes big, visible, trustworthy and pleasant are connected with Novita's work at fairs (Figure 11).

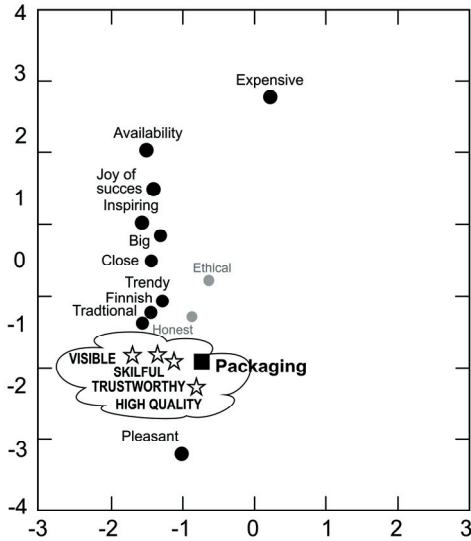


Figure 10:
The brand experience map of the packaging as a tool of brand communication

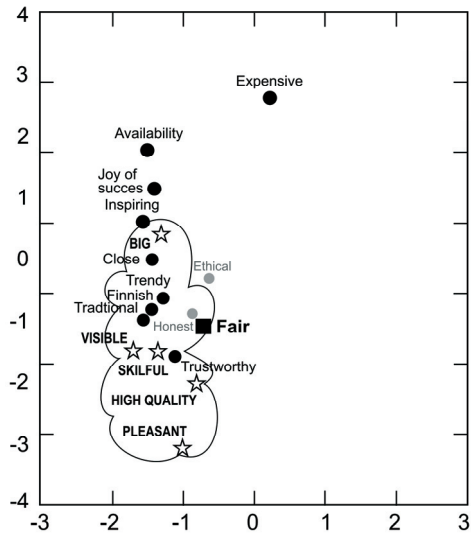


Figure 11:
The brand experience map of the fair as a tool of brand communication

4. Discussion

The results indicate that the magazine and the Neulomo community were in this case study the most important tools of brand building for the Novita-brand. To please the customers, it's also important for Novita to be present at fairs. It was shown, that Novita succeeds well in brand communication, but Facebook and emails don't have role in brand building, at least as they are used at the time of carrying out this case study.

The brand experience map indicates which attributes are and are not emphasized in the customers' minds. As the Novita Company was involved in the first part of the study where important attributes were collected, it can be used to compare how successful the company is in communicating different values. Thus, it shows the direction for better communication between brand owner and customer. According to this case study, Novita should pay more attention to the attributes honest and ethical, and consider how these attributes could be expressed in a better way in their communication.

The results also indicate that loyalty has very much to do with the product itself, the yarn, in addition to communication. The most important communication channels, magazine and the Neulomo community, have a very important impact on loyalty. Other channels, emails, Facebook, Lanka-deli, fairs or packaging, were not mentioned by the consumers although Novita sees them as important parts of the brand building.

It is important for the brand owner to understand which issues have an effect on loyalty. The Neulomo members rave over the importance of the internet community - they spend a lot of time there. However, if there was another similar community available, would the members leave this one? Based on the observations from this study, the interaction with the members is the key issue. That is, keeping the Neulomo community satisfied in a way that they feel that Novita Company listens to them and appreciates their opinions and activities is of major importance. This has made it possible for Novita to obtain such loyal customers and it is also a way to maintain loyalty.

As this case study was carried out in a project that aims at taking a look into the future of printed magazines, it was of specific interest to consider what the role of the magazine in brand building is. It was quite obvious, that the magazine itself as an artefact is important for the Neulomo members. This is very well in accordance with the studies of Luomanen (2010) and Peteri (2006). From company point of view, also the magazine has an important role in building customer loyalty. Brand communication was strongly connected to the magazine. However, the magazine today is not used for interactive communication with the Neulomo members as the internet community is. It is very important to take into account that as interactivity with the Neulomo members is one of the key elements in building and maintaining loyalty, this should most certainly also be considered from the viewpoint of the printed magazine. Interactivity could also be utilized to attract new customers to buy the magazine and bring them to the Neulomo community.

5. Conclusions

Based on the experiences from this case study with Novita it can be concluded that the brand experience map suits well for research purposes. With the use of the map we are able to visualize the viewpoints of the brand owner and its customers in the same figure, and present the current situation of how the customers find the brand. Interpreting the brand experience map gives important information for improving the brand communication and stressing which are the attributes the brand owner should pay attention to in order to change or strengthen the experience the brand evokes in the customers' minds. By repeating the measurements after the brand owner has made an attempt to change or strengthen the experience and drawing a new version of the experience map, we are able to show how the situation has changed.

In the media environment we live at today, the channels people use for communication are ever increasing and therefore also very challenging to study. In addition, very few studies take into account the strengths of printed products in the media mix. However, printed magazines can still have an important role, and this role may very well be taken into account as one channel among others with an approach as presented in this study. As the roles of different channels are not static, and new ones come along, the results of this study may also change over time, even if no action is taken from the brand owners' side. Hence, in cases where the brand experience map is used, its role can be active as presented above in showing how to affect the brand experience of the customers or passive in assisting in the observation of the customers and giving the brand owner information of the direction into which its customer's values are moving.

Acknowledgements

This study was carried out as a part of Tekes funded project "Future of the Magazine". Authors would like to thank Tekes for funding, Sappi Fine paper for steering the research and Novita for joining the project as a case company.

References

- Aikala, M., Arvola, A., Heiniö, R.-L., (2011) *Tuntutestausmenetelmän kehittäminen pakkauksille. VTT Working Papers 160. VTT, Finland. 24 pages. (in Finnish).*
- Aikala, M., Nieminen, S., Poropudas, L., Seisto, A., (2003) *The end user aspects in print product development. 30th IARIGAI Conference, 7-10 September, 2003, Dubrovnik, Croatia, 11p.*
- Brakus, J., Schmitt, B., Zarantonello, L., (2009) *Brand Experience: What Is It? How Is It Measured? Does It Affect Loyalty? Journal of Marketing 73(May 2009), 52-68.*
- Jackson, J. E., (2003) *A User's guide to principal components. John Wiley & Sons, USA 2003, 569p.*
- Luomanen, J., (2010) *Living with the Media. Analysing Talk about Information and Communication Technology. Doctoral dissertation. Published in the series of Media Studies, Tampere University Press.*
- Malär, L., Krohmer, H., Hoyer, W., Nyffenegger, B., (2011) *Emotional Brand Attachment and Brand Personality: The Relative Importance of the Actual and the Ideal Self. Journal of Marketing 75(July 2011), 35-62.*
- Mensonen, A., Aikala, M., Laine, J., (2010) *Multisensory evaluation of the paper products. 37th IARIGAI Conference, 12-15 September, 2010, Montreal, Canada.*
- Mensonen, A., Hakola, J., (2012) *Novel value perceptions and business opportunities through packaging customization. International Journal of Business and Social Science 3(2012)5.*
- Peteri, V., (2006) *Home by media. A study on domestication of media technologies. Doctoral dissertation. Published in the series of Media Studies, Tampere University Press.*
- Thomson, M., MacInnis, D., Park, W., (2005) *The Ties That Bind: Measuring the Strength of Consumers' Emotional Attachments to Brands. Journal of consumer psychology 15(2005)1, 77-91.*
- Zarantello, L., Schmitt, B., *Using the brand experience scale to profile consumers and predict consumer behaviour. Brand management 17(2010)7: 532-540.*
- Yoo, B., Donthu, N., *Developing and validating a multidimensional consumer-based brand equity scale. Journal of Business research 52(2001), 1-14.*



On the definition of a multi-criteria model for the evaluation and adoption of packaging

Marios Tsigonias^{1,2,3}, *Nikolas Kakizis*³, *George Romanos*³, *Antonios Tsigonias*¹,
*Diana Tsimis*¹, *Anastasios Politis*^{1,2}, *Dimitrios Zevgolis*²

¹ Technological Educational Institute of Athens

Dept. of Graphic Arts Technology

Ag. Spyridonos, GR-12210 Egaleo, Greece

E-mails: mtsigon@chem.demokritos.gr; antonio_tsigonias@yahoo.gr; ditsimis@teiath.gr;
politisresearch@techlink.gr

² Hellenic Open University

School of Applied Arts

18, Parodos Aristotelous St., GR-26335 Patra, Greece

E-mail: zevgolis@eap.gr

³ National Center of Scientific Research "Demokritos"

Terma Patriarchou Grigoriou & Neapoleos

GR-15310, Ag. Paraskevi, Greece

E-mails: kakizis@chem.demokritos.gr; groman@chem.demokritos.gr

Abstract

Packaging, in all its facets and applications, is a complex industrial process characterized by a multi-disciplinary technological and scientific dimension. To this end, packaging systems and solutions can be considered the product of a technological and scientific process that validate and integrate into a single product entity results, conclusions, trends and cumulative experience from a multitude of sources ranging from technological innovation to socioeconomic trends and liberal arts. The current paper proposes a multi-criterion, multi-tier model suitable for the analysis and assessment of packaging processes and the resulting products. The Packaging Multi-Criteria Analysis (PMCA) model provides an integrated method for not only the post-implementation assessment of packaging systems, but also for the design, feasibility and expected socioeconomic and artistic impact of new approaches in the development of packaging processes in general. The PMCA is expected to provide orientation as well as practical guidance on the decision making process pertaining to the development of new packaging systems that will be well adopted to a wide range of business, marketing or other needs.

Keywords: packaging, multi-criteria analysis, packaging planning, packaging evaluation, packaging systems assessment, packaging performance index - PPI

1. Introduction - Multi-criteria analysis (MCA)

The words criterion and attribute are often used synonymously in the MCA-relative literature (Unknown, 2009). In this manner, an attribute usually refers to a measurable criterion and a multi-criteria analysis constitutes an approach aimed at comparing different forms of input or output and integrating them in a coherent form. Nevertheless, decision-making, correlation of non-homogeneous information, (i.e. artistic value of product, process costs, environmental impact, current consumer trends, etc.) and resolution of particularly complex problems, is not possible to be carried-out by means of a one-dimensional analysis or through a simple two-parameter optimization process. This has led to the development of new multivariable or multi-criteria analysis methods. Thus, an MCA analysis method can be regarded as an advanced form of operational research and decision making at both theoretical and practical levels. MCA methodologies are nowadays being regarded as essential decision support and operational planning and design tools with the primary scope of reducing the confusion caused in cases involving many different criteria and sources of information that relate to specific options. (Janssen, 2001; Brown, Joulert, 2011; Atanackovic et al., 1998; Giampietroa et al., 2006; Voropai, Ivanova, 2002).

Essentially, an MCA method achieves the composition and management of a large body of information, a comprehensive look on all aspects of the problem, criteria - factors that influence the decision making process (Doubos, Zopounidis, 2004). However, it is of utmost significance for an MCA to maintain the pre-

ferences, views, opinion and ideas of the end-user and/or the stakeholder and capitalize on the end-user's experience and specific knowhow, while at the same time maintaining the impartial participation of the stakeholder in the MCA process, (Sheppard, Meitner, 2005; Harrison, Qureshi, 2000). Therefore, the key success-factor of an MCA process is the realization of a balanced synthesis of the stakeholders group that will implement the MCA in the light of policy-making and system preferences and values used by the stakeholder, balancing between all stakeholders, adjusting where necessary and proportionate to the objectives, attribute special weights to the factors taken into consideration so as the final decision values may reflect the stakeholders experiences and know-how (Doubos, Zopounidis, 2004; Doubos, 2007).

Adopting this pragmatic approach has better results of an MCA process as the management of inhomogeneous information and sizeable data discourages analysts and decision makers in other circumstances. The development of an MCA process and the selection of an MCA model and specific parameters is directly related to the approach used in the composition of all parameters involved into reaching rational and well-informed decisions. To this end, the main purpose of MCA is to support decision makers facing problems based on non-homogeneous, multi-variable parameters and information. Typically, an MCA approach attempts to correlate under a single functional and coherent framework loosely related parameters in cases where a unique optimal solution does not exist and it is therefore necessary to use stakeholders experiences and preferences to differentiate between solutions and assess alternative decision scenarios.

2. The proposed packaging multi-criteria analysis model (PMCA)

Packaging design and evolution, is a multi-disciplinary, multi parametric process that needs to take into consideration different, even contradictive criteria such as:

- Graphic and Manufacturing Design;
- Marketing – Branding;
- Materials and manufacturing processes;
- Logistics and supply chain support;
- Environmental impact;
- Capital and operational costs;
- Legislation;
- Innovation and adoption of new or breakthrough technologies.

The values and weighing of each of these criteria are depended to the valuation and data/information fusion process of many sub-criteria, which are combined and valued so as to provide a combined value. To this effect, the process of designing and development an MCA method for the analysis and assessment of packaging systems and processes is a complex combinational process that has to abide to conditions pertaining to:

- internal consistency and logical soundness;
- transparency;
- ease of use;
- data requirements not inconsistent with the importance of the issue being considered;
- realistic time and manpower resource requirements for the analysis process;
- ability to provide an audit trail, and
- software availability, where needed.

The combination of the criteria and the prior conditions used results in the formulation of the MCA backbone. In order to evolve the process and taking into consideration that an MCA technique commonly applies numerical analysis to a performance matrix in two stages, the next MCA process steps are identified in the forms of Scoring and Weighting of criteria. In scoring, the expected consequences of each option are assigned a numerical score on a strength of preference scale for each option for each criterion. More preferred options score higher on the scale, and less preferred options score lower. In practice, scales extending from 0 to 100 are used, where 0 represents a real or hypothetical least preferred option, and 100 is associated with a real or hypothetical most preferred option. All options considered in the MCA would then fall between 0 and 100. In the weighting process, numerical weights are assigned to define, for each criterion, the relative valuations.

In this manner, the implementation of the PMCA model follows two main stages or phases. Phase 1 is thus determined by the successful completion of the following tasks:

1. Criteria identification and definition,
2. Criterion-specific stakeholders/experts group formulation;
3. Identification of contributing sub-criteria for each criterion;
4. Determination of sub-criteria valuation methods (numerical assessment and calibration, consumer polling, end-users/experts polling etc.);
5. Determination of weighing factor per sub-criterion;
6. Assessment of each sub-criterion and averaging of values so as to reach a criterion value.

Phase 2 of the PMCA process involves the combination of the weighted criteria into a two-dimensional graphical representation that allows for the reaching of informed decisions. The scoring of each criterion is the combined value of the weighed sub-criteria derived by means of equation 1.

$$\beta = \frac{\alpha_1\beta_1 + \alpha_2\beta_2 + \dots + \alpha_\mu\beta_\mu}{\alpha_1 + \alpha_2 + \dots + \alpha_\mu} \tag{1}$$

Where $\alpha_1, \alpha_2, \dots, \alpha_\mu$ are the weighing factors and $\beta_1, \beta_2, \dots, \beta_\mu$ the criterion values of each sub-criterion and μ is the number of sub-criteria that consist the specific criterion. The combination of the values of all criteria results in Equation 2.

$$PPI = \frac{\alpha_1\beta_1\alpha_2\beta_2 + \alpha_2\beta_2\alpha_3\beta_3 + \dots + \alpha_v\beta_v\alpha_1\beta_1}{\alpha_1\alpha_2 + \alpha_2\alpha_3 + \dots + \alpha_v\alpha_1} \tag{2}$$

Where similarly α_i is the weighing factor and β_i the criterion value of each criterion contributing to the determination and valuation of the Packaging Performance Index, or PPI. PPI may also be subsequently derived by Equation 3 which is a more comprehensive version of Equation 2.

$$PPI = \frac{\sum_{i=1}^v [(\alpha_i\beta_i)(\alpha_{i+1}\beta_{i+1})] + \alpha_v\beta_v\alpha_1\beta_1}{\sum_{i=1}^v (\alpha_i\alpha_{i+1}) + \alpha_v\alpha_1} \tag{2}$$

The values for each criterion derived by the application of Equation 1 may be plotted into a two-dimensional plot, as presented in Figure 1.

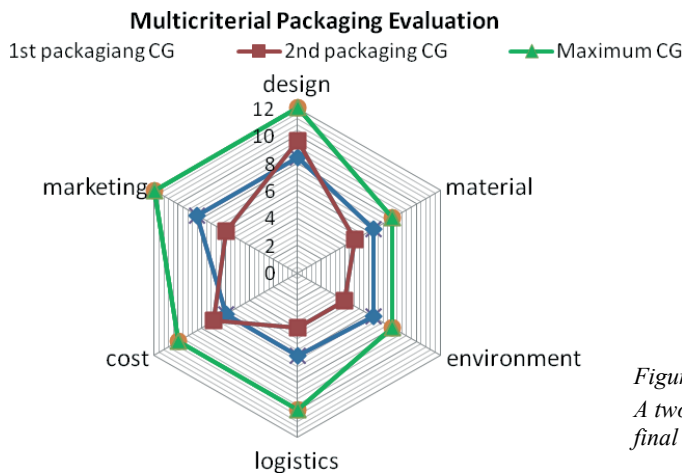


Figure 1: A two dimensional plot of the PMCA model final implementation results

3. Applying the proposed PMCA model

In this paragraph we are going to present the use of the PMCA Model through a case study. For this purpose we are testing the two phase PMCA in a case of milk packaging reconstruction that occurred as an outcome of the dissertation of Ms Maria Psarogiannakopoulou during her studies in the Graphic Arts Technology De-

partment (TEI of Athens). Ms Psarogiannakopoulou attempted to propose a new series of packaging for fresh milk products. Some of her new design proposals are depicted in Figure 1b. Her alternative proposals did not limited by graphic and constructive design improvements but many more suggestions were included in the final packaging proposals such as marketing and material improvements, environmental benefits etc.



Figure 2: a) The existing packaging (©Friesland Campina) and b) The new packaging proposal (©Psarogiannakopoulou Maria)

In order to evaluate the new packaging proposal compared to the existing one the two phase PMCA Model was used. In the first phase 6 basic criteria are sort out. Each criterion is evaluated by an independent special-ists group. Methodology that each group evaluates the sub-criteria of their field may depends on the criterion. Some evaluation procedures may exploit the authority of the experts groups but the majority of the criteria are evaluated after thorough researches in the market or after strict laboratory quality controls and comprehensive studies. The use of some auxiliary evaluation tables is extremely useful in the first phase of analysis. The first phase evaluation procedure, criterion by criterion, is depicted indicative on the Tables 1 to 6.

Table 1: First phase analysis, evaluation of the 1st Criterion (Design) performance

Criterion	Sub-criterion	Alternative Packaging Performance					
		Existing packaging	New packaging	Ideal solution	Very good	Sufficient	Non axeptable limit
1st Criterion Design	Visual Communication	6	7	8	7	6	5
	Graphic Design	10	11	12	10	8	6
	Constructive Design	7	7	8	7	6	5
	Technical Printing Issues	7	7	8	7	6	5
	Technical Construction Issues	7	7	8	7	6	5
	Legislation	6	6	6	5	4	3
1st Criterion Performance		43 (0.86)	45 (0.90)	50 (1.0)	43	36	29

Table 2: First phase analysis, evaluation of the 2nd Criterion (Marketing - Branding) performance

Criterion	Sub-criterion	Alternative Packaging Performance					
		Existing packaging	New packaging	Ideal solution	Very good	Sufficient	Non axeptable limit
2nd Criterion Marketing - Branding	Visual Communication	5	6	7	6	5	4
	Consumers pshycology	9	10	11	10	8	6
	Marketing research	6	6	7	6	5	4
	Branding Strategy	6	7	7	6	5	4
	Competition - Innovation	6	6	7	6	5	4
	Economical Issues	5	5	6	5	4	3
	Legislation	5	5	5	5	4	3
2nd Criterion Performance		42 (0.84)	45 (0.90)	50 (1.0)	44	36	28

Table 3: First phase analysis, evaluation of the 3rd Criterion (Materials - Construction) performance

Criterion	Sub-criterion	Alternative Packaging		Ideal	Very good	Sufficient	Non axeptable
		Existing	New				
3 rd Criterion Materials - Construction	Physicochemical	7	7	8	7	6	5
	Printability	10	10	12	10	8	6
	Formability	7	7	8	7	6	5
	Construction	7	7	8	7	6	5
	Environment	7	7	8	7	6	5
	Legislation	6	6	6	5	4	3
3rd Criterion		44	44	50	43	36	29

Table 4: First phase analysis, evaluation of the 4th Criterion (Logistics) performance

Criterion	Sub-criterion	Alternative Packaging Performance		Ideal solution	Very good	Sufficient	Non axeptable limit
		Existing packaging	New packaging				
4 th Criterion Logistics	Labeling	6	6	7	6	5	4
	Protection and Safety	9	9	10	9	8	6
	Secontary –tertiary packaging	6	7	7	6	5	4
	Innovative technologies	6	6	7	6	5	4
	Energy & Transportation Costs	6	6	7	6	5	4
	Batches recalls	6	6	7	6	5	4
	Legislation	6	6	5	5	4	3
4th Criterion Performance		45 (0.90)	46 (0.92)	50 (1.0)	44	37	29

Table 5: First phase analysis, evaluation of the 5th Criterion (Environment) performance

Criterion	Sub-criterion	Alternative Packaging Performance		Ideal solution	Very good	Sufficient	Non axeptable limit
		Existing packaging	New packaging				
5 th Criterion Environment	Production pollutants	7	7	8	7	6	5
	Transportation pollutants	10	11	12	10	8	6
	Packaging pollutants	7	7	8	7	6	5
	Recyclability or Degradability potential	7	7	8	7	6	5
	Waste handling	7	7	8	7	6	5
	Legislation	6	6	6	5	4	3
5th Criterion Performance		44 (0.88)	45 (0.90)	50 (1.0)	43	36	29

Table 6: First phase analysis, evaluation of the 6th Criterion (Cost) performance

Criterion	Sub-criterion	Alternative Packaging Performance		Ideal solution	Very good	Sufficient	Non axeptable limit
		Existing packaging	New packaging				
6 th Criterion Cost	Production Cost	6	6	7	6	5	4
	Filling Cost	8	9	10	10	8	6
	Transportation Cost	6	6	7	6	5	4
	Recall & Defective Cost	6	6	7	6	5	4
	Packaging Cost vs Product Price	6	6	7	6	5	4
	Advertisement Cost	5	5	6	5	4	3
	Waste handling Cost	6	6	6	5	4	3
6th Criterion Performance		43 (0.86)	44 (0.88)	50 (1.0)	44	36	28

Table 7: Second phase analysis, evaluation of the 6 Criteria performance (Packaging Performance Index)

	Criterion 1 Design	Criterion 2 Marketing	Criterion 3 Materials	Criterion 4 Logistics	Criterion 5 Environment	Criterion 6 Cost	
	α_1	α_2	α_3	α_4	α_5	α_6	
Weighting Factor	20%	20%	15%	15%	15%	15%	
	β_1	β_2	β_3	β_4	β_5	β_6	PPI
Existing packaging Criterion Value	0.86	0.84	0.88	0.90	0.88	0.86	0.7518 or 75.18%
New packaging Criterion Value	0.90	0.90	0.88	0.92	0.90	0.88	0.7906 or 79.06%

In the second phase another independent experts group is going to determine the Weighting Factor of each Criterion. In our Case the experts group decided to value the first two Criteria slightly higher than the rest four. This was done because of the Branding Strategy that has to be reinforced in this particular scenario. With the use of Equation 1 all Criterion values are calculated for both Existing packaging and New packaging Solutions. Finally we may work out the data on Table 7 and with the use of Equation 3 we may calculate the Packaging Performance Indexes for both alternative packaging solutions.

In the Table 7 the optimum packaging solution is clearly indicated. On the other hand there is no other information offered such as weighted criterion values. For these purposes the 2 dimensional diagrammes are much more convenient. In Figure 3 the alternative packaging solutions are compared in a manner that not only indicates the optimum one but also provides us with much more descriptive characteristics.

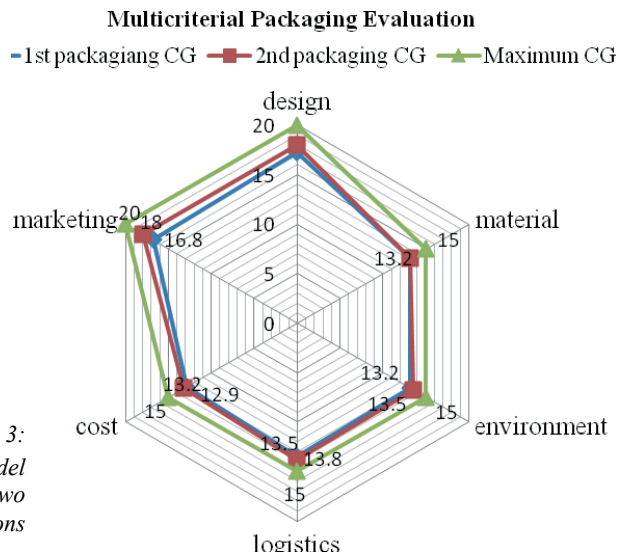


Figure 3: A two dimensional diagramme of the PMCA model with the final implementation results of the two alternative packaging solutions

4. Discussion and conclusions

In this paper a multi-criteria analysis model (PMCA) is proposed for the evaluation of packaging design strategy. PMCA is an indicative solution that is able to work functionally in most packaging design related situations but it is strictly recommended to work on the model and reconstruct it before use. It is impossible for a single model to describe every situation since packaging is a complex, multi-disciplinary field that involves so many materials, processes and ideas. This is the reason that a general and quite simple two phase (stage) model was suggested that allows for easy of use and high levels of parameterization for implementation under different conditions, scenarios and user specific requirements. For more complex situations, reconstruction of the model and transformation into a three stage evaluation model would be more appropriate by a possible subsequent increase of the criteria and the sub-criteria that are evaluated in each stage. For less complex situations, some of the valuated sub-criteria may not be taken into consideration or even implement an even simpler one stage model. The main advantages of the use of a multi-criteria packaging evaluation model can be depicted in Figure 4.

In general the PMCA allows for:

- Quantification and qualification of a complex decision making process;
- Visualization of alternative solutions and scenarios;
- Optimization of processes and resources used;
- Implementation of a structured decision making process.

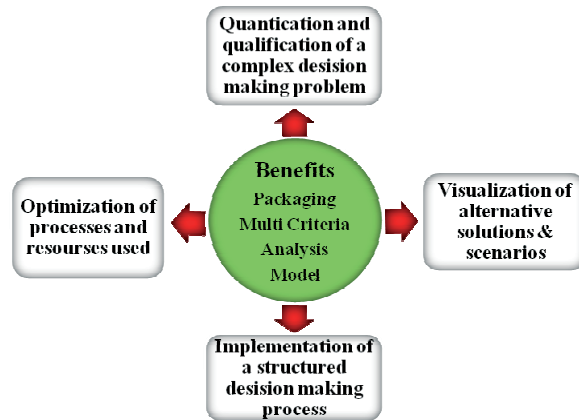


Figure 4: Benefits and expected impact of the implementation of the PMCA model in the packaging industry

In overall the proposed PMCA model and methodology framework, can be reasonably assumed that it follows a Linear Additive Model (LAM) (Uknown, 2009). In addition to that and depending on the fact that in many cases pairwise comparisons, between either different criteria or between options and alternative scenarios need to be carried-out it is subsequently deducted that in many cases the LAM evolves into an Analytical Hierarchy Process (AHP) as the decision maker/expert under the process of assessing weights, is asked a series of questions, each of which determines how important one particular criterion is relative to another for the decision, or the scenario being addressed (Shim, 1989). In general the proposed PMCA model follows the LAM approach as it assess and valuates criteria that are preferentially independent of each other. The linear model shows how an option's values on the many criteria can be combined into one overall value. This is done by multiplying the value score on each criterion by the weight of that criterion, and then adding all those weighted scores together. However, this simple arithmetic is only appropriate if the criteria are mutually preference independent. LMA models have a well-established record of providing robust and effective support to decision-makers working on a range of problems and in various circumstances. However and since a sizeable "uncertainty" is inherent to the overall process of reaching a decision for the packaging system and/or process, further examination and research may be required and an uncertainty factor to be formally integrated in the PMCA model.

References

- "Multi-criteria analysis: a manual", (2009), *Communities and local Government Publications, London*.
- Atanackovic, D., McGillis, D. T., Galiana, F. D., (1998), "The application of multi-criteria analysis to substation design", *IEEE Transactions on Power Systems, Vol. 13, No. 3*.
- Brown, C. A., Joulert, A., (2003), "Using multicriteria analysis to develop environmental flow scenarios for rivers targeted for water resource management", *Water SA, Vol. 29, No 4*.
- Doubos, M., (2007), "Multivariable decision support systems, Lecture Notes", *Technical University of Crete, Department of Manufacturing and Production Engineers*.
- Doubos, M., Zopounidis, K., (2004), "Multivariable decision making - Methodological approaches and applications".
- Giampietroa, M., Mayumib, K., Munda, G., (2006), "Integrated assessment and energy analysis: Quality assurance in multi-criteria analysis of sustainability", *Energy 31: 59-86*.
- Harrison, S. R., Qureshi, M. E., (2000) "Choice of stakeholder groups and members in multi-criteria decision models", *Natural Resources Forum 24, 11- 19*.

Janssen, R., (2001), *"On the Use of Multi-Criteria Analysis in Environmental Impact Assessment in The Netherlands"*, *J. Multi-Crit. Decis. Anal.* 10: 101-109.

Sheppard, S. R. J., Meitner, M., (2005) *"Using multi-criteria analysis and visualization for sustainable forest management planning with stakeholder groups"*, *Forest Ecology and Management* 207: 171-187.

Shim, J. P., (1989), *"Bibliographical research on the analytic hierarchy process (AHP)"*, *Socio-Economic Planning Sciences*, 23: 161-167.

Voropai, N. I., Ivanova, E. Yu., (2002), *"Multi-criteria decision analysis techniques in electric power systems expansion planning"*, *Electrical Power and Energy Systems* 24: 71-78.

The emotional impact of packaging design. An eye tracking analysis

Ulrich Nikolaus, Denise Lipfert

HTWK
Leipzig University of Applied Sciences
Gutenbergplatz 2 - 4, D-04103 Leipzig, Germany
E-mail: nikolaus@fbm.htwk-leipzig.de

Abstract

Improvement of merchandise appeal, increasing the willingness to buy, advertisement of product modifications - there are several reasons why packages are often designed to have an emotional impact on consumers. In this paper, the emphasis is set on user reactions to packaging design.

We present the results of an eye tracking study, where user reactions to (prescription only) pharmaceutical packaging with rather simple, restrained designs are compared to the more sumptuous styling of chocolate boxes. Differences in user reaction/information reception are described and implications for packaging design discussed.

Keywords: packaging; paper and ink interaction; print quality and measurement

1. Introduction

Product packaging has to fulfill multiple functions: in addition to the physical protection of the product, it has to relay a wide range of information (cf. Berndt & Sellschopf 2011) - e.g. on product properties, its application or usage, origin and price.

In addition, it is an important marketing instrument as well - ensuring brand recognition, product differentiation and increasing the willingness to buy (cf. Hinz & Weller 2011). An important task in packaging design is to create designs that reconcile all of these requirements, in order to satisfy the consumer's need for information while simultaneously creating a favorable emotional impact desired by the producer.

As it is difficult to achieve all of these objectives at the same time, packaging design often needs to compromise, only partially achieving one aim in order to reach an objective with a higher priority. Evidently, it is dependent on the product which of these requirements is more important: In pharmaceutical packaging, for instance, customer information on active ingredients and dosage is certainly much more important than it is in chocolate packaging - where, on the other hand, marketing goals may be of a higher significance.

Thus, objectives in packaging design differ, leading to a different use of visual components (text, images, color etc.) depending on whether the main focus is more on information transfer or rather on stimulating emotional responses. By using different layouts and designs, designers intend to cause different user reactions, thus hoping to initiate changes in the customer's perception and cognition.

Increasing the emotional appeal of products has recently become a major trend in brand communication (cf. Munzinger & Musiol 2009, 125; Busch 2007, 5). Today, products have to compete with hundreds of others in the shelves (Munzinger & Musiol 2009, 235), whose properties are becoming increasingly similar (cf. Hinz & Weller 2011, 234). This decrease in product differentiation makes it necessary to find other ways to distinguish a product or offering from its competitors. As the emotional impact of a product (or its packaging) is considered to influence the consumer's behavior, motivation and (buying) decisions (cf. Bittner & Schwarz 2010, 18) it is supposed to be an interesting tool to stir desire and produce sales (Munzinger & Musiol 2009, 16).

It is generally assumed that packaging design indeed *does* stimulate emotions, and that the emotional impact packaging design has on consumers is influenced by such factors as the size or shape of the packaging, graphic and surface design, color or typography (cf. Hinz & Weller 2011, 236; Duchowski 2007, 263). These visual marketing stimuli are thought to influence the consumer's perception and information processing (cf. Wedel & Pieters 2006, 37 ff.), thereby attracting and guiding his attention (Munzinger & Musiol 2009, 50 f).

While some authors are convinced that emotions are the key to improve sales, discuss case studies and promote "emotional selling" (e.g. Bittner & Schwarz 2010), others state a lack of literature or well-developed theories (Tapio Neuwirth 2008, 25) or note that some methods used in practice are based upon outdated beliefs and theories on advertising appeal (Munzinger & Musiol 2009, 215).

Recently, eye tracking has been considered to be a reliable tool to measure user reactions to visual stimuli (Busch 2007, 5). Wedel and Pieters (2006, 2) state that in the last decade, there has been a rapid growth in commercial applications of eye-tracking technology to assess the effectiveness of visual marketing efforts - and that the recognition of the central role of attention in consumers' cognitive processes and behavior and the realization that eye movements are an accurate reflection of these processes has furthered the use of eye-movement research in academia as well (l.c., 45). Though they concede that more research is needed to address the effects of the informational and emotional content of visual marketing stimuli on attention (l.c., 60), and Duchowski (2007, 262) states that the use of eye trackers is not often well documented or otherwise advertised (he speculates that advertising companies do not wish to disclose the usage of eye trackers because they fear that this might be perceived by the buying public as somewhat devious (l.c., 274)), they also consider eye trackers to be valuable tools in marketing research (l.c.).

Although most of the research published addresses issues like copy testing, print advertising, or ad placement and is not especially focused on packaging design (l.c.; Busch 2007; Wedel & Pieters 2006), some of the results describing user reactions to these visual stimuli may certainly apply accordingly to packaging.

Some results that might be applicable in general are, for instance, that *pictures* have a high tendency to attract attention (Wedel & Pieters 2006, 50), are traditionally believed to have a higher emotional impact on consumers than textual information (Munzinger & Musiol 2009, 67) and therefore may be particularly suited to add an emotional appeal to a product (Busch 2007, 5). *Brand or logo elements* are also considered to be crucial in integrating information and in routing the consumer's attention (Wedel & Pieters 2006, 51). Besides, it seems that the style of a pictorial is able to influence the emotional appeal - color photos, for instance, tend to be interpreted as realistic and honest, whereas black and white photos create a more nostalgic and outdated impression (Seeger 2009, 366).

Compared to *text*, pictures are said to have some additional advantages - for instance, that pictures are better suited to catch the viewer's attention and could be processed more quickly (Busch 2007, 40 f.) - which might lead to the assumption that reading is a rather tedious task and that text, therefore, is not very well suited for marketing purposes.

Using eye tracking technology, assumptions like these can now be put to a test, and it can be determined if results from other fields of application are valid for packaging design as well.

The aim of this study was to identify differences in consumer reaction to various packaging designs. Objectives of research were to find out, if specific viewing patterns could be identified for emotional appealing and non-emotional packaging designs, respectively, and if characteristic differences could be detected. Next, it was to be determined which design elements (product names, product shots, brand names, logos etc.) got most of the attention, and which ones attracted the attention of the viewers first. Regarding the relationship between images and text, it was to be tested if pictorial elements got higher attention values than textual elements, and if this was always the case (or if, for instance, pharmaceutical packages got higher attention values for text and chocolate boxes higher values for pictures). At last, in a post-test survey, the test participants were asked to assess the emotional impact of the test samples and to specify which design elements influenced this assessment most.

Half of the designs that were chosen for the test were packages for prescription-only drugs. As they are not to be sold over the counter, marketing issues can be assumed to be of minor importance, the main focus being on information transfer. These packages were assumed to have a rather simple, restrained design. To obtain a sufficient amount of test samples, two pharmacies that deliver presorted drugs to nursing homes were asked to collect their left over packages over a period of two weeks. As it turned out, not all prescription-only drugs had minimalistic packaging designs. Therefore, the following criteria were defined that were likely to increase the emotional impact of a packaging design in the view of the authors: nonstandard typography, multi-colored designs or colored backgrounds, color gradients, ornamental images or elaborate logos, trim lines, gloss lamination or embossment. For the test, six test samples were chosen at random that met at most two of the criteria named above. As a control element, one package was chosen that met five of the above criteria (five being the maximal number of matches that any of the packaging designs achieved).

The other half of the test samples were chocolate boxes that had a more salient, sumptuous styling. Here the design was focused on providing buying incentives and increasing the merchandise appeal, whereas product information was of minor importance (at least compared to pharmaceutical packaging). To find packages with a rather high merchandising appeal, the authors decided to choose products that were both well-known and successful. The samples were selected by analyzing the best seller list of a specialist web shop for chocolates and other sweets (details can be found in Lipfert 2012, 38 f.). Again, the choice was narrowed by defining certain criteria: All seasonal goods and packages with obtrusive discount markers were excluded as well as those with transparencies, holograms, embossment or other effects. For the sake of simplicity, all samples had to be available in German stores as well. As before, six test samples were chosen, supplemented by one control element that contained less images and more text and was therefore assumed to be less emotional than the others.

2. Research and methods

The eye tracking tests that will be described in this paper was performed at the Leipzig University of Applied Sciences (HTWK Leipzig) in October 2011 (Lipfert 2012). The research design of this study being as follows:

Subjects:

Twenty fourth-year students (14 males, 6 females) studying Media Technology at HTWK Leipzig were recruited for the experiments. They had normal or corrected vision, and their ages ranged from 18 to 34 years (23.3 on average). Although they all attended basic lectures on visual media design in their first year, none of them had special knowledge in packaging design.

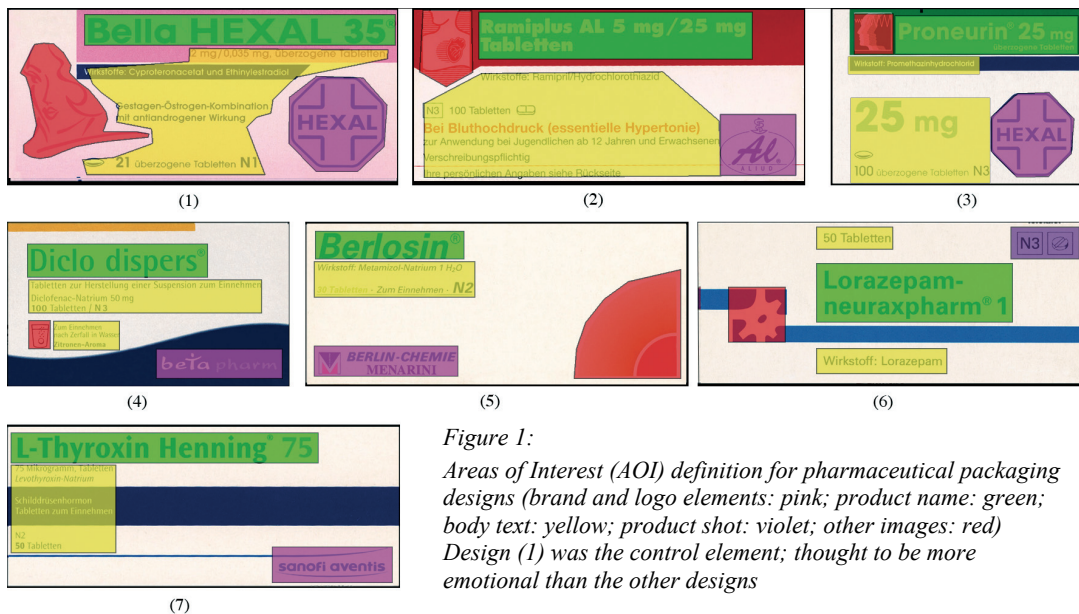


Figure 1:

Areas of Interest (AOI) definition for pharmaceutical packaging designs (brand and logo elements: pink; product name: green; body text: yellow; product shot: violet; other images: red) Design (1) was the control element; thought to be more emotional than the other designs

Stimuli:

Because the eye tracking system used for this test was computer-based, two-dimensional reproductions of the fourteen sample packaging designs were shown to the test participants on a 17" computer screen in random order¹. To use the screen resolution to its full capacity, all samples were in landscape format, and to improve the quality of the samples, all packages were both scanned and reproduced photographically and then combined and retouched using an image processing program to obtain a realistic recreation.

These fourteen designs (seven chocolate boxes and seven pharmaceutical packages) were then shown to the subjects on a dark background; one sample at a time, each display lasting five seconds. All participants saw the pharmaceutical packages first and the chocolate boxes afterward. Within each group of packaging

¹ For a more detailed discussion on using digital images instead of real packages for the visual assessment of visual packaging designs, please cf. (Laine et al. 2010).

designs, the stimuli were displayed in random order. Using eye tracking technology, the overall distribution of attention was analyzed in order to identify differences in user reaction.

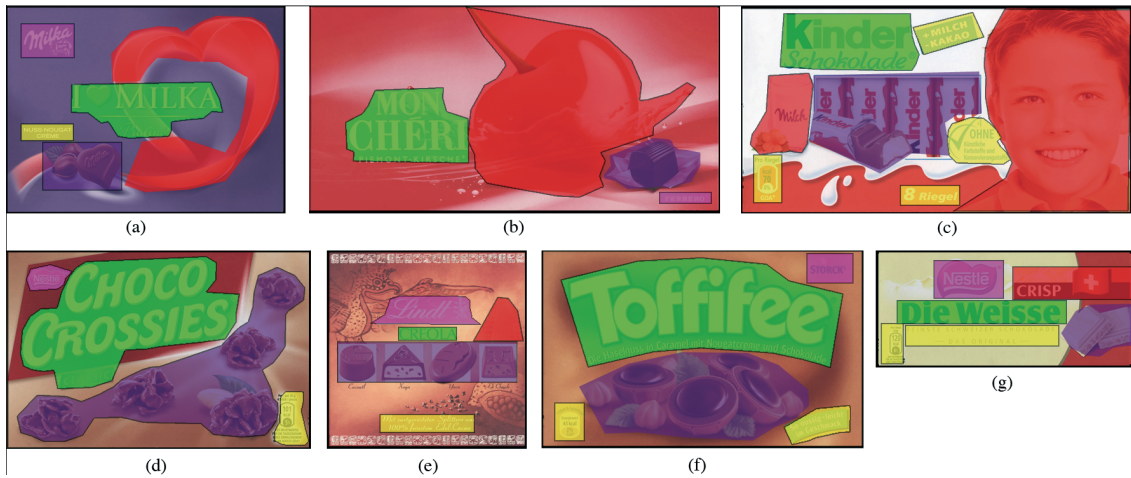


Figure 2: Areas of Interest (AOI) definition for chocolate boxes (brand and logo elements: pink; product name: green; body text: yellow; product shot: violet; other images: red) Design (g) was the control element; thought to be more simple, restrained than the other designs

Apparatus and procedure:

The stimuli were presented on a NYAN 2 XT/EDGE eye tracking system produced by Interactive Minds, Dresden (Interactive Minds 2012). A Samsung SyncMaster 17" TFT display with 1280 × 1024 pixel resolution was used at a sampling rate of 60 Hz rate and 0.45° accuracy. The samples were slightly enlarged in order to compensate for the lower resolution of computer screens.

Then, user reactions were recorded and their visual scan paths analyzed. In order to assess the relative importance of the main visual components on the sample packages (brand name, logo, product name, product shot etc.). Areas of Interest (AOI) were defined beforehand for each of these elements in order to compare hit rates, the time to first fixation, gaze durations etc. These Areas of Interest are shown in Figure 1 and Figure 2, respectively.

After the test, the participants were asked to complete a questionnaire, inquiring at the outset to name those designs that were already known to them prior to the test and to rate the display time (too short/too long). Furthermore, they were asked to assess for each design, whether it was rather informative than emotional (or vice versa), and to name those visual components most important for this decision.

3. Results

In a first step, the overall emotional impact the presented stimuli had on the test participants was to be determined. To do this, the test subjects were asked to rank all packaging designs by using a 7-point Likert scale ranging from very emotional (+3) to very restrained (-3)². As the results in Figure 3 show, all pharmaceutical packages were assigned non-emotional values (the control element being the only exception), whereas all but two chocolate boxes were placed on the emotional side (one of these two being the control element). Thus, the assessment of the test subjects was more or less consistent with the expectations of the study design.

In a next step, it was to be determined if this difference in emotional appeal triggered different information reception strategies that led to observable variations in eye movements. A comparison of various scan paths (mapping the eye movement of a test subjects to the corresponding stimulus) allowed for a quick first estimate.

² In order to prevent a distortion of the eye tracking test results, this question was included in the post-test-questionnaire. Before answering the question, the corresponding packaging design was displayed to the test participants for another second, which was assumed to be long enough to recall but not long enough to extract new information, which might possibly have influenced the answers in the post-test survey.

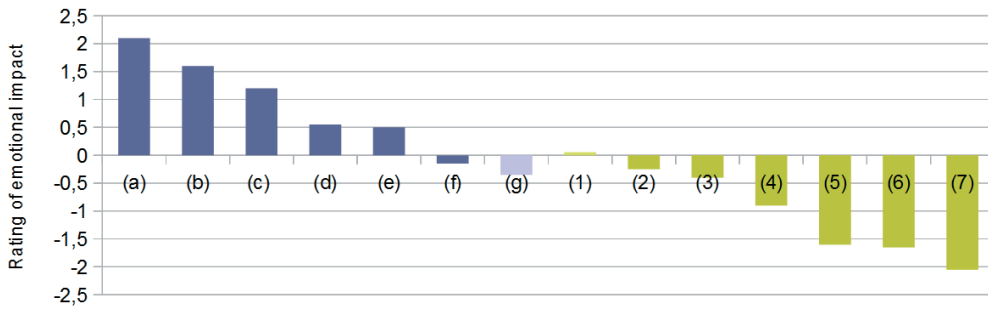


Figure 3: Rating of the emotional impact of all stimuli by test participants in a post-test survey using a 7-point Likert scale. Chocolate boxes are marked (a) - (g); pharmaceutical packages (1) - (7). Please note that (g) and (1) are control elements

For pharmaceutical packaging, the results were largely as expected. The scan paths of the participants were more or less homogeneous, their eye movement essentially following a standard reading pattern (cf. Figure 4). The measurements for the Time to First Fixation in Table 1 (i) show that for all stimuli, the attention of the test participants focused first on text elements; either on the product name or the body text (there was an almost equal distribution between these two). Furthermore, text elements were not only the first to be fixated, they also got the longest viewing time (cf. Table 1 (ii)). Pictorial elements, on the other hand, received considerably less attention - with two notable exceptions: The (in the original multicolored) logo in Figure 1 (5) and the rather unusual, gear-wheel like object in Figure 1 (6) were the only ones to receive a significantly higher attention. The results for design (1), which was supposed to be the control element, did not differ significantly from the other designs in the test



Figure 4: Sample scan paths from pharmaceutical packaging design analysis. Each circle visualizes a fixation of the viewer. The numbers in the upper half of the circle specify the order in which the fixations were made, the number in the lower half and the size of the circles visualize gaze duration

For pharmaceutical packaging, the results were largely as expected. The scan paths of the participants were more or less homogeneous, their eye movement essentially following a standard reading pattern (cf. Figure 4). The measurements for the Time to First Fixation in Table 1 (i) show that for all stimuli, the attention of the test participants focused first on text elements; either on the product name or the body text (there was an almost equal distribution between these two). Furthermore, text elements were not only the first to be fixated, they also got the longest viewing time (cf. Table 1 (ii)). Pictorial elements, on the other hand, received considerably less attention - with two notable exceptions: The (in the original multicolored) logo in Figure 1 (5) and the rather unusual, gear-wheel like object in Figure 1 (6) were the only ones to receive a significantly higher attention. The results for design (1), which was supposed to be the control element, did not differ significantly from the other designs in the test.

In the post-test survey, the test participants were asked to specify, which design elements had influenced their rating shown in Figure 3 most. All test subjects ascribed the highest influence values to the design color and the text elements. The only pictorial elements that got significantly higher ratings were the stylized outlines of four heads that can be found in the upper left corner of Figure 1 (3). Interestingly, this design was rated as the second most emotional of all packaging designs (the control element excluded). With the exception of design in Figure 1 (3), which was familiar to 7 out of 20 test participants, all other designs were unknown to all but one or two test subjects.

Table 1: Eye tracking results for prescription-only pharmaceutical packaging designs (average of all individual results). (i): The Time to First Fixation (in seconds) indicates, when a certain Area of Interest (AOI) was first focused. (ii): The Gaze Duration (in seconds) indicates the average viewing time for a certain AOI. The expression "n.a." (not available) indicates there is no such design element in this particular packaging design. The earliest and second earliest values (or highest and second highest, respectively) are marked for clarity

Time to first fixation	(1)	(2)	(3)	(4)	(5)	(6)	(7)
Product name	0.67	0.78	0.81	0.43	1.17	0.28	0.56
Body text	0.62	0.56	0.76	0.92	0.54	2.11	0.55
Brand / Logo	2.23	4.01	2.31	3.4	2.35	n.a.	2.98
Other images	2.1	1.24	2.06	3.42	2.99	2.25	n.a.
Product shot	n.a.	n.a.	n.a.	n.a.	n.a.	2.6	n.a.

(i)

Gaze duration	(1)	(2)	(3)	(4)	(5)	(6)	(7)
Product name	0.67	0.86	1.31	0.91	0.55	1.4	0.95
Body text ³	2.44	2.36	0.87	1.47	1.54	0.57	2.26
Brand / Logo	0.13	0.11	0.34	0.36	0.68	n.a.	0.31
Other images ³	0.28	0.14	0.15	0.07	0.41	0.61	n.a.
Product shot	n.a.	n.a.	n.a.	n.a.	n.a.	0.39	n.a.

(ii)

Compared to the pharmaceutical packaging designs, the eye tracking results for the chocolate packaging proved to be more ambiguous. Here, no uniform viewing patterns could be detected; the scan paths showed more variation from one test subject to another (cf. Figure 5).



Figure 5: Sample scan paths from chocolate box design analysis. Each circle visualizes a fixation of the viewer. The numbers in the upper half of the circle specify the order in which the fixations were made, the number in the lower half and the size of the circles visualize gaze duration

The values for Time to First Fixation in Table 2 (i) show that, again, the name of the product (i.e. a text element) was the item that first grabbed the attention of the test participants. In general, the product shot and brand or logo elements came second and third. Whereas the quite prominent red cherry in Figure 2 (b) got the attention of the test subjects comparatively early, other quite noticeable pictorial elements like the red heart in Figure 2 (a) or the boy's face in (c) attracted the attention of the test participants comparatively late. Furthermore, the pictorial of the Swiss flag in Figure 2 (g) obviously caught the participants' eye sooner than the corresponding product shot.

A comparison of Table 2 (i) and (ii) shows that whereas brand or logo elements grabbed the subjects' attention quite early in the scanning process, it was obviously only viewed for a short time, because the gaze duration values are comparatively low (though they are still higher than the corresponding gaze duration values for pharmaceutical packaging). Body text, on the other hand, grabbed the participants' attention rather late, but it kept their attention longer than the brand/logo elements. Apart from that, product names, product shots and other pictorials got, on average, most of the attention.

The gaze duration was longest for the product name in Table 2 (a), (b) and (f), and longest for the product shot in Table 2 (c), (d) and (e). In Table 2 (g), the Swiss flag got more viewing time than the corresponding product shot. Remarkable are the high gaze duration values for the logo element in Figure 2 (a), the big red cherry in Figure 2 (b) and the boy's face in Figure 2 (c).

³ For designs that included more than one body text element or more than one image apart from the product shot and the brand and logo elements, the gaze duration for that body text / image element that got the most attention is shown.

Table 2 (i): Eye tracking results for chocolate box designs (average of all individual results). (i): The Time to First Fixation (in seconds) indicates, when a certain Area of Interest (AOI) was first focused. (ii): The Gaze Duration (in seconds) indicates the average viewing time for a certain AOI. The expression "n.a." (not available) indicates there is no such design element in this particular packaging design. The three earliest (or highest) values are marked for clarity

Time to first fixation	(a)	(b)	(c)	(d)	(e)	(f)	(g)	Gaze duration	(a)	(b)	(c)	(d)	(e)	(f)	(g)
Product name	0.32	0.41	1.03	0.47	0.72	0.44	0.64	Product name	1.43	1.34	0.46	1.02	0.27	1.45	0.58
Body text	2.63	n.a.	1.84	2.47	2.57	3.0	2.01	Body text ⁴	0.35	n.a.	0.37	0.81	0.48	0.48	0.57
Brand / Logo	1.76	2.38	n.a.	1.93	0.91	2.06	1.33	Brand / Logo	0.53	0.22	n.a.	0.37	0.41	0.3	0.49
Other images	2.47	0.87	4.29	n.a.	1.3	n.a.	1.37	Other images ⁴	0.32	1.03	0.73	n.a.	0.29	n.a.	0.67
Product shot	2.34	1.87	0.49	1.38	0.89	1.96	2.51	Product shot	0.48	0.51	0.73	1.21	0.87	0.75	0.54

(i) (ii)

Results from the post-test survey show that, apart from Figure 2 (e) and (g), all packaging designs were known to almost all of the participants. When asked to assess which design elements influenced their rating of the emotional impact (shown in Figure 2) most, color and the product shot were mentioned most often (14.4 and 9.6 times out of 20, respectively). Product names, body texts and brand/logo elements were mentioned less frequently (5.6; 3.0 and 3.3 times, respectively). Here, the test subjects could add elements of their own to the given list, and three design elements were named remarkably often: the boy's face in Figure 2 (c), the heart and the word "love" in design (a).

4. Discussion

Interpreting the results, first, it has to be stated that there definitely is a difference in the information reception processes reflected in the eye tracking results. The homogeneous, reading-order based scan paths recorded while showing the pharmaceutical stimuli certainly differ from the more irregular, less predictable patterns for chocolate boxes. However, the two examples inserted as control elements (design (I) that was considered to be quite elaborate for a prescription-only packaging and design (g) that was thought to be rather austere for a chocolate design) showed only minor differences compared to the other designs of the same group. This could mean that their emotional appeal is either too weak to elicit significant changes in the participants' reactions, or that there may be different viewing strategies that could have been learned beforehand and are activated if the viewer looks at a pharmaceutical package or a chocolate box, respectively.

Assessing the relative importance of the various elements used in packaging design, it has to be stated that pictorial elements got less attention from the test participants than expected. We assumed that the attention of the subjects would focus - at least while looking at the chocolate boxes - first and foremost on the graphic elements of the packages. It turned out, however, that the product name (a text item) was the most important element for all viewers. It caught the participants' attention sooner and held it longer than the pictorial elements - which would support results in ad design stating that text elements (most notably: headlines) may be more important than previously thought (cf. Busch 2007, 40; Wedel & Pieters 2006, 49). Though pictorials do have a high tendency to attract attention (and have been assigned a certain influence on the emotional appeal of a packaging design in the post-test survey), their influence tends to be over-estimated. In particular, the size of a certain pictorial does not seem to be the primary factor in capturing the viewer's attention (as the comparatively high attention values for the rather small brand element in Figure 6 (i) compared to the huge red heart or the rather high values for the product shot in Figure 6 (ii) compared to the big red cherry) show. This, again, is consistent with findings in (Wedel & Pieters 2006, 51). Thus, images got less attention than assumed; especially background-images got low attention values, even if they were big in size and clearly intended to be "key visuals".

⁴ For designs that included more than one body text element or more than one image apart from the product shot and the brand and logo elements, the gaze duration for that body text / image element that got the most attention is shown.

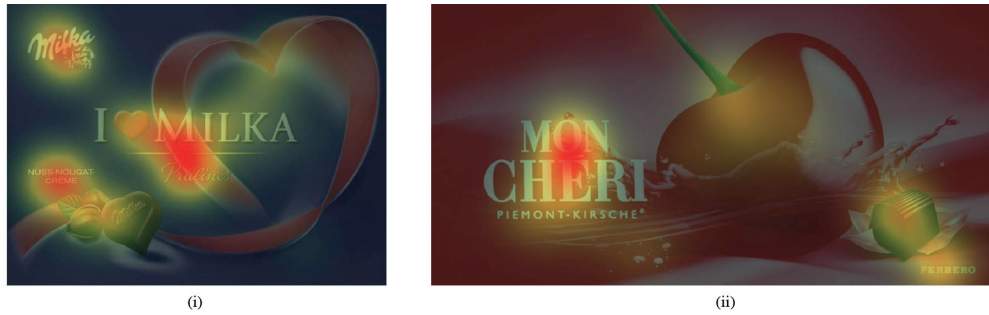


Figure 6: Sample heat maps from packaging design analysis. Those areas of the stimuli that received most attention from the test participants are marked with colored spots (red means high levels of attention, followed by yellow and green). Areas that got only minor attention are darkened

The assumption that certain key stimuli like erotic signals or pictures showing children, animals or faces get a higher visual attention (Munzinger & Musiol 2009, 86, 97; Seeger 2009, 364; Busch 2007, 6) could at least be confirmed for the faces in the designs (4), (7) and (c): Though they did not belong to those components that grabbed the viewer's attention early, they tended to get a higher gaze duration and were mentioned by the participants as having an influence on the emotional appeal in the post-test survey.

While pictorials got less attention than assumed, text elements got more. Especially the product name is standing out, because it got not only very early fixations, but also long gaze durations. Thus, it seems to be the key design element that viewers use to identify a certain package design and to employ it as a visual anchor for the subsequent viewing process. This, again, is consistent with findings from ad design, where the headline of an ad has been attributed a pivotal role (cf. Duchowski 2007, 264; Wedel & Pieters 2006, 50 f.). Other design elements that are used for identification seem to be the brand and logo elements: though they get comparatively low gaze durations, they get their first fixations comparatively early. Results in (Wedel & Pieters 2006, 52) and (Duchowski 2007, 265) point to a crucial role of brand and logo elements in routing the viewers' attention and in promoting accurate brand memory (although additional research seems to be necessary).

Considering its relatively small size, body text seems to get comparatively high attention values. This is certainly so for the pharmaceutical packages, but also for the text elements on chocolate boxes (considering the minor percentage of design space they get). Though, according to the post-test survey, text seems to play an important role in rating the emotional appeal of a packaging design as non-emotional, they do grab the viewer's attention, and can, therefore, not be neglected in packaging design. Again, various results from ad design emphasize the relative importance of body text (cf. Duchowski 2007, 264 ff.; Busch 2007, 40).

Furthermore, the familiarity of packaging seems to be a factor that may not be neglected. As mentioned before, results from the post-test survey showed that most of the chocolate box designs were known to the test participants, whereas most of the pharmaceutical packaging designs were not. According to results from (Wedel & Pieters 2006, 60 f.), this has to be taken into account, because familiar designs "require and attract less attention than unfamiliar ads because they are easier to process. ... Familiarity decreases attention to the brand, does not affect pictorial attention, but increases attention to the text". The authors suggest that familiar designs can be learned and that, on repeated viewing, only one or two basic features are used by the viewers while trying to identify a brand rapidly and accurately (l.c., 55). Consequently, in the post-test survey, when asked to assess the display duration of five seconds that was predefined for each stimulus, test participants tended to assess this period as being too short for the pharmaceutical packaging designs, but not so for the chocolate boxes (Lipfert 2012, 66): possibly, because this period of time is long enough for recognition, but too short for an all-embracing scan of an unknown design. Therefore, it might be interesting to repeat the eye tracking test using chocolate boxes that are comparatively unknown to the test subjects, in order to determine if this has a significant impact on their viewing strategies.

One final result that could be derived from the survey conducted at the end of the usability test showed that the subjects attributed a much higher emotional values to the *coloring* of the packaging than to the images. In fact, when asked to specify which design element influenced their rating of the emotional appeal of the packaging most, color got the highest values (on average 16.9 mentions out of 20 for packaging designs and 14.4 for chocolate boxes, respectively), followed, for the pharmaceutical designs, by textual and brand/logo elements (7.9 and 3.7 mentions, respectively) and, for the chocolate boxes, by product shot and product name (9.6 and 5.6 mentions, respectively).

Thus, color seems to play a most important role in influencing the emotional impact of a packaging design. Unfortunately, these effects are hard to explore using eye tracking technology, if the whole package is designed in a bright violet or red (as Figure 2 (a) and (b)): if the background, product shot and additional images are all designed in different shades of the same color, it is hard to determine by looking at scan paths and gaze durations, if the attention of the viewers is more on the shown objects or on their color values. Color is an inherent value of all objects that cannot be separated from the other properties of a design element.

5. Conclusions

Summarizing, it can be said that by comparing both groups of packaging designs, differences in user reaction could certainly be detected: The visual scan paths were more predictable for the pharmaceutical packages than for the more marketing-oriented designs of the chocolate boxes. However, the importance of text elements even for the more emotional designs seems to be higher, whereas the importance of images seems to be lower than originally assumed. The coloring of the packaging, on the other hand, seems to have a much higher emotional impact on consumers; its importance should likewise not be underestimated.

An interesting finding is that apparently minor details of the packaging design like the insertion of a stylized head in a logo, the usage of the word "love" in a brand name or a Swiss flag can have a significant influence on viewing strategies and on the emotional impact of a packaging design. This reconfirms the common rule that in graphic design, details matter - and even small changes can significantly improve (or else: impair) the emotional appeal of a (packaging) design.

Thus, careful planning and execution and analysis of packaging designs are crucial to ensure consumer acceptance and economic success of the corresponding products (Hinz & Weller 2011, 227). As this study indicates, eye tracking can play a valuable role in evaluating, understanding and improving existing packaging designs. As of now, however, these examinations tend to raise as many new questions as they may answer, because the information reception and the subsequent cognitive processes are quite complex and still not fully understood. Therefore, eye tracking still requires some expertise and poses some challenges (Duchowski 2007, 301); sometimes results are not completely consistent across studies (Wedel & Pieters 2006, 55), some are "underresearched" (i.e., 52) and some factors need to be further investigated (i.e., 65). Nonetheless, as eye tracking is entering into mainstream science and is becoming continuously easier to use (Duchowski 2007, VII; 301) it may become a valuable tool to increase the visual efficiency and the emotional appeal of packaging designs.

Acknowledgments

The authors would like to thank all students of the Leipzig University of Applied Sciences (HTWK) that volunteered for their participation in the test. Special thanks to Eugen Herzau and Katharina Roerber for fruitful discussions, to André Göhlich (all HTWK Leipzig) for his help in preparing the test and in visualizing the results and to Nadia Nikolaus for proof-reading and most helpful suggestions.

References

- Berghaus, N., (2005). *Eye-Tracking im stationären Einzelhandel: Eine empirische Analyse der Wahrnehmung von Kunden am Point of Purchase*. Lohmar: EUL.
- Berndt, D., Sellschopf, L., (2011). *Verpackungsfunktionen*. In: Kaßmann, Monika (ed.): *Grundlagen der Verpackung. Leitfaden für die fächerübergreifende Verpackungsausbildung*. Beuth: Berlin Vienna Zürich.
- Bittner, G., Schwarz, E., (2010). *Emotion Selling. Messbar mehr verkaufen durch neue Erkenntnisse der Neurokommunikation*. Wiesbaden: Gabler.
- Busch, H., (2007). *Eye Tracking. Die Kunst des Augenblickes*. Berlin: VDZ.
- Duchowski, A. T., (2007). *Eye Tracking Methodology: Theory and Practice*. London: Springer
- Hinz, K., Weller, B., (2011). *Planung und Gestaltung von Verpackungen*. In: Kaßmann, Monika (ed.): *Grundlagen der Verpackung. Leitfaden für die fächerübergreifende Verpackungsausbildung*. Beuth: Berlin Vienna Zürich
- Interactive Minds (2012). *Eyegaze Edge System*. Retrieved 2012-07-13 from: <http://www.interactive-minds.com/de/eyetracker/eyegaze-edge>

Laine, Janne; Rusko, Elina; Arvola, Anne Pajukunta Janne; Nurmi, Olli, (2010). Computer-displayed images in the subjective assessment of visual packaging designs. In: Enlund, Nils; Lovreček, Mladen (ed.): Advances in printing and media technology XXXVII. Darmstadt: International Association of Research Organisations for the Information Media and Graphic Arts Industries (IARIGAI)

Lipfert, D., (2012). Emotionale Wirkung von Verpackungsdesign - eine Nutzeranalyse mittels Eye-Tracking. Diploma thesis. HTWK Leipzig: Leipzig

Munzinger, U., Musiol, K. G., (2009). Markenkommunikation. Wie Marken Zielgruppen erreichen und Begehren auslösen. Munich: mi-Wirtschaftsbuch

Nielsen, J., Pernice, K., (2010). Eyetracking web usability. Berkeley, Calif.: New Riders.

Seeger, H., (2009). Praxisbuch Packaging. Wie Verpackungsdesign Produkte verkauft. Munich: mi Wirtschaftsbuch.

Tapio Neuwirth, E., (2008). He knows the customs of the customer (Profile Jens Nordfält). In: SCA Shape 3 (2008), pages 23-25

Wedel, M., Pieters, R., (2006). Eye tracking for visual marketing. Foundations and trends in marketing. Boston: now Publ.

Index of authors

- (von) Arx, Urs 97
 Ahtik, Jure 91
 Aikala, Maiju 271
- Bablyuk, Evgeny 61
 Backhaus, Johannes 227
 Batagelj, Boštjan 83
 Baumann, Reinhard 33, 43
 Bernet, Pascal 97
 Beynon, David 169
 Bircher, Fritz 97
 Bitsch, Thorsten 221
 Blohm, Erik 261
 Bogataj, Urška 83
 Borbély, Ákos 115
 Bornemann, Nils 221
 Bould, David 187
 Bračko, Sabina 313
 Budimir, Ivan 107
- Cheng, Ssu-Yi 241
 Claypole, James 207
 Claypole, Timothy 153, 169, 181, 187
- Davies, Glyn R. 181
 Deganello, Davide 153, 207
 Deger, Wolfgang 33
 Desch, Michael 253
 Dörsam, Edgar 47, 69, 159, 175, 221, 253
 Držková, Markéta 17, 75
 Dziallas, Holger 33
- Đokić, Miloje 83
- Enlund, Nils 3
 Enns, Eugen 33
 Espig, Michael 43
- Fleming, Paul 53
 Fukushima, Hiroyuki 53
- Galton, David 181
 Galus, Matthias 213
 Gane, Patrick 195
 Gatsou, Chrysoula 293
 Gregor Svetec, Diana 83
 Griesheimer, Stefan 175
 Guck, Tim 221
- Hall, Richard 181
 Hamblyn, Anja 153
 Hamblyn, Simon 181
 Harri, Liliya 245
 Heinz, Sebastian 43
 Hoić, Ana 123
 Horváth, Csaba 117, 139
 Hsieh, Yung-Cheng 241
 Husovska, Veronika 53
- Izdebska, Joanna 233, 245
- Jesenko, Janko 131
 Jewell, Eifion 187
 Jutila, Eveliina 195
 Juhola, Helene 23
- Kakizis, Nikolas 329
 Kao, Chih-Cheng 241
 Kaplanová, Marie 17
 Klanjšek Gunde, Marta 11
 Knox, Mike 53
 Kohl, Albert 33
 Krause, Reinhold 97
 Kuula, Timo 271
- Laine, Janne 321
 Lee, Kuo-Kun 241
 Lipfert, Denise 337
 Lumby, Natalia 303
 Lyashenko, Alexandra 69
- Maček, Marijan 83
 Markkula, Kristiina 27
 Massfelder, Daniel 159
 Mensonen, Aino 321
 Milosavljević, Dragan 227
 Morić Kolarić, Branka 107
 Mozetič, Miran 5
 Možina, Klementina 145, 287, 313
 Muck, Tadeja 83
- Nagornova, Irina 61
 Neumann, Jann 159, 253
 Nikolaus, Ulrich 337
- Pavlovič, Leon 83
 Pekarovicova, Alexandra 53
 Peřinka, Nikola 17, 75
 Petek, Bojan 131, 281
 Pivar, Matej 83
 Podsiadlo, Halina 245
 Politis, Anastasios 293, 329

- Praprotnik, Ana 281
Pavlovič, Leon 83
Pekarovicova, Alexandra 53
Peřinka, Nikola 17, 75
Petek, Bojan 131, 281
Pivar, Matej 83
Podsiadło, Halina 245
Politis, Anastasios 293, 329
Praprotnik, Ana 281
- Rat, Blaž 287, 313
Rättö, Peter 261
Ridgway, Catherine 195
Roberts, Kathy 53
Roch, Martin 75
Romanos, George 329
- Salun, Larisa 69
Sauer, Hans-Martin 47
Schär, Manfred 97
Seisto, Anu 271, 321
Selbmann, Karl-Heinz 97
Siegel, Frank 33, 43
Spiehl, Dieter 253
Stahl, Simon 47
Stark, André 43
- Syrová, Lucie 17
Syrový, Tomáš 17, 75
Szentgyörgyvölgyi, Rozália 117
Szymanowski, Maciej 233
- Theopold, Alexandra 159
Trost, Thomas 261
Tsigonias, Antonios 329
Tsigonias, Marios 329
Tsimis, Diana 329
Urbanc, Tanja 145
- Vadnjal, Klemen 281
Vatrapu, Ravi 271
- Weichmann, Armin 213
Willert, Andreas 33, 43
Williams, Phylip 207
Wolber, Tim 213
- Zevgolis, Dimitrios 293, 329
- Žiljak Stanimirović, Ivana 123
Žiljak Vujić, Jana 107, 123
- Żolek-Tryznowska, Zuzanna 233



Call for papers

The Journal of Print and Media Technology Research is a peer-reviewed periodical, published quarterly by [iarigai](http://www.iarigai.org), the International Association of Research Organizations for the Information, Media and Graphic Arts Industries.

Authors are invited to prepare and submit complete, previously unpublished and original works, which are not under review in any other journals and/or conferences.

The journal will consider for publishing papers on fundamental and applied aspects of at least, but not limited to, the following topics:

- ⊕ Printing technology and related processes
Conventional and special printing; Packaging, Printed functionality (incl. polymer electronics, sensors, and biomaterials); Printed decorations; Printing materials; Process control
- ⊕ Premedia technology and processes
Color reproduction and color management; Image and reproduction quality; Image carriers (physical and virtual); Workflow and management
- ⊕ Emerging media and future trends
Media industry developments; Developing media communications value systems; Cross-media publishing
- ⊕ Social impact
Media in a sustainable society; Consumer perception and media use

Submissions for the journal are accepted at any time. If meeting the general criteria and ethic standards of the scientific publication, they will be rapidly forwarded to peer-review by experts of high scientific competence, carefully evaluated, selected and edited. Once accepted and edited, the papers will be printed and published as soon as possible.

There is no entry and/or publishing fee for authors.

Authors are asked to strictly follow the guidelines for preparation of a paper (see abbreviated version on inside back cover). Complete guidelines can be downloaded from

<http://www.iarigai.org/publications/>

Papers not complying with the guidelines will be returned to authors for revision.

Submissions and queries should be directed to

journal@iarigai.org or office@iarigai.org

Subscriptions 2013

Journal of Print and Media Technology Research is published in print version and distributed by subscription only, solely or in package with the annual edition of the Advances in Printing and Media Technology. The following subscription models are available:



Journal of Print and Media Technology Research*

A peer-reviewed quarterly
ISSN 2223-8905

- | | |
|--------------------------------------------------------------------------------------------------------------------------------|----------------|
| A Regular annual subscription (4 issues p. a.) | 300 EUR |
| B Members of iarigai - one copy (4 issues) free of charge
Additional copies for members - discount 20% | 240 EUR |



Advances in Printing and Media Technology - Vol. 40**

(hard bound book with selected and edited full conference papers)
ISSN 2225-6067, ISBN 978-3-9812704-5-7

- | | |
|-------------------------------------------------------------------------------------------------------------------|----------------|
| C Regular rate per copy | 155 EUR |
| D Members of iarigai - one copy free of charge
Additional copy for members - discount 20% | 124 EUR |



Two-in-one package (JPMT and Advances - Vol. 40)**

(valid only if ordered together)

- | | |
|-------------------------------------------------------------------------------------------------------------------------------------------------------|----------------|
| E Annual subscription to the journal + current volume of the Advances in Print & Media Technology Research (full regular price 455 EUR) | 359 EUR |
| F Additional package for members (extra discount 26 EUR) | 333 EUR |

Select one of the offered subscription models (A - F) and place your order online at:

<http://www.iarigai.org/publications>

(open: Order/Subscribe here)

or send an e-mail order to: office@iarigai.org

* Single copies of JPMT can be purchased only if available and upon a separate request

** Vol. 40 of the Advances In printing and Media Technology will be published in November 2013